

**Controls on the deposition, accumulation and preservation of mixed
fluvial and marginal-marine successions in coastal-plain settings.**

Michelle Nicole Shiers

***Submitted in accordance with the requirements for the degree of
Doctor of Philosophy***

The University of Leeds

School of Earth and Environment

December 2016

The candidate confirms that the work submitted is her own, except where work which has formed part of jointly-authored publications has been included. The contribution of the candidate and the other authors to this work has been explicitly indicated below. The candidate confirms that appropriate credit has been given within the thesis where reference has been made to the work of others.

The thesis comprises three chapters that were prepared for publication and have been subsequently modified for inclusion in this thesis. the current status of these components of the manuscript, at the time of submission, is as follows:

Chapter 4:

Shiers, M.N., Mountney, N.P., Hodgson, D.M. and Cobain, S.L. 2014. Depositional controls on tidally influenced fluvial successions, Neslen Formation, Utah, USA. *Sedimentary Geology*, 311, 1-16. DOI: 10.1016/j.sedgeo.2014.06.005.

Shiers, M.N. – Main author. Responsible for data collection, processing, collation and interpretation, and writing of the manuscript.

Mountney, N.P. – In-depth discussion and detailed review of the manuscript

Hodgson, D.M. – In-depth discussion and detailed review of the manuscript

Cobain, S.L. – Assistance in data collection and discussions

Chapter 5:

Shiers M.N., Hodgson D.M. and Mountney N.P. 2017. Process Response to Marine Influence in Lower Coastal Plain Strata: Campanian Neslen Formation, Utah, USA. *Journal of Sedimentary Research*, 87, 168-187. DOI: 10.2110/jsr.2017.7.

Shiers, M.N. – Main author. Responsible for data collection, processing, collation and interpretation, and writing of the manuscript.

Mountney, N.P. – In-depth discussion and detailed review of the manuscript

Hodgson, D.M. – In-depth discussion and detailed review of the manuscript

Chapter 6:

Shiers M. N., Mountney N.P., Hodgson D.M. and Colombera L. (in preparation). Controls on the facies distribution and heterogeneity of lower coastal plain fluvial point-bar elements.

Shiers, M.N. – Main author. Responsible for data collection, processing, collation and interpretation, and writing of the manuscript.

Mountney, N.P. – In-depth discussion and detailed review of the manuscript

Hodgson, D.M. – In-depth discussion and detailed review of the manuscript

Colombera, L. – Data processing using the Fluvial Architecture Knowledge Transfer System (FAKTS) database developed by the Fluvial Research Group at the University of Leeds.

Parts of the Discussion (Chapter 7) also form part of a published paper:

Colombera C., **Shiers M.N.** and Mountney N.P., 2016. Assessment of Backwater Controls on the Architecture of Tributary-Channel Fills in a Tide-Influenced Coastal-Plain Succession: Campanian Neslen Formation, U.S.A. *Journal of Sedimentary Research*, 86, 476-497. DOI: 10.2110/jsr.2016.33.

Colombera, L. – Main author. Responsible for data collection, processing, collation and interpretation, and writing of the manuscript.

Shiers, M.N. – Data collection, in-depth discussion and detailed review of the manuscript.

Mountney, N.P. – In-depth discussion and detailed review of the manuscript.

This copy has been supplied on the understanding that it is copyright material and that no quotation from the thesis may be published without proper acknowledgement.

© 2016 The University of Leeds and Michelle Nicole Shiers

Acknowledgements

Firstly I would like to thank my supervisors, Dave Hodgson and Nigel Mountney. I appreciate all of the opportunities and experiences I have received during my PhD studies, including being involved in additional field experience in South Africa, attending conferences and sponsors meetings. I am really grateful for the support, guidance and encouragement you have given me over the years. Thank you to Luca Colombera for your advice; I have enjoyed the opportunity to work and published papers with you.

I would also like to thank the sponsors of FRG-ERG (AREVA, BHP Billiton, ConocoPhillips, Det Norske, Murphy Oil Corporation, Nexen, Saudi Aramco, Shell, Tullow, Woodside and YPF) for financial support. Special thanks to Nexen for their provision of an internship in their London (Uxbridge) office; the experience that I gained from this has significantly enhanced my understanding of hydrocarbon exploration geology.

I am especially grateful to the people who assisted me during my field work: Tom Wiggins, Sarah Cobain, Luca Colombera, Catherine Russell, Cathey Burns, Luke Beirne and Camille Steel; I certainly couldn't have done it without you and it would definitely have been a lot less fun. Sarah, you put up with me and helped me find the best sources of alcohol in Utah; Camille, you kept me calm through the thunderstorms and car crashes. Fieldwork was certainly a lot more fun with a 'gang': Catherine, Cathey, Luke and Luca, I will never forget sitting on the rim of the Book Cliffs watching the sun set with you all.

Thank you to everyone in the department (both past and present) who have helped me in so many ways; from cups of tea (or glasses of wine) to proofreading abstracts and practicing presentations, giving advice and just being around when a shoulder was needed; you have all made it possible for me to get to this point. Of particular mention are Tom Fletcher, Yvonne Sychala, Menno Hofstra, Janet Richardson, Hannah Brooks, Andrea Ortiz-Karpf, Sarah Cobain, Catherine Russell and Cathey Burns; it wouldn't have been the same without you. Thanks to all my friends from Leeds for providing fun away from the geology world. Life in Leeds would definitely have been more difficult without the Danow's and Magzimof's; you have no idea how much I appreciate everything you have done for me, providing me with continuous support and a place to retreat when it all got too much.

Most importantly, to my family, thanks for the years of support, hugs, encouragement, phone calls and nagging; thank you to Elliot, Victoria, Grandma and Grandpa. Finally, to my amazing parents, I will never be able to thank you enough for the unwavering love and support you have given me, being there truly whenever it was needed; I knew I could always ask for help no matter the time, place or reason and you would be there with a listening ear and a home cooked meal. I am more grateful than you will ever know.

Abstract

Discerning the roles of autogenic and allogenic controls on the deposition, accumulation and preservation of sedimentary successions requires characterisation at a variety of scales. This is especially true for paralic environments where the preserved stratigraphic record is complicated by spatial and temporal interactions of fluvial, wave and tidal processes.

The Campanian Neslen Formation (Utah) represents a marine influenced fluvial succession that accumulated in a humid, low-latitude coastal plain. Detailed lithofacies, architectural element and sequence stratigraphic analyses of the succession has involved the collection of 106 sedimentary logs, 194 architectural panels, 2000 paleocurrent readings, analysis of ichnofacies, and the tracing of key stratal surfaces in order to elucidate the relative balance of autogenic and allogenic processes. Outcrops in a range of orientations relative to the palaeoshoreline, enable the geometries of complicated architectural elements to be constrained. Mapping of channelised elements in three dimensions and the quantified analysis of their facies and geometry has been undertaken. Study sites, average spacing 3 km, have been used to produce a regional-scale correlation between sub-environments.

The lower Neslen Formation accumulated as part of a high-accommodation, transgressive succession with variable influence from marine processes. Point-bar elements in the lower Neslen Formation are isolated and lithofacies assemblages within these elements deviate from widely used facies models as a result of the combined effects of low fluvial discharge and the presence of raised mires, which acted to modify channel dynamics. High-resolution correlation of strata have enabled identification of a several marine-influenced intervals and hence a refined sequence stratigraphic framework is proposed. The upper Neslen Formation is interpreted to represent part of a lower accommodation, highstand succession within which channelised elements became increasingly amalgamated upwards.

This study demonstrates a rare example of the transfer of the fluvial-to-marine transition zone into the stratigraphic record and the implications of this for the distribution of reservoir heterogeneities. In contrast with previous studies that emphasise sea-level change as the dominant control on paralic successions; this stratigraphic dataset demonstrates the extent to which autogenic processes can modify the allogenic stratigraphic signature.

Table of Contents

Submitted in accordance with the requirements for the degree of Doctor of Philosophy.....	i
Table of Contents	vi
List of Tables	xiv
List of Figures	xv
1 Introduction.....	1
1.1 Project Rationale.....	1
1.2 Aims and Objectives.....	3
1.3 Research Questions	3
1.4 Methods.....	10
1.4.1 Field Techniques.....	10
1.4.1.1 Sedimentary graphic logs.....	10
1.4.1.2 Lithofacies analysis.....	10
1.4.1.3 Stratigraphic panels	11
1.4.1.4 Architectural elements.....	11
1.4.1.5 Palaeocurrent analysis	11
1.5 Thesis Layout.....	12
Chapter 1: Introduction	12
Chapter 2: Literature Review	12
Chapter 3: Geological Setting	12
Chapter 4: Depositional controls on a marine influenced fluvial succession	13
Chapter 5: Response of a coal-bearing coastal plain succession to marine transgression.....	13
Chapter 6: Controls on the depositional architecture of lower coastal plain fluvial point-bar elements.....	14
Chapter 7: Discussion.....	14
Chapter 8: Conclusions and future work	14
2 Literature Review	15
2.1 Fluvial depositional systems	15
2.1.1 Meandering fluvial environments.....	18
2.2 Point-bar elements	20
2.3 Marginal marine systems.....	24
2.3.1 Coastal process classification	25

2.3.2	Autogenic Controls.....	28
2.4	Fluvial-to-marine transition zone.....	30
2.4.1	Modern and ancient studies	32
2.4.1.1	Marine indicators	32
2.4.1.1.1	Sedimentary indicators.....	32
2.4.1.1.2	Ichnological indicators	34
2.4.2	Sequence stratigraphy.....	35
2.4.3	The backwater effect.....	36
2.5	Coal deposits and their significance.....	38
2.5.1	Controls	38
2.5.2	Sequence stratigraphy.....	39
2.6	Summary	41
3	Geological Setting	42
3.1	Tectonic Setting and Basin Evolution.....	42
3.1.1	Tectonic Evolution.....	42
3.1.2	Western Interior Seaway.....	43
3.1.2.1	Transgression and Regression.....	43
3.1.2.2	Tidal Range.....	46
3.2	Climate	47
3.3	Mesaverde Group Stratigraphy.....	48
3.4	Neslen Formation.....	50
3.4.1	Palaeoenvironment.....	50
3.4.2	Sequence Stratigraphy	53
3.4.3	Marine Indicators	57
3.4.4	Study area and interval	58
3.5	Summary	59
4	Depositional controls on a marine influenced fluvial succession	60
4.1	Introduction	60
4.2	Geological Setting	64
4.3	Methods.....	67
4.4	Facies and Architectural Elements.....	70
4.4.1	Architectural Element S ₁ : Multistorey multilateral sandstone element	76
4.4.1.1	Description	76
4.4.1.2	Interpretation.....	76

4.4.2	Architectural Element S ₂ : Ribbon channel-fill element.....	76
4.4.2.1	Description	76
4.4.2.2	Interpretation.....	77
4.4.3	Architectural Element S ₃ : Lenticular sandstone-dominated element 77	
4.4.3.1	Description	77
4.4.3.2	Interpretation.....	78
4.4.4	Architectural Element S ₄ : Heterogeneous lenticular element.....	78
4.4.4.1	Description	78
4.4.4.2	Interpretation.....	79
4.4.5	Architectural Element S ₅ : Amalgamated inclined heterolithic stratification (IHS) element	79
4.4.5.1	Description	79
4.4.5.2	Interpretation.....	79
4.4.6	Architectural Element S ₆ : Tabular sandstone element	80
4.4.6.1	Description	80
4.4.6.2	Interpretation.....	80
4.4.7	Architectural Element S ₇ : Coarsening-upwards sandstone element	81
4.4.7.1	Description	81
4.4.7.2	Interpretation.....	82
4.4.8	Architectural Element F ₁ : Small-scale sandstone and siltstone	82
4.4.8.1	Description	82
4.4.8.2	Interpretation.....	82
4.4.9	Architectural Element F ₂ : Fining-upwards mudstone and siltstone.....	83
4.4.9.1	Description	83
4.4.9.2	Interpretation.....	83
4.4.10	Architectural Element F ₃ : Coal-prone element	83
4.4.10.1	Description	83
4.4.10.2	Interpretation.....	84
4.5	The Stratigraphic Succession and Depositional Environment	88
4.5.1	Palisade Zone	89
4.5.2	Ballard Zone	91
4.5.3	Chesterfield Zone	91
4.5.4	Depositional Environments.....	92

4.6	Discussion.....	93
4.6.1	Overall trends in channel stacking	93
4.6.2	Controls on sand-body stacking patterns.....	99
4.7	Summary	101
5	Response of a Coal-Bearing Coastal Plain Succession to Marine Transgression: Campanian Neslen Formation, Utah, USA	103
5.1	Introduction	103
5.2	Geological Setting	107
5.3	Methods	115
5.4	Results	121
5.4.1	Lower Palisade Zone.....	121
5.4.1.1	Description	121
5.4.1.2	Interpretation.....	121
5.4.2	Palisade Coal Zone.....	122
5.4.2.1	Description	122
5.4.2.2	Interpretation.....	122
5.4.3	Middle Palisade Zone	123
5.4.3.1	Description	123
5.4.3.2	Interpretation.....	124
5.4.4	Upper Palisade Zone.....	125
5.4.4.1	Description	125
5.4.4.2	Interpretation.....	125
5.4.5	Ballard Zone.....	125
5.4.5.1	Description	125
5.4.5.2	Interpretation.....	126
5.4.6	Basal Ballard and Thompson Canyon Sandstone Beds	126
5.4.6.1	Description	126
5.4.6.2	Interpretation.....	127
5.5	Discussion.....	130
5.5.1	Stratigraphic variations	130
5.5.2	Marine-influenced packages	131
5.5.2.1	Allogenic processes	131
5.5.2.2	Autogenic processes.....	133
5.6	Summary	134

6	Controls on the depositional architecture of fluvial point-bar elements in a coastal plain setting	136
6.1	Introduction	136
6.2	Geological Setting	141
6.3	Methods.....	142
6.4	Results.....	143
6.4.1	Type I146	
6.4.1.1	Description	146
6.4.1.2	Interpretation.....	147
6.4.2	Type II.....	148
6.4.2.1	Description	148
6.4.2.2	Interpretation.....	151
6.4.3	Type III.....	151
6.4.3.1	Description	151
6.4.3.2	Interpretation.....	152
6.4.4	Type IV.....	154
6.4.4.1	Description	154
6.4.4.2	Interpretation.....	154
6.4.5	Point-bar element type summary	156
6.5	Discussion.....	158
6.5.1	Controlling Factors in the Neslen Formation	158
6.5.1.1	Systems tract and A:S ratio	159
6.5.1.2	Marine influence	160
6.5.1.3	Spatial variability.....	161
6.5.1.4	Presence of coal beds.....	162
6.5.1.5	Grain size.....	163
6.5.1.6	Flow velocity	163
6.5.2	Comparison of the Neslen Formation to FAKTS and literature...	166
6.5.2.1	Systems tract and A:S ratio	166
6.5.2.2	Marine influence	167
6.5.2.3	Presence of coal beds.....	167
6.5.2.4	Grain size.....	168
6.5.2.5	Flow velocity	168
6.6	Summary	168

7	Discussion	170
7.1	Research question one: What are the sedimentological and stratigraphic expressions of the fluvial-to-marine transition zone?	170
7.1.1	Marine influence in fluvial deposits	170
7.1.2	Stratigraphic expression of the FMTZ	174
7.1.3	Preservation of marine influence	176
7.1.4	Research question one summary	176
7.2	Research questions two and three: What is the balance of allogenic and autogenic processes in coastal plain settings?	177
7.2.1	Research question 2: What are the main controls on deposition and vertical accumulation of fluvial and marginal marine strata?.....	177
7.2.1.1	Tectonics	178
7.2.1.1.1	Basin subsidence and accommodation	180
7.2.1.1.2	Source area uplift and sediment supply	183
7.2.1.2	Eustasy.....	183
7.2.1.2.1	Shoreline processes	184
7.2.1.3	Sequence stratigraphy	184
7.2.1.4	Climate	185
7.2.1.5	Research question two summary.....	186
7.2.2	Research question 3: To what extent are autogenic processes important in producing the observed stratigraphic architecture of fluvial and marine deposits?	187
7.2.2.1	Avulsion.....	187
7.2.2.2	Presence of mires.....	188
7.2.2.3	Backwater hydrodynamics	190
7.2.2.4	Autostratigraphy	193
7.2.2.5	Delta-lobe switching.....	194
7.2.2.6	Shifting palaeoenvironments	195
7.2.2.7	Research question three summary	197
7.2.3	Research questions two and three synthesis.....	197
7.2.3.1	Increase in the aspect ratio, thickness and amalgamation of channelised elements in the upper Neslen Formation .	200
7.2.3.2	Occurrence of repeated marine influenced intervals..	200
7.2.3.3	Change from marine influence in the lower Neslen Formation to fluvial dominance in the upper Neslen Formation	201

7.2.3.4	Decrease in the quality, occurrence and thickness of coal upwards through the Neslen Formation	201
7.2.3.5	Occurrence of point-bar assemblages that do not conform to typical facies model.....	201
7.3	Research question four: How can palaeoenvironmental models of ancient marginal marine systems be constrained?	202
7.3.1	Depositional models and modern analogues	202
7.3.1.1	Palisade Zone: upper to lower delta plain/coastal plain	203
7.3.1.2	Ballard Zone: upper delta plain.....	205
7.3.1.3	Thompson Canyon Sandstone Bed and Basal Ballard Sandstone Bed: Reworked barrier and washover sandstones.....	205
7.3.1.4	Chesterfield Zone: Alluvial plain.....	206
7.3.2	Research question four summary	207
7.4	Research question five: What is the impact of marine processes on the reservoir potential of sand bodies in lower fluvial plain, coastal plain and marine marginal setting?	212
7.4.1	Heterogeneity in the Neslen Formation	212
7.4.1.1	Tidal influence	214
7.4.1.2	Wave influence	215
7.4.2	Point-bar elements.....	215
7.4.3	Research question five summary	215
8	Conclusions and Future Work	217
8.1	Conclusions	217
8.2	Recommendations for future research.....	219
8.2.1	Palynological and mineralogical analysis of sediments within the Neslen Formation.....	219
8.2.2	Three dimensional modelling of channelised elements	219
8.2.3	Down-dip correlation of Neslen Formation strata.....	220
8.2.4	Comparison to other ancient successions	220

References	222
Appendix A	260
Appendix B	262
Appendix C	274
Appendix D	293
Appendix E	305
Appendix F	306
Appendix G	318
Appendix H	331
Appendix I	335

List of Tables

Table 4-1: Table describing and interpreting the facies observed in architectural elements of the Neslen Formation.....	73
Table 4-2: Change in relative proportions of the architectural elements by area between the depositional zones of the Neslen Formation.	92
Table 5-1: Table describing the geometry, facies and ichnology of representative architectural elements of the lower Neslen Formation	114
Table 6-1: Table summarising key variables for the interpretation of different point-bar element types within the Neslen Formation.....	147
Table 6-2: Table showing quantitative analysis of channels in the Neslen Formation separated by element type.....	165
Table 7-1: Table showing the reliability of a series of a series of sedimentological and ichnological marine indicators.....	171
Table 7-2: Table describing the possible autogenic and allogenic processes which many have generated the preserved stratigraphic architecture	200

List of Figures

Figure 1.1: Map depicting the main sites of data collection in this study of the sedimentology of the Neslen Formation, Utah, USA.....	9
Figure 2.1: Simplified model of fluvial systems.....	15
Figure 2.2: The occurrence conditions of common sand bedforms	16
Figure 2.3: Classification of channel plan-view geometry.....	17
Figure 2.4: Channel plan-view geometry.....	18
Figure 2.5: Architectural elements in meandering fluvial systems.....	19
Figure 2.6: Common terminology used in analysis of meandering systems and point bars.....	20
Figure 2.7: Descriptive terminology for point-bar architecture 6.....	21
Figure 2.8: Models of inclined heterolithic strata.....	23
Figure 2.9: Plan view maps for idealised coastal depositional systems	24
Figure 2.10: Schematic diagram illustrating the division of deltas into fluvial-dominated, wave-dominated and tide-dominated types.....	25
Figure 2.12: Coastal process classification ternary plots.....	26
Figure 2.11: Schematic diagram showing how coastal environments evolve through transgression and progradation cycles.....	26
Figure 2.13: Representative schematic plan view models of the 15 classification categories in the coastal process classification.....	27
Figure 2.14: Image of modern coastline.....	28
Figure 2.15: The delta cycle.....	29
Figure 2.16: Diagram showing the changes in facies, energy, grain size, salinity and channel morphology through the fluvial-to-marine transition zone.....	30
Figure 2.17: Stratigraphic architecture of fluvial depositional sequence influenced by base-level fluctuations.....	37
Figure 2.18: Long profile view sketch of a floodplain profile, showing the relationships between tidal effects, brackish water effects and backwater effects.....	38
Figure 2.19: Relation of rate of change of base level to coal thickness and geometry.....	40
Figure 2.20: Idealised curve to show the relationship between accommodation change, peat production, peat facies and resultant coal types.....	41
Figure 3.1: Generalised map of the Western Interior Seaway.....	42
Figure 3.2: Figures showing the evolution of the Western Interior Seaway through time, adapted after Blakey 2016.....	45
Figure 3.3: Cross section of the sedimentary infill of the Western Interior Basin,..	46

Figure 3.4 Stratigraphy of part of the Mesaverde Group succession and overlying strata in the Book Cliffs.	49
Figure 3.5: General depositional setting for the western margins of the Western Interior Seaway during the Late Cretaceous.	51
Figure 3.6: Estuarine depositional model for the Neslen Formation.	51
Figure 3.7: Summary of Campanian clastic wedges in the foreland basin.....	55
Figure 3.8: Interpretations of the sequence stratigraphy of the upper Mesaverde Group).	56
Figure 3.9: Location of outcrops investigated in this study	58
Figure 3.10: Schematic diagram showing the relative position and size of study areas investigated in each chapter.....	59
Figure 4.1: Conceptual model of marine influenced environments illustrating the variability and complexity present within the marine influenced fluvial zone.....	62
Figure 4.2: Stratigraphy of the Mesaverde Group and overlying successions	63
Figure 4.3: Location maps of the study area.	64
Figure 4-4: Composite graphic sedimentary log	66
Figure 4.5: Example stratigraphic panel from the Neslen Formation.....	68
Figure 4.6: Example of reconstructed channels at different time periods A-Dc.....	69
Figure 4.7: Representative lithofacies of the Neslen Formation.....	75
Figure 4.8: Schematic depositional settings for architectural elements within the Neslen Formation and representative interpreted photographs.	88
Figure 4.9: Simplified maps through time (A-D) of the Neslen Formation outcrop.	90
Figure 4.10: Depositional models of the palaeoenvironment represented by the Neslen Formation through time.....	98
Figure 4.11: Allogenic, autogenic or combined forcing mechanisms y.....	100
Figure 5.1: Sequence Stratigraphic framework of the Book Cliffs.....	106
Figure 5.2: Stratigraphy of the Mesaverde Group in the Book Cliffs.....	108
Figure 5.3: Location maps of the study area8.....	109
Figure 5-4: Sedimentary logs recorded at each study locality	116
Figure 5.5: Sedimentary facies and ichnology observed within the Neslen Formation.).....	117
Figure 5.6: Representative architectural elements of the Neslen Formation.	118
Figure 5.7: Correlation panel of the logged sections.....	120
Figure 5.8: Summary of vertical trends through the lower Neslen Formation.	129
Figure 5.9: Modified sea-level curve for the lower Neslen Formation.	132
Figure 6.1: Conceptual model of point-bar elements.	139

Figure 6.2: Quantitative proportions of facies within modern and ancient successions analysed using data present in the FAKTS databases.....	140
Figure 6.3: Study location map.	141
Figure 6.4: Simplified stratigraphy of the Neslen Formation	142
Figure 6.5: Representative photographs of sedimentary facies observed within point-bar elements of the Neslen Formation.....	145
Figure 6.6: Quantitative analysis of facies of point-bar elements of the Neslen Formation.....	146
Figure 6.7: Example of a type I point-bar element within the Neslen Formation.	149
Figure 6.8: Example of a type II point-bar element within the Neslen Formation	150
Figure 6.9: Example of a type III point-bar element within the Neslen Formation H.	153
Figure 6.10: Example of a type IV point-bar element within the Neslen Formation.....	155
Figure 6.11: Quantitative proportions of facies within the Neslen Formation	157
Figure 6.12: Schematic panel showing the location of each point-bar element examined in this study in relation to the interpreted sequence stratigraphic framework.....	159
Figure 6.13: Schematic diagram showing the possible spatial zones for deposition of the different type of point-bar elements.....	162
Figure 6.14: Schematic models of point-bar models.	166
Figure 7.1: Schematic facies models of point-bar elements in the Neslen Formation with the relative amount of marine influence indicated.	173
Figure 7.2: Panel showing the heterogeneity of point bar elements in the Neslen Formation.....	173
Figure 7.3: Large-scale correlation panel.	175
Figure 7.4: Upstream and downstream relative influence of allogenic controls....	178
Figure 7.5: Allogenic interactions and feedback loops	179
Figure 7.6: Sequential schematic section across a foreland basin showing a cycle of thrust-load induced subsidence.....	182
Figure 7.7: Schematic diagram showing the effects which ombrotrophic mires have on fluvial systems on the coastal plain, and at the shoreline	189
Figure 7.8: Data panel showing the stratigraphic relationship between different channelised architectural elements in the Neslen Formation.....	191
Figure 7.9: Interpreted depositional zones of the backwater plain	193
Figure 7.10: Schematic diagram showing the possible palaeoenvironments for deposition of the TCSB.	195
Figure 7.11: Schematic diagram showing how different depositional zones in the Neslen Formation	196

Figure 7.12: Main allogenic controls responsible for deposition of different depositional intervals of the Neslen Formation. 198

Figure 7.13: Generalised depositional model of a fluvio-deltaic depositional environment. 204

Figure 7.14: Modern analogue for the Palisade Zone of the Neslen Formation. .. 208

Figure 7.15: Modern analogue for the Ballard of the Neslen Formation..... 209

Figure 7.16: Modern analogues for sandbodies such as the Thompson Canyon Sandstone Bed. 210

Figure 7.17: Modern Analogue for the Chesterfield Zone of the Neslen Formation. 211

Figure 7.18: Figure showing the different scales of heterogeneity observed in the Neslen Formtions 213

1 Introduction

This chapter provides an overview of the thesis and its structure. Key research questions are described at the outset and the rationale behind the research is explained.

Each subsequent chapter is outlined in turn in order to summarise the principal components of the thesis. The primary case study for this research was conducted through sedimentological analysis of part of the Cretaceous Neslen Formation, Book Cliffs, Utah, USA, and this succession is briefly introduced.

1.1 Project Rationale

Marginal marine deposits accumulate in a wide range of depositional environments that are governed by different process regimes, and which respond to changes in sea level and sediment supply in different ways. Changes in sea level, accommodation and sediment supply (dominantly allogenic parameters) control the large-scale stratigraphic architectures of marginal marine environments, and gaining an improved understanding of how these controls influence processes of sedimentation is important in reconstructing palaeogeographic settings, e.g. changes in shoreline trajectory amongst others. Given future projected rises in global sea level, understanding the process response to marine transgression across low-lying coastal-plain areas is more pertinent than ever. Furthermore, marginal marine deposits (sediment deposited at, or close to the shoreline) are important hydrocarbon reservoirs, as sources for high-quality aggregates, precious minerals and metals, and as potential sites for the underground storage of carbon dioxide.

There remains widespread debate as to the relative importance of different external controls on the evolution of marginal marine systems, and in the accumulated sedimentary and stratigraphic architecture of paralic successions. For example, several studies have questioned the applicability of long-established sequence-stratigraphic models to successions of non-marine origin (e.g. Weissmann et al. 2000; Muto et al. 2016; Hampson 2016).

The complicated interaction of marginal marine process regimes with fluvial systems is recorded in the stratigraphic architecture of such deposits. The accumulation of marginal marine and fluvial deposits through time result in paralic successions, i.e. the interfingering of fluvial and marginal marine deposits. A variety of allogenic and autogenic processes, which collectively exert a variety of controls on palaeoenvironmental development, serve to modify the deposition, accumulation and preservation of sediment through the fluvial-to-

marine transition zone (FMTZ). The FMTZ changes position over time in response to variations in fluvial discharge, tidal range and wave action (Dalrymple and Choi 2007, Martinius and Gowland 2011). The relative effect of wave, tidal and fluvial processes on sedimentation varies systematically through the FMTZ. The preserved record of the effects of controls on processes of deposition, accumulation and preservation of sediment are expressed at different scales in the stratigraphic architecture of sedimentary successions.

The FMTZ is defined as 'that part of the river which lies between the landward limit of observable effects of tidally induced flow deceleration at low river discharge, and the most seaward occurrence of a textural or structural fluvial signature at high river stage' (van den Berg et al. 2007, p289). Several recent studies have been undertaken in an attempt to characterise the deposits of the FMTZ in both modern and ancient settings (e.g. Shanley et al. 1992; van den Berg et al. 2007; Gugliotta et al. 2016). The interplay of processes of deposition, accumulation and preservation of sedimentary deposits of fluvial, wave and tidal origin recorded within a sequence stratigraphic framework have been studied previously (e.g. Shanley et al. 1994; Dalrymple and Choi 2007). However, our understanding of modern FMTZs and their preserved sedimentary products in the stratigraphic record, including their response to accommodation and sediment supply variations in time and space, remain relatively poorly documented and understood.

Although the sedimentary geology of marginal marine and fluvial successions as well as the transition between them has been investigated by several studies (e.g. Browne and Naish 2003; Dalrymple and Choi 2007; Gugliotta et al. 2016), the changes in sedimentology across a range of scales that encompasses lithofacies-, architectural element-, system- and sequence- to sequence set-scales have not been documented. This study seeks to address this shortcoming. High-resolution, multi-scale studies are used to establish the controls on deposition, accumulation and preservation of deposits of an exhumed ancient paralic succession within the context of a broader sequence stratigraphic framework. The mechanisms and balance of autogenic and allogenic controls are examined in relation to the stratigraphic expression of a paralic succession, in terms of architectural element stacking patterns, and the internal lithofacies composition of elements of mixed fluvial and marine-influenced fluvial origin present within such a succession. One avenue of investigation are the spatial and temporal changes in the character of architectural elements such as point-bar elements in stratigraphic successions.

1.2 Aims and Objectives

The aim of this study is to understand the controls on the deposition, accumulation and preservation of mixed fluvial and marginal marine successions and their variability spatially through the FMTZ. Specific objectives of this research are as follows:

- (i) Document the variety and organisation of lithofacies present within the marine-influenced fluvial system;
- (ii) Assess the controls on the pattern of stacking of fluvial, tidal and marine-influenced sand-bodies;
- (iii) Evaluate the degree to which a sequence stratigraphic framework can be applied to a relatively up-dip section of a fluvial system in a lower coastal plain succession;
- (iv) Develop an understanding of the controls on the internal character of fluvial and marine-influenced point-bar elements developed in a FMTZ setting;
- (v) Present and discuss the stratigraphic significance of evidence that provides a better understanding of the interplay of autogenic and allogenic controls on the sedimentary evolution of paralic successions.

1.3 Research Questions

The following research questions have been developed to frame the research programme. The rationale for addressing these questions is provided here, and the questions will be explicitly answered in Chapter 7 (Discussion):

1. What are the sedimentological and stratigraphic expressions of the fluvial-to-marine transition zone?

Rationale: The complexity and variation within and through the fluvial-to-marine transition zone has been the focus of much recent research (e.g. Fedo and Cooper 1990; Shanley et al. 1992; Bose and Cakraborty 1994; Ghosh et al. 2005; Cummings et al. 2006; Eriksson et al. 2006; Van den Berg et al. 2007; Flaig et al. 2009; Corbett et al. 2011; Ashour et al. 2012; Bhattacharya et al. 2012; Sisulak and Dashtgard 2012; La Croix and Dashtgard 2015; Olariu et al. 2015; Shchepetkina et al. 2016; Gugliotta et al. 2016). Research efforts to date have been focused on gaining an improved understanding of how lithofacies distributions change through this transition zone (e.g. Dalrymple et al. 1991; 1992; Browne and Naish 2003; Cummings et al. 2006; Dalrymple and Choi 2007; Gugliotta 2016). The extent to which marine (i.e. tidal and wave) processes impact on the fluvial realm is difficult to interpret from outcrop studies. Many sedimentological indicators may also form in purely fluvial environments, leading to the over-estimation of tidal influence in depositional and

reservoir models. Conversely, marine processes may be under-represented in the rock record as they commonly accumulate during episodes of low fluvial discharge in fine grained deposits, and hence have the tendency to be overprinted or eroded out by fluvial deposits during high fluvial flow.

Data collected from analysis of modern rivers (Choi et al. 2004; van den Berg et al. 2007; Dashtgard et al. 2012; Czarnecki et al. 2014; La Croix and Dashtgard 2015; Shchepetkina et al. 2016), and the analysis of modern marginal marine systems platform geometries via satellite imagery, can be applied to aid the interpretation of the geological significance of stratal relationships observed in ancient exhumed successions. These approaches require careful consideration in their application because data collected from modern systems are, by definition, representative of systems developed during sea-level highstand. Hence, modern systems represent poor analogues to ancient successions that accumulated variably during episodes of lowstand, transgression and highstand within sedimentary basins.

Gaining a more comprehensive understanding of how different factors interact to control resultant sedimentary architecture needs careful and detailed analysis of the significance of preserved stratigraphic trends. From an applied standpoint, understanding these controls is important in successfully characterising petroleum reservoirs hosted in paralic successions. Furthermore, an understanding of the processes controlling the deposition, accumulation and preservation of sediment within the fluvial-to-marine transition zone is necessary to make appropriate and justified palaeo-environmental and sequence-stratigraphic interpretations of sedimentary successions.

2. What are the main controls on deposition and vertical accumulation of fluvial and marginal marine strata?

Rationale: The principal controls on deposition, accumulation and preservation of sediments in both fluvial and paralic environments have long been attributed to allogenic processes of tectonics, climate change and eustasy (e.g., Leeder 1977; Bridge and Leeder 1979; Bristow and Best 1993; Cecil et al. 1993; Mackey and Bridge 1995; Heller and Paola 1996; Blum and Törnqvist 2000; Hampson et al. 2012; Miall et al. 2014a). Fundamentally, tectonics and eustasy control the generation of accommodation space and the rate at which this space is filled is governed by sediment supply, which itself is partly influenced by tectonics and climate (Castelltort and Van Den Driessche 2003; Armitage et al. 2011). These large-scale, extrinsic controls are interrelated, and drive changes in other, autogenic, parameters such as avulsion frequency and delta-lobe switching.

The role of allogenic processes in controlling stratigraphy, and in particular fluvial architecture, has been extensively investigated (e.g. Allen and Posamentier 1993; Aitken and

Flint 1994; Leeder and Stewart 1996; Ethridge et al. 1998; Blum and Törnqvist 2000; Cohen et al. 2005; Ethridge et al. 2005; Ambrose et al. 2009; Abels et al. 2013), with much research having focussed on fluvial response to changes in base level (e.g. Allen and Posamentier 1993; Aitken and Flint 1994; Leeder and Stewart 1996; Ethridge et al. 2005; Holbrook et al. 2006; Holbrook and Bhattacharya 2012). The rate of base-level rise can exert a profound effect on the timing and degree to which alluvial aggradation occurs, and the extent to which tidal effects are reflected upstream from contemporaneous shoreline deposits.

Marginal marine successions are interpreted in terms of sequence stratigraphy through the identification of key correlatable surfaces (van Wagoner et al. 1988; 1990; 1991; Allen and Posamentier 1993; Vail 1987). The theory of sequence stratigraphy was developed based on the stratal architectures exposed in continuous, large-scale outcrops composed of strata representative of marginal-marine and shallow-marine palaeoenvironments analysed using relatively widely spaced study sites (e.g. the late Cretaceous Star Point Sandstone, Blackhawk Formation, lower Castlegate Sandstone and related strata exposed in the Wasatch Plateau and Book Cliffs, Utah and Colorado, USA). Conceptual sequence stratigraphic models remain largely unchanged and widely applied (e.g. Shanley and McCabe 1994; Blum and Törnqvist 2000; Catuneanu et al. 2009; Neal and Abreu 2009; Jerolmack and Paola 2010). Sequence stratigraphic theory states that the principal drivers of stratal architecture are relative variations in sea-level or base-level. Understanding the principles of sequence stratigraphy and their relation to climate, tectonics and eustasy is vital in discerning the relative importance of allogenic processes in controlling the deposition and vertical accumulation of fluvial and marginal marine strata

3. To what extent are autogenic processes important in producing the observed stratigraphic architecture of fluvial and marine deposits?

Rationale: The validity of models which propose that allogenic controls exert by far the most dominant influence on the generation of large-scale sedimentary architectures is starting to be questioned. Recently, the influence of autogenic processes in modifying the sedimentary architecture of fluvial and paralic successions has been increasingly recognised (e.g. Hampson et al. 2016; Muto et al. 2007; Colombera et al. 2015; 2016a). Examples of autogenic processes which are important in fluvial and marginal marine deposits include: self-organisation (autostratigraphy; Muto et al. 2001; 2007; 2016), whereby there is a threshold to progradation following which there is autoretreat of the shoreline; avulsion dynamics (Stouthamer et al. 2011) i.e. the style and frequency of channel switching; and compactional subsidence (Brain et al. 2016) which is the rate at which the sediment auto-compacts after deposition.

An additional notable autogenic control in humid climatic settings is the presence of peat mires (Cecil 1990). Peat mires can have various influences on fluvial depositional systems through the generation of anomalous accommodation space due to rapid compaction as organic material accumulates (Ryer and Langer 1980; Fielding 1985; Courel 1987; Bohacs and Suter 1997; Holz et al. 2002) or due to the capacity of peat mires to be resistant to erosion (McCabe 1985; Eble et al. 1994; Jerrett et al. 2011b). As such, the type of peat mires and their development can modify the accumulation and preservation potential of sediment due to differential accommodation space and altering the hydrodynamics of fluvial flow.

Understanding the relative importance of autogenic and allogenic controls on sedimentation is crucial for understanding how such mechanisms are responsible for determining the resulting depositional architecture (Blum and Törnqvist 2000; Stouthamer and Berendsen 2007; Hajek et al. 2012). Discerning the relative influence of autogenic and allogenic processes is made complicated by the lack of quantitative understanding of autogenic processes and their interactions with allogenic forcing mechanisms. The ability of deposits influenced by autogenic processes to partly overprint, obscure and be confused with deposits influenced by allogenic processes, such as basin subsidence and sediment supply (Hajek et al. 2010, 2012), means that discerning the relative role of allogenic and autogenic processes requires detailed analysis.

4. How can palaeoenvironmental models of ancient marginal marine systems be constrained?

Rationale: Well-constrained palaeoenvironmental models have been produced for fluvial (e.g. Cant and Walker 1978; Fielding 1985; Abdul Aziz et al. 2003; Santos et al. 2012; Ghazi and Mountney 2012; Medici et al. 2015) and shallow and deep marine (e.g. Gardiner and Hiscott 1988; Driese et al. 1991; Gowland 1996; Figueiredo et al. 2010; Nelson et al. 2011) systems. However, the development of widely applicable models of marginal marine systems, including the FMTZ, are complicated by the wide range of sub-environments and temporal and spatial interactions of process regimes. Several site-specific palaeoenvironmental and depositional models for these systems have been developed (e.g. McIlroy 2006; Stuart 2015; Gomis-Cartesio et al. 2016). However, the development of generic models that can be applied to the construction of palaeoenvironmental models of marginal marine systems requires high-resolution, three-dimensional analysis of ancient outcrops at a variety of scales. System-scale reconstructions are largely qualitative and necessarily use widely spaced study sites and extrapolate changes in architecture and facies (e.g. Ryer 1981; Tew and Mancini 1995; McCarthy et al. 1999; Hampson et al. 2012; 2013; Longhitano and Steel 2016). This means that the reconstructions often exclude important

details, such as the maximum landward extent of marine influence. Reconstruction of individual architectural elements, can be used to construct palaeoenvironmental models of local depositional environments. Analysis of point-bar elements (e.g. Ghinassi et al. 2014; Bhattacharya et al. 2015; Wu et al. 2015) can be used to infer the palaeoenvironment of the parent river. Quantitative data collected from outcrops which describe the geometry, dimensions and lithofacies of architectural elements are important in constraining these palaeoenvironmental models.

It is often difficult to fully reconstruct palaeoenvironment using outcrop data alone. Therefore, the use of modern analogues (e.g. Miall 2005; Stuart 2015) to add detail on the planform geometry and relationships between architectural elements is a vital component. However, the choice of modern analogue needs to be appropriate with consideration of scale, latitude, climate, and character of drainage and sedimentary basin.

5. What is the impact of marine processes on the reservoir potential of sand bodies in lower fluvial plain, coastal plain and marine marginal setting?

Rationale: Understanding the controls on the heterogeneity, connectivity and large-scale architecture of paralic reservoirs is vital for the exploitation of hydrocarbon-bearing successions. Outcrop analogue successions are routinely used in the development of geological 3D models with which to characterise subsurface reservoirs that cannot themselves be examined in detail. In order to efficiently extract hydrocarbons from subsurface reservoirs, analysis of architectural elements in three-dimensions and at high resolution are required, analogous outcropping successions are commonly used to achieve this due to the inherent limitations of traditional techniques e.g. seismic reflection profiles amongst others.

Wave processes can modify sediment through winnowing of muds to produce higher quality reservoir sandstones (e.g. Dreyer et al. 2005) and can also introduce stratigraphic complexity to paralic successions. Tidal processes can have major impacts on hydrocarbon exploration and development through the introduction of finer grained sediment (partially due to flocculation of muds within the turbidity maximum zone) (La Croix and Dashtgard 2014; Gugliotta et al. 2016). Significant modification of facies can be introduced by tidal processes within point-bar elements, for example in the form of mud-clast conglomerates and significant heterogeneities generated by mud-draped bounding surfaces (Homewood and Allen 1981; Nio and Yang 1991; Shanley et al., 1992; Dalrymple and Choi 2007; La Croix and Dashtgard 2015; Capelle et al. 2016) and tidal rhythmites (Dalrymple et al. 1991; Nio and Yang 1991; Eriksson and Simpson 2000; Ghosh et al. 2004; Bhattacharya et al. 2015; Choi and Kim 2016), which can act as baffles to fluid flow (Tyler and Finley 1992; Hogan and Sutton 2014). Through quantified lithofacies analysis of multiple

architectural elements in three-dimensions the controls on heterogeneities can be more readily discerned (Ellison 2004; Pranter et al. 2007; Musial et al. 2013).

Much attention has been paid to the characterisation of point-bar elements in terms of their evolutionary processes (Ghinassi et al. 2014; Ielpi and Ghinassi 2014; Wu et al. 2015), their heterogeneity (lithological, geometrical and topological) (Willis 1989; Pearson and Gingras 2006; Willis and Tang 2010; Labrecque et al. 2011; Musial et al. 2012; 2013; Nardin et al. 2013), and modelling fluid flow through such deposits (Ellison 2004; Pranter et al. 2007; Donselaar and Overeem 2008; Willis and Tang 2010). Three-dimensional characterisation of sedimentary successions of fluvial origin developed in humid climate settings has been carried out for individual point-bar elements in ancient outcrops (e.g. Ghinassi et al. 2014; Ielpi and Ghinassi 2014; Bhattacharya et al. 2015; Wu et al. 2016). However, few of these studies are quantitative in form, and few encompass data across multiple case studies (cf. Miall 1988; Colombera et al. 2013; 2017). Quantitative data is vital in generating models that accurately capture facies distributions, including the development of inclined heterolithic stratification (IHS; Thomas et al. 1987; Choi et al. 2004; Dalrymple and Choi 2007; Choi 2011; Sisulak and Dashtgard 2012), and the deposition of heterolithic facies (e.g. flaser, lenticular and wavy bedding). Detailed three-dimensional analyses of exhumed fluvial successions at a scale typical of reservoirs have rarely been attempted (e.g. Deutsch and Wang 1996; Corbeanu et al. 2001; Martinus and Næss 2005; Anderson et al. 2006; Keogh et al. 2007; Pranter et al. 2008; 2011; 2014). Application of detailed outcrop analysis across a range of architectural elements and systems tracts is required for the development of more accurate models of reservoirs hosted in sedimentary successions of lower fluvial plain, coastal plain and marine marginal origin.

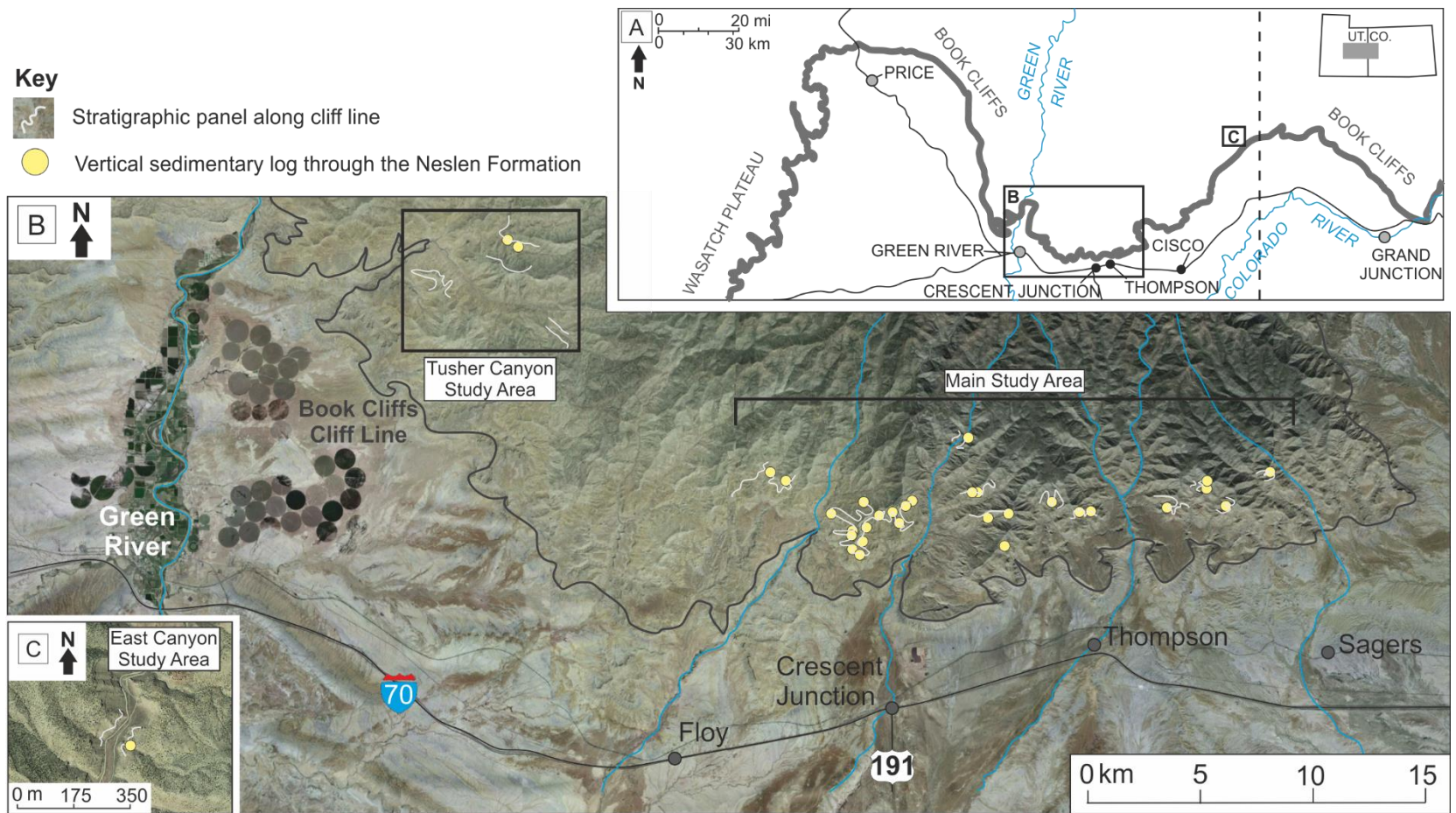


Figure 1.1: Map depicting the main sites of data collection in this study of the sedimentology of the Neslen Formation, Utah, USA. A) Location map showing the position of the Book cliffs. B Main study location where the majority of the data collected for this study were acquired. C) Subsidiary, down-dip study location at East Canyon.

1.4 Methods

In order to answer the research questions presented above, the Cretaceous Neslen Formation (Mesaverde Group, Book Cliffs, Utah, USA) was chosen as a suitable case study of a succession laid down in a fluvial dominated, marginal marine environment. The Neslen Formation has excellent exposure over extensive distances (10's of km) with multiple cliff lines arranged at varying orientations to each other such that it provides quasi-3D control. The outcrop consists of cliff-forming sandstones with intervening slope-forming finer grained units. The main area of study is from 3 km west of Floy Canyon in the west to Sagers Canyon in the east, with subsidiary study sites at Tusher Canyon and East Canyon (Fig. 1.1). Additional observations of modern systems complement the primary field-derived data set collected as an integral part of this study. More detail on the stratigraphic context, sequence stratigraphic framework, and sedimentology of the Neslen Formation, and the basin is provided in Chapter 3.

1.4.1 Field Techniques

Data for this project were collected during four field seasons between 2012 and 2015, totalling approximately five months of work in the field.

1.4.1.1 Sedimentary graphic logs

Sedimentary graphic measured logs have been collected to document the vertical facies and architectural element distribution within the Neslen Formation. In total, 106 sedimentary graphic logs were measured across the central Book Cliffs region, recording a total of ~3000 m of sedimentary succession. Of these logs, 16 captured the full thickness of the Neslen Formation, 15 encompass the lower part of the Neslen Formation, and 75 detail individual architectural elements (e.g. channel bodies) in parts of the succession that are especially well exposed (Fig. 1.1). The resolution of logging undertaken was dependent on the size and detail required; regional logs were measured at a resolution of 50 mm, whereas detailed local logs were measured at a resolution of 10 mm.

1.4.1.2 Lithofacies analysis

Using measured logs, a series of 14 lithofacies have been identified. These lithofacies have been defined based upon the recognition of characteristic sediment textures and structures. Lithofacies have been interpreted in terms of depositional or post-depositional processes. The lithofacies presented in this thesis are described and interpreted in chapter 4 following an adapted version of the commonly employed scheme presented in the seminal

works by Miall (1978, 1996). The identified and defined lithofacies are referenced throughout this thesis.

1.4.1.3 Stratigraphic panels

A total of 194 stratigraphic panels have been compiled. These encompass cliff outcrops that are collectively ~20 km in lateral extent, and arranged at varying orientations to each other (Fig. 1.1). Architectural panels have been generated from direct field measurement, supported by analysis of photographs and in-field sketches. The panels themselves enable the geometry and distribution of architectural elements recorded in one-dimensional form in the graphic sedimentary logs to be discerned in a quantitative manner in two or, in some cases, three dimensions. Panels enable relationships between neighbouring elements to be discerned. These panels have been constructed by lateral tracing and correlation of key surfaces in the field, by walking out key stratal surfaces. Such observations are supported by analyses of high-resolution photomontages. Architectural panels have been tied to vertical measured sections (graphic sedimentary logs) to enable the generation quantitative depositional models that encompass the detailed sedimentology and large scale architectural element relationships.

1.4.1.4 Architectural elements

Architectural elements are components of a depositional system that are equivalent to, or smaller than, a channelised sandstone and larger than an individual facies unit and are characterised by a distinctive internal facies assemblage and external geometry (Miall 1996). Data collected in the form of sedimentary logs and stratigraphic panels, combined with interpretation of constituent and genetically related assemblages (associations) of lithofacies has enabled a series of 10 architectural elements to be identified within the Neslen Formation strata. Descriptions and interpretations of each architectural element are described in chapter 4 and are referenced in chapter 5.

1.4.1.5 Palaeocurrent analysis

Palaeocurrent data have been collected to determine spatial and temporal trends in channel and shoreline orientation, and to enable the reconstruction of aspects of architectural elements, such as the geometry and growth trajectory of point-bar elements. Analysis of palaeocurrent data has enabled establishment of the role of fluvial, tide and wave processes in influencing localised palaeoflow direction. Two-thousand palaeocurrent indicators have been collected from a wide range of architectural elements. Palaeocurrent data were collected from a range of sedimentary structures including ripples crests, dip-directions of ripple foreset strata, cross-bedding foreset azimuths, groove casts, channel axes and margins and dip direction of lateral accretion surfaces. Of the palaeocurrent

readings collected, 1021 were from point-bar elements, 207 were from distributary channel fill elements, 203 were from bay-fill sandstone elements and 316 were from tabular reworked barrier elements; the remainder were from other element types.

1.5 Thesis Layout

Within this body of work, chapters 1-3 constitute the introductory part of the thesis; these chapters include a review of the background to the research topic, the study area and the stratigraphy. The research questions are addressed in three separate chapters (4-6). The research questions are then discussed in more general terms in chapter 7, and are synthesised in the conclusions in chapter 8. Sequentially through chapters four to six, the thesis focuses in on bodies of strata representing accumulation events over progressively shorter temporal time scales and more detailed analyses. Within each data chapter (4-6) there exists modest restatement of key background information so as to frame and reiterate key observations, thereby serving to remind the reader of salient points relating to the background geology.

Chapter 1: Introduction

Chapter 1 introduces the research rationale, aim, objectives, key research questions and data collection methods.

Chapter 2: Literature Review

This chapter provides a short review of published literature pertinent to key concepts covered in this thesis, including an overview of aspects of the sedimentary geology of fluvial systems developed in humid climate environments, paralic systems (importance, features and key concepts), schemes for the classification for coastal process and their deposits, and the fluvial-to-marine transition zone including a summary of its likely impact on the preserved stratigraphy, point bars, and marine indicators and the importance of the backwater effect (Lamb et al. 2012; Blum et al. 2013).

Chapter 3: Geological Setting

Chapter 3 covers the geological and stratigraphic setting of the Neslen Formation, placing it into an overall palaeogeographic and environment setting, and summarising the sequence stratigraphy of the upper Mesaverde Group succession of which the Neslen Formation forms a part.

Chapter 4: Depositional controls on a marine influenced fluvial succession

(Paper 1: Depositional controls on a tidally influenced fluvial succession, Neslen Formation, Utah, USA: *Sedimentary Geology* vol. 311, pp. 1-16, 2014. DOI: 10.1016/j.sedgeo.2014.06.005)

This chapter discusses the stratigraphic architecture of marginal-marine successions and considers how such successions record the interplay of autogenic and allogenic processes. Detailed mapping in three dimensions of architectural relationships between sandstone bodies has enabled documentation of lateral and vertical changes in the style of channel-body stacking and analysis of the distribution of sedimentary evidence for tidal influence. Architectural element stacking patterns show an increase in the size, mean grain size and degree of amalgamation of channel sandbodies upwards. Lateral changes in the distribution of architectural elements are also established. These changes can be explained through allogenic changes in sediment supply or accommodation generation, or through autogenic avulsion and progradation.

Chapter 5: Response of a coal-bearing coastal plain succession to marine transgression

(Paper 2: Response of a coal-bearing coastal plain succession to marine transgression: Campanian Neslen Formation, Utah, USA *Journal of Sedimentary Research*, vol. 87, pp. 168-187. DOI: 10.2110/jsr.2017.7)

This chapter focuses on developing an improved understanding of the process response of shorelines to changes in relative sea level on low-gradient coastal plains in order to enable detailed palaeogeographic reconstructions, and to better predict lithological heterogeneity in hydrocarbon reservoirs. Lateral variations in the occurrence of architectural elements demonstrate an increase in marine influence down-dip as part of the FMTZ. The lower Neslen Formation is interpreted to record overall transgression, as evidenced by the increase in the intensity of marine processes upwards. The occurrence of multiple flooding surfaces are interpreted to have been generated in response to the balance of progradation with minor variations in the rate of change of relative sea level, the effects of which were initially buffered by the presence of raised peat mires.

Chapter 6: Controls on the depositional architecture of lower coastal plain fluvial point-bar elements

This chapter focuses on the lithofacies distribution and external geometry of point-bar elements in the Neslen Formation. Detailed analysis of 41 point-bar elements is used to identify four distinct point-bar element 'types'. Two of the point-bar types identified do not conform to traditional depositional models. A relational database, which stores examples of the facies proportions and geometry of numerous point-bar elements documented from many successions worldwide, is used to compare facies assemblages and aspect ratios of point-bar elements in the Neslen Formation with other comparable successions. The occurrence of atypical point-bar elements are discussed in terms of allogenic and autogenic processes and are attributed to low stream power and hence lower sediment supply. There is an upwards increase in the width-to-thickness aspect ratio and amalgamation of point bar elements. This is interpreted to reflect a temporal decrease in the rate of accommodation generation combined with an increase in sediment supply.

Chapter 7: Discussion

This chapter summarises answers to the questions posed in Chapter 1. This chapter integrates and summarises the results of all preceding chapters and presents a wider discussion of the controls on the deposition and preservation of sediment in paralic successions (including within the FMTZ). This chapter incorporates examples from modern and ancient marine influenced systems worldwide. This discussion enables the wider applicability and context of the detailed case study of the Neslen Formation to be considered in relation to analogous sedimentary systems and the controls that operate upon them more generally.

Chapter 8: Conclusions and future work

This chapter summarises the main findings of this thesis and includes additional comments. Topics for future work are also presented.

2 Literature Review

This chapter provides an overview of past and current concepts relating to controls on the geomorphic and sedimentary evolution of fluvial and marginal marine systems in general, and of the fluvial-to-marine transition zone, in particular. The fluvial-to-marine transition zone is defined and discussed with reference to the typical stratigraphic architecture of preserved examples of such successions and sedimentological evidence for marine processes that operate within this realm. The sedimentary architecture of fluvial and fluvial-related point bars, and their preserved elements in both modern settings and ancient outcrops is considered.

2.1 Fluvial depositional systems

Fluvial systems are the primary mechanism for transporting sediment from the hinterland to marine environments. Clastic sediments are carried in fluvial systems via debris flow, bedload and suspended-load transport processes. Fluvial depositional environments are complicated and highly variable. Fluvial sedimentary successions are characterised by a wide range of associated deposits, including lateral and downstream accretion barform elements, and channel-fill elements; one common type of barform that commonly accumulates in response to the meandering (migration) of river channels is the point-bar element, which is commonly associated with lateral accretion; such types account for a significant proportion of sandstone bodies within the Neslen Formation and hence are discussed in detail in section 2.2, below. Beyond the confines of the main channel, overbank elements include crevasse channels and splays, and floodplain fines (Fig. 2.1). The

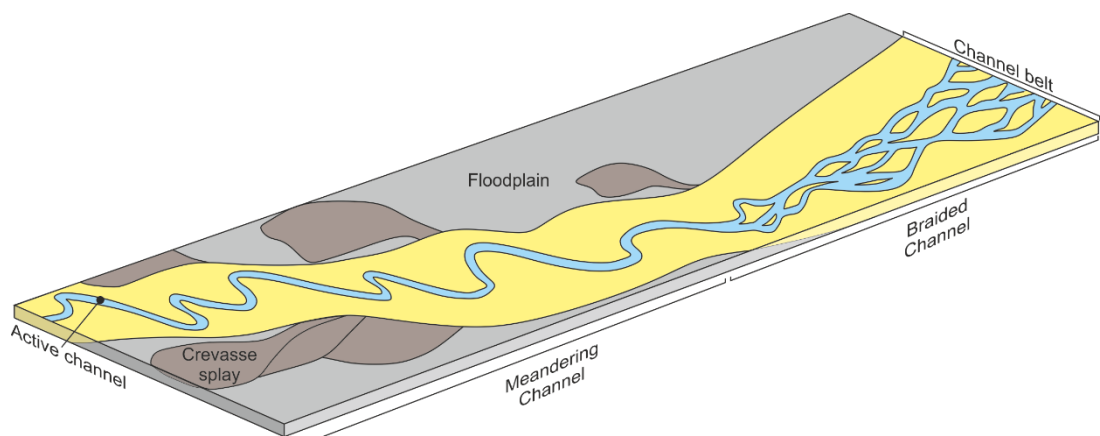


Figure 2.1: Simplified model showing the proportion of relatively more sand dominated portions of fluvial systems within the channel belt and finer grained portions within the floodplain.

dimensions and internal architecture of these elements are dependent on each other, and a series of allogenic and autogenic controls operate to govern the resultant form of each sub-environment.

Following transport, processes of deposition of sediment generate a predictable suite of sedimentary structures, which represent accumulations of features such as bedforms that accumulate and migrate over time, leaving behind bodies of strata as preserved architectural elements. Sediment arranged into bedforms can be defined as a single geometrical element (Bridge 1993) and such accumulations are important as their migration creates a variety of recognisable sedimentary structures that can be used to determine a specific palaeoenvironment of deposition. The specific sedimentary bedforms generated, as well as properties such as channel stability, are dependent on factors such as current flow velocity and sediment grain size (Harms et al. 1975; Collinson 1996; Blum et al. 2013) (Fig.2.2).

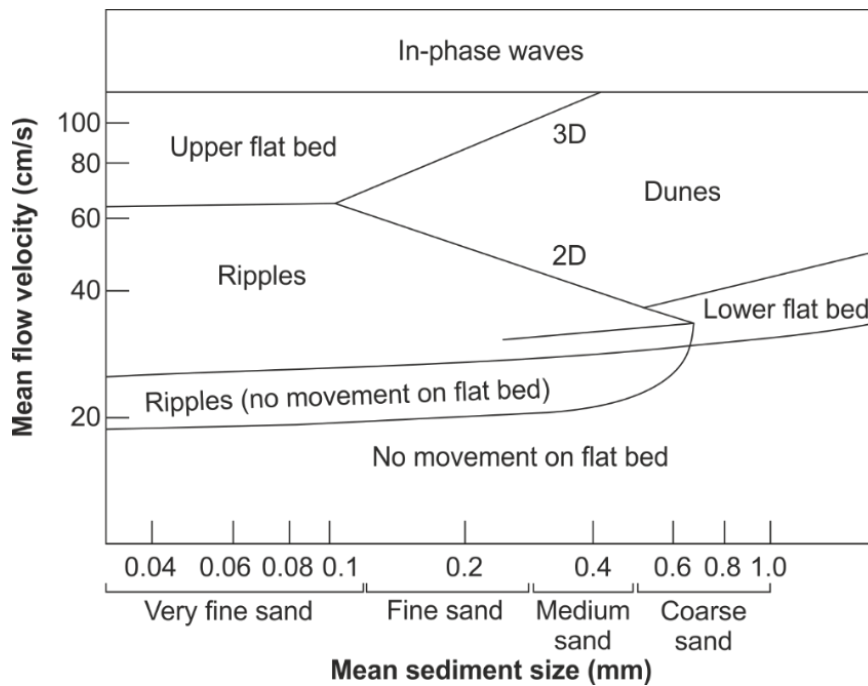


Figure 2.2: The occurrence conditions of common sand bedforms plotted in the field of current velocity and sediment grain size, adapted after Harms 1975; Collinson 1996.

Rivers are commonly classified into four end-members: straight, braided, anastomosing and meandering (Schumm 1985; Leopold et al. 1995). These types are distinguished by the degree of sinuosity each river channel and the planform arrangement of the channels present (Fig. 2.3). First-order controls on fluvial systems are catchment drainage area, fluvial system length and gradient (Syvitski and Milliman 2007; Blum et al. 2013)(Fig. 2.4). Differences in channel patterns reflect stream power (discharge and channel slope), bed material grain size, and the presence (or absence) of bank stabilising agents such as vegetation, mud or peat (Dade and Friend 1998; Dade 2000; Church 2006, Blum et al. 2013).

The Neslen Formation is interpreted as having arisen via the accumulation of the deposits of dominantly high-sinuosity, meandering channels (Willis 2000; Hettinger and Kirschbaum 2003; Kirschbaum and Hettinger 2004; Cole 2008; Olariu et al. 2015). Hence, specific attention is herein paid to this type of deposit. Other types of channel bodies are interpreted to reflect deposition from relatively low-sinuosity channels (Colombera et al. 2016) within the Neslen Formation are interpreted as backwater channels and are discussed below.

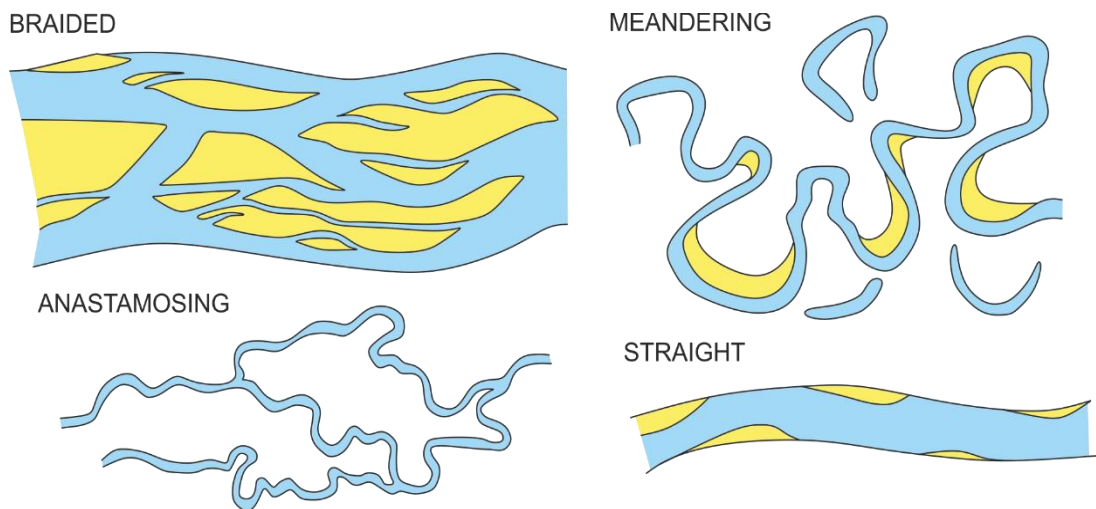


Figure 2.3: Classification of channel plan-view geometry, adapted after Schumm 1985

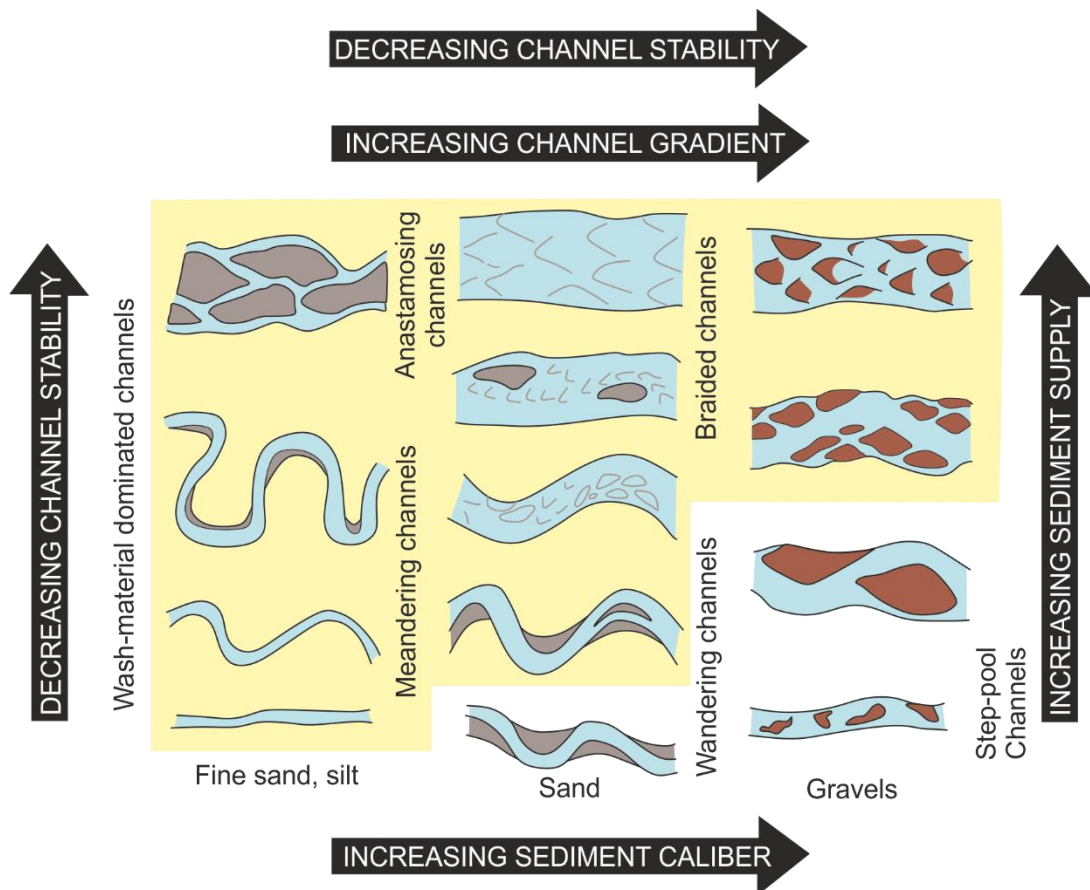


Figure 2.4: Classification of channel plan-view geometry. Channel types highlighted in the yellow box are common to alluvial rivers and are more likely to be preserved in the stratigraphic record, adapted after Church 2006; Blum 2013.

2.1.1 Meandering fluvial environments

The majority of meandering fluvial systems are characterised by a mix of both bedload and suspended load. The channel-fill succession occurs principally as a result of lateral migration of the active channel (Nichols et al. 2009). In meandering rivers, channel plan forms typically have a higher sinuosity than braided systems (Figs. 2.3, 2.4), and commonly transport both fine- and coarse-grained material. Meandering fluvial systems comprise a series of sub-components, each with their own defining characteristics, the accumulated sedimentary deposits of which are preserved as architectural elements (Fig. 2.5) (section 1.4.1.4) and have been described extensively by Miall (1985; 1988; 1996). Most meandering fluvial systems have extensive associated floodplains which are episodically inundated by water and sediment when higher river discharge events exceed or break through the channel levees.

The development and evolution of meandering fluvial systems are controlled by a combination of processes. Allogenic processes are dependent on three main factors: eustatic variations, tectonics and climate, which in turn control accommodation space and

sediment supply (Miall 2014a). Autogenic processes also typically exert a significant influence: progradation of coastal distributive fluvial systems (DFS's – Weissmann et al. 2013 and references therein), construction of delta lobes and their ultimate abandonment due to switching (Blum and Roberts, 2012), and major nodal avulsions (Jones and Schumm 2009; Hofmann et al. 2011) have each been shown to fundamentally control preserved architectural expression.

Processes whereby the meandering river-channel deposits accumulate are dominantly via one of four mechanisms: (i) by a shift in channel position (i.e., lateral or downstream accretion), whereby the position of the channel moves laterally with time (Friend et al. 1979); (ii) by avulsion, where a channel segment jumps position on its floodplain, commonly in response to a flood event (Smith et al. 1989); (iii) by neck cut-off of a closing meander loop due to bend tightening (Erskine et al. 1992); (iv) by chute cut-off (Constantine et al. 2009). In the aftermath of an avulsion event, or a neck or chute cut-off event where by a meander loop becomes truncated, sediment is deposited as the flow in the old river course decelerates and reduces in volume. A reduced rate of water supply in the original channel course decreases the capacity of the channel to carry sediment and the locus of sediment transport is progressively diverted into a new channel. Abandoned channel reaches tend to become filled by relatively fine-grained material as the remaining flow within them becomes sluggish. This favours sediment accumulation dominantly from suspended load or via river floods from the new course over the old channel.

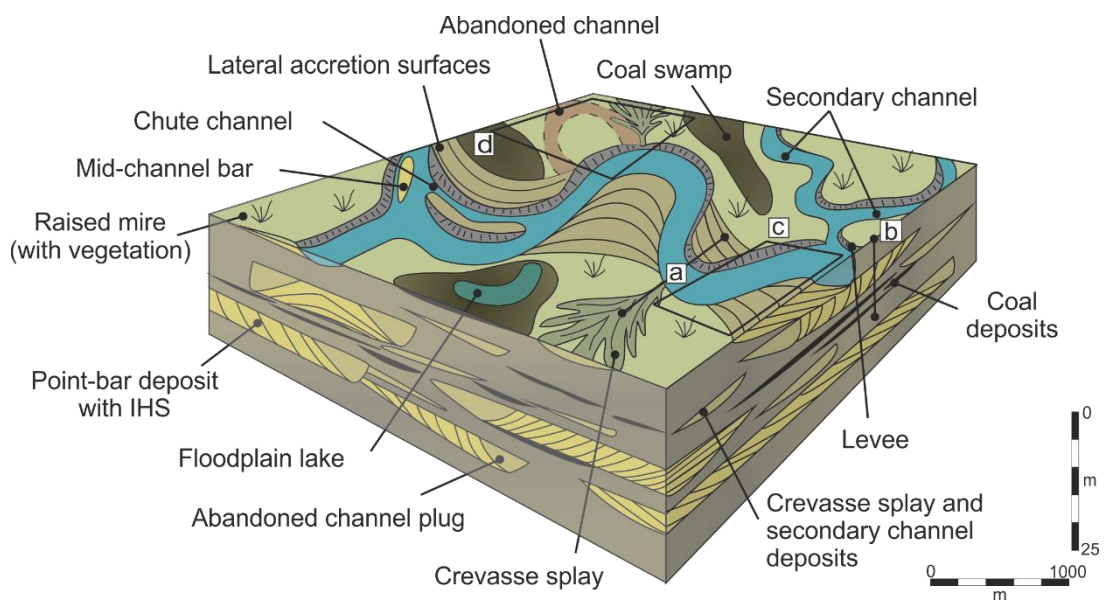


Figure 2.5: Architectural elements in meandering fluvial systems.

Stratigraphically, the preserved products of multiple avulsions are expressed as channel bodies that commonly occur stacked and offset via the process of compensational channel stacking (Straub et al. 2009). Early analyses of stacking patterns were provided by the models of Leeder (1977), Allen (1978) and Bridge and Leeder (1979), commonly referred to as ‘LAB’ models. Factors known to affect the style of stacking of channelised sand bodies in floodplain successions include, but are not limited to, avulsion type and frequency, the ratio of basin width to channel-belt width, style of sediment compaction, discharge magnitude and distribution, slope, topography and sediment load type and yield (Leeder 1977; Bridge and Leeder 1979; Bristow and Best 1993; Mackey and Bridge 1995; Heller and Paola 1996). LAB models suggest that the interconnectedness (i.e. degree of amalgamation) of fluvial sandstone bodies is inversely proportional to the rate of deposition of sediment. As such, changes in channel-body stacking patterns, are argued to be related to the rate of change of subsidence within the basin (Heller and Paola 1996). However, recognition of high- or low- accommodation systems tracts based solely on patterns of channel-body interpretations may be misleading as cannibalisation of the floodplain may not be the cause of the occurrence of packages of strata characterised by high-channel density or sheet-like geometries (Colombera et al. 2015). Instead, changes in amalgamation and aspect ratio of channel bodies might arise as a consequence of autogenic changes in, for example, avulsion frequency as a function of gradient generated by differential sedimentation between channel belts and the adjacent floodplain.

2.2 Point-bar elements

Point bars are common features of fluvial depositional systems; they most usually form through progressive lateral accretion of sediment on the inner banks of meander bends in fluvial and marine-influenced fluvial environments (Fig. 2.6). The growth and evolution of point bars commonly results in the accumulation of a characteristic succession of lithofacies

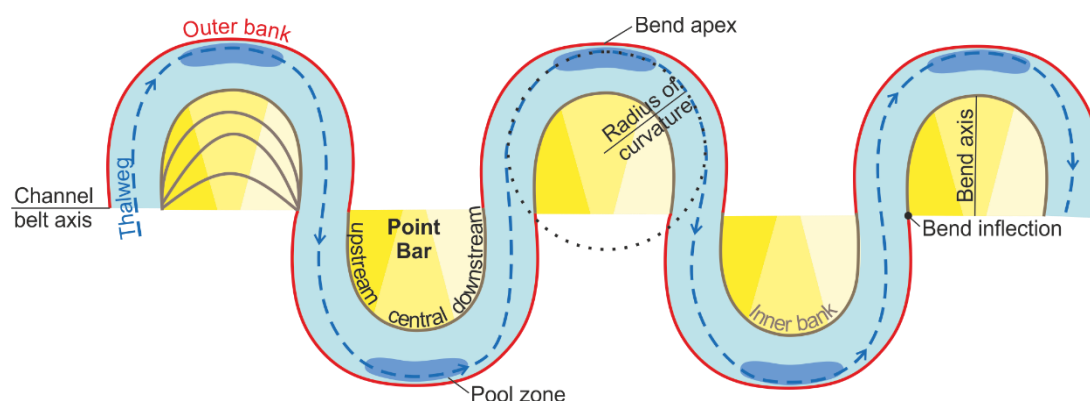


Figure 2.6: Common terminology used in analysis of meandering systems and point bars, adapted after Ielpi and Ghinassi 2014 and references therein.

(Visher 1960,1965, 1972; Allen 1964, 1965, 1970; McGowen and Garner 1970; Bluck 1971; Schumm and Khan 1972;; Barwis 1977; Jackson II 1976; 78; Miall 1977; 1985; 1988; Nanson 1980; Harms et al. 1982; Nanson and Page 1983; Smith 1987; Cloyd et al. 1990; Allen 1991; Nio and Yang 1991; Rasanen et al, 1995; Galloway and Hobday 1996; Fenies and Faugères 1998; Leeder 1999; Brekke and Couch 2011; Ghazi and Mountney 2011; Ghinassi et al. 2014; Ielpi and Ghinassi 2014; ; Johnson and Dashtgard 2014; Wu et al. 2015). The base of point-bar elements is a concave upwards erosional bounding surface, filled with a sedimentary sequence that commonly fines upwards overall (Bernard et al. 1962; Allen 1963; Walker 1984; Collinson 1996; Miall, 1996). Thin sheets of bedload gravels are deposited during maximum velocity in the deepest part of the channel (the thalweg; Fig. 2.6). Such deposits are preserved as channel lags at the base of point-bar elements. The faster flow in deeper parts of the channel favours the development of subaqueous dunes that generate trough and planar cross-bedded sandstone units as they migrate (Fig. 2.7). Higher up on the inner bank, ripples form to produce climbing ripple cross-lamination in fine-grained sand (Nichols 2009) (Fig. 2.7). Lateral migration of the channel allows point-bar deposits to accumulate via lateral accretion. Lateral accretion occurs whereby there is erosion on the outer bend of a meander and deposition on the inner bend; thereby leading to the progressive lateral migration of the inner channel bank and its associated deposits over the channel base. The resultant facies succession is expressed as an upward decrease in both grain size and cross-bedded sets. At bankfull stage helical flow generates a vertical circulation that occurred normal to the river bank and carries bottom sediment load up the sloping face of the point bar (Galloway and Hobday, 1983). Therefore, the coarsest sediments tend to accumulate in the basal part of the channel, whereas the finest sediments tend to accumulate in upper

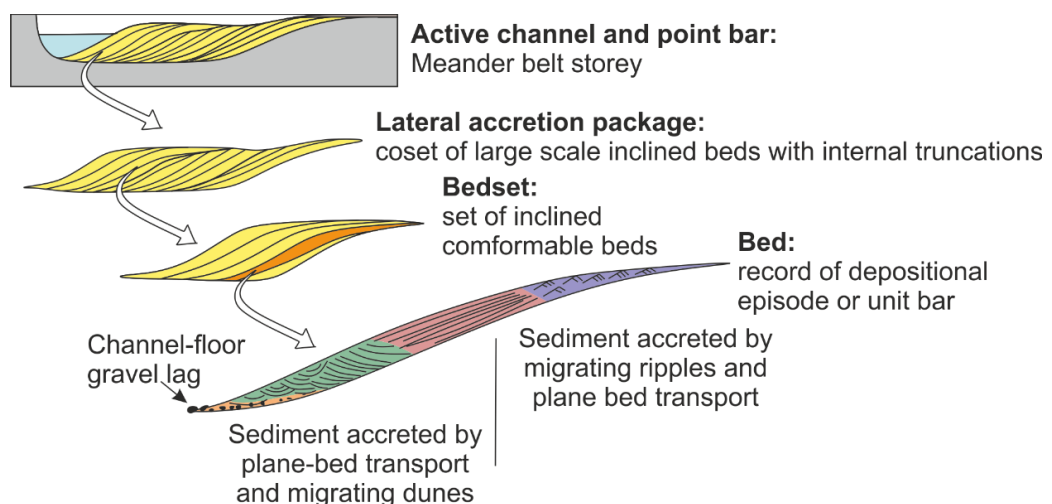
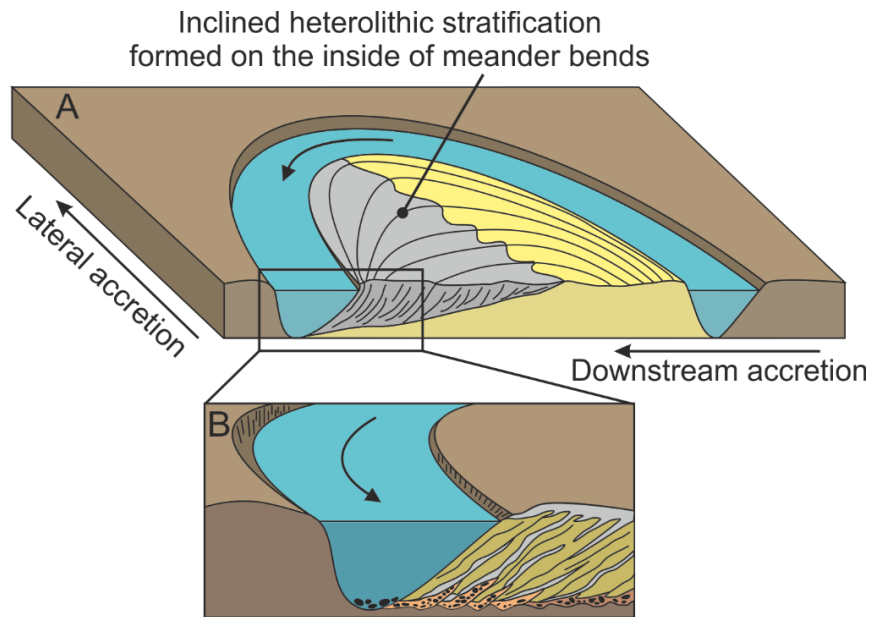


Figure 2.7: Descriptive terminology for point-bar architecture(adapted after Bridge 1993, 2003, Ghinassi et al. 2014. Facies colours correspond to the facies presented in Chapter 6.

part of the point bar (Fig. 2.7). Stages in the lateral migration of point bars of meandering channels can sometimes be recognised as inclined surfaces commonly referred to as lateral accretion surfaces (Allen, 1963) or scroll-bar surfaces (Fig. 2.7).

The growth, sedimentary architecture and internal facies of the deposit may be complex and varied depending on their evolution and controls of the formative river (Schumm and Khan 1972; Hickin 1974; Jin and Schumm 1987; Smith 1998; Peakall et al. 2007; Duan and Julien 2010; Soltan and Mountney 2016). Point bars form through a combination of expansion, translation, rotation and downstream migration (cf. Ielpi and Ghinassi 2014; Ghinassi et al. 2014) and the deposits which are preserved record the evolution of an individual point bar, or even a particular part of a single point bar. Patterns of point-bar evolution commonly occur in combination (Jackson 1976), giving rise to many variations of the aforementioned “normal” facies model. The plan-form evolution of point bars, together with the bankfull depth of the channel and rate of aggradation, determines the bedding architecture, connectivity, shape, geometry and heterogeneity of the resulting sandbody (Miall 1988; Willis 1989; Bridge 2003; Willis and Tang 2010; Ghinassi et al. 2014; Colombero et al. 2016c). A plethora of research carried out on the sedimentology of point-bar deposits has utilised studies of both modern systems (e.g. Smith 1998; Choi et al. 2004; Smith et al. 2009; Hooke and Yorke 2011; Choi 2011; Kasvi et al. 2013; Johnson and Dashtgard 2014) and ancient outcrops (e.g. Nanson 1980; Miall 1985; Turner and Eriksson 1999; Hovikovski et al. 2008; Ghazi and Mountney 2009; Li et al. 2010; Hubbard et al. 2011; Labrecque et al. 2011; Ielpi and Ghinassi 2014; Ghinassi et al. 2014; Wu et al. 2015; Jablonski and Dalrymple 2016), as well as computational modelling (e.g. Bridge and Leeder 1979; Willis 1989; Sun et al. 2001; Willis and Tang 2010; Duan and Julien 2011; Yan et al. 2016) and physical modelling (e.g. Schumm and Khan 1972; Smith 1998; Peakall et al. 2007). The aim of much of this work has been to characterise the facies, lithological heterogeneity, geometry and mechanisms of formation of different types of point-bar deposits.

Point bars in marine-influenced environments may be modified by tidal processes, which commonly cause the development of inclined heterolithic stratification (IHS; Thomas et al. 1987). Inclined heterolithic stratification deposits consist of inclined units of alternating sandstone and mudstone/siltstone that are separated by inclined surfaces produced by either non-deposition or erosion (Thomas et al. 1987). Although IHS can form in exclusively fluvial environments, it is more likely to develop in tidally influenced fluvial environments (Dalrymple and Choi, 2007). Inclined heterolithic stratification most commonly forms as lateral accretion deposits (Fig. 2.8) on inclined point-bar surfaces on the inner bank of a channel bend. Inclined heterolithic stratification deposits are likely to be coarser grained where they accumulated at the inner parts of the tidal-fluvial transition compared to those deposited towards the mouth of the fluvial system (Dalrymple and Choi, 2007). This is



Angle of IHS can vary between 1-34° but are commonly around 12°

Figure 2.8: Models of inclined heterolithic strata (IHS) A) the distribution of sand and fines around a point-bar element, adapted after Fustic et al. 2012. B) Hypothetical distribution of fines within and basal conglomerate within IHS. Grey areas represent fine grained silt or mud, yellow is dominantly sandstone and orange is commonly conglomerate, adapted after Thomas et al. 1987.

because mud- and silt-sized particles are deposited close to the turbidity maximum zone (section 2.4 below)

IHS in ancient (e.g. Shanley et al.1992; Corbeau et al. 2004; Pranter et al. 2007; Johnson et al. 2016) and modern (e.g. Choi et al. 2004; Hovikovski et al. 2008; Choi 2010; 2011; Sisulak and Dashtgard 2012; Johnson and Dashtgard 2014) successions have been increasingly investigated in recent years in order to provide analogues for major subsurface hydrocarbon reservoir plays, notably the Cretaceous McMurray Formation, Alberta, Canada, within which large-scale point-bar deposits exhibit IHS (cf. Smith 1987; Fustic 2007; Patruyo et al. 2009; Labrecque et al. 2011; Fustic et al. 2012; Jablonski 2012). The sand dominated McMurray Formation hosts significant volumes of heavy oil, yet the lithological heterogeneity arising from IHS deposits means that the reservoir is compartmentalised and problematic to develop (Fustic et al. 2012). The study of Fustic et al. (2012) helps to refine depositional models and decrease uncertainty in petroleum system behaviour.

Most ancient IHS deposits are erosionally based, overlie a basal lag conglomerate (and often an inclined-stratified basal sandstone), exhibit an overall fining upward of sediment and decrease in scale of sedimentary-structures, and contain evidence of palaeoflows directed parallel to their inclined units' strike (Fig. 2.7). Distinguishing IHS of

fully fluvial origin from that of marine-influenced origin relies on a series of criteria; not all such criteria will necessarily be observed in the deposits of a single point bar but a combination of their occurrence can allow an interpretation of tidally influenced point-bar deposits:

- i. Channel lag deposits that contain shell debris of brackish or full-marine fauna;
- ii. Deposits from the upper part of a point-bar element that comprise wave and current ripple bedding with lenticular and flaser bedding;
- iii. Interbedded sand and mud, which constitutes much of the deposit;
- iv. Plant material deposited on point bar inclined surfaces will be dominated by tidal salt marsh species indicative of brackish water;
- v. Palaeoflow directions may be bimodal to bipolar, reflecting flow reversals; individual beds may show ripple strata and ripple forms indicative of migration in opposite directions;
- vi. Herringbone stratification within the upper parts of point-bar elements;
- vii. The occurrence of trace fossils interpreted to reflect marine or brackish water deposition.

2.3 Marginal marine systems

Marginal marine systems include a range of environments, the principal ones being tidal flats, estuaries (tide and wave dominated), lagoons, strandplain, barriers, beaches and deltas (Figs. 2.9). The type of environment occurring at a coastline is dependent on a range

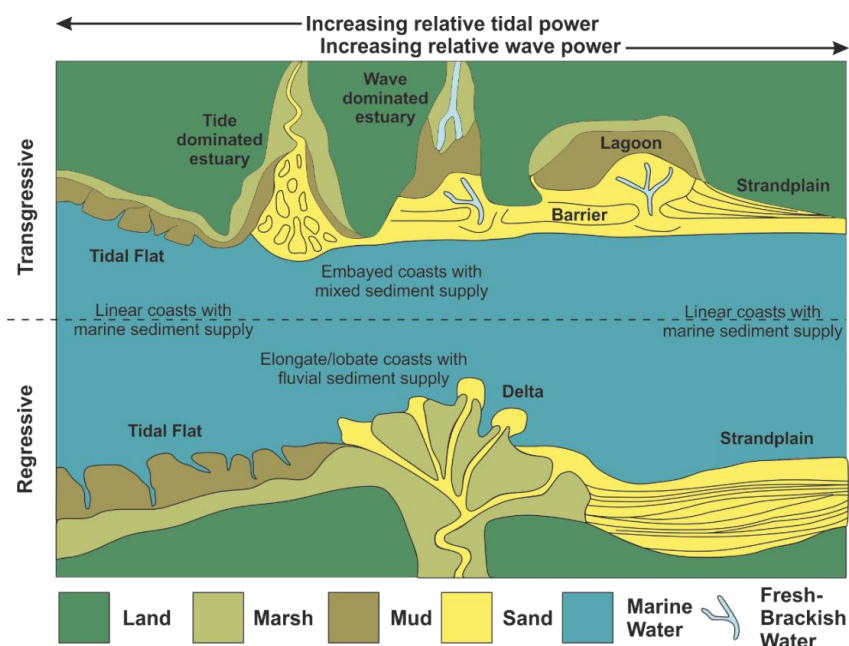


Figure 2.9: Plan view maps for idealised coastal depositional systems showing key relationships and different geomorphologies, adapted after Harris et al. 2002.

of factors including the sediment supply (as a function of climate and tectonics), relative tidal, wave and fluvial power (see below), the presence of embayments and whether the coastline is regressive or transgressive in nature (Fig. 2.9).

2.3.1 Coastal process classification

Within sedimentology, paralic and shallow marine depositional systems are commonly described using a ternary classification based upon the relative importance of fluvial, tidal and wave processes on sculpting the shoreline geomorphology (Galloway 1975; Fig. 2.10). Different combinations of processes will alter the coastline morphology and the distribution of sandbodies within a depositional environment; in the accumulated sedimentary record, they will introduce different types of lithological heterogeneity, understanding of which is important for assessing hydrocarbon behaviour in shallow-marine reservoirs (Ainsworth 2010). The ternary process-based classification scheme was introduced in the 1970s to classify modern deltas (Galloway 1975). This was later modified to include a third axis to account for grain size (Orton and Reading 1993; Fig. 2.11).

In more recent works, the ternary coastal process classification scheme has been further refined (Fig 2.12; Ainsworth et al. 2011). The refined classification scheme uses discrete categories that are based on a dominant process, as well as a secondary and tertiary process clarifiers (Fig. 2.12). Combinations of processes are considered in terms of their

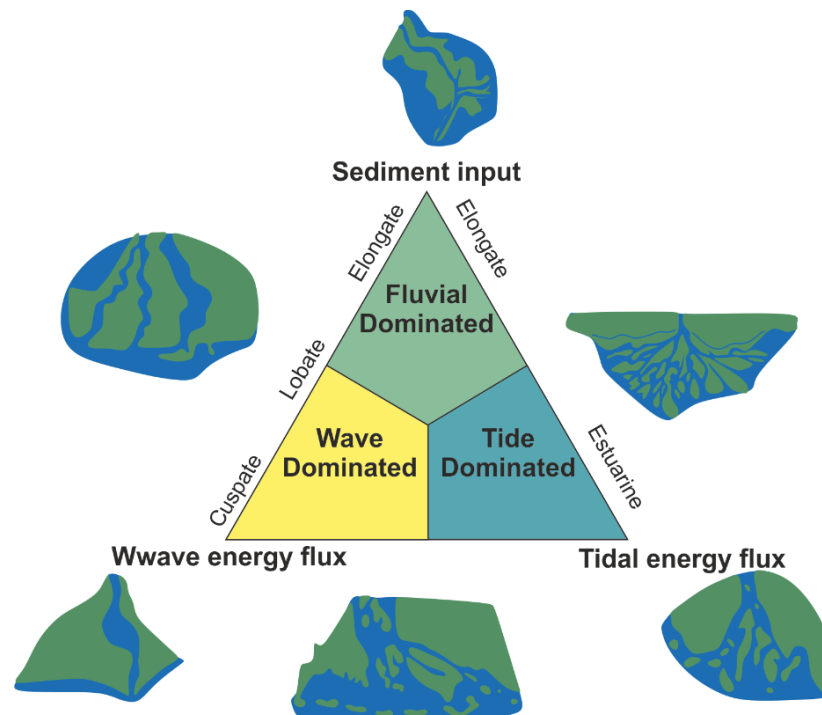


Figure 2.10: Schematic diagram illustrating the division of deltas into fluvial-dominated, wave-dominated and tide-dominated types. The relative importance of sediment input, wave energy flux, and tidal energy flux determine the morphology and internal stratigraphy of the delta, adapted after Galloway 1975.

expected influence upon shoreline sedimentary systems. The result of the classification is that 15 possible categories of shoreline depositional process combinations exist (Fig. 2.13). It is important to emphasise that many coastal sub-environments commonly exist in close proximity to each other (Fig. 2.14) and will show complicated spatial and temporal relationships.

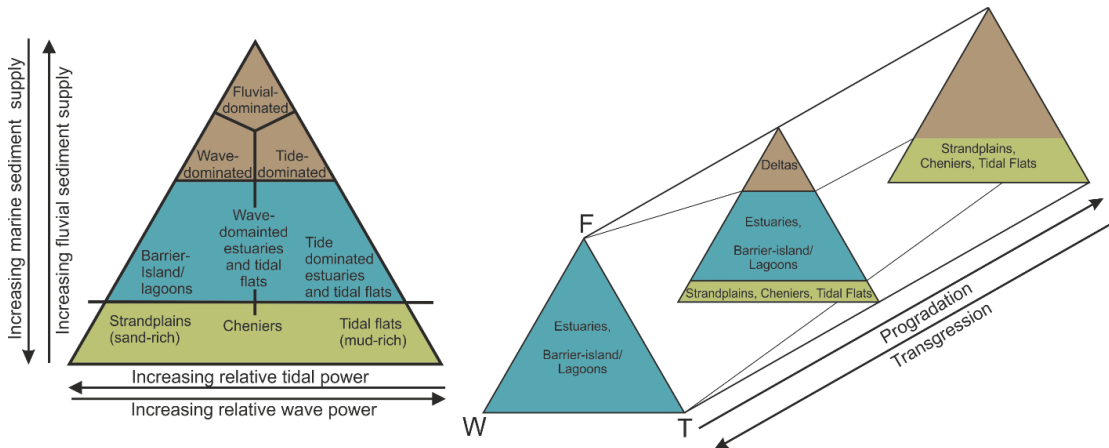


Figure 2.12: Schematic diagram showing how coastal environments evolve through transgression and progradation cycles. As progradation increases estuarine systems give way to deltaic and tidal environments, the opposite occurs during transgression, adapted after Reading and Collinson 1996.

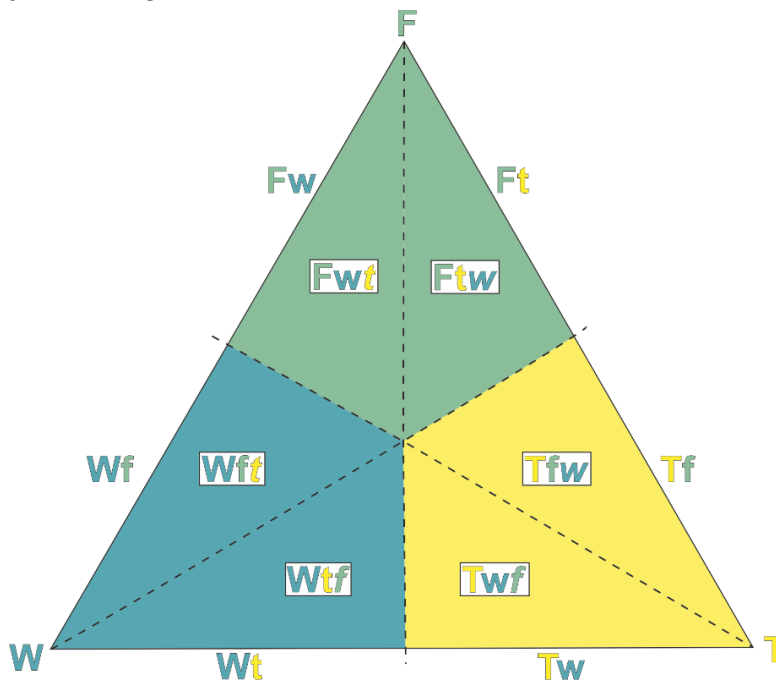


Figure 2.11: Coastal process classification ternary plots, adapted after Ainsworth et al. 2011. F = Fluvial dominated; W = Wave dominated; T = Tide dominated. Capital letters indicate the dominant process, bold lower case letters indicate a process which influences an environment and lower case letters in italics, indicate a process which modifies the environment.

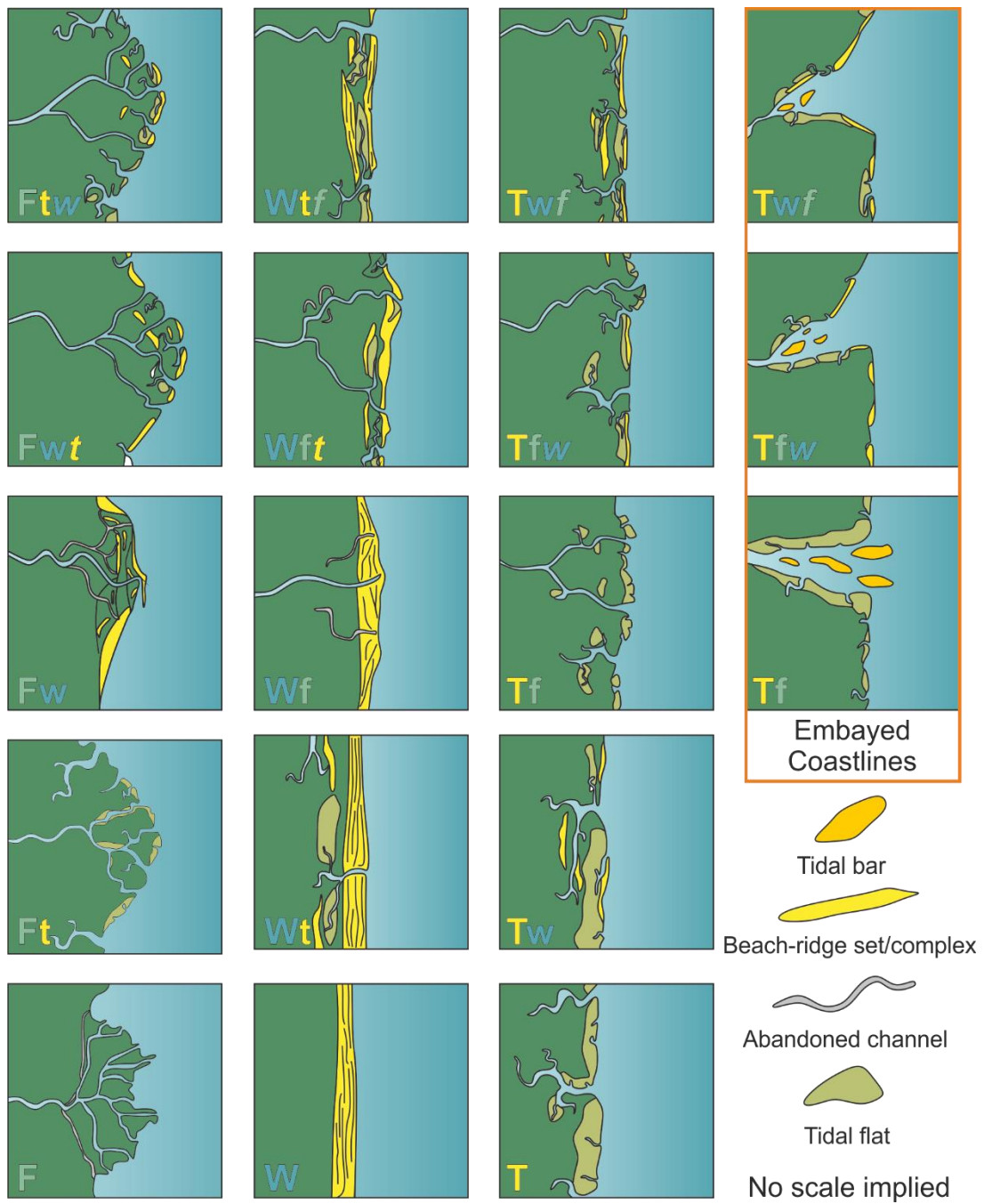


Figure 2.13: Representative schematic plan view models of the 15 classification categories in the coastal process classification presented in Fig. 2.12, adapted after Ainsworth 2011.

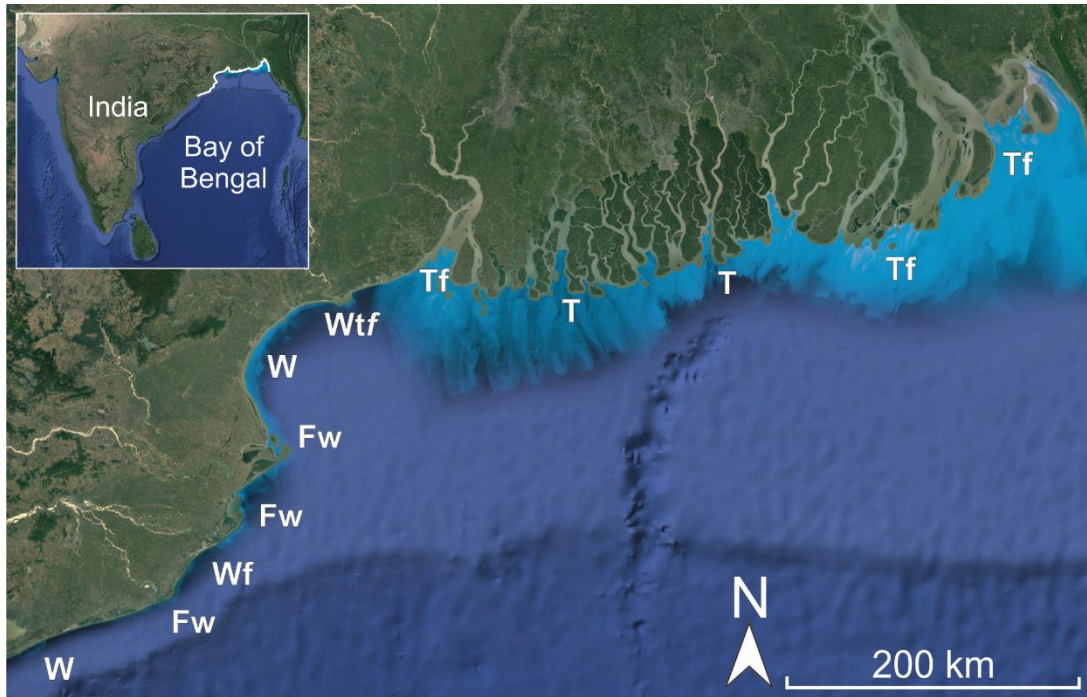


Figure 2.14: Image of modern coastline showing how depositional process dominance results in different coastline morphologies and how dominant processes can change laterally over relatively short distances. Images courtesy of Google Earth.

2.3.2 Autogenic Controls

Recent research has assigned increased significance to the influence of autogenic controls, with many studies recognising how continental successions preserve patterns of stratal architecture that are most readily explained by self-organisation behaviour over basin-filling time scales of 10^3 - 10^6 years (Hampson 2016). Regressive shorelines can turn around to transgression without the imposition of any changes in the rate of accommodation generation or sediment supply; this processes, which is termed autoretreat (Muto and Steel 1992), is caused by the inability of a fixed rate of sediment supply to fill the growing area behind the shoreline.

Deltaic systems are subject to additional autogenic processes of delta lobe abandonment. Following abandonment, individual deltas go through a predictable succession of events, known as the delta cycle (Fig. 2.15), which includes subsidence, ravinement and landward translation of the marsh shoreline, and marine reworking of delta-front sands to construct transgressive barrier-island arcs, and, eventually, submerged sand shoals (Coleman and Gagliano 1964; Coleman 1988; Penland et al. 1988, 1989; Roberts 1997; Flocks et al. 2009).

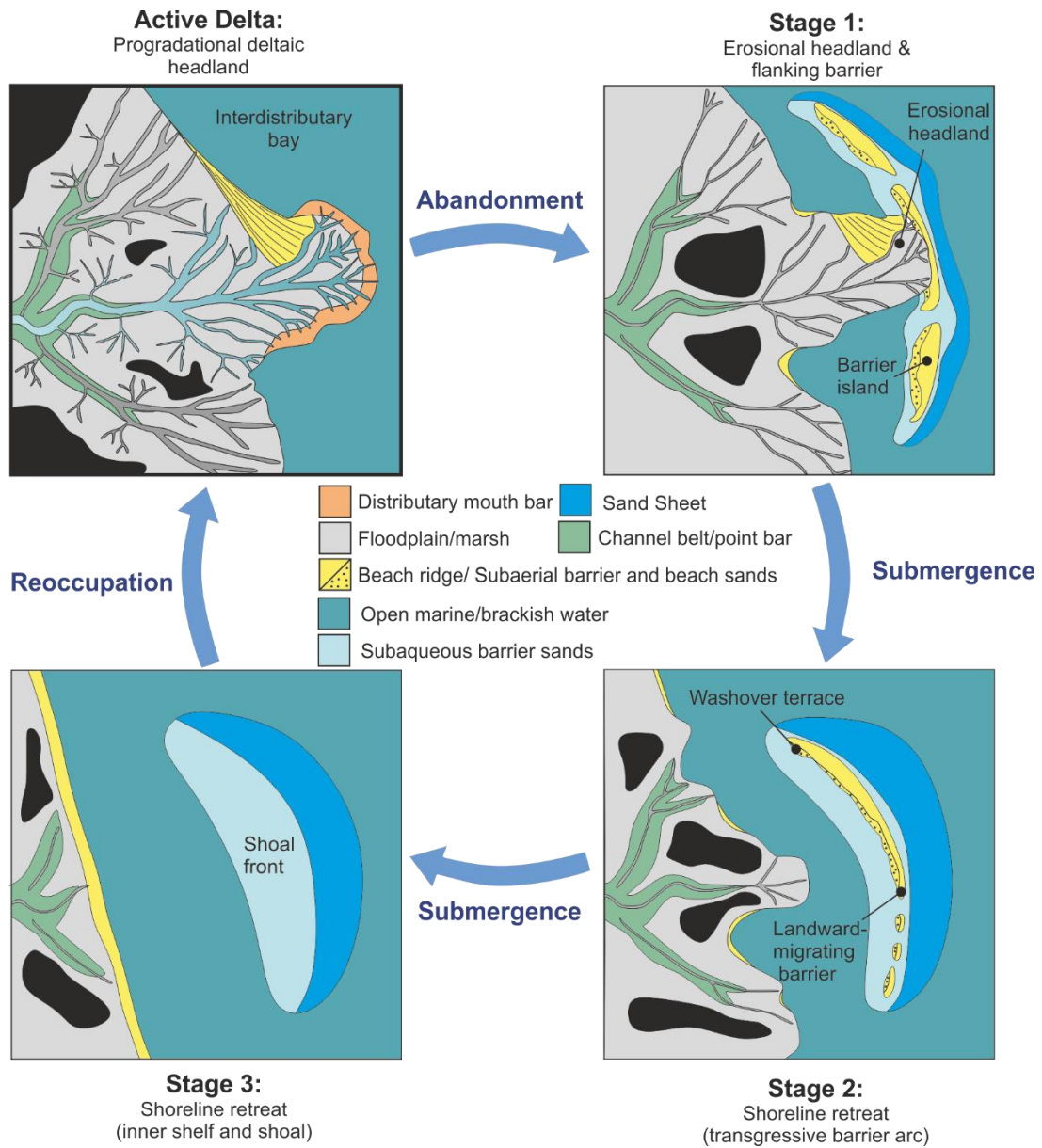


Figure 2.15: The delta cycle, illustrating natural evolution of deltas following avulsion and relocation of feeder fluvial channels, adapted after Penland et al. 1988; Blum and Roberts 2012.

2.4 Fluvial-to-marine transition zone

The transition zone between fully fluvial and fully marine environments is called the fluvial-to-marine transition zone (FMTZ; Fig. 2.16). The FMTZ is defined by the upstream limit of marine processes and the downstream extent of fluvial processes (van den Berg et al. 2007) (chapter 1). In a landward direction, marine processes become progressively replaced by fluvial processes (Fig. 2.16). The assemblage of sedimentary structures (considered

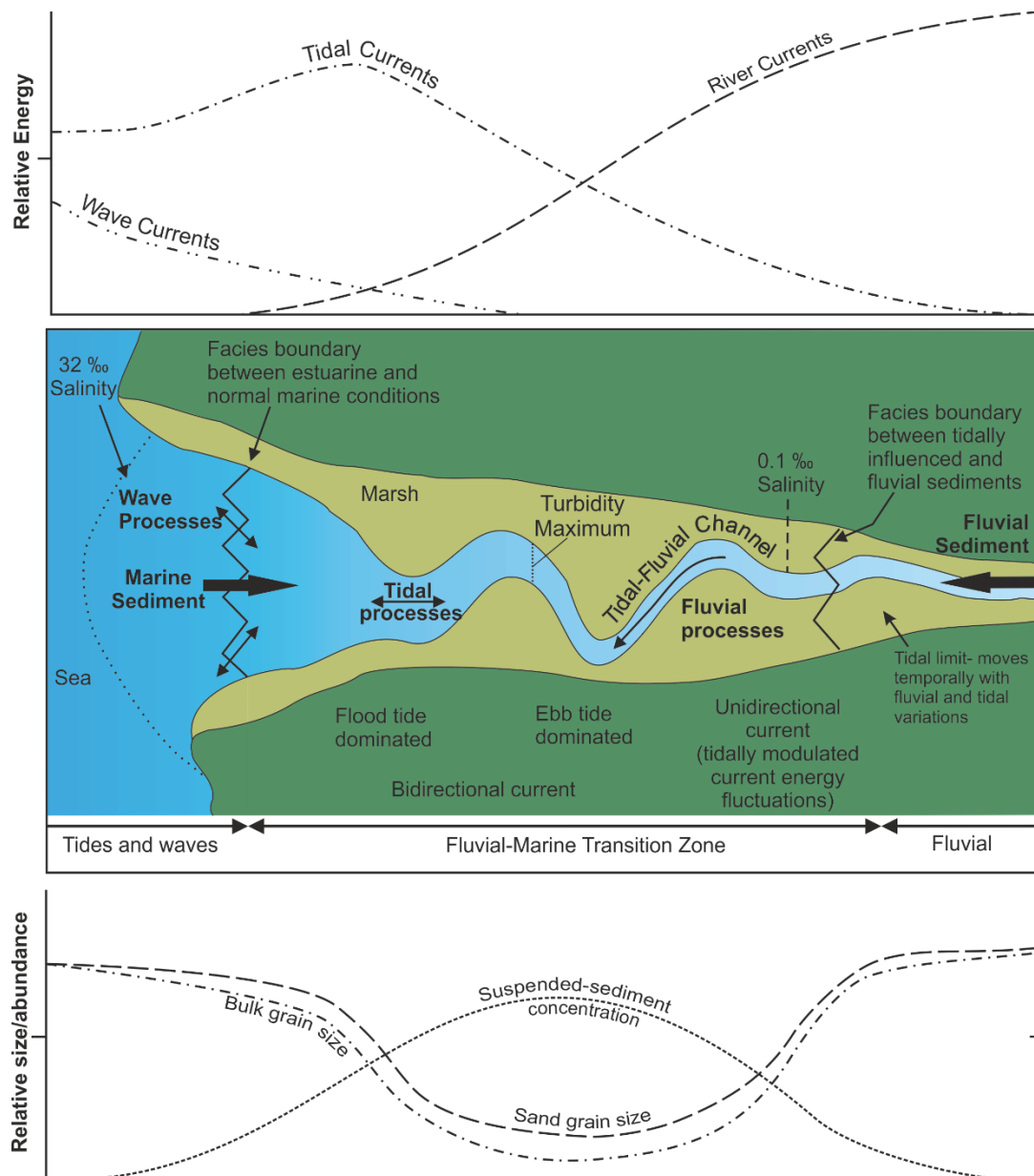


Figure 2.16: Diagram showing the changes in facies, energy, grain size, salinity and channel morphology through the fluvial-to-marine transition zone and the relevant processes, adapted after Dalrymple et al. 1992; Martinius and Gowland 2011, Dalrymple and Choi 2007; van den Berg and van Gelder 2007.

below) indicative of marine processes can occur over distances of several tens to hundreds of kilometres within the FMTZ and can vary greatly with distance and time through the transition zone. The FMTZ is not static but moves relative to the tidal regime and fluvial discharge and wave action (Dalrymple and Choi 2007; Martinius and Gowland 2011; Dalrymple et al. 2015) and the relative effect of these processes on the sedimentation process varies systematically through the fluvial-marine transition. In distributive systems such as deltas, the FMTZ will be different for each active major channel depending on its configuration (e.g. longitudinal section, slope gradient) and the relative strength of river and tidal currents (Blum et al. 2013).

The maximum documented distance of tidal-penetration into a modern river is in the Amazon River, in which tidal influence is detectable up to 800 km landward of the coast (Dalrymple et al. 2015). Even rivers of medium size have tidal-penetration distances up to hundreds of kilometres in low gradient, coastal plain settings (Dyer 1997; van den Berg et al. 2007; Dalrymple et al 2015). The extent of the fluvial-tidal transition zone will vary in length due to the gradient of the fluvial system (Martinius and Gowland 2011) caused by the longer distance of tidal penetration (cf. Dalrymple 2010).

The presence of tidal process is associated with high proportions of suspended sediment concentration along an area of the FMTZ that it is known as the turbidity maximum (TM) or turbidity maximum zone (Schubel 1968; Fig. 2.16). The link between tides and the deposition of mud at the turbidity maximum is due to the presence of brackish water that helps the flocculation of clay size particles (McCave 1970; Silverberg and Sundby 1979; van den Berg et al. 2007; La Croix and Dashtgard 2014). Moreover, this process is assisted by the physical process of the tidal currents that can transport the suspended sediment landward, whereas bedload material might still be subject to a residual component of seaward transport via fluvial flow (Dalrymple and Choi 2007). As it is part of the FMTZ, the TM is also not fixed spatially or temporally in space but will be displaced along the river profile in response to periodic changes in fluvial and tidal and wave process (Uncles et al. 2006; La Croix and Dashtgard 2014). Mud deposits, typically in the form of drapes on bar-front surfaces, are present in accumulated bedforms in the FMTZ. Such drapes commonly exhibit a greater silt fraction than mud deposits in estuarine slack water settings (van den Berg et al. 2007).

2.4.1 Modern and ancient studies

Detailed studies of modern FMTZ systems have been undertaken in relatively few locations: the macrotidal Han River delta, Korea (Choi et al. 2004), Fraser River, Canada (Dashtgard et al. 2012; Sisulak and Dashtgard 2012; Czarnecki et al. 2014; Dashtgard and La Croix 2015), Rhine-Meuse Rivers, The Netherlands and Germany (van den Berg et al. 2007), Ogeechee River, Georgia (Shchepetkina et al. 2016), Niger Delta, Nigeria (Oomkens 1974), Mahakam Delta, Indonesia (Allen et al. 1976; Salahuddin and Lambiase 2013). Few modern studies have been carried out in humid, coal-bearing environments. More have been undertaken in temperate or high-latitude climate settings; this has restricted our understanding of the FMTZ in humid climatic settings.

Studies of ancient outcropping successions which are interpreted to represent deposition within FMTZ settings have become increasingly numerous in recent years, encompassing a wide range of climatic, tectonic and basinal regimes (e.g. Fedo and Cooper 1990; Shanley et al. 1992; Lanier et al. 1993; Bose and Cakraborty 1994; Makhlof 2003; Ghosh et al. 2005; Cummings et al. 2006; Eriksson et al. 2006; Flaig et al. 2009; Corbett et al. 2011; Ashour et al. 2012; Bhattacharya et al. 2012; Olariu et al. 2015). Much of this research has been promoted by the discovery and exploration of large oil reserves held in marine-influenced fluvial reservoirs, notably the McMurray Formation (Alberta, Canada) and Mungaroo Formation (NW shelf, Australia), Burgan Field (Kuwait), Brent Group and Statfjord Formation (North sea, UK).

2.4.1.1 *Marine indicators*

2.4.1.1.1 *Sedimentary indicators*

Recognition of marine influence in systems dominated by fluvial processes requires careful examination of the sedimentary structures and ichnology present. There are few sedimentary structures which can be used to unequivocally confirm marine (i.e. tidal or wave) influence (Shanley et al. 1992). However, an assemblage of structures can be used collectively to provide evidence of marine processes (Martinius and Gowland 2011). Sedimentary signatures of marine influence commonly consist of evidence for fluctuations in the energy and direction of the current, often in a manner indicative of rhythmic, periodic

variation due to tidal processes (Collinson et al. 2006). These flow fluctuations can manifest themselves in the sedimentary record in a variety of ways, as considered below.

One of the most commonly recognised tidal structures is that of tidal rhythmites (cf. Visser 1980). Rhythmites are defined as 'repetitive tidal signals developed as very thin strata in a wide range of tide dominated systems' (Longhitano et al. 2012) where variations in the thickness of sand and mud laminae or the thickness of climbing-ripple cross laminations show a rhythmic trend through or along a bed set. Tidal rhythmites commonly occur in association with inclined heterolithic stratification (Choi 2011) where the rhythmites most typically occupy the upper part of a fining-upward channel-fill succession. These trends can be attributed to variations in tidal currents through time and are the most reliable 'stand-alone' tidal indicator (Dalrymple 2010).

Erosional surfaces within cross-bed sets may be interpreted as reactivation surfaces connected to ebb-modulated fluctuations in flow velocity (cf. Nio and Yang 1991; Brettle et al. 2002). Reactivation surfaces between cross-bedding or sigmoidal bedding are gently dipping erosion surfaces that become slightly convex upward in an upstream direction within a single cross-bed set (Bhattacharya et al. 2012). In fluvial deposits this structure can be attributed to reflect stage fluctuations and subsequent modification of bedforms (Shanley et al. 1992). Alternatively, in tidal deposits, reactivation surfaces can be attributed to reversals in flow direction such that a bedforms leeside is episodically or periodically partially eroded and planed (Collinson et al. 2006), resulting in substantial bedform modification. Multiple reactivation surfaces that have a common spacing are most common in tidal environments (Shanley et al. 1992; Bhattacharya et al. 2012) and are commonly draped by fine sediments (clay, mudstone etc.) due to changes in flow velocity and/or direction due to the influence of tides.

Alternations in current energy can manifest as lenticular, flaser and wavy bedding; units of ripple-laminated sandstone broken up by interlaminations and lenses of finer grained sediment (silt and mud). Where sand dominates and mud drapes are subordinate, as in flaser bedding, the muddy sediment occurs as thin, discontinuous laminae, which drape ripple forms or are confined to ripple troughs. Where fine grained sediment dominates sand may occur as isolated ripple form sets; lenticular bedding. There is a continuous gradation in the proportions of sandstone and mudstone/siltstone, with wavy bedding being used to

define intermediate proportions of sandstone and mudstone (Collinson et al. 2006). The use of these structures as tidal indicators is contentious, as they can also form in fully fluvial environments where the flow regime changes over time, especially in ephemeral fluvial systems (Picard and High 1973). The identification of rhythmic alternations of sandstone and siltstone can be used to infer tidal causation of heterogeneity due to the daily or seasonal changes in tides (Reineck and Wunderlich 1968; Demowbray 1983, Shanley et al. 1992).

Ripple lamination in which foresets dip in opposite directions can manifest as herringbone cross-lamination, symmetrical ripple-lamination or as isolated occurrences of the reverse direction of climbing ripples. Current reversals may occur due to the influence of tidal processes (Shanley et al. 1992). In some cases, such as in the reverse direction of climbing ripples, the products of a dominant (commonly flood) and minor (ebb) current can be interpreted (cf. Gugliotta et al. 2016).

Cracks developed on the base of sandstone beds occur commonly 1-2 cm deep and 4-5 mm deep as isolated or branching casts. Where there is a lack of association of beds with evidence of sub-aerial exposure, such structures are likely to be syneresis cracks (Collinson et al. 2006). Syneresis cracks form within muddy sediments under conditions of varying salinity and in response to tension as muddy, water-saturated sediments lose water to an overlying aqueous layer causing cracks to form (Plummer and Gostin 1981; Shanley et al. 1992).

2.4.1.1.2 Ichnological indicators

Deposits within the fluvial-to marine transition zone (FMTZ) will, to some degree, have accumulated in a zone of transition from fresh to marine water; hence, such deposits are considered to record accumulation in a brackish water zone. Brackish-water trace fossil assemblages are defined on the basis of combinations of ichnogenera, low bed ichnodiversity, diminutive size and shallow penetration (Bromley 1996; Gingras et al. 2012). Such forms reflect the highly stressed habitat that the FMTZ represents, with temporally and spatially variable water salinity. Since many ichnogenera attributed to brackish conditions are also found in normal marine salinity environments, the ichnofacies assemblage and considerations of size and diversity are important. The fundamental characteristics of the brackish-water ichnofacies model were developed by Pemberton et al. (1982) and refined by Beynon et al. (1988).

The main suite of trace fossils that have been identified as being indicative of a brackish waters are: *Arenicolites*, *Chondrites*, *Conichnus*, *Gryolithes*, *Monocraterion*, *Ophiomorpha*, *Palaeophycus*, *Planolites*, *Scolicia*, *Skolithos* and *Teichichnus*, *Teredolites*, and *Thalassinoides*. Other trace fossils have also been recognised in deposits with a saline water influence. These include, but are not confined to: *Acritarchs*, *Anorichnus*, *Asterosmona*, *Aulichnites*, *Bergaureia*, *Cylindrichnus*, *Helminthopsis*, *Medousichnus*, *Rhizocorallium*, *Rosselia*, and *Terebellina* (Howard and Frey 1984; Pemberton and Wightman 1992; Pemberton and MacEachern 1995; Gingras et al. 2012).

2.4.2 Sequence stratigraphy

Sequence stratigraphy is the study of rock relationships within a chronostratigraphic framework of repetitive, genetically related strata bounded by surfaces of erosion or non-deposition, or their correlative conformities (van Wagoner et al. 1988). Sequence stratigraphy was initially developed as a concept applied principally to shallow-marine deposits (Vail et al. 1987) but was extended to include interpretation of coastal fluvial deposits in the models of Posamentier and Vail (1988) and Posamentier et al. (1988). The concept of systems tracts was introduced to define a linkage of contemporaneous depositional systems, forming the sub-division of a sequence (Vail et al. 1977). A sequence can be subdivided into systems tracts, which are defined by their position within the sequence and by the stacking patterns of parasequence sets and parasequences bounded by marine-flooding surfaces. Sequences and their stratal components are interpreted to form in response to the interaction between the rates of eustasy, subsidence, and sediment supply.

Deposits of the FMTZ have been variably placed within different systems tracts. Many authors interpret the deposits of the FMTZ as being temporally equivalent to marine maximum flooding surfaces and are transgressive in nature (Cummings et al. 2006; Dalrymple and Choi 2007; Fig. 2.17). Where the deposits are interpreted to have formed during a transgressive systems tract (TST), the progression from amalgamated sandstones (within a lowstand systems tract; LST) into more isolated and tidally influenced deposits reflects a relatively rapid rate at which accommodation space is created relative to sediment supply (Shanley and McCabe, 1994). During early sea-level rise (LST) tidal processes are significant, because of the constriction of tidal flows in the estuaries and embayments; as sea level rises further to a point where it can extend over the adjacent interfluvium (i.e. at the beginning of the TST) tidal processes remain important as the shoreline remains significantly rugose; a characteristic of transgressive shorelines (Longhitano et al. 2012).

Tidally influenced fluvial deposits have also been cited to form at the greatest extent of sub-aerial exposure and erosion, where incised valleys flood and estuaries begin to form

(Plink-Björklund 2005, Aschoff and Steel 2011a). In the LST model, during progradation, fluvial channels grade seaward and upwards into tidally influenced fluvial deposits and are characterised by thin bedded, ripple-laminated very-fine to fine-grained sandstones and plane-parallel laminated sandstones and mudstones (Plink-Björklund 2005). The transition from fluvial to tidally influenced fluvial deposits upwards is interpreted by these authors as evidence for deposition during sea-level rise.

Strong tidal influence is common during sea-level fall as well as rise, and factors such as shoreline morphology, basin width, bathymetry, proximity to shelf edge, shelf width and shelf angle that directly produce tidal responses (Longhitano et al. 2012). In shallow seaways, such as the Western Interior Seaway, a further consideration is that sea-level fall can cause an increase in tidal influence due to seaway narrowing causing a reduced wave fetch and the constriction of tidal currents (Longhitano et al. 2012).

2.4.3 The backwater effect

The backwater zone of a river is defined as ‘the distal reach where the streambed drops below sea level, resulting in river-flow deceleration’ (Chatanantavet et al. 2012; Colombera et al. 2016). Significant recognition is now given to the role of backwater hydraulics as a control on fluvio-deltaic morphodynamics (e.g. Chatanantavet et al. 2012; Lamb et al. 2012; Nittrouer et al. 2012; Chatanantavet and Lamb 2014; Ganti et al. 2014; Colombera et al. 2016), and this has raised awareness of its potential importance as a factor controlling sedimentary architecture in the preserved stratigraphy of corresponding preserved successions (Lamb et al. 2012; Blum et al. 2013). The backwater zone overlaps with the FMTZ (Fig. 2.18) and the lithological and architectural character of channels within this zone will be influenced by these processes. The backwater zone can extend 100s of kilometres upstream from saltwater intrusions or from the landward-most effects of tidal action that would produce discernible marine indicators in preserved fluvial channel-fill deposits (Li et al. 2006). This is because, rather than overtopping the banks (and levees) during flooding (Sambrook Smith et al. 2010), channels within the backwater zone will be subject to water-surface drawdown during flood events. Channels interpreted as distributary channel-fills in the backwater zone are presented in chapters 4 and 5 and discussed further in chapter 7.

INCISED VALLEYS FORMED DURING FALLING STAGE

BYPASS CHANNELS FORMED DURING FALLING STAGE

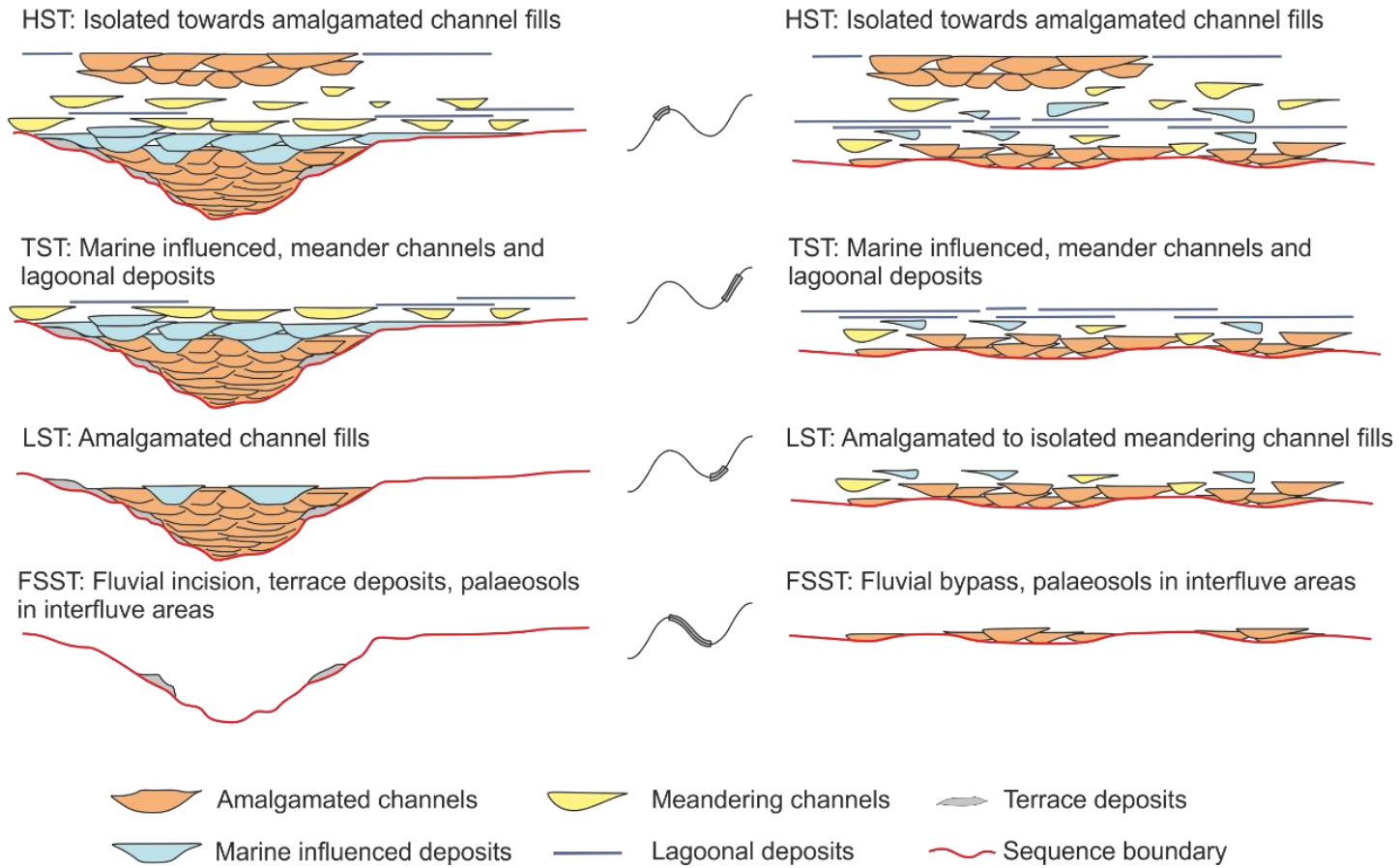


Figure 2.17: Stratigraphic architecture of fluvial depositional sequence influenced by base-level fluctuations., adapted after Shanley and McCabe 1991; Van Strien 2010.

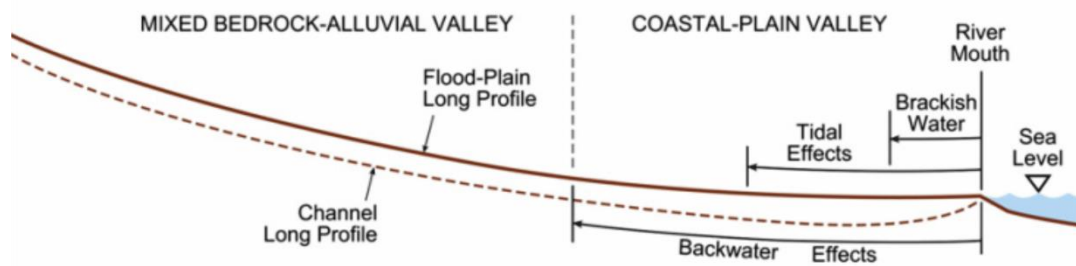


Figure 2.18: Long profile view sketch of a floodplain profile, showing the relationships between tidal effects, brackish water effects and backwater effects and their relative extents upstream, adapted after Li et al. 2006. The limit of tidal effects is the up-dip extent of the FMTZ.

2.5 Coal deposits and their significance

Coal seams form in a broad spectrum of depositional systems, from alluvial fan settings, to strandplains, to subaqueous settings (e.g. mangrove swamps). The environments of deposition of coal have been discussed by many authors (e.g. McCabe 1984; 1987; Fielding 1985; 1987; Jerrett et al. 2011a; b). The Neslen Formation is interpreted as having been deposited in a fluvial to deltaic environmental setting and hence specific consideration is given to these depositional environments herein.

Coal forms from the accumulation of vegetation debris, commonly in environments that are in close proximity to sites of clastic accumulation, such as crevasse splays on floodplains (Gersib and McCabe 1981) or in interdistributary bays or levees (Baganz et al. 1975). The introduction of clastic material hampers the formation of high-quality coal. As such, peat deposits, which form high-quality coal seams, tend to accumulate in regions restricted from the regular introduction of clastic material, notably in raised mires (see below).

2.5.1 Controls

The fundamental control on coal formation and preservation is the accommodation rate in relation to rate of peat production (Cross 1988). Factors such as climate (e.g. Parrish et al. 1982), tectonics (e.g. Fielding 1987) and eustasy (e.g. Ryer 1981) are important in modifying how the peat accumulates, is preserved, and how it converts into coal upon burial. The type of flora, peat accumulation rates and groundwater table are also important considerations (Bohacs and Suter 1997; Holz et al. 2002). A continuously rising water table,

relative to the sediment surface, generates the accommodation for peat to accumulate (Diessel 1992). If the rate of accommodation generation is exceeded by the rate of peat production, then available accommodation for further accumulation becomes limited and the mire is more likely to be eroded. Conversely, if the rate of accommodation generation exceeds the rate of peat production, the mire can become drowned by marine transgression, convert into a lagoon, or be overwhelmed by clastic sedimentation (Bohacs and Suter 1997).

Coal seams are produced in raised (ombrotrophic) or low-lying (rheotrophic) mires. Coals with inorganic mineral content below 10% have been interpreted as the products of ancient ombrotrophic mires (Clymo 1987; Diessel et al. 2000; Davies et al. 2005; Jerrett et al. 2011b); these are-rain fed mires which build up above the regional water table and are able to restrict clastic influx. Rheotrophic mires are ground-water fed and accumulate in depressions. Hence, rheotrophic mires have a high potential to accumulate clastic detritus via fluvial or marine inundation; they commonly have a higher detrital mineral content and a high syngenetic pyrite content, which indicates the influence of brackish water (Cohen et al. 1987; Petersen and Andjersberg 1996; Jerrett et al. 2011b, c). Controls on the occurrence of ombrotrophic or rheotrophic mires is influenced by the presence of groundwater and the balance of evaporation and evapotranspiration (Jerrett et al. 2011b, c).

2.5.2 Sequence stratigraphy

Within a depositional sequence, the occurrence and distribution of paralic coals is predictable. For a given peat production rate, the occurrence of paralic coals may vary significantly due to variations in the local rate of change in accommodation (Gastaldo et al. 1993; Aitken and Flint 1995; Bohacs and Suter 1997). Lower accommodation rates favour initiation of mires earlier in the LST and later in the HST, whereas higher rates would delay or prevent peat accumulation (Flint et al. 1995; Fig. 2.19).

During the LST, the low rate of accommodation generation creates space that is rapidly filled vertically initially then horizontally, forming continuous coal seams which decrease in quality upwards (Fig. 2.19; Flint et al. 1995). In the late lowstand and initial transgression the increasing rate of accommodation generation allows peat to accumulate in place, and the mires tend to remain isolated, forming laterally discontinuous seams (Fig. 2.19). As transgression continues, only thin, discontinuous coals are formed as the high rate of accommodation generation precludes mires accumulation until the accommodation is filled, mires are stressed and eventually inundated and preservation decreases. In the late TST and initial HST the accommodation rate permits the formation of thick, isolated coal seams which increase in continuity upwards (Fig. 2.19).

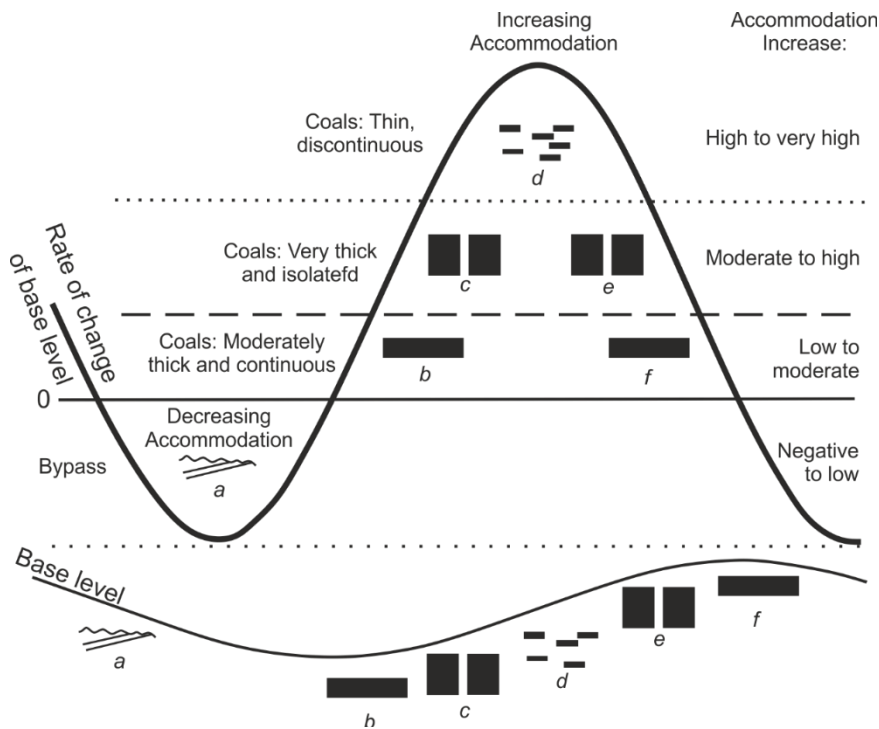


Figure 2.19: Relation of rate of change of base level to coal thickness and geometry for a given peat production, adapted after Bohacs and Suter 1997.

Interpreting key sequence stratigraphic surfaces in terrestrial sequences can be achieved through careful analysis of coal-bearing strata (Diessel et al. 2000; Wadsworth et al. 2002; Jerrett et al. 2011a, b, c)(Fig. 2.20). The succession can 'wet' or 'dry' upwards: drying-up successions correspond to a decrease in the ratio of accommodation rate: peat production rate; the converse is the case for wetting-up successions. In a drying-up succession, the point at which a coal seam overlies clastic sediments composed of marine, lagoonal or lacustrine strata represents a territorialisation surface in response to shallowing upwards (Fig. 2.20; Diessel et al. 2000).

Continued decrease in accommodation (Fig. 2.20) results in zero accommodation, terminating peat accumulation; this can produce an erosional sub-aerial exposure surface (ES; Moore 1995). In a 'wetting-up' succession coal seam located above sub-aerial, terrigenous strata represents a paludification surface (PS); such a surface represents the end of peat accumulation as it cannot keep pace with increasing accommodation. In such a case peat production is gradually replaced by marine, lagoonal or lacustrine sedimentation (Diessel et al. 2000). If clastic input is low or there is an abrupt increase in accommodation then the contact between the coal seam and overlying marine, lacustrine or lagoonal sediment is abrupt and interpreted as a flooding surface (FS; Fig. 2.20). If this surface shows evidence of erosion or reworking it may instead be interpreted as the transgressive surface (TS; Fig. 2.20). The point at which there is turnaround between a drying-up sequence and

wetting-up sequence can be interpreted as a sequence boundary (SB or maximum flooding surface (MFS) depending on the trend of increasing or decreasing accommodation (Fig. 2.20) The recognition of sequence boundaries and maximum flooding surfaces within a coal deposit can only be recognised based upon careful, chemical analysis of the accumulation, or by the identification of laterally extensive partings within the coal seams (seam splits) (Jerrett et al. 2011a).

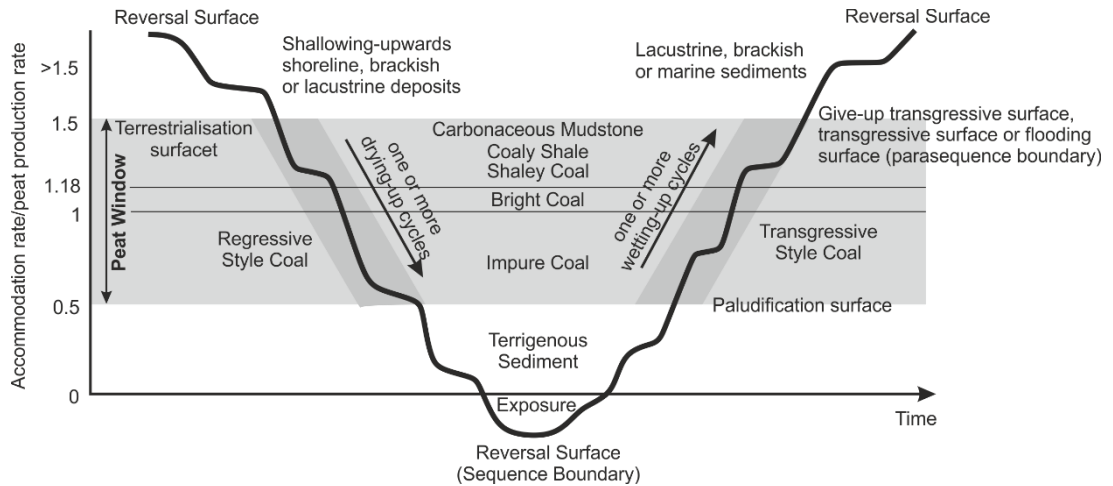


Figure 2.20: Idealised curve to show the relationship between accommodation change, peat production, peat facies and resultant coal types. The drying up cycles correspond to decreasing accommodation and wetting up cycles correspond to increasing accommodation, adapted after Wadsworth et al. 2003, Jerrett et al. 2011b.

2.6 Summary

Fluvial, tidal and wave processes vary temporally and spatially through the fluvial-to-marine transition zone and controls (both autogenic and allogenic) on these processes are difficult to discern from outcrop of ancient fluvial and paralic systems. Where a coastal plain system is characterised by a low-gradient, fluvial channels are likely to be influenced by tidal and backwater processes. Point-bar elements which accumulate under these conditions will likely preserve deposits that reflect the interaction of multiple processes. The interaction of competing peat mires and fluvial systems on the coastal plain further complicates the resultant stratigraphy.

3 Geological Setting

This chapter summarises the regional and local geological setting of the study area, encompassing the stratigraphy of the Mesaverde Group. This chapter also summarises the palaeogeographic and palaeoenvironmental interpretations of the region for the Upper Cretaceous in general, and of the time of accumulation of the Neslen Formation, in particular.

3.1 Tectonic Setting and Basin Evolution

3.1.1 Tectonic Evolution

The Sevier orogenic belt, which is commonly also referred to as the Sevier thrust belt, together with the associated Cretaceous foreland basin on its eastern side evolved over a period of 70 million years from the Aptian to Maastrichtian (Jordan 1981, Aschoff and Steel 2011a). The foreland basin was ~300 km wide (in central Utah) and extended over 2000 km north-to-south (DeCelles 2004). The Sevier orogenic belt is defined as a 'narrow zone of



Figure 3.1: Generalised map of the Western Interior Seaway showing the maximum extent of marine inundation across the continental plate (pale blue), the landmass (dark green) and the orogenic belt (brown). Major tectonic boundaries are also shown; tick on overriding plate. Adapted after Miall et al. 2008

regional scale thin- and thick- skinned thrust faults and related folds that extends from the Canadian portion of the Cordillera south to southeastern California' (DeCelles 2004, p. 118).

The orogen developed in response to subduction of the Farallon plate at the western margin of North America, which caused shortening within the Sevier thrust belt and Laramide structures (Aschoff and Steel 2011b) (Fig. 3.1). Collision occurred at a rate of ~8mm/year in the Late Jurassic, increasing to 150 mm/year by the Paleocene, with abrupt increases in early, mid-, and latest Cretaceous (DeCelles 2004). The Sevier orogenic belt took up most of the regional shortening in the area through displacement on the Canyon Range (Neocomian-Aptian), Pavant (Aptian-Albian), Paxton (Cenomanian-Campanian) and Gunnison (late Campanian-Paleocene) thrust systems (Decelles et al. 1995). There was a progressive transition from thin- to thick-skinned deformation caused by gradual shallowing of the subducting slab. Many authors have argued that this transition resulted in pulses of increased sediment supply within the foreland basin (e.g. Aschoff and Steel 2011a). Episodes of thrust faulting therefore likely controlled the patterns of sedimentation as clastic detritus was shed into the foreland basin (Goldstrand 1994). The Laramide Orogeny, which occurred after the Sevier Orogeny, from the late Cretaceous (70-80 Ma) to 35-55 Ma and was driven by shallow subduction of the Farallon and Kula plates beneath the North American plate (DeCelles 2004). The Sevier and Laramide "events" are not temporally distinct but represent local and regional response to different styles of deformation (Cross 1986). The change from Sevier thin-skinned thrusting to Laramide basement-involved uplifts in the study area occurred during the late Campanian (Willis 2000). The Laramide Orogeny resulted in a series of intermontane structural basins; e.g. Uinta Basin, Utah; and adjacent mountain blocks.

3.1.2 Western Interior Seaway

3.1.2.1 *Transgression and Regression*

The North American Cordilleran foreland basin was occupied by the Western Interior Seaway (WIS) during the Cretaceous. This foreland basin extended from present-day Canada to the Gulf of Mexico (Jordan 1981; Robinson Roberts and Kirschbaum 1995; Aschoff and Steel 2011a; b) (Fig. 3.1). The WIS was characterised by relatively shallow water depths along its length, rarely exceeding 100 m, and by low-gradient margins (e.g. Kauffman 1977), except for localised areas in the proximity of the forebulge zone or adjacent to isolated intra-basinal highs (Plint et al. 1993; Longhitano and Steel 2016).

The basin developed from the late Jurassic through Paleocene times (Aschoff and Steel 2011b) due to tectonic thickening of the crust and lithospheric loading which caused downwarping in the foreland basin (Jordan 1981). The basin reached its maximum extent in

the Turonian (Kirschbaum and Hettinger 2004). The seaway was present for 35 Myr's, before the sea drained from the interior for the last time in the Maastrichtian (Robinson Roberts and Kirshbaum 1995). The sedimentary fill of the basin thickens westward and Cretaceous sediments constitute much of the accumulated succession (Aschoff and Steel 2011b), which exceeds 2 km in thickness in the centre of the basin (van Wagoner 1995). The north-south trending Sevier orogenic belt is the main sediment source for the basin. The majority of clastic detritus was shed from uplifted highlands and was transported eastward across a relatively narrow, low-lying coastal plain towards the shore of the WIS. The palaeo-shoreline of the WIS is thought to have been characterised by orientations from northwest-southeast to northeast-southwest (Aschoff and Steel 2011b).

The seaway was initially flooded from the north in the Aptian (Robinson Roberts and Kirshbaum 1995; Fig. 3.2). During the late Aptian to early Albian an extensive northern arm of the seaway and a minor southern arm encroached slowly and irregularly into the basin until the two arms joined during the Cenomanian (Fig. 3.2a-c). The Cenomanian is a period of overall transgression and the central part of the seaway is represented by a record of continuous deposition of marine shale (Robinson Roberts and Kirshbaum 1995) (Fig. 3.2d). In the early to middle Turonian, the sea continued to transgress far into central Utah to produce a dominantly north-south trending coastline (Franczyk et al. 1992) (Fig. 3.2e). The first major regression occurred in the late Turonian, following which the shoreline prograded to the east across Wyoming (Robinson Roberts and Kirshbaum 1995), producing a northeast trending shoreline (Franczyk et al. 1992). In the mid Coniacian, a major transgression occurred; interrupted by three minor regressive phases (Robinson Roberts and Kirshbaum 1995). At this time the marine shoreline was located relatively proximal to the highlands of the Sevier thrust belt (Franczyk et al. 1992). Towards the late Santonian (Fig. 3.2f) the marine shoreline gradually prograded eastward before another transgression pushed the shoreline westward in latest Santonian to earliest Campanian times (Franczyk et al. 1992) (Fig. 3.2g).

During the Campanian a series of gradual shoreline regressions (Fig. 3.2g) occurred, resulting in the withdrawal of the seaway from the majority of Utah by the late Campanian (Fig. 3.2h). This event occurred in response to (i) the slowing and cessation of basin

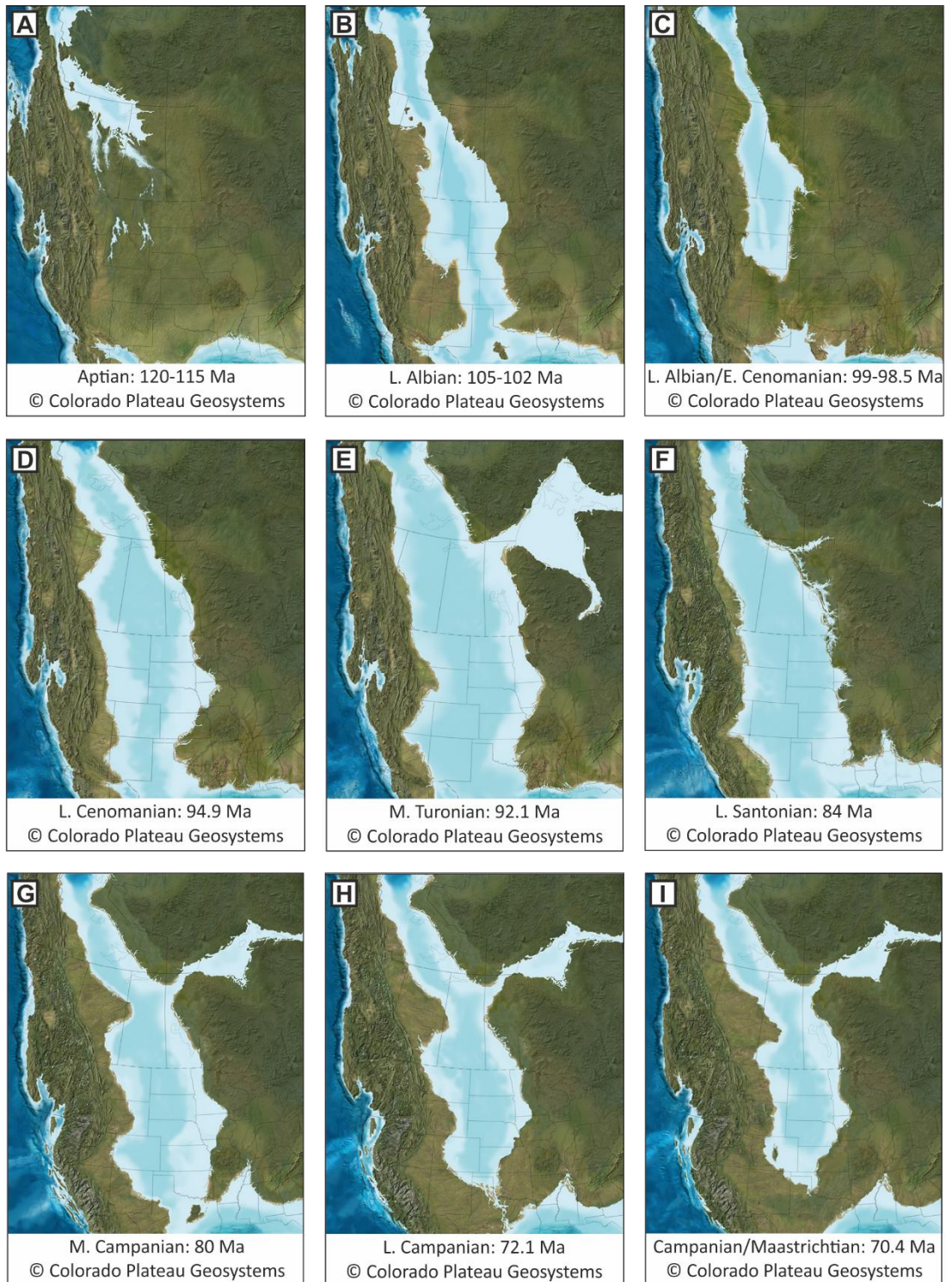


Figure 3.2: Figures showing the evolution of the Western Interior Seaway through time, adapted after Blakey 2016.

subsidence along the western margin of the Western Interior Seaway, and/or (ii) an increase in clastic sediment supply from the west. By the end of Campanian the seaway had mostly retreated from Utah and overall regression continued through the Maastrichtian (Fig. 3.2i). The seaway had retreated fully from Utah by the end of the Cretaceous (Blakey and Ranney 2008); details of the palaeogeography of that time and up to the Oligocene are covered extensively in Franczyk et al. (1992).

A wedge of siliclastic strata (van Wagoner 1995; Fig. 3.3) forms the majority of the infill of the Cordilleran Western Interior Basin. From the late Cretaceous through Paleocene, the basin was locally punctuated by Laramide structures, which produced smaller basins within the Western Interior Seaway (e.g. Uinta and Piceance Basins) (Aschoff and Steel 2011a).

3.1.2.2 Tidal Range

Shallow epeiric seaways are commonly dominated by tidal action (Longhitano and Steel 2016); in such seaways, there is commonly a correlation between tidal amplitudes, tidal current velocities and shelf width. Within the WIS, the large-scale effect of tidal waves entering the seaway from the Gulf of Mexico produced significant anticlockwise tidal flow patterns (Dalrymple 2010; Longhitano and Steel 2016). However, the predominantly shallow water depth of the seaway during the Campanian (the time of deposition of the Neslen Formation), as well as the restricted opening of the seaway to the open ocean (Figs. 3.1, 3.2), would likely have acted to dampen tidal forces and the tidal range in the southern reaches of the seaway (Steel et al. 2012).

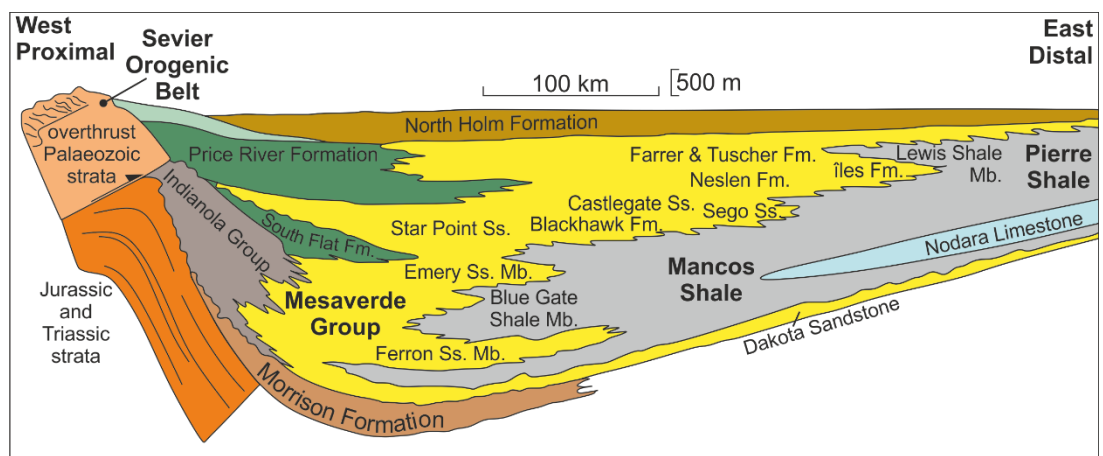


Figure 3.3: Cross section of the sedimentary infill of the Western Interior Basin, adapted after Kauffman 1977; Seymour and Fielding 2013; Armstrong 1968.

Modelling of tidal and storm conditions within the WIS was undertaken by Eriksen and Slingerland (1990) using a multi-layer, numerical model of turbulent flow in shallow seas, and was based on bathymetry and palaeogeography as postulated by Kauffman (1984). Later modelling was been carried out by Slingerland et al. (1996) and Slingerland and Keen (1999) who demonstrated the hypothesised anticlockwise gyre of normal surface circulation patterns. Overall the WIS was dominated by storms (passing west to east) and hurricanes (moving north), which promoted southerly longshore drift across the west coast of the seaway; the overall tidal regime was microtidal (0-2 m tidal range) on the south-western coastline (Longhitano and Steel 2012).

Localised amplification of tides at the coastline likely played a significant role in the generation and preservation of deposits along the western margins of the seaway, which record strong tidal processes locally (Mellere and Steel 1995; 2000; Nummedal and Riley 1999; Hampson et al. 2008; Legler et al. 2014; Steel et al. 2012). Amplification is attributed an increase in tidal power through narrow, shallow straits and embayments, which formed from the subtle growth of tectonic structures on the sea floor (Yoshida et al. 2007; Nyberg and Howell 2016). Eastern Utah and Western Colorado lay within one notable embayment: the 'Utah Bight' (Zapp and Cobban 1960; McGookey et al. 1972; Legler et al. 2014). This resulted in accumulation of the tide-influenced to tide-dominated Sego Sandstone, deposits of which are indicative of a microtidal to mesotidal regime within the embayment.

3.2 Climate

During the Cretaceous, the palaeoclimate of western North America changed from a relatively more arid regime that characterised the earlier Mesozoic times across what is now the western USA, to a significantly more humid regime in the Cretaceous (Fillmore 2011). This change occurred as the North American continent drifted northwards to between 30° and 60° N. From oxygen isotope analysis of fossil shells, sea temperatures are reported to have been up to 15°C warmer than those of similar latitudes today (Fillmore 2011). The climate of Utah in the Upper Cretaceous was humid and subtropical (Fillmore 2011), with potentially monsoonal conditions (Foreman et al. 2015). During the Campanian – the specific time interval for this work – the study area occupied a subtropical palaeolatitude (approximately. 42°N) and experienced a warm, humid climate (Bhattacharya and MacEachern 2009).

3.3 Mesaverde Group Stratigraphy

The Mesaverde Group is a 1500 m thick succession of Upper Cretaceous strata that is especially well exposed along the Book Cliffs of eastern Utah and western Colorado. The Book Cliffs extend for approximately 200 km and form the eroded southern margin of the Uinta and Piceance Basins (Lawton and Bradford, 2011). The Mesaverde Group comprises deposits of fluvial and proximal marine origin arranged in an overall progradational trend where the various formations that comprise the group intertongue with the deeper-water deposits of the Mancos Shale (Fig. 3.3), which is extensive over large parts of eastern Utah, Colorado and Wyoming (Steel et al. 2012).

The stratigraphic subdivision of the Mesaverde Group is summarised by a number of authors (e.g. Weimer 1960; Warner 1964; Roehler 1990; Miall 1993; Olsen et al. 1995; Willis 2000; Cole and Cumella 2003; Hettinger and Kirschbaum 2003; Johnson 2003; Bullimore et al. 2008; Steel et al. 2011). Formations that comprise the group accumulated in the Campanian; the names assigned to some of these formations change across the Utah-Colorado border (Fig. 3.4). In Utah, the Mesaverde Group is split into the Star Point Sandstone, Blackhawk Formation, Castlegate Sandstone (including the Bluecastle Tongue), Segó Sandstone, Neslen Formation, Price River Formation, Farrer Formation and the Tuscher Formation (Fig. 3.4). In Colorado the Mesaverde Group is composed of the Castlegate Sandstone, Segó Sandstone, Îles Formation (often referred to as the Mount Garfield Formation) and Williams Fork Formation (Kirschbaum and Hettinger 2004) (Fig. 3.4).

Overall, the Mesaverde Group in Utah is divided into an upper and lower part. The lower part comprises the Star Point Sandstone, Blackhawk Formation and the Castlegate Sandstone. The Buck Tongue, stratigraphically above the Castlegate Sandstone, separates the upper and lower parts of the group. This tongue of shale, which is of offshore marine origin, records an abrupt landward shift in deposition due to either tectonic subsidence or an increase in relative sea level (Willis and Gabel 2003). The upper part comprises the Segó Sandstone, Neslen Formation, Bluecastle Tongue, Farrer Formation and Tuscher Formation (McLaurin and Steel 2000; Willis and Gabel 2001; 2003).

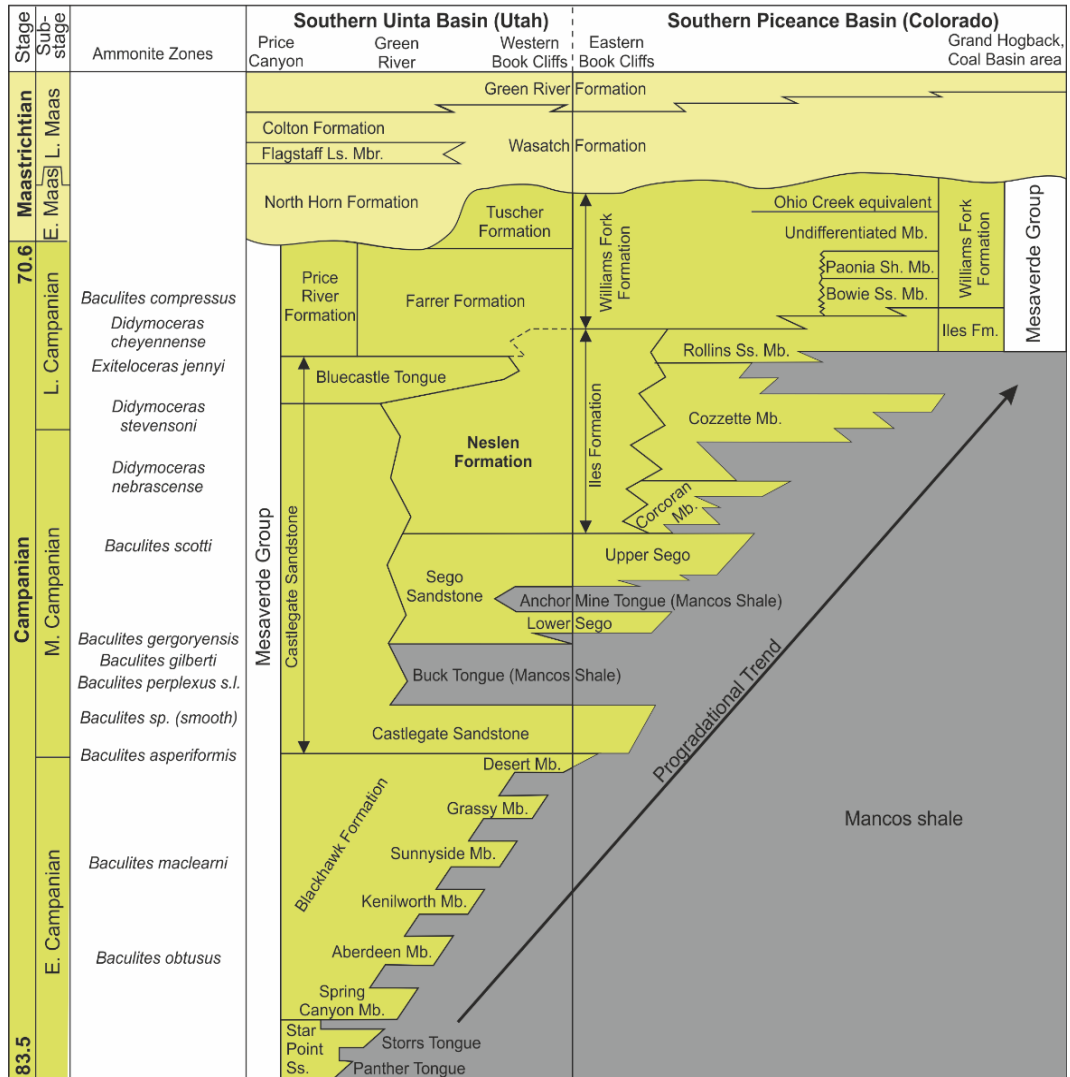


Figure 3.4 Stratigraphy of part of the Mesaverde Group succession and overlying strata in the Book Cliffs region from Price (Utah) to Grand Hogback (Colorado), adapted after Kirschbaum and Hettinger 2004.

Since the 1980s, the outcropping successions exposed in the Book Cliffs have been a testing ground for the development of concepts in sequence stratigraphic analysis (Chapter 2). Early sequence stratigraphic work focused on the lower Mesaverde Group (Blackhawk Formation and Castlegate Sandstone); the upper Mesaverde Group remains relatively understudied. In recent years, the regional sequence stratigraphic framework for the Upper Mesaverde Group from Tusher Canyon (Utah) down-dip (i.e. eastwards) to Book Cliffs Mine, Grand Junction (Colorado) has been established (e.g. McLaurin and Steel 2000; Hettinger and Kirschbaum 2002; Kirschbaum and Hettinger 2004; Kirschbaum and Spear 2012). This allows for studied deposits of the Neslen Formation to be placed within a regional sequence stratigraphic context (see section 3.4.2 below).

3.4 Neslen Formation

The Neslen Formation is defined on the basis of the occurrence of coal-bearing strata above the Segó Sandstone (Fisher 1936). The sedimentology of this formation has been described by many authors (Young 1957; Lawton, 1986; Pitman et al. 1986; Franczyk et al. 1990; Gualtieri 1991; Robinson Roberts and Kirschbaum 1995; Olsen et al., 1995; van Wagoner 1995; McLaurin and Steel 2000; Willis 2000; Hettinger and Kirshbaum 2002; Kirschbaum and Hettinger 2004; Aschoff and Steel 2011a, 2011b; Olariu et la. 2015). Deposits of the Neslen Formation comprise approximately 50% fine-grained units and 50% cliff-forming sandstones interbedded with coal beds that are themselves each up to 1 m thick (Lawton 1986; Gualtieri 1991). Siltstones are dominantly carbonaceous. Sandstones are dominantly very fine-grained.

The base of the Neslen Formation has a gradational and intertonguing relationship with the uppermost upward-coarsening cycle of the underlying Segó Sandstone (Pitman et al. 1987). The Neslen Formation is replaced westward (i.e. palaeo-landward) into the Castlegate Sandstone near Green River and eastward (i.e. palaeo-seaward) into the lower part of the Îles Formation (Fig. 3.4). The thickness of the Neslen Formation varies from 40 m at Tusher Canyon to over 120 m at the Utah–Colorado border.

3.4.1 Palaeoenvironment

The Neslen Formation comprises tabular and lenticular sandstones within slope-forming organic rich mudstone and siltstones. The overall palaeoenvironmental context of the Neslen Formation (Fig. 3.5) has been interpreted as strandplain (Gualtieri 1991), delta plain (Karaman 2012; O’Brien 2015; Gates and Scheetz 2015; Burton et al. 2016) or estuarine complex (Willis 2000; Kirschbaum and Hettinger 2004; Cole 2008; Fig. 3.6). The time-equivalent Îles Formation in Colorado is interpreted as a prograding delta complex (Boyles and Scott 1982; Young 1983; Gomez-Veroiza and Steel 2010; Cole and Cumella 2003; Kirschbaum and Cumella 2015) or as vertically stacked, wave-dominated shorelines (Kirschbaum and Hettinger 1998). The Neslen Formation was deposited as part of a low-gradient, low-relief fluvial floodplain and coastal plain (Lawton 1986; Pitman et al. 1987).

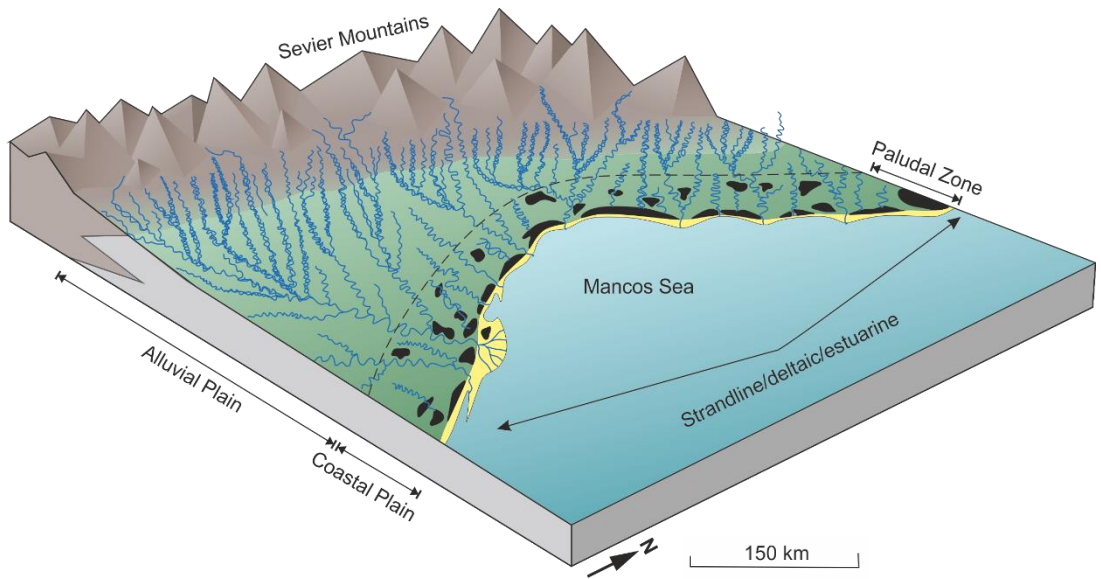


Figure 3.5: General depositional setting for the western margins of the Western Interior Seaway during the Late Cretaceous, adapted after Ryer and McPhillips 1963; Cole 2008.

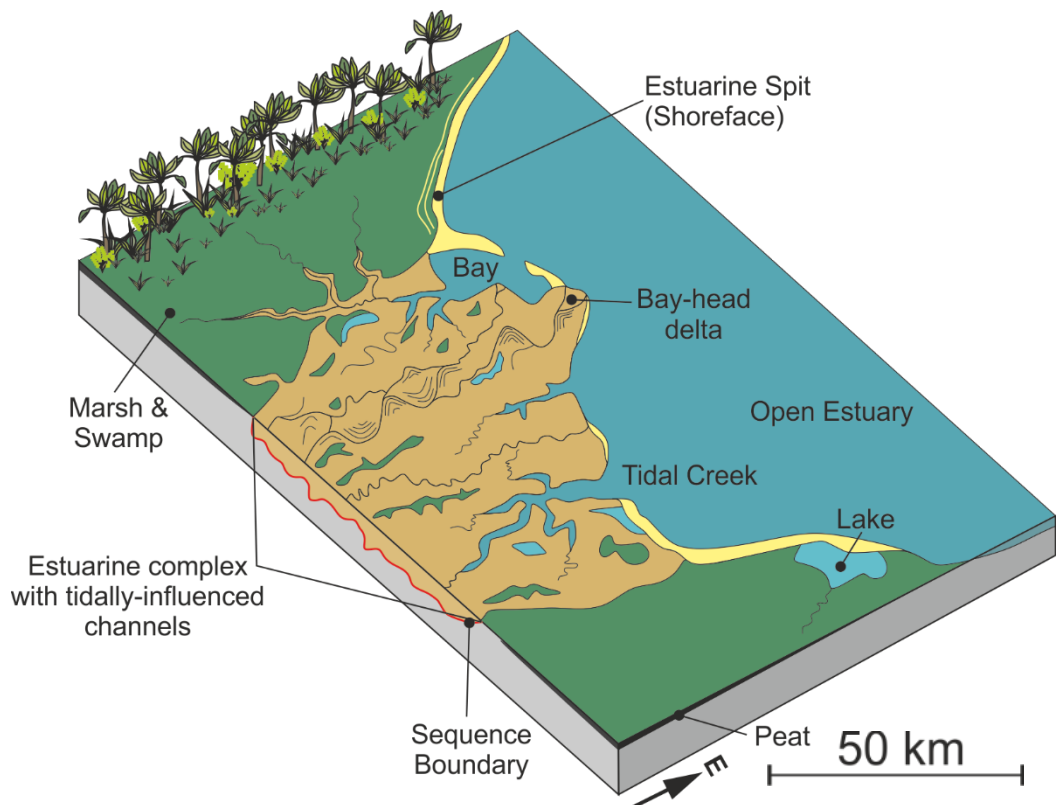


Figure 3.6: Estuarine depositional model for the Neslen Formation, adapted after Cole, 2008. The vegetation is not drawn to scale.

The westward (i.e. palaeo-landward) transition of coeval Neslen and upper Castlegate depositional environments from tidal flat to meander belt deposits records a lateral coarsening of lithologies toward the Sevier Orogenic Belt. Overall, the proportion of sandstone preserved within the formation increases upward (Pitman et al. 1987). The Neslen Formation records an upward change from deposits of tidal-flat origin near its base, passing up through sandstone of probable distributary channel origin, to tidally influenced fluvial deposits, into a section dominated by deposits of fluvial meander-belt origin (Lawton 1986; Willis 2000). The lower parts of the formation accumulated in brackish water and fresh water environments in a coastal-plain setting that was characterised by various sub-environments, including tidal flats, lagoons, bays, marshes and oyster reefs (Pitman et al. 1987; Chan and Pfaff 1991). The upper Neslen Formation was deposited in upper coastal-plain and lower alluvial-plain settings that were characterised by meandering rivers that crossed extensive flood plains (Pitman et al. 1987).

Lenticular sand-bodies in the Neslen Formation have a bimodal distribution of width-to-thickness aspect ratios, either between 10:1 and 30:1, or 100:1 or greater (Gualtieri 1991); those with smaller aspect ratios are interpreted as channel scour-and-fill deposits. Bodies with larger aspect ratios have been interpreted as the product of infill of tidally influenced fluvial and fluvial channels (Kirschbaum and Hettinger 2004; Aschoff and Steel 2011b), deposits in the fills of which are indicative of low-energy fluvial systems (Gualtieri 1991). Meandering streams are suggested by common inclined lateral accretion deposits and frequent burrowed and rooted crevasse-splay deposits in the siltstone dominated parts of the succession (Lawton 1986). The thickness and lateral extent of the channel-fill sandstone deposits indicates that many of the rivers were short-headed streams draining the upper coastal and lower alluvial plains (Keighin and Fouch 1981; Pitman et al. 1987).

Within the Neslen Formation, notable tabular sandstone bodies include the Thompson Canyon Sandstone Bed (TCSB) and Sulphur Canyon Sandstone Bed (SCSB) (Fisher 1936), which are composed of clean, well-sorted quartz sandstones that are laterally continuous and traceable for several tens of kilometres (Kirschbaum and Hettinger 2004). The units are dominated by wavy-lenticular bedding and symmetrical wave rippled sandstone beds that are locally bioturbated and burrowed by *Ophiomorpha*; isolated occurrences of hummocky cross-stratification are noted. These beds have been variably interpreted as reworked sandy sediment deposited in a bay-shore environment (Gualtieri 1991), a tidal bar (Hettinger and Kirschbaum 2002), or a beach or tidal flat (Kirschbaum and Hettinger 2004). Cole (2008) interprets the TCSB as a marginal marine sandstone bounded at its base by a transgressive surface of marine erosion.

Four coal zones are recognised within the succession: the lowermost Palisade Coal Zone, the Ballard Coal Zone, the Chesterfield Coal Zone and the Carbonera Coal Zone (Fisher 1936; Gualtieri 1991; Kirschbaum and Hettinger 2004; Cole 2008). The Carbonera Coal Zone is located in the upper Neslen equivalent strata of Colorado. The Palisade Coal Zone (Lower Coal Zone of Gualtieri 1991) consists of a series of 1 to 9 coal beds that occur close to the top of the Segó Sandstone, coal beds range in thickness from 0.025 to 1 m (Gualtieri 1991). The Palisade Coal Zone may stratigraphically correlate to the Anchor Coal Zone (Young 1955) of the Îles Formation. The Ballard Coal Zone consists of 1 to 4 coal beds, which range in thickness from 0.03 to 1 m, the thickness of the zone ranges from 0.2 to 5 m, and occurs beneath and is associated with the presence of the TCSB. The Chesterfield Coal Zone lies stratigraphically above the TCSB (Fisher 1936) and consists of 1 to 6 coal beds, which ranging in thickness from 0.025 to 2.13 m within a zone that itself ranges in thickness from 0.13 to 10 m (Gualtieri 1991).

3.4.2 Sequence Stratigraphy

The Neslen Formation is interpreted to have been deposited as part of a clastic wedge that accumulated under conditions of low rates of accommodation generation (Ashoff and Steel 2011b 'wedge B', consisting of the Neslen Formation, Segó, Corcoran and Cozzette Sandstones). The progradation distance of the clastic wedge was anomalously high: up to 400 km rather than 250 km for other parts of the Mesaverde succession (Ashoff and Steel 2011b; Fig. 3.7). Tidal deposits are present within the transgressive and regressive parts of the sandstone tongues (Ashoff and Steel 2011b).

Contrasting sequence stratigraphic interpretations have been proposed for the Neslen Formation. Defining flooding surfaces and sequence boundaries as well as their correlation is often contentious; within the Neslen Formation authors present different interpretations as laid out below.

A sequence boundary at the top of the Neslen Formation – termed the Bluecastle Sequence Boundary – is interpreted by many authors (Yoshida et al. 1996; McLaurin and Steel 2000; Hettinger and Kirschbaum 2003; Fig. 3.8).

Willis (2000) presents a sequence stratigraphic interpretation of the Upper Castlegate Sandstone, Segó Sandstone and the Neslen Formation between Helper and Pinto Wash West. He splits the succession into three sequences. Each sequence is ~100 m thick and is considered to have developed over a period of one-to-three million years in duration. These sequences themselves each contain several nested, higher-frequency stratigraphic sequences. Within the Neslen Formation, no higher frequency sequences were identified

(Willis 2000) and no sequence boundary was identified at the contact between the Sego Sandstone and Neslen Formation.

Yoshida et al. (1996) interpret the lowermost strata of the Neslen Formation as a lowstand systems tract (LST), with a transgressive systems tract (TST) overlying this; these two systems tracts are separated by a significant flooding surface (Fig. 3.8a). Towards the middle of the formation, a sequence boundary separates the TST from an overlying LST. No highstand systems tracts (HST) are interpreted to have been preserved. The base of the LST is dominated by fluvial channel sandstone bodies that are overlain by finer-grained units. McLaurin and Steel (2000) also split the Neslen Formation into two sequences (Fig. 3.9b) with a sequence boundary towards the middle of the formation. However the flooding surface is placed towards the base of the formation.

Hettinger and Kirschbaum (2000) argue that the Neslen Formation within the study area is bounded at both its base and top by sequence boundaries (Fig. 3.8c). A low-order boundary is inferred from the presence of a laterally persistent channel sandstone complex which is typically coarser-grained than the underlying strata located towards the middle of the Neslen Formation and which separates coastal plain facies below from dominantly fluvial facies above.

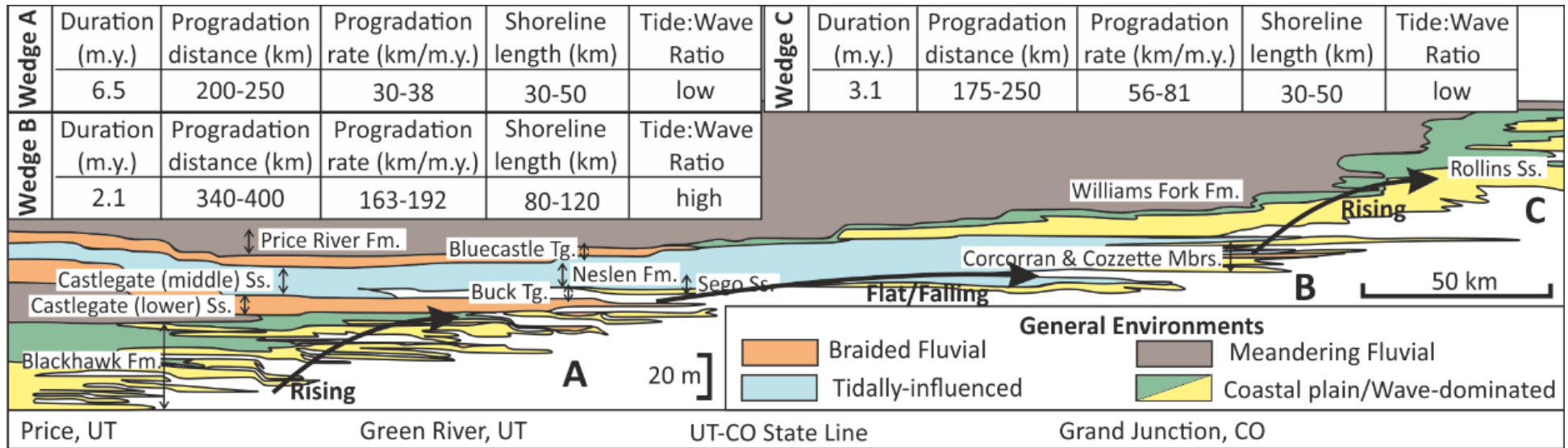


Figure 3.7: Summary of Campanian clastic wedges in the foreland basin showing units and stacking trajectories, and environments of deposition. Abbreviations: Formation (Fm.), Sandstone (Ss.), Tongue (Tg.), adapted after Aschoff and Steel 2011b.

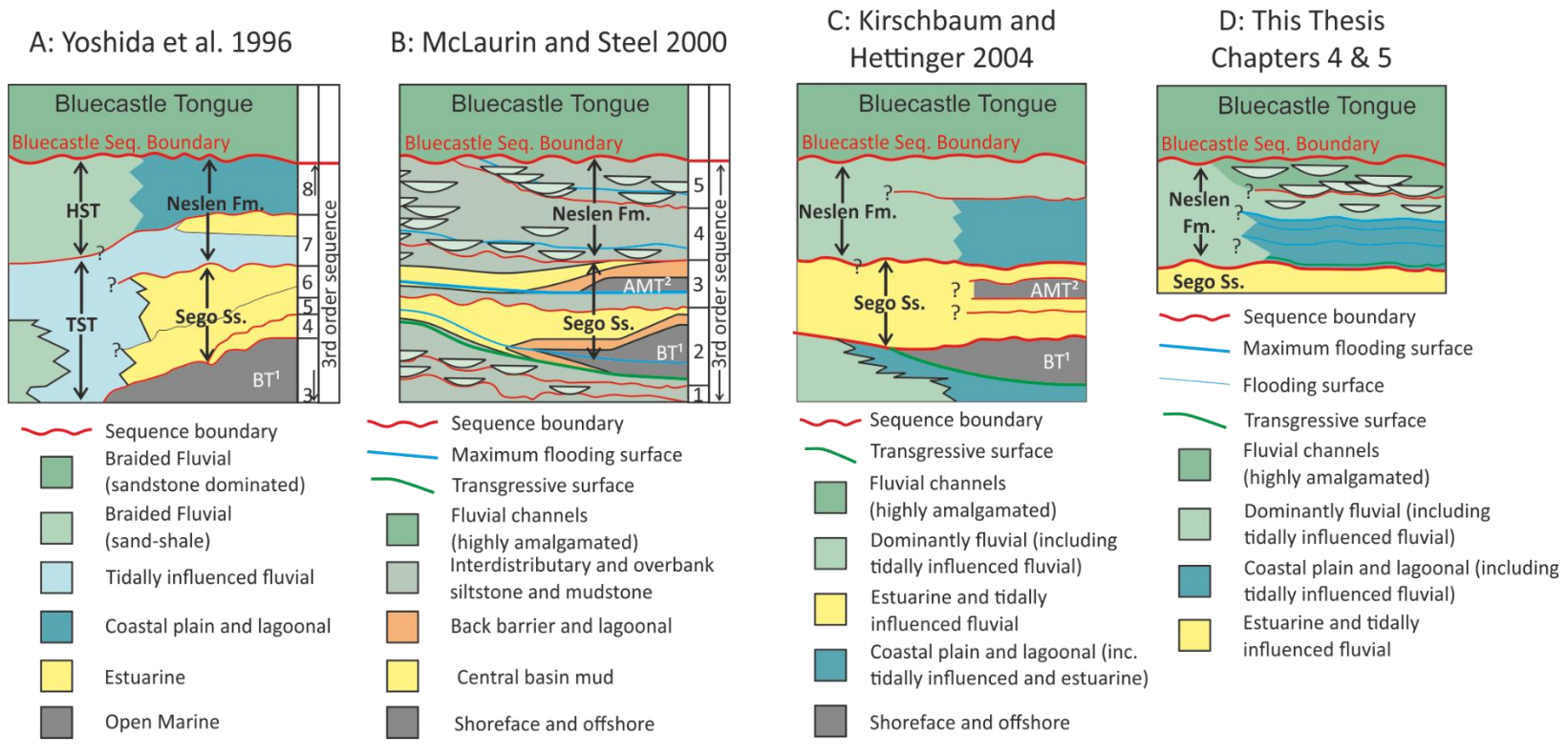


Figure 3.8: Interpretations of the sequence stratigraphy of the upper Mesaverde Group. The interpretations of Yoshida et al. 1996; McLaurin and Steel 2000 and Kirschbaum and Hettinger 2004 are compared to interpretations made in chapters 4 and 5. Abbreviations: Sandstone (Ss.), Formation (Fm.), Sequence (Seq.), Transgressive Systems Tract (TST), Highstand Systems Tract (HST), Buck Tongue (BT), Anchor Mine Tongue (AMT).

3.4.3 Marine Indicators

The Neslen Formation has been widely interpreted previously as being tidally influenced (Boyles and Scott 1982; Young 1983; Lawton 1986; Willis 2000; McLaurin and Steel 2000; Cole and Cumella 2003; Kirschbaum and Hettinger 2004; Tabet et al. 2008; Gomez-Veroiza and Steel 2010; Karaman 2012; Kirschbaum and Spear 2012; Kirschbaum and Cumella 2015; O'Brien 2015; Olariu 2015; Gates and Scheetz 2015; Burton et al. 2016). This interpretation is made based upon the presence of a range of sedimentary and ichnological indicators in the Neslen Formation.

Sedimentary indicators include draped ripples (both asymmetrical; and symmetrical forms) for which drapes consist of mud, silt or carbonaceous material and are single or double in character; double drapes are more diagnostic of tidal influence (Willis 2000). Beds exhibiting asymmetrical ripple lamination show ambiguous indications of bi-directional flow whereby foreset azimuths within a genetically related ripple-laminated bed dip in opposing directions and thereby record sediment transport that occurred in opposing directions (Willis 2000; Dalrymple et al. 2015; Olariu et al. 2015). Current energy fluctuations caused by either seasonal or tidal discharge variations are recorded by the presence of flaser, wavy or lenticular bedding (Willis 2000), where ripple-laminated sandstone occurs interbedded with mudstone or siltstone. Tidal rhythmites (cf. Kvale 2012) are present in the upper part of some sandstone beds within point-bar elements defined by variations in lamina thicknesses (Dalrymple et al. 2015; Olariu et al. 2015). Muddy intervals only rarely exhibit rhythmic thickness variations reflecting cessation/reduction of river flow due to tidal influence that allowed suspended sediment to settle to the bed (Dalrymple et al. 2015). Multiple reactivation surfaces in beds exhibiting cross bedding (Willis 2000) are also used as evidence to suggest tidal influence (Shanley et al. 1992).

Trace fossils identified within the Neslen Formation include *Arenicolites*, *Diplocraterion*, *Ophiomorpha*, *Skolithos*, *Teichichnus*, *Teredolites*, *Thalassinoides*, *Planolites* and *Rhizocorallium* (Willis 2000; Olariu et al. 2015). These are mostly associated with muddier intervals. Commonly, trace fossils occur in ichno-monospecific assemblages. Such low-diversity assemblages of trace fossils include forms that are typical of marine environments from the *Skolithos* and *Cruziana* ichnofacies; these are typical of assemblages found in brackish-water, marginal-marine environments (Pemberton and Wightman 1992). *Teredolites* (Willis 2000) consists of club-shaped borings preserved through colonisation of xylic (woodground) substrates in marine and marginal-marine environments. *Teredolites* borings are produced in wood substrates primarily by *teredinid* and *pholadid bivalves* (Savrda 1991, Bromley et al 1984).

3.4.4 Study area and interval

The stratigraphy of the Neslen Formation has been investigated between Floy Canyon and Tusher Canyon (Fig. 3.9b), with subsidiary study locations at Tusher Canyon and East Canyon (Fig. 3.9). The main cliff line is oriented E-W (Fig. 3.10) but numerous canyon exposures provide three-dimensional constraint (<5 km) on the stratigraphic architecture. This thesis describes deposits through the full thickness of the Neslen Formation around Crescent Butte (Fig.3.10) where there is continuous exposure along the entire cliff line (Chapter 4). Deposits from intervals in the lower Neslen Formation have been analysed by placing each study site along a dip-transect (Fig. 3.10) (Chapter 5). Detailed study of individual point-bar elements (Fig. 3.10) at all levels of the stratigraphy has also been carried out (Chapter 6). Progressively through the thesis the study of each chapter (chapters 4 to 6) focuses on progressively smaller packages of strata and attempts analysis in increasing detail.

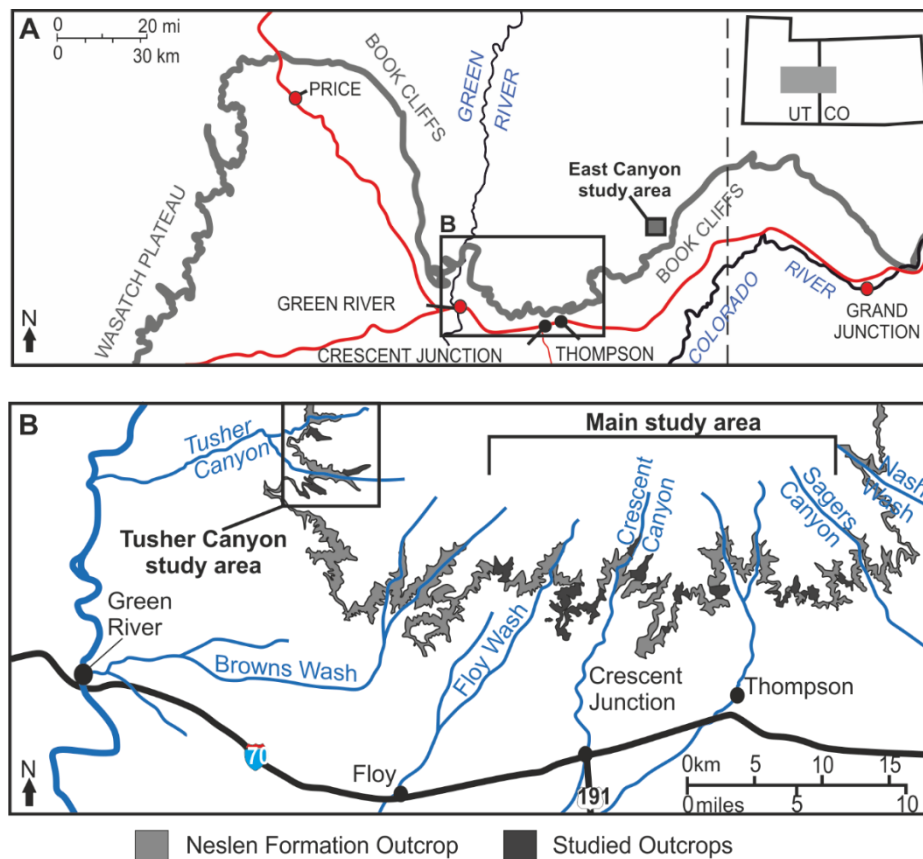


Figure 3.9: Location of outcrops investigated in this study. A) With relation to the wider context of the Book Cliffs, B) Extent of outcrop studied in relation to the total Neslen Formation Outcrop

3.5 Summary

Subduction of the Farallon plate beneath North America during the Cretaceous produced the Sevier Orogenic Belt and associated Western Interior Seaway. The seaway was progressively filled by offshore shale, shallow-marine sandstone, fluvial sandstone and coastal plain siltstone, shale and coal as a sediment pile up to 2 km thick accumulated. Overall, the WIS had a microtidal range. However, embayments may have served to locally amplify the tidal signature preserved in the sedimentary record. The climate was overall humid throughout the Campanian, initiating the formation of laterally extensive coal zones in the Neslen Formation.

The Neslen Formation was deposited during the Campanian as part of the upper Mesaverde Group on the margin of the Western Interior Seaway. The Neslen Formation is composed of channelised sandstone elements (which are variably influenced by marine processes) and sandstones of shallow-marine origin encased within organic-rich mudstone and siltstone deposits. Analysis of the Neslen has been carried out at various scales in order to examine the relative roles of autogenic and allogenic processes on producing the preserved stratigraphy and examines the role of marine processes on the fluvial system

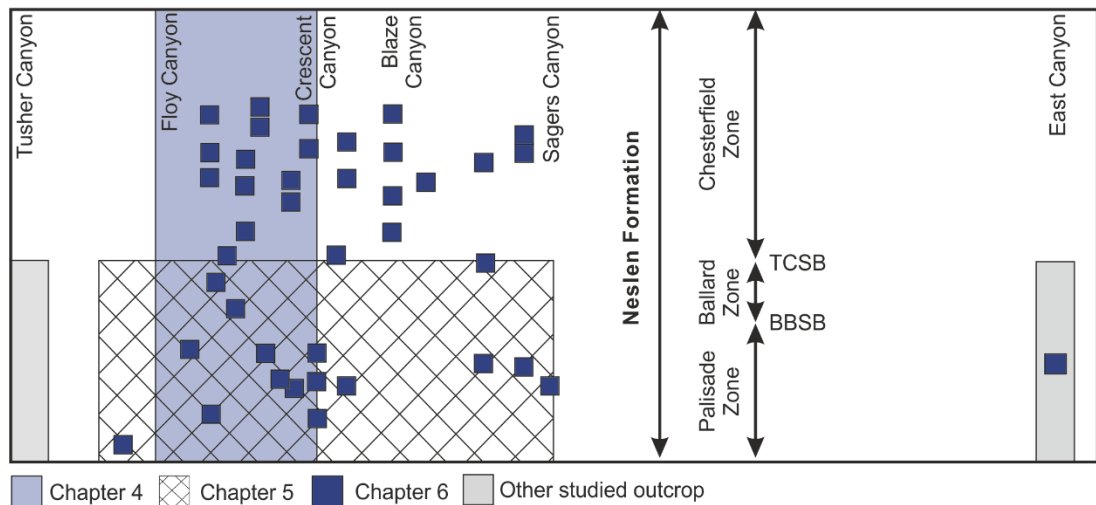


Figure 3.10: Schematic diagram showing the relative position and size of study areas investigated in each chapter.

4 Depositional controls on a marine influenced fluvial succession

The stratigraphic architecture of marginal marine successions records the interplay of autogenic and allogenic processes, and discerning their relative role in governing the morphology of the palaeoenvironment and the architecture of the preserved sedimentary succession is not straightforward. The Campanian Neslen Formation, Mesaverde Group, Utah, is a marine influenced fluvial succession sourced from the Sevier Orogen, which prograded eastwards into the Western Interior Seaway. Detailed mapping in three dimensions of architectural relationships between sandstone bodies has enabled documentation of lateral and vertical changes in the style of channel-body stacking and analysis of the distribution of sedimentary evidence for tidal influence. Upwards, through the succession, sandstone channel bodies become larger and more amalgamated. Laterally, the dominant style of channel bodies changes such that ribbon channel-fills are restricted to the east of the study area whereas lateral accretion deposits dominate to the west.

Combined allogenic and autogenic controls gave rise to the observed stratigraphy. A temporal decrease in the rate of accommodation generation resulted in an upward increase in amalgamation of sand-bodies. Autogenic processes likely played a significant role in moderating the preserved succession: up-succession changes in the style of stacking of channelised bodies could have arisen either from progradation of a distributive fluvial system or from an upstream nodal avulsion of a major trunk channel; accumulation of tide influenced, wave dominated units likely record episodes of delta-lobe abandonment, subsidence and submergence to allow accumulation of near shore sand bars with associated washover complexes.

4.1 Introduction

The majority of published studies of marine influenced systems are those associated with estuaries and incised valleys rather than non-confined coastal alluvial plains (e.g., Dalrymple et al. 1992; Shanley and McCabe 1994; Plink-Björklund 2005; Dalrymple and Choi 2007). There are numerous published studies of the sedimentology of the tidal-to-fluvial transition zone in both ancient (e.g. Shanley et al. 1992; Bose and Chakraborty 1994; Shanley and McCabe 1995; Yoshida 2000; Ghosh et al. 2005; van den Berg et al. 2007; Flaig et al. 2011; Corbett et al. 2011; Ashour et al. 2012; Bhattacharya et al. 2012) and modern (e.g., Choi et al. 2004; Nanson et al. 2013; Lambiase 2013; Vakarelov and Ainsworth 2013) settings. Few of these studies have integrated sedimentological relationships with detailed analyses of the style of stacking and hence connectivity of channel bodies that record different degrees of tidal-influence. However, the discovery and exploration of large oil reserves held in tidally influenced fluvial reservoirs, including the Cretaceous McMurray Formation,

Alberta, Canada, have focussed attention on these successions (e.g. Hubbard et al. 2011; Fustic et al. 2012; Musial et al. 2012).

Conceptual models (e.g., Dalrymple and Choi 2007; Figs. 2.16; 4.1) identify a suite of dynamic processes that compete within tidally influenced environments. Recognition and characterisation of tidally influenced fluvial deposits is challenging because the energy of the system changes both spatially (upstream to downstream) and temporally as a function of the relative roles played by competing tidal, wave and fluvial forces (Fig. 4.1). Fluvial discharge varies seasonally or in a pseudo-random manner in response to major flood events (Leopold 1964; Miall 2013). Tidal currents are modulated by the interplay of semi-diurnal (or diurnal), monthly (spring-neap) and annual cycles. Typically, the effects of these processes diminish upstream in the zone of tidal influence (Dalrymple and Choi 2007; van den Berg et al. 2007). Furthermore, few sedimentary structures alone serve as unequivocal evidence for tidal currents; rather, the interpretation of such processes from outcrop successions is reliant on the occurrence of an assemblage of sedimentary structures, in combination with palaeontological and ichnological salinity indicators (Shanley et al. 1992) as described in section 2.4.

The pattern of stacking of channel bodies on delta plains is controlled by extrinsic and intrinsic factors, in a similar manner to fluvial successions. Early analyses of such stacking patterns (e.g., Leeder 1977; Allen 1978; Bridge and Leeder 1979) argued that the degree of amalgamation of fluvial sandstone bodies is inversely proportional to the sedimentation rate. As such, changes in channel-body stacking patterns reflect the rate of change of subsidence within the basin (Heller and Paola 1996; section 2.3).

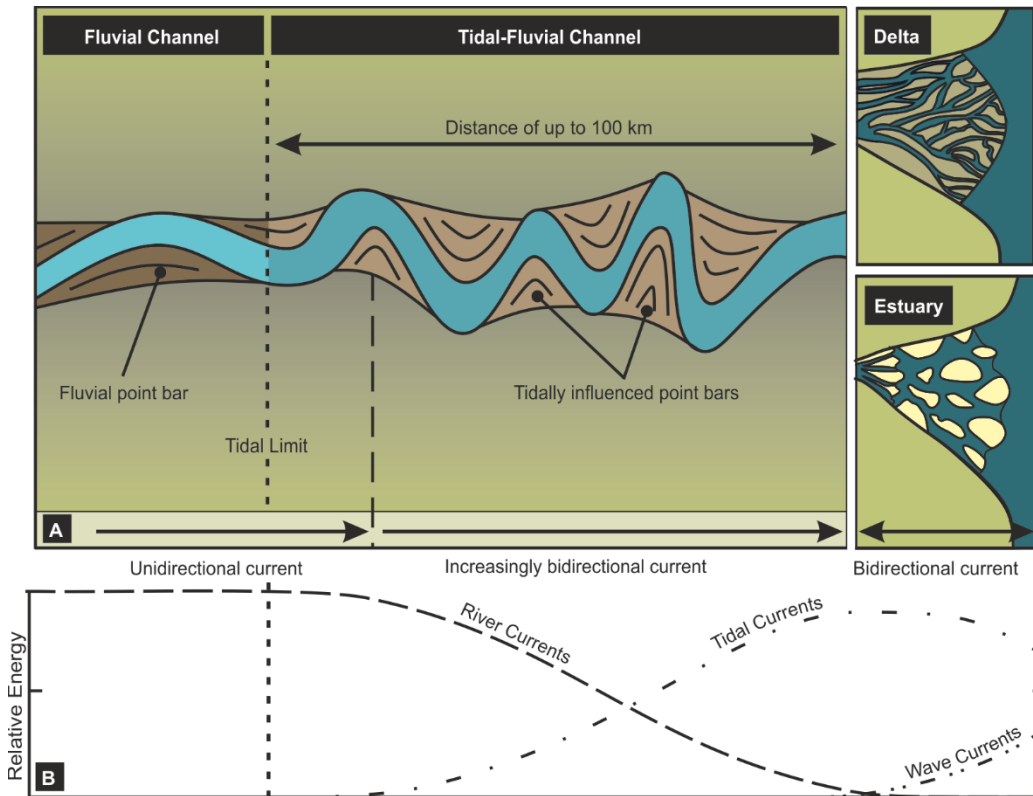


Figure 4.1: A) Conceptual model of marine influenced environments illustrating the variability and complexity present within the marine influenced fluvial zone. B) Graph showing the temporal variation of the energy regimes within marine influenced systems. Modified after Dalrymple and Choi (2007)

Decryption of the controls on deltaic and fluvial architectures in coastal systems requires detailed analysis of continuous, laterally extensive outcrops that allows for the reconstruction of three-dimensional geometries and trends of architectural elements together with their relationship to one another. Studies based on one- or two-dimensional datasets (e.g. Holbrook 2001; Hampson et al. 2012), with three-dimensional constraints (e.g. McLaurin and Steel, 2007; Pranter and Sommer 2011; Trendell et al., 2013) or with control in one direction (e.g. Hampson et al. 2013; Legler et al. 2013) do not allow for channel bodies or channel belts to be accurately projected beyond the cliff line. Studies that do benefit from three-dimensional data sets, however, commonly examine vertical cliff sections for which it is not possible to gather detailed sedimentological information or palaeoflows (e.g., Deveugle et al. 2011).

The Neslen Formation of the Mesaverde Group, Book Cliffs, eastern Utah, USA (Fig. 4.2), however, benefits from three-dimensional outcrop expression that enables accurate reconstruction of channel-body and channel-belt orientations together with detailed facies analysis within settings representative of zones of transition from fluvial to tidal dominance (Fig. 4.3).

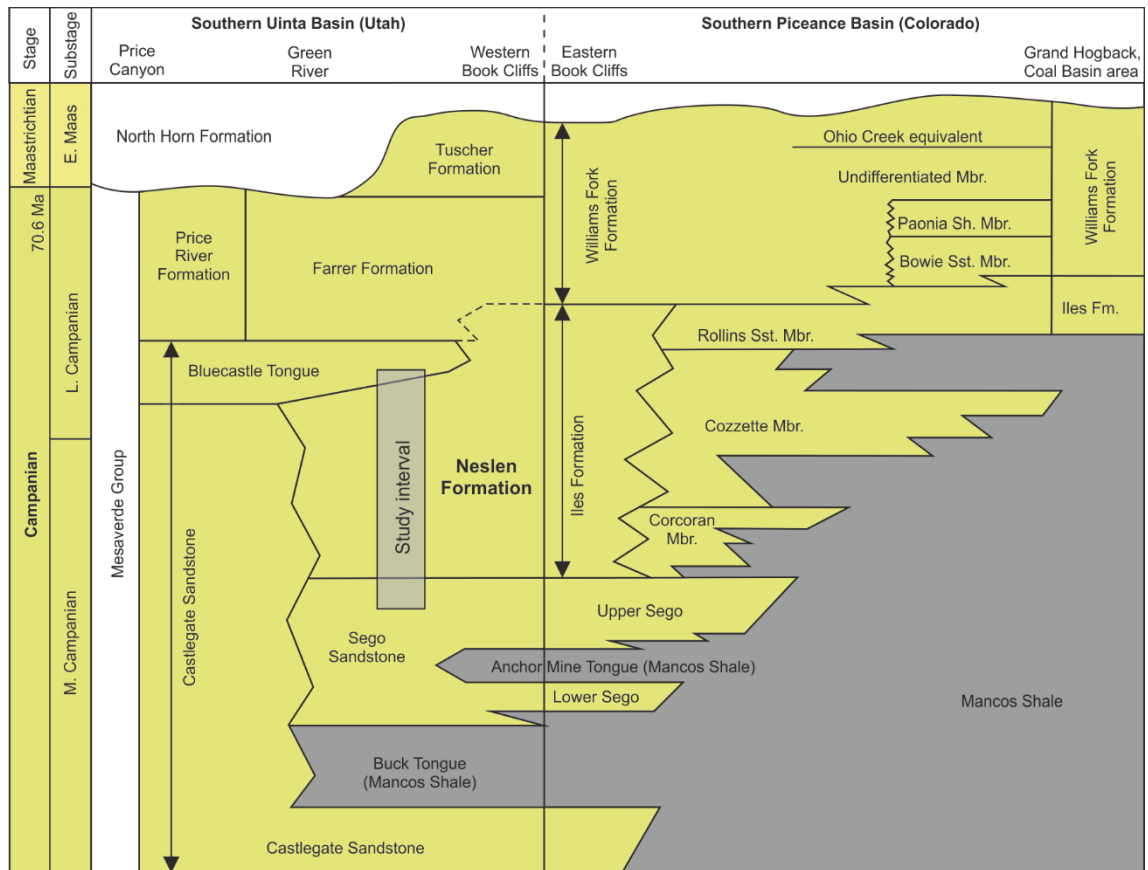


Figure 4.2: Stratigraphy of the Mesaverde Group and overlying successions in the Book Cliffs region from Price (UT) to Grand Hogback (CO). Modified after Kirschbaum and Hettinger (2004).

As such, the Neslen succession is well suited to determination of the relative roles of allogenic factors such as changes in relative sea-level, sediment supply and basin subsidence, tectonism and climate (Dalrymple and Choi 2007 Gawthorpe and Colella 2009; Hampson et al. 2013; Hampson 2016) and autogenic factors such as progradation of a distributive fluvial system, delta lobe switching and major nodal avulsion (Jones and Schumm 2009; Hofmann et al. 2011; Blum and Roberts 2012; Weissmann et al. 2013) each of which may act to control coastal plain and delta morphology and preserved architecture.

The aim of this study is to demonstrate the combined allogenic and autogenic factors that control the transition from tidally influenced to exclusively fluvial sedimentation in the marginal marine setting represented by part of the Neslen Formation. Specific objectives are: (i) document the lithofacies present; (ii) characterise the three-dimensional architecture of tidally influenced fluvial deposits; (iii) assess the controls on the pattern of stacking of fluvial, tidal and tidally influenced sand-bodies, and (iv) evaluate the degree to which a sequence stratigraphic framework can be applied to a relatively up-dip section of the Neslen Formation. Traditionally, the stratigraphy of the Mesaverde Group has been interpreted dominantly in terms of sedimentary response to allogenic processes. This work

redresses the balance by identifying a range of autogenic processes that might alternatively have given rise to the preserved stratigraphic expression.

4.2 Geological Setting

The Neslen Formation crops out along the Book Cliffs of eastern Utah as part of the extensively studied Upper Cretaceous Mesaverde Group (Lawton 1985; Olsen et al. 1995; van Wagoner 1995; McLaurin and Steel 2000; Hettinger and Kirshbaum 2003; Kirschbaum

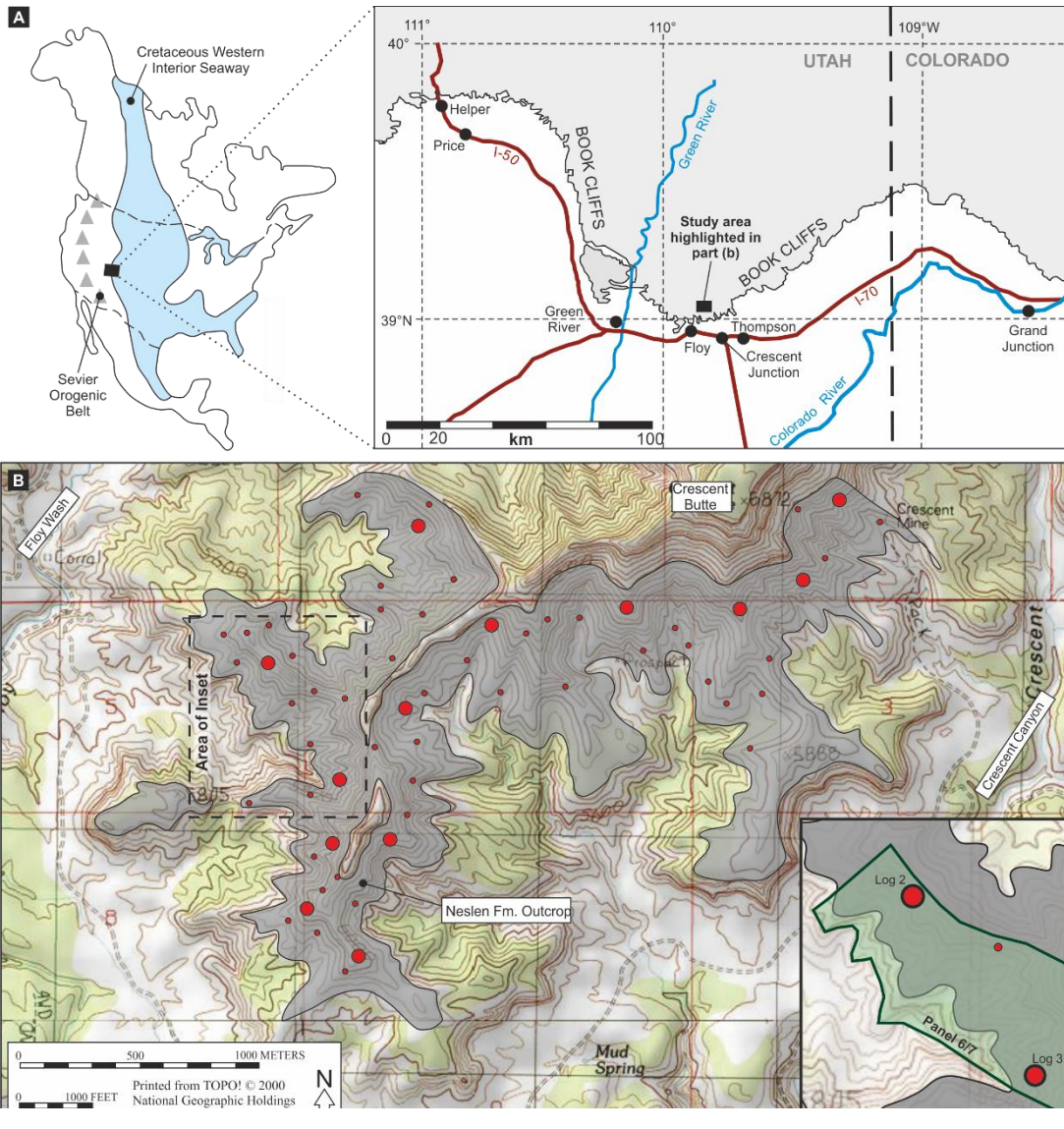


Figure 4.3: Location maps of the study area. A) Map illustrating the position of the cretaceous Western Interior Seaway in the USA. Modified after Taylor and Machent (2011). B) Topographic map of the study area. Neslen Formation outcrop is shown by the shaded area. Inset shows the approximate coverage of panel 2.3/2.4 shown in Fig. 4.5. Locations of measured sections through at least half of the Neslen Formation are represented by large red circles; smaller circles denote the location of sections measured through individual architectural elements or groups of elements. Highlighted section locations represent the sections shown in Fig. 4.4. The position of logs collected in this study are shown in Appendix A.

and Hettinger 2004; Aschoff and Steel 2011a, b; Fig. 4.2) which forms the eroded southern margin of the Uinta Basin (Lawton and Bradford 2011). The Mesaverde Group contains several siliciclastic wedges (Fig. 4.2) sourced from the Sevier Orogenic Belt that prograded eastward to the accompanying foreland basin occupied by the Western Interior Seaway (Armstrong 1968; Krystinik and Blakeney DeJarnett 1995; McLaurin and Steel 2007; Miall et al. 2008; Aschoff and Steel 2011b; Fig. 4.3). The Campanian Neslen Formation was deposited in a low gradient, low relief coastal plain system.

The formation passes westward (landward) into the Castlegate Sandstone near Green River and eastward (seaward) into the lower part of the Mount Garfield Formation – the paralic coastal and shallow-marine Cozzette and Corcoran members of the Iles Formation of Hettinger and Kirshbaum (2003) and Kirschbaum and Hettinger (2004) (Fig. 4.2).

The Neslen Formation thickens seaward from 40 m at Tusher Canyon to over 120 m at the Utah-Colorado border. Tidal process and brackish-water indicators have been inferred from sedimentological evidence in the lower and middle parts of the formation (Willis, 2000; Hettinger and Kirshbaum 2003; Kirschbaum and Hettinger 2004). Sand-bodies in the Neslen Formation have been interpreted as the product of infill of distributary channels, sinuous tidally influenced fluvial channels and fluvial channels (Kirschbaum and Hettinger 2004; Aschoff and Steel 2011b).

Three distinct intervals have been identified in the Neslen Formation based on the presence of thin coal beds between channelised sand-bodies: the lowermost Palisade Coal Zone, the Ballard Coal Zone and the uppermost Chesterfield Coal Zone (Gualtieri 1991; Hettinger and Kirshbaum 2003; Kirschbaum and Hettinger 2004; Cole 2008), in this study the more general terms Palisade Zone, Ballard Zone and Chesterfield Zone are used in order to split up the stratigraphy (Fig. 4.4).

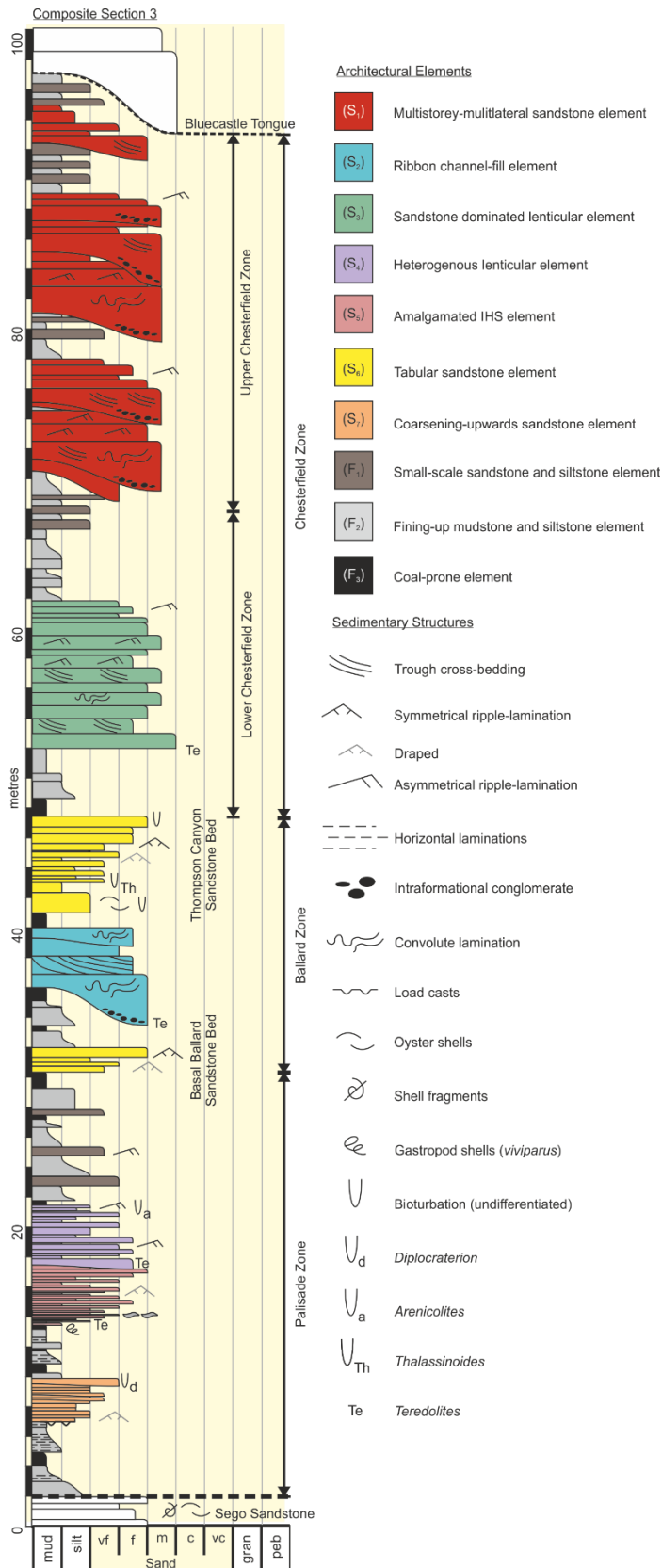


Figure 4-4: Composite graphic sedimentary log recorded from the Neslen Formation, the location of which is represented by section 3.1 and 3.2 (Fig. 4.5) and highlighted by the locations outlined in Fig. 4.3. Stratigraphic zones are based on the coal zones defined by previous workers (e.g. Gaultieri 1998; Hettinger and Kirschbaum 2003; Cole 2008). Sedimentary logs collected in this study are shown in Appendix B.

4.3 Methods

The dataset for this study was acquired from the Neslen Formation between Floy Wash and Crescent Canyon where the outcrop provides continuous exposure of units of fluvial and marginal marine strata around a set of cliff lines (13 km in length) arranged in a three-dimensional outcrop pattern that provides excellent strike and dip control (Fig. 4.3b). Fifty-five vertical sections have been measured through the Neslen Formation (Fig. 4.3b; Appendix A, B) that record changes in lithology, grain size, sedimentary structures and the occurrence of trace and body fossils (Fig. 4.4; Appendix B).

Fifty stratigraphic panels were constructed by walking out and tracing sand-bodies to document their lateral changes, record quantitative information (thicknesses, internal lithofacies arrangements, attitudes and styles of juxtapositions of elements), and measure the attitude of key stratal surfaces. Sand-body positions were mapped using GPS with photographic panels used to provide additional information for parts of cliff-lines that could not be accessed directly (Fig. 4.5; Appendix C). Nine-hundred-and-fifty palaeocurrent measurements were recorded from cross-bedded sets, ripple laminations, scour marks and lateral accretion surfaces (rose diagrams in Fig. 4.6; Appendix D). Vertical profiles (Fig. 4.4; Appendix A, B) were collated with stratigraphic panel data to provide continuous lateral and vertical coverage through the outcrop section (e.g. Fig. 4.5; Appendix C). This approach permitted characterisation of the fine-grained, slope-forming units in greater detail. Integration of the data recorded has enabled individual channel bodies and multi-storey channel belts to be traced in three dimensions around adjoining cliff-lines (Fig. 4.6; Appendix D).

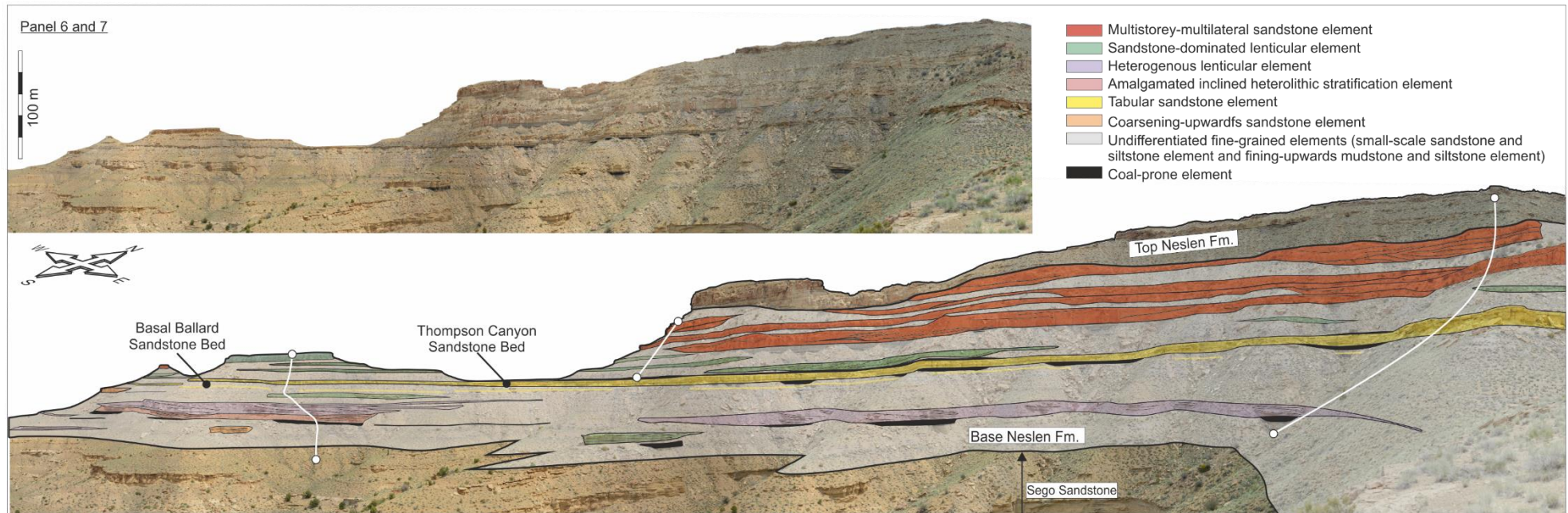


Figure 4.5: Example stratigraphic panel from the Neslen Formation, the location of which is shown in the inset in Fig. 4.3B. Colours in the interpreted panel represent discrete architectural elements. A composite log using sections 3.1 and 3.2 is shown in Fig. 4.4. Stratigraphic panels were collected almost continuously around the study area and are shown in Appendix C.

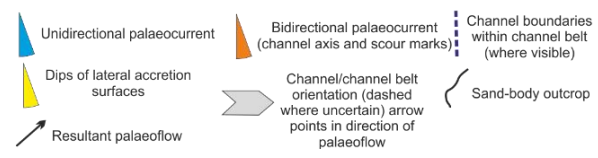
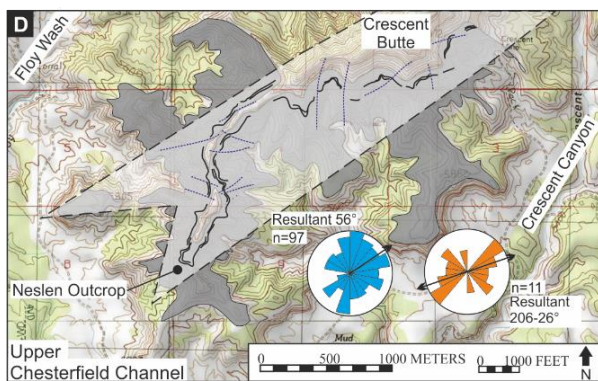
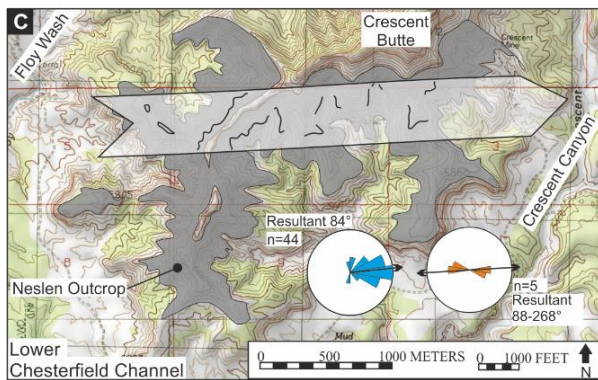
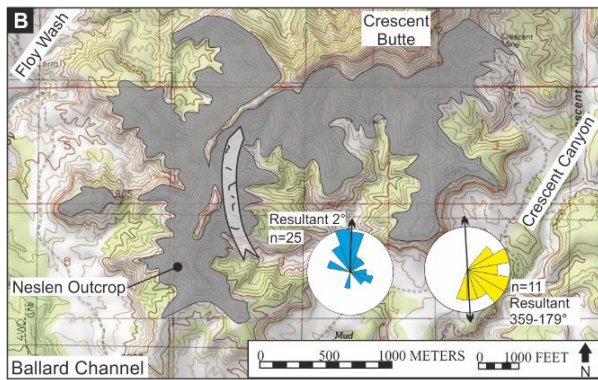
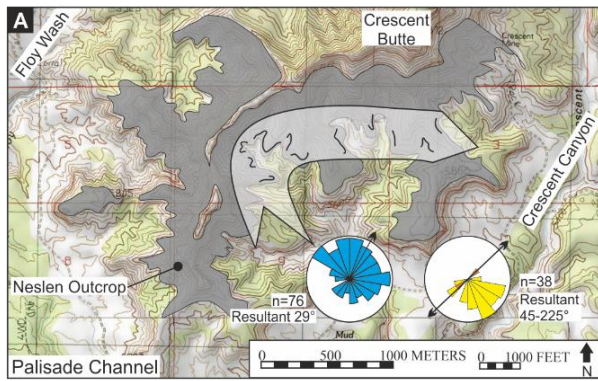


Figure 4.6: Example of reconstructed channels at different time periods A-D. Further examples are provided in Appendix D. Reconstructions are based on outcrop geometries, sedimentology and palaeocurrent data measured from a variety of sedimentary structures (cross-bedding, ripple cross-laminations, ripple forms, lateral accretion surfaces, channel axis orientations and scour marks) as shown by the rose diagrams. Sequence of planview palaeo-orientations of channel bodies and channel-belts from the lower to upper parts of the formation are shown. Base maps from TOPO! Software, 2000, National Geographic.

4.4 Facies and Architectural Elements

Sixteen lithofacies (Fig. 4.7; Table 4.1) have been identified in the Neslen Formation and these occur as associations present in ten distinct architectural elements, assigned to two element groups: sandstone-dominated elements (S_1 - S_7 ; Fig. 4.9a-g) and those dominated by fines (F_1 - F_3 ; Fig. 4.9h-j). Architectural elements are components of a depositional system that are equivalent in size to or smaller than a channelised sandstone and larger than an individual facies unit, and are characterised internally by a distinctive facies assemblage, internal geometry, external form and vertical profile (cf. Miall 1985, 1996). The terms used herein to categorise the channelised sandstone bodies composed of one or multiple elements are as follows (cf. Miall 1996): a channel-fill is a deposit formed through the direct infill of a single channel. A channelised element is a deposit formed via deposition associated with the development of a single channel, including processes of channel-fill, lateral and downstream accretion. A series of individual channelised elements stacked together form a multi-storey, multi-lateral sandstone complex. These elements and compound elements are used as building blocks that stack together to form a larger depositional sequence (*sensu* Mitchum et al. 1977).

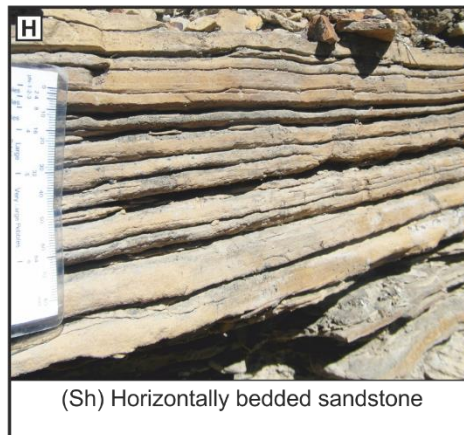
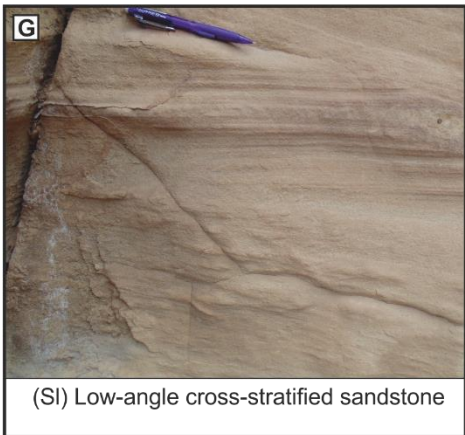
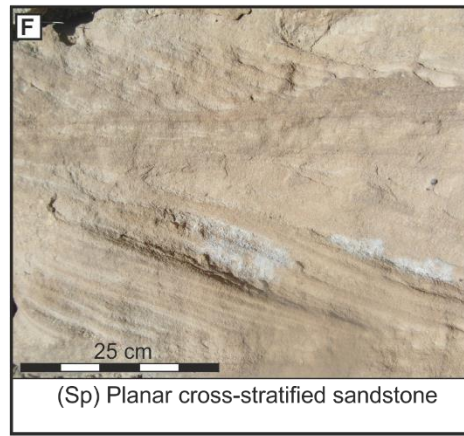
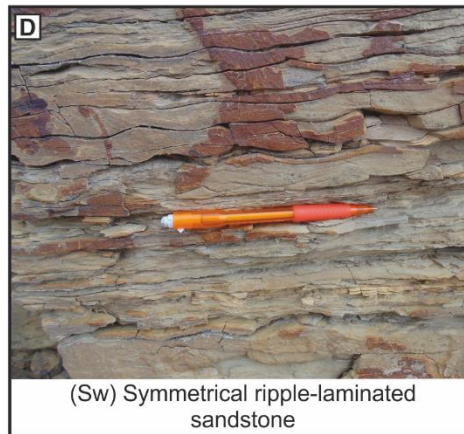
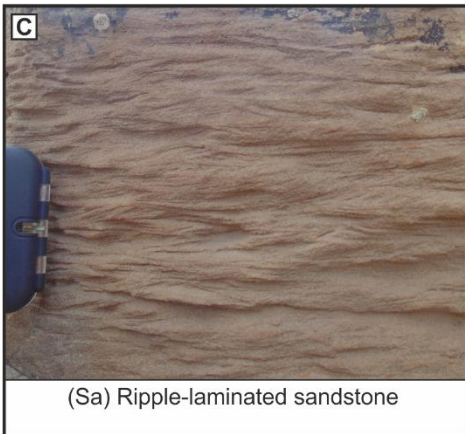
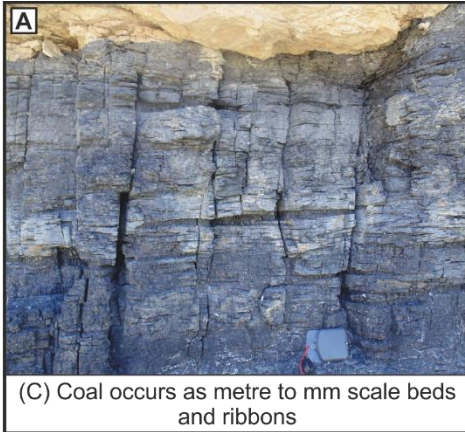
Facies	Description	Interpretation
Gh - Matrix supported conglomerate (occasionally stratified)	Intraformational conglomerate made up of sandy, muddy or sideritic granule- to cobble sized clasts which is angular to well-rounded and massive or crudely horizontally laminated. Occurring at the base of elements or lining erosional surfaces	Deposition as channel lags or scour fills of bedload sediment that was reworking of the coastal plain
Sm – Massive Sandstone	Moderately sorted, fine to medium grained sandstone which is massive or faintly laminated. Often exhibiting normal grading and may contain granule sized muddy clasts. Occurring in dm-cm- thick tabular to lenticular beds within point bar elements	Product of rapid deposition of sand under high energy conditions associated with high-flow stage especially in beds containing clasts. Post depositional origin cannot be discounted unless beds are associated with an erosional base.
Sh – Horizontally stratified sandstone	Fine-grained sandstone with planar horizontal bedding arranged into dm-beds. Beds defined by minor grain size variations.	Deposition in either the upper- or lower- flow regime
St – Trough cross-stratified sandstone	Fine grained trough cross-stratified sandstone arranged in 10 to 50 cm thick sets. Sideritic and/or muddy pebbles and granules commonly distributed along the foresets. dm- to m-thick lenticular or tabular beds; sharp bases.	Cross-strata are the product of migrating dunes with sinuous crest lines (i.e. they are 3D). Clusters of pebbles indicate periods of high-energy flow.
Sp – Planar cross-stratified sandstone	Very fine to medium grained sandstone with flat upper and lower bounding surfaces and approximately parallel cross-bedding.	Cross-strata are the product of migrating dunes with straight crest lines (i.e. they are 2D).
Sl – Low-angle cross-stratified sandstone	Fine grained low-angle cross-stratified sandstone (<15°). Sets are 10-15 cm thick and occur within tabular beds which are dm-thick.	Deposition either (i) in upper- or lower-flow-regime plane-bed field on existing low-relief topography, or (ii) by migrating low-relief 3D bedforms. In latter case, the deposits may have developed under

transitional flow regimes, and represent bedforms such as washed-out dunes (cf. Fielding 2006).

Sa – Ripple cross-laminated sandstone	Fine to very fine, ripple cross-laminated sandstone, occasionally climbing at subcritical angles or climbing in opposite directions. Mud, silt or organic drapes are occasionally observed. Cm- to dm-thick lenticular or tabular beds; sharp or gradational contacts.	Accumulation as a result of migrating asymmetrical ripples. Climbing cross-lamination indicates high rates of suspension fallout combined with bedload traction. Draped ripples indicate periods of low current velocity, possibly influenced by tides
Sw – Symmetrical ripple cross-laminated sandstone	Fine to very fine, symmetrical ripple cross-laminated sandstone. Cm-dm-thick tabular beds with sharp or gradational contacts. Mud, silt or organic drapes are occasionally observed.	Product of accumulation of wave ripples generated on the surface of a standing body of water (De Raaf et al. 1977) or due to current reversals as a result of tidal action (Shanley et al. 1992). Draped ripples indicate periods of low velocity, possibly influenced by tides.
Sd –Deformed sandstone	Fine to medium, moderately to well-sorted sandstone; laminae contorted dm- m-sized fold structures	Product of post-depositional deformation of cross-stratified sandy deposits, probably in response to fluidisation (cf. Owen 1995)
Ss Internally scoured sandstone	Fine to medium grained sandstone with internal erosion surfaces, often lined with a lag. Erosional surfaces can have decimetre scale relief.	Internal erosion indicates the occurrence of multiple flows with varying energies capable of scouring previously deposited sediment.
H – Heterolithic sandstone (wavy, flaser and lenticular bedding)	Units of ripple cross-laminated sandstone where the sands are interbedded with intercalations of mud and silt to varying proportions. Where sandstone dominates as in flaser bedding, fines drape ripple forms and may be discontinuous. Lenticular bedding preserves sandstone isolated ripple sets. Wavy bedding describes intermediate proportions of sandstone and fines.	Heterolithic deposits record deposition under fluctuating flow conditions. Higher energy, unidirectional ripples result in the accumulation of ripple laminated sandstone. Low flow conditions result in the accumulation of varying proportions of fine grained material. Fine grained material may be a result of deposition of fluid-muds due to flocculation.

Si – Interbedded sandstone and siltstone	Interbedded fine sandstone and siltstone accumulated as mm-scale sandstone–siltstone couplets (cf. Rahmani 1988) which are horizontally laminated. The thickness of laminae in some cases exhibit subtle rhythmicity.	Alternations of sandstone and siltstone result from alternations of flow energy which may be as a result of fluvial discharge variations or where rhythmicity is observed it may be due to tidal forcing.
Sf – Fossiliferous sandstone	Predominantly gastropod-rich fossil beds (Viviparus) associated with wood (often bored by Teredolites) and bivalves. Beds are up to 50 cm thick and generally fine upwards.	Sheltered marine, brackish water conditions, likely deposited as a storm lag in a sheltered lagoon environment.
Fsm – Massive mudstone and siltstone	Accumulations of mudstone and siltstone, occasionally mottled or burrowed, dm-thick beds.	Deposition in low energy conditions, likely from suspension settling, massive nature may be due to post depositional bioturbation. Deposition of mudstone may be as a result of deposition through fluid muds.
Fl – Laminated mudstone and siltstone	Laminated and interlaminated mudstone and siltstone with occasional very-fine sandstone lenses, laminations are mm-scale.	Laminated mudstone and siltstone deposited as a result of settling from suspension under low flow conditions.
C – Coal	Organic rich accumulations of coal in mm-sized laminations or as clasts of coalified vegetation.	Deposition as reworked clasts of peat or vegetation which subsequently is compacted into coal.

Table 4-1: Table describing and interpreting the facies observed in architectural elements of the Neslen Formation



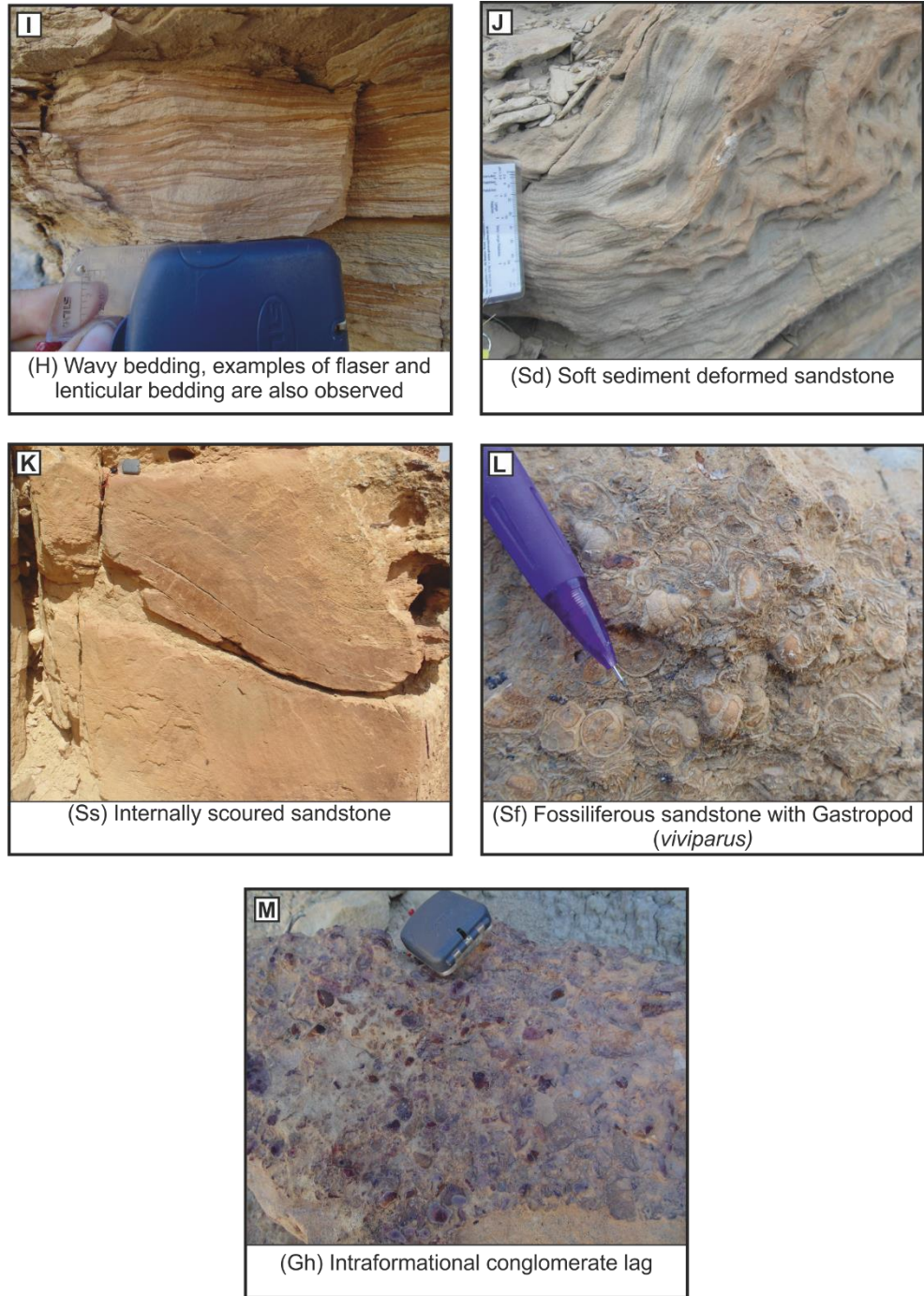


Figure 4.7: Representative lithofacies of the Neslen Formation. A) Coal overlain by a channelised sandstone bed; lenses of higher-quality coal formed from coalified wood. B) Laminated and massive mudstone and siltstone. C) Ripple-laminated sandstone in the upper part of a channelised element. D) Symmetrical ripple-laminated sandstone observed in a tabular sandstone element. E) Trough cross-bedded sandstone within a ribbon channel fill-element. F) Planar cross-bedded sandstone. G) Low-angle laminated sandstone. H) Horizontally laminated sandstone, occasionally interbedded with fine-grained sediment (Si). I) Heterolithic sandstone; ripple-laminated sandstone with intervening fine-grained sediment in varying proportions to produce wavy, flaser or lenticular bedding. J) Soft-sediment deformed sandstone, examples at different scales (dm-m) are observed. K) Internally scoured sandstone observed within an amalgamated channel-fill element. L) Fossiliferous sandstone with shell fragments including the gastropod *viviparus* (centre of photograph). M) Intraformational conglomerate forming a lag at the base of a channelised element.

4.4.1 Architectural Element S₁: Multistorey multilateral sandstone element

4.4.1.1 Description

This element (Fig. 4.9a) is made up of individual channel elements stacked together to form multi-storey, multi-lateral channel elements (Figs. 4.5; 4.9a). Individual channel elements are 4-8 m thick; true widths exceed 400 m but few can be traced across their full extent. Channelised elements exhibit up to 6 m of basal incision and pass laterally into overbank sandstone elements (F₁; Fig. 4.4; 4.9a). Channel elements stack to form 10-20 m thick channel complexes that are at least 800 m wide (Figs. 4.5; 4.6d). Inclined surfaces within channel complexes are not uncommon, where identified they dip at angles of 10-20°, in directions close to perpendicular to palaeoflow (as revealed by small-scale sedimentary structures). Sandstones comprising channel-body fills are fine-to-medium grained, well-sorted and arranged into fining-upward sets. Representative facies for individual storeys comprise basal intraformational conglomerate lying atop a scour surface (Gh; Table 4.1; Fig. 4.7d), trough and planar cross-bedded sandstone sets (Sp, Sx; Table 4.1; Figs. 4.7h, i) with or without lags of intraformational conglomerate, convolute laminated sandstone (Sd; Table 4.1; Fig. 4.7m) and massive sandstone (Sm; Table 4.1) with current ripple-laminated sandstone in their upper parts (Sa; Table 4.1; Fig. 4.7j).

4.4.1.2 Interpretation

The association of facies in this element records highly erosive channelised flows, as indicated by the amount of incision and the occurrence of basal conglomerate lag deposits. Gradual upward fining, and the change from cross-bedded sandstone to ripple-laminated sandstone, indicates a decrease in energy as infilling of the channel progressed. Inclined surfaces are interpreted to have arisen via dominantly lateral accretion with subsidiary downstream accretion (cf. Bridge 2006). The dominance of cross-bedding indicates the migration and accumulation of dunes within the channel. The high levels of amalgamation record repeated cut-and-fill processes (Collinson et al. 2006) within a long-lived channel or repeated avulsions (Stouthamer 2007). The tendency of individual channelised elements to gradually thin and pinch-out laterally into overbank sandstones (F₁; Fig. 4.9a, 4.9h), together with the occurrence of accretion surfaces, and an absence of indicators for tidal influence, indicates a high-energy channelised fluvial regime.

4.4.2 Architectural Element S₂: Ribbon channel-fill element

4.4.2.1 Description

Ribbon channel-fill elements (*sensu* Miall 2013) exhibit abrupt pinch-outs with steep cut-banks (inclined at 30-50°); they rarely connect to overbank sandstones laterally (Fig. 4.9b). Examples of this element exhibit 4-7 m of incision where the erosional relief is also the total thickness of the channel at its axis. These channel forms are 100-400 m wide (Fig. 4.6c) and exhibit low width-to-thickness ratios of 10-15. The fill of these elements is

generally aggradational, arranged into sets separated by erosional surfaces. Intraformational conglomerate lags (up to 70 mm thick; Gh; Table 4.1; Fig. 4.7d) are present directly overlying scour surfaces. Cross-bedding (Table 4.1; Figs. 4.7g, 4.7h) is common at the base with low-angle-inclined laminations (Sl; Table 4.1; Fig. 4.7g) passing upwards and laterally into ripple cross-lamination (Sa; Table 4.1; Fig. 4.7j). Cross-stratification with tangential bases and lower angle top-set laminae are identified as sigmoidal cosets; rare convex-up cross-bed structures are also recognised. Some sandstone sets are characterised by a single organic-rich drape on the surfaces of cross-bed toe-set and fore-set deposits. The base of ribbon channel-fill elements occasionally exhibits mono-species assemblages of *Thalassinoides* or *Skolithos* trace fossils, and the channel lag may include clasts of *Teredolites* bored wood.

4.4.2.2 Interpretation

Within ribbon channel-fills (Miall 1996), the range of sedimentary structures indicates a fill style dominated by migration and accumulation of three-dimensional dunes where drapes may indicate some tidal influence. Low-angle-inclined laminations indicate either deposition on existing low-relief topography or migrating low-relief bedforms. Ripple cross-laminations that record climb at high angles indicate high rates of deposition from suspension combined with bed load traction (Collinson et al. 2006). Sigmoidal structures and convex-upward structures typically indicate flow conditions transitional between the upper and lower flow regime (Fielding 2006); sigmoidal bedding and the preservation of relic dune topography has also been noted in association with tidal bundles (Shanley et al. 1992; Plink-Björklund 2005). The rare occurrence of structures indicative of tidal influence suggests some modification by tidal currents; however, the majority of sets record unidirectional flow. One possible interpretation is that the channel fill may have been influenced by processes within a backwater environment (Lamb et al. 2012). The lack of unequivocal tidal indicators in the sand-bodies could be due to overprint by flood-related drawdown during development of the channels; a process known to occur in response to floods which increase scouring in the backwater zone (Lamb et al. 2012; Nittrouer et al. 2012). The trace fossil assemblage in the base of these elements indicates a brackish water influence (Bromley et al. 1996) This hypothesis is further supported by the aggradational nature of the sand-bodies, the common occurrence of internal scours and the geometry of the channel-fills (Chatanantavet et al. 2012). Overall, ribbon channel-fill elements are interpreted as the sandstone infill of distributary channels in the upper delta plain.

4.4.3 Architectural Element S₃: Lenticular sandstone-dominated element

4.4.3.1 Description

Lenticular sandstone-dominated elements are 2-6 m thick (Figs. 4.4; 4.9c), although incision at the base of these elements is only up to 3 m deep. The lowermost infill of the

element is fine-to-medium grained, whereas the middle and upper part of the infill is very fine-to-fine grained sandstone; deposits are moderately to well sorted. Inclined surfaces within the elements dip at 6-20° at a high angle relative to palaeoflow (as revealed by the azimuth of dipping cross-beds). These channelised elements vary in width from 90 to 500 m (Fig. 4.6c). Beds vary in thickness from 5-40 cm and thin upwards; they commonly have a lenticular form and down lap abruptly onto lower beds or onto the basal surface of the element. Lithofacies associations that comprise the fill of this element include, but are not limited to, massive-to-faintly-laminated sandstone (Sm; Table 4.1) with ripple cross-laminated sandstone (Sa; Table 4.1; Fig. 4.7j), and occasional occurrences of trough and planar cross-bedding (Sp/Sx; Table 4.1; Fig 4.7h, i).

4.4.3.2 Interpretation

Lithofacies associated with this element indicate that they were formed as point-bar elements adjacent to channels which were subject to stable energy conditions with unidirectional flow orientation and no evidence for current reversal. The balance of incision versus thickness of channelised elements indicates a high degree of levee confinement (cf. Fielding 1986). The azimuth of inclined surfaces in relation to sets of cross-strata demonstrates a dominance of lateral accretion which is typical in style to that observed in point-bar settings (Bridge et al. 2006). This channel element represents a meandering channelised deposit; the absence of tidal indicators indicates a fluvial origin.

4.4.4 Architectural Element S₄: Heterogeneous lenticular element

4.4.4.1 Description

Heterogeneous lenticular elements (S₄; Fig. 4.9d) are up to 5 m thick and 50-300 m wide (Figs. 4.4, 4.6a). These elements comprise alternating tabular to wedge-shaped beds of well-sorted, fine-to-medium sandstone and laminated siltstone. Beds dip at 5-25° and pass laterally into overbank elements (F₁ and F₂, Fig. 4.5). The sandstones are organised into beds ranging in thickness between 0.05-0.5 m and display a range of facies including ripple cross-lamination (Sr; Fig. 4.7j), horizontal lamination (Sh; Table 4.1; Fig. 4.7f) and low-angle cross-lamination. Single and double drapes on ripple foresets (Fig. 4.7f) are observed although there is no evidence for rhythmicity. Finer-grained beds are 5-10 cm thick, and vary in geometry; some pinch out gradually, whereas others have a constant thickness; fine beds are composed of massive to laminated mudstone and siltstone (Fsm/FI; Figs. Table 4.1; 4.7b, c) as well as heterolithic deposits such as wavy and flaser bedding (H; Table 4.1; Fig. 4.7l). Evidence for current reversal includes opposing dip directions within ripple foresets. Trace fossils including *Arenicolites*, *Diplocraterion*, *Rhizocorallium* and root traces are common within mono-species assemblages especially in the upper, typically finer parts of lateral accretion sets (bioturbation index value of 3; Taylor and Goldring 1993); *Teredolites* (bored woodground) is common in the channel lag at the base of these elements.

4.4.4.2 Interpretation

The geometry of the elements is similar to that of S_3 above, with inclined surfaces representing point-bar deposits that likely developed during lateral accretion. Where recognised elsewhere, the heterolithic style of the lateral accretion deposit has commonly been termed Inclined Heterolithic Stratification (IHS) and although such deposits are known to form in some purely fluvial environments, many authors have noted its widespread occurrence in tidally influenced systems (e.g. Thomas et al. 1987; Shanley et al. 1992; Choi 2011; Fustic et al. 2012). These elements were deposited adjacent to tidally influenced rivers where the alternating sandstone and finer sediment beds are attributed to alternations in the energy of the system. Specifically, the occurrence of single and double mud drapes supports a tidal interpretation (Shanley et al. 1992). The presence of ichnofacies typical of brackish water, in combination with evidence for current reversals, demonstrates that these elements were influenced by tidal currents, indicating accumulation within the fluvial-to-tidal transition zone (cf. Shanley et al. 1992; van den Berg et al. 2007).

4.4.5 Architectural Element S_5 : Amalgamated inclined heterolithic stratification (IHS) element

4.4.5.1 Description

This element (Fig. 4.9e) consists of stacked heterolithic bed-sets of alternating sandstone, siltstone and mudstone inclined from 4-8°, with variable dip azimuths and internal truncation surfaces. Amalgamated bed sets coarsen upwards and stack to form elements up to 16 m thick that can be traced for up to 150 m. Sandstone beds comprise massive (Sm; Fig. 4.7e) and laminated sandstone (Sl; Fig. 4.7f) flaser, lenticular and wavy bedded sandstone (H; Fig. 4.7l), sandy ripple forms with single- and double-drapes of mud, carbonaceous and related organic material (Sa; Fig. 4.7j). Finer-grained beds are generally laminated, mottled or massive (Fl/Fm; Fig 4.7b; c). Exposure of this architectural element is often poor due to the style of weathering, which hinders detailed observations. Rare beds composed of gastropod shells (*Viviparus*), together with bivalves and large pieces of bored wood (*Teredolites*) are present towards the base of these elements. Other trace fossils associated with this element are *Medousichnus*, *Planolites* and *Palaeophycus*.

4.4.5.2 Interpretation

Inclined stratification with clinofolds at varying angles on a small scale (<20 m in height) may indicate a deltaic environment of limited lateral extent – possibly a Gilbert-type delta or bay-head delta. Sedimentary, palaeontological and ichnological evidence indicates a sheltered marine environment: the mono-species ichnological assemblage is attributed to a quiet-water coastal margin environment that was subject to variable salinity levels, as is common in lagoons, restricted bays and interdistributary bays (cf. Joeckel and Korus 2012), typical of bay-head delta environments (Syvitski and Farrow 1983).

4.4.6 Architectural Element S₆: Tabular sandstone element

4.4.6.1 Description

Two major examples of this element are present within the study area: the Thompson Canyon Sandstone Bed (TCSB) and the Basal Ballard Sandstone Bed (BBSB) (Fig. 4.9f); other thinner, more isolated examples are also observed within the Palisade Zone (Figs. 5.5; 5.8). Both the BBSB and TCSB examples can be traced near-continuously around the studied 13 km cliff-line (Fig. 4.5). The TCSB is the best-exposed example and can be split informally into a lower and upper part. The lower part comprises siltstone to very fine-grained grey sandstone and is characterised by heavily bioturbated beds (bioturbation index up to 5; some containing shell fragments (Fig. 4.9f)). This lower part is 1-1.5 m thick and is topped by a darker grey siltstone bed up to 1 m thick, which contains two siderite-rich layers in the uppermost 0.2 m. Abundant examples of *Thalassinoides* are present on the base. The overlying upper part of the TCSB comprises thickening and coarsening upward fine- to medium-grained, well sorted, very clean sandstone (Fig. 4.9f). Beds have a variable dip with shallowly dipping clinofolds (up to 7°) commonly directed towards the west. Beds commonly show symmetrical ripple lamination (Sw; Table 4.1; Fig. 4.7k), with mud drapes in the lower beds; other beds exhibit horizontal laminations (Sh; Fig. 4.7f), or are massive (Sm). Bioturbation, trace fossils (*Arenicolites*, *Begueria*, *Planolites*, and *Ophiomorpha*) and roots traces are abundant in the top beds of this element. Individual beds are 50-150 mm thick and are commonly tabular in nature (although some exhibit an undulating top surface), wedging-out gradually over tens to hundreds of metres. Although the TCSB is the best-developed example of this element, other instances, including the BBSB, show similar facies associations and architectures. This element is commonly underlain and overlain by coal (F₃; Fig. 4.7a).

4.4.6.2 Interpretation

The lower division of the TCSB represents a lagoonal-fill deposited in a low-energy setting, which was subject to intense bioturbation that masks original sedimentary structures. The upper division of the TCSB with clinofolds shallowly dipping towards the west indicates progradation in a landward direction. Symmetrical ripple laminations with mud drapes are typical of tidal environments modulated by storm conditions. Trace fossils are of a relatively limited size and diversity and may represent a stressed brackish-water environment (Bromley 1996). A shallow-water, restricted marine environment in which symmetrical wave ripples and brackish water trace fossils could be preserved is envisaged. Possible sites for such accumulation include wash-over fans (represented by the upper part of the element) that built over a lagoon (represented by the lower part); in this case the progradation was in a landward direction from a barrier island, with wash-over sands accumulating over more inboard lagoonal sediments. The preferred interpretation is of a laterally extensive back-stepping barrier (cf. Bridges 1976; Hobday and Jackson 1979;

Galloway 1986; Willis and Moslow 1994) with associated washover complex similar to that inferred for the Atlantic coast of the USA (Swift 1975; Swift et al. 1985; Kraft et al. 1987). Preservation of a barrier complex is likely to be via transgressive submergence (cf. Penland et al. 1988), in-place drowning (cf. Sanders and Kumar 1975) or shoreface retreat (cf. Penland et al. 1988). Where barriers are drowned in place then sands would be preserved as isolated ribbons at successive locations (Sanders and Kumar 1975) this is likely to be the mode of preservation for any thin examples of this element in the Palisade Zone with limited lateral extent. Transgressive submergence is the preferred mode of preservation and predicts the generation of shelf sand bodies (barrier complexes and sheet sands) without preservation of the shoreline sands they are derived from (Penland et al. 1988). Shoreface retreat is discounted due to the lack of erosional unconformity or ravinement surface observed within the Lower Neslen Formation (Cattaneo and Steel 2003). The high degree of preservation of the barrier complexes is inferred to have been due to rapid compaction of underlying sediment which allows submergence below wave base (cf. Percival 1992).

Other interpretations include a large mouth bar, bay fill, or part of a wave-dominated estuary. A mouth bar or bay fill sub-environment is here discounted because of the great lateral extent of the bodies; the TCSB can be traced for up to 45 km (Gualtieri 1991), and the BBSB up to 18 km (chapter 5). A wave-dominated estuary hypothesis is discounted due to the lack of evidence of a feeding fluvial system. Previous workers have attributed this element to a sand-flat-to-shoreface setting or a sand spit (Kirschbaum and Hettlinger 2004). The possibility that laterally extensive tabular sandbodies are the product of forced-regression must also be considered. Forced regression is defined as shoreline retreat under relative sea-level fall (Posamentier et al. 1992; Ainsworth and Pattison 1994; Posamentier and Morris 2000). During relative sea level fall, sharp based shoreface deposits form which are relatively coarse grained (Posamentier et al. 1992) and are overlain by an erosional unconformity as the upper surface is subject to incision and bypass. The sharp based nature of the base of tabular sandbodies can be interpreted as regressive surfaces of marine erosion formed during falls in relative sea level with the sandstone itself deposited during forced regression of the shoreline (cf. Fitzsimmons and Johnson 2000). However, the absence of evidence within the study area of incision into the upper surface, and the high down-dip extent of both the TCSB and BBSB do not conform to this model. The presence of landward dipping (i.e. westward) clinofolds are counter to seaward-dipping clinofolds which would be expected to form during forced regression (Posamentier and Morris 2000).

4.4.7 Architectural Element S₇: Coarsening-upwards sandstone element

4.4.7.1 *Description*

Coarsening-upwards sandstone elements (Fig. 4.9g) are up to 5 m thick and 100s of metres in lateral extent, exhibit a distinctive thickening and coarsening-upward trend from very fine- to fine-grained sandstone and are characterised internally by horizontal

laminations (Sh; Table 4.1; Fig. 4.7f), ripple laminations (Sa; Table 4.1; Fig. 4.7j) often with single or double mud drapes, and bioturbation (*Ophiomorpha*, *Rhizocorallium* and *Diplocraterion*). Interbedded sandstone and laminated siltstone beds exhibit load casts and convolute lamination (Sd; Table 4.1; Fig. 4.7m) and lenticular, flaser and wavy bedding (H; Table 4.1; Fig. 4.7l). Bases of these elements are generally erosional and exhibit variable incision up to 30 cm. In the upper parts of these elements beds are thicker and bed boundaries become increasingly erosive, many have lags of intraformational conglomerate (Gh; Table 4.1; Fig. 4.7d) and some preserve root traces.

4.4.7.2 Interpretation

Heterolithic small-scale coarsening-upwards elements record an upward shallowing, with progradation in varying orientations. These elements include a wide range of different sub-environments, including overbank areas subject to episodic flooding, crevasse channels and splays, levees, sand spits, minor mouth bars, avulsion deposits and bay-mouth sequences (Elliott 1974). The size and geometry of the sand-bodies, the predominance of tidal indicators and the presence of brackish-water ichnofacies, together with their association with tidally influenced fluvial strata (S_4), indicates environments such as crevasse deltas and minor mouth bars (Elliott 1974; Joeckel and Korus 2012) influenced significantly by marine incursion.

4.4.8 Architectural Element F₁: Small-scale sandstone and siltstone

4.4.8.1 Description

This element (Fig. 4.9h) is composed of thin beds of very-fine- to fine-grained sandstone and siltstone (<1 m thick), commonly associated with element F₂. Dips of laminations and beds are 2-5°. Exposure of sedimentary structures is often poor due to weathering and the occurrence of unidentifiable post-depositional concretions. The sandstone beds are tabular and pinch out laterally into fining-upward floodplain elements (F₂) gradually over tens to hundreds of metres. The bases of some of the sandstones record localized erosion but incision is no more than 0.3 m. Deposits of these elements exhibit a fining-upward trend. Associated lithofacies comprise massive sandstone (Sm; Fig. 4.7e), horizontally laminated sandstone (Sh; Fig. 4.7f) and massive to laminated siltstone (Fl/Fm; Fig. 4.7b,c), climbing-ripple laminated sandstone and current-ripple laminated sandstone (Sa; Fig. 4.7j).

4.4.8.2 Interpretation

These small-scale sandstone and siltstone elements are attributed to rapid deposition of sand by unconfined flows in levees, crevasse splays and crevasse channels (McCabe, 1987). Objective criteria for distinguishing between these sub-environments in the field are limited. Masking of the original grain size and sedimentary structures by post-depositional nodules means that their separation through traditional lithofacies analysis is

difficult. The fine-sand size of grains in these deposits indicates a low-energy environment and climbing-ripple strata indicate rapidly waning flows. Where incision is observed, the deposit is interpreted as being more proximal to the parent channel and deposited in a slightly higher-energy environment (cf. Fielding 1984; Guion et al. 1995). The overbank sandstones were deposited as a result of break-out from the main channel, which led to rapid deposition from unconfined flow on the floodplain in proximal parts of crevasse splays and channels (cf. Guion et al. 1995).

4.4.9 Architectural Element F₂: Fining-upwards mudstone and siltstone

4.4.9.1 Description

This element (Fig. 4.9i) is composed of brown to black mudstone and siltstone beds arranged in fining-up packages, which are up to 5 m thick (Fig. 4.4) and tens to hundreds of metres in lateral extent. Deposits gradually fine upward to laminated (Fl; Fig. 4.7b) and massive silty-mudstone and subsequently to mudstone (Fm; Fig. 4.7c). Fine grained elements can be split into two associations based on the arrangement of architectural elements and sedimentary features. The first type (A) exhibits sulphur staining, wood fragments and impressions, small fragments of amber, coalified debris and rooted horizons, this type is commonly overlain by coal seams and grades upwards from element F₁. The second type (B) is notably absent from coal or amber or evidence of vegetation, and occasionally exhibits bioturbation (bioturbation index 0-3) and is underlain by elements S₄-S₆.

4.4.9.2 Interpretation

The very-fine grained nature of this floodplain element indicates accumulation in settings characterised by very-low energy conditions. Type A elements are interpreted as being part of a waning flood deposit, likely in the distal parts of crevasse splays and related overbank sub-environments (Guion et al. 1995). Roots, amber and wood fragments all indicate the presence of vegetation on the floodplain. Type B elements are interpreted having accumulated in quiet water brackish settings such as lagoons (Horne et al. 1978). The two sub-elements are not always readily discernible and association with other elements must be considered.

4.4.10 Architectural Element F₃: Coal-prone element

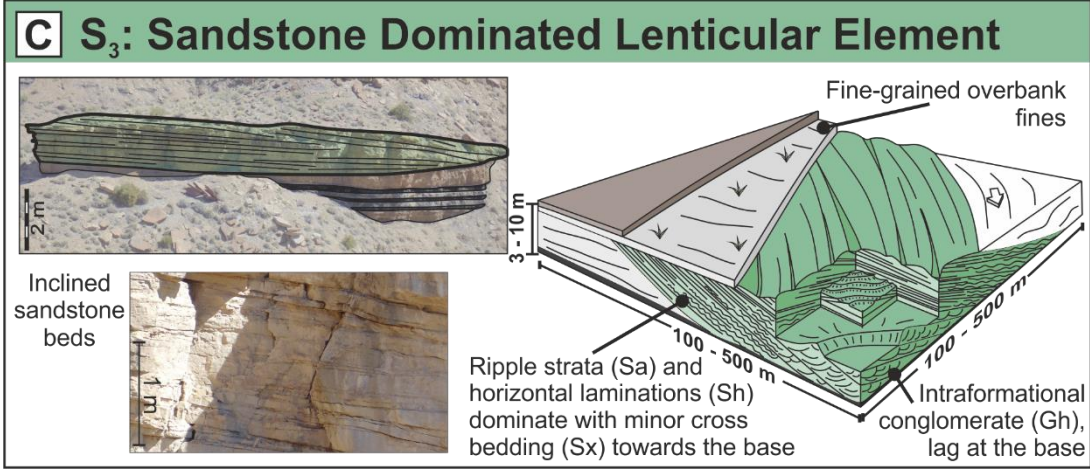
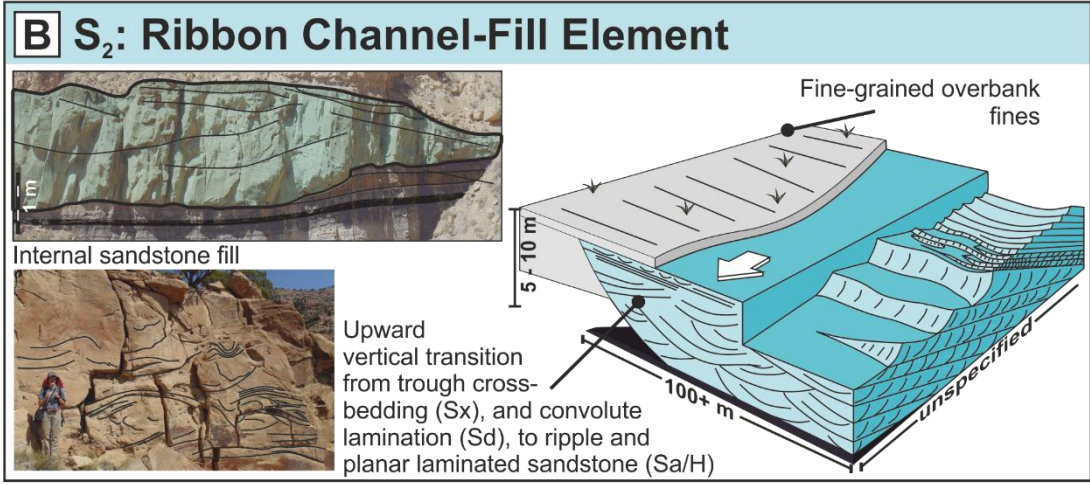
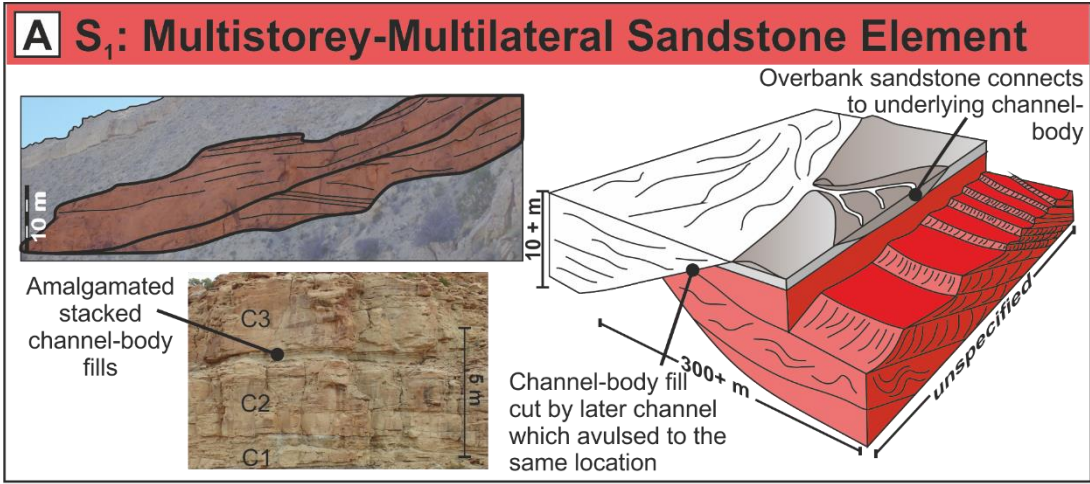
4.4.10.1 Description

Coal (Fig. 4.9j) occurs on a range of scales from mm-sized ribbons to metre-thick beds of considerable lateral extent (Fig. 4.7a) lying above fining-upward floodplain elements (F₂; Figs. 4.4, 4.5). In many places the black coals show sulphur staining and contain amber, wood fragments and localised sandstone clasts. Coals in the Ballard Zone occur as extensive

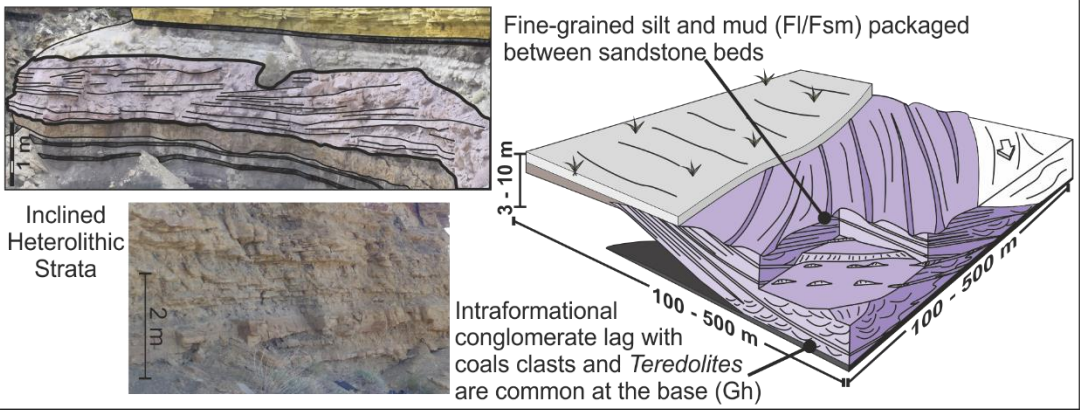
sheets, contrastingly in the Palisade Zone coals are thinner and discontinuous. Around the field area coals continually occur at the same stratigraphic levels.

4.4.10.2 Interpretation

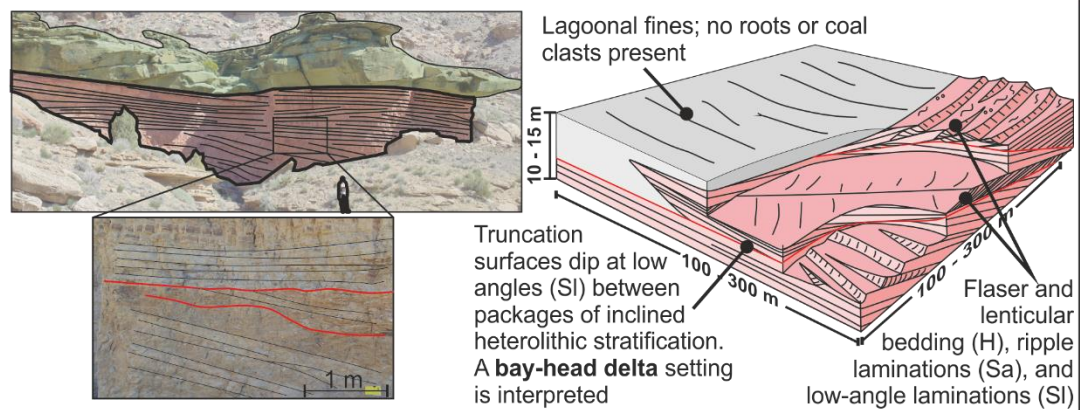
Peat mires form in humid, swampy conditions in areas where rainfall exceeds evaporation and organic growth is rapid (Guion et al. 1995). Low ash, ombrotrophic coals, such as the ones in the Neslen Formation, formed in raised swamp environments in which there was low clastic input and low subsidence (McCabe 1987; Guion et al. 1995). Coals present in the Blackhawk Formation and Castlegate Sandstone have been interpreted by previous authors as raised mire deposits (Davies et al. 2006; Jerrett et al. 2011a,b). Coals formed in paralic coastal or deltaic settings that were subject to the influence of a continuously rising mire water table (base level) relative to the sediment surface which generated the accommodation required for sustained episodes of peat accumulation (Davies et al. 2006); a similar environment is envisioned for these deposits. Coals in the Neslen Formation were deposited in close proximity to sites of active clastic accumulation (channelised deposits; S₂ to S₄ and overbank sandstones; F₁), as such in order for coals to develop to a high quality, they must be raised up such that the peat is able to form without clastic input.



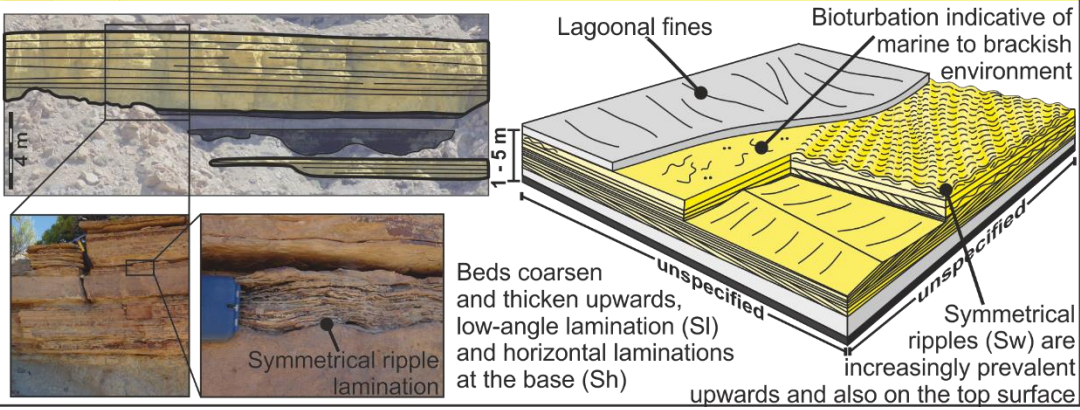
D S₄: Heterogenous Lenticular Element



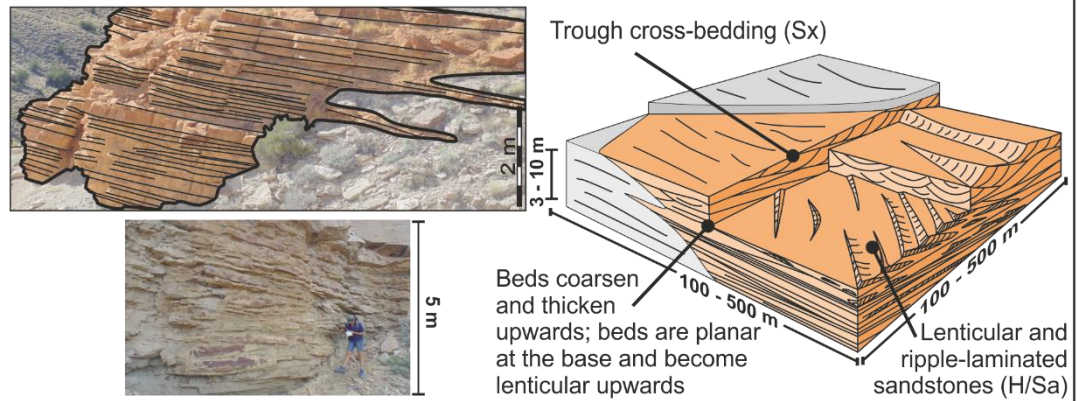
E S₅: Amalgamated IHS Element



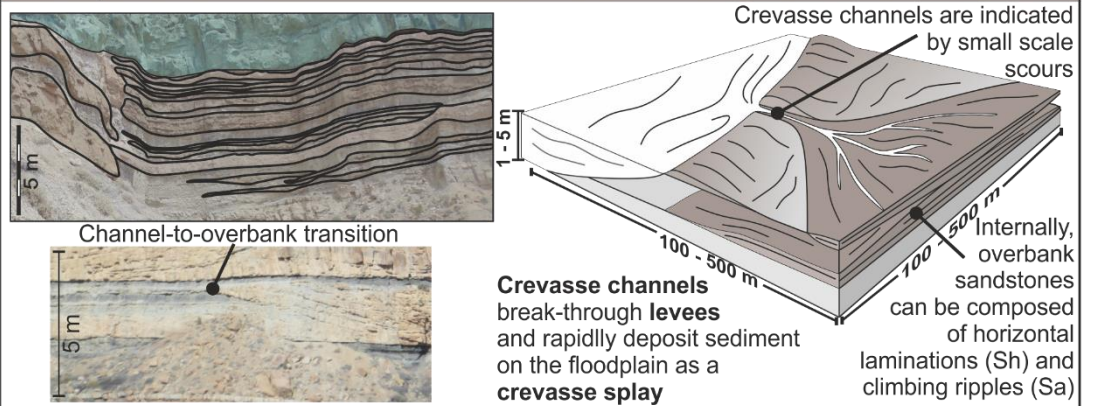
F S₆: Tabular Sandstone Element



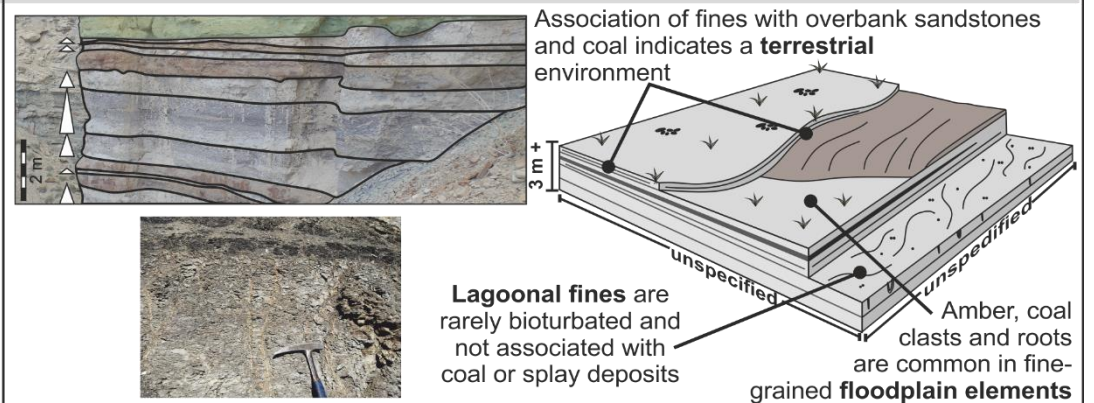
G S₇: Coarsening-upwards Sandstone Element



H F₁: Small-scale Sandstone and Siltstone Element



I F₂: Fining-upwards Siltstone and Mudstone



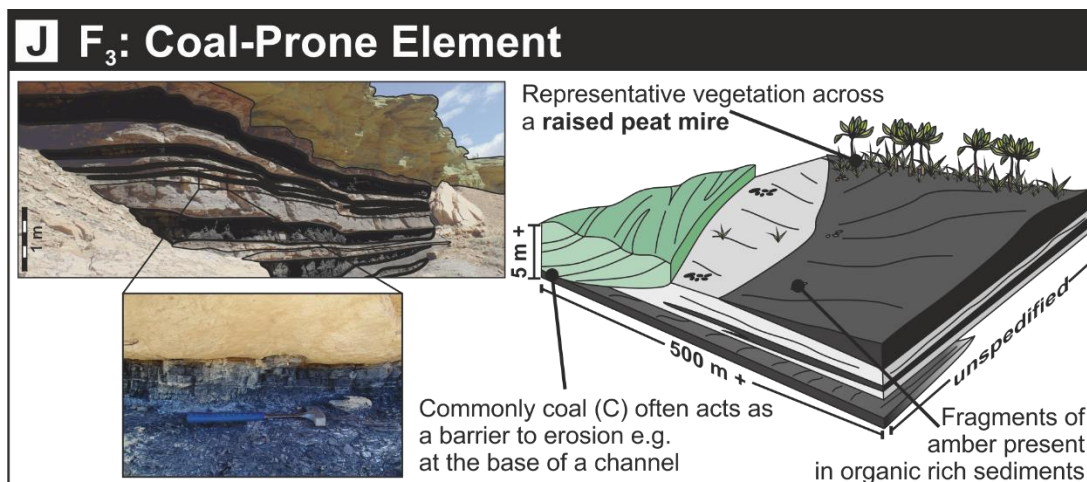


Figure 4.8: Schematic depositional settings for architectural elements within the Neslen Formation and representative interpreted photographs. A) Multistorey-multialateral sandstone element. B) Ribbon channel-fill element. C) Sandstone-dominated lenticular element. D) Heterogeneous lenticular element. E) Amalgamated inclined heterolithic strata element. F) Tabular sandstone element. G) Coarsening-upwards sandstone element. H) Small-scale sandstone and siltstone element. I) Fining-upwards siltstone and mudstone element. J) Coal-prone element.

4.5 The Stratigraphic Succession and Depositional Environment

The lithostratigraphy of the Neslen Formation has been subdivided previously by Gualtieri (1991), Hettinger and Kirshbaum (2003), Kirschbaum and Hettinger (2004) and Cole (2008) into a series of coal zones or coal-bearing intervals, and this subdivision is employed here. Additionally, in the region of study, the formation can be further subdivided based on the presence of the laterally extensive, tabular sandstone elements (S_6 ; Fig. 4.9f) and the formation is informally subdivided into a series of zones (Fig. 4.4).

The lowermost Palisade Zone spans a stratigraphic interval from a prominent oyster bed that serves as a local marker at the top of the underlying Segoe Sandstone (Willis, 2000; Hettinger and Kirschbaum, 2003) to the base of the BBSB (Basal Ballard Sandstone Bed), a thickness of ~30 m (Fig. 4.4). Within this zone fine-grained elements (F_1 - F_3) dominate over subsidiary channelised and bay-fill elements (S_3 - S_5 ; S_7 ; Table 4.2).

The overlying Ballard Zone – which is bounded by the BBSB at its base and the TCSB (Thompson Canyon Sandstone Bed) at its top (Fig. 4.4), both examples of the tabular sandstone element (S_6) – is typically 10 m thick. This zone is dominated by coal-bearing floodplain elements (F_3) and organic-rich examples of fining-upward floodplain facies successions (F_2 ; Table 4.2).

The top of the TCSB marks the lower boundary of the Chesterfield Zone (Fig. 4.4), which in this region is informally split into a part dominated by sandstone-prone lateral accretion elements (S_3) with subordinate ribbon channel-fill elements (S_2) and an upper part dominated by amalgamated channel-fill elements (S_1). Channelised elements in the lower Chesterfield Zone are isolated and encased within floodplain-fine elements (F_2) that preserve significantly less organic matter and relatively thinner coals than in equivalent floodplain elements lower in the succession. The upper Chesterfield Zone is characterised by a further decrease in the proportion of floodplain-fine elements (F_2 - F_3) but an increase in abundance of overbank sandstone elements (F_1 ; Table 4.2).

Passing upward through the Neslen Formation, evidence for tidal influence decreases within the sandstone elements; exceptions to this trend are the BBSB and TCSB in the middle part of the formation, which exhibit evidence for accumulation under the influence of mixed wave and tide action. A marked decrease in sedimentary structures indicative of tidal influence in channelised elements is noted above the level of the TCSB, with the only tidal indicators above this level occurring at the base of the Chesterfield Zone.

4.5.1 Palisade Zone

Upwards through the Palisade Zone, a shift from dominantly heterolithic lateral accretion elements (S_4) to sandstone-prone elements (S_3) is observed. The widths of channelised elements in this zone are highly variable from less than 100 m to ~500 m (Appendix D). Channel elements with lower lateral extent tend to crop out towards the eastern part of the study area (Fig. 4.9a). Palaeoflow indicators demonstrate considerable variability across the study area; a general trend of southerly palaeoflow is identified in the west of the study area, whereas in the centre and east, palaeoflow is directed between NE and SE (Fig. 4.9a). Channelised elements exhibit moderate connectivity within this zone; although direct amalgamation of sand-bodies does not occur, overbank sandstone elements (F_1) serve to connect the otherwise isolated channel-fill elements. The occurrence of overbank sandstone elements is greater in the east, though this may be an apparent trend where steeper slopes tend to increase exposure of such elements.

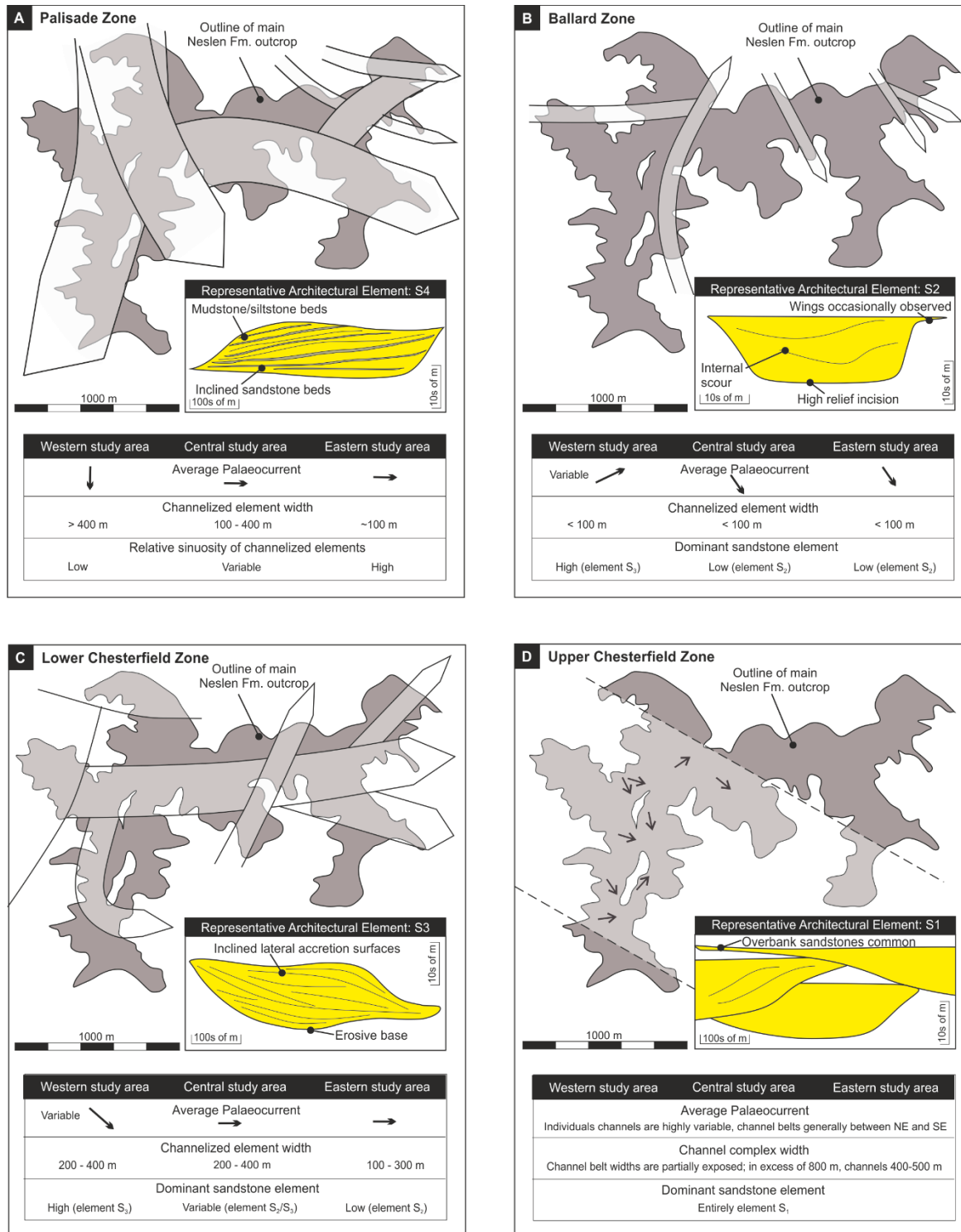


Figure 4.9: Simplified maps through time (A-D) of the Neslen Formation outcrop. A summary of the channel architectures, geometries and channel-body orientations together with spatial variations from west to east in the field area are indicated for the stratigraphic zones shown in Fig. 4.4.

4.5.2 Ballard Zone

Channelised sandstone elements are rare in this zone, with geometries that reflect the effects of differential compaction associated with encasing coals. All such elements have a limited lateral extent; widths do not exceed 100 m (Fig. 4.6b). The majority of channelised bodies are ribbon-channel-fill elements (S_2 ; Table 4.2), confined to the eastern part of the study area with a consistent palaeocurrent towards the SE. In the western study area, a small number of sandstone-prone lateral accretion elements (S_3) are present and these exhibit evidence for variably oriented palaeoflow. Channelised sandstone elements exhibit low connectivity: with the majority of examples isolated within coal-bearing floodplain-fine elements (F_2 and F_3). Overbank sandstone elements are notably absent.

4.5.3 Chesterfield Zone

Within the Chesterfield Zone, the boundary between the lower and upper part takes the form of a sandstone facies transition whereby the lower and upper parts exhibit local variations in thickness (Figs. 4.4; 4.5). The entire Chesterfield Zone is ~50 m thick and the upper boundary is marked by an abrupt increase in grain size and a slight change in the colour of sand-bodies (from beige to brown) at the base of the overlying Bluecastle Tongue (Franczyk et al. 1992).

Channelised elements in the lower Chesterfield Zone are represented by both ribbon channel-fill elements (S_2) and sandstone-prone lateral accretion elements (S_3), with a decrease in the occurrence of ribbon channel-fills upwards (Fig. 4.4). From west to east across the study area, channel-element architectures vary in a similar way to those in the Ballard Zone, with ribbon channel-fill elements more common in the east (Fig. 4.9c). Widths of channelised elements vary from 100-700 m. Channelised elements have basal surfaces that record greater erosion than those lower in the formation, with up to 8 m of incisional relief. Overbank sandstone elements (F_1) serve to connect some otherwise isolated channelised sand-bodies, but tend to be poorly exposed.

Individual storeys in channelised elements of the upper Chesterfield Zone are up to 8 m thick and multi-storey compound elements can exceed 20 m (Fig. 4.4); these channelised sandstone bodies are therefore considerably thicker than those in the lower parts of the formation. Measurements relating to the geometry and orientation of individual channelised elements present in the upper Chesterfield Zone (Fig.4.9d) are more difficult to obtain because such elements crop out as cliff-forming sandstone bodies. Overall palaeocurrents vary from NE- to SE-directed, which is in close agreement with other

measured channel orientations. Connectivity of channelised sandstone elements in this zone is high due to the degree of amalgamation of channelised bodies which form laterally extensive multi-storey and multi-lateral channel-belts (Fig. 4.5). Additionally, the majority of the overbank elements preserved in this zone are overbank sandstone elements

(F₁) although preservation of floodplain fines (F₂) between sandstone units is noted in some places (Table 4.2).

4.5.4 Depositional Environments

Each zone exhibits different facies and architectural-element character, suggesting that each represents a subtly different palaeoenvironmental setting within the overall depositional system. Furthermore, changes in the sedimentological character of the zones occur in a predictable manner up-succession and analysis of these trends is herein used to propose a suite of depositional models with which to account for the progressive temporal evolution of the succession.

Here, the style of channel and channel-belt stacking and plan form geometries, together with the change in facies and architectural elements up through the Neslen Formation, have been integrated with previously proposed models (Gualtieri 1991; Hettinger and Kirshbaum 2003; Kirschbaum and Hettinger 2004; Cole 2008) to reconstruct the depositional environment in an unprecedented level of detail.

U. Chesterfield	50 (7)	0	0	0	0	0	0	20 (38)	30 (4)	0
L. Chesterfield	0	10 (5)	20 (13)	0	0	0	0	5 (8)	63 (5)	2 (1)
Ballard (inc. BBSB, TCSB)	0	10 (4)	5 (2)	0	0	20 (2)	0	0	45 (2)	20 (3)
Palisade	0	0	7 (4)	8 (16)	3 (5)	0	2 (14)	10 (15)	65 (6)	5 (4)

Table 4-2: Change in relative proportions of the architectural elements by area between the depositional zones of the Neslen Formation: values derived from quantitative analysis of two-dimensional stratigraphic panels. Bracketed numbers refer to the number of outcrops in the study area used to calculate the proportion of architectural element outcrop.

The Palisade Zone (Fig. 4.10a) represents a delta plain to fluvial floodplain setting. Channel bodies in this zone – many of which show evidence for tidal influence – are isolated and exhibit variable thicknesses and orientations (Fig. 4.4, 4.8; Appendix D). Channels meandered through an environment of raised mires that gave rise to accumulation of coals and fine-grained sediment. This zone was characterised by overbank swamp regions subject to episodic low-energy flows, within which limited and sporadic siliciclastic input was derived from flood events via crevasse splays (F_1).

The overlying BBSB represents a response to a rise in relative sea level, which resulted in the accumulation of tide influenced, wave dominated sandstones of paralic-to-shallow marine origin (Kirschbaum and Hettlinger 2004). The environment of deposition in the Ballard Zone was dominated by organic-rich muds and coals (F_2 and F_3) that accumulated in extensive raised mires and poorly drained floodplains in a sub-environment proximal to the palaeo-shoreline, channels were rare, small and mostly isolated (Fig. 4.10b).

The TCSB (Fig. 4.10c) represents a return to a wave dominated environment; the lower parts of the TCSB represent a quiet, shallow, brackish-water lagoon setting; the upper part represents a wash-over fan system that built over this lagoon in response to landward retreat of the shoreline system, possibly driven by modest relative sea-level rise.

The overlying lower Chesterfield Zone records a change in palaeoenvironment back to emergent conditions (Fig. 4.10c). The base of this zone records the last high-quality coal in the formation. The increase of channel-body dimensions indicates more highly erosive flows than those observed in the Palisade and Ballard Zones, in response to a higher-energy environment. The trend of temporally increasing energy regime is continued into the upper Chesterfield Zone (Fig. 4.10d) where channel elements are thicker and wider, with greater incisional relief at their bases, and increasingly amalgamated. Palaeocurrents remained directed generally eastward indicating flow towards a north-south oriented palaeo-shoreline (Johnson 2003; Miall 2008).

4.6 Discussion

4.6.1 Overall trends in channel stacking

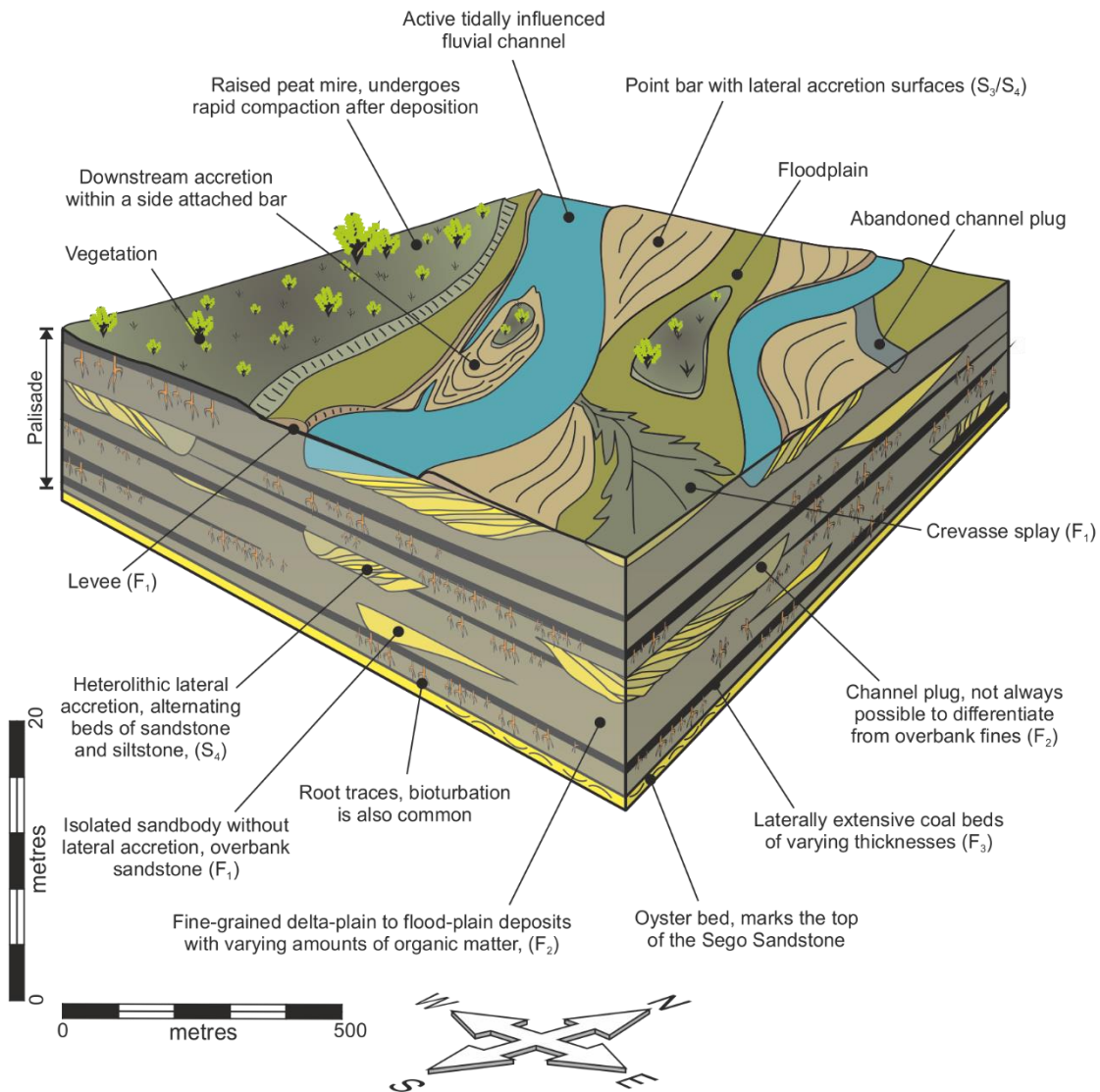
Major trends in preserved channelised element width, orientation and density of stacking between the identified zones are summarised in Figure 4.10. Upwards through the formation, systematic changes in the style and distribution of types of channelised elements are noted (Figs. 4.8, 4.10). The Palisade Zone is dominated by isolated heterolithic lateral accretion elements (S_4), the Ballard Zone by ribbon channel elements (S_2), the lower Chesterfield Zone exhibits examples of both ribbon channel elements (S_2) and sandstone-prone lateral accretion elements (S_3), and the upper Chesterfield Zone is dominated by amalgamated channel-fill elements (S_1). Isolated sandstone-prone lateral-accretion

elements also occur in the upper parts of the Palisade Zone and in the western part of the Ballard Zone (Table 4.1). These changes are mirrored by changes in channelised element size which tend to increase in both width and thickness towards the top of the formation (Figs. 4.4, 4.5). The mean grain size of channelised sandstones also increases upwards through the formation, from very-fine to fine-grained sandstone in the Palisade Zone to medium grained sandstone in the top of the upper Chesterfield Zone (Fig. 4.4; Appendix B).

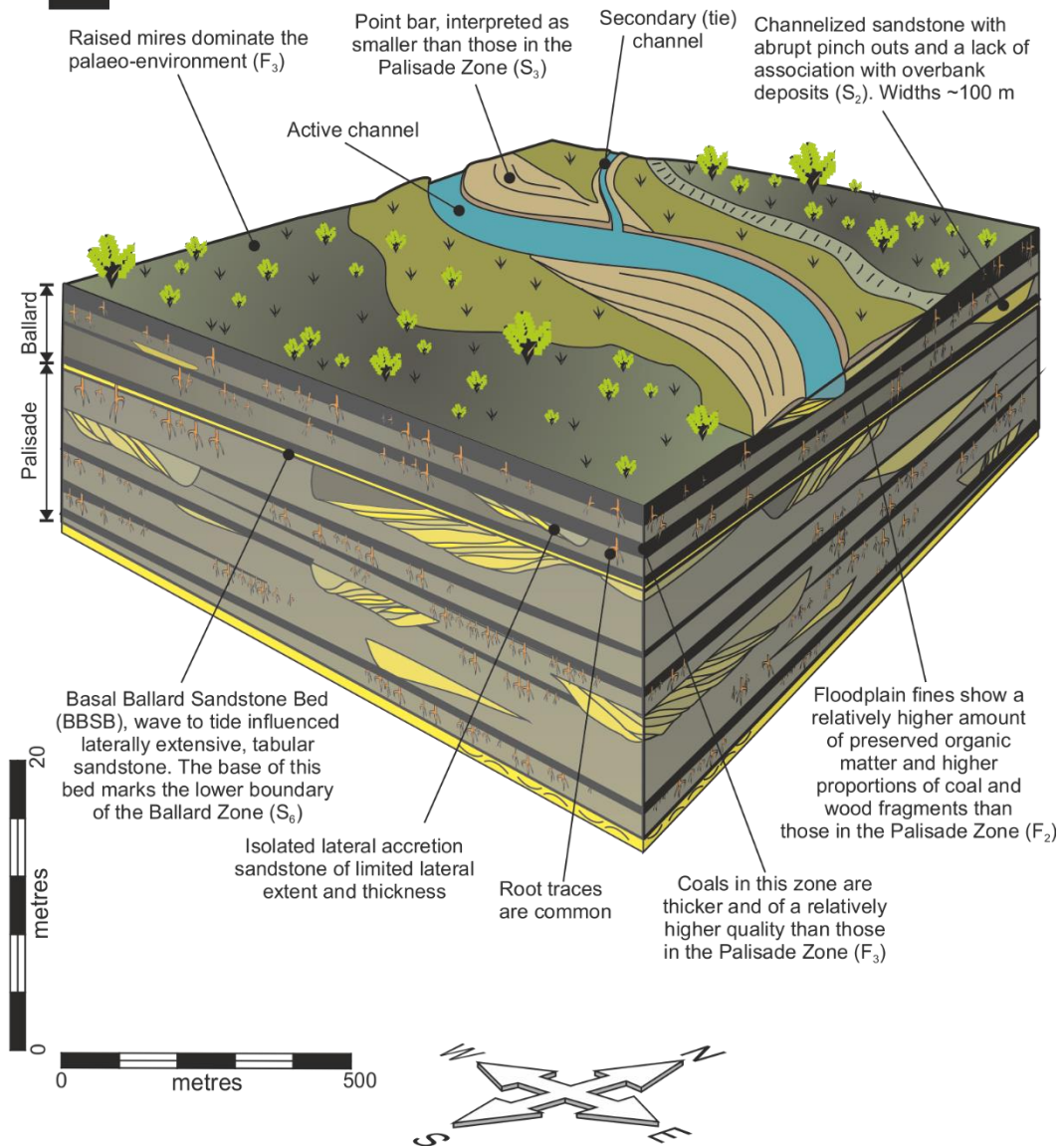
An overall regional eastward palaeocurrent trend for Cretaceous successions of the margin of the Western Interior Seaway has been documented by many authors (e.g., Kauffmann 1977; Johnson 2003; Miall et al. 2008; Fillmore 2011). Tracing of channelised elements reveals significant local variability in palaeocurrents both within and between zones (Fig. 4.8). Channel orientations in the Palisade Zone are oriented to the south in the western part of the study region but are generally east-directed in the rest of the study region (Fig. 4.8a; Appendix D). There is also an apparent decrease in the preserved width of channelised elements towards the east (Fig. 4.8). This spatial variability in channel orientation arises as a consequence of the high sinuosity of the palaeochannel networks.

Within the Ballard and lower Chesterfield Zones (Fig. 4.8b,c; Appendix D), trends exist in distribution of channelised elements: ribbon channel-fill elements are confined to the eastern part of the study region and these exhibit generally east-directed palaeocurrents; sandstone-prone lateral accretion elements dominate in the western part of the study region and exhibit more variable palaeocurrents. This spatial variability is likely to be due to the occurrence of coeval channels, whereby sinuous channels dominated by lateral accretion deposits occurred inland in comparison to distributary channels which were confined to coastline proximal settings.

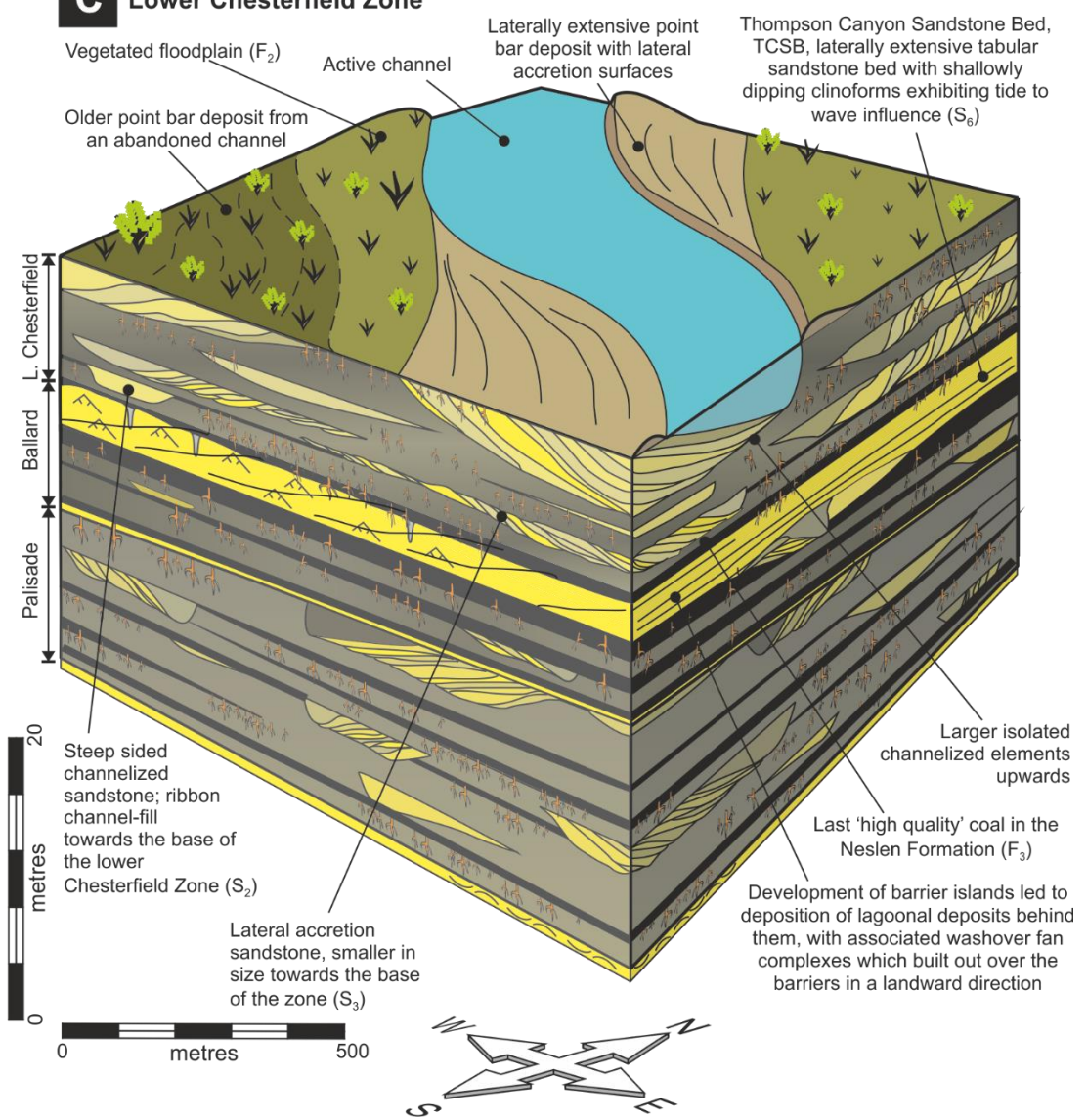
A Palisade Zone



B Ballard Zone



C Lower Chesterfield Zone



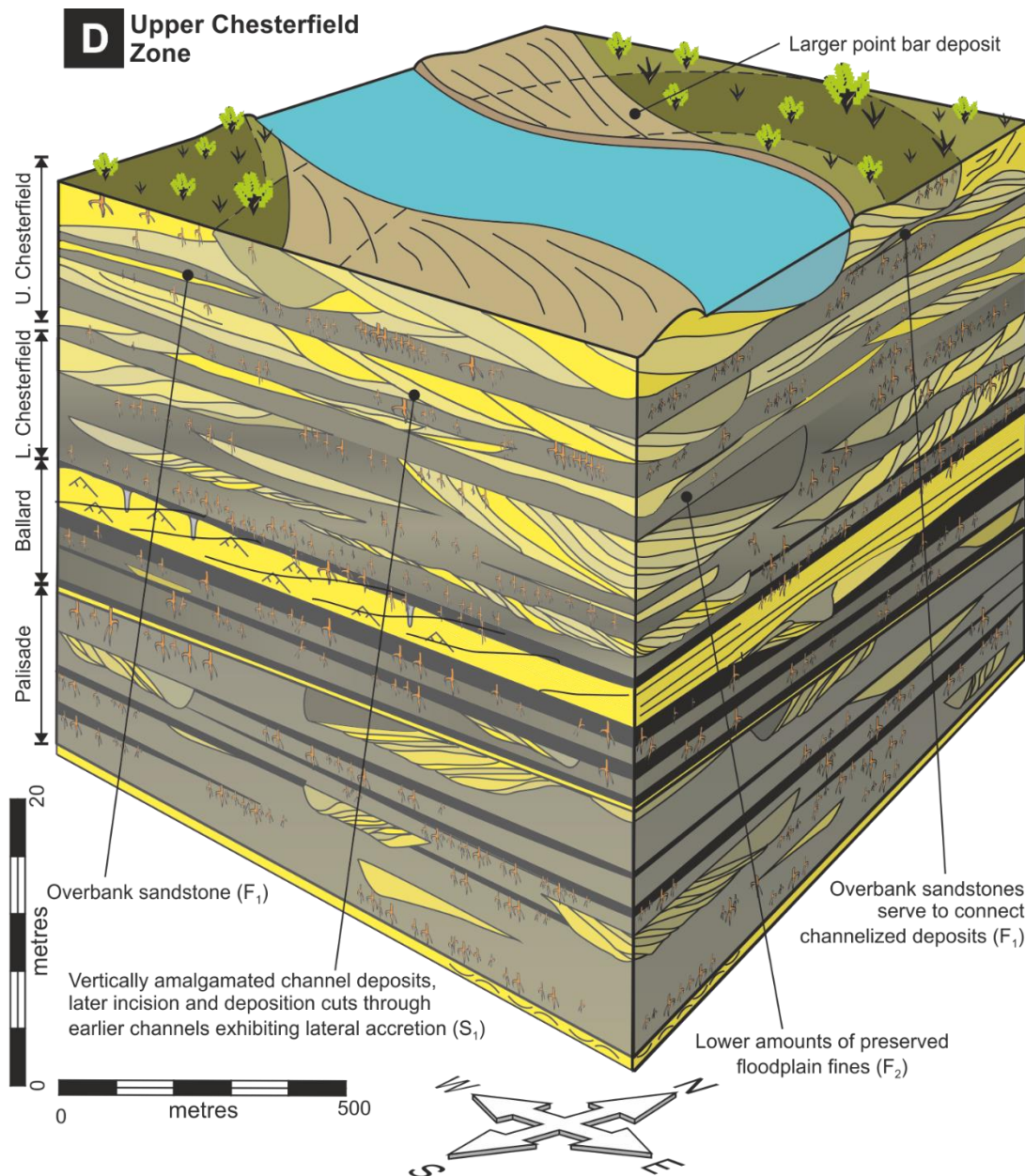


Figure 4.10: Depositional models of the palaeoenvironment represented by the Neslen Formation through time. Models accurately portray the dimensions and orientations of channelised elements recorded from the study area. A) Palisade Zone in which the depositional environment is dominated by floodplain fines and coals (F_2 , F_3) with small channels (S_3 , S_4), which vary in orientations between W-E and N-S due to their inherent sinuosity; overbank sandstone bodies (F_1) are common. B) Ballard Zone is dominated by raised peat mires, with only rare through-going channels that are of limited lateral extent and mostly of distributary channel-fill type (S_2). C) Lower Chesterfield Zone in which larger channels undertook lateral accretion (S_3), narrower distributary channel-fill elements are also common (S_2); channel size increases up through the zone and many channel forms show marked incision at their bases. D) Upper Chesterfield Zone is dominated by channel-bodies which are highly amalgamated (S_1); overbank sandstone elements (F_1) are common.

4.6.2 Controls on sand-body stacking patterns

The upward change in the observed pattern of stacking of channelised sand-bodies in the Neslen Formation can be explained in terms of a response to the interplay of allogenic and autogenic processes. Various combinations of these potential controlling factors can act to generate a similar stratigraphic architecture (Fig. 4.11).

Allogenic mechanisms through a change in accommodation generation may account for the increase in channel amalgamation upwards. A transgressive systems tract is recorded by the lowermost Palisade Zone of the Neslen Formation (e.g. Olsen et al. 1995; Kirschbaum and Hettinger 2004). Above the level of the TCSB, the Chesterfield Zone corresponds to a highstand systems tract (Kirschbaum and Hettinger 2004). The base of the TCSB represents a maximum flooding surface (Chapter 5). The sandstone body of the BBSB represents a minor marine flooding event and associated parasequence.

All channelised depositional systems are subject to autogenic processes (e.g. avulsion) and the role and significance of such controls must not be discounted. Overall, the coastal alluvial plain represented by the Neslen Formation may have been part of a type of distributive fluvial system (cf. Weissmann et al. 2005, 2010a, b, 2013; Hartley et al. 2010) the autogenic progradation of which could account for the overall transition from smaller, isolated, tidally influenced channelised elements in the Palisade Zone to progressively larger channels and eventually amalgamated channel-fills in the upper Chesterfield Zone (Fig. 4.4). The TCSB and BBSB can also be attributed to intrinsic processes (Fig. 4.11): in the event of delta abandonment the underlying sediments would have been subject to auto-compaction (Wellner et al. 2005), especially where thick underlying mire deposits are present, leading to subsidence, submergence and related shoreline retreat, thereby enabling a transgressive barrier to form (cf. Blum and Roberts 2012). Washover terraces would then have built out over lagoonal deposits through barrier rollover (Mellett et al. 2012) to form the sheltered, brackish-water tide influenced, wave dominated units represented by the TCSB and BBSB.

Given that the depositional environment was proximal to the shoreline of the Western Interior Seaway, which is known to have been subject to coeval shoreline transgressions and regressions (Ryer 1983; Johnson et al 2003; Miall et al. 2008) it is unlikely that a solely autogenic generation of the system occurred and thus a combined autogenic and allogenic processes are deemed the most likely (Fig. 4.11).

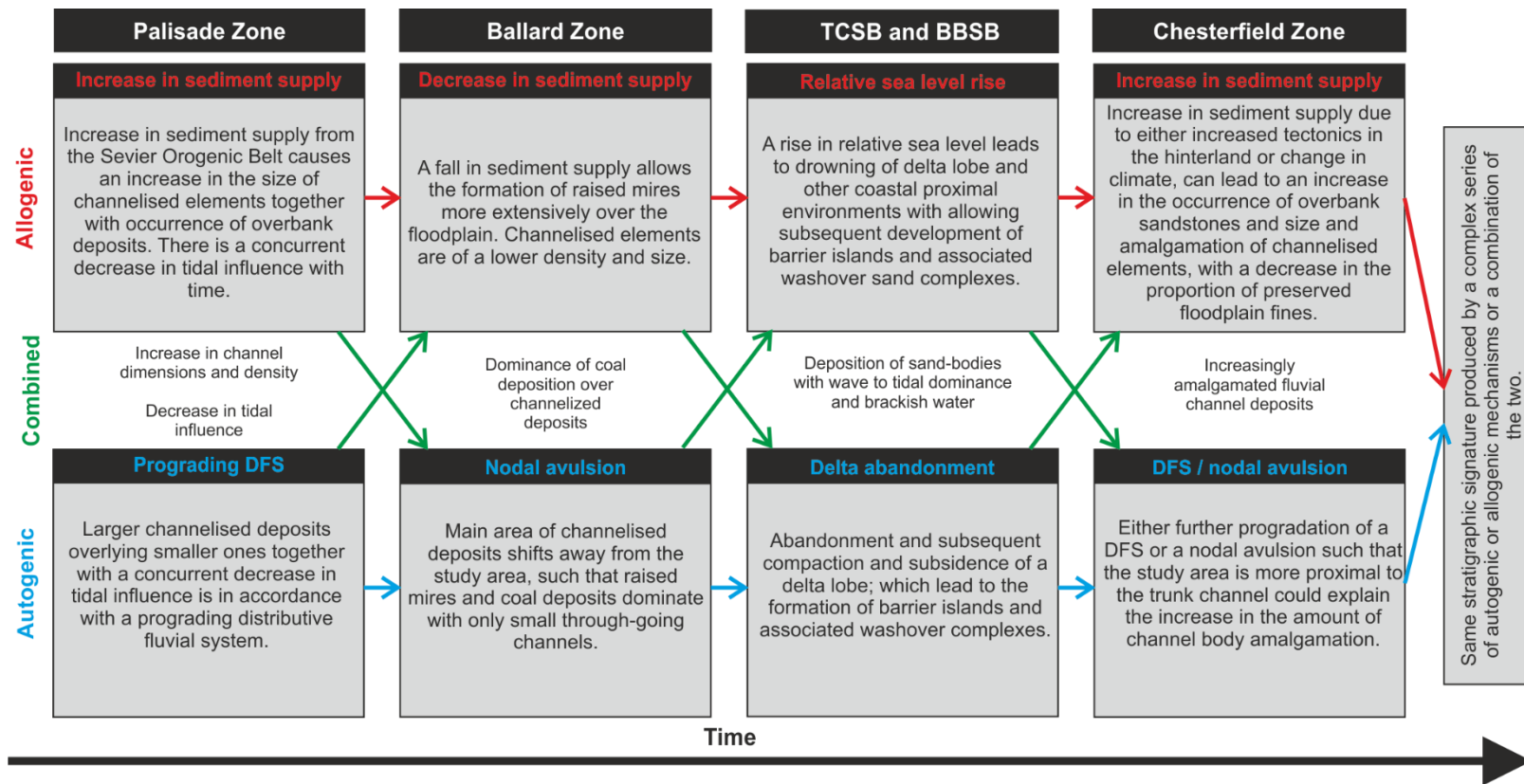


Figure 4.11: Allogenic, autogenic or combined forcing mechanisms that control marine influenced of fluvial environments can generate identical preserved stratigraphic successions. Red lines show solely allogenic mechanisms whereas blue lines show autogenic mechanisms. Green lines illustrate how combined allogenic and autogenic processes could have also given rise to the Neslen Formation stratigraphy.

Although this study has considered only a small area within a larger depositional system, the three-dimensional nature of the outcropping succession allows the interplay and relative roles of autogenic and allogenic controls to be reconstructed (Fig. 4.11). The patterns and trends revealed by this dataset, such as variations in planform geometries and spatial changes in the channel-fill style, likely reflect local variations on the regional system. Variations in local palaeocurrents, channel dimensions and changes in sand-body stacking likely occurred due to inherent properties of the system such as channel meandering and avulsion; such changes could not have been discerned to this level of detail by two-dimensional studies.

The marginal-marine palaeoenvironmental setting of this succession provides direct evidence of relative base-level change through time; this enables broad allogenic changes to be discerned (in terms of base-level control) from autogenic processes. The lateral continuity of coal zones in the Neslen Formation (Gualtieri 1991) indicates regional modification by allogenic processes. The overall up-succession change in channel dimensions and evidence for tidal influence reflects a trend of decreasing rate of accommodation generation combined with a stable or increasing rate of sediment supply (Fig. 4.11).

Localised complexities such as the spatial variations in channel element orientations are attributed to autogenic processes that operated over short time scales. For example, the Ballard Zone is anomalous within the overall succession because it records a decrease in the proportion and size of channelised elements together with the increase in the dominance of coals (Table 4.1). This can be explained in terms of an autogenic process whereby an up-stream nodal avulsion could have led to deposition of a greater proportion of channelised elements in a location outside the study area such that with the studied area was more distal to the trunk channel, thereby leaving it starved of sediment input and hence dominated by coals and floodplain fines (F₂-F₃).

4.7 Summary

The Neslen Formation accumulated in a tidally influenced, marginal marine setting and exhibits a range of mixed tidally influenced, fluvial dominated and bay-fill deposits in its lower part, with exclusively fluvial deposits dominated by multi-storey, multi-lateral sandstone bodies in its upper part. A gradual upward transition from tidally influenced to exclusively fluvial sedimentation is interrupted by two prominent sandstone elements (BBSB and TCSB) that indicate tide influenced, wave dominated sedimentation in washover fan and lagoon complexes.

Mapping of channelised elements has enabled quantification of the impact of the upward transition from tidally influenced to fluvial deposition; in terms of channel dimensions and orientations: (i) the dominant architectural style changes from smaller channelised elements characterised by inclined heterolithic strata, to sandstone-prone elements characterised by lateral accretion within the Palisade Zone; (ii) in the Ballard Zone, the dominant channelised element type are ribbon channel elements; (iii) the lower Chesterfield Zone is dominated by sandstone-prone lateral accretion elements and ribbon channel-fill elements; and (iv) in the upper Chesterfield Zone is dominated by amalgamated channel-fill elements.

The preserved style of stratigraphic architecture can be accounted for by a combination of allogenic and autogenic processes. Allogenic processes were responsible for generating the gross-scale upward change in stratigraphic architecture whereby the broader sequence framework records a transgressive systems tract passing upwards into a highstand systems tract. Autogenic processes gave rise to local variations and complexities in the architectural style.

5 Response of a Coal-Bearing Coastal Plain Succession to Marine Transgression: Campanian Neslen Formation, Utah, USA

The process regime of low-gradient coastal plains, delta plains and shorelines can change during transgression. In ancient successions, accurate assessment of the nature of marine influence is needed to produce detailed palaeogeographic reconstructions, and to better predict lithological heterogeneity in hydrocarbon reservoirs. The Campanian lower Neslen Formation represents a fluvial-dominated and tide- and wave-influenced coastal-plain and delta-plain succession that accumulated along the margins of the Western Interior Seaway, USA. The succession records the interactions of multiple coeval sedimentary environments that accumulated during a period of relative sea-level rise.

A high-resolution data set based on closely spaced study sites employs vertical sedimentary graphical logs and stratigraphic panels for the recognition and correlation of a series of stratal packages. Each package represents the deposits of different palaeoenvironments and process regimes within the context of an established regional sequence stratigraphic framework. Down-dip variations in the occurrence of architectural elements within each package demonstrate increasing marine influence as part of the fluvial-to-marine transition zone.

Three marine-influenced packages are recognised. These exhibit evidence for an increase in the intensity of marine processes upwards as part of an overall transgression through the lower Neslen Formation. These marine-influenced packages likely correlate down-dip to flooding surfaces within the time-equivalent Îles Formation. The stratigraphic arrangement of these packages is attributed to minor rises in sea level, the effects of which were initially buffered by the presence of raised peat mires. Post-depositional auto-compaction of these mires resulted in marine incursion over broad areas of the coastal plain. Results demonstrate that autogenic processes modified the process response to overall rise in relative sea level through time. Understanding the complicated interplay of processes in low-gradient, coal-bearing, paralic settings requires analysis of high-resolution stratigraphic data to discern the relative role of autogenic and allogenic controls.

5.1 Introduction

Stratigraphic successions of mixed fluvial and marginal marine (paralic) origin, in which sediments are delivered by rivers and redistributed by waves and tides represent

important archives of shoreline responses to sea-level change (Coleman and Wright 1975; Galloway 1975; Boyd et al. 1992; Ainsworth et al. 2011). Many modern coastal systems are undergoing transgression, and sedimentary process regimes vary systematically through the fluvial-to-marine transition zone (FMTZ; section 1.1) (Fedo and Cooper 1990; Boyd et al. 1992; Dalrymple and Choi 2007; Martinus and Gowland 2011) (Fig. 5.1). Studies of ancient transgressive paralic successions (e.g. Devine 1991; Valasek 1995; Sixsmith et al. 2008; Kieft et al. 2011; Leva Lopez et al. 2016) help to constrain the long-term sedimentary and stratigraphic response of FMTZs to autogenic and allogenic controls.

In ancient transgressive paralic successions, numerous allogenic and autogenic factors influence the interplay of fluvial, tidal and wave processes. Allogenic factors include tectonic setting, shelf width, climate, sediment supply rate and delivery mechanism, sea-level rise, and ocean basin morphology (Coleman and Wright 1975; Galloway 1975; Boyd et al. 1992; Bhattacharya and Giosan 2003; Nyberg and Howell 2016). Autogenic processes include switching of delta lobes (Coleman 1988; Tornqvist et al. 2008; Blum and Roberts 2012), autostratigraphy (Muto 2001; Muto and Steel 2002; Muto et al. 2007) and channel avulsion (Allen 1965; Richards et al. 1993; Stouthamer et al. 2011). However, unravelling the relative influence of autogenic and allogenic processes is a challenge and the interpretation of paralic strata commonly excludes the impact which autogenic processes have on the preservation of strata e.g. spatial partitioning of environments and promotes solely allogenic analysis.

In paralic successions, the tracing of flooding surfaces up-dip into the non-marine realm requires careful consideration. Correlative surfaces to marine flooding surfaces in the coastal plain realm can be expressed by deposits that record marine influence (McLaurin and Steel 2000), may be absent through up-dip erosion by fluvial processes (Yoshida et al. 1996; Hettinger and Kirschbaum 2003). A notable autogenic control in many low-latitude paralic systems is the development of peat mires (Frazier and Osanik 1969; Fielding 1987; Bohacs and Suter 1997; Davies et al. 2006; Jerrett et al. 2011a, b). Prior to compaction, topographically elevated peat mires can act as buffers to limit transgression; raised mires develop above the level of fluvial or marine inundation (Eble et al. 1994; Kamola and Van Wagoner 1995; Jerrett et al. 2011a) and the cohesive nature of the sediment that comprises such bodies means that they are able to withstand erosional processes (McCabe 1985), limiting the depth of fluvial and/or tidal erosion. Volume reduction associated with the auto-compaction of mires upon initial burial, and their transformation to coal, typically occurs rapidly (Ryer and Langer 1980; Fielding 1985; Courel 1987; Bohacs and Suter 1997; Nadon 1998; Holz et al. 2002). Hence, such processes cause significant local variations in accommodation. Localised areas of enhanced accommodation may be filled by fluvial

crevasse-splay deposits (van Asselen et al. 2009), or may result in marine incursion anomalously far inland (Kosters and Bailey 1983; Kamola and Van Wagoner 1995; Jerrett et al. 2011a, b). Understanding the origin of flooding surfaces is important in extending sequence stratigraphic interpretations up-dip from the coastal realm. Such interpretations can be used to enhance interpretation of paralic strata establishing likely trends in facies, architectural elements and intervals of marine influence from up-dip to down-dip and hence can improve prediction of the distribution of reservoir-quality sand bodies.

The Campanian lower Neslen Formation (upper Mesaverde Group), Book Cliffs, eastern Utah, the focus of this work, records accumulation in the lower part of a coastal plain and delta-plain system (Young 1955; 1957; Fisher et al. 1960; Keighin and Fouch 1981; Franczyk et al. 1990; Willis 2000; Hettlinger and Kirschbaum 2003; Kirschbaum and Hettlinger 2004; Cole 2008; Shiers et al. 2014; Olariu et al. 2015; Colombera et al. 2016). The well-established regional sequence stratigraphic framework (Fig. 5.2), extensive marker beds that subdivide the stratigraphy (Fig. 5.3), and outcrops with strike- and dip-oriented control permit a rare opportunity to document the preserved record of mixed process response of coal-bearing paralic successions during an episode of overall transgression through the lower Neslen Formation. Specific objectives are as follows: (i) to explain the origin of the preserved depositional architecture that arose in response to multiple laterally extensive, small scale relative sea-level rises; and (ii) to discuss the interplay of autogenic and allogenic controls on the sedimentary evolution of low-gradient coal-bearing paralic successions during transgression.

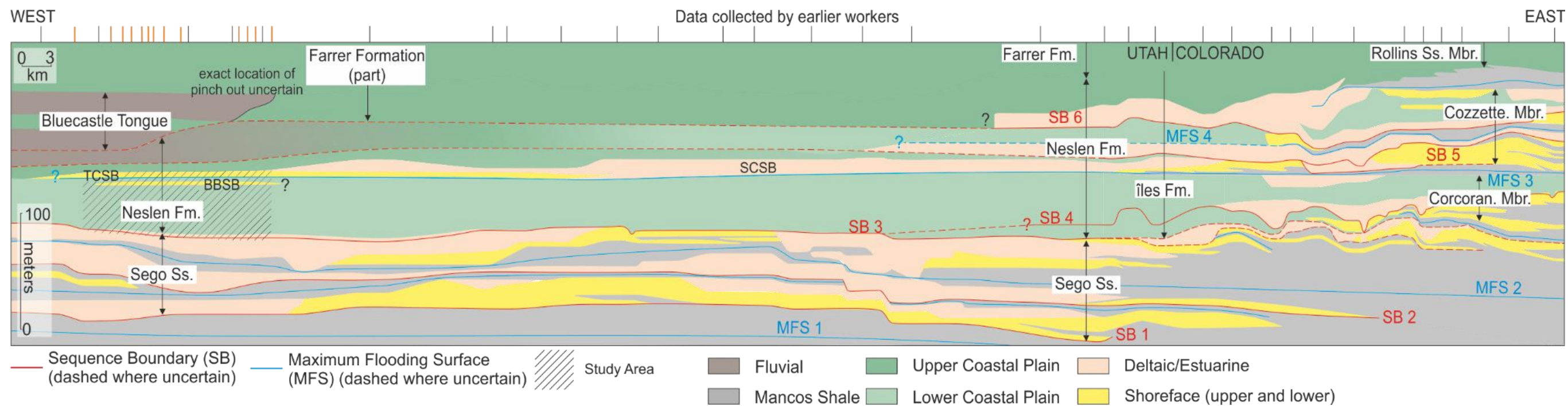


Figure 5.1: Sequence Stratigraphic framework of the Book Cliffs, from Tusher Canyon (west) to Lipan Wash (CO) (Line of section is shown in Fig. 5.4). The panel is based upon works by Kirschbaum and Hettinger (2004); Kirschbaum and Spear (2012) and Shiers et al. (2014); and has necessitated grouping of depositional environments in order to integrate multiple interpretations. Marker beds (Kirschbaum and Spear 2012; Shiers et al. 2014) are indicated including the Sulphur Canyon Sandstone Bed (SCSB), Thompson Canyon Sandstone Bed (TCSB) and Basal Ballard Sandstone Bed (BBSB). The TCSB and SCSB are marine sandstone bodies interpreted by previous workers. Sequence boundaries and flooding surfaces are numbered in ascending order. Locations for this study are indicated in red, location names are shown on Fig. 5.4.

5.2 Geological Setting

The Upper Mesaverde Group is exposed along the Book Cliffs of eastern Utah and western Colorado. It comprises stratal successions of shallow-marine, coastal and fluvial origin that accumulated during the Late Campanian (~72 Ma) as part of a clastic wedge that prograded eastwards from the Sevier Orogenic Belt towards the Western Interior Seaway (WIS) (Kauffman 1977; Miall et al. 2008). The western coastline of the WIS was oriented north-south, although many local embayments are postulated (Robinson Roberts and Kirschbaum 1995; Miall et al. 2008). The coastal plain was low gradient (2.5×10^{-4} m/m; Colombera et al. 2016) and low relief (Cole and Cummella 2003), meaning that minor sea-level change resulted in widespread transgression or re-exposure of the coastal plain during regression. The seaway is estimated to have had a microtidal range of 0 to 2 m (Steel et al. 2012).

A sequence stratigraphic framework for the Mesaverde Group is well established (Figs. 5.2, 5.3) (e.g. Miall 1993; O'Byrne and Flint 1995; Olsen et al. 1995; Willis 2000; Yoshida 2000; Miall and Arush 2001; Davies et al. 2006; Rittersbacher et al. 2014). The Buck Tongue, stratigraphically above the Castlegate Sandstone (Figs. 5.2, 5.3a), records an abrupt landward shift in deposition due to either tectonic subsidence or an increase in relative sea level (Willis and Gabel 2003). Above this, renewed progradation of the clastic wedge (Wedge B Fig. 3.7; Aschoff and Steel 2011a) resulted in accumulation of the upper Mesaverde Group: the Segoe Sandstone, Neslen Formation, Bluecastle Tongue, Tusher Formation, and Farrer Formation (McLaurin and Steel 2000; Willis and Gabel 2001, 2003). The regional sequence stratigraphic framework of the Upper Mesaverde Group from Tusher Canyon (Utah) down-dip (i.e. eastwards) to Book Cliffs Mine, Grand Junction (Colorado) has been established by previous workers (e.g. McLaurin and Steel 2000; Hettinger and Kirschbaum 2002; Kirschbaum and Hettinger 2004; Kirschbaum and Spear 2012; Shiers et al. 2014) (Fig. 5.2).

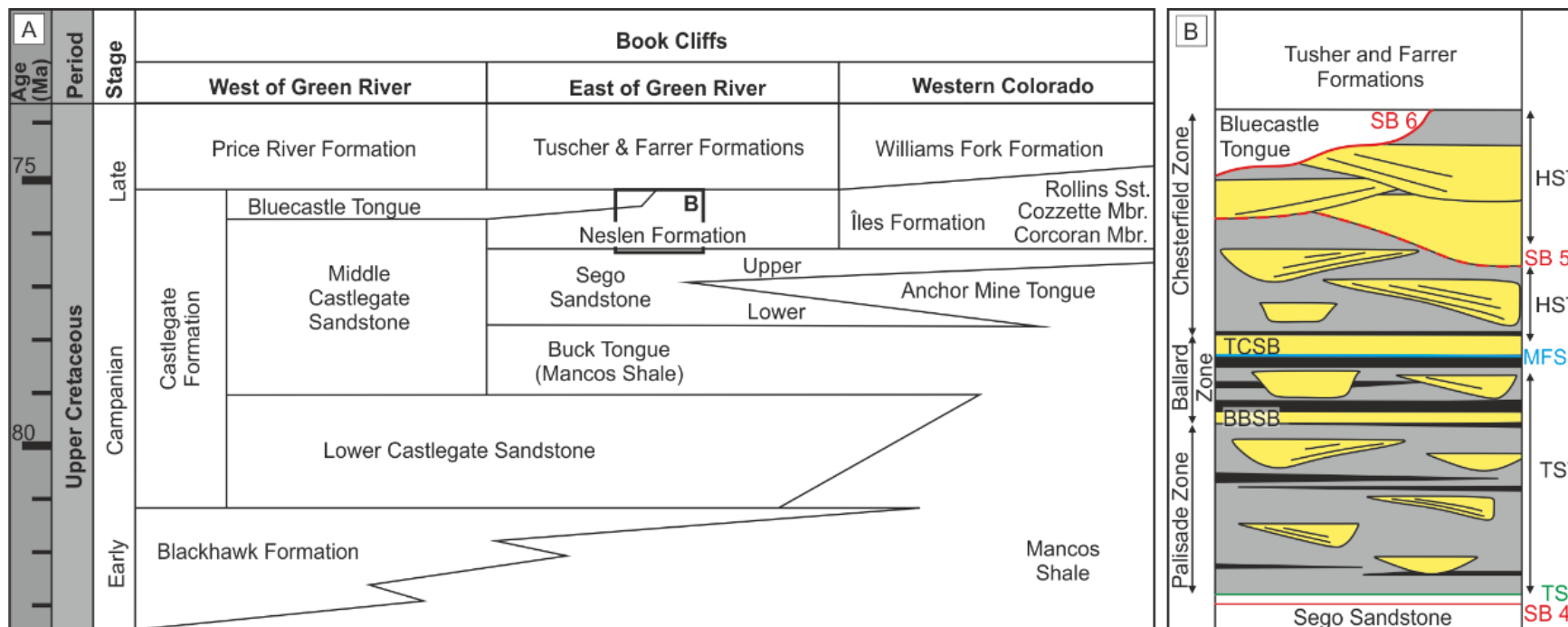


Figure 5.2: A) Stratigraphy of the Mesaverde Group in the Book Cliffs between Price (UT) and Grand Hogback (CO) modified after Kirschbaum and Hettinger 2004. B) Informal stratigraphic subdivision of the Neslen Formation (cf. Shiers et al. 2014) within the study area. Zones within the formation are highlighted and a schematic representation of the stacking of sand bodies (yellow), coal (black) and floodplain fines (gray) is indicated. Sequence boundaries and flooding surfaces are indicated on Figure 5.2. TCSB – Thompson Canyon Sandstone Bed, BBSB – Basal Ballard Sandstone Bed. SB stands for Sequence Boundary, TS is Transgressive Surface and MFS is Maximum Flooding Surface, numbered surfaces refer to the surfaces in Figure 5.2.

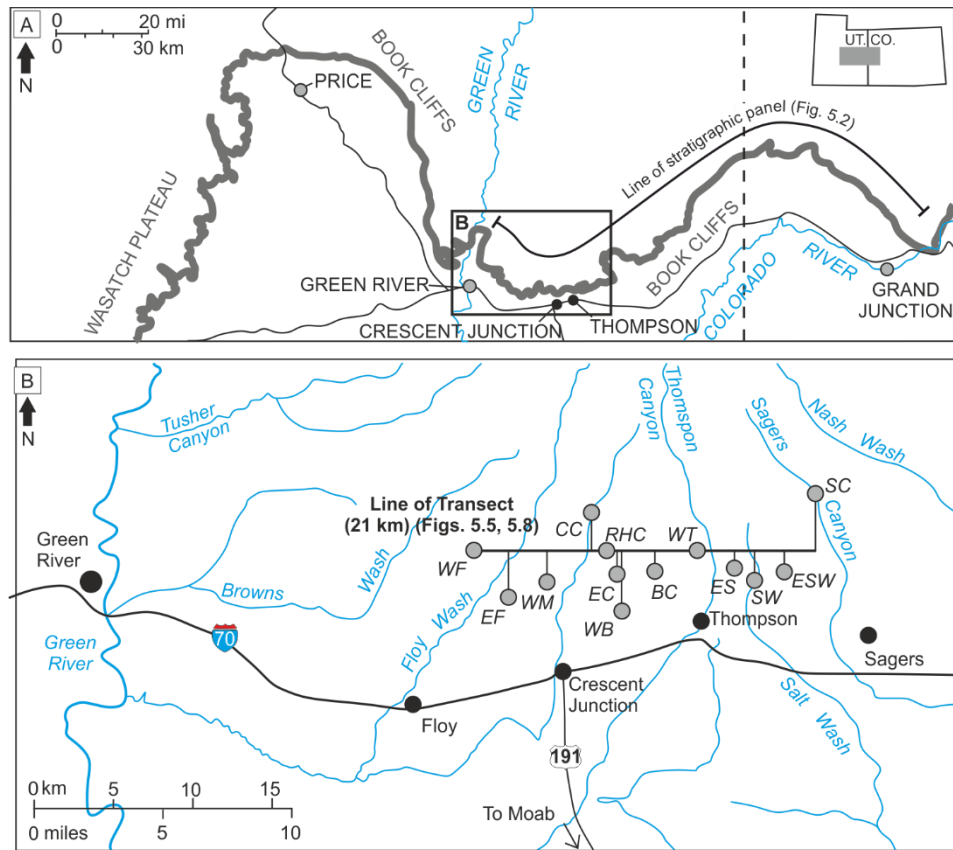


Figure 5.3: Location maps of the study area. A) Map illustrating the position of the study area along the Book Cliffs (modified after Taylor and Machent 2011). B) Location of each study locality projected onto a west-east transect; (WF = West Floy Canyon; EF = East Floy Canyon; WM = West Crescent Mine; CC = Crescent Canyon; RHC = Right Hand Crescent Canyon; EC = East Crescent Canyon; WB = West Blaze Canyon; BC = Blaze Canyon; WT = West Thompson Canyon; ES = East Sego Canyon; SW = Salt Wash; ESW = East Salt Wash; SC = Sagers Canyon). Each study locality is composed of measured vertical profiles (Fig. 5.5) and stratigraphic panels. Line of transect is indicated by the orange line, and is shown on Figs. 5.5, 5.8.

Sequence stratigraphic interpretations of the Neslen Formation vary; Figure 5.2 presents a generalised panel that is a compilation of the interpretations of Hettinger and Kirschbaum (2003) together with observations by these authors of the stratigraphy (Shiers et al. 2014). The position of sequence boundaries within the Neslen Formation is contentious (Fig. 3.8): Yoshida et al. (1996) argued for a sequence boundary in the lower part of the formation; McLaurin and Steel (2000) and Hettinger and Kirschbaum (2003) argued for a sequence boundary in the middle to upper part. Willis (2000) interprets the entire lower Neslen Formation as a lowstand systems tract (LST), with no sequence boundaries identified. Kirschbaum and Hettinger (2004) identify a thin shoreface sandstone in Colorado, the base of which they interpret as a Maximum Flooding Surface (MFS); coastal plain strata below this shoreface sandstone are assigned to a transgressive systems tract (TST). This shoreface

sandstone is likely equivalent to the laterally extensive Thompson Canyon Sandstone Bed (TCSB) present in the vicinity of this study, which is also of marine shoreface origin (Kirschbaum and Spear 2012; Cole 2008; Shiers et al. 2014). The TCSB is recognized in Utah sections of the Neslen Formation between Horse Canyon and Buck Canyon, a distance of 45 km (Gualtieri 1991), and the base is interpreted as a MFS (Cole 2008). Strata of the lower Neslen Formation below the MFS represented by the TCSB are therefore assigned to a TST, whereas overlying strata of the upper Neslen Formation are assigned to a highstand systems tract (HST) (Figs. 3.8d; 5.2).

The Neslen Formation has been subdivided into three zones based on the occurrence of coal and laterally extensive tabular sandstone bodies (Shiers et al. 2014; Figs. 5.2, 5.3b). The lower two – the Palisade and Ballard zones – are the focus here. The lowermost Palisade Zone (Fig. 5.3b) is dominated by coal, siltstone and mudstone of fluvial floodplain origin, with rare channelised sandstone, coarsening-upwards sandstones and inclined heterolithic strata (Shiers et al. 2014). The overlying Ballard Zone is composed almost exclusively of coal and organic-rich mudstone and siltstone, and is bounded by two prominent tabular sandstone elements (Table 5.1): the lower Basal Ballard Sandstone Bed (BBSB) and the upper TCSB. The TCSB has been variably interpreted as representing a beach or tidal flat (Kirschbaum and Hettinger 2004), tidal bars (Hettinger and Kirschbaum 2002); a marine sandstone bounded at its base by a transgressive surface of marine erosion (Cole 2008). The TCSB was identified in all sections of this study, implying lateral continuity over this distance (Figs. 5.2, 5.3b). The BBSB was first identified by Shiers et al. (2014) and can be identified in all but one section in this study. The Chesterfield Zone – the uppermost of the three zones – overlies the TCSB and represents the upper part of the Neslen Formation. The Chesterfield Zone is composed dominantly of fluvial channel sandstones that become increasingly amalgamated upwards (Shiers et al. 2014; section 6.5). The Neslen Formation is overlain unconformably by the Bluecastle Tongue or conformably by the Farrer Formation (Figs. 5.2, 5.3) (Cole 2008; Lawton and Bradford 2011).

The lower Neslen Formation (below the base of the TCSB; Fig. 5.2) (Pitman et al. 1986; Franzcyk et al. 1990; Gualtieri 1991; Robinson Roberts and Kirschbaum 1995; Willis 2000; Hettinger and Kirschbaum 2002; Kirschbaum and Hettinger 2004; Cole 2008; Shiers et al. 2014; Olariu et al. 2015; Colombera et al. 2016), represents a tide- and wave-influenced coastal plain and delta-plain succession, which accumulated landward of a wave-dominated shoreline located in what is now western Colorado: the Îles Formation (Figs. 5.2, 5.3) (Kirschbaum and Hettinger 1998; Willis and Gabel 2003). The strata of the lower Neslen Formation pass basinward into time equivalent strata of the Îles Formation (Corcoran and Cozette members) (Kirschbaum and Hettinger 2004) (Fig. 5.2).

Architectural element	Geometry and dimensions	Description	Ichnology	Relationship to other elements	Interpretation
S₂- Ribbon channel-fill	Abrupt pinch-outs with steep cut-banks (35°). Basal incision 4-7 m which is equal to the element thickness. Width 35-200 m and low aspect ratio of 10-15.	Aggradational fine- to medium-grained sandstone arranged into sets separated by erosion surfaces. Scour surfaces overlain by intraformational conglomerate. Cross bedding is common towards the base, passing upwards into ripple cross-laminated sandstone. Sigmoidal co-sets; convex-up cross bedding are recognized. Drapes of siltstone and carbonaceous material occur. No Lateral accretion surfaces are observed.	BI 1; examples of <i>Skolithos</i> and <i>Arenicolites</i> towards the base of the element.	Erosionally overlie elements F ₁ , F ₂ and F ₃ .	Distributary channels (Miall 1996), unidirectional flow with migrating, large-scale dunes and minor modification by tidal currents (drapes on foresets) in a backwater environment (cf. Colombera et al. 2016)
S₃- Sandstone- dominated lenticular	Commonly exhibit a lenticular form with thicknesses of 2-6 m and with basal incision up to 3 m deep. Width of 90-500 m. Inclined surfaces dip at 6-20°.	Fining upwards from fine-grained to very fine-grained sandstone. Lenticular beds (5-40 cm) downlap onto lower beds or the basal surface. Lithofacies include massive-to-faintly laminated sandstone with ripples, climbing ripple cross-lamination and cross-bedding.	BI 1-2 in beds at the top of element.	Erosionally overlie elements F ₁ , F ₂ and F ₃ .	Channelised unidirectional flow with a high degree of levee confinement. Dominance of lateral accretion typical of fluvial point bars (cf. Bridge, 2006).

<p>S₄- Heterogenous Lenticular</p>	<p>Thicknesses up to 5 m and 50-300 m wide. Bed surfaces dip at 5-25°.</p>	<p>Alternating tabular- to wedge-shaped beds of well-sorted, fine-grained sandstone and siltstone. Sandstone beds (0.05-1 m thick) display ripple cross-lamination, horizontal lamination and low-angle cross-lamination. Single and double drapes on ripple foresets are common. Rare occurrences of opposing dip directions in ripple foresets. Siltstone beds (5-10 cm thick) exhibit lenticular-flaser-wavy laminations.</p>	<p>BI 0-3 (higher in upper parts of element) including <i>Arenicolites</i>, <i>Diplocraterion</i>, <i>Rhizocorallium</i>. <i>Teredolites</i> is common at the base.</p>	<p>Commonly pass laterally into and erosionally overlie elements F₁, F₂ and F₃.</p>	<p>Inclined surfaces represent lateral accretion in heterolithic point bars (Inclined Heterolithic Stratification; Thomas et al. 1987). Presence of brackish water ichnofacies, draped ripples and current reversals indicate marine influence on these deposits (Shanley et al. 1992).</p>
<p>S₅- Amalgamated IHS</p>	<p>Beds are horizontal or inclined up to 8° within elements that are up to 16 m thick. Within each element, packages attain a maximum thickness of 4 m and can be traced laterally for up to 150 m.</p>	<p>Stacked heterolithic bed-sets of alternating sandstone, siltstone and mudstone. Overall the beds within each package thicken and coarsen upwards. Sandstone beds are massive to laminated and exhibit ripples with single- and double-drapes of mud and carbonaceous material. Finer- grained beds are generally laminated to massive but in places also exhibit flaser, lenticular and wavy bedding.</p>	<p>BI 0-3 with <i>Medousichnus</i>, <i>Planolites</i> and <i>Palaeophycus</i>. Gastropod (<i>Viviparus</i>) and bivalve fragments with <i>Teredolites</i> at the base.</p>	<p>Commonly overlies elements F₁-F₃. Lateral relationships are typically poorly exposed.</p>	<p>Inclined clinofolds at varying angles on a small scale indicate a small-scale prograding delta (crevasse delta, Gilbert-type delta or bay-head delta) in a sheltered marine environment (Syvitski and Farrow 1983; Joeckel and Korus 2012). A fluvial interpretation is rejected based upon the ichnology and the thickening and coarsening upwards trend within each package.</p>

<p>S₆ Tabular sandstone</p>	<p>Thickness varies from 1-6 m (for the sandy upper part). The finer, lower part (where present) is 1-1.5 m thick. Lateral extent is 100s m to 10s of km. In some areas, shallowly dipping (up to 7°) clinofolds dipping to the west are observed. Beds are tabular, wedging out over 100s of metres.</p>	<p>Examples of this element occur in, but are not exclusive to, the TCSB and BBSB. The finer-grained lower part of this element is only observed in examples in the TCSB and is composed of heavily bioturbated dark grey siltstone and very fine-grained sandstone containing shell fragments and siderite bands. The sandy upper part is observed in all examples and comprises thickening- and coarsening-up packages of clean, well sorted sandstone. Where not obscured by bioturbation, beds are 50-150 mm thick and exhibit symmetrical ripple-lamination (mud draped in lower beds), and horizontal lamination.</p>	<p>Lower TCSB – heavily bioturbated (BI 5) overprinting of original sedimentary structures. <i>Thalassinoides</i> abundant on the base. Upper TCSB and other examples: BI 0-5 increases both upwards down-dip. Bioturbation includes <i>Arenicolites</i>, <i>Bergueria Planolites</i> and <i>Ophiomorpha</i>. Crawling and root traces on top surfaces.</p>	<p>Commonly underlain and overlain by thick, well developed coal (F₃) or by floodplain or lagoonal fines (F₂). Lateral transitions at the point of pinch out are not directly observed.</p>	<p>The lower division represents a lagoonal setting, subject to intense bioturbation. Sedimentary structures and ichnology in the upper part represent a brackish water, wave dominated environment e.g. washover fans, shoreface, or a sand-spit (Kirschbaum and Hettlinger 2004). A retreating barrier bar interpretation is favoured based on the geometry and scale of the elements (Penland et al. 1988). A bay-fill is discounted due to the down-dip extent of the bodies and the lack of erosional surface.</p>
<p>S₇- Coarsening-upwards sandstone</p>	<p>Elements up to 5 m thick and 20-100 m in lateral extent. Erosion at the base of the element is up to 30 cm. Bed boundaries become increasingly erosive upwards.</p>	<p>Thickening- and coarsening-upwards from very fine- to fine-grained sandstone characterised by horizontal and ripple laminations, commonly with single or double drapes (mud, silt or carbonaceous). Interbedded sandstone and siltstone beds exhibit load casts and convolute lamination and lenticular, flaser and wavy bedding. Intraformational conglomerate occurs on internal scour surfaces.</p>	<p>BI 0-3 including <i>Ophiomorpha</i>, <i>Rhizocorallium</i> and <i>Diplocraterion</i>. Root traces towards the top.</p>	<p>Commonly overlies elements F₁-F₃. Lateral relationships are typically poorly exposed</p>	<p>Tide and wave influence, brackish water ichnology and shallowing upwards succession indicates environments such as crevasse deltas or mouth-bars (Joeckel and Korus 2012).</p>

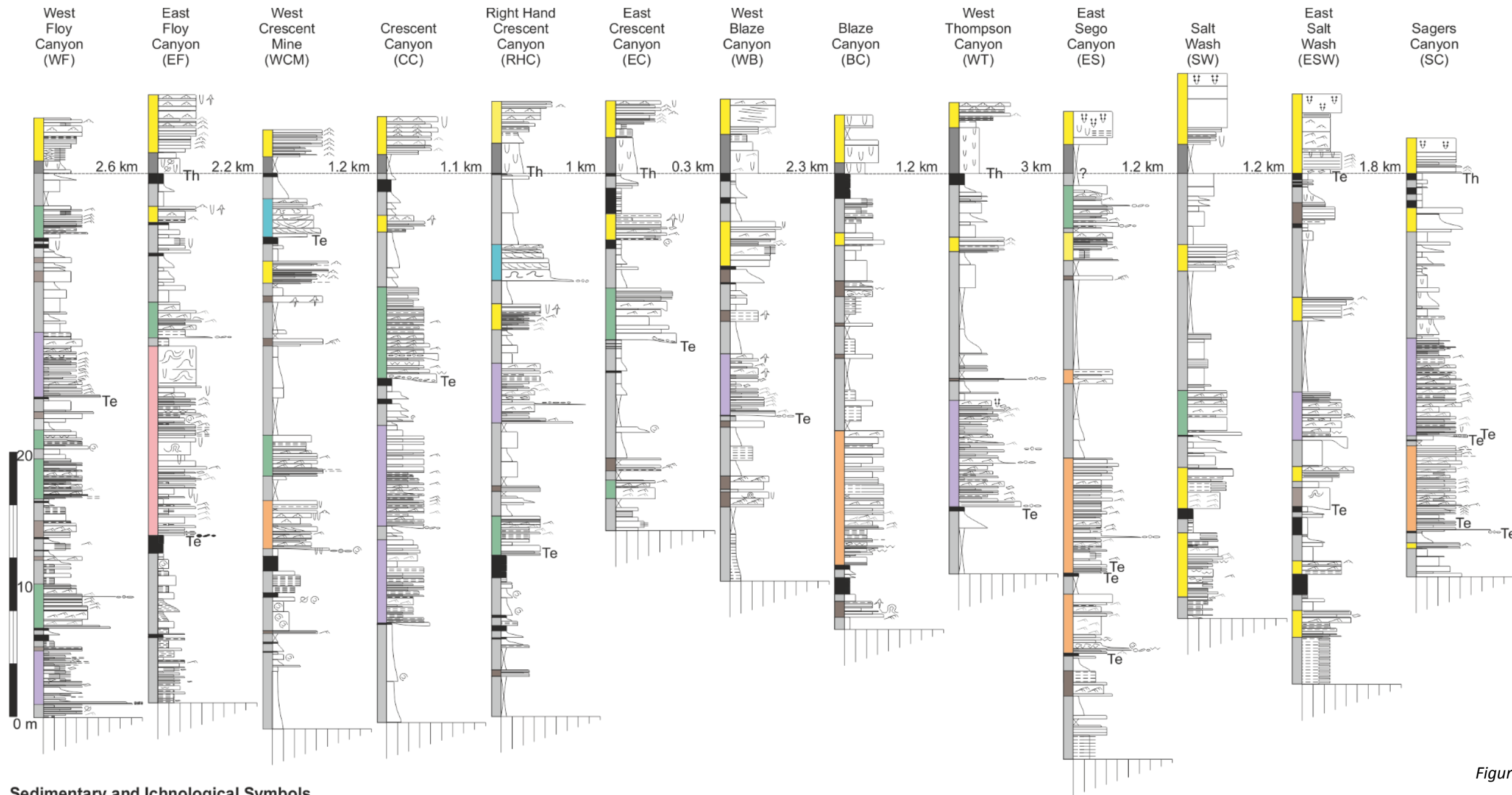
F₁- Small-scale sandstone and siltstone	Elements are less than 2 m thick and pinch out gradually over tens to hundreds of metres. Localised erosion up to 30 cm at the base.	Very fine- to fine-grained sandstone and siltstone. Beds dip in varying orientations at low angles (2-5°). Weathering and the occurrence of post-depositional concretions obscure sedimentary structures. Lithofacies include massive sandstone, climbing and current ripple and horizontal laminations	BI 0. Rare root casts are preserved.	Passes laterally and vertically into element F ₂ ; commonly overlies element F ₁ .	Un-confined flows on levees, crevasse channel and splays. Incision indicates slightly higher energy flows (Guion et al. 1995; Mjos et al. 2009).
F₂- Finning- upwards mudstone and siltstone	Packages are up to 5 m thick and have a lateral extent of tens to hundreds of metres.	Brown to black mudstone and siltstone arranged into fining upwards packages. A: Common sulfur staining, wood fragments, coalified wood debris and rooted horizons. B: Passes vertically from laminated siltstone to massive mudstone, notably absent of rooted horizons, deformed (flattened) coal and amber clasts.	A: BI 0. Occasional root casts are preserved. B: BI 0-3 Some bioturbation of indeterminate origin.	A: Overlain by coals of element F ₃ , commonly grades upwards from F ₁ . B: Commonly overlain or underlain by elements S ₅ -S ₇ .	A: Accumulation in low-energy settings such as distal crevasse splays (Guion et al. 1995). B: Accumulation in quiet water brackish settings such as lagoons (Horne et al. 1978). The two sub-elements are not always readily discernible and association with other elements must be considered.
F₃- Coal-prone	Various scales are preserved from mm-sized ribbons to metre-thick beds of tens to hundreds of metres lateral extent.	Black, friable coals containing amber and wood fragments, as well as sandstone clasts. Coals do not occur as simple sheets but interfinger with clastic facies.	Lenses of sand can represent sandy infill of burrows.	Commonly occur at the top of element F ₂ and are commonly overlain by sandier elements (F ₁ , S ₂ -S ₇)	Coals formed in raised peat mires in humid, swampy conditions (Davies et al. 2006; Jerrett et al. 2011a).

Table 5-1: Table describing the geometry, facies and ichnology of representative architectural elements of the lower Neslen Formation. Each element is interpreted in terms of representative sub-environments.

5.3 Methods

Thirteen study areas have been analysed over a 21 km-long dip section (Floy Canyon to Sagers Canyon; Fig. 5.4). Sedimentary logs collected through the lower Neslen Formation (i.e. the Palisade and Ballard zones; Fig. 5.3b) have been projected onto an east-to-west transect aligned oblique or perpendicular to the shoreline of the Western Interior Seaway (Robinson Roberts and Kirschbaum 1995; Aschoff and Steel 2011b) (Figs. 5.4, 5.5). In total, forty-two vertical sedimentary profiles (total length = 840 m; Appendix E; F), 106 stratigraphic panels (Appendix G) that record stratigraphic architectural relationships (total width = 5000 m) and 408 palaeocurrent readings (measured from cross-bedded sets, ripple laminations, scour marks and lateral accretion surfaces) were collected from the base of the Neslen Formation to the top of the TCSB.

Each log records lithofacies (Table 4.1; Fig. 4.7) and ichnological information (Figs. 5.5, 5.6). In total, nine architectural elements (Figs. 4.8; 5.7) have been interpreted in the lower Neslen Formation (cf. Shiers et al. 2014). Multistory, multilateral channel elements (S_1) are not observed in this part of the stratigraphy (chapter 4). The architectural elements are based upon the vertical and lateral distribution of facies and their stratigraphic context as recorded on the stratigraphic panels; these are described in Table 5.1; for extended description and interpretation of architectural elements see section 4.4. Architectural elements in the lower Neslen Formation comprise bodies of strata interpreted to represent the following sub-environment types: S_2 : Ribbon channel-fill elements: distributary channels; S_3 : Lenticular sandstone-dominated elements: fluvial point bars; S_4 : Lenticular heterogeneous elements: tidally influenced point bars; S_5 : Amalgamated inclined heterolithic strata: bay-head deltas; S_6 : Tabular sandstone element: reworked barrier sandstones; S_7 : Coarsening-upwards sandstone element: bay-fill sandstones, including mouth bars; F_1 : Small scale sandstone and siltstone: fluvial overbank; F_2 : Fining upwards siltstone and mudstone : lagoonal or fluvial floodplain origin; F_3 : coal-prone mires (Figs. 5.7).



Sedimentary and Ichnological Symbols

- | | | | | | |
|---|---------------------------------|-----------------------|----------------------|--------------------|--------------------|
| Symmetrical Lamination (grey if draped) | Horizontal Lamination | <i>Teredolites</i> | Trough Cross-Bedding | Lenticular Bedding | <i>Ophiomorpha</i> |
| Asymmetrical Ripple Lamination (grey if draped) | Wavy Bedding | <i>Thalassinoides</i> | Low-angle Lamination | Wood Fragments | Shell Fragments |
| Flaser Bedding | Bioturbation (undifferentiated) | Convolute Lamination | Clasts | Root Traces | |

Architectural Elements

- | | | | | |
|--------------------------------------|---|---|--|------------------|
| Ribbon channel-fill element | Lenticular sandstone dominated element | Lenticular heterogenous element | Amalgamated inclined heterolithic stratification | Tabular sandston |
| Coarsening-upwards sandstone element | Small-scale sandstone and siltstone element | Fining-upwards mudstone and siltstone element | Coal-prone element | Bioturbated mud: |

Grain-size Scale

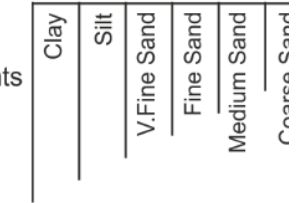


Figure 5-4: Sedimentary logs recorded at each study locality, detailing the facies and ichnology alongside the interpreted architectural elements. Logs are hung from the base of the Thompson Canyon Sandstone Bed which acts as a marker for the succession. Refer to Figure 5.2 for study locations.

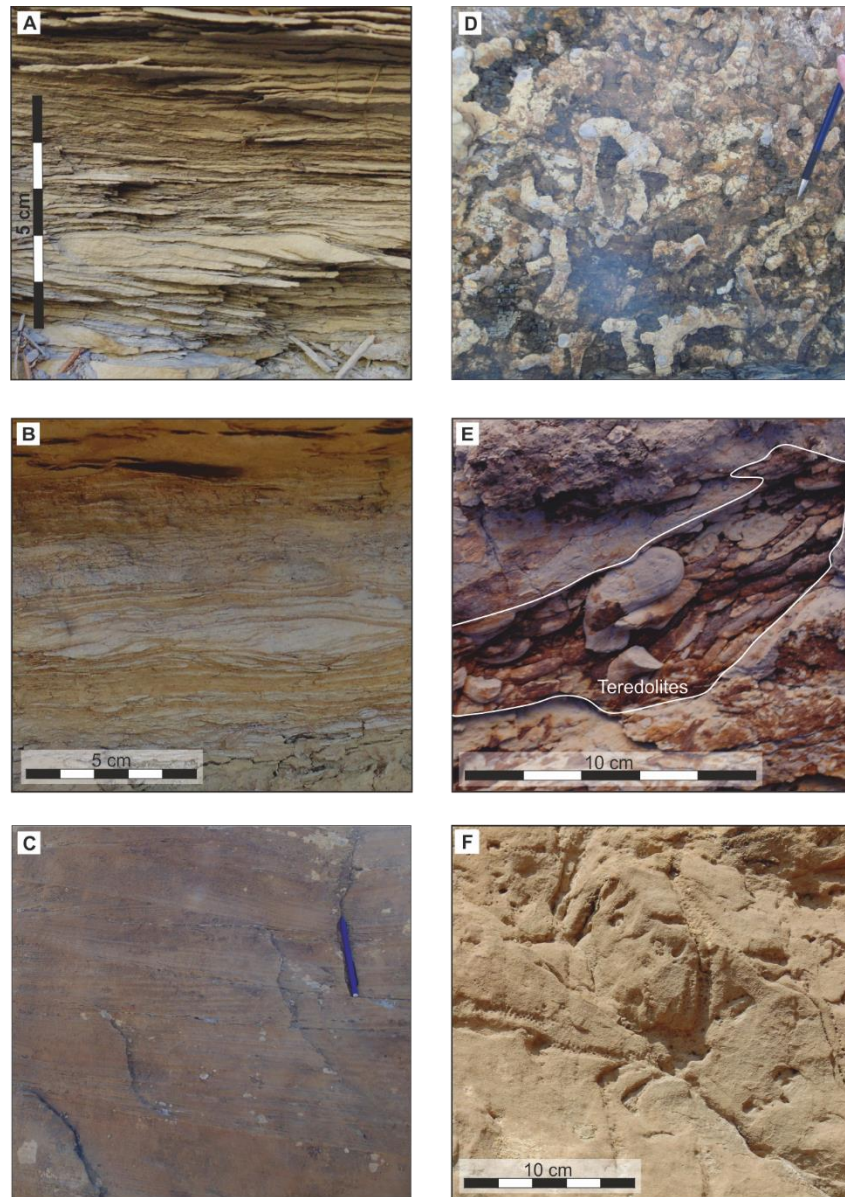


Figure 5.5: Sedimentary facies and ichnology observed within the Neslen Formation. A) Wavy and flaser bedding (H) within a coarsening-upwards sandstone element (S_7), draped asymmetrical ripples (S_a) are visible in the lower part of the photograph. (S_6). B) Silt-draped asymmetric ripples (S_a) within a lenticular sandstone dominated element (S_3). C) Sandstone exhibiting cross-bedding (S_x) with multiple reactivation surfaces within a ribbon channel-fill element (S_2). D) *Thalassinoides* observed at base of the lower TCSB; Thompson Canyon Sandstone Bed; (S_6). E) *Teredolites* bored wood found in the base of a lenticular heterogenous element (S_4). F) Highly bioturbated sandstone of the TCSB (S_6) examples of *Ophiomorpha* are common; bioturbation index of 3 (Taylor and Goldring 1993)

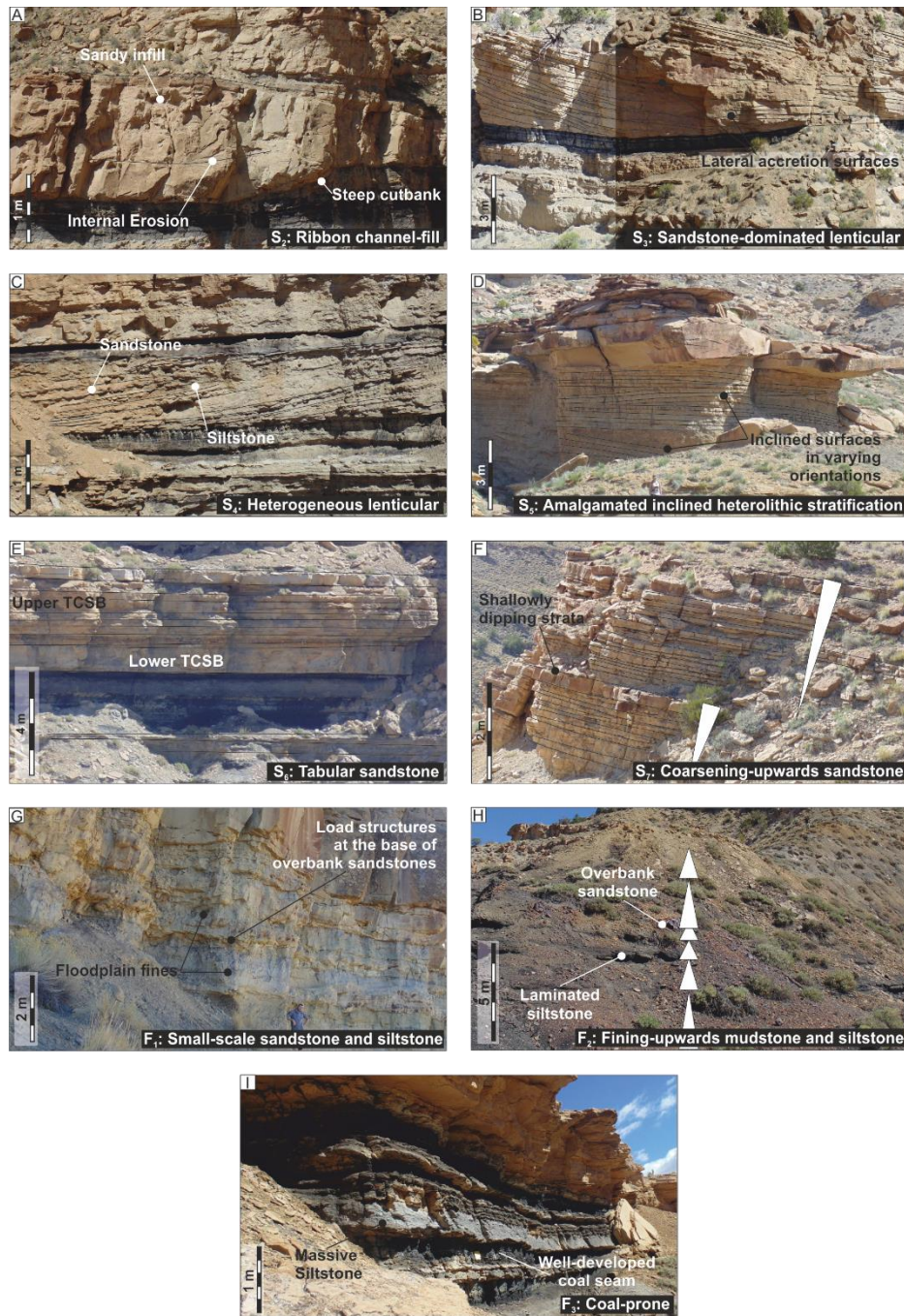


Figure 5.6: Representative architectural elements of the Neslen Formation; description and interpretation of elements can be found in Table 5.1. A) Ribbon channel-fill element (S_2). B) Sandstone-dominated lenticular element (S_3). C) Lenticular heterogeneous element (S_4). D) Amalgamated inclined heterolithic stratification (S_5). E) Tabular sandstone element (S_6). F) Coarsening-upwards sandstone element (S_7). G) Stacked small-scale sandstone and siltstone elements (F_1). H) Repeated arrangements of fining-upwards mudstone and siltstone elements (F_2). I) Coal-prone elements (F_3), interbedded with examples of F_1 and F_2 .

The method through which the logged sections have been correlated is outlined in Appendix G, identification of key stratal surfaces and coal zones within the stratigraphy allow correlation of seven lithostratigraphic packages (Fig. 5.8), each of which represents time-equivalent depositional sub-environments. Correlation was refined through careful analysis of the facies within each architectural element, as well as their relationship to surrounding elements (Fig. 5.5; Appendix G).

The depiction of the seven lithostratigraphic packages on a correlation panel (Fig. 5.8) has been used to analyse the vertical and lateral changes in the proportions of constituent architectural elements (Fig. 5.9A). The proportion of architectural elements within each lithostratigraphic package is calculated from the cumulative logged thickness of each architectural element within that interval compared to the total sum of the thickness of the interval at each study site. Trends can also be established through analysis of, palaeocurrent patterns within each interval (Fig. 5.9B), and the occurrence of sedimentary tidal and ichnological brackish water indicators (Fig. 5.9C). Palaeogeographic maps (Fig. 5.9D) have been developed for each depositional interval. These have been constructed through analysis of the facies and architectural-element facies associations. Plan-view dimensions of elements were garnered from the lateral extent of elements on stratigraphic panels, and informed by imagery of modern systems.

ye

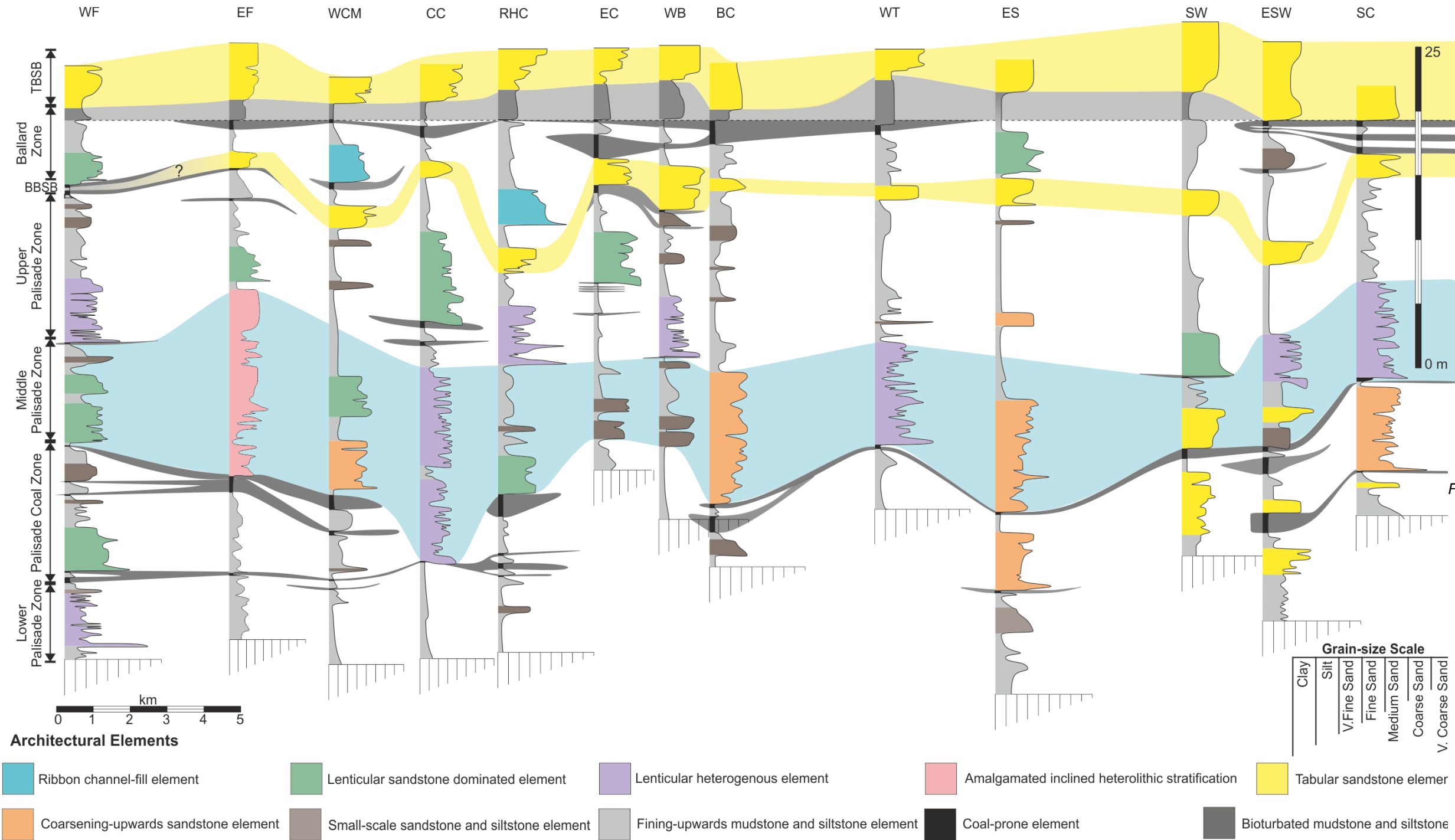


Figure 5.7: Correlation panel of the logged sections located along the line of section (to scale) (Figure 5.4). Interpreted packages (see text) are indicated as are marker units: Basal Ballard Sandstone Bed and Thompson Canyon Sandstone Bed. Shaded dark grey regions represent coal-bed correlations. The workflow for producing this figure, and the subsequent synthesis facies panel (Fig. 5.10) is shown in Appendix G.

5.4 Results

5.4.1 Lower Palisade Zone

5.4.1.1 Description

The Lower Palisade Zone (average thickness 4.7 m) is the package from the top of the Sege Sandstone to the first coal bed in the Lower Neslen Formation (Fig. 5.8). The lower Palisade Zone is dominated by fining-upwards mudstone and siltstone elements (F_2 ; 81%), (Table 5.1; Fig. 5.9-1A), which contain abundant amber and compacted fragments of vegetation (which now appear as flattened clasts of coal), with rare thin sandstones and siltstones (F_1 ; Table 5.1; 7.5%). Laterally, the type of sandstone dominated elements within the Lower Palisade Zone varies (Fig. 5.8). At West Floy, small (up to 4 m thick and 150 m wide) heterogeneous lenticular elements (Fig. 5.7b) are present (S_3 ; Table 5.1). Towards the east (East Salt Wash and Sagers Canyon), thin tabular sandstone elements (Fig. 5.7e) occur and are characterised internally by clinofolds that dip shallowly ($<5^\circ$) towards the west (S_6 ; Table 5.1), and thicken- and coarsen-upwards. Sedimentary structures (Fig. 5.9-1C) observed in heterogeneous lenticular elements (S_4) and tabular sandstone elements (S_6) (Table 5.1) notably include wavy and lenticular bedding (Fig. 5.6a), and single and double mud draped ripples (Fig. 5.6a, b). Palaeoflow is predominantly towards the east (Fig. 5.9-1B).

5.4.1.2 Interpretation

In the western part of the study area, the fine-grained elements are interpreted as part of a non-marine environment due to the presence of coal and amber (Fig. 5.7h) (cf. Guion et al. 1995). In the eastern part of the study area, however, the lack of these identifying features and indistinct bioturbation in some outcrops may indicate a lagoonal environment (Horne et al. 1978) (Fig. 5.5; Table 5.1). The inferred lateral change in environment from east to west is reinforced by the decrease in abundance of sandstone-dominated elements interpreted to represent lateral accretion elements (S_3 and S_4) and the increase in occurrence of tabular sandstone elements which record a dominance of wave processes. Tabular sandstone elements (S_6) are interpreted as small back-stepping barrier complexes based on the architecture and the facies assemblages (Table 5.1; section 4.4.6), which were likely preserved via in place drowning as isolated ribbons (Fig. 5.8) (Sanders and Kumar 1975; Penland et al. 1988). In the western parts of the study area, lenticular sand bodies in the lower Palisade Zone are interpreted as tidally influenced point-bar elements based on their geometry, together with evidence of alternating current energy in the form of wavy and lenticular bedding, and single and double mud-draped ripples (Fig. 5.9-1C; Table 5.1). Sedimentary structures within sandstone-dominated elements, specifically the

occurrence of double mud drapes, indicate current energies that fluctuated, possibly due to tidal forcing (Shanley et al. 1992; Lavigne 1999). The change in architectural elements from western to eastern parts of the study area represents a change from fluvially dominated to marine dominated energy regimes as part of the FMTZ.

5.4.2 Palisade Coal Zone

5.4.2.1 Description

The Palisade Coal Zone lies stratigraphically above the Lower Palisade Zone (Fig. 5.8). It is characterised by coal-prone floodplain elements that comprise 26.5% of the package (Fig. 5.9-2A). Individual coal beds (Fig. 5.7i) vary in thickness, up to 1 m and are discontinuous at outcrop but can be traced laterally for 100s of metres at each study site. Fine-grained elements (F₂; Fig. 5.7g) are abundant in this package (46.5 %; Fig. 5.9-2A). Sandstone-prone elements such as coarsening-upwards sandstone elements (S₇; 4%; Fig. 5.7f) and sandstone dominated lenticular elements (S₃; 5.5%) are present in minor amounts (Fig. 5.9-2A). The type of sandstone-prone elements changes in a down-dip direction (i.e. to the east; Fig. 5.8) from lenticular sandstone dominated elements (S₃) (Fig. 5.7b, c) (3 to 7 m thick), to large coarsening-upwards sandstones up to 8m thick (S₇; Fig. 5.7f) and tabular sandstone elements (S₆; Fig. 5.7e). In the eastern part of the study area (Fig. 5.8; between East Sege to Sagers Canyon), mono-ichnospecific assemblages of ichnogenera such as *Rhizocorallium* are observed within coarsening-upwards sandstones elements (S₇) and towards the top of lenticular heterogeneous elements (S₄). Additionally, in this vicinity, *Teredolites* bored wood (Fig. 5.6e) is abundant at the base of these elements (S₄ and S₇) These elements are characterised by lithofacies defined by the following types of sedimentary structures: uni- and bi-directional ripples draped with a combination of silt and carbonaceous material; lenticular, flaser, and wavy bedding (Fig. 5.5d); sets of uni-directional ripple strata that record sediment transport in opposing directions (Fig. 5.9-2C). Palaeoflow directions are dominantly towards the east and northeast (Fig. 5.9-2B).

5.4.2.2 Interpretation

The abundance of coal indicates the dominance of mires (cf. Davies et al. 2006), likely in a flood basin that additionally comprised fine-grained siltstone and mudstone with minor sandstones of crevasse-splay origin (Table 5.1; Fig. 5.9-2D). Mires within the Neslen Formation are interpreted as partly ombrotrophic in origin (coals with mineral contents below 10 %, building up above flooding levels; Spears 1987; Davies et al. 2005). This interpretation of ombrotrophic mires is equivocal without detailed analysis of the inorganic mineral volume. However, this interpretation is supported by an important consideration: raised mires self-exclude clastic detritus and allow the organic material to develop good

quality coals (such as those in the Neslen Formation, with low clastic content; Tabet et al. 2008) in close proximity to active clastic fluvial systems (Clymo 1987) (Table 5.1; Fig. 5.8). The same reasoning was used to support the interpretation of accumulation of coals in largely ombrotrophic mires within the underlying Blackhawk Formation (Davies et al, 2006). The Blackhawk Formation formed in similar depositional settings under similar climatic regimes to those of the Neslen Formation (Davies et al. 2006). The interpretation of ombrotrophic mires is important as they serve to stabilise fluvial channel position and limit channel migration (the majority of palaeoflow orientations are directed towards the north and east (Fig. 5.9-2B). The observed trace fossils, their lack of diversity and diminutive size of their occurrence within architectural elements towards the east of the studied section (Figs. 5.5, 5.8) is indicative of an environment that was subject to brackish-water influence (Bromley 1996; Gingras et al. 2012). Within sandstone-dominated architectural elements, drapes on ripple foresets and opposing directions of currents recorded by current ripple cross-laminated strata can be interpreted as having been modified by tides (Shanley et al. 1992). Symmetrical ripples are interpreted as wave ripples generated on the bottom of a standing body of water (De Raaf et al. 1977). In this case, the association of symmetrical ripples with brackish-water ichnogenera indicates an environment of deposition such as a lagoon.

5.4.3 Middle Palisade Zone

5.4.3.1 Description

This package (Fig. 5.8) is dominated by a range of sandstone-prone elements (66 %; Fig. 5.9-3A), subordinate fine-grained elements commonly contain plant debris (as fragments of flattened coal) and rooted horizons in the west. Sandstone-prone (S_3 ; Fig. 5.7b) and heterolithic (S_4 ; Fig. 5.7c) lenticular elements interpreted to represent lateral accretion occur predominantly in the west, whereas coarsening-up sandstone elements up to 10 m thick (S_6 ; Fig. 5.7f) and tabular barrier sandstone elements up to 6 m thick (S_6 ; Fig. 5.7e) are more common in the east (Fig. 5.8). Tabular sandstone elements can be traced laterally for up to 500 m in dip-oriented sections (average 300 m). A variety of trace fossils characterise the Middle Palisade Zone, notably *Arenicolites*, *Teredolites* (Fig. 5.6e), *Ophiomorpha* (Fig. 5.6f), *Rhizocorallium*, with an increase in bioturbation intensity and diversity towards the east, from 1 to 5 (Taylor and Goldring 1993). Trace fossils commonly occur as mono-ichnospecific assemblages towards the top of beds and are of a limited size but a high density. Within all sandstone elements (S_3 to S_7), silt-draped ripples are abundant (Fig. 5.6a, b), as are lenticular, wavy and flaser bedding (Figs. 5.6a, 5.9-3C), and rare symmetrical ripple lamination (Fig. 5.9-3C). Where more than one sandstone-dominated element is observed within the Middle Palisade Zone, the lowermost element is either a coarsening-upwards

sandstone or tabular sandstone element (S_6 or S_7), and the upper is either a sandstone-dominated or heterolithic lenticular element (S_3 or S_4) (e.g. West Crescent Mine and East Salt Wash). Palaeocurrents in this package (Fig. 5.9-3B) show a wide range: the dominant direction is towards the SE, with subordinate trends to the north and south.

5.4.3.2 Interpretation

The dominant depositional environment interpreted from both the ichnological assemblage, density and size of traces is a brackish-water to marine setting (Bromley 1996; Gingras et al. 2012), although *Teredolites* can be rafted up-stream into fresh water settings (Shanley et al. 1992; Lavigne 1999). Sedimentary structures indicative of tidal influence (Shanley et al. 1992) occur within sandstones throughout this package and are present at the most up-dip localities (West Floy; Fig. 5.5). Fine-grained elements (F_2 ; Table 5.1) in this package are indicative of either floodplain or lagoonal environments, depending on the presence or absence of plant material with rooted horizons, or bioturbation indicative of the terrestrial nature of siltstone and mudstone beds (Horne et al. 1978; Guion et al. 1995) (Table 5.1). The tabular sandstone elements (S_6) are interpreted as minor washover fans constructed from a distal barrier or spit and preserved via in-place drowning (Sanders and Kumar 1975; Penland et al. 1988) (Table 5.1; Fig. 5.9-3D). The wide variability of palaeocurrents (Fig. 5.9-3B) is attributed to a combination of flow reversals within channelised elements (S_3 , S_4) and the sinuous nature of the channels and modification at the shoreline, for example by longshore currents (Fig. 5.9-3D) (Shanley et al. 1992; Bhattacharya and Giosan 2003). The change in process influence between lower and upper elements within the Middle Palisade Zone, with underlying elements being more marine influenced and upper elements more fluvial influenced, is interpreted to record an initial marine incursion and the subsequent filling of accommodation in response to progradation of fluvial systems as part of a transgressive interval (Fig. 5.9).

The wide range of architectural elements (S_3 to S_7) within the Middle Palisade Zone is indicative of modification by a variety of combinations of fluvial, wave and tide processes (Table 5.1). There is a down-dip change in architectural elements whereby, towards the west, fluvial elements (S_{3-4}) occur encased within floodplain fines (F_2 ; Table 5.1), whereas to the east marine influenced elements are encased within fine-grained lagoonal deposits (Figs. 5.5, 5.8). The spatial variability of multiple coeval sub-environments likely records the interplay of fluvial, wave and tidal processes.

5.4.4 Upper Palisade Zone

5.4.4.1 Description

This package (Fig. 5.8) is dominated by fine-grained deposits (66%; F₂), small-scale sandstones and siltstones (5%; F₁; Fig. 5.7G), lenticular elements (S₃ and S₄; 24%; Figs. 5.7B, C; 5.9-4A), and coarsening-upwards sandstones (1%; S₇; Fig. 5.7E). Within this package, coal (4% overall) decreases in abundance to the east (Figs. 5.5, 5.8). The occurrence of sandstone dominated elements (S₃ and S₄) decreases to the east (Fig. 5.8). Palaeocurrents exhibit wide variability (Fig. 5.9-4B) but are overall directed towards the east. Sedimentary structures include lenticular bedding, mud and carbonaceous draped ripple forms (Fig. 6A) and *Teredolites* bored wood (Fig. 5.6E) within the basal-most parts of lateral accretion elements (S₃; Fig. 5.9-4C).

5.4.4.2 Interpretation

The palaeoenvironment was dominated by a floodplain containing small raised mires traversed by small sinuous channels (Fig. 5.9-4D). Draped ripples present within sandstone-prone lateral accretion elements (S₃; Fig. 5.8) suggests fluctuating flow energies, which were likely caused by tidal or discharge variations (cf. Thomas et al. 1987). The decrease in the occurrence of lateral accretion deposits towards the east may be due to the line of outcrop failing to intersect major channel bodies (Fig. 5.9-4D). Alternatively, this may reflect lateral changes through the FMTZ. The presence of *Teredolites* indicates close proximity to a brackish environment, likely within the zone of tidal push (Shanley et al. 1992; Lavigne 1999).

5.4.5 Ballard Zone

5.4.5.1 Description

Occurring stratigraphically between the BBSB and TCSB (Fig. 5.8), this package has large proportions of coal (15%; F₃; Fig. 5.9-6A), with seams up to 3 m thick, which previous authors have named the Ballard Coal Zone (Cole 2008; Shiers et al. 2014). Within this package, there occur a high proportion of organic-prone, fine-grained elements (67%; F₂; Fig. 5.7H) with intervening ribbon channel-fill elements (S₂), which are 3-7 m thick (Table 5.1) and small (5 m thick) lenticular sandstone elements (S₃), which together make up 15% of the package (Fig. 5.8). Within the ribbon channel-fills (S₂) (Fig. 5.7A), carbonaceous and mud drapes on foresets and bottomsets of cross-beds, and rare mud drapes on ripple forms on the uppermost surface of the elements are observed (Fig. 5.9-6C). Palaeocurrents within these bodies are aligned to the south and east (Fig. 5.9-6B), indicating that channel-fills are oriented in this direction, and are surrounded by dominantly coal-prone floodplain (F₂, F₃;

Fig. 5.9-6D). Bioturbation (*Skolithos* and *Arenicolites*, *Thalassinoides*) are observed in abundance within mono-specific assemblages in the basal-most parts of elements, as are lags containing fossil wood debris with *Teredolites* (Fig. 5.6E).

5.4.5.2 Interpretation

Fine-grained deposits (F_2) in this package are interpreted to be of terrestrial origin due to the high organic content, as well as the presence of rooted horizons (Fig. 5.8). Distributary channel-fill elements are interpreted based on the arrangement of internal lithofacies and the external geometry of the sand bodies (Colombera et al. 2016) (Table 5.1). Ichnogenera present within the base of these channelised elements indicate deposition within marine-to-brackish water (Tonkin 2012). However, the majority of the channel-fills show little evidence of modification by marine processes. This may be due to overprinting of marine influence during river floods (Colombera et al. 2016). Sandstone-dominated lateral accretion elements (S_3) do not record indicators of marine influence, and are interpreted as meandering fluvial channels, possibly tie channels between larger distributary channels (Fig. 5.9-6D) within a delta-plain setting. Overall this package is interpreted as fluvially dominated with some minor modification by tides within the lower parts of distributary channel fills.

5.4.6 Basal Ballard and Thompson Canyon Sandstone Beds

5.4.6.1 Description

Bounding the Ballard Zone at the base is the Basal Ballard Sandstone Bed (BBSB) and at the top is the Thompson Canyon Sandstone Bed (TCSB); both form distinctive tabular marker sandstone bodies (Table 5.1; Fig. 5.6E). The TCSB is made up of a lower fine-grained package and an upper tabular sandstone body (Table 5.1; Fig. 5.5). Together, they are commonly bounded above and below by coals (Figs. 5.5, 5.8, 5.10B). Palaeocurrents measured from ripple forms in the BBSB and TCSB are predominantly directed towards the southeast and east, respectively (Fig. 5.9-5B, 7B). The BBSB pinches out between the East Floy and West Floy study sites over a distance of 2.5 km (Fig. 5.8). This pinch-out is marked at West Floy by a thin siltstone between two coal beds; the siltstone contains a mono-species assemblage of *Arenicolites* of diminutive size.

The lower portion of the TCSB has abundant *Thalassinoides* (Fig. 5.6D) directly below the base (Fig. 5.5). The lower part of the TCSB is fine-grained and heavily bioturbated, masking any original sedimentary structures (Table 5.1). Bioturbation within the reworked barrier sandstone elements (S_6), including the upper portion of the TCSB, comprises *Ophiomorpha* (Fig. 5.6F), *Planolites*, *Bergaueria*, and *Arenicolites*, which increase in intensity and abundance towards the east. Sedimentary structures within sandy portions of the BBSB

and TCSB include low-angle laminations, symmetrical ripple lamination, and asymmetrical ripple lamination that exhibits both single and double mud and silt drapes in the lowermost beds of the element (S₆; Table 5.1).

5.4.6.2 Interpretation

The ichnology of the siltstone that marks the pinch-out of the BBSB around Floy Canyon is low diversity and traces are of a limited size, therefore most likely representing a marine or brackish environment (cf. Tonkin 2012). The increase in intensity and diversity of the bioturbation within the BBSB and TCSB (increasing towards the east from a BI of 1 to 5; Fig. 5.6F) indicates an environment that became increasingly marine influenced with more stable salinity to the east (cf. Bromley 1996; Tonkin 2012). The sedimentary structures in the TCSB and BBSB (Table 5.1) indicate the influence of wave processes, with drapes on the ripples indicative of tidal influence.

The lower portion of the TCSB is interpreted as lagoonal or interdistributary bay fines, whilst the upper part and the BBSB are interpreted as part of a back-stepping barrier complex (Table 5.1). Preservation of the unit indicates that transgressive submergence (cf. Penland et al. 1988), in-place drowning (cf. Sanders and Kumar 1975) or shoreface retreat (cf. Penland et al. 1988) of the barrier complex has occurred. The style and stratigraphic expression of barrier retreat, or rollover, is controlled by the interplay of substrate slope, sediment supply, rate of sea-level rise and back-barrier accommodation (Mellett et al. 2012). Where barriers are drowned in place then sands would be preserved as isolated ribbons at successive locations (Sanders and Kumar 1975), counter to the laterally extensive sand bodies of the BBSB and TCSB. Barrier rollover retreat leads to the formation of a sand blanket that infills the back barrier and overlying lagoonal sediments. Barrier retreat is most commonly associated with an erosional unconformity or ravinement surface (Cattaneo and Steel 2003), such surfaces are not observed within the Lower Neslen Formation. Transgressive submergence is therefore the most likely mode of preservation of shelf sand bodies (barrier complexes and sheet sands) without the preservation of the shoreline sands these bodies were derived from (Penland et al. 1988). Such sand bodies preserved via transgressive submergence likely accumulated down-drift of transgressed delta complexes. Coarsening-upwards trends within tabular sandstone elements are interpreted to reflect migration of linear, storm-generated sandbars.

The TCSB and BBSB are considered to be marker horizons within the studied stratigraphy. The interpretation of the TCSB and BBSB as being deposited as part of a back-stepping barrier complex has implications for the interpreted sequence stratigraphy of the lower Neslen Formation. The facies dislocation at the base of the elements (heavily marine bioturbated (BI of 4-5) is juxtaposed on top of coal; the base of the marine siltstone is

commonly covered with *Thalassinoides*) indicates a major change in depositional environment across this surface, and leads to its interpretation as a flooding surface. The interpretation that the base of laterally extensive tabular sandstone elements as a flooding surface is further justified by the presence of prominent coal horizons (Fig. 5.8). It is common for thick coals to be topped by flooding surfaces and capped by marine beds (Arditto 1987; 1991; Flint et al. 1995). This assigns the TCSB and BBSB as transgressive barrier island complexes in which the initial origin of the sand has been obliterated and sediment has been reworked into extensive sand sheets (cf. Bridges 1976; Hobday and Jackson 1979; Galloway 1986; Willis and Moslow 1994) and is in accordance with models proposed for the Atlantic coastline of the USA where barriers have prograded in a landward direction (cf. Swift 1975; Swift et al. 1985; Kraft et al. 1987).

A rejection of a forced regressive shoreface origin for tabular sandstone elements is laid out in chapter 4. Although individual stratigraphic logs through the TCSB superficially appear similar to a prograding shoreface parasequence, topped by a flooding surface is discounted based on the facies within the architectural elements; and the facies juxtaposition at the base of the elements.

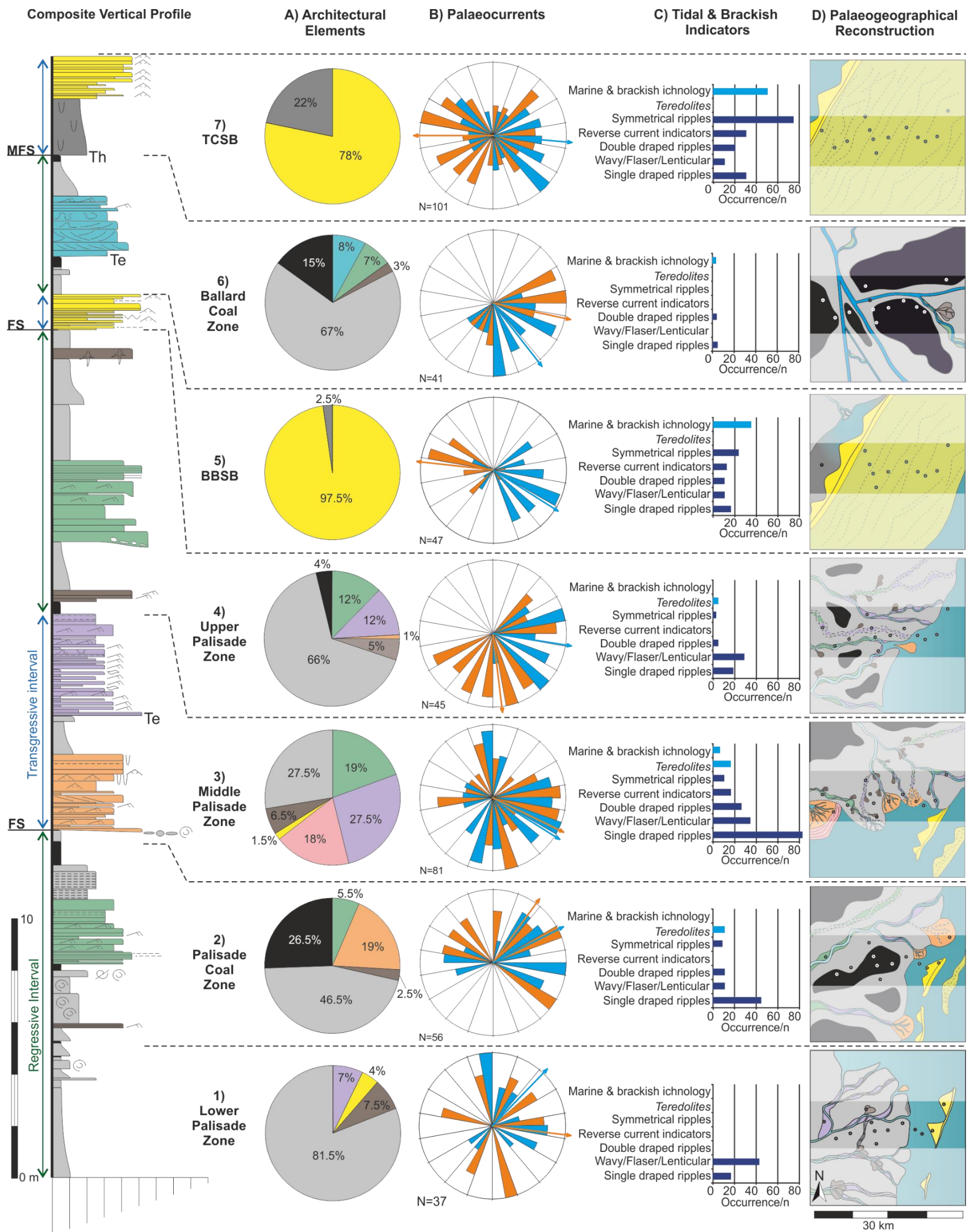


Figure 5.8: Summary of vertical trends through the lower Neslen Formation. An idealized, composite sedimentary section is shown on the left-hand side and is divided into the interpreted depositional packages. Regressive intervals (green) and transgressive intervals (blue) are indicated the line of section along with the position of interpreted flooding surfaces. A) Architectural element proportions (for key see Figure 5.7). B) Summary paleocurrent orientations for each package; orange represents bedding or lateral accretion surfaces, blue represents the dip direction of ripples and cross-bedded strata. C) Occurrence of key indicators of marine (tidal and wave indicators) and brackish water conditions. Sedimentary indicators (dark blue) are interpreted to represent fluctuations in current energy and directions. Marine to brackish ichnogenera includes *Ophiomorpha*, *Arenicolites*, *Thalassinoides*, *Rhizocorallium*, *Bergaueria*, and *Diplocraterion*. D) Paleogeographic reconstruction for each package; accurate in the proportion and dimensions of architectural elements and paleoflows. Circles represent study sites. See Figure 5.5 for key.

5.5 Discussion

5.5.1 Stratigraphic variations

Vertical and lateral trends within and between the depositional packages are important in understanding the temporal and spatial variations in the sedimentary succession. Within the majority of depositional packages, there is a down-dip (i.e. west to east) variability in architectural elements from dominantly fluvial with higher proportions of coal dominated elements, to architectural elements which exhibit marine influence encased within coal-poor, fine-grained mudstone and siltstone (Figs. 5.5, 5.8). The Middle Palisade Zone (MPZ) records a change from dominantly fluvial elements encased within floodplain fines in the west, to marine-influenced elements encapsulated by fine-grained elements of lagoon origin in the east (Fig. 5.9-3D). Packages were increasingly influenced by marine processes towards the east as part of the FMTZ (Fig. 5.1c). Architectural elements deposited within a depositional package were not necessarily coeval. Examination of the relative change in elements, sedimentary structures and ichnology (Fig. 5.5) recorded at study locations in close proximity to each other are required to recognise these changes. Stratigraphically, the palaeoenvironment changes from a fluvial dominated delta plain, which is influenced to some extent by tidal processes, to a wave dominated shoreline system (Fig. 5.9D).

The sandstone dominated MPZ contains abundant marine indicators (Figs. 5.5, 5.9-3C) within a thin interval (8 m average thickness) and lies stratigraphically between the Palisade Coal Zone and Upper Palisade Zone, which themselves contain relatively fewer marine indicators within sandstone elements (Fig. 5.9C). Architectural elements within the MPZ record significant spatial variability (Fig. 5.9-3D) within an overall shallowing upwards trend, which continues into the Upper Palisade Zone (Fig. 5.8). The MPZ records deposition within a lower delta-plain setting that was substantially modified by marine processes, given the presence of structures indicative of tidal influence as well as brackish water ichnology. This markedly marine-influenced package occurs at a point in the stratigraphy that has not been accounted for by previous sequence stratigraphic interpretations (e.g. Hettlinger and Kirshbaum 2003; Aschoff and Steel 2011 a, b) (Figs. 3.8; 5.2). The marine influenced nature of the MPZ is similar to that described for the middle Castlegate Sandstone (McLaurin and Steel 2000).

The BBSB and TCSB are interpreted as variably wave-dominated, back-stepping barrier complexes (Sanders and Kumar 1975; Penland et al. 1988). The greater thickness and extent of the TCSB, together with the more intense bioturbation, and the occurrence of trace

fossils such as *Ophiomorpha* (Fig. 5.6f), are indicative of greater open-marine conditions than the BBSB. This shows that, overall, the MPZ, BBSB and TCSB become increasingly modified by marine processes upwards (Fig. 5.10). The shift in relative marine conditions is not necessarily a function of a proximal-distal relationship, rather changes in the rate of deposition from the MPZ to the BBSB and TCSB or lateral changes in palaeoenvironment to a more protected coastal setting or could also be important.

5.5.2 Marine-influenced packages

Prediction of the way in which marine-influenced packages correlate with down-dip flooding surfaces and shoreface deposits, and the controls on their occurrence within the stratigraphy, is important for gaining an improved understanding of the way in which coastal plains respond to sea-level change. The controls on the occurrence and position of the MPZ, BBSB and TCSB can be attributed to autogenic or allogenic processes, as considered below.

5.5.2.1 Allogenic processes

Correlations of the lower Neslen Formation indicate that the TCSB is contiguous to the tongue of mudstone between the Corcoran and Cozzette members of the Îles Formation (Kirschbaum and Spear 2012; MFS 3: Fig. 5.2). The base of the TCSB is interpreted as the MFS. This is supported by the sharp contact of the lower TCSB which has abundant *Thalassinoides* directly below its base (Fig. 5.6d), a thickening and coarsening upward trend within the TCSB, and an underlying, well-developed coal seam (Fig. 5.10b). The base of the TCSB represents an abrupt and significant deepening in depositional environment from peat mire to lagoonal fines and wave-modified sandstone (Fig. 5.10). The base of the BBSB, which has a lateral extent of at least 18 km, displays a facies dislocation at its base from coal to wave-modified sandstone (S_6). Additionally, it possesses a similar internal lithofacies composition and architecture to the TCSB, and therefore likely represents a minor flooding surface (FS; Fig. 5.10).

The MPZ contains a wide range of architectural elements, which contain abundant evidence for marine influence. As a marine-influenced package additional to, and lower in the stratigraphy than, the BBSB and TCSB, it is likely that this package correlates down dip to minor tongues of the Mancos Shale within the Corcoran Member (Fig. 5.2); this correlation has not been previously proposed. The marine incursion responsible for deposition of the MPZ is therefore interpreted as the most landward expression of transgression that was on-going further seaward (cf. Rudolph et al. 2015), similar to that described in the Castlegate Formation (McLaurin and Steel 2000).

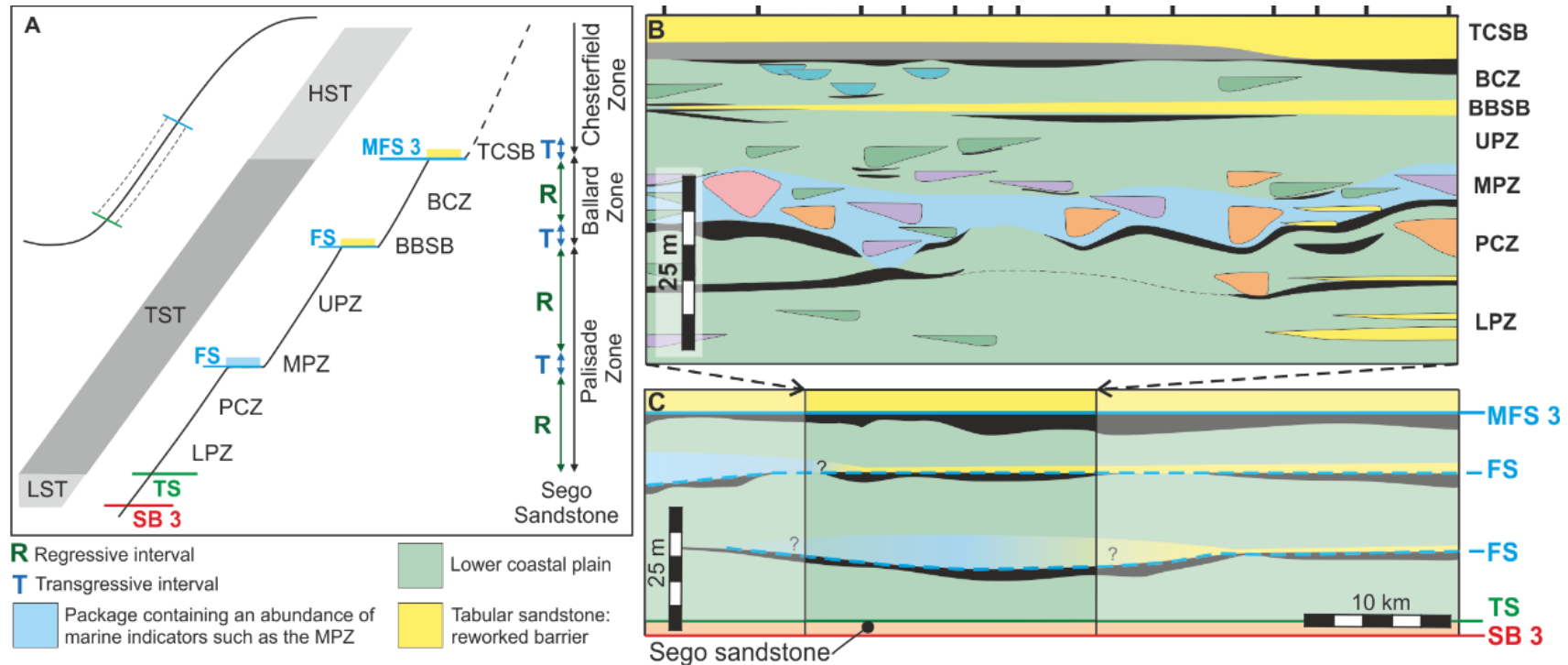


Figure 5.9: A) Modified sea-level curve for the lower Neslen Formation; sequence boundaries and flooding surfaces are named on Figure 5.2. Depositional packages are as follows: Lower Palisade Zone (LPZ), Palisade Coal Zone (PCZ), Middle Palisade Zone (MPZ), Upper Palisade Zone (UPZ), Basal Ballard Sandstone Bed (BBSB), Ballard Coal Zone (BCZ) and Thompson Canyon Sandstone Bed (upper and lower) (TCSB). Intervals of regression (R; green) and transgression (T; blue) are indicated along the sea-level curve. B) Dip-cross section of the lower Neslen Formation; geometries of sandbodies are schematic. C) Relationship of the lower Neslen Formation within the broader sequence stratigraphic panel (Fig. 5.2). Key for architectural elements is shown in Figure 5.5.

The successive increase in marine processes preserved upwards from the MPZ to the BBSB and ultimately to the TCSB indicates that the lower Neslen Formation records an overall episode of transgression punctuated by variations in the rate of sea-level change or in sediment supply, which modify the rate of transgression (Fig. 5.10a). No relative sea-level fall is interpreted between flooding surfaces, rather a decrease in rate of relative sea-level rise relative to the rate of sediment supply results in the deposition of regressive, progradational intervals (Figs. 5.9, 5.10a). The low gradient of the coastal delta plain (Colombera et al. 2016) means that even minor relative sea-level rise would flood broad portions of the coastal plain. The refined stratigraphic framework (Fig. 5.10a) exhibits a series of retrogradationally stacked wave-dominated sandstones within a net transgressive tract (Fig. 5.10c).

5.5.2.2 Autogenic processes

Autogenic processes such as coal compaction and delta auto-retreat are important considerations when analysing the cause of overall transgression within a paralic succession.

Marine-influenced packages (MPZ, BBSB and TCSB) may have been produced by purely autogenic processes intrinsic to the evolution of the system. These packages may be referred to as 'auto-breaks' within an overall progradational sequence (Fig. 5.2) which was subject to auto-retreat (the landward retreat of a shoreline which occurs inevitably, under conditions of constant rate of relative sea-level rise and without change in basin conditions: Muto and Steel 1992; 1997).

The MPZ and TCSB are underlain by coal zones, and the BBSB is underlain by coal in four up-dip and central localities (Fig. 5.8). The distribution of coal through the Neslen Formation can be used to explain the location of marine-influenced packages, as well as their thickness and internal character. It is common for significant coal deposits to accumulate above and landward of shoreface sandstone bodies (Ryer 1981; Cross 1988; Jerrett et al. 2011a, b). This suggests that the up-dip limit of shorefaces (i.e. the extent of transgression) is defined by the seaward-most position of raised coal mires. This is because raised mires withstand erosion and hence are able to buffer transgression (McCabe 1985; Kamola and Van Wagoner 1995; Jerrett et al. 2011b). Mires and swamps in coastal-plain and delta-plain settings can rapidly compact to a level that is equal to or lower than sea level (e.g. Mississippi region – St Bernard and Lafourche deltas; Blum and Roberts 2009; California – Sacramento-San Joaquin Delta; Miller et al. 2008; Ganges–Brahmaputra Delta; Schmidt 2015). Auto-compaction of coal occurs rapidly following deposition (Fielding 1984; 1985; Nadon 1998; Ryer and Langer 1980; Courel 1987), which encourages marine inundation over broad areas of the coastal plain adjacent to sites of clastic accumulation that compact less (Kosters and

Bailey 1983; van Asselen et al. 2009; Jerrett et al. 2011a, b). Such a process means that transgression in response to low-amplitude sea-level rise can occur passively (i.e. with low energy) over a low-relief and low-gradient coastal plain. This differential compaction can also explain the juxtaposition of architectural elements observed within the Neslen Formation (e.g. MPZ; Fig. 5.9-3D) and the occurrence of marine-influenced or marine-dominated intervals (MPZ, BBSB and TCSB; Figs. 5.8, 5.10). Differential compaction, and the subsequent filling of the newly generated accommodation might also play a role in sediment partitioning by reducing the delivery of sediment to the shoreline, and hence decreasing the rate of delta or shoreface progradation and favoring barrier preservation in a similar way to the behavior of local accommodation created by growth faults proximal to the shelf edge (cf. Olariu and Olariu 2015).

Relative sea-level rise may be driven by autogenic coal compaction, rather than eustatic sea-level change. This is notably evident in the MPZ; where more than one architectural element is observed, the lower is more influenced by marine processes (Figs. 5.8, 5.10). The thickness of coal seams is greatest where there is no underlying sandstone (e.g. Palisade Coal Zone at East Floy) and thinnest where sandstone-dominated elements occur (e.g. Ballard Coal Zone at Right Hand Crescent). This is due to differential rates and amounts of compaction of sandstone-prone elements compared to fine-grained and coal-prone elements (F_2 and F_3). A sandstone element (S_2 to S_7) will undergo less post-depositional compaction than an adjacent fine-grained elements (F_2 and F_3). As such, the accommodation generated after deposition will be greatest above a fine grained, or coal prone element. Where coal fills this accommodation, the deposits will be thinner where they overlie a sandstone-prone element (Fig. 5.8). Differential compaction explains why the MPZ, BBSB and TCSB are thickest where they overly thick in place coal accumulations where they show an increase in abundance of marine indicators (Figs. 5.8, 5.10b).

5.6 Summary

Use of a dataset with closely spaced sections, has allowed the correlation of paralic strata within the coal-bearing lower Neslen Formation. This method has enabled recognition of discrete stratal packages within an ancient low-gradient, low-relief coastal plain and shoreline succession, which records sedimentological and stratigraphical evidence for modification by interplay of fluvial, wave and tidal processes.

Correlation of marine-influenced packages helps to refine the established sequence stratigraphic framework, which overall indicates that the lower Neslen Formation accumulated as part of a long-term TST. The deposition and preservation of three marine

influenced packages (MPZ, BBSB and TCSB) arose in response to three laterally extensive, but small scale cycles of relative sea-level change, which increased in amplitude over time (i.e. upwards in the succession). The base of the TCSB marks a regional maximum flooding surface, which likely correlates down-dip to a tongue of Mancos Shale between the Corcoran and Cozzette members of the Îles Formation of open marine origin. The BBSB and MPZ record minor floods across the coastal plain as part of an overall episode of punctuated relative sea-level rise.

The impact of peat-developing environments in low-gradient coastal plains is significant. Peat mires initially act as buffers to sea-level rise. Following deposition, auto-compaction of peat during its transformation to coal reaches a threshold level beyond which widespread marine incursion may occur rapidly over the coastal plain. Lateral variability in the distribution of peat mires across a low-gradient coastal plain result in shifting patterns of accommodation generation. This may result in the juxtaposition of a broad range of depositional environments, leading to the preservation of complicated facies patterns and architectural relationships.

Overall, this study shows that the interplay of autogenic and allogenic controls on the sedimentary evolution of the succession is complicated. The role of autogenic processes, such as coal compaction, is often overlooked but the rate and extent of marine transgression associated with moderate relative sea-level rise in low-gradient, low relief coastal settings may be driven by auto-compaction of peat mires in the coastal plain.

6 Controls on the depositional architecture of fluvial point-bar elements in a coastal plain setting

The internal and external architecture of point-bar elements record the evolution of the associated channel through time. This chapter aims to refine traditional facies models that describe the anatomy of fluvial point-bar elements and to discuss the autogenic and allogenic controls on their formation.

Within the Campanian Neslen Formation, 41 point-bar elements located within an established sequence stratigraphic framework have been analysed through combined use of sedimentary logs, stratigraphic panels and palaeocurrent analysis. Results show that individual point-bar elements increase in width-to-thickness aspect ratio and become increasingly amalgamated upwards. Four distinct point-bar element types are identified based upon their lithofacies assemblages and external geometry. Two of these point-bar types conform to traditional facies models; however two exhibit an unusually low proportion of cross-bedded sandstone and a higher proportion of massive sandstone, horizontally laminated sandstone and ripple-laminated sandstone. The occurrence of these atypical point-bar assemblages is restricted to the lower and middle parts of the Neslen Formation. A relational database, which provides data on the geometry of point-bar elements and facies proportions, is used to compare the lithofacies arrangement and architecture of point-bar elements from the Neslen Formation to those in other humid-climate, coastal-plain successions.

The upward increase in aspect ratio and amalgamation of point-bar elements through the Neslen Formation reflects an upward decrease in the rate of accommodation generation and/or increase in the rate of sediment supply. The deposition of point-bar elements with lower proportions of cross-bedded sandstone in the lower Neslen Formation can be attributed to low stream power linked to the lower rates of sediment supply that are interpreted for this interval. The high level of detail used to analyse the point-bar elements in this study allows for the recognition of previously under-described point-bar assemblages.

6.1 Introduction

Studies of point bars in both fluvial and tidal environments (e.g. Visher 1965; Allen 1965; 1983; McGowen and Garner 1970; Barwis 1977; Jackson II 1976; 1978; Miall 1977; 1985; 1988; Nanson 1980; Harms et al. 1982; Nanson and Page 1983; Smith 1987; Cloyd et

al. 1990; Allen 1991; Nio and Yang 1991; Rasanen et al 1995; Galloway and Hobday 1996; Fenies and Faugères 1998; Leeder 1999; Brekke and Couch 2011; Johnson and Dashtgard 2014) identify a series of commonly occurring lithofacies and depict their proportions, dimensions and transitions, often in the form of facies models (Fig. 6.1a). Many of these facies models also relate the sedimentology to fundamental flow processes; for example the common fining upwards of point-bar elements (Bernard et al. 1962; Allen 1963; Miall 1996) records energy dissipation through filling of the associated channel. However, there are many variations to the typical facies assemblages displayed in Figure 6.1a (e.g. Doeglas 1962; Thomas et al. 1987; Smith et al. 2009), many of these are recorded in the Fluvial Architecture Knowledge Transfer System (FAKTS), a relational database that includes lithofacies proportions and geometries of fluvial deposits from a wide variety of successions (Colombera et al. 2012; 2013a, b) (Fig. 6.2a). The documented variability in the lithofacies assemblage of point-bar elements (Fig. 6.2b-h) and the range of width-to-thickness aspect ratios (Fig. 6.2i), mean no single facies model can be applied universally to account for stratigraphic complexity in fluvial point-bar deposits. For example, many fluvial point-bar elements are heterolithic (e.g. McMurray Formation, Fig. 6.2b; Fairlight Clay Formation, Fig. 6.2d; Wessex Formation, Fig. 6.2g) and are characterised by inclined heterolithic stratification (IHS; Fig. 6.1b) (Weimer et al. 1982; Demowbray 1983; Thomas et al. 1987; Shanley et al. 1992; Turner and Eriksson 1999; Choi et al. 2004; 2010; 2011; Dalrymple and Choi 2007; Hovikoski et al. 2008; Choi 2011; Brekke and Couch 2011; Sisulak and Dashtgard 2012; Johnson and Dashtgard 2014). Stratigraphic heterogeneity represented by IHS most commonly takes the form of mud-draping on bar fronts (Fig. 6.1b), whereby mud is deposited during episodes of reduced flow, which can be associated with tidal processes (e.g. Weimer et al. 1982; Thomas et al. 1987; Shanley et al. 1992; Choi et al. 2004; Dalrymple and Choi 2007; Hovikoski et al. 2008; Sisulak and Dashtgard 2012; Johnson and Dashtgard 2014). In other cases this draping is associated with secondary or counter currents, for example during the development of counter point bars in fully fluvial settings (e.g. Smith et al. 2009).

There are three main allogenic controls influence point-bar architecture (Cecil et al. 1993; Blum and Törnqvist 2000; Hampson et al. 2012; Shiers et al. 2014) and stacking patterns (Leeder 1977; Bridge and Leeder 1979; Bristow and Best 1993; Mackey and Bridge 1995; Heller and Paola 1996): tectonism, climate change and eustasy (Miall 2014), which impact upon a range of parameters, including hinterland geology, flood basin size, longitudinal river profile, river sinuosity, base-level position and rate of change, rate of accommodation generation, bedload type, vegetation type and abundance, soil and floodplain type, levee development, channel sinuosity, gradient and relief of the alluvial-coastal plain, and degree of marine influence and backwater length (Schumm 1968; Steel

and Aasheim 1978, Miall 1987; Einsele 1992; Cecil et al. 1993; Wallinga et al. 2004; Erkens et al. 2009; Hampson et al. 2012; Miall 2014; Ielpi and Ghinassi 2014; Miall 2014; Colombera et al. 2016; Nyberg and Howell 2016). Autogenic controls are also important; these include mechanisms of channel avulsion, auto-compaction of floodplain sediments and the style of fluvial system (i.e. distributive vs. tributive) (Stouthamer and Berendsen 2007; Jones and Schumm 2009; Erkens et al. 2009; Miall 2014; Shiers et al. 2014). From an applied standpoint, understanding these controls will allow enhanced understanding of the distribution of facies, including the development of IHS (Thomas et al. 1987; Choi 2011; Sisulak and Dashtgard 2012), and the deposition of heterolithic facies (e.g. flaser, lenticular and wavy bedding). This will have major implications on hydrocarbon reservoir behaviour, and on water flow and contaminant transport in groundwater aquifers. Fine-grained deposits tend to act as baffles or even barriers to fluid flow (mesoscopic heterogeneity: Tyler and Finley 1991; Miall 2014).

Relatively few studies have integrated detailed sedimentological data of multiple point-bar deposits distributed laterally and vertically through a succession for which an established sequence stratigraphic framework – and hence accommodation state – is well constrained. The aim of this study is to discuss the controls that give rise to a varied range of facies distributions within point-bar elements present in a fluvial succession. To achieve this aim, a detailed study of exhumed point-bar elements in the Campanian Neslen Formation of Utah has been undertaken. Specific objectives of this study are as follows: (i) to describe the typical facies arrangements of point-bar elements within the Neslen Formation; (ii) to establish how point-bar elements accumulate vertically through the formation; (iii) to compare and contrast the architecture and facies distributions of point-bar elements in the Neslen Formation to both previously proposed facies models and other comparable successions; and (iv) to develop an understanding of the controls on both the internal lithofacies within point-bar elements and their vertical stacking.

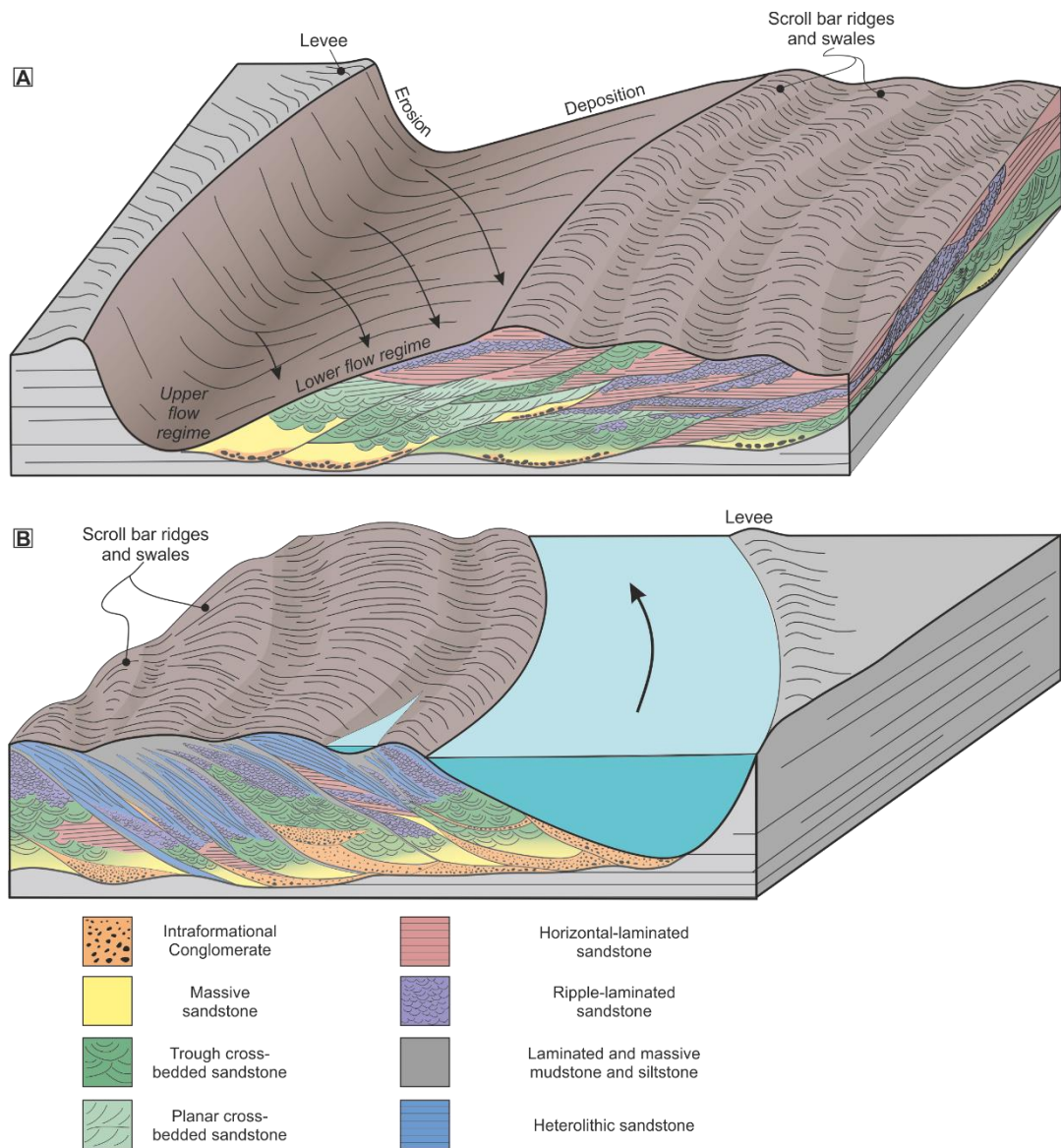


Figure 6.1: Conceptual model of point-bar elements. A) Three-dimensional depositional model of facies and architecture of a sandstone-dominated point-bar element (adapted after Cant and Walker 1978; Nanson 1980; Allen 1982; Walker 1984; Miall 1985; Miall 1988; Ghazi and Mountney 2009; Colombera et al. 2013b). B) Three-dimensional depositional model of facies and architecture of a heterolithic point-bar element (adapted in part from Thomas et al. 1987; Smith et al. 2009; Labrecque et al. 2011; Fustic et al. 2012; Musial et al. 2012).

6.2 Geological Setting

Data have been collected from 41 exhumed point-bar elements identified in the Campanian Neslen Formation, which forms part of the Upper Cretaceous Mesaverde Group and crops out along the Book Cliffs of eastern Utah (Fig. 6.3). The Neslen Formation was deposited in a low-gradient (Colombera et al. 2016), low-relief (Cole and Cumella 2003) lower fluvial plain and coastal plain setting. The succession comprises sandstones encased within argillaceous, commonly coal-bearing strata (Young 1957; Fisher et al. 1960; Willis 2000; Cole 2008; Colombera et al. 2016; Shiers et al. 2014; Chapter 5).

The succession is interpreted as the accumulated sedimentary record of fluvial floodplain, upper- and lower-delta plain palaeoenvironments (Kirschbaum and Hettinger 2004; Aschoff and Steel 2011a; Shiers et al. 2014; Chapter 5). Tabular sandstone bodies present within the Neslen Formation are interpreted as being of barrier origin (Chapter 5) and include the Thompson Canyon Sandstone Bed (TCSB), which has a lateral continuity of at least 45 km (Gualtieri 1991), and the Basal Ballard Sandstone Bed (BBSB), which has a lateral continuity of at least 18 km (Chapter 5). These architectural elements, together with the presence of laterally extensive coal zones, form stratigraphic references for observations of adjoining packages of strata (cf. Colombera et al. 2016) (Fig. 6.4).

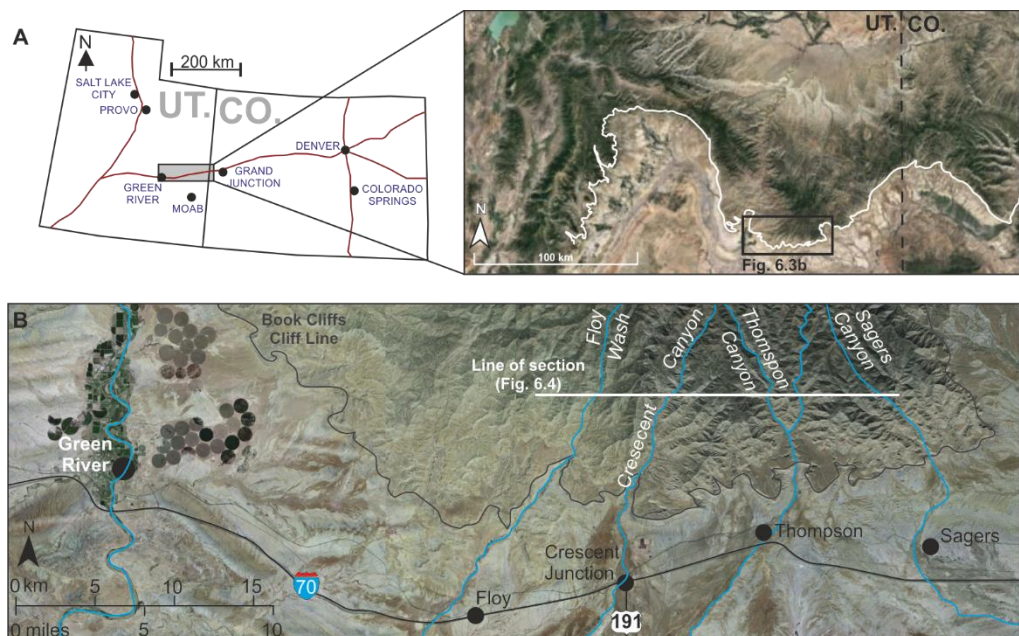


Figure 6.3: Study location map. A) Location of the study area in the Book Cliffs. B) Location of the studied stratigraphy between Floy Canyon and Saggers Canyon (Fig. 6.4). GoogleEarth ©. UT = Utah, CO = Colorado.

6.3 Methods

Field-based outcrop investigation involved the recognition of sedimentary bodies considered representative of fluvial point-bar deposits. Architectural elements selected for detailed study were characterised at outcrop by their facies succession, occurrence of inclined surfaces, and external geometry, together with palaeocurrent analysis. Field study has focused on the identification and facies characterisation of 41 sand bodies interpreted to have accumulated as point bars in response to the evolution of meandering fluvial channels. The stratigraphic position of studied point-bar elements was determined in relation to the top of the underlying Sege Sandstone, as well as their position relative to the marker beds of the TCSB and BBSB (cf. Colombera et al. 2016).

The studied point-bar elements are distributed laterally and vertically through the Neslen Formation (Figs. 6.3, 6.4). Twenty studied outcrops are located in the lower Neslen Formation: 13 in the Palisade Zone; 3 in the Ballard Zone. Four examples are in the lower Chesterfield Zone (Fig. 6.4). A further 22 sandstone bodies were investigated from the upper Chesterfield Zone (Fig. 6.4). For the studied point-bar elements, the external geometries (width and depth), internal lithofacies and bounding-surface orientations were measured. The relationship of point-bar elements to surrounding elements was captured through the

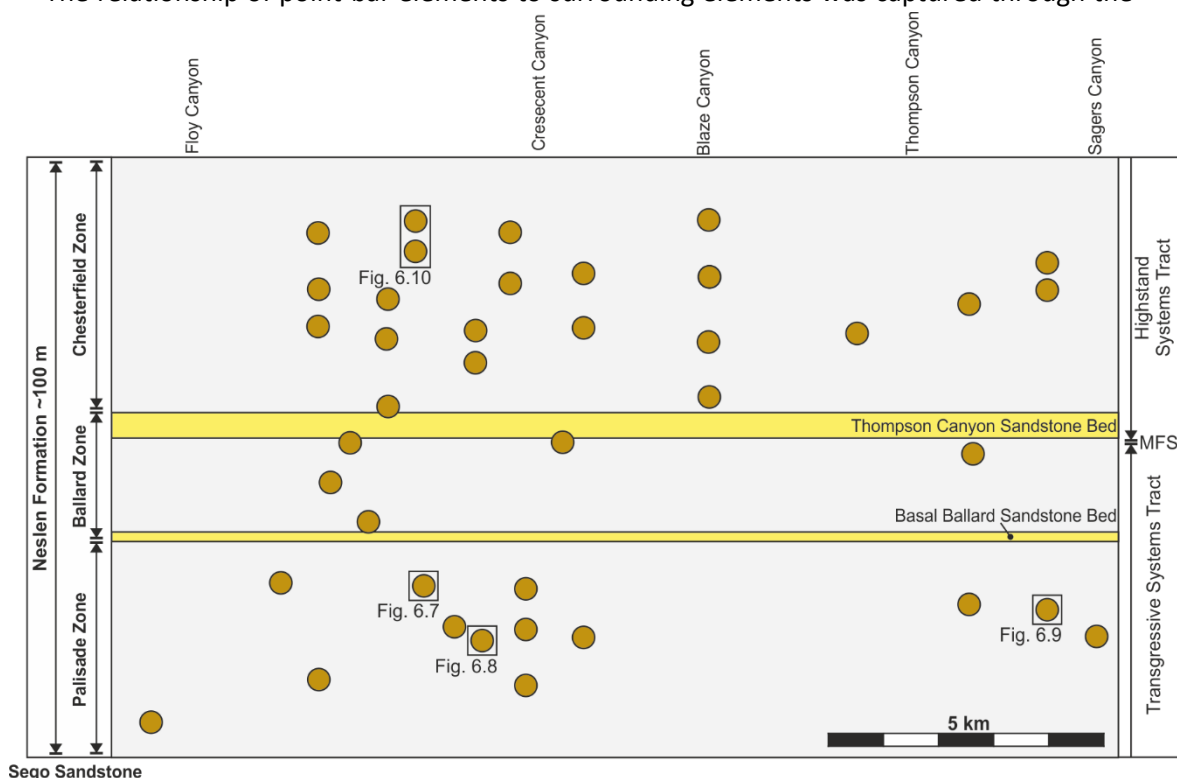


Figure 6.4: Simplified stratigraphy of the Neslen Formation (cf. Shiers et al. 2014; 2016) and the stratigraphic position of outcrops with studied point-bar elements.

construction of measured architectural-element panels. Internal lithofacies distributions were described and logged (total number of logs = 65) at millimetre to centimetre scale (covering a total of 400 m). Trace fossils are ascribed to ichnological assemblages. Palaeocurrent readings (n = 1021) were determined from the dip direction of foresets of cross bedding and ripple lamination, as well as the dip azimuths of bounding surfaces of lateral accretion sets. Channelised sand bodies in the upper Chesterfield Zone (Fig. 6.4) are highly amalgamated (Shiers et al. 2014) and analysis of these bodies was restricted (due to the nature of the cliff-forming outcrop) to single vertical logs and photographic stratigraphic panels.

The sequence stratigraphic framework of the Neslen Formation has been established within Chapters 4 and 5. This framework has allowed each studied point-bar element to be associated to a systems tract, such that differences in point-bar internal facies distributions can be related to different accommodation settings.

Quantitative analysis of lithofacies and geometries for each studied point-bar element have been determined by coding the collated data within the Fluvial Architecture Knowledge Transfer System (FAKTS; Colombera et al. 2012; 2013a; b). Bespoke database queries allow characterisation of the internal facies and bar dimensions to yield quantitative representations of the elements. Calculation of facies proportions within point-bar elements are recorded as a fraction of the logged sections within point-bar elements, where the base and top of the element is well defined. Lithological heterogeneity within point-bar elements is defined as the thickness proportion of fine-grained lithofacies (silt and finer) relative to the total logged thickness. The aspect ratio of point-bar elements is calculated as a ratio between the maximum logged thickness and the minimum known width of the element. The true width of the element is calculated through mapping of the point-bar elements around cliff lines combined with the measurement of palaeocurrents. A partial width is used to calculate the aspect ratio of point-bar elements where the outcrop is obscured and an apparent width is recorded where an outcrop lacks sufficient palaeocurrent indicators to establish the true width (cf. Geehan and Underwood, 1993). Utilising the FAKTS database facilitates recognition of similarities and disparities between individual point-bar elements, and has enabled the construction of a quantitative facies model using a database approach (Colombera et al., 2013a). The FAKTS database has additionally enabled point-bar elements from different systems to be compared to those studied in the Neslen Formation (Fig. 6.2a).

6.4 Results

Three different types of channel element have been previously identified in the Neslen Formation: distributary channel elements (or ribbon channel-fill elements) (Shiers et

al. 2014; Colombera et al. 2016; Chapter 5); sandstone-dominated point-bar elements (alternatively referred to as fluvial channel sandstones) (Willis 2000; Kirschbaum and Hettlinger 2004; Cole 2008; Shiers et al. 2014; 2016; Colombera et al. 2016); heterolithic point-bar elements (alternatively referred to as inclined heterolithic strata or tidally influenced channels) (Willis 2000; Kirschbaum and Hettlinger 2004; Shiers et al. 2014; Olariu et al. 2015; Colombera et al. 2016). Amalgamated channel elements of the upper Chesterfield Zone are interpreted as fluvial point bars (Shiers et al. 2014). The lithological character of infill of fluvial channels by point-bar architectural elements is represented by 14 lithofacies (Figs. 4.7; 6.5; Table 4.1). The facies are interpreted in terms of depositional or post-depositional processes

The average internal facies proportions of point-bar elements of the Neslen Formation (Fig. 6.6b) are similar to other systems analysed using the FAKTS database (Fig. 6.2a), and the width-to-thickness aspect ratios of the bar forms are similar to those of other successions deposited in humid climates (Figs. 6.2i, 6.6c) (Colombera et al. 2012; 2013a; b). However, detailed analysis reveals that there is variety in the facies proportions and aspect ratio between point-bar elements within the Neslen Formation. The variation in facies proportions and aspect ratio between the 41 analysed point-bar elements permits identification of four element 'types' (Table 6.1).

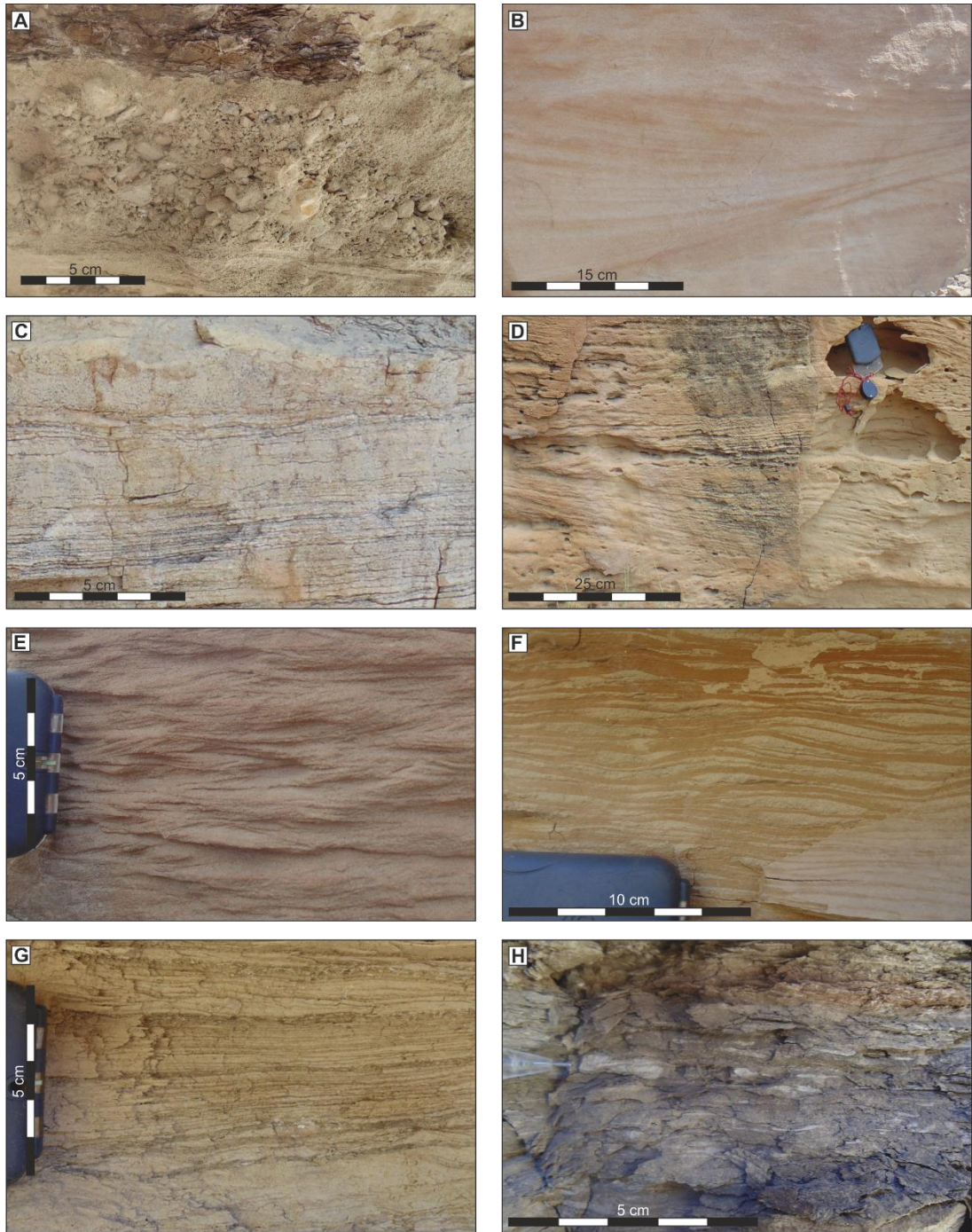


Figure 6.5: Representative photographs of sedimentary facies observed within point-bar elements of the Neslen Formation. A) Intraformational conglomerate (Gh) found at the base of elements and on erosional surfaces. B) Trough cross-bedded sandstone (Sx). C) Horizontally laminated sandstone (Sh). D) Low-angle laminated sandstone (Sl). E) Ripple cross-laminated sandstone (Sa). F) Heterolithic lenticular and wavy sandstone with intervening siltstone laminations (H). G) Horizontally interbedded sandstone and siltstone (Si). H) Massive (Fsm) and laminated (Fl) mudstone and siltstone.

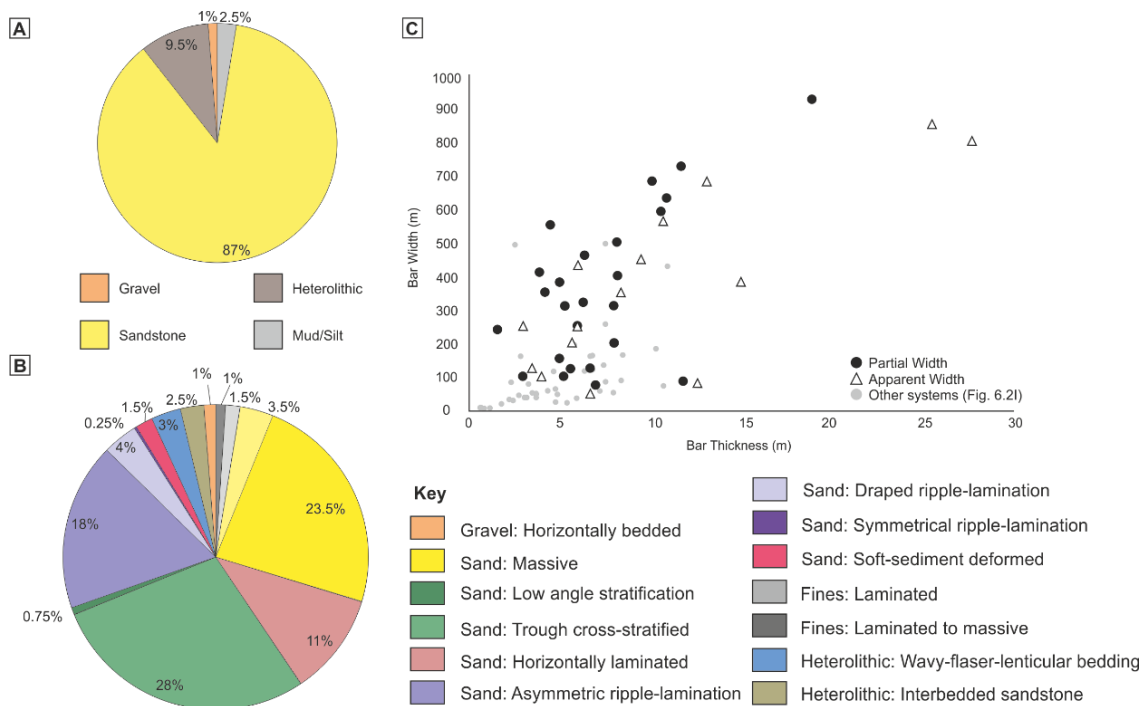


Figure 6.6: Quantitative analysis of facies of point-bar elements of the Neslen Formation carried out using the FAKTS database. A) Lithology of all studied point-bar elements in the Neslen Formation. B) Facies proportions of all studied point-bar elements within the Neslen Formation. C) Graph showing aspect ratio of all studied point-bar elements in the Neslen Formation in comparison to other bars analysed in the FAKTS database (Fig. 6.21).

6.4.1 Type I

6.4.1.1 Description

Type I point-bar elements (Table 6.2; Fig. 6.7; Appendix H) are characterised by high proportions of well sorted ripple laminated sandstone, mud, silt and carbonaceous draped ripple-laminated sandstone (17.6 to 68 %) (Fig. 6.7), no cross-bedding is observed. Thirteen elements of this type are identified. Elements are 3 to 12 m thick, and exhibit a wide range of width to thickness ratios (between 1:10 and 1:83; Table 6.2; Fig. 6.11f). The proportion of horizontally laminated sandstone in these types of elements is 8 to 24%. The dip of point bar accretion surfaces is 10 to 20°. Heterogeneity within this type of element is generally low (0 to 3.6%); two instances of higher heterogeneity also occur (16.7 %, 17.6 %).

Commonly, the lowermost 0.5 m of the fill exhibits wood fragments and intraformational conglomerate (Gh) within massive, fine and medium grained sandstone. *Teredolites* and *Thalassinoides* are observed within channel lags at the base of the elements. Ripples are dominantly asymmetrical (Fig. 6.7f), and are commonly draped by mud, silt or carbonaceous material; both single and double drapes are observed. Vertically, the changes

in facies are subtle; ripple lamination (Fig 6.7c) gives way upwards to draped ripple lamination and heterolithic deposits of wavy and flaser bedding (H), and then interbedded siltstone and sandstone laminae (Si) (Fig. 6.7d, f).

6.4.1.2 Interpretation

The dominantly lateral direction of accretion within these point-bar elements is demonstrated by the high angle between the palaeo-flow direction indicated by ripple cross-laminae dip directions and the accretion direction in bar-form elements demonstrated by the azimuth of dipping bar surfaces (Fig. 6.7h). The proportions of facies are distinctive; in particular, there is a low incidence of occurrence of cross-bedded sandstone and a high proportion of ripple laminated sandstone, including draped ripples (Table 6.1). Rippled sandstone is the product of deposition by migrating asymmetrical ripples (Collinson et al. 2006) under waning traction flows (Simons et al. 1960; Visher 1965). Horizontal laminated sandstone (Sh; Table 4.1; Fig. 6.5c) was deposited from traction flows in either the upper or lower flow regime plane-bed field, with finer grained laminations reflecting minor energy

	Type I	Type II	Type III	Type IV	
Number of elements	13	4	2	22	
Thickness range (m) (average)	3-12.6 (6.4)	3.5-12.6 (5.8)	5.7-15 (10.35)	4-25 (10.6)	
Aspect ratio range (average)	7-83 (36)	30-40 (20)	25-40 (30)	33-150 (71)	
Lateral accretion angle (°)	10-20	5-10	10-15	<10	
Heterogeneity range /% (average/ %)	0-17.6 (7)	0.5-23.5 (10.5)	0.5-9 (4)	0-12.5 (0.75)	
Average Facies proportions (%)	Sm	26.5	48.5	22.5	19
	Sh	15	19	21.5	7.5
	Sx	0.5	1	34	50.25
	Sa	40	5	11.5	13
	H	7.5	9	0	0
	Si	6	6.5	0	0
	Gh	3	0	3.5	2.5
Bioturbation	Ar, Te, Th throughout	Te and Th prevalent	Minor Te, Me at base	Minor Te at base of lowermost elements	

Table 6-1: Table summarising key variables for the interpretation of different point-bar element types within the Neslen Formation. Sm = massive sandstone, Sh = horizontally laminated sandstone, Sx = trough cross-bedded sandstone, Sa = asymmetrical ripple-laminated sandstone, H = heterolithic sandstone, Si = interbedded sandstone and siltstone, Gh = intraformational conglomerate. Te = Teredolites. Me = Medousichnus, Th = Thallassinoides, Ar = Arenicolites

fluctuations (Simons et al. 1960; Visser 1965; Fielding et al. 2006). Heterolithic facies (H) indicates deposition under fluctuating flow energies (potentially modulated by tidal influence); there is a balance between deposition of mud from suspension and sand deposition either from suspension or as saltating bedload via migrating unidirectional ripples (Miranda et al. 2009). The occurrence of heterolithic facies and the presence of *Teredolites* and *Thalassinoides* trace fossils can be used to infer marine influence in these deposits (Bromley 1996).

Overall the facies architecture of this type of point bar is interpreted to reflect deposition under low flow velocities in the lower flow regime (Wakelin-King and Webb 2007), which may have been modified to some degree by marine processes.

6.4.2 Type II

6.4.2.1 Description

Type II point-bar elements (Table 6.2; Fig. 6.8; Appendix H) are classified based upon the dominance of massive sandstone (30 to 68%; Fig. 6.8g) and the small proportion of ripple laminated sandstone (<12%). Four examples of this element are identified; they are 3.5 to 12.6 m thick and have width-to-thickness ratios of 30 to 40 (Table 6.2). The dip of point bar accretion surfaces is 5 to 10°. Examples of this type of point-bar element have a high proportion of mudstone and siltstone present (up to 23.5%; Fig. 6.8g), arranged in heterolithic packages (Figs. 6.8b; 6.8e).

The proportion of horizontally laminated sandstones (Sh; Fig. 6.8d) varies from 6 to 32%. Sandstone beds in these elements thin upward, from 0.2 to 0.8 m thick at the base, to 0.05 to 0.5 m thick in the upper parts of the elements. Fining upward trends are not always apparent (Fig. 6.8b). The thickness of fine-grained beds increases upwards; towards the base of the elements, mudstone and siltstone exist as mm- to cm-thick beds; in the upper parts of the elements individual fine-grained beds are up to 0.5 m thick. Interbedded sandstone and siltstone beds (Si) and heterolithic sandstones (H) commonly exhibit weak rhythmicity of laminae thicknesses. Massive sandstones occur in beds which commonly exhibit scoured bases. Trace fossils such as *Teredolites* and *Thalassinoides* are present in the basal-most beds of some examples (e.g. Fig. 6.8c) as mono-specific assemblages.

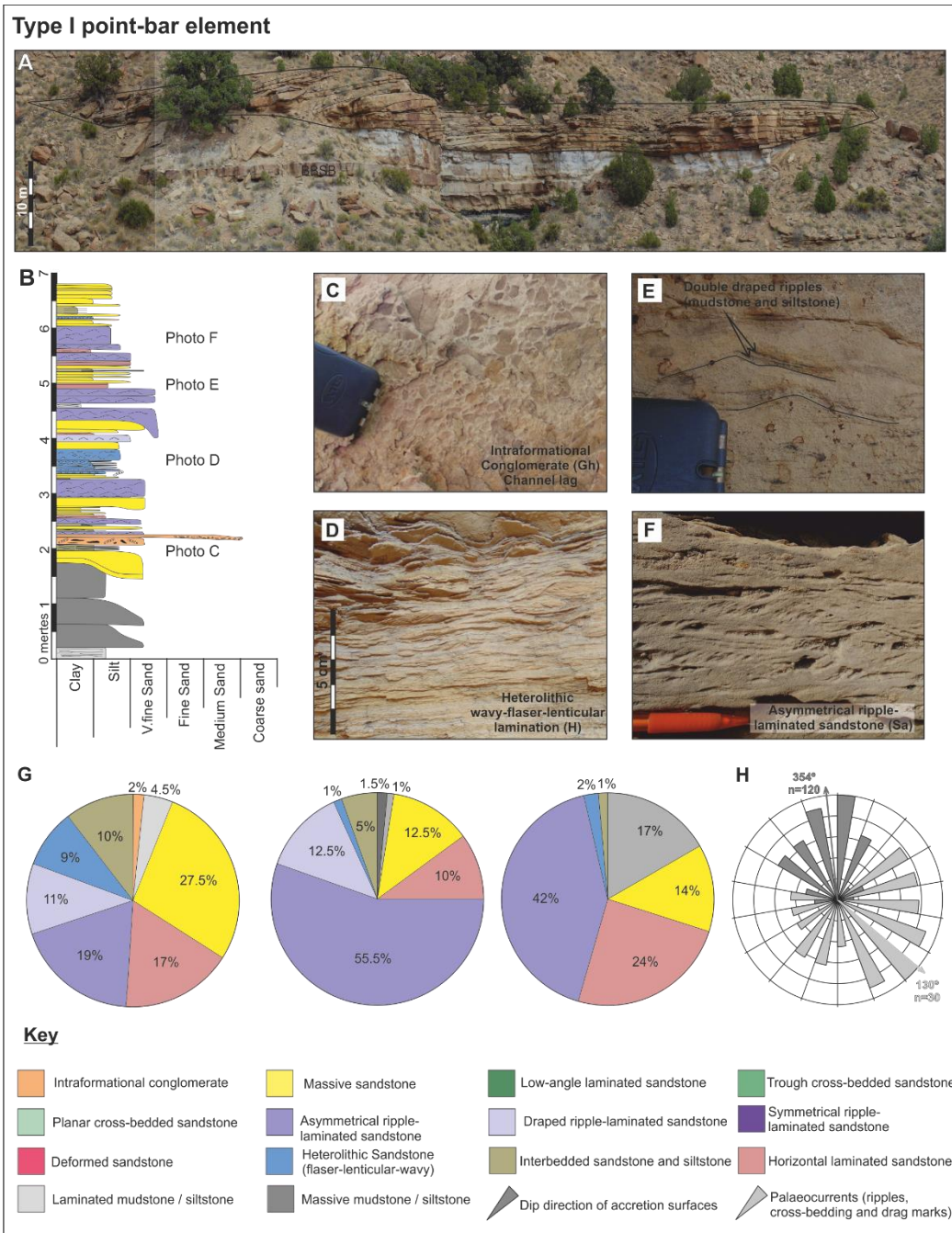


Figure 6.7: Example of a type I point-bar element within the Neslen Formation. A) Photograph panel of a representative type I point-bar element located at Crescent Canyon (Fig. 6.4); inclined surfaces dip at 10 to 15°. B) Representative logged section through a type I point-bar element. C) Photograph of intraformational conglomerate (Gh) with rounded mud clasts up to 3 cm long at the base of the point-bar element. D) Detailed photograph of interbedded sandstone and laminated siltstone (Si). E) Photograph of horizontally interbedded sandstone and siltstone (Si). F) Photograph of asymmetrical ripple-laminated sandstone (Sa). G) Representative facies proportions within examples of type I point-bar elements. H) Palaeocurrent data for the studied example shown in (A). Further examples can be found in Appendix H.

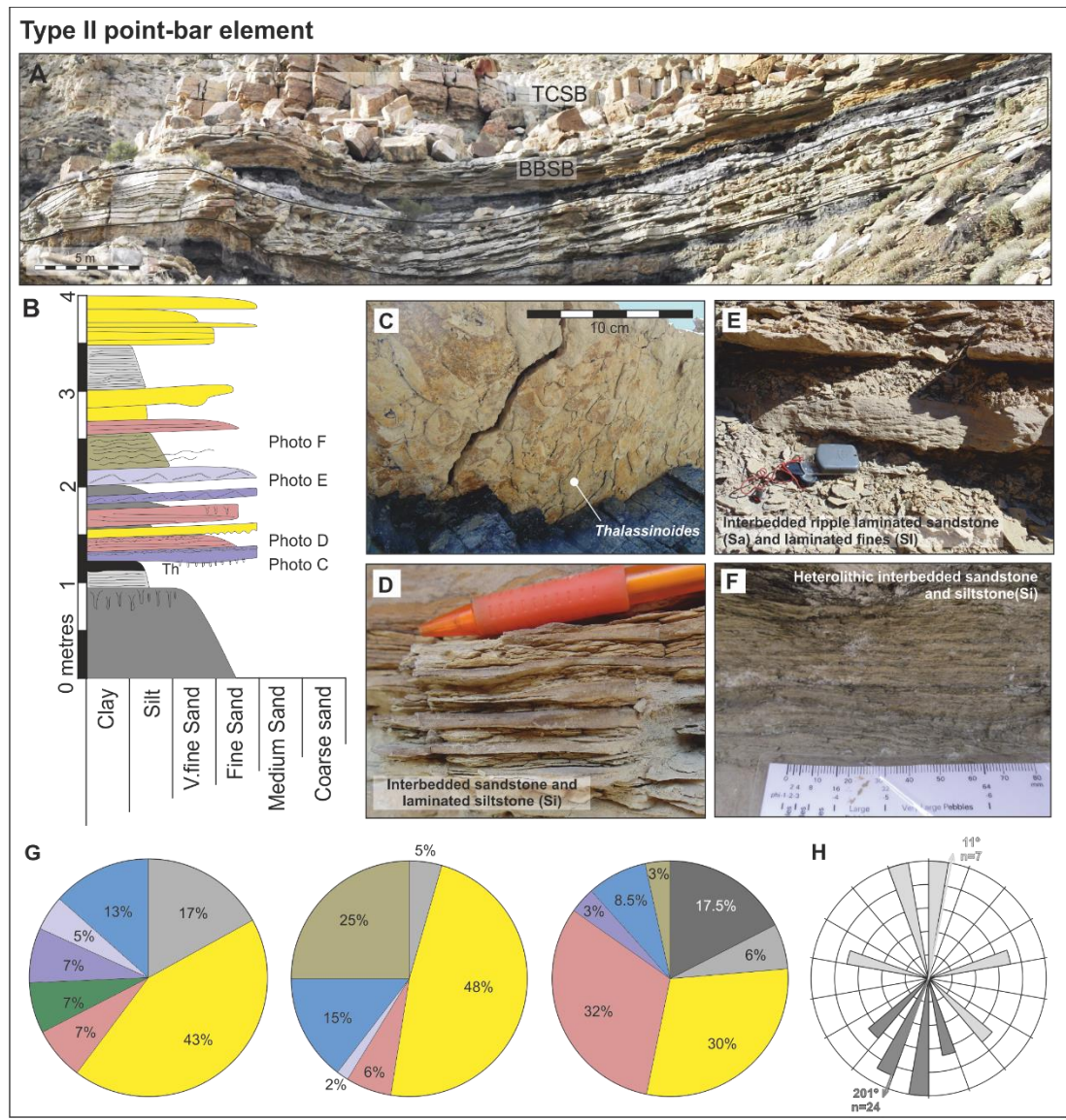


Figure 6.8: Example of a type II point-bar element within the Neslen Formation. A) Photograph panel of a type II point-bar element; inclined surfaces dip at 5 to 10° (Figs. 6.3, 6.4) TCSB = Thompson Canyon Sandstone Bed, BBSB = Basal Ballard Sandstone Bed. B) Logged section through type II point-bar element with alternating sandstone and siltstone beds. C) Photograph showing abundant *Thalassinoides* on the base of the point-bar element. D) Photograph showing horizontally laminated sandstone with interbedded siltstone (Sh and Si). E) Ripple-laminated sandstone beds (Sa) with intervening laminated siltstones (Si). F) Pinstriped interbedded siltstone and sandstone (Si) within which sandstone laminae thicken upwards. G) Constituent facies proportions for type II point-bar elements. H) Palaeocurrent data for the studied example shown in (A); there is a high angle between the azimuth of dip direction of accretion surfaces and that of ripple lamination indicating the dominance of lateral accretion. For key for facies colours refer to Fig. 6.7. Further examples can be found in Appendix H.

6.4.2.2 Interpretation

Similar to type I point-bar elements, these bodies are interpreted as laterally accreting point bars (Fig. 6.8h). These elements have the highest proportion of preserved fines (Figs. 6.8g; 6.11c). The proportion of mudstone and siltstone which occur alternating with sandstone beds in inclined packages within the elements defines them as IHS; other occurrences of which have widely been cited as being a product of tidal influence (Shanley et al. 1992; Dalrymple and Choi 2007), although they can also occur in fluvial and ephemeral fluvial systems (Thomas 1987; Lynds and Hajek 2006; Archer 1995; Kvale et al. 1995; Kvale 2012). Here, a tidal-influence interpretation is supported by the presence of mono-specific assemblages of trace fossils interpreted to reflect brackish or saline depositional environments. Sedimentological evidence of tidal influence includes the presence of interbedded sandstone and siltstone (Si, H; Figs. 6.8; 6.11c), repeating beds of which show weak rhythmicity. The high proportion of massive sandstone (Sm; Figs. 6.8; 6.11c) is interpreted to reflect rapid deposition of sediment with a narrow grain size range, from concentrated flows, locally filling scours (Collinson et al. 2006). Massive sandstones could also be the result of post-depositional modification through fluidisation, although no evidence of this is observed. Low proportions of cross-bedding may be due to finer grain size or a lower flow velocity than is required for sandstone to accumulate as dune-scale bedforms (Harms et al 1975).

The facies within these bodies demonstrates that the sediment accumulated under fluctuating energy conditions, which may be due to marine influence; this interpretation is further supported by the presence of an ichnofacies indicative of brackish water conditions (Bromley 1996).

6.4.3 Type III

6.4.3.1 Description

Type III point-bar elements (Table 6.2; Fig. 6.9a) in the Neslen Formation are characterised by relatively high proportions of cross-bedded sandstone (over 30%) and low to medium heterogeneity (0.5 to 9% fines) (Figs. 6.9g, 6.11d). Two of the studied point-bar elements fit into this classification (aspect ratios 25 and 40; point-bar element thicknesses of 5.7 m and 15 m). Beds have tangential geometries at the base, wedging out laterally over 3 to 5 m (Fig. 6.9a). The dip of point bar accretion surfaces is 10 to 15°.

The beds thin- and fine-upwards, from fine and medium-grained sandstone at the base, to very fine-grained sandstone at the top of the element (Fig. 6.9b). The basal deposits are characterized by gravel to pebble mud clasts (Figs. 6.5a; 6.9b,c), and trace fossils (*Teredolites* and *Medousichnus*). Massive or cross-bedded sandstone (Sm/Sx) are common

in the lowermost parts of type III element fills, with sets typically partitioned by erosion surfaces. Upwards, type III point-bar elements are dominated by cross-bedded sandstone (Fig. 6.9b, d). Progressively, upwards, the thickness of cross-bedded sandstones decreases (from ~0.5 m thick beds towards the base to 0.2 m thick in the upper parts of elements) and ripple laminated (Sr; Figs. 6.9b; 6.9e), massive (Sm) and horizontally laminated (Sh) sandstone facies become more common (Fig. 6.9g).

6.4.3.2 Interpretation

The high angle between the palaeoflow direction indicated by cross-laminae dip directions and the accretion direction in bar-form elements demonstrated by the azimuth of dipping bar surfaces supports a dominant lateral direction of accretion (Fig. 6.9h; Bridge 2006). The presence of large proportions of trough cross-bedding (St; Fig. 6.5b) within examples of this element is interpreted as deposition by migrating subaqueous dunes (Table 6.1). In some cases, cross bedded sandstones exhibit multiple reactivation surfaces, which might indicate variations in flow energy and/or direction, potentially due to tidal processes (Shanley et al. 1992), or changes in river discharge. The presence of *Medouscihnus* can indicate tidal influence; *Teredolites* (bored wood) is typical of both marine and brackish environments; however individual logs can be pushed (rafted) upstream within the backwater zone (Savrda 1991). The proportion of trough and planar cross-bedded sandstone in all lateral-accretion elements in the FAKTS database is 35% (Fig. 6.2a); this is similar to the proportion preserved in type III point-bar elements (26%). The amount of ripple lamination in type III point-bar elements is 11% (Fig. 6.11d) and in all point-bar elements is 9% (Fig. 6.2a).

This element is interpreted as lateral accretion deposits formed from fluvially dominated meandering channels that traversed the coastal plain (Kirschbaum and Hettinger 2004; Aschoff and Steel 2011b).

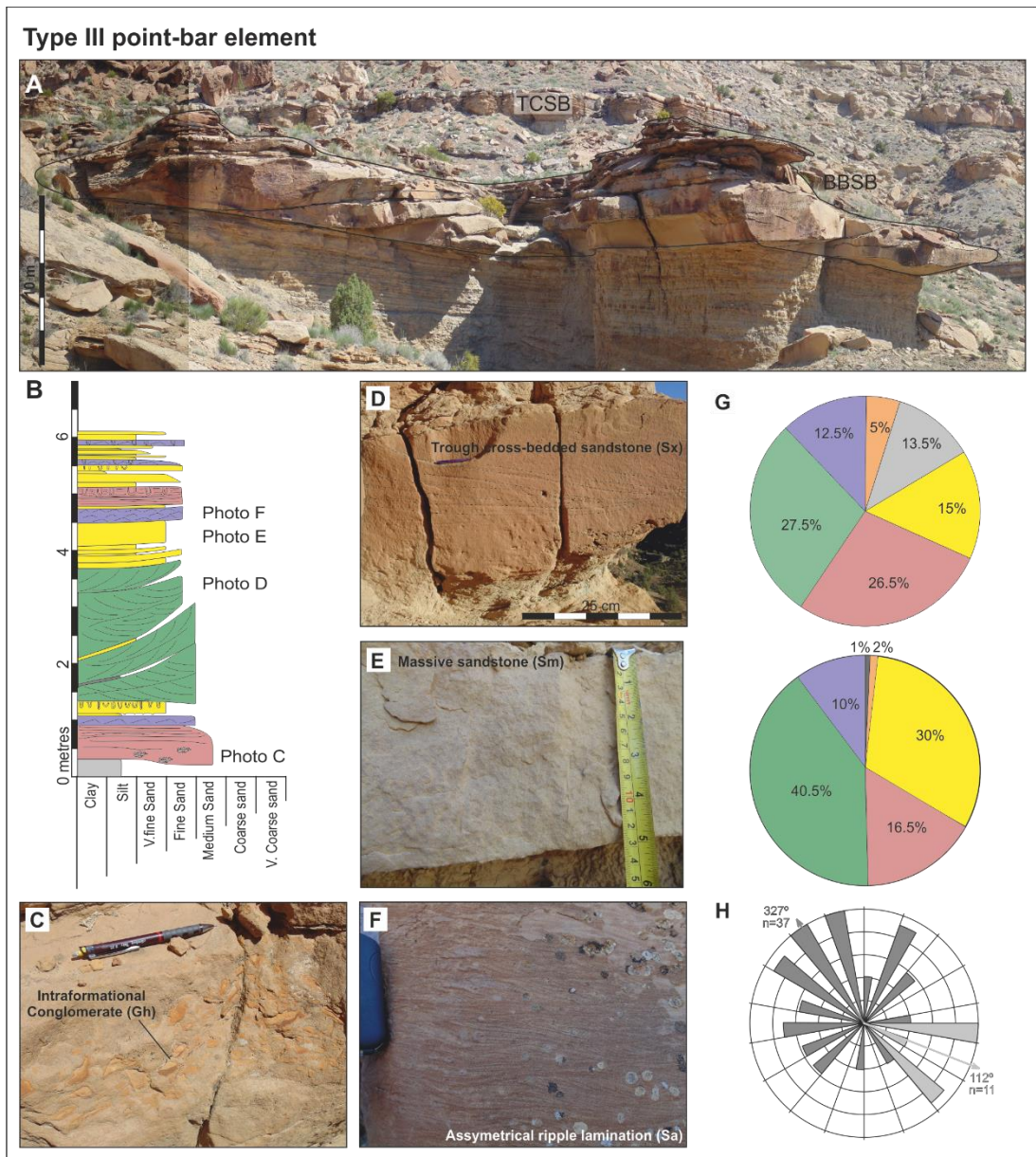


Figure 6.9: Example of a type III point-bar element within the Neslen Formation. A) Photograph panel of a point-bar element showing the sigmoidal shape of beds (Figs. 6.3, 6.4), TCSB = Thompson Canyon Sandstone Bed. B) Logged section through a type III point-bar element. C) Photograph of intraformational conglomerate (Gh) found at the base of a type III point-bar element. D) Photograph of trough cross-bedded sandstone (Sx). E) Photograph of massive sandstone bed (Sm). F) Photograph of asymmetrical ripple-laminated sandstone (Sa). G) Constituent facies proportions for type I point-bar elements. (H) Palaeocurrent data for the studied example shown in (A); there is a high angle between the azimuth of dip direction of accretion surfaces and that of ripple lamination indicating the dominance of lateral accretion. For key for facies colours refer to Fig. 6.7. Further examples can be found in Appendix H.

6.4.4 Type IV

6.4.4.1 Description

Type IV point bars (Appendix H; Table 6.2; Fig. 6.10) exhibit a high proportion of cross-bedded sandstone (49%). Twenty point-bars of this type are identified within the upper Chesterfield Zone. Elements are 4 to 25 m thick (average: 10.2 m), and possess high aspect ratios: 33 to 150 (average is 71) (Fig. 6.11f). Inclined accretion surfaces are less common than in other point-bar types, but where observed dip at moderate angles, up to 10° (Fig. 6.10a; Table 6.2). Type IV elements generally have low heterogeneity; on average <0.75%, with one example of 12.5% (Figs. 6.10, 6.11e, Table 6.2). Elements of this type are commonly vertically and laterally amalgamated, forming extensive sandstone belts in the upper Chesterfield Zone (Fig. 6.12) (*sensu* Shiers et al. 2014; section 4.5.3).

Erosion surfaces separating individual channel elements are commonly observed; with metre-scale relief and intraformational conglomerate preserved in the lowermost beds (Fig. 6.10b). Cross-bedded sandstone and massive sandstone dominates, passing upwards to ripple laminated and horizontally laminated sandstone (Fig. 6.10b). Bioturbation within these elements is not discernible.

6.4.4.2 Interpretation

The facies assemblage within these bodies is similar to type III point-bar elements; however, they are distinguished by their thickness and aspect ratio (Table 6.2; Fig. 6.11f), as well as the degree of amalgamation (Fig. 6.10a; Shiers et al. 2014).

Where it has been possible to measure the orientation of cross-bedding and lateral accretion surfaces within the same point bar element there is a high relative angle between them indicating a dominance of lateral accretion. The vertical succession of facies reflects lower velocity flows developing progressively through filling of the channel (Visher 1965). The particularly thick and amalgamated nature of these point-bar elements is interpreted to reflect low accommodation on the floodplain where channels cannibalised the underlying floodplain and earlier channelised deposits (Leeder 1977; Allen 1978; Bridge and Leeder 1979; Heller and Paola 1996; Shiers et al. 2014). The incised basal contacts of the point-bar elements indicates the high energy within the associated channel. The lack of marine indicators in these bodies indicates deposition in a dominantly fluvial setting.

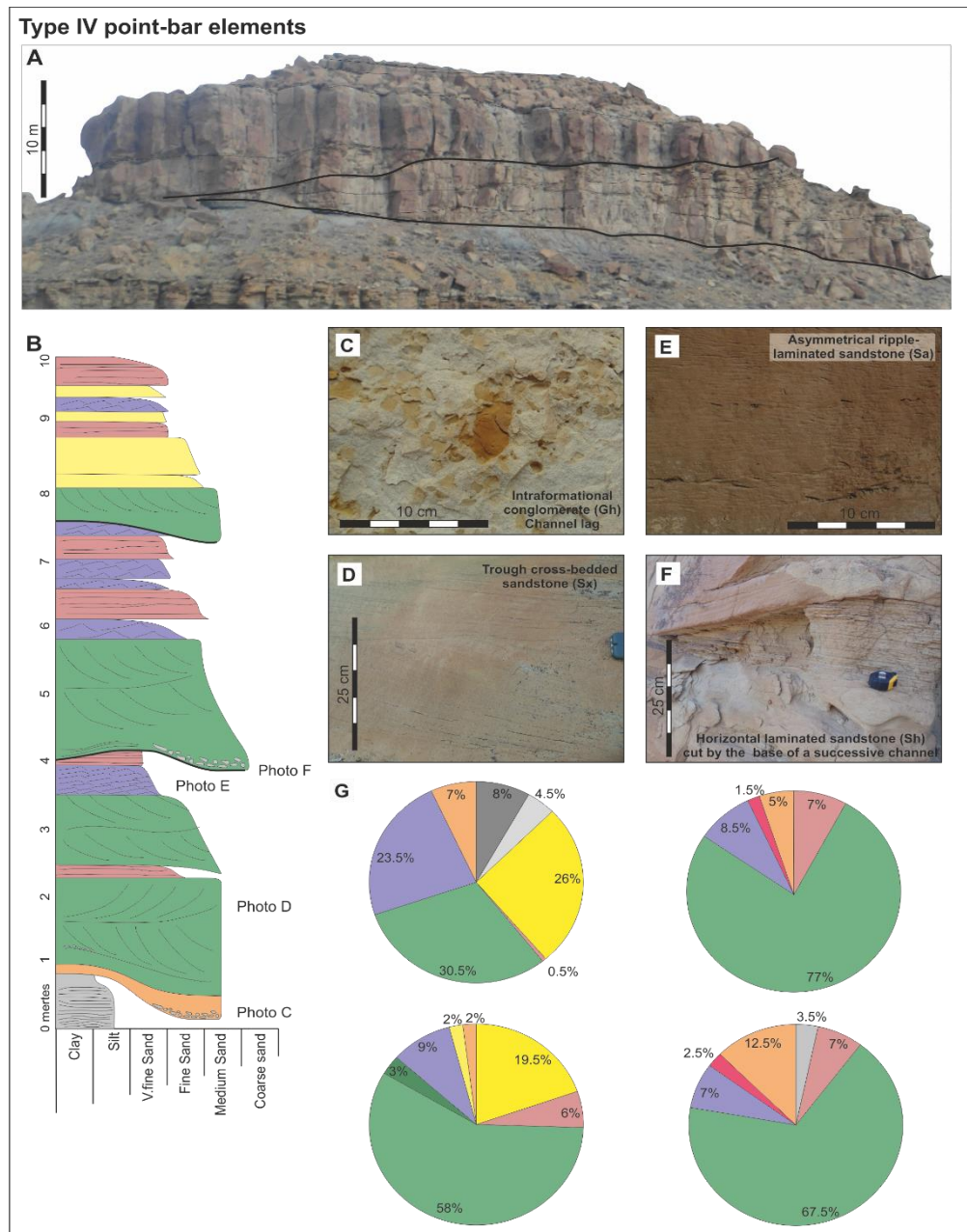


Figure 6.10: Example of a type IV point-bar element within the Neslen Formation. A) Photograph panel of representative type IV point-bar elements; thicker lines show the basal incision surface of individual point-bar elements. B) Representative logged section through typical type IV point-bar elements showing erosive surfaces at the base of each point-bar element, and the vertical transition from cross-bedded to ripple laminated sandstone. C) Photograph of intraformational conglomerate (Gh). D) Photograph of trough cross-bedded sandstone (Sx). E) Photograph showing horizontally laminated sandstone (Sh) cut it into by an overlying point-bar element. F) Asymmetrical ripple-laminated sandstone (Sa). G) Representative facies proportions within examples of type IV point-bar elements. For key for facies colours refer to Fig. 6.7. Further examples can be found in Appendix H.

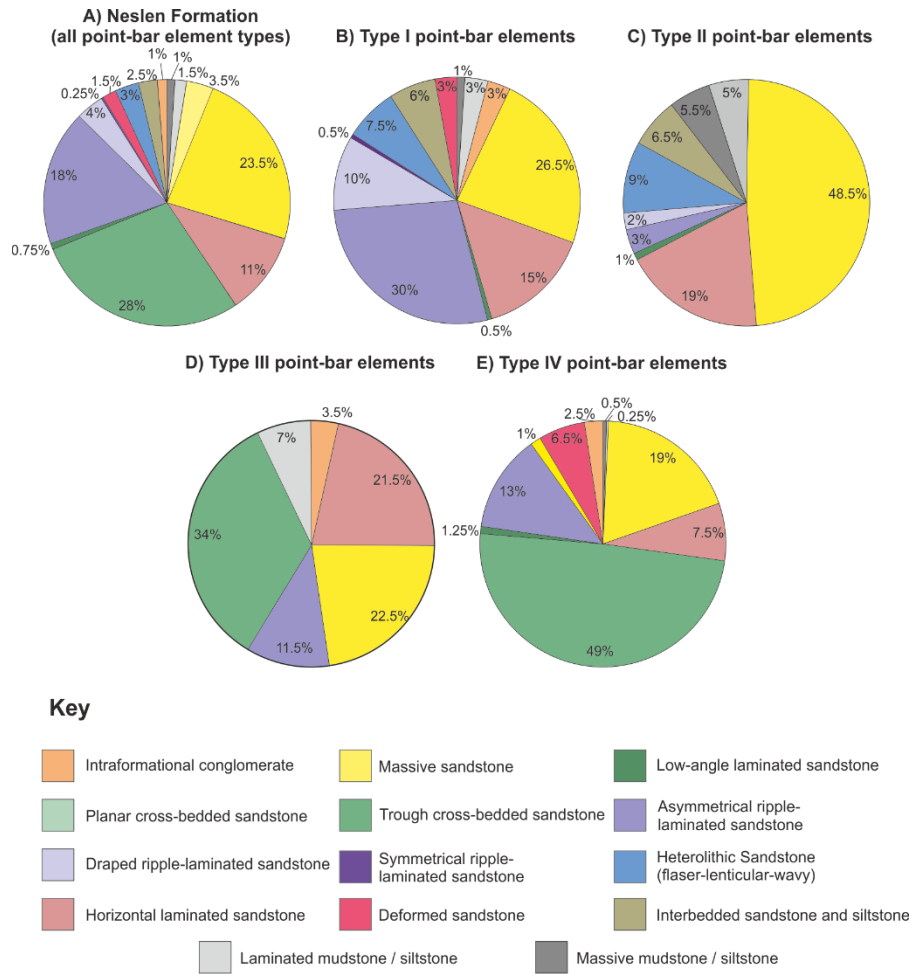
6.4.5 Point-bar element type summary

The proportions of facies, and the observed vertical transitions preserved in type III and IV point-bar elements (Figs. 6.9, 6.10) is similar to many other point-bar elements, e.g., those interpreted in the Scalby Formation (Fig. 6.2f), which was deposited in humid subtropical conditions (Nami and Leeder 1977; Ielpi and Ghinassi 2014), and those of point-bar elements in the lower Williams Fork Formation (Fig. 6.2e) (Pranther et al. 2007). Type III and IV point-bar elements are also similar to the facies proportions in all point-bar elements analysed within the FAKTS database (Fig. 6.2a) and published models (Fig. 6.1). The vertical transition of facies (Figs. 6.9b, 6.10b) demonstrates that, progressively, as the point bar developed, the preserved facies reflect lower flow velocities through progressive accumulation on the inner bend of the migrating channel element.

Type I and II point-bar elements (Figs. 6.7, 6.8) are dissimilar to the models presented in the literature (Fig. 6.1), as well as to the facies proportions of most successions analysed in the FAKTS database (Fig. 6.2a). The Wessex and Green River formations (Fig. 6.2g, 6.2h) also exhibit a dominance of ripple-laminated sandstone for their constituent point-bar elements, although these elements still additionally contain significant proportions of cross-bedded sandstone. Point bars that are dominated by ripple strata are described by Miall (1985; his model 7), and are interpreted in that study as representative of deposition from highly sinuous, suspended-load dominated rivers. No systems analysed in FAKTS exhibit similar facies proportions shown for these types of elements (Figs. 6.11b, c).

The aspect ratios of type I, II and III point-bar elements is similar to those of other point-bar elements in the FAKTS database (Fig. 6.11). The aspect ratio of type IV point-bar elements is higher than that of other systems; this is likely to be due to the highly amalgamated nature of these sandbodies and a substrate with limited cohesion. Where the nature of the outcrop does not permit the identification of the base of each point-bar element within a channel-belt, the thickness of the point-bar element may be overestimated; this risk is minimised through the combined use of stratigraphic panels and sedimentary logs.

Across all analysed elements, the grain size of cross-bedded sandstones (fine-to-medium grained and medium-grained sandstone; Figs. 6.9b; 6.10b) is consistently coarser than that of ripple-laminated sandstone beds (very fine- to fine-grained sandstone; Figs. 6.7b, 6.8b).



F) Aspect ratio of Neslen Formation point-bar elements separated by element type

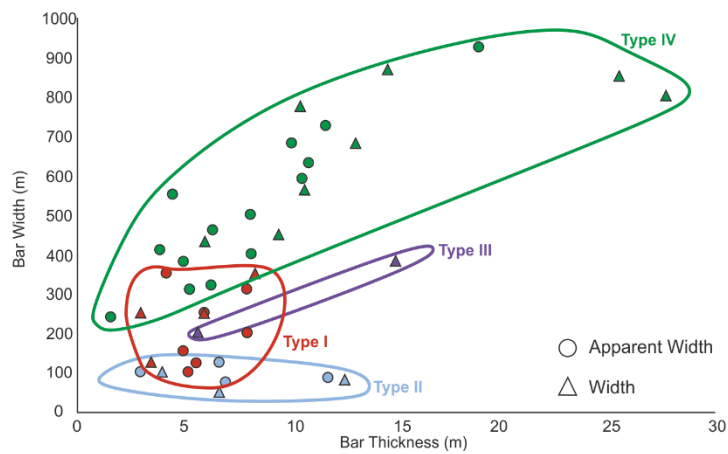


Figure 6.11: A) Quantitative proportions of facies within the Neslen Formation. B-E) Quantitative proportion of facies within the four interpreted point-bar element types of the Neslen Formation. F) Graph showing the aspect ratio of point-bar elements in the Neslen Formation separated by element type.

Marine influence is interpreted within point-bar elements classified as types I and II from the facies and ichnology evident within these bodies. Sedimentary indicators occur in the form of single and double draped ripples (Sa), wavy, flaser and lenticular sandstones (H) and interbedded sandstone and siltstone (Si) which can show subtle rhythmicity. Although these structures themselves merely indicate fluctuating flow energies, potentially caused by tidal fluctuations, the accompanying ichnological evidence (*Teredolites*, *Thalassinoides*) supports the interpretation of marine influence in type I and II point-bar elements.

6.5 Discussion

The presented results are discussed in two ways: i) in terms of the vertical changes of point-bar character (geometry, facies and amalgamation); ii) the occurrence of atypical point-bar assemblages in the lower Neslen Formation. The controls on both of these are presented in section 6.5.1 below and the compared to data from other systems analysed using FAKTS (section 6.5.2)

6.5.1 Controlling Factors in the Neslen Formation

Vertically through the Neslen Formation, there is a systematic change in channel type (Fig. 6.12). Type I point-bar elements are abundant throughout the Palisade, Ballard and lower Chesterfield Zones. Type II elements are restricted to the Palisade Zone. Type III elements occur towards the middle of the formation (upper Palisade and lower Chesterfield zones). Type IV point bars occur exclusively within the upper Chesterfield Zone. The stratigraphic increase in aspect ratio (width:thickness ratio) of the point-bar elements means that the sandstone bodies are increasingly wide for a given thickness (Fig. 6.12).

Type I and II point-bar elements in the lower Neslen Formation also display a series of sedimentological and ichnological indicators of marine influence. These elements are smaller and more heterolithic point-bar elements with a low relative proportion of cross-bedded sandstone, and higher proportion of ripple-laminated, and horizontally laminated sandstone (Fig. 6.11).

The controls on the stacking and facies assemblage of the point-bar elements are varied, encompassing allogenic and autogenic processes and are discussed below.

6.5.1.1 Systems tract and A:S ratio

In the lower Neslen Formation, interpreted as a transgressive systems tract (TST) (Chapter 5), point-bar elements are predominantly type I and II elements. In the upper Neslen Formation, interpreted as the highstand systems tract (HST), there is a change from type I and III elements to solely type IV elements upwards. This is concurrent with an increase in amalgamation of the sandstone bodies. There is a statistically significant increase in the aspect ratio of point-bar elements through the Neslen Formation with an abrupt increase across the TCSB (tested using ANOVA analysis: significance level = 0.05, p value = 0.001), the base of which is interpreted as the maximum flooding surface (Cole 2008; Chapter 5) (Fig. 6.12).

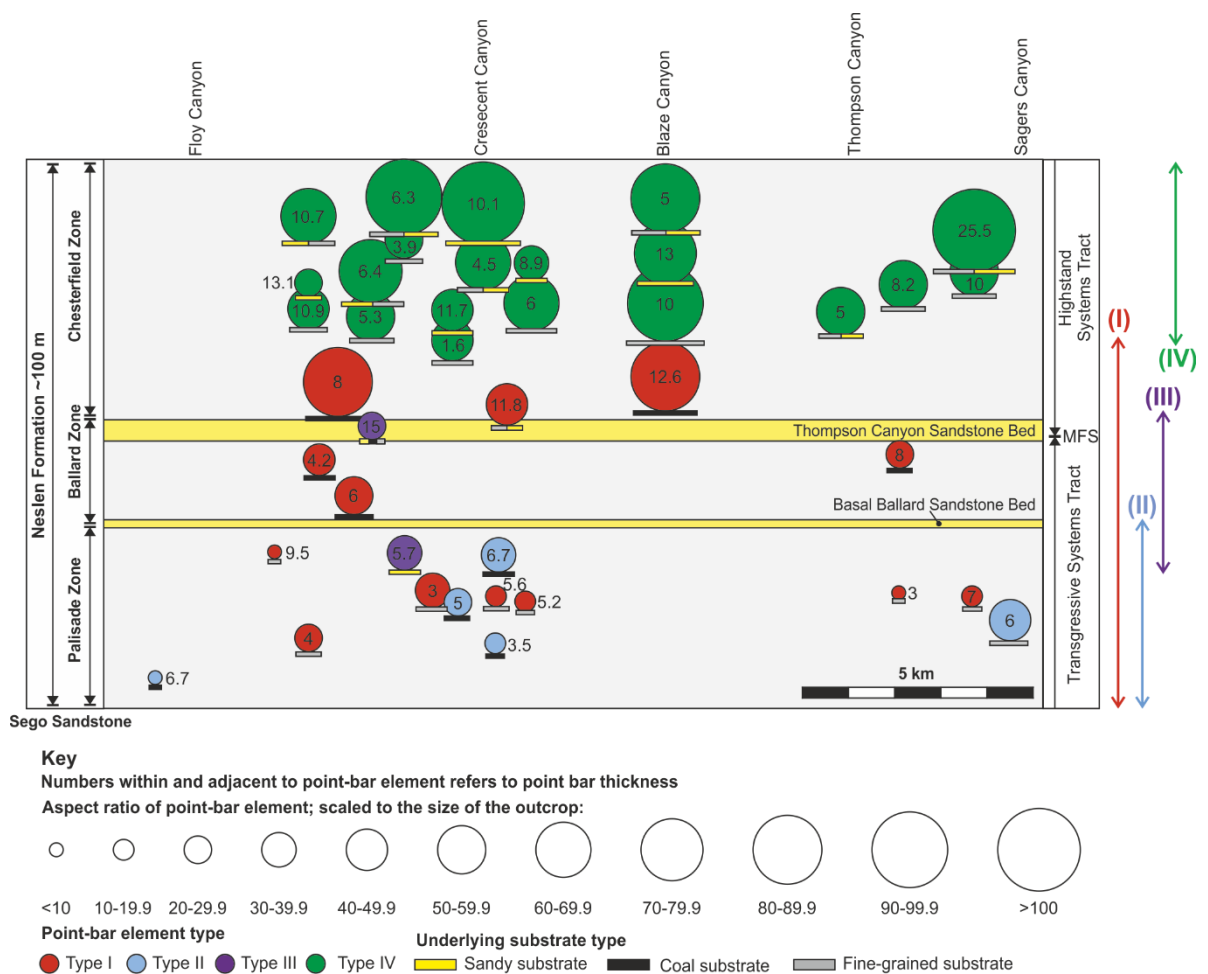


Figure 6.12: Schematic panel showing the location of each point-bar element examined in this study in relation to the interpreted sequence stratigraphic framework. Each point-bar element is colour coded to represent the interpreted element type (I, II, III or IV) and is shown in relation to each element's underlying substrate, as well as scaled in proportion to the aspect ratio of the outcrop. Numbers within examples refer to the maximum logged thickness of the point-bar element in metres.

The interplay of eustasy, tectonics, sediment supply and compaction is widely accepted as a control on the stacking of fluvial systems (e.g. Leeder 1977; Allen 1978; Bridge and Leeder 1979; Aitken and Flint 1995; Heller and Paola 1996; Currie 1997; S nderholm and Tirsgaard 1998; Huerta et al. 2011; Foix et al. 2013). Channel-body stacking is commonly expected to inversely correlate with aggradation rate, thereby also affecting the geometry and connectedness of channel deposits. These assumptions are often made on the basis of results from a suite of numerical models known as the Leeder-Allen-Bridge (LAB) models of alluvial architecture (Leeder 1978; Allen 1978; Bridge and Leeder 1979). Periods of low accommodation on the floodplain promote extensive reworking of fine-grained overbank material due to lateral channel migration or avulsion (Posamentier and Vail 1988; Holbrook 1996). During periods of increased accommodation generation an increased proportion of overbank material is preserved and reworking of channel deposits is limited.

Upwards through the Neslen Formation, the succession was controlled by an upward decrease in accommodation or increase in sediment supply from TST to HST (Shiers et al. 2014; Chapter 5). This change caused the rivers to traverse their floodplains, increasing the degree of reworking of existing sediment (cf. Wright and Marriott 1993). This situation arose due to the higher gradient of the fluvial plain (associated with regression of the seaway, progradation of the coastal plain or increased sediment supply) and delivery of relatively coarse sediment (cf. Chan and Pfaff 1991) which resulted in an increase in stream power and the proportion of transported bedload sediment, which facilitated a change from high- to low-sinuosity channels (cf. Legarretta et al. 1993; Wright and Marriott 1993; Aitken and Flint 1995; Burns et al. 1997; Currie 1997; Holbrook 1996; Rogers 1998; Flint et al. 2001). Contrastingly, within a TST, channels are typically smaller, and more sinuous.

Stream power (as a function of sediment supply) is directly proportional to discharge and gradient and inversely proportional to the channel width, thus, may result in the preferential accumulation of sediment into dunes rather than ripple-sized features for a given grain size (Harms 1975). The role of accommodation change in governing the internal lithofacies character of point-bar elements is less well understood.

6.5.1.2 Marine influence

The lower Neslen Formation is moderately influenced by marine processes (Lawton 1986; Pitman et al 1987; Kirschbaum and Hettinger 2004; Gualtieri 1991; Karaman 2012; O'Brien 2015; Gates and Scheetz 2015; Burton et al. 2016; chapter 5). The overall progradation of the Neslen Formation through time (chapter 5) means that facies belts also prograded eastward overall. The upper Neslen Formation represents alluvial channels which formed up-dip of any discernible influence of marine) or backwater processes (Shiers et al. 2014). This indicates that the change from isolated (types I, II and III) to amalgamated point-

bar elements (type IV) may correlate with the change in hydrodynamics of the channels due to the absence of backwater processes (cf. Colombera et al. 2015). Further discussion of this is presented in chapter 7.

The influence of marine processes on the facies assemblage of point-bar elements is well documented (Weimer et al. 1982; Thomas et al. 1987; Shanley et al. 1992; Choi et al. 2004; Dalrymple and Choi 2007; Hovikoski et al. 2008; Sisulak and Dashtgard 2012; Johnson and Dashtgard 2014). Type I and II point-bar elements are interpreted to have been subject to tide influence. This interpretation is made based on the preservation of significant heterogeneities (Figs. 6.7g, 6.8g, 6.11b, 6.11c), either as individual beds of mudstone and siltstone (forming IHS) or heterolithic packages (H, Si, draped ripples; Table 4.1). The abundance of heterolithic facies, which in some cases shows subtle rhythmicity, supports that channel flow was modulated by tidal processes (van den Berg et al. 2007). Type I and II elements also exhibit abundant trace fossils, which are indicative of deposition in a stressed, brackish water environment (Table 6.1; Bromley 1996; Gingras et al. 2012). The influence of tides may have modulated the channel flow; causing repeated fluctuations in velocity and hence the introduction of significant heterogeneities. However, the lack of down-dip changes in the type of point-bar element (Fig. 6.12) indicates that proximity to the shoreline was not a major influence on the observed facies assemblages, or that the area covered by this study was not sufficiently large to detect such changes.

6.5.1.3 Spatial variability

The vertical change in the occurrence of different point-bar element types can be explained by spatial variation in coeval facies belts and changes in marine influence up-dip from the coastline. The amount of marine influence interpreted is highest in type II point-bar elements, with minor influence by tidal processes interpreted for type I point bar elements. Minor evidence of brackish water ichnofacies at the base type III point-bar elements indicates that they were deposited closer to the coastline than type IV point-bar elements which are interpreted to have been deposited up-dip of the limit of marine and backwater influence (Fig. 6.13). Thus, the vertical changes in types of point-bar element could have originated through shifting of these facies belts through time.

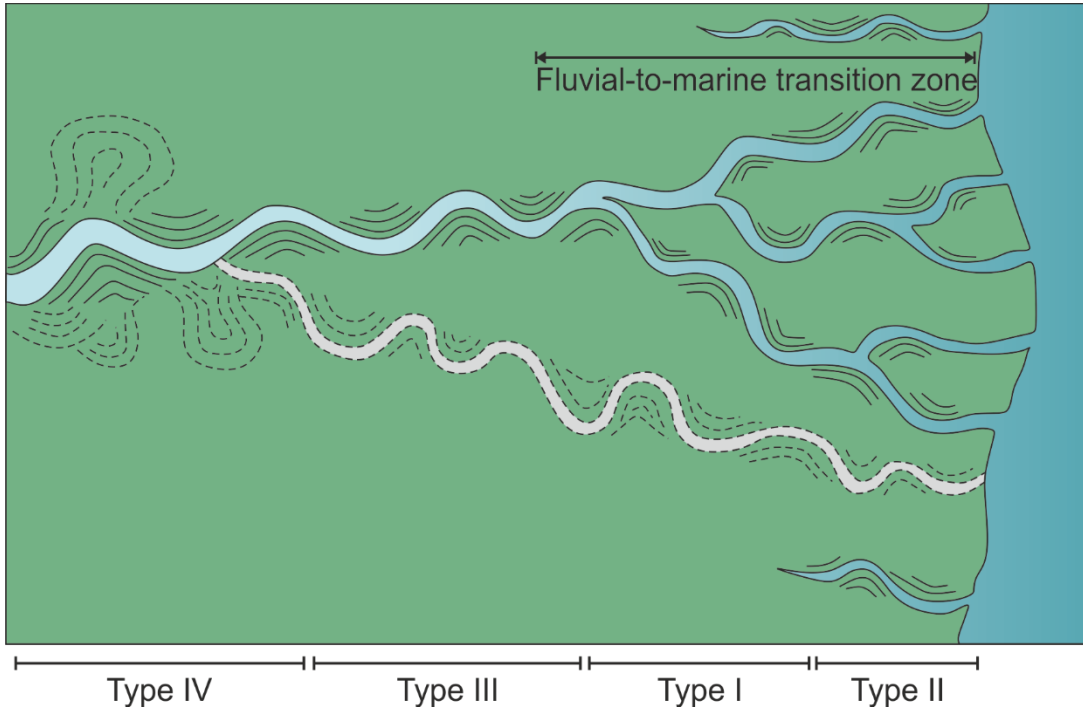


Figure 6.13: Schematic diagram showing the possible spatial zones for deposition of the different type of point-bar elements with relation to the limit of marine influence (tidal and backwater processes)

The change from dominantly type III to type IV point-bar elements in the upper Neslen Formation can be explained by a decrease in the rate of relative sea-level rise from the TST to HST (section 6.5.1.1 above), which led to regional shifts in facies belts, due to progradation of the coastal plain through time (at much slower rates, by one to several orders of magnitude, than those assumed for the LAB models; Miall 2014a). This means that the depositional environment within the study area changed from a coastal plain (modified to some degree by marine and backwater processes) in the lower Chesterfield Zone to a fluvially dominated alluvial plain in the upper Chesterfield Zone (Fig. 6.13).

6.5.1.4 Presence of coal beds

Vertically there is a decrease in the occurrence and quality of coal beds in the Neslen Formation; both of these changes can be caused by the same processes (e.g. changes in climate, accommodation or DFS progradation), or else the change in the abundance of coal could itself be the causative factor.

The presence of laterally extensive, ombrotrophic mires in the lower Neslen Formation (chapter 5) could have been preserved to form coals only where the overall increase in accommodation approximately equals the accumulation rate of peat (see discussions in Speiker 1949; Young 1955; Teichmüller 1962; Bloom and Ellis 1965; Rampino

and Sanders 1981; Tissot and Welte 1984; Courel 1989; Allen 1990; McCabe 1991). The production of peat can also generate localised topographic lows through rapid compaction of organic matter following accumulation (Bohacs and Suter 1997) which modify the avulsion frequency and controlled the location of channels. The avulsion of a channel which is contained within a topographic low will require more energy, hence the avulsion frequency would be lower than for coastal plains which lack mires.

Point-bar elements underlain by coal are exclusively categorised as type I or II elements (Fig. 6.12). The aspect ratio of point-bar elements that have an underlying coal-prone substrate are generally lower than those with sandy or mudstone/siltstone substrates (Fig. 6.12). Therefore, it is likely that channel evolution (through incision and accretion) was controlled by the presence of mires either adjacent to, or underlying the channel. Incision and accretion of the channel was likely limited by the higher relief of ombrotrophic mires (chapter 5) and their ability to withstand erosion (McCabe 1985). The presence of a mire would therefore likely limit the size of point-bar elements, as well as influence the morphodynamics of the river and hence the internal lithofacies character of the developing point bars.

6.5.1.5 Grain size

The average grain size of point-bar elements generally increases through the Neslen Formation, with type I and II point-bar elements composed predominantly of very-fine to medium grained sandstone (Figs. 6.7b, 6.8b), whereas type III and IV elements are composed predominantly of fine-to-medium grained sandstone (Fig. 6.9b, 6.10b). The grain size of sandstones in ripple-laminated sandstone beds is finer than that in cross-bedded sandstone beds. This likely reflects higher stream power within associated channels during deposition of cross-stratified beds. The increase in grain size upwards through the Neslen Formation, as well as the increase in aspect ratio and amalgamation of the point-bar elements, is likely reflects an increase in stream power over the time interval represented by accumulation of the Neslen Formation (see section 6.5.1.5). Therefore, the disparity in grain-sizes between the different types of point bar elements is thought to be causative; a product of the same process forming the unusual point-bar assemblages of type I and II elements.

6.5.1.6 Flow velocity

The palaeoflow velocity within the channels associated with ancient point-bar elements is difficult to determine. Numerous equations have been produced which relate channel dimensions to sinuosity, water discharge and gradient (e.g. Leopold and Wolman 1960; Schumm 1963; 1972; Williams 1986; Bridge and Mackey 1993; Table 6.3). These calculations often negate short time-scale discharge variations (e.g. individual flood events).

Generally, the calculated flow velocity (see Table 6.3) for the channels associated with Neslen Formation point-bar elements increase upwards through the Neslen Formation and that calculated for type I and II point-bar elements is significantly lower than those calculated for type III and IV elements.

The low discharge velocities in the lower Neslen Formation may be attributed to allogenic controls such as low channel gradients, or times of especially low river flow through an overall drier climate. This would indicate that, if a change in the river discharge was the controlling factor, during times of accumulation and preservation of the deposits of the Palisade, Ballard and lower Chesterfield zones, then flow velocity and/or channel gradients would have been lower than at the time of emplacement of deposits of the upper Chesterfield zone, or during deposition of other units on the margins of the WIS (Table 6.3). A drier climate model, with more extreme variations in flow velocity, is herein discounted because of the association of good-quality coals with the Palisade and Ballard zones (Fig. 6.12; chapter 5). A floodplain gradient for the Neslen Formation of $\sim 2.5 \times 10^{-4}$ m/m is inferred from the gradient of transgressive surfaces traced by Aschoff and Steel (2011a). The low basin gradient may have resulted from the interference between Sevier-style tectonics, Laramide-style tectonics, and dynamic subsidence; this would offer explanation of the observed extensive transgressions, which are partially attributed to eustatic fluctuations (Aschoff and Steel 2011; Chapter 5). Type I and type II point-bar elements are attributed to channels within which the stream power was reduced and sediment was not capable of accumulating into dune-sized features (Fig. 6.14). This situation could have arisen in channels located off-axis from the main trunk channel belt, or within a palaeoenvironment within which multiple contemporaneous channels were active e.g. a delta plain setting (Fig. 6.13). There is no link between the proportion of preserved fines within the point bars and the flow velocity. This is because the calculated flow velocities are time and depth averaged, and fine-grained sediments are attributed to periods of low river flow.

	Unit	Equation		Neslen Fm.	Type I	Type II	Type III	Type IV	McMurray Fm.	Ferron Ss.	Lower Williams Fork Fm.	Scalby Ss.	Wesse x Fm.	Green River Fm.
Maximum Bankfull depth (D)	m	Measured		8.8	6.4	5.8	10.35	10.6	30-40	7	6.65	6.65	3.24	6.5
Bankfull width (W)	m	$8.88(0.5D)^{1.82}$ Or measured	(1)	131.7	73.8	61.7	176.9	184.7	500-548	290	281	165	100	74
Channel belt width (Wm)	m	$148 \times D^{1.52}$	(2)	4035	2486	2141	5164	5354	40,308	2850	2636	2636	883	2546
W:D (F)	/	W/D	(3)	15	11.5	10.6	17	17.4	13.9-18.3	41.4	42.3	24.8	30.86	11.4
Wavelength (λ)	m	$10.9 \times W^{1.01}$	(4)	1507	839	700	2030	2121	5500-6400	3345	3241	1892	1141	842
Sinuosity (P)	/	$3.5F^{-0.27}$	(5)	1.7	1.8	1.9	1.6	1.6	1.6-2.4	1.3	1.2	1.5	1.4	1.8
Mean annual discharge (Qm)	m ³ /s	$\frac{W^{2.43}}{18 \times F^{1.13}}$	(6)	368	121.8	86	655 rev	709	10,978	796	719	361	83.5	123
Mean annual flood (Qma)	m ³ /s	$16 \left(\frac{W^{1.56}}{F^{0.66}} \right)$	(7)	5425	2620	2090	7916	8338	43,994	9511	8927	5534	2193	2645

Table 6-2: Table showing quantitative analysis of channels in the Neslen Formation separated by element type, compared to other systems on the margins of the Western Interior Seaway (green) and humid-climate successions generally (orange). Maximum bankfull depth is interpreted from the average point-bar thickness assuming no compaction. A minor error is introduced where the maximum bankfull depth is used to calculate the bankfull width and channel belt width as these calculations require D to refer to the mean bankfull depth (Bridge and Tye 2000). Sources for equations: (1) Bridge and Mackey (1993); (2) Williams (1986); (4) Leopold and Wolman (1960); (5) Schumm (1963); (6, 7, 8) Schumm (1972).

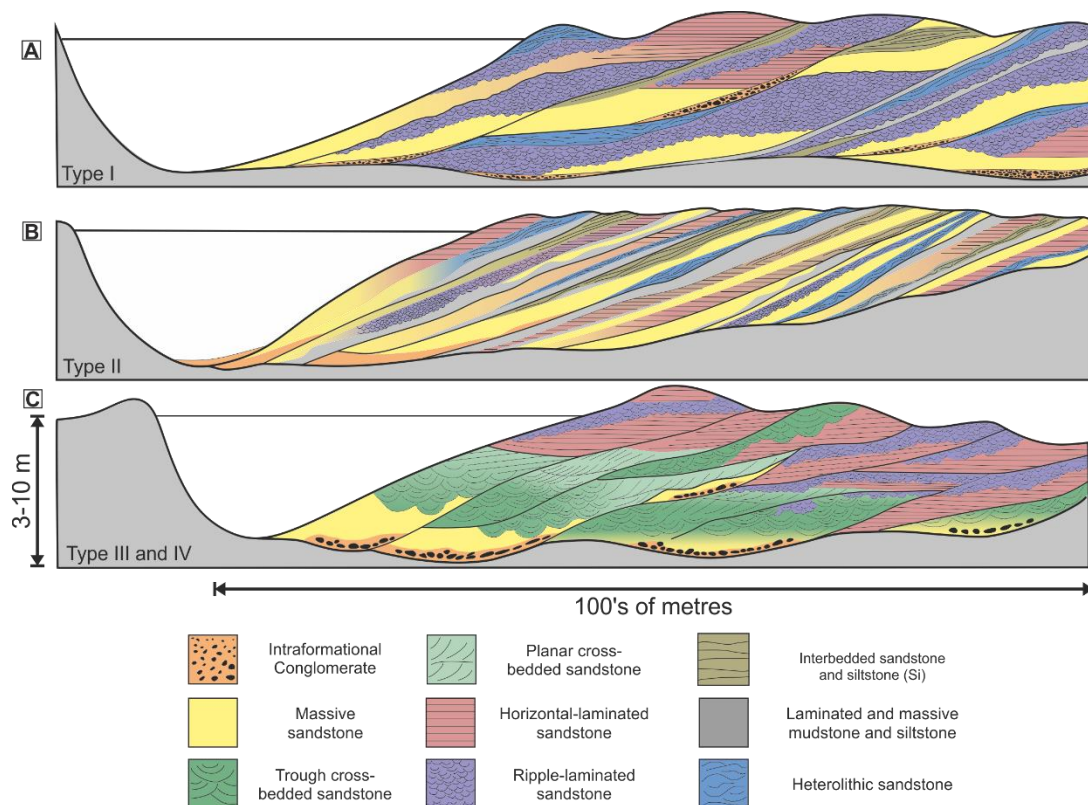


Figure 6.14: Schematic models of point-bar models. A) Ripple-dominated (type I) point-bar element. B) Heterolithic (type II) point-bar element lacking cross-bedded sandstone. C) point bar element that conforms to traditional facies models (type III and IV).

6.5.2 Comparison of the Neslen Formation to FAKTS and literature

In the Neslen Formation there exist established trends between the types of point-bar element and their style of vertical stacking. Analysis shows that these trends are likely due to an interplay of accommodation space (likely influenced by the presence of coal and marine processes), grain size and flow velocity. Analysis using FAKTS can be used to test if these trends can be observed in other ancient successions of other humid climate and coastal plain systems interpreted as having been deposited in humid and/or coastal plain environments.

6.5.2.1 Systems tract and A:S ratio

The relationship between the rate of accommodation generation and geometry, channel-body density and amalgamation has been established through case-study analyses using FAKTS (Colombera et al. 2015). Results show that, in many case studies, there is no direct correlation between accommodation space and channel geometry, density and amalgamation; in contrast to stratigraphic or numerical models (presented in Section 6.5.1.1). Testing of these long-held relationships (Miall 2014a; Colombera et al. 2015), have shown that the use of channel-body characteristics alone for the identification of high- and low-accommodation systems tracts is not justified in all depositional settings. This is because

of the disparity between the instantaneous accumulation rate for an active river, versus long term, time-averaged accumulation rates calculated for ancient successions where there are long periods without sedimentation (Miall 2014b). However, the stacking of channelised elements observed in the Neslen Formation remains consistent with the relationships predicted by stratigraphic models as well as those observed in other formations (e.g. Breathitt Group, Aitken and Flint 1995; Ericson Sandstone, Martinsen et al. 1999; Blackhawk Formation, Hampson et al 2012; Fig. 7.5). This shows that the relationship of stacking patterns with accommodation space is complicated; fluvial systems are subject to an interplay of multiple controls.

Sediment supply is assumed to be constant in many sequence stratigraphic models (e.g. Posamentier and Vail 1988); this is likely a gross over simplification. Sediment supply is highly significant as a control on the architecture of fluvial and shallow-marine systems (Posamentier and Allen 1993; Schlager 1993; Schumm 1993; Wescott 1993). Variations in sediment supply cannot be tested using FAKTS due to a lack of suitable data from published studies. It is difficult to correlate pulses in sediment supply from the hinterland to depositional intervals which contain higher proportion of sandstone in the floodplain-coastal plain without precise dating of relatively thin intervals of the stratigraphy, which themselves are expected to represent relatively short-lived geologic episodes.

6.5.2.2 Marine influence

The link between point-bars interpreted to have been modified by tidal processes and the lack of cross-bedded sandstone (and concurrent high proportion of ripple-laminated and horizontally laminated sandstone) is not observed within other formations (e.g. Weimer et al. 1982; Thomas et al. 1987; Shanley et al. 1992; Bose and Chakraborty 1994; Choi et al. 2004; Dalrymple and Choi 2007; van den Berg et al. 2007; Hovikoski et al. 2008; Matinius and Gowland 2011; Sisulak and Dashtgard 2012; Johnson and Dashtgard 2014; Legler et al. 2014). None of the successions interpreted as having been laid down in environments proximal to the marine realm show similar facies assemblages to the Neslen Formation. This indicates that, although marine processes may have been responsible for the introduction of significant heterogeneities within point-bar elements, they are unlikely to be the dominant control on the occurrence of cross-bedding within these elements.

6.5.2.3 Presence of coal beds

Other coal-bearing systems analysed using FAKTS do not exhibit similar facies assemblages to type I or II point-bar elements of the Neslen Formation. Other coal-bearing systems documented in the literature (e.g. Ferron Sandstone, Ryer 1981; Raniganj coal measures, Casshyap and Kumar 1987; Straight Cliffs Formation, Shanley et al. 1992; Weisselster Basin, Halfar et al. 1998; Lopingian coal measures, Wang et al. 2011) do not

report instances of facies assemblages similar to those in the type I or II point-bar elements reported for the Neslen Formation. This indicates that, although there is a strong relationship between the presence of coal substrates and the occurrence of type I and II facies assemblages (Figs. 11b;c; 12), this relationship has not hitherto been established in other successions.

6.5.2.4 Grain size

The point-bar elements analysed using the FAKTS database possess a wide variety of grain sizes. For example, sandstone units in the Green River Formation (Fig. 6.2h) and Ferron Sandstone (Fig. 6.2c), which are representative of the component lithofacies of point-bar elements, are generally fine-to medium-grained (Cotter 1971; Shuster and Steidtmann 1987), yet their facies proportions are dissimilar to each other. The Wessex Formation, UK (Stewart 1983), has similar proportions of preserved fines (i.e. heterogeneity) and relative proportions of cross-bedded to ripple laminated sandstone as the McMurray Formation, Alberta (Jablonski et al. 2012) (Fig. 6.2b, 6.2g), however the grain size of sandstone units are different (Insole et al. 1994; Insole and Hutt 1994; Labrecque et al. 2011). This suggests that grain size is unlikely to be the primary controlling factor governing the internal facies architecture of point-bar elements.

6.5.2.5 Flow velocity

Comparing the preserved internal lithofacies (Figs. 6.2b-h) with the flow velocity and sinuosity (Table 6.3) shows that systems for which channels are calculated to have low mean annual discharge values (<150 m³/s) have greater proportions of ripple-laminated sandstone preserved in the associated point-bar elements (e.g. Green River Formation, Wessex Formation). This correlation between the proportion of ripple lamination and the mean annual discharge indicates that those channels who have an overall lower flow are more likely to have associated point-bar elements with type I or II facies assemblages. No other studied successions documented in the literature have a similarly low proportion of cross-bedded sandstone as the type I or II point-bar elements studied here.

6.6 Summary

Quantitative analysis of 41 point-bar elements from the Cretaceous Neslen Formation has allowed four point-bar element types to be distinguished based on their internal facies types, proportions and geometry. Type I and II point-bar elements are characterised internally by a distinctive lack of cross-bedding and are instead dominated by ripple-laminated sandstone and massive, horizontally laminated sandstone, respectively. Type III and IV point-bar elements are similar to many others from other successions based on analysis using the FAKTS database; these types conform to traditional point-bar models.

Upwards through the Neslen Formation there are a series of changes in the character of point-bar elements: i) an increase in the aspect ratio of point-bar elements; ii) an increase in the thickness and amalgamation of point-bar elements; iii) a decrease in heterogeneity; iv) a change from dominantly type I and II point-bar elements in the lower Neslen Formation to type III and IV point-bar elements in the upper part.

Vertical changes in channel-body stacking identified in the Neslen Formation are interpreted to have been caused by dominantly allogenic processes. A vertical increase in sediment supply and/or a decrease in the rate of accommodation generation were two probable controls, which likely also resulted in an upwards decrease in the occurrence of coal beds. In the lower Neslen Formation, point-bar elements that exhibit an abundance of ripple and horizontally laminated and massive sandstone, and a corresponding absence of cross-bedded sandstone, are recognised. The deposition of these less common types of point-bar elements (i.e. types I and II) can be attributed to low stream power for this interval. Other important considerations in the deposition of unusual point bar assemblages include the fine-grained nature of the sediment and the presence of mires.

7 Discussion

This Chapter integrates the results of all preceding Chapters and presents a wider discussion that introduces examples from modern coastal systems and from other ancient preserved successions considered to be analogous in part to the Neslen Formation. The overall depositional context of the Neslen Formation is reconstructed. Factors that govern the style of preservation of sedimentary indicators of marine influence in ancient strata are considered. The extrinsic and intrinsic controls on the deposition, accumulation and preservation of coastal successions are discussed. The subsurface reservoir implications of this study are also considered.

This Chapter will address each of the research questions presented in Chapter 1 in turn; and discuss the wider significance of the results of this thesis. A summary for each research question is presented.

7.1 *Research question one: What are the sedimentological and stratigraphic expressions of the fluvial-to-marine transition zone?*

The fluvial-to-marine transition zone (FMTZ) separates fully fluvial from fully marine sedimentation processes (Chapter 2). The vertical accumulation of fluvial, FMTZ and marine deposits (also referred to as paralic successions) is complicated due to the spatially and temporally transitional nature of the FMTZ. Here, paralic deposits from humid-climate environmental settings have been studied at a range of scales to capture the sedimentological and stratigraphic expression of the FMTZ (chapters 4-6). Justified interpretation of marine influence in fluvial deposits relies on the identification of a suite of sedimentary and ichnological indicators; these are discussed below. Several authors have suggested previously that the deposits of the FMTZ show predictable transitions down-dip in terms of sediment character, facies, ichnology, and geometries (in both plan-form and cross-section) of architectural elements (Dalrymple et al. 1991; 1992; 2003; Buatois et al. 1997; Pemberton et al. 2001; Browne and Naish 2003; MacEachern et al. 2005; Cummings et al. 2006; Dalrymple and Choi 2007; Gugliotta 2016). The occurrence of down-dip changes in facies and architectural elements has been tested for the lower Neslen Formation (chapter 5); general aspects of these changes are discussed below.

7.1.1 Marine influence in fluvial deposits

The sedimentary response to the fluctuating energy conditions within the FMTZ results in the accumulation of a specific suite of sedimentary structures (as described in section 2.4.1.1). The majority of these sedimentary indicators accumulate as the result of fluctuating energy and/or direction of flow within the system (for example in channels).

These fluctuations can be caused by modulation of the flow due to tidal processes as well as the influence of storms. However, this is not definitive as similar processes can occur in fully fluvial settings e.g. ephemeral fluvial environments subject to episodic flow regimes (Picard and High 1973). The identification of a suite of trace fossils indicative of stressed brackish water conditions can also be used to infer marine influence on fluvial deposits (section 2.4.1.1.2). A summary of the marine sedimentary indicators identified in deposits of the Neslen Formation and a ranking as to their reliability as marine indicators is shown in Table 7.1.

Structure/Trace fossil	Reliability (1-3, 1 is high, 3 is low)
<i>Teredolites</i>	2: Teredolites bored wood can be rafted upstream, in which case it must be within the tidal push zone.
<i>Thalassinoides</i>	1: Found in shallow marine and deep marine environments.
<i>Lockeia</i>	3: Can be found in any aquatic environment.
<i>Bergaueria</i>	1: Found in shallow marine and deep marine environments.
<i>Ophiomorpha</i>	1: Prolific in marine shoreface environments, brackish water, sandy substrates common.
<i>Rhizocoralium</i>	1: Found in shallow marine and deep marine environments.
<i>Arenicolites</i>	3: Can be found in Aeolian, marine, freshwater and fluvial environments.
<i>Skolithos</i>	3: Can be found in a wide range of depositional environments.
Draped bedforms	1/2: Drapes of mud, silt or carbonaceous material can form on ripples and on cross-bedding foresets. They indicate alternations in the energy of the current which can be due to tidal processes or discharge variations; where rhythmic thickness variations are apparent they are attributed to tidal processes.
Mud-chip conglomerate	3: Whilst many authors cite this structure as occurring in tidally influenced point bars it can occur in any depositional environment.
Wavy-flaser-lenticular bedding	1/2: Bed which preserve varying proportions of mudstone/siltstone and sandstone form due to alternations in the energy of the current which can be due to tidal processes or discharge variations; where rhythmic thickness variations are apparent they are attributed to tidal processes.
Wave ripples	1: Symmetrical wave ripples commonly form in environments influenced by waves and tides.
Sandstone deposits with bidirectional ripples	2: Formation of occasional bi-directionality in ripple-laminated beds can form in any fluvial environments due to the presence of eddies.
Cross-bedding with multiple reactivation surfaces	2: Multiple reactivation surfaces can also occur from changes in fluvial flow e.g. in ephemeral fluvial systems

Table 7-1: Table showing the reliability of a series of a series of sedimentological and ichnological marine indicators.

Within the lower Neslen Formation, the most abundant marine indicators are found within the Middle Palisade Zone (MPZ); a marine influenced depositional package is interpreted to represent a transgressive interval (chapter 5). Similar marine influenced intervals can, in some cases, be interpreted as zones of flooding in other successions (e.g. Gastaldo et al. 1993; Aitken and Flint 1995; McLaurin and Steel 2000). In the case of the Neslen Formation, the shallowing-upward trend observed in the succession within the MPZ indicates that the base of the interval is interpreted as a flooding surface (Figure 5.10). Within the Neslen Formation, heterolithic point-bar elements contain a high proportion of marine indicators (Chapters 4 and 6; Fig. 7.1) in accordance with many interpretations of heterolithic and marine-influenced point bars described in the literature (e.g. Thomas et al. 1987; Smith 1989; Corbeau et al. 2004; Dalrymple and Choi 2007; Fustic 2007; Pranter et al. 2007; Patruyo et al. 2009; Labrecque et al. 2011; Fustic et al. 2012; Jablonski 2012; Sisulak et al. 2012; Sisulak and Dashtgard 2012; Johnson and Dashtgard 2014; Shanley et al. 2012; Sambrook Smith et al. 2016). It follows that the MPZ should therefore contain a high proportion of heterolithic point-bar elements. This hypothesis can readily be tested by comparing the correlations made in Chapter 5, with the locations of type II point-bar elements (Fig. 7.1) analysed in Chapter 6 (Fig. 7.2). This analysis shows that those point bars with the highest heterogeneity (over 20 % of the logged section is made up of siltstone or mudstone; Fig. 7.1) are preferentially found within the MPZ, with only a single occurrence in each of the Lower Palisade and Palisade Coal Zones. The MPZ also contains point-bar elements which have a moderate level of heterogeneity (10-20 %), with other occurrences of such types restricted to the Ballard Zone (Fig. 7.2). This shows that there is a weak correlation of marine-influenced intervals with the occurrence of heterolithic point bars in the Neslen Formation.

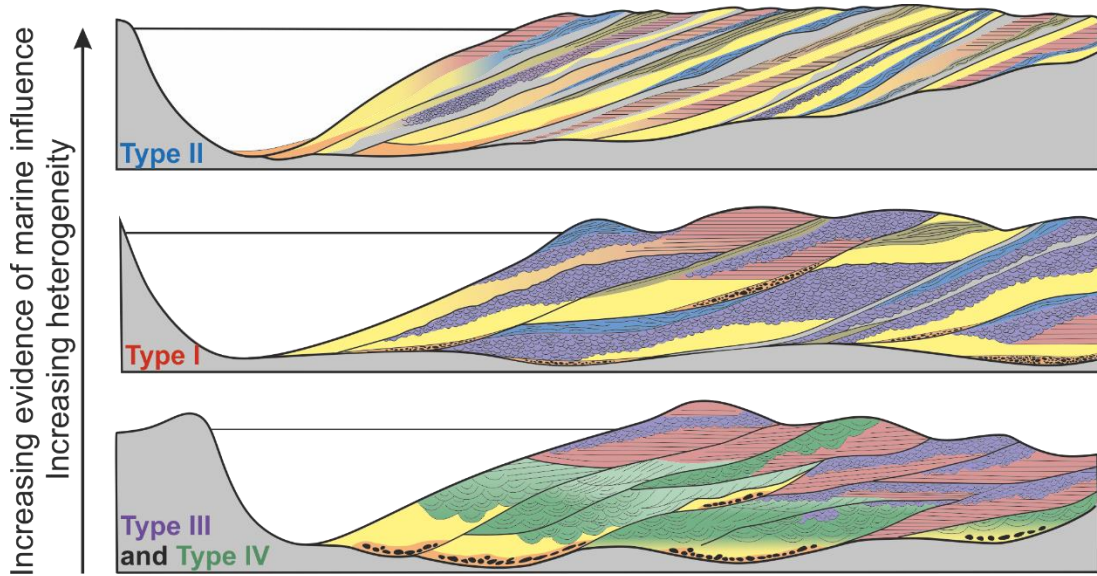


Figure 7.1: Schematic facies models of point-bar elements in the Neslen Formation with the relative amount of marine influence indicated.

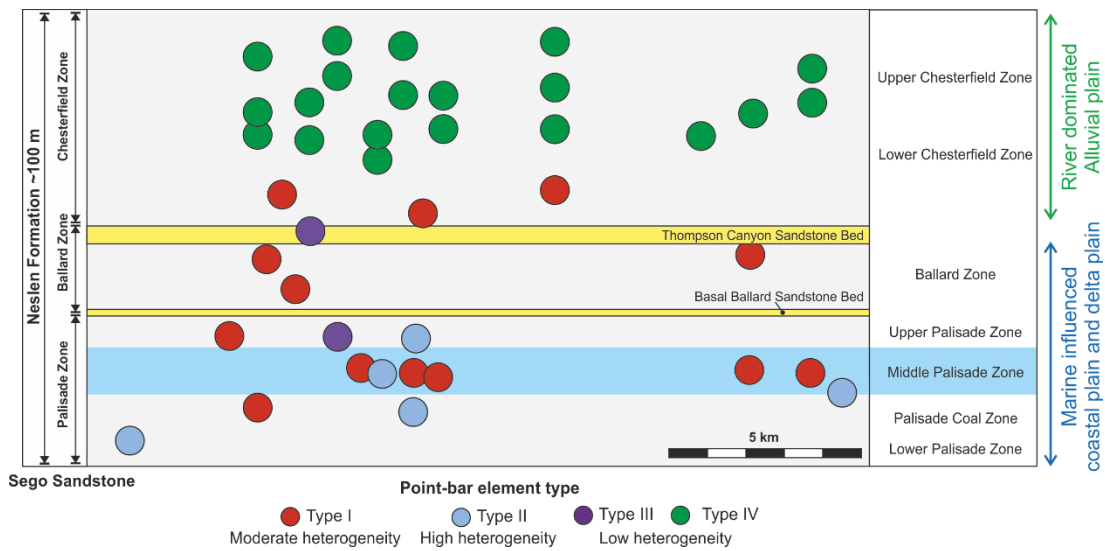


Figure 7.2: Panel showing the heterogeneity of point bar elements in the Neslen Formation and the interpreted depositional intervals: the Middle Palisade Zone is highlighted in blue.

7.1.2 Stratigraphic expression of the FMTZ

Many studies which attempt to correlate packages of marine-influenced strata are undertaken using study sites that are many kilometres apart (e.g. Shanley and McCabe 1994; Blum and Torqvist 2000; Catuneanu et al. 2009; Neal and Abreu 2009; Jerolmack and Paola 2010); this means that our understanding of how deposits of the FMTZ are transferred into the stratigraphic record are likely oversimplified. For example, if the marine-influenced strata of the Neslen Formation was analysed using only sedimentary logs at Tusher Canyon; Floy Canyon and Sagers Canyon (effectively reducing the available dataset by 60%) then the way in which the FMTZ is interpreted to have been preserved in the stratigraphic record would have been very different (Fig. 7.3). Using widely spaced study sites, the general trends identified through the formation (e.g. large-scale patterns of channel amalgamation) can still be recognised; however different depositional intervals interpreted for the lower Neslen Formation (chapter 5) could not be discerned using such an approach. Identification of time-equivalent packages (chapter 5) has been achieved through analysis of closely spaced study sites (2-3 km apart) which have been used to determine the three-dimensional architecture of the deposits. Recognition of these packages has helped to develop a greater understanding of how the Neslen Formation accumulated through time; furthermore, it has enabled reconstruction of the way in which the geomorphic FMTZ has been transferred into the stratigraphic record. Within each depositional interval (e.g. Middle Palisade Zone; Upper Palisade Zone; Chapter 5) there is a change from fluvial-dominated elements in the up-dip parts of the study area, to wave and tidal-influenced elements in the down-dip regions (Fig. 5.8). However, the transition is not simple: some marine-influenced deposits are identified in relatively up-dip regions and fluvial-dominated deposits are identified in relatively down-dip positions. This is likely to be due to the limitations of a large-scale correlation panel which is essentially two-dimensional and hence does not take into account variability in the preservation of landforms around what is inferred to have been a highly rugose coastline.

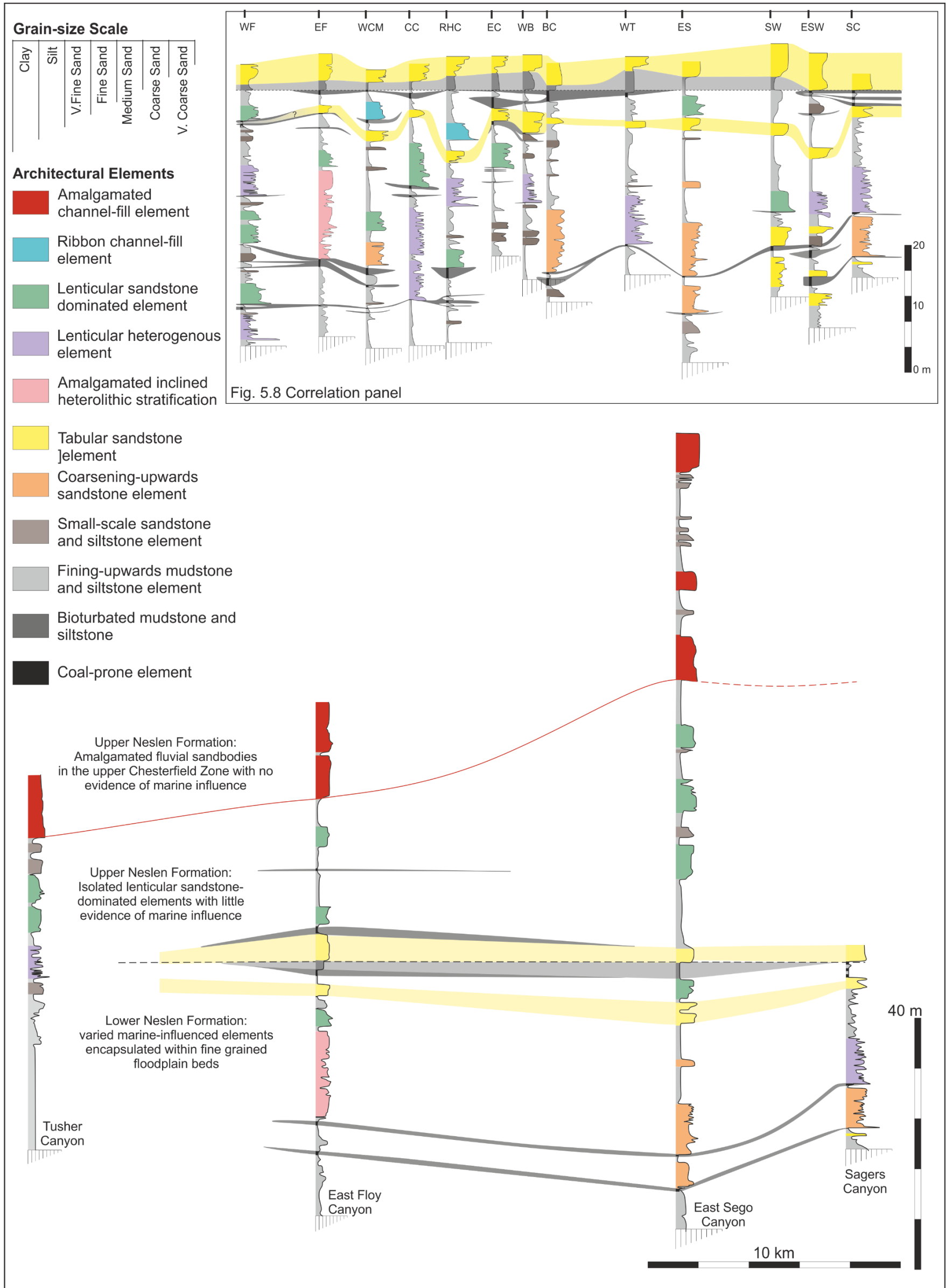


Figure 7.3: Large-scale correlation panel using widely spaced vertical profiles. The contrast with correlation panel used in Chapter 5 is emphasised by showing Figure 5.8 alongside it at the same scale.

7.1.3 Preservation of marine influence

The extent of tidal influence inland from a coeval shoreline is dependent on a range of factors: primarily the coastal-plain gradient, the tidal range at the coast and fluvial discharge (Dalrymple et al. 2015). However, none of these criteria can be easily calculated for ancient successions. The tidal extent for ancient successions is therefore calculated as the maximum distance between a contemporaneous shoreline and channel deposits for which a tidal signature can be discerned from the sedimentary structures and/or ichnology. Such a physical link is difficult to determine. As well as this, many facies have been considered previously as exclusively indicative of tidal processes, rather than the result of mixed fluvial-tidal interactions (with possible overall fluvial dominance). This means that overall the amount of tidal processes interpreted to have influenced ancient successions is difficult to estimate. Some successions may have been subject to the overestimation of tidal influence (e.g. Lajas Formation; Gugliotta 2016) whereas others may have had previous fluvial interpretations changed to reflect previously overlooked tidal influence (e.g. Hawkesbury Sandstone; Miall and Jones 2003)

Calculation of the extent of the FMTZ using the distance from the shoreline to the limit of tidal influence likely underestimates the extent of tidal processes upstream due to the overprinting and reworking of tidal processes commonly deposited during periods of low river flow (Dalrymple et al. 2015). This is important, especially in humid-climate systems such as the Neslen Formation, due to the occurrence of high precipitation events that could cause high-discharge floods (Huber et al. 2002; Miller et al. 2013), which have the potential to overprint the record of tidal processes. Counter to this, since evidence of tidal influence on fluvial sediment deposition in the rock record can be subtle and ambiguous, particularly in the upper reaches of such systems where the tidal influence diminishes, they can easily be overlooked, potentially leading to further underestimates of the length of the FMTZ.

Overall this work has demonstrated that within the Neslen Formation marine influence is variably preserved in the lower parts of the succession (chapters 4, 5 and 6). The distance from the coeval shoreline, however, remains difficult to estimate.

7.1.4 Research question one summary

This thesis has detailed the indicators of marine influence observed in fluvial-dominated palaeoenvironments located in humid climatic settings; although few of the sedimentary indicators identified in the Neslen Formation (draped ripples, flaser-wavy lenticular bedding, IHS) provide unequivocal proof of tidal influence, the combination of a series of sedimentary structures combined with the interpretation of trace fossils typical of brackish water settings (e.g. *Rhizocorallium*, *Arenicolites*, *Teredolites*, *Thalassinoides*) allows for a more confident interpretation of marine-influenced fluvial strata.

The stratigraphic expression of the FMTZ in terms of the up-dip to down-dip transition of facies, architectural elements and ichnology is not simple. This study has emphasised that, in order to recognise ancient deposits of a FMTZ, intervals of stratigraphy which are approximately time-correlative need to be studied via detailed sedimentological analysis of closely spaced study sites.

7.2 Research questions two and three: What is the balance of allogenic and autogenic processes in coastal plain settings?

This part of the research has worked to establish the balance of allogenic and autogenic mechanisms in generating the preserved stratal architecture of the Neslen Formation. The balance of processes interpreted for the Neslen Formation can then be used to better understand the deposition, accumulation and preservation of other marginal marine systems. In the Neslen Formation the stratal architectures observed can be summarised as follows:

- Overall change from marine influenced strata in the lower Neslen Formation to fluvially dominated in the upper Neslen Formation,
- Decrease in coal quality, occurrence and thickness upwards,
- Vertical change in point-bar element facies upwards,
- Vertical increase in point-bar element amalgamation,
- Increase in point-bar element thickness and aspect ratio upwards, and,
- The occurrence of repeated marine influenced intervals in the lower to middle parts of the Formation.

The possible role of allogenic (section 7.2.1; research question 2) and autogenic (section 7.2.2; research question 3) processes are discussed separately below and synthesised in Section 7.2.3.

7.2.1 Research question 2: What are the main controls on deposition and vertical accumulation of fluvial and marginal marine strata?

The primary allogenic forcing mechanisms are driven by changes in climate, tectonics (which controls basin subsidence and source area uplift) and eustasy (Fig. 7.4) (Shanley and McCabe 1994). Fundamentally, these factors control the ratio between accommodation and sediment supply (A:S ratio). The subsequent processes are highly interdependent and result in a complicated series of interactions and feedback loops, the result of which control the preserved sedimentary architecture of fluvial and marginal marine systems (Fig. 7.5) (Shanley and McCabe 1994).

This section will present discussion of the importance of tectonics, climate and eustasy in controlling the depositional architecture of channel elements, their style of stacking and amalgamation, and the response of the coastal plain system to transgression.

The relative importance of these controls in governing the observed stratigraphic architecture of the Neslen Formation (Chapters 4-6) will be discussed.

7.2.1.1 Tectonics

The tectonic setting of the studied basin controls many factors which will impact on the deposition of sediment in fluvial and marginal marine settings. Tectonic style and activity governs the rate, amount and location of subsidence generated within an evolving basin (Leeder 1993), commonly driven by movement on basin-bounding faults, for example. Relative uplift in the source area controls sediment supply (Hovius 1998).

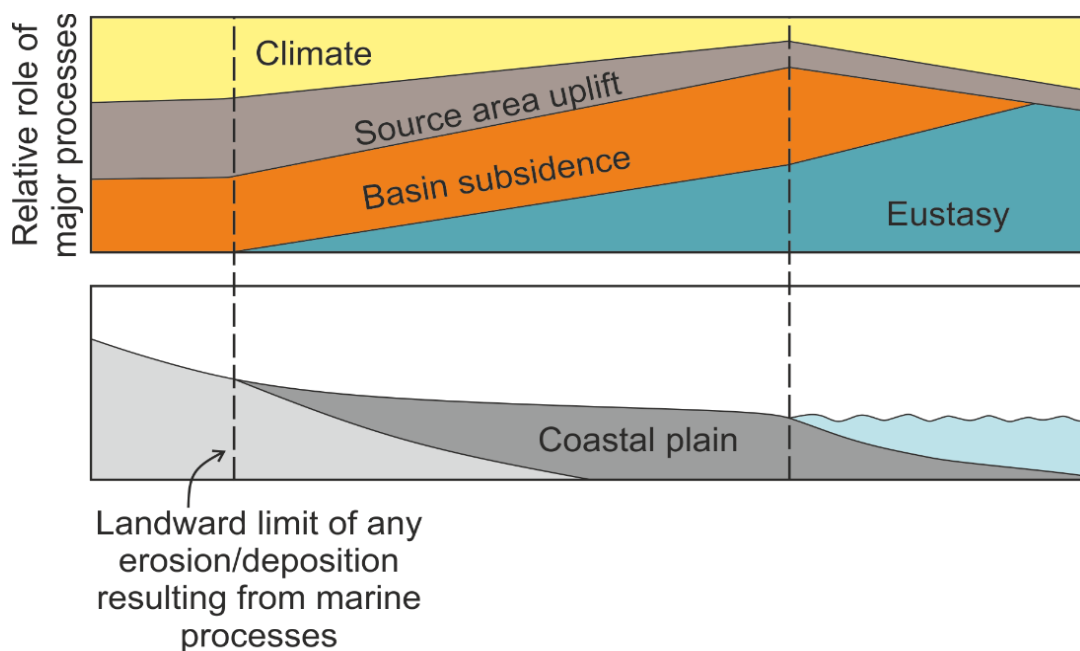


Figure 7.4: Upstream and downstream relative influence of allogenic controls on fluvial and marginal marine architecture (adapted after Shanley and McCabe 1994)

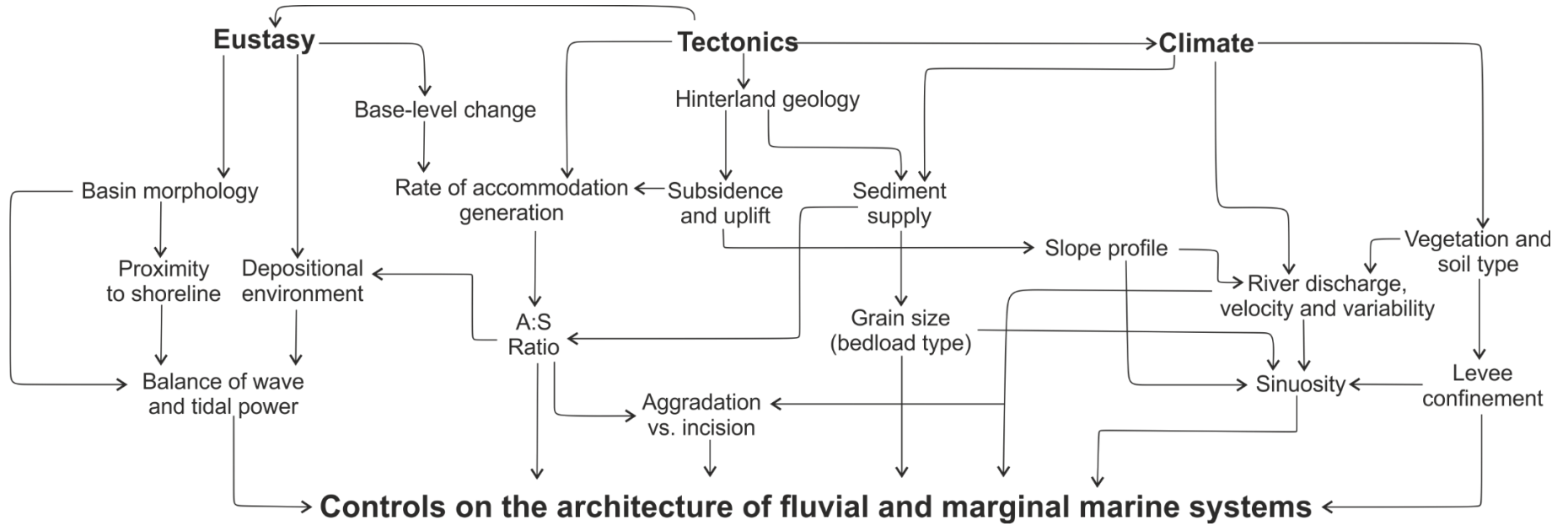


Figure 7.5: Figure showing the complicated allogenic interactions and feedback loops that can affect the controls on the architecture of fluvial and marginal marine environments

7.2.1.1.1 Basin subsidence and accommodation

Within orogenic belts, load build-up causes flexure of the crust which leads to subsidence and the development of a foreland basin (Yingling and Heller 1992). The Neslen Formation was deposited in the Western Interior Seaway (WIS); the foreland basin associated with the Sevier Orogenic Belt (See Chapter 2 for details). The subsidence across the basin controls the amount of space available for deposition and the rate at which it is generated (accompanied by sea-level changes (Section 7.2.3) and autogenic factors (Section 7.3) discussed below). The rate at which accommodation is generated is a major control on the vertical accumulation of channel bodies in non-marine environments; however, of greater importance is the balance of accommodation generation with sediment supply.

The rate of sediment supply to the margins of the WIS outpaces the rate of subsidence leading to extensive progradation (Aschoff and Steel 2011b). However, the chronostratigraphy is poorly constrained, hence no absolute values as to rates can be provided. The generic statements of sediment supply and subsidence rates do not take into account variations in accumulation rate of sediment, which may have been modified by a wide range of different processes (section 7.3).

The gradient of the floodplain and coastal plain are also a function of the rate of basin subsidence and will have a major influence on the velocity of fluvial flow and hence the ability of water flowing in channels to carry sediment.

Two popular and widely adopted types of model to account for response of fluvial systems to base-level change are those of (i) Wright and Marriot (1993) and Shanley and McCabe (1994), so-called 'WMSM' models, and (ii) those of Allen (1978), Leeder (1978), Bridge and Leeder (1979), Bridge and Mackey (1993) and Mackey and Bridge (1995), so-called 'LAB' models (Fig.2.17). The premise of these models is that changes of accommodation exert a critical control on alluvial architecture whereby channel-stacking patterns are the basis for the differentiation between high- and low-accommodation systems tracts (Miall 2014a). During episodes of high rates of accommodation generation, channel bodies become filled and buried before the active channel returns to re-occupy the original site of deposition on the floodplain. During low rates of accommodation generation, channels migrate and relocate frequently, eroding their own earlier deposits such that fluvial successions are more likely to accumulate amalgamated and vertically stacked (i.e. multi-storey) sand bodies. However, much discussion has been made of the applicability of the rates used in both the LAB and WMSM models, which assume an accommodation rate up to three orders of magnitude greater than that typically represented in the rock record (Miall 2014a). In the Neslen Formation, the overall trend in stacking patterns (Chapters 4 and 6) is concordant with an overall decrease in the rate of accommodation generation or an increase in the rate of sediment supply through time, as proposed by LAB models. The stacking of

channelised elements (Fig. 6.12) is similar to that described by Olsen (1995) and models of tectonic forcing (e.g. Willis 2000) (Fig. 7.6). Although these models are constructed for dominantly alluvial sequences, many of the same trends predicted by these models can be observed in paralic successions such as the Neslen Formation. The upwards decrease in the rate of accommodation generation is likely linked to the overall progradation of the coastal plain in the upper Neslen Formation (chapter 4).

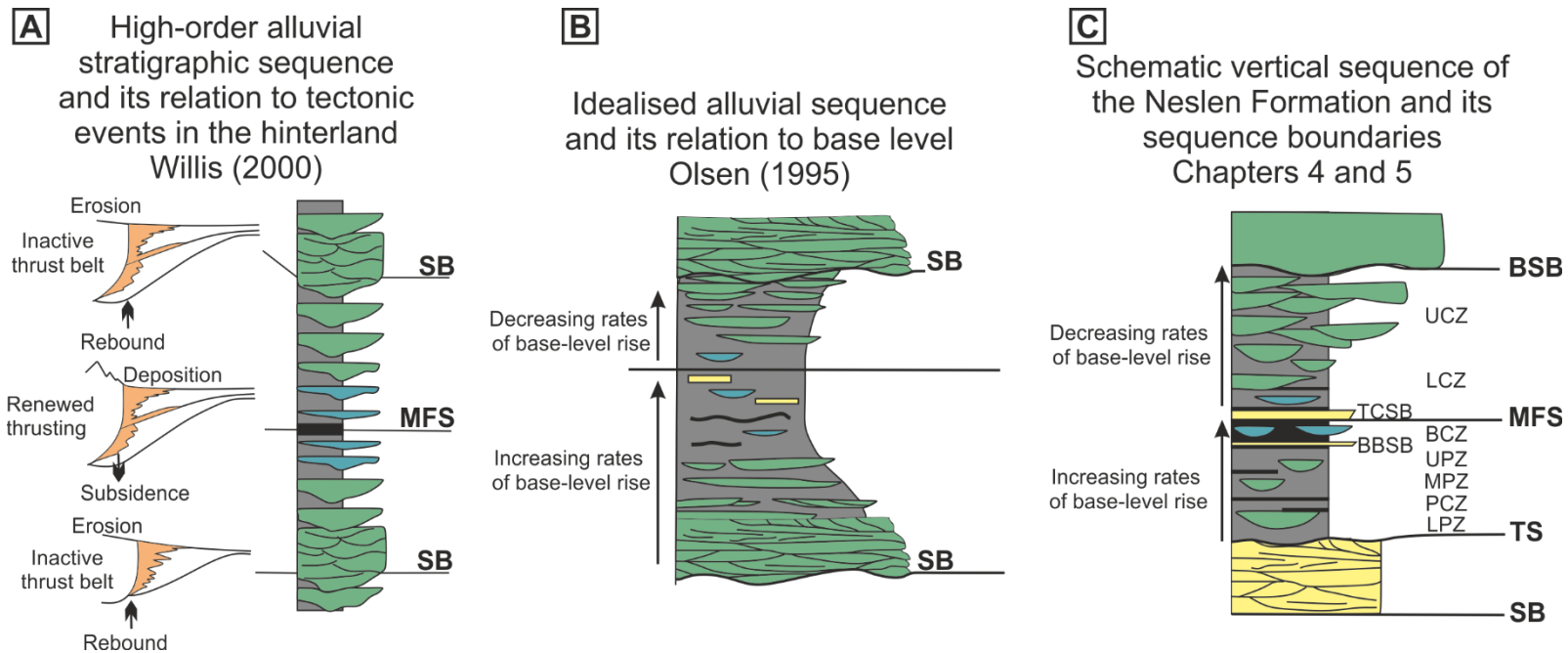


Figure 7.6: A) Sequential schematic section across a foreland basin showing a cycle of thrust-load induced subsidence and the high-order alluvial stratigraphic sequence, adapted after Willis 2000. B) Idealised alluvial sequence with bounding unconformities, adapted after Olsen et al. 1995. C) Idealised vertical sequence of the Neslen Formation interpreted in this thesis, with interpreted key surfaces and depositional intervals. SB = Sequence Boundary, MFS = Maximum Flooding Surface, BSB = Bluecastle Sequence Boundary, TS = Transgressive Surface, LPZ = Lower Palisade Zone, PCZ = Palisade Coal Zone, MPZ = Middle Palisade Zone, UPZ = Upper Palisade Zone, BCZ = Ballard Coal Zone, LCZ = Lower Chesterfield Zone, UCZ = Upper Chesterfield Zone, BBSB = Basal Ballard Sandstone Bed, TCSB = Thompson Canyon Sandstone Bed. Dominantly fluvial sandstones are shown in green, marine influenced deposits are in blue, marine dominated deposits are in yellow.

7.2.1.1.2 Source area uplift and sediment supply

Periods of increased sedimentation in clastic wedges can be tied to periods of tectonic activity in the hinterland (Leeder 2011); this requires integrated tectonic and sedimentological analysis for the correlation of strata using geochronology and/or accurate mineralogical analysis in order to establish sediment provenance. Cretaceous strata of the Mesaverde Group form a series of clastic wedges that prograded eastward from the Sevier orogenic belt. The Sevier orogenic belt is a late Mesozoic and early Cenozoic fold-thrust belt (Yingling and Heller 1992) from which clastic material was shed into the WIS from rising thrust sheets (Jordan 1981). Overall, sediment supply through the Late Cretaceous was high; due to uplift in the thrust belt, which then shed clastic detritus into the developing basin. The rate of sediment supply was enhanced by the warm, wet climate (Aschoff and Steel 2011b). The cliff-forming lower Castlegate Sandstone has been interpreted as a depositional response to an episode of uplift within the orogen (van de Graaf 1972), coincident with movement on either the Meade-Crawford (Fouch et al. 1983) or Charleston-Nebo (Lawton 1983) thrust systems.

Deposits of the middle Castlegate Sandstone, which is time equivalent to the Neslen Formation, are interpreted to represent a decreased rate of sediment influx or more rapid subsidence in the basin (Lawton 1986). The overall increase in sediment supply that is inferred to have taken place through the accumulation of the Neslen Formation (chapters 4 and 6) occurred over a timescale too short to link to a specific thrusting event (although a well-defined timescale for the Neslen Formation is lacking). The absence of growth strata used to infer tectonic activity proximal to the hinterland (Aschoff and Steel 2011b) indicates that increased sediment supply may alternatively be linked to changes in climate (e.g. higher rates of precipitation; see section 7.2.2). Aschoff and Steel (2011b) divided the Mesaverde Group into three clastic wedges (Fig. 3.7). Of these, wedge B, which comprises the Middle Castlegate Sandstone, Sego Sandstone, Neslen Formation, Corcoran and Cozzette Members of the Îles Formation, apparently prograded much further into the basin in response to a combination of an increased rate of sediment supply and a decreased rate of accommodation generation. A direct relationship between the foreland stratigraphy and the tectonic history may, in some cases, be indistinguishable due to the effects of subsidence transmitted from thrust loads (Beaumont et al. 1993). Hence, the possibility of correlating changes in the stratigraphic architecture of the Neslen Formation to tectonic events in the hinterland has not been possible.

7.2.1.2 Eustasy

Changes in the rate of eustatic sea-level rise and fall will directly affect the deposition of sediment proximal to the shoreline through the rate of generation of accommodation. The

rate at which accommodation is generated or filled will govern the stacking patterns of shoreline strata (Posamentier and Vail 1988; Posamentier et al 1993; Shanley and McCabe 1994; Blum and Törnqvist 2000) and the position of key stratal surfaces, such as sequence boundaries and marine flooding surfaces, which can be correlated up-dip into marine-influenced fluvial strata and, in some cases, into fully fluvial successions. Changes in eustatic sea level can be related to the preservation of marine influence in fluvial strata; for example, episodes of transgression are related to intervals of marine-influence preserved in paralic strata and can also change the balance of processes affecting the shoreline (Fig. 2.17).

7.2.1.2.1 Shoreline processes

The balance of wave and tidal processes incident on a shoreline can have major effects on the depositional architecture of the resultant succession (Ainsworth 2011). Wave activity and processes tend to induce the development of a linear to lobate shoreline planform morphology through redistribution of sediment. In contrast, tidal processes tend to result in the development of highly rugose, funnel-shaped shorelines. Wave action promotes development of barriers, particularly during marine transgression, which are typically laterally extensive and relatively straight. The seaward parts of these features are subject to the full force of any wave processes (Davis and Hayes 1984; Ainsworth et al. 2011). Highly embayed or funnel-shaped coastal morphologies have the potential to amplify the tidal wave as it moves into an area, thereby increasing the potential for increased tidally generated current velocities and the transport of sediment because of tides (Ainsworth et al. 2011).

The Neslen Formation is interpreted to have a wave-dominated shoreline, as revealed by the sedimentary structures within tabular sandstone elements (including the TCSB and BBSB; chapters 4 and 5). Evidence of the action of wave processes is recorded in a change from the dominant tidal processes interpreted from shorelines of the underlying Segó Sandstone (Van Wagoner 1991; Willis and Gabel 2001; 2003; Legler et al. 2014, Cappelle et al. 2016). This change could have originated due to transgression in a shallow seaway, such as the WIS, which can reduce the tidal range as the seaway widens and tidal currents become less constricted. Locally, transgression can also cause tidal amplification at river mouths, evidence of this is not observed in the study area of the Neslen Formation. The wave fetch may also increase (Longhitano et al. 2012).

7.2.1.3 Sequence stratigraphy

Fluvial systems are expected to have certain characters depending on their position within a sequence stratigraphic framework (e.g. Fig. 2.17), as predicted by the LAB and WMSM models discussed above (section 7.2.1.1). As described in Chapter 6, channelised elements in the lower Neslen Formation represent deposits of the TST, whereas those in the

upper Neslen Formation represent the HST, with a corresponding change in aspect ratio and amalgamation of channelised deposits (Figure 7.1;). This change in architectural style between the two systems tracts is in agreement with the predictions of the conceptual models proposed by Posamentier and Vail (1988) and WMSM models (Bridge and Mackey 1993; Mackey and Bridge 1995). Channel elements within the TST tend to be isolated and have a heterolithic fill, whereas those within the HST tend to be more amalgamated and have a sandstone fill. Within the Neslen Formation, the most laterally extensive, and, superficially, the most well-developed coals are found within the Ballard Zone, directly beneath the base of the TCSB (interpreted as the MFS; section 5.5.2.1). Examples from the Cretaceous Western Interior Basin in Utah (Ryer 1981; 1984) and the San Juan Basin of New Mexico (Sears et al. 1941; Fassett and Hinds 1971) illustrate that the thickest and most extensive delta-plain coals are restricted to the transgressive maximum (Aitken and Flint 1995). This shows that the response of the coastal plain to relative sea-level change includes changes to the floodplain substrate and pattern of stacking of channelised elements.

It is common for episodes of transgression to be represented in the stratigraphic record as strata of coastal plain origin that contain evidence for marine influence (Shanley and McCabe 1991, 1993; Shanley et al. 1992; Aitken and Flint 1995; McLaurin and Steel 2000; Fig. 2.17). This is concordant with that observed in the lower Neslen Formation, which is interpreted as a TST and which contains significant evidence of marine influence (chapter 5). The interpretation of the punctuated transgression in the Neslen Formation is similar to interpretations made in other larger-scale studies (e.g. Aschoff and Steel 2011a) which interpret the preserved succession of the Neslen Formation to record an overall long-term eustatic sea-level rise; however variations in the rate of sea-level rise coupled with high sediment supply has been shown to result in the occurrence of minor regressive intervals (chapter 5).

7.2.1.4 Climate

Climate controls fluvial and paralic systems in a variety of ways. It controls discharge rate and sediment supply through precipitation, e.g. rainfall floods (Benedetti 2003; Holbrook et al. 2006). It also impacts chemical and physical weathering and the occurrence of landslides, and hence the rates of exhumation of source rocks and the rate and calibre of the sediment supply. Other climatic effects include the flood interval, flood intensity and groundwater levels, as well as the development of mires and vegetation on the floodplain, which play an important role in stabilising the substrate. Seasonal fluctuations in discharge and sediment supply (e.g. through monsoonal climates) are represented by variations in grain size within architectural elements expressing variations in flow strength (Jablonski and Dalrymple 2014). Seasonal fluctuations in discharge can result in grain-size variations and, hence, the development of significant heterogeneities in fluvial deposits; these can

potentially be mistakenly be interpreted as evidence of tidal influence (cf. Gugliotta et al. 2016).

Overall, the Neslen Formation is considered to have been deposited during an episode of greenhouse climatic conditions (Huber et al. 2002) and, hence, the palaeoenvironment was subject to high-precipitation events that resulted in high frequency of fluvial flood events (Miller et al. 2013). Such behaviour encouraged development of a thick regolith and widespread ombrotrophic mires (chapter 5). Evidence of seasonal sedimentation patterns in the Neslen Formation can be inferred for those point-bar elements with significant heterogeneities (S_4) but which lack either ichnological evidence of marine processes or rhythmicity (chapter 6). Within amalgamated channel-fill elements (S_1), which lack any true evidence of marine processes, the presence of fine-grained laminae on cross-bed surfaces, and regular changes in grain size from medium- to fine-grained sandstone indicates some fluctuation in flow regime (chapter 4). Yoshida et al. (1998) state that there is no evidence of a change in climate through the studied interval to suggest that changes in fluvial channel stacking are the result of climatically-induced changes in sediment supply. However, this observation does not consider or account for the decrease in the abundance and quality of coal deposits upwards through the Neslen Formation. This said, there is no evidence of aridity in the form of calcretes, desiccation cracks or evaporate deposits, which may indicate a significant fluctuation in paleoclimate and episodic changes to a more arid climate regime (Willis 2000). However, the upwards decrease in abundance, quality and thickness of coal deposits (Figs. 4.4; 5.9; Table 4.2) could have arisen in response to a slight change to a less humid climate. Changes in the climatic system would also affect precipitation and hence discharge variability inherent to a dominantly humid-climate system (Fricke et al. 2010). Alternatively, the decrease in coal occurrence upwards may have been partially driven by climatically driven variations in sediment supply or be linked to changes in accommodation.

7.2.1.5 Research question two summary

This study has discussed the influence of climate, tectonics and eustasy on fluvial stacking and paralic strata located on the margins of the WIS, developed in a humid climatic setting. Stratigraphic changes which are attributed to dominantly allogenic processes include the increase in amalgamation of channelised elements upwards and the change from marine influence in the lower Neslen Formation to fluvial dominance in the upper Neslen Formation. Although these observations have been made previously (e.g. Lawton 1986; Pitman et al. 1987; Franczyk et al. 1989; Willis 2000), high-resolution analysis has allowed for these large-scale trends to be attributed more definitively to allogenic controls. The increase in channel amalgamation is hence interpreted to reflect a combination of a decrease in the rate of accommodation generation and higher sediment supply. The change from marine-

influenced to fluvially dominated strata is interpreted to reflect progradation of the coastal plain as part of a HST, in accordance with traditional sequence stratigraphic models. Climate is not considered to have been a major control on the observed stratal architectures, rather, the change in occurrence and quality of coal upwards is considered to be a function of the increase in sediment supply.

7.2.2 Research question 3: To what extent are autogenic processes important in producing the observed stratigraphic architecture of fluvial and marine deposits?

Recent research (summarised by Hampson et al. 2016) has emphasised the importance of autogenic processes on the preserved fluvial and paralic succession through self-organisation (autostratigraphy; Muto et al. 2001; 2016), avulsion dynamics (Stouthamer and Berendsen 2011), and compactional subsidence (Brain et al. 2016). Understanding the relative importance of autogenic and allogenic controls on sedimentation is crucial for understanding how such mechanisms are responsible for determining the resultant depositional architecture (Blum and Törnqvist 2000; Stouthamer and Berendsen 2007; Hajek et al. 2012). Discerning the relative influence of autogenic and allogenic processes is complicated because autogenic processes can obscure and overprint allogenic processes, such as basin subsidence and sediment supply (Hajek et al. 2010; 2012)

7.2.2.1 *Avulsion*

Avulsion – the switching of channels to new positions on the floodplain (Smith et al. 1989; Mohrig et al. 2000; Slingerland and Smith 2004) – is the main process by which coarse-grained channel deposits are emplaced into the floodplain (Miall 2014). Avulsion is commonly regarded as an autogenic process is modulated by allogenic processes, including changes to rates of sediment supply and fluvial discharge (Stouthamer and Berendsen 2007). Avulsion typically occurs when a river exceeds a geomorphological threshold related to local topographic gradients, such that the channel relocates to a topographic low on the floodplain or reoccupies a previously abandoned channel location (Mohrig et al. 2000; Slingerland and Smith 2004). Floodplains which contain raised mires (see Section 7.3.2) can influence avulsion through the generation of heightened topographic relief on the floodplain. Avulsion commonly results from the erosion of channel banks, forming a crevasse channel, which will either form a progradational crevasse splay delta, or an incisional crevasse channel (Smith et al. 1989; Mohrig et al. 2000; Hajek and Edmonds 2014). The available preservation space, floodplain gradient, sediment supply and the channel aggradation rate act to determine the avulsion frequency (Bryant et al. 1995; Tornqvist and Bridge 2002; Postma 2014). Major avulsion in a delta plain can cause delta-lobe switching downstream (Section 7.3.5) (Edmonds et al. 2009).

The channel body organisation observed in the Neslen Formation, which is characterised by an increase in amalgamation (i.e. channel body proximity) within the upper Neslen Formation (Chapters 4 and 6), likely arose as the result of changes in basin boundary conditions (i.e. allogenic processes). Highly detailed analysis of a three-dimensional part of the cliff line around Crescent Butte (Chapter 4) shows an absence of channel-body clustering at all depositional intervals of the Neslen Formation, which would result from long-term self-organisation via avulsion (cf. Hajek et al. 2010). The upper Chesterfield Zone channels are therefore interpreted to record repeated occupation of the same site on an extensive floodplain after avulsion (cf. Hampson et al. 2013). Multi-storey sandbodies of the upper Chesterfield Zone record vertical stacking of channel-belt deposits without evidence of a master bounding erosion surface that defines a palaeovalley. Within the upper Chesterfield Zone it is considered that the amalgamation of channels represents long term switching of channel position over floodplain which has low rates of accommodation generation (section 7.2.1.1.1).

7.2.2.2 *Presence of mires*

The formation of mires on the floodplain or coastal plain can affect depositional processes in these locations through changes in accommodation. The presence of peat impedes drainage over wide areas (Thomas 1992). There can be a decrease in accommodation space in localised regions due to the presence of ombrotrophic (i.e. raised) mires. Raised mires form in regions where the annual precipitation exceeds evaporation and where there are no dry periods (Moore 1987). The presence of raised mires in close proximity to the shoreline can influence the response of the coastal plain to sea-level change. Cretaceous coals that accumulated along the coastal plain of the Western Interior Seaway developed in palaeogeographic settings above and landward of shoreline facies within many progradational units. This relationship has been observed in many successions, associated with both transgressive (Dakota Sandstone) and (Straight Cliffs Formation) and regressive (Ferron Sandstone, Emery Sandstone) systems tracts. Coals within the Neslen Formation are thickest and of a higher quality within the Ballard Coal Zone (chapters 4 and 5); beneath the MFS. Throughout the lower Neslen Formation coal beds are associated spatially with marine influenced intervals (chapter 5). In the case of the Neslen Formation the position of coal zones is thought to be a function of the ability of ombrotrophic mires to buffer initial sea-level rise, but on compaction allows for rapid, passive, marine incursion across the coastal plain (Kamola and Van Wagoner 1995) (Fig. 7.7).

Ombrotrophic mires can create extensive regions raised above the normal level of the floodplain, and above the depth of channel incision (Fig. 7.7); which can have implications for channel behaviour. Flow within a channel will preferentially avoid a resistant substrate (such as an incised valley margin, or resistant meander-belt deposits such as abandoned

channel fills or fine-grained counter point bar units, peat mires or lacustrine deposits; Labrecque et al. 2011) and hence the expansion and sinuosity of the meander is restricted (Brice, 1974; Keller, 1972; Hooke, 1984; Smith et al., 2009; Fustic et al., 2011). The presence of a coal-prone substrate is a possible control on the formation of point-bar elements which do not conform to the typical facies models displayed in Figure. 6.1 (chapter 6).

Analysis of stacking patterns of channels within the Palisade and Ballard zones (i.e. those that are coal-prone) does not exhibit any clustering as may be predicted (McCabe 1984) (Chapter 4). This is may be because avulsion frequency during the time of deposition was not sufficiently high to result in clustering of channel elements. Avulsion frequency is controlled by the floodplain gradient and rates of deposition (Tornqvist and Bridge 2002). In the Mesaverde Group as a whole rates of sediment supply were generally high (Aschoff and Steel 2011a) and hence the interpreted low avulsion frequency for the Palisade Zone is more likely linked to the low gradient of the floodplain. Low sediment supply inferred for the Palisade Zone due to the occurrence of type I and II point-bar element (chapter 6) may be due to high-frequency changes in sediment supply through the Neslen Formation.

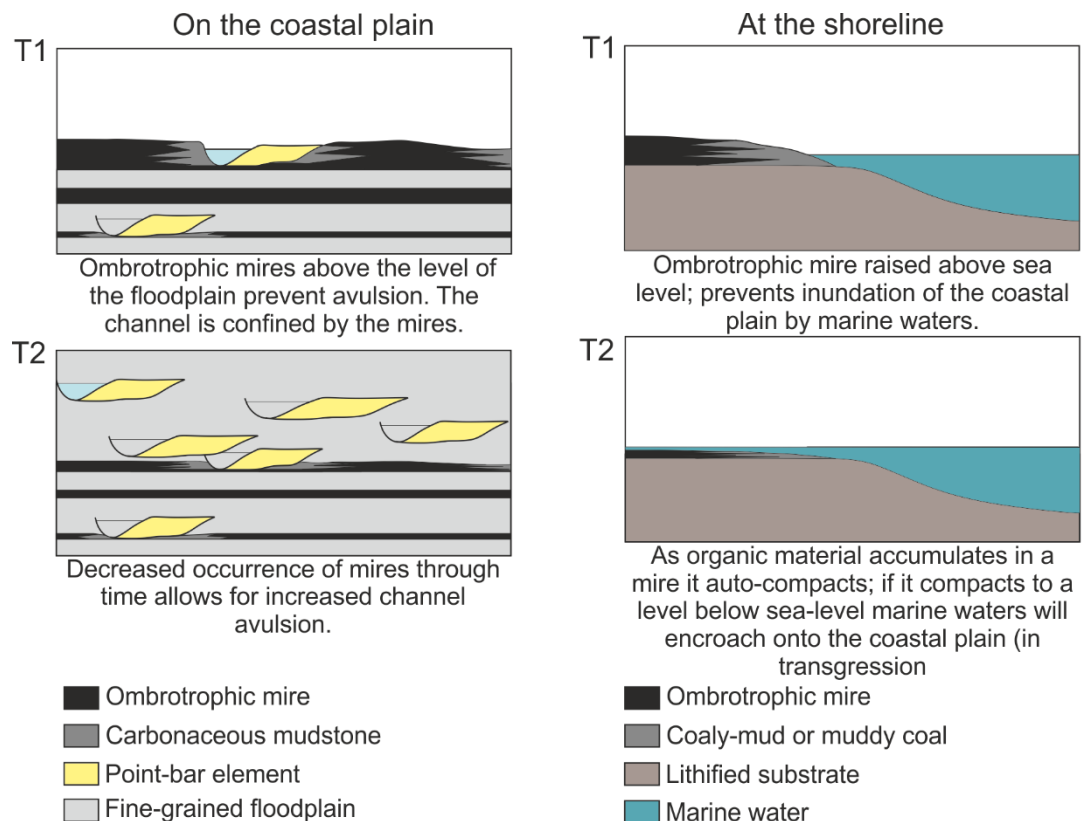


Figure 7.7: Schematic diagram showing the effects which ombrotrophic mires have on fluvial systems on the coastal plain, and at the shoreline at two time intervals (T1 and T2).

7.2.2.3 Backwater hydrodynamics

The backwater zone of a river is defined as the distal reach where the streambed drops below sea level, resulting in river-flow deceleration on approach to the static water body into which it discharges (cf. Chatanantavet et al. 2012). Significant recognition is now given to the role of backwater hydraulics as a control on channel morphodynamics (Chatanantavet et al. 2012; Lamb et al. 2012; Nittrouer et al. 2012; Chatanantavet and Lamb 2014; Ganti et al. 2014), and this has raised awareness of its potential importance as a factor controlling sedimentary architecture in ancient stratigraphy (Lamb et al. 2012; Blum et al. 2013). In several modern wave-dominated deltas, the 'backwater reach' coincides with the location at which the trunk river channel branches downstream at the apex of the delta to form a distributary channel network (Jerolmack and Swenson 2007; Hartley et al. 2016).

On the basis of observations from modern depositional systems and results from numerical models (Chatanantavet et al. 2012; Lamb et al. 2012; Blum et al. 2013; Chatanantavet and Lamb 2014), it is possible to hypothesise the influence that backwater processes have on the sedimentary architecture of distributary-channel fills in lower-delta-plain settings. The depositional architecture of distributary channel-fills is described in Chapter 4; the facies organisation of these bodies is dominated by a limited number of facies: massive (Sm), horizontally laminated (Sh), cross-bedded (Sx) sandstones with beds of convolute laminations (Sd) commonly present. Overall, the bodies are described as having a low aspect ratio (on average 1:16); with steep, erosional channel-body margins (cut banks of at least 35°) and a sandstone-dominated channel-fill without associated lateral accretion surfaces. The lithofacies of the dominantly aggradational infill can be described by the model presented by Colombera et al. (2016). These bodies also contain cryptic indicators of tidal influence and brackish water (cf. Colombera et al. 2016); these include organic and muddy drapes on cross-bedding foresets, herringbone cross-bedding, trace fossils such as *Skolithos* and *Ophiomorpha* in accordance with deposits laid down in coastal plain environments whose constituent channels contain evidence of tidal influence (e.g. Okolo 1983; Hopkins 1985; Dreyer 1990; Kirschbaum and McCabe 1992; Olsen 1993; Plink-Björklund 2008).

Colombera et al. (2015) used Neslen Formation strata to suggest that the zone of backwater influence extended approximately 30 km up-dip from the contiguous shoreline. The occurrence of distributary channel-fill elements is restricted to areas around Crescent Butte (chapter 4; Fig. 4.10), although this may be due to a combination of channel orientation and outcrop. West of the East study site (chapter 5; Fig. 5.8) no distributary channel elements are observed, this indicates the approximate limit of backwater processes for the Ballard Zone and lower Chesterfield Zone was around Floy Canyon and hence the contiguous shoreline was located around Cisco (UT) (Fig. 1.1). The position of the shoreline was highly variable at this time; thus, the maximum limit of backwater processes was also variable.

Given this, Cisco merely represents the point of transgression for the Ballard Zone and lower Chesterfield Zone; it is likely that the shoreline transgressed further into Utah during deposition of the BBSB and TCSB (chapter 5)

The combination of data presented in Colombera et al. (2016), together with that presented in this thesis (chapter 4; Appendix D), can be used to test how stratigraphic variations in channel-body architecture is related to the control exerted by backwater processes. Placing the relative position and aspect ratio of distributary channel bodies (S_2) within the stratigraphic context of the Neslen Formation (Fig. 7.8), which incorporates the aspect ratio of barform deposits (S_3/S_4) has allowed for improved understanding of backwater processes in the Neslen Formation:

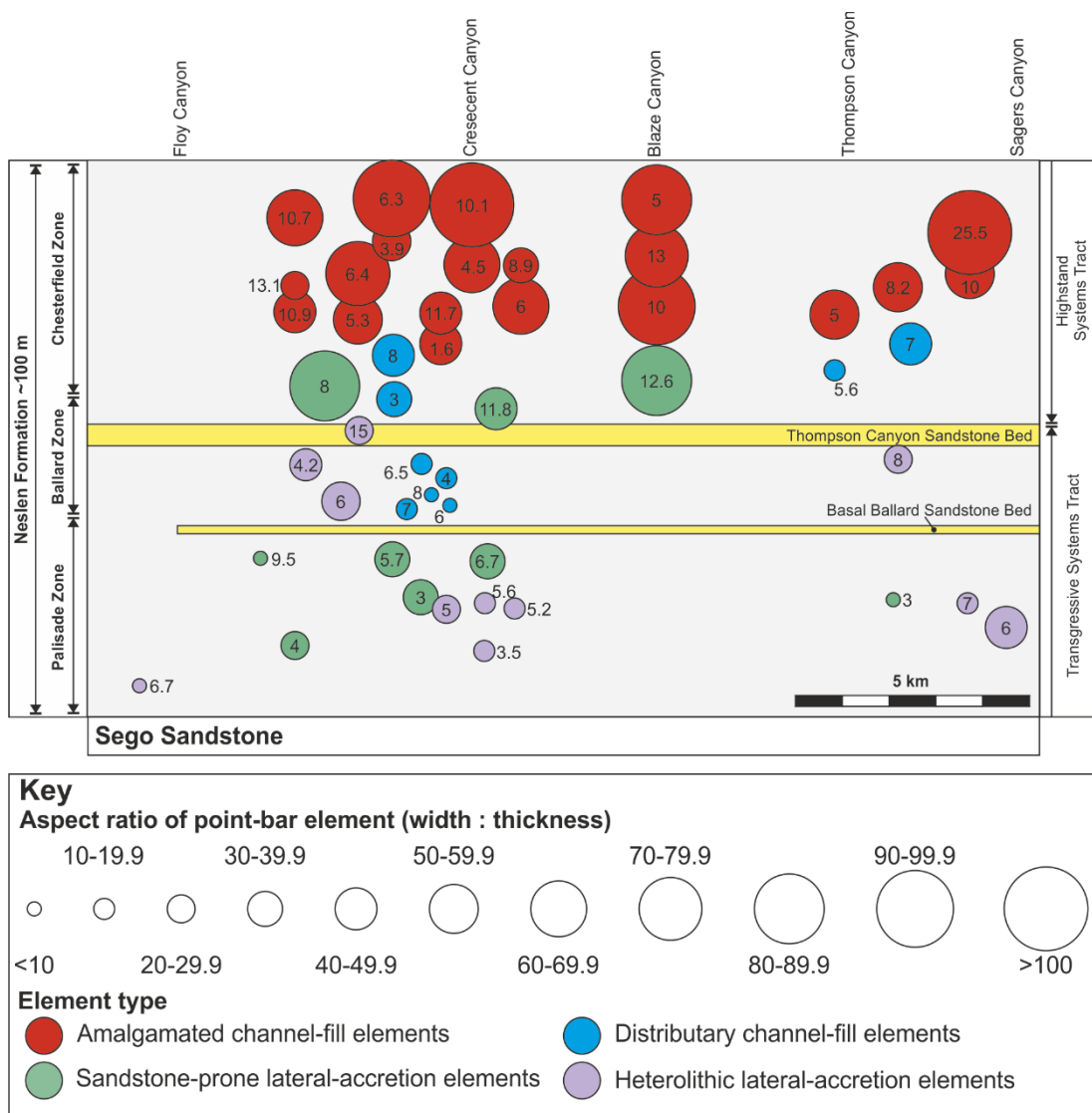


Figure 7.8: Data panel showing the stratigraphic relationship between different channelised architectural elements in the Neslen Formation. Distributary channel-fill elements are restricted to the Ballard and lower Chesterfield Zones, and their aspect ratio is larger in the lower Chesterfield Zone.

Distributary channel-fill elements occur in the same stratigraphic interval as sandstone-prone point-bar elements (majority type I but also type III; Chapter 6). Sandstone-prone point-bar elements (S_3) in modern systems are likely to have been deposited in the upper backwater zone, where they undertook rapid migration (cf. Blum et al. 2013). By contrast, the distributary channel-fill elements are interpreted to represent laterally stable, low sinuosity channels in the coastal plain (Colombera et al. 2016; see section 7.3 for further consideration of the relative location of channel types on the coastal plain). Although these elements occur together within the Ballard Zone and lower Chesterfield Zone, it remains unclear whether they occurred in the same geomorphic context and were contiguous; especially given the especially low gradient of the coastal plain where even minor sea-level changes would have resulted in significant shifts in the position of the shoreline (as discussed in chapter 5).

The aspect ratio of analysed distributary channel-fill elements is lower in the Ballard Zone than in the lower Chesterfield Zone (Fig. 7.8). This is likely due to the position of the shoreline in relation to the depositional environment. The aspect ratio of channel bodies (W:T) is predicted to decrease seaward (Colombera et al. 2015), and hence the studied Ballard Zone channels are interpreted to have been located closer to the shoreline than those in the lower Chesterfield Zone.

The majority of distributary channel-fill elements (S_2 ; chapters 4 and 5) occur in close proximity to marine-dominated sandstone elements of the BBSB and TCSB (Fig. 7.8) within the Ballard and lower Chesterfield Zones (chapters 4 and 5). This indicates that the occurrence of backwater processes at this location is related to the processes resulting in the formation of flooding surfaces (chapter 5). Episodes of relative rise in sea level which resulted in deposition of the BBSB and TCSB shifted the zone of backwater influence to portions of the Neslen Formation up-dip of the study area, compared to its position during periods of lower sea-level. During deposition of the upper Chesterfield Zone, the limit of backwater processes is predicted to have been further east; i.e. down-dip of the study location. Backwater processes extend further upstream than tidal processes and the influence of brackish water (Fig. 2.17). Hence, the Ballard Coal Zone represents the most up-dip part of the coastal plain which is modified by marine processes. This means that the depositional zones of the Neslen Formation (chapters 4 and 5) can be placed on a longitudinal profile (Fig. 7.9). The lack of any marine indicators in point-bar elements of the Ballard Coal Zone (chapter 5) indicates that the area of deposition was located up-dip from the effect of tidal processes.

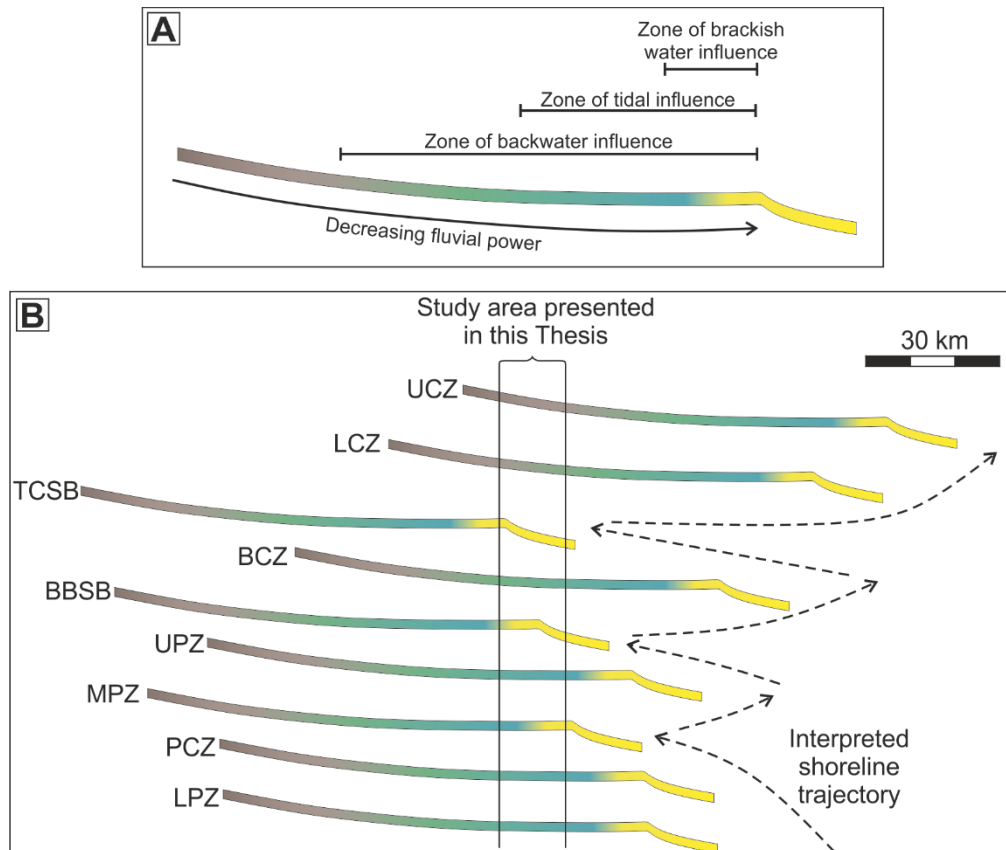


Figure 7.9: Interpreted depositional zones of the backwater plain, from the shoreline (dominated by marine processes in yellow), through the zones of tidal and marine influence (blue) and backwater influence (green) into the fully fluvial domain (brown). B) The vertical evolution of the Neslen Formation showing the change in palaeoenvironment interpreted for the study area upwards and the interpreted shoreline trajectory.

7.2.2.4 Autostratigraphy

During progradation there is increased sediment storage on the coastal plain (Hampson 2016). This limits the extent of progradation, eventually resulting in autogenic retreat of the shoreline; in autostratigraphy or autoretreat (Muto and Steel 1992; Muto et al. 2016). The results of numerical and physical stratigraphic modelling used to explain autostratigraphy, are difficult to test using outcrop and subsurface data with only limited observations made on such datasets (e.g. Muto and steel 1992; 2002; Muto et al. 2007; Van Heist et al. 2001; Paola and Martin 2012; Hampson 2016).

The progradation of the coastal plain of the lower Neslen Formation was punctuated by several flooding surfaces that could have arisen through autoretreat of the shoreline (*sensu* Muto and Steel 1992). However, the differentiation between forcing mechanisms that can result in the same preserved stratigraphy as autostratigraphy, e.g. pulses of sedimentary supply and changes in the floodplain gradient, is not possible using outcrop data alone (cf. Kim et al. 2006; Hampson 2016). Analysis in the down-dip regions of the Neslen Formation –

and its equivalent in Colorado, the Îles Formation – is required to establish whether the shoreline trajectories are concave landward, reflecting a decreasing rate of progradation during aggradation as predicted in autostratigraphy (Muto and Steel 1992; Muto et al. 2007).

7.2.2.5 Delta-lobe switching

Autogenic delta-lobe switching occurs over relatively small temporal (< 100 kyr) and spatial scales (10s of km²) (Coleman and Gagliano 1964; Fig. 2.15). Lobe switching is less pronounced in wave-dominated delta systems, because waves and storms act to suppress deltaic distributaries and lobes. Their geomorphological threshold(s) required to switch their positions are not reached through redistribution of river-supplied sediment offshore and alongshore (e.g. Coleman and Wright 1975).

Much research relating to delta-lobe switching has been carried out on the Mississippi Delta (Penland and Boyd 1981; Penland and Suter 1983; Penland et al. 1985; Courel 1987; Penland et al. 1988; Roberts and Coleman 1996; Roberts 1997; Blum and Roberts 2012). Mapping of delta lobes which are interpreted to have accumulated over the last 7500 years have been carried out. Delta-lobe switching has also been recognised in other modern systems e.g. the Ebro Delta (Sornoza et al. 1998), the Po Delta (Correggiari et al. 2005). Recognition of delta-lobe switching in ancient exhumed successions is difficult due to the nature of the processes, whereby the location of deposition shifts and hence is difficult to analyse through outcrop studies. Strata of the Blackhawk Formation contain a subtle but pervasive architectural motif that may be attributed to delta-lobe switching (Hampson 2016).

A series of stages occur in the abandonment of delta lobes (Penland and Boyd 1981; Penland and Suter 1983; Penland et al. 1985; Courel 1987; Penland et al. 1988; Roberts and Coleman 1996; Roberts 1997; Blum and Roberts 2012). Initial abandonment leads to the formation of an erosional headland with flanking barriers (Penland et al. 1985; Penland et al. 1988; Roberts and Coleman 1996; Blum and Roberts 2012) with a complicated arrangement of architectural elements similar to that of the Middle Palisade Zone (chapter 5). Subsequent submergence (caused by auto-compaction) leads to shoreline retreat and the formation of a widespread transgressive barrier system (Penland and Suter 1983); such systems could be represented in the Neslen Formation by the Basal Ballard Sandstone Bed and Thompson Canyon Sandstone Bed (chapter 5; Fig. 7.10). Continued submergence leads to further shoreline retreat and the formation of an inner shelf sand shoal until the area of the coastline was reoccupied (Blum and Roberts 2012). This sequence of abandonment can be used to explain the short time scale fluctuations in marine-influenced intervals observed in the lower Neslen Formation (Chapter 5). Periods of rapid, localised deposition alternating with longer hiatuses are hypothesised for models of delta avulsion. In the Neslen Formation, these

hiatuses may be represented by the formation of coals which take long periods of time to accumulate in comparison to clastic material. To definitively establish whether the succession was formed due to multiple delta-lobe avulsions detailed studies would need to be carried out in down-dip regions and correlated to the study area represented in chapters 4 and 5.

7.2.2.6 *Shifting palaeoenvironments*

Shifting loci of deposition at the coastline would result in significant spatial complexity. It is well known that adjacent parts of the coastline have different balances of fluvial, tidal and wave processes incident on them (cf. Ainsworth et al. 2010; Amir Hassan 2013) (Fig. 2.14). In the lower Neslen Formation, type I and II point bar elements interpreted as having been deposited in a palaeoenvironment with multiple contiguous channels (chapter 6). Therefore, it follows that there existed multiple points of fluvial input and channels which traversed the alluvial plain (Fig. 7.11). In the Neslen Formation, it is hypothesised that at the mouth of each trunk river a delta has the potential to develop. Each individual delta will have the ability to prograde and avulse independently. This can result in a highly rugose coastline (unless longshore processes act to rapidly smooth the shoreline) and hence encourage the amplification of tidal processes. The intervening areas between

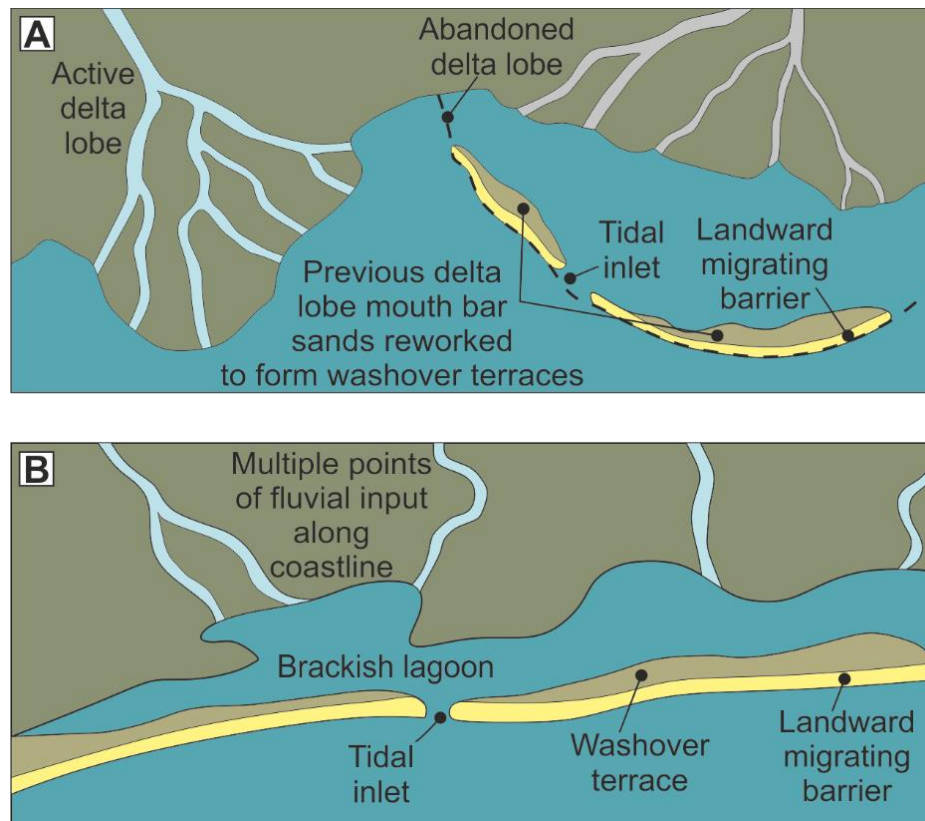


Figure 7.10: Schematic diagram showing the possible palaeoenvironments for deposition of the TCSB: A) development of washover terraces following delta-lobe switching and, B) the formation of laterally extensive spits and barriers along a strandplain coastline.

fluvial input will be less significantly modified by fluvial processes and might instead be likely dominated by wave processes (Fig. 7.10).

This has implications for the development of different depositional environments inferred for the lower Neslen Formation; wave-dominated strandplain, fluvial dominated deltas and tidally influenced lower coastal plain. Through time as the different palaeoenvironments indicated in Figure 7.11 shift position (the lateral arrangement in the figure is intended for illustrative purposes only) it will lead to the vertical accumulation of different depositional environments upwards without the need to invoke allogenic changes in sea level or sediment supply to produce the observed stratigraphy.

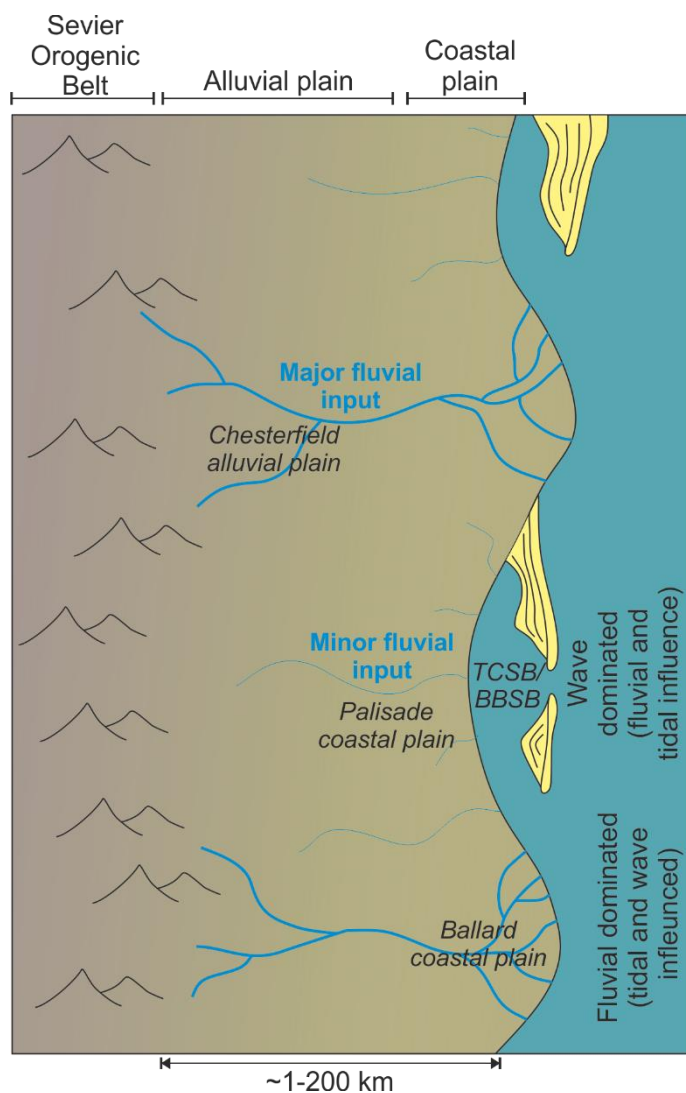


Figure 7.11: Schematic diagram showing how different depositional zones in the Neslen Formation (the Palisade Zone, Ballard Zone, and TCSB) can exist simultaneously at the shoreline due to lateral variations in processes. The vertical succession in the Neslen Formation may have accumulated simply by switching of the palaeoenvironment through time.

7.2.2.7 Research question three summary

This part of the research has worked to redress the long held interpretation of paralic strata, especially of the Book Cliffs, as being driven by allogenic changes. In the Neslen Formation the presence of raised mires is an important control that has previously been underestimated in its ability to modify the hydrodynamics of fluvial flow, as shown by the presence in the Neslen Formation of point-bar facies which do not conform to traditional depositional models. The data set presented here shows the correlation between coal zone and overlying marine-influenced or marine-dominated intervals and hence their ability to buffer sea-level rise; an interpretation that is important in mitigating the effects of sea-level rise.

The influence of backwater processes on paralic strata has also been highlighted. Backwater processes in the Neslen Formation are most easily recognised in the Ballard and lower Chesterfield Zones where distributary channels are interpreted. The position and aspect ratio of distributary channel-elements can be used to infer distance to the palaeoshoreline and changes in the palaeogeography.

Distinguishing the importance of autostratigraphy has not been possible without detailed analysis of down-dip, age-equivalent strata to the Neslen Formation. Other autogenic processes are thought to be less significant in the formation of the observed stratigraphic architecture; whilst avulsion of channels certainly occurred during deposition of the Neslen Formation, it is not considered to be a major control on the key changes in the stratal architecture outlined in section 7.2.2. The possibility that shifting palaeoenvironments and delta-lobe avulsion contributed to the stratal architecture cannot be discounted using the current dataset; this is because the outcrop belt is essentially 2D in nature and along-strike variability cannot easily be discerned.

7.2.3 Research questions two and three synthesis

As described in sections 7.2.1 and 7.2.2, the trends in stratigraphic architecture observed in the Neslen Formation can occur either by solely autogenic or allogenic processes (Table 7.2). In reality, it is likely that a combination of these mechanisms were responsible for generating and preserving the architecture of the Neslen Formation, and allogensis and autogenesis cannot necessarily be treated as separate end-member behaviours. This section will address each of the stratal architectures, summarised in section 7.2.1, and the preferred interpretation as to the dominant controls of their formation. The main allogenic controls for each part of the stratigraphy (Palisade Zone, Ballard Zone and Chesterfield Zone) are outlined in Figure 7.12.



Figure 7.12: Figure showing the variation in the main allogenic controls responsible for deposition of different depositional intervals of the Neslen Formation (A-D).

Architectural Patterns	Possible autogenic controls	Possible allogenic controls
Increase in the aspect ratio and thickness of channelised sandbodies upwards.	Increase in the ability of the channels to erode and migrate e.g. due to less cohesive substrate	<u>Increase in sediment supply.</u> <u>Increase in river discharge.</u> <u>Decrease in the rate of generation of accommodation space</u>
Increase in amalgamation of point-bar elements in the upper Neslen Formation.	Increased avulsion frequency.	<u>Increase in sediment supply.</u> <u>Increase in river discharge.</u> <u>Decrease in the rate of generation of accommodation space.</u>
Occurrence of repeated marine influenced intervals	Localised, high-frequency delta lobe switching. Autoretreat of the shoreline. <u>Compaction of laterally extensive ombrotrophic mires below sea level.</u> Shifting depositional environments.	<u>High frequency, low-amplitude sea level variations as part of overall transgression with intervening regressive periods where the delta plain prograded.</u>
The change from marine influence in the lower parts of the formation to dominantly fluvial processes in the upper parts.	Shifting depositional environments.	<u>Rapid progradation of the coastal plain as part of a highstand systems tract.</u>
Decrease in the quality, occurrence and thickness of coal upwards through the Neslen Formation.	Unlikely	Change in climate. <u>Change in sediment supply or accommodation space</u> Changes in floodplain drainage
Occurrence of point-bar assemblages that do not conform to typical facies models.	<u>Low fluvial discharge as a function of multiple contemporaneous channels.</u>	Low fluvial discharge as a function of changes in climate. Low floodplain gradient.

<u>Influence of coal-prone</u> <u>substrate modifying the flow</u> <u>hydrodynamics.</u>
--

Table 7-2: Table describing the possible autogenic and allogenic processes which may have generated the preserved stratigraphic architecture observed in the Neslen Formation. The preferred controls are emphasised by being underlined.

7.2.3.1 Increase in the aspect ratio, thickness and amalgamation of channelised elements in the upper Neslen Formation

The change from thinner, isolated channelised sandbodies (S_2 , S_3 and S_4) with a lower aspect ratio in the Palisade, Ballard and lower Chesterfield Zones to thicker, highly amalgamated channelised elements (S_1) in the upper Chesterfield Zone (Chapters 4 and 6) is interpreted to reflect wholly allogenic processes. The channelised elements in the upper Chesterfield Zone are interpreted as type IV point-bar elements, these elements show a higher fluvial discharge in channels than other point-bar elements in the Neslen Formation (Table 6.2). The higher fluvial discharge likely also means that sediment supply in the upper Chesterfield Zone was correspondingly higher.

The possibility of this change being due to the progradation of a distributive fluvial system or nodal avulsion, outlined in Chapter 4 (Fig. 4.11), is discounted based on the lack of down-dip changes in point-bar facies and geometry outlined in Chapter 6 (Fig. 6.12, 7.8).

7.2.3.2 Occurrence of repeated marine influenced intervals

The occurrence of repeater marine influenced intervals (the MPZ, BBSB and TCSB) described in chapter 5 are considered to have arisen as a result of combined allogenic and autogenic factors. It is considered unlikely that the presence of repeated marine-influenced intervals was a response solely to allogenic processes due to their apparent high-frequency of occurrence. The occurrence of raised mires on the floodplain initially served to buffer periods of transgression (Section 7.2.2.2). Intervals of stratigraphy which exhibited thinner or lower occurrences of coals are concurrent with periods of progradation of the coastal plain; relative sea level fall (Chapter 5). As the peat compacted it allowed passive encroachment of marine waters over the low gradient coastal plain.

The possibility that autoretreat of the coastal plain (Section 7.2.2.4) contributed to the occurrence of repeated marine intervals cannot be discounted based on the essentially two-dimensional outcrop-belt analysed in this thesis.

7.2.3.3 Change from marine influence in the lower Neslen Formation to fluvial dominance in the upper Neslen Formation

The upwards change in the interpreted amount of marine influence which modified the deposition, accumulation and preservation of the sediments on the Neslen Formation coastal plain shows an initial increase from marine influence in the Palisade Zone, to marine influence to dominance in the Ballard Zone and then fluvial dominance in the Chesterfield Zone. This change can be explained by lateral shifts in palaeoenvironment as described in section 7.2.2.6. However discerning this mechanism from allogenic mechanisms without along-strike datasets is not possible.

The overall change from marine influence in the lower and middle parts of the formation to fluvial dominance in the upper parts is ascribed to progradation of the coastal plain, such that through time the study area was located progressively further from the shoreline through time.

7.2.3.4 Decrease in the quality, occurrence and thickness of coal upwards through the Neslen Formation

The thickness, occurrence and quality of the coal in the Neslen Formation decreases upwards overall; this can be explained by a change to a drier climate, an increase in sediment supply or a decrease in accommodation space. A further possibility is a decrease in preservation of peat due to an increase in fluvial activity (discharge and sediment supply). A drier climate is discounted due to the concurrent increase in size and grain size of channelised elements; indicating an increase in fluvial discharge and sediment supply which are therefore likely to be the contributing factor.

7.2.3.5 Occurrence of point-bar assemblages that do not conform to typical facies model

As discussed in chapter 6, the point-bar elements in the lower Neslen Formation do not always conform to typical facies models. The possible autogenic and allogenic processes that contribute to the formation of these atypical facies assemblages are described in section 6.5. Overall the anomalously low proportions of cross-bedded sandstone and high proportions of massive sandstone, ripple-laminated sandstone and horizontally laminated sandstone are interpreted to form as a function of low stream power and low sediment supply as a function of multiple contemporaneous, marine influenced channels across a paludal floodplain.

7.3 Research question four: How can palaeoenvironmental models of ancient marginal marine systems be constrained?

This thesis presents high-resolution datasets collected from outcrop studies of the Neslen Formation (presented in Chapters 4 to 6) and uses them to refine the palaeogeographic interpretations for this stratigraphic interval. The reconstruction of marginal marine palaeoenvironments using ancient core, seismic or outcrop datasets, which are refined using data from modern systems, is a long-established technique (e.g. Le Blanc 1975; Snedden and Bergman 1999; Yoshida et al. 2004; Howell et al. 2008; Ainsworth et al. 2008; 2010; Stuart 2015; Gugliotta et al. 2016; van Cappelle et al. 2016).

There is general consensus amongst published studies that the Neslen Formation was deposited in a setting that comprised meandering fluvial, paludal (i.e. marsh) and lagoonal environments, with some degree of marine influence (Lawton 1986; Pitman et al. 1987; Kirschbaum and Hettinger 1998; 2004; Willis 2000; Cole 2008; Olariu et al. 2015; Chapters 4 and 5). The upper Neslen Formation is universally interpreted as having accumulated as the result of dominantly fluvial sedimentation, whereby meandering channels migrated across an alluvial plain (Lawton 1986; Pitman et al. 1987; Kirschbaum and Hettinger 1998; 2004; Chapters 4 and 6). However, many authors disagree as to whether the marine influenced part of the Neslen Formation was part of an estuarine (Kirschbaum and Hettinger 1998; 2004; Willis 2000; Cole 2008; Olariu et al. 2015), deltaic (Lawton 1986; Aschoff and Steel 2011a,b; Colombera et al. 2015; O'Brien 2015; Andresden 2016) or coastal plain (Pitman et al 1987; Franczyk et al. 1989) environment. Within this study, no evidence has been forthcoming to indicate the presence of an incisional surface that would support the interpretation of the Neslen Formation representing the infill of an incised valley fill. The presence of distributary channel fills (Lawton 1986; Colombera et al. 2016; Chapters 4 and 5) supports the interpretation that the lower Neslen Formation was deposited in a lower to upper delta-plain environmental setting.

7.3.1 Depositional models and modern analogues

The Neslen Formation deposits encountered in this study reveal a range of evidence to support the interpretation of several localised depositional sub-environments: (i) lower delta plain and coastal plain including bay-fill sandstones and tidally influenced point bars; (ii) upper coastal plain-delta plain including distributary channel network; (iii) wave dominated reworked barriers; (iv) alluvial plain deposits. Figure 7.13 presents a generalised fluvio-deltaic depositional setting with possible location of the studied intervals of the Neslen Formation annotated. This model was produced using high-resolution datasets complimented by modern analogue studies to produce palaeogeographical maps and hence can be used to inform studies of hydrocarbon reservoirs (section 7.4).

For each of the studied intervals of the Neslen Formation (Palisade Zone, Ballard Zone, the TCSB and the Chesterfield Zone: chapter 4) an attempt has been made to assign a suitable modern analogue. Whilst the palaeoenvironment of each interval of the Neslen Formation can be established (sections 7.3.1.1-7.3.1.4 below); no single modern system can seek to represent it accurately. This is because images of modern systems represent a snapshot in time whereas palaeoenvironmental reconstruction of the Neslen Formation has necessarily taken place over time intervals. As well as this, the Neslen Formation was deposited on the margins of an epeiric seaway. However, no modern epeiric seaways of a similar scale exist and hence no presently active system can be considered as a true analogue.

7.3.1.1 Palisade Zone: upper to lower delta plain/coastal plain

The Palisade Zone is characterised by a combination of point-bars interpreted as the result of meandering river behaviour which are occasionally modified by marine processes, bay-fill sandstones and crevasse splays and coal. The depositional environment for the Palisade Zone is interpreted as lower coastal plain and delta plain settings with multiple contemporaneous fluvial channels associated with type I and II point-bar elements (chapter 6). Overall, there are changes in marine influence towards the east, reflecting the proximity to the shoreline. Intervals of increased marine influence within the Palisade Zone (Middle Palisade Zone; chapter 5) are interpreted to be represent a depositional environment relatively closer to the shoreline.

A modern analogue for the Palisade Zone is the lower delta plains of the Rufiji River Delta (Tanzania), which has a network of sinuous contemporaneous channels with associated point-bar elements and intervening vegetated floodplain (Fig. 7.14). The Rufiji Delta contains mangrove swamp; an environment conducive to the formation of peat. This modern system was selected based on the superficial similarity in the depositional elements observed and the similar climatic regime; other analogous modern systems include: the upper delta plain of the Niger Delta (Nigeria; Oomkens 1974), Mahajamba River, north-western Madagascar.

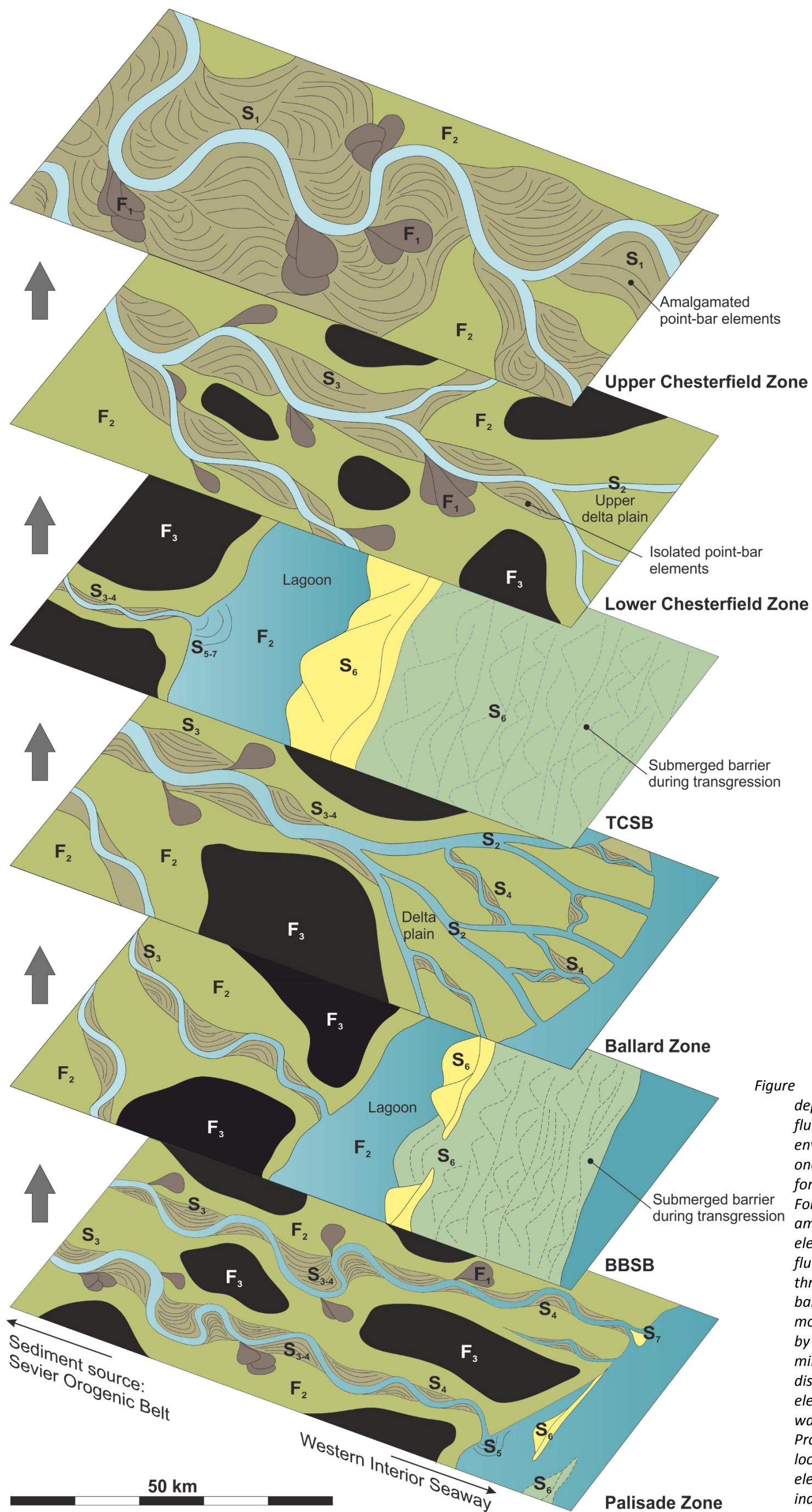


Figure 7.13: Generalised depositional model of a fluvio-deltaic depositional environment, such as the one that would have formed the Neslen Formation, passing from amalgamated channel elements which were fluvially dominated; through to isolated point-bar elements which we modified to some degree by marine processes, mires, bay-fill sandstones, distributary channel elements and reworked washover sandstones. Prospective relative locations of architectural elements (S₁-S₇) are indicated.

7.3.1.2 Ballard Zone: upper delta plain

The Ballard Zone was dominated by coal-prone floodplain elements which were laterally extensive and well-developed indicating the formation of ombrotrophic mires in landward of the backshore bays and lagoons. Distributary channel-fills and lateral accretion point-bar elements are observed in the Ballard Zone. Point-bar elements in the Ballard Zone do not contain many marine indicators, this indicates that the Ballard Zone represents the preserved record of sediment accumulation in an upper delta plain setting, up-dip from the limit of tidal influence on sedimentary structures but within the backwater zone (Blum et al. 2013; Colombera et al. 2016). An appropriate modern analogue is identified in the Mahakam River Delta (Fig. 7.15). At this location distributary channels dominate with subordinate, sinuous channels, which are thinner than distributary channels and have associated point-bar elements linked with them. The distributary channels of the Mahakam delta are 10-20 m thick (Lambiase et al. 2016), greater than those of similar channels of the Neslen Formation (3-8 m thick; section 7.2.2.3; Colombera et al. 2016); however the aspect ratios are similar along with the facies observed within the channel-fill (Lambiase et al. 2016).

7.3.1.3 Thompson Canyon Sandstone Bed and Basal Ballard Sandstone Bed: Reworked barrier and washover sandstones

The marker units of the TCSB and the BBSB are composed of a lower, heavily bioturbated, organic rich siltstone and very fine sandstone which is interpreted as being of lagoonal origin and an upper tabular sandstone which has significant marine and brackish water ichnospecies such that the sandstone bodies are interpreted as having been modified by wave processes. The depositional environment interpreted for the TCSB (chapters 4 and 5) is concordant with models of backstepping barriers and washover sand complexes (collectively referred to as a barrier-fan complex) in the literature (e.g. Horne et al. 1979; Kamola and Wagoner 1995) developed during transgression. Overall, the development of the TCSB is similar to the evolution of parasequences in the Spring Canyon Member (Blackhawk Formation, Utah)(Kamola and van Wagoner 1995): during transgression the strandline migrated landward until it encountered peat mires, which buffered relative sea level rise (cf. Shanley and McCabe 1995; chapter 5), and development of a bay/lagoon and barrier islands over the former coastal plain. As the relative sea level rise slowed, transport of sediment to the shoreline led to rapid progradation of the shoreline, represented by the Chesterfield Zone. The occurrence of raised mires immediately landward of the shoreline enhanced preservation of the underlying parasequence (Kamola and van Wagoner 1995). Lateral to the barrier-fan complex it is likely that other depositional environments were also present, e.g. fluvial dominated deltas as discussed above, flood-tidal deltas and tidal inlet sandstones. Other interpretations for the formation of wave dominated parasequences encased within dominantly coastal and alluvial plain strata include: mouth bar, bay-fill

sandstone, or part of a wave dominated estuary (section 4.4.6.2). The abrupt contact at the base and top of these bodies, their internal facies and down-dip extent eliminates mouth bar or bay-fill interpretations. The interpretation of any part of the Neslen Formation as estuarine is rejected based on the lack of a feeding fluvial system or basal incisional surface. Barrier deposits can form in a variety of environments but develop most easily on wave-dominated coasts with a microtidal range (Leeder 1999). The barrier complex could have formed through reworking of submerging delta lobes (section 7.3.6 above). Alternatively, it could have formed through longshore drift.

An analogous system, in terms of morphology, is the western Mexican coast (Isla del Itamura; western Mexico; Fig 7.16). These are laterally extensive barriers with a region of washover sandstones. Over time these barriers could prograde landward over lagoonal fines to form deposits such as those observed in the TCSB. Further analogous systems can be found along the eastern seaboard of the United States which exhibit similar processes to that proposed for the TCSB and other barrier-fan complexes (Swift 1975; Swift et al. 1985; Kraft et al. 1987).

7.3.1.4 Chesterfield Zone: Alluvial plain

The Chesterfield Zone is dominated by fluvial deposits, which become increasingly amalgamated upwards through the succession. The depositional environment for the Chesterfield Zone is interpreted to be dominantly within the alluvial plain. The channel elements in the upper Chesterfield Zone are interpreted as high-energy channel-fill and associated laterally migrating (and potentially downstream migrating) point-bar elements. The lack of marine indicators implies a purely fluvial regime. Deposits within the lower Chesterfield Zone were affected by backwater processes; resulting in deposition and preservation of distributary channel-fills together with isolated fluvial dominated point-bar elements. As such, the location of deposition is considered to have been relatively down-dip from the upper Chesterfield Zone.

A possible modern analogue is the up-stream region of the Mississippi River (Louisiana/Mississippi USA). Sinuous channels exhibit cross-cutting relationships preserving large point-bar elements over a wide area (Fig. 7.17) and are analogous to the upper Chesterfield Zone although within a valley-fill. The lower Chesterfield Zone was located relatively down-dip from the deposits of the upper Chesterfield Zone (Fig. 7.17b) The Mississippi River has relatively rapid subsidence rates which prevents peat accumulation (Kosters et al. 1987). Other analogous systems include: Niger River (Nigeria) and parts of the Indus River (India).

7.3.2 Research question four summary

This section presents a highly constrained and detailed summary of the palaeoenvironment of the Neslen Formation. High-resolution analysis and interpretation of narrow intervals of strata which are approximately time equivalent allows for subtle changes in the palaeoenvironment to be readily discerned. A selection of suitable modern analogues for different depositional intervals are detailed, modern analogues are used to constrain plan-form geometries and the relationship between different depositional environments. This method can easily be applied to other successions which have laterally extensive outcrop belts. Data gathered from individual marginal marine successions analysed using high-resolution analysis can be used to produce generic marginal marine models.

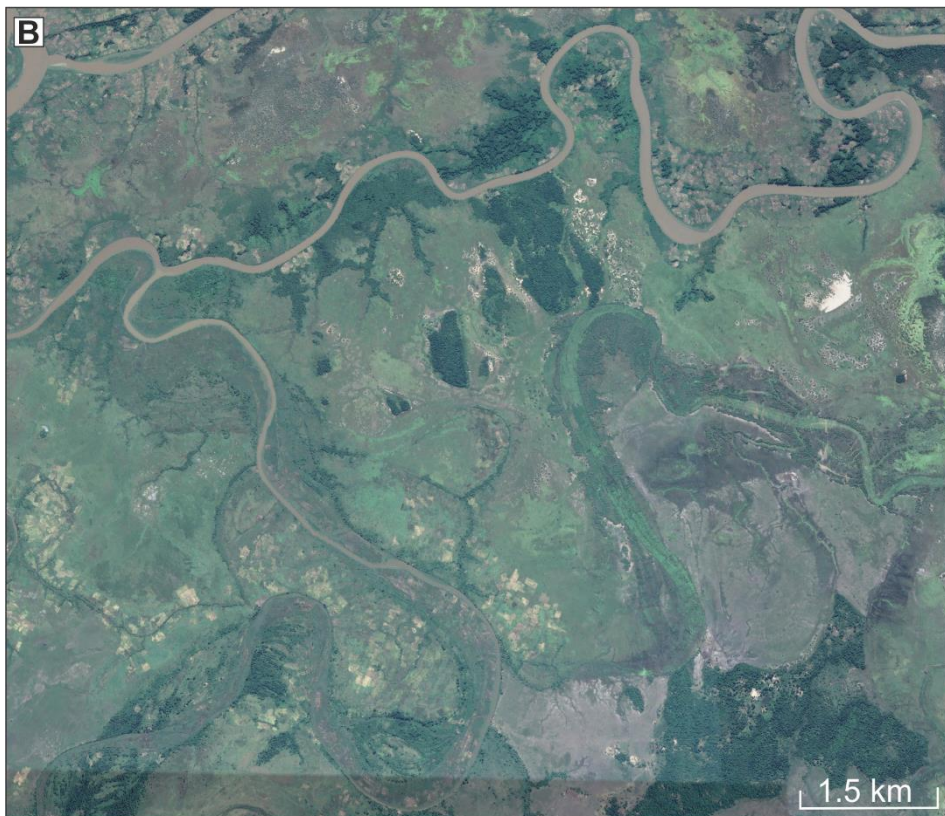


Figure 7.14: Modern analogue for the Palisade Zone of the Neslen Formation at the Rufiji River Delta (Tanzania). A) shows the large scale architecture, image centred around UTM 7 52,57.69-S; 39 18,53.75-E. B) Detail of the area emphasising the presence of multiple contemporaneous channels with associated point-bar elements.

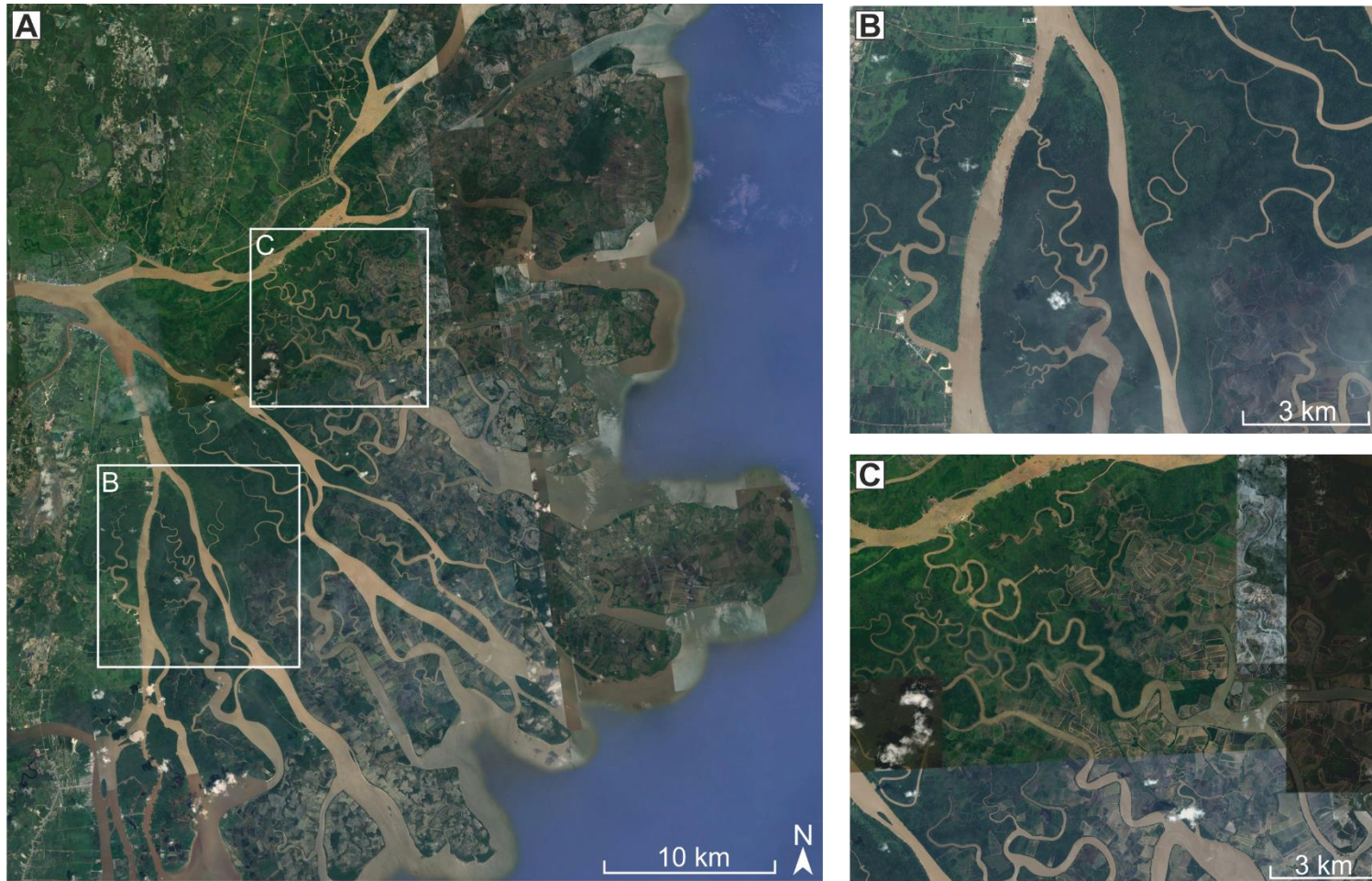


Figure 7.15: Modern analogue for the Ballard of the Neslen Formation at the Mahakam Delta. A) shows the large scale architecture, image centred around UTM 0 40, 46.22-S; 24 53.28-E. B) Detail of the area emphasising the presence of distributary channels. C) Detail of sinuous channels which exist in the areas between distributary channels.



Figure 7.16: Modern analogues for sandbodies such as the Thompson Canyon Sandstone Bed at the Western Mexican coast (Isla de Altamura) barrier-strandplain shoreline. A) Large scale architecture of the coastline, image centred around UTM 26 31,49.24-N; 97 18,48.44-W. B) Detail of barrier complex with associated landward lagoon.

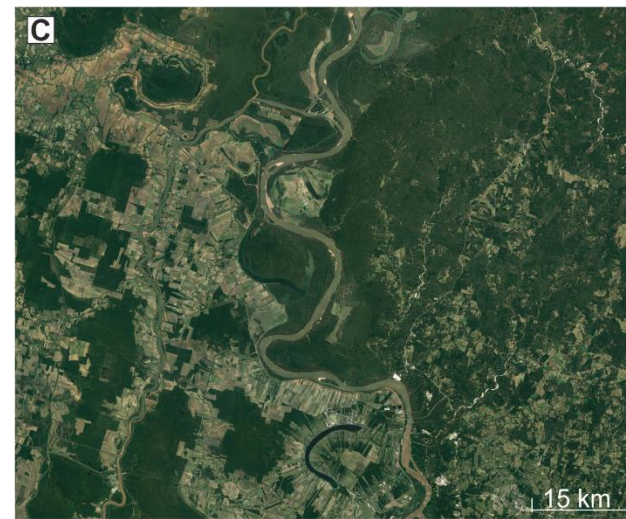
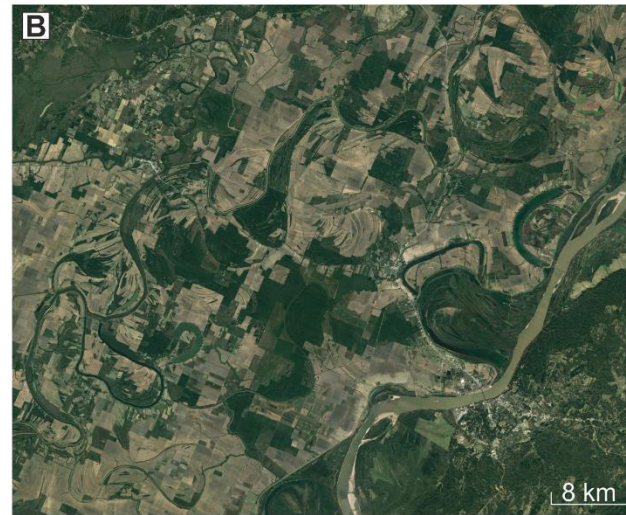
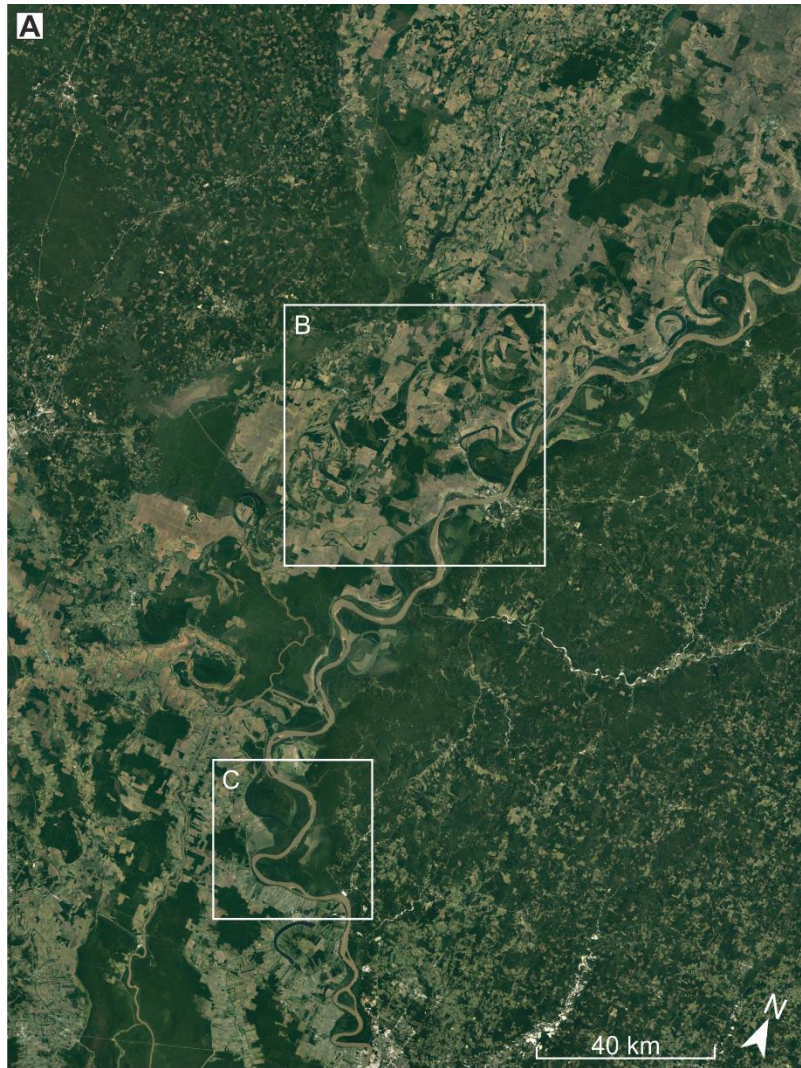


Figure 7.17: Modern Analogue for the Chesterfield Zone of the Neslen Formation, the Mississippi River. A) Large scale architecture of the alluvial plain showing the decrease in reworking in a downstream direction, image centred around UTM 31 22,37.64-N; 91 31,37.79-W. B) Detail of a part of the Mississippi River which shows multiple active and abandoned point-bar elements analogous to the upper Chesterfield Zone. C) Single active river with associated point bars, isolated within the floodplain, this part of the Mississippi River is analogous to the lower Chesterfield Zone.

7.4 Research question five: What is the impact of marine processes on the reservoir potential of sand bodies in lower fluvial plain, coastal plain and marine marginal setting?

7.4.1 Heterogeneity in the Neslen Formation

Reservoir heterogeneity is considered at a range of scales: megascopic, macroscopic, mesoscopic and microscopic (cf. Tyler and Finney 1991). At the scale of the studied stratigraphy sandstones within the lower Neslen Formation are commonly encased within floodplain, or lagoonal mudstone and siltstone, and hence the lower part of the Neslen Formation has a greater heterogeneity (low net:gross) than the upper Neslen Formation (Fig. 7.18a). This megascopic heterogeneity is attributed to allogenic processes of accommodation space and sediment supply rather than marine processes.

Architectural elements of the Neslen Formation display macroscopic and mesoscopic heterogeneity (cf. Tyler and Finney 1991) within coarsening-upwards bay-fill sandstone (S_5/S_7) and heterolithic point-bar elements (S_4) (Chapter 4). Mesoscopic Heterogeneities in these deposits occur at a range of scales, from mm-thick drapes on ripples (mud, silt or carbonaceous; Fig. 7.18b), to cm-thick laminae within heterolithic sets of wavy or lenticular bedding (Fig. 7.18c) and dm-thick fine grained beds of mudstone or siltstone (Fig. 7.18d). Microscopic heterogeneity will likely be present within architectural elements of the Neslen Formation but were beyond the scope of this work. This study has aimed to improve understanding of the occurrence and distribution of lithological heterogeneities (chapter 6) at the meso- and macro-scale to refine databases for petroleum modelling of fluvial systems. Meso-scale and macro-scale heterogeneity within architectural elements of the lower and middle parts of the Neslen Formation can arise from fluvial variations in current energy; however, given the marine influence present in these parts of the stratigraphy it is likely that tidal processes played a role in introducing some of these heterogeneities.

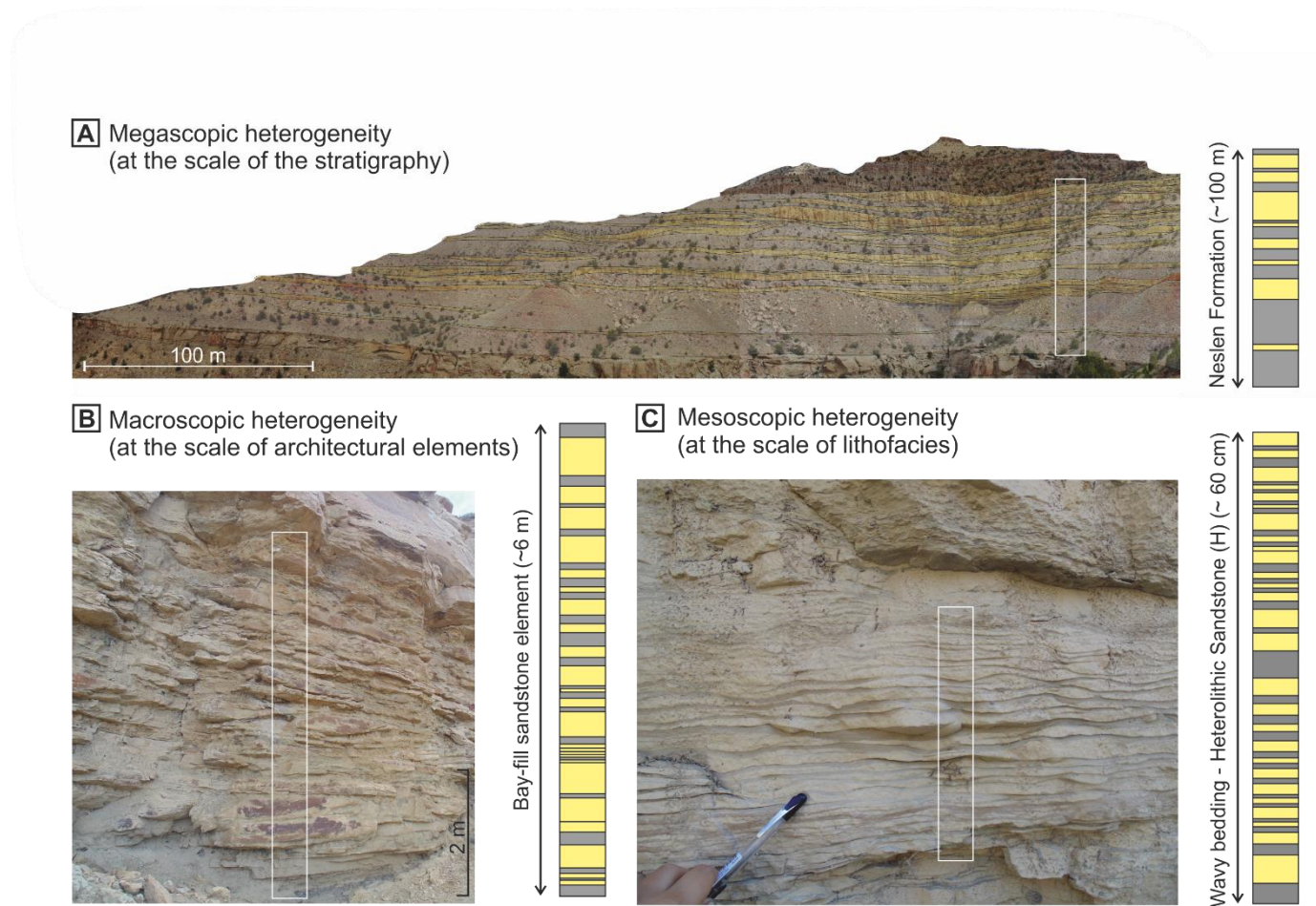


Figure 7.18: Figure showing the different scales of heterogeneity observed in the Neslen Formation, yellow represents sandstone, grey is fine-grained sediment. A) Heterogeneity at the scale of the stratigraphy, B) Heterogeneity at the scale of the architectural element, C) Heterogeneity at the scale of the lithofacies

7.4.1.1 Tidal influence

Typically, deposits influenced by tidal processes have high mesoscopic and microscopic heterogeneity due to fluctuating current energies (finer-grained sediment deposited during tidally modulated low-flow stage) as well as the high proportion of suspended sediment in a region proximal to the turbidity maximum, a part of the FMTZ (Purnachandra Rao et al. 2011; La Croix and Dashtgard 2014). Additionally, where there is an influx of brackish waters into the fluvial realm, deposition and accumulation of mud is promoted due to the flocculation of clays (La Croix and Dashtgard 2014). Specifically, analysis of the internal lithological heterogeneity of point-bar deposits has become increasingly important in recent years; such deposits have become targets for the discovery and exploitation of large oil reservoirs held in fluvial and tidally influenced fluvial reservoirs (e.g. McMurray Formation: Hubbard et al. 2011; Fustic et al. 2012; Musial et al. 2012). Tidal reworking can affect reservoir quality at the delta mouth either by acting to winnow fines from the sands or by reducing permeability in distributary channels by the introduction of increased amounts of fine-grained detritus (Purnachandra Rao et al. 2011). Understanding the processes by which heterogeneities are introduced and their occurrence and distribution is vital for predicting reservoir behaviour.

Sedimentary cores are commonly used to analyse subsurface deposits in an attempt to assess reservoir potential; identifying architectural elements (Chapter 4) can be achieved through analysis of the grain-size profile, as well as lithofacies. Bodies composed of mouth-bar and crevasse-delta deposits, for example, can be recognised from their coarsening-upward profiles (Elliott 1974). However, differentiation of these sub-environments is difficult using solely one-dimensional analysis. Point-bar and channel-fill elements might be characterised by fining-upward-trends (Miall 1985), not all point-bar elements possess such a trend (Chapter 6). Recognition of tidal indicators (such as those described in Section 2.4.1) requires careful, facies-scale analysis, specifically of finer-grained elements. Correct identification of ichnological evidence with which to reconstruct palaeoenvironmental salinity levels is also important. Such approaches are important in establishing whether these heterogeneities were introduced as a consequence of seasonal variations in flow or spring-neap, or diurnal cycles related to tidal action (Gugliotta et al. 2016).

Recognition of the FMTZ in the subsurface is challenging; even where cores are accompanied by detailed seismic information. A detailed set of criteria are required to definitively assess whether a deposit accumulated in a part of the FMTZ (Table 7.1). A more complete understanding of the FMTZ will allow outcrops to be assigned to appropriate positions along the transition zone; this is important in assessing the length of the FMTZ and the distance of the deposit from its contiguous shoreline.

7.4.1.2 *Wave influence*

Wave processes, together with longshore currents, enhance overall reservoir potential in deltas by redistributing sand as beaches in the interdistributary areas. Wave modification acts to winnow fine-grained material out of sandstones, thereby increasing their reservoir quality (cf. Tyler et al. 1987; Anderson 1991; Dutton et al. 1991; Harris 1992; LePain and Kirkham 2012; Williams 2015). Evidence for this is observed in the Neslen Formation in the tabular sandstones bodies (the Basal Ballard Sandstone Bed and Thompson Canyon Sandstone Bed), which are composed of well-sorted, well-rounded quartz grains with an overall high net:gross ratio, and are interpreted as having been modified dominantly by wave processes.

7.4.2 Point-bar elements

The reservoir potential of point-bar elements is governed by the presence of mesoscopic and microscopic heterogeneities which controls the permeability of the sandstone, as well as the connectivity between sandstone bodies. Point-bar elements in the lower Neslen Formation are isolated and are heterolithic, meaning they make relatively poor-quality reservoir intervals. In contrast to this, point-bar elements in the upper Neslen Formation have very low heterogeneity and are highly amalgamated, and hence would provide an efficient and well-connected reservoir volume. Efficient recovery of hydrocarbons hosted within fluvial successions containing point-bar elements requires understanding of the internal facies arrangements (cf. Chapter 6). Characterising the facies within point-bar elements in subsurface reservoirs (e.g. McMurray Formation, Labrecque et al. 2011; Mungaroo Formation, Stuart 2015) is complicated and, hence, it is common for analogues of outcropping successions to be used. Data from outcropping successions can be used to refine models constructed using limited data on facies in core studies, as demonstrated in Figure 2.18); although it is important to note differences in scale between subsurface and outcropping successions. For example, the point-bar elements of the McMurray Formation (Table 6.2) are much larger than those in the Neslen Formation; this means that while depositional models may not always be applicable, the data presented in this thesis broadens our understanding of the range of internal lithofacies distribution within point-bar elements.

7.4.3 Research question five summary

Marine processes can have a positive and negative impact on the reservoir potential of sandbodies. Within the Neslen Formation wave processes act to winnow finer grained material from sand and hence improve the overall net: gross of sandbodies such as the TCSB

and BBSB which are interpreted as reworked barrier and washover sand complexes. Within the lower Neslen Formation, macroscopic and mesoscopic heterogeneities are considered to be due to the influence of tidal processes; these occur in point-bar elements and bay-fill sandstone elements. This ability to place architectural elements within a stratigraphic framework emphasises the way in which marine processes are interpreted to have had the most influence on the reservoir potential of sandbodies during transgressive intervals.

8 Conclusions and Future Work

This Chapter summarises the main findings of this study, and considers possible future work that could be undertaken to build upon the outcomes of this research.

8.1 Conclusions

The transfer of an ancient fluvial-to-marine transition zone (FMTZ) into the stratigraphic record is expressed as a range of subtle, typically gradual, changes in the style of preservation of architectural elements. This is associated with changes in lithofacies characterised by a suite of marine indicators indicative of sedimentation in relatively up-dip (fluvial) to relatively down-dip (coastal) positions. The transition is not simple and can only be recognised through interpretation of stratigraphic intervals that can be shown to be time-equivalent (i.e. time-correlative). In the Neslen Formation, the FMTZ is at least 20 km in length; the backwater length is hypothesised to be approximately 30 km. There is a disparity between the length of the FMTZ and limit of backwater processes measured in modern systems (commonly many 10s to 100s of km) and that hypothesised in many ancient successions (commonly many 10s of km). This is likely due to the effectiveness of river floods as agents to overprint the subtle indicators of marine influence deposited during low-flow periods. In the Neslen Formation, palaeo-rivers were likely smaller than most of the large modern systems that have been studied for assessment of the length of the backwater zone and the FMTZ; as such the corresponding distance upstream limit of marine influence was also shorter in the Neslen Formation case example than many modern examples.

This thesis has presented data at a wide range of spatial scales (10^2 - 10^4 m), analysis of which has yielded results that can be used to detail the heterogeneity and connectivity of reservoir-prone sandstone units. These data can reduce uncertainty in the large-scale depositional architecture in analogous paralic successions subsurface reservoirs for oil and gas, water aquifers, and carbon sequestration.

The main stratigraphic changes observed in the Neslen Formation; outlined in section 7.2; can be explained using a combination of allogenic and autogenic processes. At the scale of individual architectural elements, the recognition of point-bar elements with unusual facies assemblages (Chapter 6) is attributed to a combination of allogenic factors (low fluvial discharge and sediment supply) combined with autogenic processes (the presence of ombrotrophic mires). These types of point-bar assemblages have not been recognised elsewhere in the rock record or in modern systems, as such it is likely that specific, autogenic, processes in the Neslen Formation played a role in controlling their

accumulation. This is important in understanding the palaeoenvironment of the Neslen Formation, as well as a consideration for the modelling of flow behaviour within ancient point-bar elements. At the formation scale, the increase in point-bar amalgamation, thickness and aspect ratio observed through the Neslen Formation (Chapters 4 and 6) is attributed to dominantly allogenic controls such as a decrease in accommodation space and increase in sediment supply; similar controls are interpreted to have been responsible for the concurrent decrease in coal quality, occurrence and thickness upwards through the Neslen Formation. Through the Neslen Formation there is an overall decrease in the amount of marine influence (Chapters 4, 5 and 6), this is attributed to overall progradation of the shoreline through time. However, the repeated intervals of marine influence in the lower part of the Neslen Formation are attributed to a combination of allogenic changes in relative sea-level buffered by the occurrence of raised mires on the coastal plain.

Within the Neslen Formation, it is possible to explain the majority of stratigraphic architectural patterns through allogenic changes in accommodation generation and sediment supply and eustatic changes in sea-level. However, autogenic processes can also generate similar stratigraphic signatures and processes, for example via delta-lobe avulsion, auto-retreat and compaction-driven subsidence. The stratigraphic response to such autogenic processes is shown to have likely partly overprinted and obscured that of allogenic processes. The extent to which autogenic processes; specifically the presence of large ombrotrophic mires on the floodplain; can modify these overarching processes has previously been underestimated.

The interplay of allogenic and autogenic controls on the sedimentary evolution of paralic successions has been documented for the Neslen Formation and overall this has increased our understanding of the dominant controls on the deposition, accumulation and preservation of sediment in marginal marine systems. This research has established a series of criteria for the extent to which a sequence stratigraphic framework can be applied to up-dip sections of the coastal plain. The parameters for establishing the reservoir prospects for successions similar to the Neslen Formation, e.g. connectivity of reservoir-prone sandbodies and heterogeneity and facies arrangement within architectural elements has also been recognised.

8.2 Recommendations for future research

The research carried out for this study could be continued and extended in a series of ways to further enhance and consolidate our understanding of the evolution of paralic sedimentary systems, as considered below.

8.2.1 Palynological and mineralogical analysis of sediments within the Neslen Formation

Analysis of fine-grained sediments using palynology would further augment the dataset presented in this thesis. Such analysis would provide a high-resolution biostratigraphic framework for the succession. Furthermore, palynological analysis would assist in the differentiation of terrestrial vs. marine-influenced parts of the succession (cf. Woollands and Haw 1976; Akyuz et al. 2016). Hence, such research would help to further refine the sequence stratigraphic framework proposed in Chapter 5.

Detailed analysis of the maceral content of coals is related to the depositional conditions in the original mire and hence would enable the interpretation of ombrotrophic mires (Chapters 5 and 6) to be made equivocally. Additionally, detailed analysis of the mineral content could also be used to identify hiatal surfaces and assist in demonstrating the effects of changes in the rates of creation and filling of accommodation (cf. Jerrett et al. 2011a, b). Such analysis would enable more quantitative analysis of the palaeoenvironmental changes that resulted in the observed vertical changes in coal quality. Provenance analysis of sandstone elements would enable differentiation of marine-sourced sediment vs. sediment sourced from the Sevier Orogenic Belt and may also enable correlation of discrete pulses of tectonic activity with sediment supply (cf. Jordt et al. 1995).

8.2.2 Three dimensional modelling of channelised elements

Three-dimensional modelling was beyond the scope of this work but could form the basis for a follow-up study to reduce uncertainty in hydrocarbon reservoir behaviour and increase hydrocarbon recovery. In particular, detailed data on facies proportions within point-bar elements and the distribution of point-bar elements provided in Chapters 4 and 6 could be applied to populate static and dynamic reservoir models through object or pixel modelling. Such analysis would enable more accurate prediction of fluid flow behaviour. Reservoir property data, e.g. heterogeneities, could be interpreted from logged sections, and stratigraphic panels can be used to quantify connectivity between the various channel deposits identified (Chapter 4). This could take the form of the construction of numerical models to simulate the evolution individual architectural elements or groups of related elements for a known set of boundary conditions using a forward stratigraphic modelling approach (cf. Yan et al. in review). Forward stratigraphic modelling at the scale of

depositional elements and systems tracts will also allow predictions about how allogenic and autogenic processes interact to give a resultant sequence stratigraphic framework.

Data from this thesis is also can contribute to quantitative facies modelling using a database approach, using techniques that have been recently developed for both fluvial systems (the Fluvial Architecture knowledge Transfer System, FAKTS, Colombera et al. 2012a, b, 2013) and for shallow-marine sedimentary systems (The Shallow-Marine Architecture Knowledge Store, SMAKS, Colombera et al. 2016b). Such database approaches for the analysis of fluvial, paralic and shallow-marine systems can be used to reveal important insights regarding the modelling of, for example, meander-belt reservoirs (Colombera et al. 2016c).

8.2.3 Down-dip correlation of Neslen Formation strata

The high-resolution data sets presented in Chapters 4 and 5 are in contrast to the majority of previous studies undertaken on the Neslen Formation, most of which have used widely spaced logged sections or well data to build a regional framework. The extension of the high-resolution analytical approach developed here to locations in the succession considered to represent palaeoenvironmental positions further down-dip would extend the correlation basinwards. Specifically, this approach would assist in characterising the expected detailed sedimentological relationships of the contiguous palaeoshoreline system. This method of analysis could provide the additional data required to gain understanding of the extent to which processes of delta-lobe switching and autostratigraphy played a role in determining the preserved stratigraphy of the succession more widely.

8.2.4 Comparison to other ancient successions

Comparison of the findings from this study with other, time-equivalent deposits along the margins of the Western Interior Seaway (e.g. Kaiparowits Formation), could be used to further discriminate between autogenic and allogenic processes. Particularly, such follow-on studies could be used to compare and contrast preserved stratigraphic architectures and hence determine whether the identified controls were operating on a basin scale (allogenic) or more locally (autogenic).

Further to this, comparison of the Neslen Formation strata with other paralic systems in different basin types and/or climatic settings would help to distinguish the extent to which these factors played a role in modifying the preserved stratigraphy. This could be achieved using the Shallow Marine Architecture Knowledge Store (SMAKS) (Colombera et al. 2016b) in order to make quantified comparisons between systems. Quantified analysis of point-bar elements in a wide range of depositional systems using FAKTS (Colombera et al. 2012 a, b) could be used to further test the controls on deposition of facies assemblages

which differ from traditional models, such as those presented in Chapter 6 (Colombera et al. 2016c).

References

- Abdul Aziz, H., Sanz-Rubio, E., Calvo, J.P., Hilgen, F.J., Krijgsman, W., 2003. Palaeoenvironmental reconstruction of a middle Miocene alluvial fan to cyclic shallow lacustrine depositional system in the Calatayud Basin (NE Spain). *Sedimentology* 50, 211-236.
- Abels, H.A., Kraus, M.J., Gingerich, P.D., 2013. Precession-scale cyclicity in the fluvial lower Eocene Willwood Formation of the Bighorn Basin, Wyoming (USA). *Sedimentology* 60, 1467-1483.
- Ainsworth, R.B., 2010. Prediction of stratigraphic compartmentalization in marginal marine reservoirs. Geological Society, London, Special Publications 347, 199-218.
- Ainsworth, R.B., Flint, S.S., Howell, J.A., 2008. Predicting coastal depositional style: influence of basin morphology and accommodation to sediment supply ratio within a sequence stratigraphic framework. *Recent Advances in Models of Siliciclastic Shallow-Marine Stratigraphy: SEPM, Special Publication 90*, 237-263.
- Ainsworth, R.B., Vakarelov, B.K., Nanson, R.A., 2011. Dynamic spatial and temporal prediction of changes in depositional processes on clastic shorelines: Toward improved subsurface uncertainty reduction and management. *AAPG Bulletin* 95, 267-297.
- Ainsworth, R.B., Pattison, S.A., 1994. Where have all the lowstands gone? Evidence for attached lowstand systems tracts in the Western Interior of North America. *Geology* 22, 415-418.
- Aitken, J.F., Flint, S.S., 1995. The application of high-resolution sequence stratigraphy to fluvial systems: a case study from the Upper Carboniferous Breathitt Group, eastern Kentucky, USA. *Sedimentology* 42, 3-30.
- Allen, J.R.L., 1963. Depositional features of Dittonian rocks: Pembrokeshire compared with the Welsh Borderland. *Geological Magazine* 100, 385-400.
- Allen, J.R., 1964. Studies in fluvial sedimentation: six cyclothems from the Lower Old Red Sandstone, Anglowelsh Basin. *Sedimentology* 3, 163-198.
- Allen, J.R., 1965. A review of the origin and characteristics of recent alluvial sediments: *Sedimentology* 5, 89-191.
- Allen, J.R., 1970. Studies in fluvial sedimentation: a comparison of fining-upwards cyclothems, with special reference to coarse-member composition and interpretation. *Journal of Sedimentary Research* 40.
- Allen, J.R., 1978. Studies in fluvial sedimentation: an exploratory quantitative model for the architecture of avulsion-controlled alluvial suites. *Sedimentary Geology* 21, 129-147.
- Allen, J.R., 1983. Studies in fluvial sedimentation: bars, bar-complexes and sandstone sheets (low-sinuosity braided streams) in the Brownstones (L. Devonian), Welsh Borders. *Sedimentary Geology* 33, 237-293.

Allen, G.P., 1991. Sedimentary processes and facies in the Gironde Estuary: a recent model for macrotidal estuarine systems, in: Smith, D.G., Reinson, G.E., Zaitlin, B.A., Rahmani, R.A. (Eds.), *Clastic Tidal Sedimentology*. Canadian Society of Petroleum Geologists Memoir, pp. 29-40.

Allen, G.P., Posamentier, H.W., 1993. Sequence stratigraphy and facies model of an incised valley fill - the Gironde Estuary, France. *Journal of Sedimentary Petrology* 63, 378-391.

Ambrose, W.A., Hentz, T.F., Bonnaffe, F., Loucks, R.G., Brown Jr, L.F., Wang, F.P., Potter, E.C., 2009. Sequence-stratigraphic controls on complex reservoir architecture of highstand fluvial-dominated deltaic and lowstand valley-fill deposits in the Upper Cretaceous (Cenomanian) Woodbine Group, East Texas field: Regional and local perspectives. *AAPG Bulletin* 93, 231-269.

Anderson, P.B., 1991. Comparison of Cretaceous landward pinch-outs of nearshore sandstones: wave-versus river-dominated deltas, east-central, Utah. *Utah Geological Association Publication* 19, 283-300.

Armitage, J.J., Duller, R.A., Whittaker, A.C., Allen, P.A., 2011. Transformation of tectonic and climatic signals from source to sedimentary archive. *Nature Geoscience* 4, 231-235.

Armstrong, R. I., 1968. Sevier orogenic belt in Nevada and Utah: *Geological Society of America Bulletin* 79, 429-458.

Aschoff, J.L., Steel, R.J., 2011a. Anatomy and development of a low-accommodation clastic wedge, upper Cretaceous, Cordilleran Foreland Basin, USA. *Sedimentary Geology* 236, 1-24.

Aschoff, J., Steel, R., 2011b. Anomalous clastic wedge development during the Sevier-Laramide transition, North American Cordilleran foreland basin, USA. *Geological Society of America Bulletin* 123, 1822-1835.

Ashour, A., Jonathan, P., Philippe, D., Mathieu, S., Philippe, S., Eddy, M., Mouloud, B., Mustafa, S., Osama, H., Michel, B., Jean-Jacques, J., Jean-Loup, R., 2012. New insight into the sedimentology and stratigraphy of the Dur At Talah tidal-fluvial transition sequence (Eocene-Oligocene, Sirt Basin, Libya). *Journal of African Earth Sciences*, v. 65, p. 72-90.

Barwis, J.H., 1977. Sedimentology of some South Carolina tidal-creek point bars, and a comparison with their fluvial counterparts, in: Miall, A.D. (Ed.), *Fluvial Sedimentology: Bedforms and Bars*. Memoir of the Canadian Society of Petroleum Geology, pp. 129-160.

Baganz, B.P., Horne, J.C., Ferm, J.C., 1975. Carboniferous and recent Mississippi lower delta plains: a comparison. *Transactions of the Gulf Coast Association of Geological Societies* 25, 183-191.

Beaumont, C., Quinlan, G., Stockmal, G., 1993. The evolution of the Western Interior Basin; causes, consequences and unsolved problems, in: Caldwell, W.G.E.,

Kauffman, E.G. (Eds.), Evolution of the Western Interior Basin. Geological Association of Canada Special Paper pp. 97-117.

Benedetti, M.M., 2003. Controls on overbank deposition in the Upper Mississippi River. *Geomorphology* 56, 271-290.

Beynon, B., Pemberton, S., Bell, D., Logan, C., 1988. Environmental implications of ichnofossils from the Lower Cretaceous Grand Rapids Formation, Cold Lake oil sands deposit, in: James, D.P., Leckie, D.A. (Eds.), *Sequences, Sedimentology: Surface and Subsurface*. Canadian Society of Petroleum Geologists Memoir, pp. 275-289.

Bhattacharya, B., Bandyopadhyay, S., Mahapatra, S., Banerjee, S., 2012. Record of tide-wave influence on the coal-bearing Permian Barakar Formation, Raniganj Basin, India. *Sedimentary Geology* 267, 25-35.

Bhattacharyya, P., Bhattacharya, J.P., Khan, S.D., 2015. Paleo-Channel Reconstruction and Grain Size Variability in Fluvial Deposits, Ferron Sandstone, Notom Delta, Hanksville, Utah. *Sedimentary Geology* 325, 17-25.

Bhattacharya, J.P., Giosan, L., 2003. Wave-influenced deltas: Geomorphological implications for facies reconstruction. *Sedimentology* 50, 187-210.

Bhattacharya, J.P., MacEachern, J.A., 2009. Hyperpycnal rivers and prodeltaic shelves in the Cretaceous seaway of North America. *Journal of Sedimentary Research* 79, 184-209.

Blakey, R., Ranney, W., 2008. *Ancient Landscapes of the Colorado Plateau*. Grand Canyon Association, Arizona.

Bloom, A.L., 1964. Peat accumulation and compaction in a Connecticut coastal marsh. *Journal of Sedimentary Research* 34.

Blum, M., Martin, J., Milliken, K., Garvin, M., 2013. Paleovalley systems: insights from Quaternary analogs and experiments. *Earth-Science Reviews* 116, 128-169.

Blum, M.D., Roberts, H.H., 2009. Drowning of the Mississippi Delta due to insufficient sediment supply and global sea-level rise. *Nature Geoscience* 2, 488-491.

Blum, M.D., Roberts, H.H., 2012. The Mississippi Delta Region: Past, Present, and Future. *Annual Review of Earth and Planetary Sciences* 40, 655-683.

Blum, M.D., Törnqvist, T.E., 2000. Fluvial responses to climate and sea-level change: a review and look forward. *Sedimentology* 47, 2-48.

Bohacs, K., Suter, J., 1997. Sequence stratigraphic distribution of coaly rocks: fundamental controls and paralic examples. *AAPG Bulletin* 81, 1612-1639.

Bose, P.K., Chakraborty, P.P., 1994. Marine to fluvial transition-Proterozoic Upper Rewa Sandstone, Maihar, India. *Sedimentary Geology* 89, 285-302.

Boyd, R., Dalrymple, R., Zaitlin, B.A., 1992. Classification of clastic coastal depositional environments *Sedimentary Geology* 80, 139-150.

Brain, M.J., 2016. Past, present and future perspectives of sediment compaction as a driver of relative sea level and coastal change. *Current Climate Change Reports* 2, 75-85.

Brekke, H., Couch, A., 2011. Use of image logs in differentiating point bar and tidal bar deposits in the Leismer area: implications for SAGD reservoir definition in the Athabasca oilsands, Extended Abstract, CSPG CSEG CWLS Convention.

Brettle, M.J., Mcilroy, D., Elliott, T., Davies, S.J., Waters, C.N., 2002. Identifying cryptic tidal influences within deltaic successions: an example from the Marsdenian (Namurian) interval of the Pennine Basin, UK. *Journal of the Geological Society* 159, 379-391.

Brice, J.C., 1974. Evolution of meander loops. *Geological Society of America Bulletin* 85, 581-586.

Bridge, J., 2006. Fluvial facies models: recent developments, in: Posamentier, H.W., Walker, R. (Eds.), *Facies Models Revisited Special Publication*, pp. 85-117.

Bridge, J.S., 1993. Description and interpretation of fluvial deposits: a critical perspective. *Sedimentology* 40, 801-810.

Bridge, J.S., Leeder, M.R., 1979. A simulation model of alluvial stratigraphy. *Sedimentology* 26, 617-644.

Bridge, J., Mackey, S., 1993. A theoretical study of fluvial sandstone body dimensions. The geological modelling of hydrocarbon reservoirs and outcrop analogues, 213-236.

Bridges, P.H., 1976. Lower Silurian transgressive barrier islands, southwest Wales. *Sedimentology* 23, 347-362.

Bristow, C., Best, J., 1993. Braided rivers: perspectives and problems. *Geological Society, London, Special Publications* 75, 1-11.

Bromley, R., 1996. *Trace Fossils: Biology, Taphonomy and Applications* Chapman Hall, London, 361 p.

Browne, G.H., Naish, T.R., 2003. Facies development and sequence architecture of a late Quaternary fluvial-marine transition, Canterbury Plains and shelf, New Zealand: implications for forced regressive deposits. *Sedimentary Geology* 158, 57-86.

Bryant, M., Falk, P., Paola, C., 1995. Experimental study of avulsion frequency and rate of deposition. *Geology* 23, 365-368.

Buatois, L.A., Mángano, G., Carr, T.C., 1999. Sedimentology and Ichnology of Paleozoic Estuarine and Shoreface Reservoirs, Morrow Sandstone, Lower Pennsylvanian of Southwest Kansas, USA, *Current Research in Earth Sciences*. Kansas Geological Survey Bulletin pp. 1-35.

Bullimore, S., Helland-Hansen, W., Henriksen, S., Steel, R., 2008. Shoreline trajectory and its impact on coastal depositional environments: an example from

Upper Cretaceous Mesaverde Group, NW Colorado. *Recent Advances in Models of Siliciclastic Shallow-Marine Stratigraphy*, 209-236.

Burns, B.A., Heller, P.L., Marzo, M., Paola, C., 1997. Fluvial response in a sequence stratigraphic framework: example from the Montserrat fan delta, Spain. *Journal of Sedimentary Research* 67, 311-321.

Burton, D., Flaig, P.P., Prather, T.J., 2016. Regional Controls On Depositional Trends In Tidally Modified Deltas: Insights From Sequence Stratigraphic Correlation and Mapping of the Loyd And Sego Sandstones, Uinta And Piceance Basins of Utah and Colorado, USA. *Journal of Sedimentary Research* 86, 763-785.

Cant, D.J., Walker, R.G., 1978. Fluvial processes and facies sequences in the sandy braided South Saskatchewan River, Canada. *Sedimentology* 25, 625-648.

Casshyap, S., Kumar, A., 1987. Fluvial architecture of the Upper Permian Raniganj coal measure in the Damodar basin, Eastern India. *Sedimentary Geology* 51, 181-213.

Castelltort, S., Van Den Driessche, J., 2003. How plausible are high-frequency sediment supply-driven cycles in the stratigraphic record? *Sedimentary Geology* 157, 3-13.

Cattaneo, A., Steel, R.J., 2003. Transgressive deposits: a review of their variability. *Earth-Science Reviews* 62, 187-228.

Catuneanu, O., Abreu, V., Bhattacharya, J., Blum, M., Dalrymple, R., Eriksson, P., Fielding, C.R., Fisher, W., Galloway, W., Gibling, M., 2009. Towards the standardization of sequence stratigraphy. *Earth-Science Reviews* 92, 1-33.

Cappelle, M., Stukins, S., Hampson, G.J., Johnson, H.D., 2016. Fluvial to tidal transition in proximal, mixed tide-influenced and wave-influenced deltaic deposits: Cretaceous lower Sego Sandstone, Utah, USA. *Sedimentology* 63, 1333-1361.

Cecil, C.B., Dulong, F.T., Cobb, J.C., 1993. Allogenic and autogenic controls on sedimentation in the Central Sumatra Basin as an analogue for Pennsylvanian coal-bearing strata in the Appalachian Basin. *Geological Society of America Special Papers* 286, 3-22.

Chan, M.A., Pfaff, B.J., 1991. Fluvial sedimentology of the Upper Cretaceous Castlegate Sandstone, Book Cliffs, Utah, in: Chidset, T.C. (Ed.), *Geology of east-central Utah*. Utah Geological Association, pp. 95-110.

Chatanantavet, P., Lamb, M.P., 2014. Sediment transport and topographic evolution of a coupled river and river plume system: An experimental and numerical study. *Journal of Geophysical Research: Earth Surface* 119, 1263-1282.

Chatanantavet, P., Lamb, M.P., Nittrouer, J.A., 2012. Backwater controls of avulsion location on deltas. *Geophysical Research Letters* 39, L01402.

Choi, K., 2011. External controls on the architecture of inclined heterolithic stratification (IHS) of macrotidal Sukmo Channel: Wave versus rainfall. *Marine Geology* 285, 17-28.

Choi, K., Kim, D.H., 2016. Morphologic and hydrodynamic controls on the occurrence of tidal bundles in an open-coast macrotidal environment, northern Gyeonggi Bay, west coast of Korea. *Sedimentary Geology* 339, 68-82.

Choi, K.S., Dalrymple, R.W., Chun, S.S., Kim, S.P., 2004. Sedimentology of Modern, Inclined Heterolithic Stratification (IHS) in the Macrotidal Han River Delta, Korea. *Journal of Sedimentary Research* 74, 677-689.

Church, M., 2006. Bed material transport and the morphology of alluvial river channels. *Annual Review Earth Planetary Science*. 34, 325-354.

Cloyd, K.C., Demicco, R.V., Spencer, R.J., 1990. Tidal channel, levee, and crevasse-splay deposits from a Cambrian tidal channel system: a new mechanism to produce shallowing-upward sequences. *Journal of Sedimentary Research* 60, 78-83.

Clymo, R., 1987. Rainwater-fed peat as a precursor of coal, in: Scott, A.C. (Ed.), *Coal and Coal Bearing Strata: Recent Advances*. Geological Society, London, Special Publications, pp. 17-23.

Cohen, A.D., Spackman, W., Raymond, R., 1987. Interpreting the characteristics of coal seams from chemical, physical and petrographic studies of peat deposits. Geological Society, London, Special Publications 32, 107-125.

Cohen, K.M., 2005. Fluvio-deltaic loodbasin deposits recording differential subsidence within a coastal prism (central Rhine-Meuse delta, The Netherlands). . IAS Special Publication 35, 295-320.

Cole, R., 2008. Characterization of fluvial sand bodies in the Neslen and lower Farrer formations (Upper Cretaceous), Lower Seego Canyon, Utah, in: Longman, M.W., Morgan, C.D. (Eds.), *Hydrocarbons Systems and Production in the Uinta Basin, Utah*. RMAG-UGA Publication 37, pp. 81-100..

Cole, R., Cumella, S., 2003. Stratigraphic architecture and reservoir characteristics of the Mesaverde Group, southern Piceance Basin, Colorado, in: Petersen, K.M., Olsen, T.M., Anderson, D.S. (Eds.), *Piceance Basin 2003 guidebook*. Rocky Mountain Association of Geologists, pp. 385-442.

Coleman, J.M., Gagliano, S.M., 1964. Cyclic sedimentation in the Mississippi River deltaic plain. *Gulf Coast Association of Geological Societies Transactions* 14, 67-80.

Coleman, J.M., Wright, L., 1975. Modern river deltas: variability of processes and sand bodies. *Deltas: Models for Exploration*, 99-149.

Coleman, J.M., 1988. Dynamic changes and processes in the Mississippi River delta. *Geological Society of America Bulletin* 100, 999-1015.

Collinson, J.D., Mountney, N., Thompson, D., 2006. *Sedimentary Structures*, 3 ed. Terra Publishing, Hertfordshire. 292 p.

Colombera, L., 2013. A database for the digitization of the sedimentary architecture of fluvial systems: uses in pure and applied research. University of Leeds.

Colombera, L., Felletti, F., Mountney, N.P., McCaffrey, W.D., 2012. A database approach for constraining stochastic simulations of the sedimentary heterogeneity of fluvial reservoirs. *AAPG Bulletin* 96, 2143-2166.

Colombera, L., Mountney, N.P., McCaffrey, W.D., 2013. A quantitative approach to fluvial facies models: methods and example results. *Sedimentology* 60, 1526-1558.

Colombera, L., Mountney, N.P., McCaffrey, W.D., 2015. A meta-study of relationships between fluvial channel-body stacking pattern and aggradation rate: Implications for sequence stratigraphy. *Geology* 43, 283-286.

Colombera, L., Shiers, M., Mountney, N., 2016a. Assessment of backwater controls on the architecture of distributary channel fills in a tide-influenced coastal-plain succession: Campanian Neslen Formation, USA. *Journal of Sedimentary Research* 86, 476-497.

Colombera, L., Mountney, N.P., Hodgson, D.M. and McCaffrey, W.D., 2016b. The Shallow-Marine Architecture Knowledge Store: a database for the characterization of shallow-marine and paralic depositional systems. *Marine and Petroleum Geology*, 75, 83-99.

Colombera, L., Mountney, N.P., Russell, C.E., Shiers, M.N. and McCaffrey, W.D., 2016c. Geometry and compartmentalization of fluvial meander-belt reservoirs at the bar-form scale: quantitative insight from outcrop, modern and subsurface analogues. *Marine and Petroleum Geology*, in review.

Constantine, J.A., McLean, S.R., Dunne, T., 2010. A mechanism of chute cutoff along large meandering rivers with uniform floodplain topography. *Geological Society of America Bulletin* 122, 855-869.

Correggiari, A., Cattaneo, A., Trincardi, F., 2005. The modern Po Delta system: lobe switching and asymmetric prodelta growth. *Marine Geology* 222, 49-74.

Cotter, E., 1971. Paleoflow characteristics of a Late Cretaceous river in Utah from analysis of sedimentary structures in the Ferron Sandstone. *Journal of Sedimentary Research* 41.

Corbeanu, R.M., Soegaard, K., Szerbiak, R.B., Thurmond, J.B., McMechan, G.A., Wang, D., Snelgrove, S., Forster, C.B., Menitove, A., 2001. Detailed internal architecture of a fluvial channel sandstone determined from outcrop, cores, and 3-D ground-penetrating radar: example from the middle Cretaceous Ferron Sandstone, east-central Utah. *AAPG Bulletin* 85, 1583-1608.

Corbeanu, R.M., Wizevich, M.C., Bhattacharya, J.P., Zeng, X., McMechan, G.A., 2004. Three-dimensional architecture of ancient lower delta-plain point bars using ground-penetrating radar, Cretaceous Ferron Sandstone, Utah. *Regional to Wellbore Analog for Fluvial-Deltaic Reservoir Modeling, The Ferron of Utah: American Association of Petroleum Geologists, Studies in Geology* 50, 427-449.

Corbett, M.J., Fielding, C.R., Birgenheier, L.P., 2011. Stratigraphy of a Cretaceous coastal-plain fluvial succession: The Campanian Masuk Formation, Henry Mountains syncline, Utah, U.S.A. *Journal of Sedimentary Research* 81, 80-96.

Courel, L., 1987, Stages in the compaction of peat; examples from the Stephanian and Permian of the Massif Central, France: *Journal of the Geological Society*, v. 144, p. 489-493.

Cross, T.A., 1986. Tectonic controls of foreland basin subsidence and Laramide style deformation, western United States. *Foreland basins*, 13-39.

Cross, T.A., 1988. Controls on coal distribution in transgressive-regressive cycles, Upper Cretaceous, Western Interior, U.S.A., in: Wilgus, C.K., Hastings, B.S., Posamentier, H.W., Van Wagoner, J.C., Ross, C.A., Kendall, C.G. (Eds.), *Sea level changes: an integrated approach: SEPM Special Publication* pp. 371-380.

Cummings, D.I., Hart, B.S., Arnott, R.W.C., 2006. Sedimentology and stratigraphy of a thick, areally extensive fluvial-marine transition, Missisauga Formation, offshore Nova Scotia, and its correlation with shelf margin and slope strata. *Bulletin of Canadian Petroleum Geology* 54, 152-174.

Currie, B.S., 1997. Sequence stratigraphy of nonmarine Jurassic–Cretaceous rocks, central Cordilleran foreland-basin system. *Geological Society of America Bulletin* 109, 1206-1222.

Czarnecki, J.M., Dashtgard, S.E., Pospelova, V., Mathewes, R.W., MacEachern, J.A., 2014. Palynology and geochemistry of channel-margin sediments across the tidal–fluvial transition, lower Fraser River, Canada: Implications for the rock record. *Marine and Petroleum Geology* 51, 152-166.

Dade, W., 2000. Grain size, sediment transport and alluvial channel pattern. *Geomorphology* 35, 119-126.

Dade, W.B., Friend, P.F., 1998. Grain-size, sediment-transport regime, and channel slope in alluvial rivers. *The Journal of Geology* 106, 661-676.

Dalrymple, R.W., 1992. Tidal Depositional Systems, in: Walker, R.G., James, N.P. (Eds.), *Facies Models- Response to Sea Level Change*, Geological Association of Canada, pp. 195-217.

Dalrymple, R.W., Baker, E.K., Harris, P.T., Hughes, M.G., 2003. Sedimentology and stratigraphy of a tide-dominated, foreland-basin delta (Fly River, Papua New Guinea), in: Sidi, F.H., Nummedal, D., Imbert, P., Darman, H., Posamentier, H.W. (Eds.), *Tropical Deltas of Southeast Asia - Sedimentology, Stratigraphy and Petroleum Geology*. SEPM Sepcial Publication, pp. 147-173.

Dalrymple, R.W., Choi, K., 2007. Morphologic and facies trends through the fluvial-marine transition in tide-dominated depositional systems: A schematic framework for environmental and sequence-stratigraphic interpretation. *Earth-Science Reviews* 81, 135-174.

Dalrymple, R.W., Kurcinka, C.E., Jablonski, B.V.J., Ichaso, A.A., Mackay, D.A., 2015. Deciphering the relative importance of fluvial and tidal processes in the

fluvial-marine transition, in: Ashworth, P.J., Best, J.L., Parsons, D.R. (Eds.), *Fluvial-Tidal Sedimentology*. Elsevier, pp. 3-45.

Dalrymple, R.W., Makino, Y., Zaitlin, B.A., 1991. Temporal and spatial patterns of rhythmite deposition on mud flats in the macrotidal Cobequid Bay-Salmon River estuary, Bay of Fundy, Canada, in: Smith, D.G., Reinson, G.E., Zaitlin, B.A., Rahmani, R.A. (Eds.), *Clastic Tidal Sedimentology*. Canadian Society of Petroleum Geologists Memoir, pp. 137-160.

Dalrymple, R.W., Zaitlin, B.A., Boyd, R., 1992. Estuarine facies models; conceptual basis and stratigraphic implications. *Journal of Sedimentary Research* 62, 1130-1146.

Dashtgard, S.E., Venditti, J.G., Hill, P.R., Sisulak, C.F., Johnson, S.M., La Croix, A.D., 2012. Sedimentation Across the Tidal-Fluvial Transition in the Lower Fraser River, Canada. *The Sedimentary Record* 10.

Davies, R., Diessel, C., Howell, J., Flint, S., Boyd, R., 2005. Vertical and lateral variation in the petrography of the Upper Cretaceous Sunnyside coal of eastern Utah, USA—implications for the recognition of high-resolution accommodation changes in paralic coal seams. *International Journal of Coal Geology* 61, 13-33.

Davies, R., Howell, J., Boyd, R., Flint, S., Diessel, C., 2006. High-resolution sequence-stratigraphic correlation between shallow-marine and terrestrial strata: Examples from the Sunnyside Member of the Cretaceous Blackhawk Formation, Book Cliffs, eastern Utah. *AAPG Bulletin* 90, 1121-1140.

Davis, R.A., Hayes, M.O., 1984. Hydrodynamics and Sedimentation in Wave-Dominated Coastal Environments What is a wave-dominated coast? *Marine Geology* 60, 313-329.

DeCelles, P.G., 2004. Late Jurassic to Eocene evolution of the Cordilleran thrust belt and foreland basin system, western U.S.A. *American Journal of Science* 304, 105-168.

Decelles, P.G., Lawton, T.F., Mitra, G., 1995. Thrust timing, growth of structural culminations, and synorogenic sedimentation in the type Sevier Orogenic Belt, Western United-States. *Geology* 23, 699-702.

Demowbray, T., 1983. The genesis of lateral accretion deposits in recent intertidal mudflat channels, Solway Firth, Scotland. *Sedimentology* 30, 425-435.

Deutsch, C.V. and Wang, L., 1996. Hierarchical object-based stochastic modeling of fluvial reservoirs. *Mathematical Geology*, 28, 857-880.

Deveugle, P.E., Jackson, M.D., Hampson, G.J., Farrell, M.E., Sprague, A.R., Stewart, J., Calvert, C.S., 2011. Characterization of stratigraphic architecture and its impact on fluid flow in a fluvial-dominated deltaic reservoir analog: Upper Cretaceous Ferron Sandstone Member, Utah. *AAPG Bulletin* 95, 693-727.

De Raaf, J.F.M., Boersma, J.R., Van Gelder, A., 1977. Wave-generated structures and sequences from a shallow marine succession, Lower Carboniferous, County Cork, Ireland. *Sedimentology* 24, 451-483.

Devine, P.E., 1991. Transgressive Origin of Channeled Estuarine Deposits in the Point Lookout Sandstone, Northwestern New Mexico: A Model for Upper Cretaceous, Cyclic Regressive Parasequences of the US Western Interior (1). *AAPG Bulletin* 75, 1039-1063.

Diessel, C.F., 1992. Coal Formation and Sequence Stratigraphy, in: Diessel, C. (Ed.), *Coal-Bearing Depositional Systems*. Springer, pp. 461-514.

Diessel, C., Boyd, R., Wadsworth, J., Leckie, D., Chalmers, G., 2000. On balanced and unbalanced accommodation/peat accumulation ratios in the Cretaceous coals from Gates Formation, Western Canada, and their sequence-stratigraphic significance. *International Journal of Coal Geology* 43, 143-186.

Doeglas, D., 1962. The structure of sedimentary deposits of braided rivers. *Sedimentology* 1, 167-190.

Donselaar, M.E., Overeem, I., 2008. Connectivity of fluvial point-bar deposits: An example from the Miocene Huesca fluvial fan, Ebro Basin, Spain. *AAPG Bulletin* 92, 1109-1129.

Dreyer, T., 1990. Sand body dimensions and infill sequences of stable, humid-climate delta plain channels, North Sea Oil and Gas Reservoirs—II. Springer, pp. 337-351.

Dreyer, T., Whitaker, M., Dexter, J., Flesche, H., Larsen, E., 2005. From spit system to tide-dominated delta: integrated reservoir model of the Upper Jurassic Sognefjord Formation on the Troll West Field, Geological Society, London, *Petroleum Geology Conference series*. Geological Society of London, pp. 423-448.

Driese, S., Fischer, M., Easthouse, K., Marks, G., Gogola, A., Schoner, A., 1991. Model for genesis of shoreface and shelf sandstone sequences, southern Appalachians: Paleoenvironmental reconstruction of an Early Silurian shelf system. *IAS Special Publication* 14, 309-338.

Duan, J.G., Julien, P.Y., 2010. Numerical simulation of meandering evolution. *Journal of Hydrology* 391, 34-46.

Dutton, S., Hamlin, H., 1991. Geologic Controls on Reservoir Properties of Frontier Formation Low-Permeability Gas Reservoirs, Moxa Arch, Wyoming, *Low Permeability Reservoirs Symposium*. Society of Petroleum Engineers.

Dyer, K.R., 1997. *Estuaries—a physical introduction*, 2 ed. Wiley, New York. P. 195

Eble, C.F., Hower, J.C., Andrews, W.M., 1994. Paleocology of the Fire Clay coal bed in a portion of the Eastern Kentucky Coal Field. *Palaeogeography, Palaeoclimatology, Palaeoecology* 106, 287-305.

Edmonds, D.A., Hoyal, D.C., Sheets, B.A., Slingerland, R.L., 2009. Predicting delta avulsions: Implications for coastal wetland restoration. *Geology* 37, 759-762.

Einsele, G., 2013. *Sedimentary basins: evolution, facies, and sediment budget*. Springer Science & Business Media. 792 p.

Elliott, T., 1974. Interdistributary bay sequences and their genesis. *Sedimentology* 21, 611-622.

Ellison, A.I., 2004. Numerical modeling of heterogeneity within a fluvial point-bar deposit using outcrop and lidar data: Williams Fork Formation, Piceance Basin, Colorado. University of Colorado, p. 231.

Eriksen, M.C., Slingerland, R., 1990. Numerical simulations of tidal and wind-driven circulation in the Cretaceous Interior Seaway of North America. *Geological Society of America Bulletin* 102, 1499-1516.

Eriksson, K.A., Simpson, E.L., 2000. Quantifying the oldest tidal record: The 3.2 Ga Moodies Group, Barberton Greenstone Belt, South Africa. *Geology* 28, 831-834.

Eriksson, K.A., Simpson, E.L., Mueller, W., 2006. An unusual fluvial to tidal transition in the mesoarchean Moodies Group, South Africa: A response to high tidal range and active tectonics. *Sedimentary Geology* 190, 13-24.

Erkens, G., Dambeck, R., Volleberg, K.P., Bouman, M.T., Bos, J.A., Cohen, K.M., Wallinga, J., Hoek, W.Z., 2009. Fluvial terrace formation in the northern Upper Rhine Graben during the last 20000 years as a result of allogenic controls and autogenic evolution. *Geomorphology* 103, 476-495.

Erskine, W., McFadden, C., Bishop, P., 1992. Alluvial cutoffs as indicators of former channel conditions. *Earth Surface Processes and Landforms* 17, 23-37.

Ethridge, F.G., 1998. Cyclic variables controlling fluvial sequence development: problems and perspectives, in: Shanley, K.W., McCabe, P.J. (Eds.), *Relative Role of Eustasy, Climate, and Tectonism in Continental Rocks*. SEPM Special Publication 59, pp. 17-29.

Ethridge, F.G., D., G., Schumm, S.A., Wood, L.J., 2005. The morphological and stratigraphical effects of base-level change: a review of experimental studies. *IAS Special Publication* 35, 213-241.

Fedo, C.M., Cooper, J.D., 1990. Braided fluvial to marine transition; the basal Lower Cambrian Wood Canyon Formation, southern Marble Mountains, Mojave Desert, California. *Journal of Sedimentary Research* 60, 220-234.

Fenies, H., Faugères, J.-C., 1998. Facies and geometry of tidal channel-fill deposits (Arcachon Lagoon, SW France). *Marine Geology* 150, 131-148.

Fielding, C.R., 1984. A coal depositional model for the Durham Coal Measures of NE England. *Journal of the Geological Society* 141, 919-931.

Fielding, C.R., 1985. Coal depositional models and the distinction between alluvial and delta plain environments. *Sedimentary Geology* 42, 41-48.

Fielding, C.R., 1986. Fluvial channel and overbank deposits from the Westphalian of the Durham coalfield, NE England *Sedimentology* 33, 119-140

Fielding, C.R., 1987. Coal depositional models for deltaic and alluvial plain sequences. *Geology* 15, 661-664.

Fielding, C.R., 2006. Upper flow regime sheets, lenses and scour fills: Extending the range of architectural elements for fluvial sediment bodies. *Sedimentary Geology* 190, 227-240.

Figueiredo, J.J., Hodgson, D.M., Flint, S.S., Kavanagh, J.P., 2010. Depositional environments and sequence stratigraphy of an exhumed Permian mudstone-dominated submarine slope succession, Karoo Basin, South Africa. *Journal of Sedimentary Research* 80, 97-118.

Fillmore, R., 2011. Geological Evolution of the Colorado Plateau of Eastern Utah and Western Colorado. University of Utah, Salt Lake City.

Fisher, D.J., 1936. The Book Cliffs Coal Field in Emery and Grand Counties, Utah, USGS Bulletin, p. 104.

Fisher, D.J., Erdmann, C.E., Reeside, J.B.J., 1960. Cretaceous and Tertiary formations of the Book Cliffs, Carbon, Emery, and Grand Counties, Utah, and Garfield and Mesa Counties, Colorado. Geological survey professional paper 332, 1-79.

Fitzsimmons, R., Johnson, S., 2000. Forced regressions: recognition, architecture and genesis in the Campanian of the Bighorn Basin, Wyoming. Geological Society, London, Special Publications 172, 113-139.

Flaig, P.P.M., Paul J.; Fiorillo, Anthony R., 2009. A tidally influenced, high-latitude coastal-plain: The Upper Cretaceous (Maastrichtian) Prince Creek Formation, North Slope, Alaska, in: Stephanie K. Davidson, Sophie Leleu, North, C.P. (Eds.), *From River to Rock Record*. SEPM Special Publication, University of Aberdeen, Scotland, pp. 233-264.

Flint, S., Aitken, J., Hampson, G., 1995. Application of sequence stratigraphy to coal-bearing coastal plain successions: implications for the UK Coal Measures. Geological Society, London, Special Publications 82, 1-16.

Flocks, J., Miner, M.D., Twichell, D.C., Lavoie, D.L., Kindinger, J., 2009. Evolution and preservation potential of fluvial and transgressive deposits on the Louisiana inner shelf: understanding depositional processes to support coastal management. *Geo-Marine Letters* 29, 359-378.

Foix, N., Paredes, J.M., Giacosa, R.E., 2013. Fluvial architecture variations linked to changes in accommodation space: Río Chico Formation (late Paleocene), Golfo San Jorge basin, Argentina. *Sedimentary Geology* 294, 342-355.

Fouch, T., Lawton, T., Nichols, D., Cashion, W., Cobban, W., 1983. Patterns and timing of synorogenic sedimentation in Upper Cretaceous rocks of central and northeast Utah, Mesozoic Palaeogeography of the West-Central United States. *Rocky Mountain Section (SEPM)*, pp. 305-336.

Franczyk, K.J., Fouch, T.D., Johnson, R.C., Molenaar, C.M., Cobban, W.A., 1992. Cretaceous and Tertiary Paleogeographic Reconstructions for the Uinta-Piceance Basin Study Area, Colorado and Utah. USGS Bulletin 1787, 1-37.

Frazier, D.E., Osanik, A., 1969. Recent Peat Deposits-Louisiana Coastal Plain. Geological Society of America Special Papers 114, 63-86.

Fricke, H.C., Foreman, B.Z., Sewall, J.O., 2010. Integrated climate model-oxygen isotope evidence for a North American monsoon during the Late Cretaceous. Earth and Planetary Science Letters 289, 11-21.

Friend, P., Slater, M., Williams, R., 1979. Vertical and lateral building of river sandstone bodies, Ebro Basin, Spain. Journal of the Geological Society 136, 39-46.

Fustic, M., 2007. Stratigraphic dip analysis—A novel application for detailed geological modeling of point bars, and predicting bitumen grade, McMurray Formation, Muskeg River Mine, northeast Alberta. Natural Resources Research 16, 31-43.

Fustic, M., Hubbard, S.M., Spencer, R., Smith, D.G., Leckie, D.A., Bennett, B., Larter, S., 2012. Recognition of down-valley translation in tidally influenced meandering fluvial deposits, Athabasca Oil Sands (Cretaceous), Alberta, Canada. Marine and Petroleum Geology 29, 219-232.

Galloway, W.E., 1975. Process framework for describing the morphologic and stratigraphic evolution of deltaic depositional systems, in: Broussard, M.L. (Ed.), Deltas – Models for exploration. Houston Geological Society, pp. 87-98.

Galloway, W.E., 1986. Reservoir facies architecture of microtidal barrier systems. AAPG Bulletin 70, 787-808.

Galloway, W.E., Hobday, D.K., 1996. Fluvial Systems, Terrigenous Clastic Depositional Systems. Springer, pp. 60-90.

Gardiner, S., Hiscott, R.N., 1988. Deep-water facies and depositional setting of the lower Conception Group (Hadrynian), southern Avalon Peninsula, Newfoundland. Canadian Journal of Earth Sciences 25, 1579-1594.

Gastaldo, R.A., Demko, T.M., Liu, Y., 1993. Application of sequence and genetic stratigraphic concepts to Carboniferous coal-bearing strata: an example from the Black Warrior basin, USA. Geologische Rundschau 82, 212-226.

Gates, T.A., Scheetz, R., 2015. A new saurolophine hadrosaurid (Dinosauria: Ornithomimidae) from the Campanian of Utah, North America. Journal of Systematic Palaeontology 13, 711-725.

Ganti, V., Chu, Z., Lamb, M.P., Nittrouer, J.A., Parker, G., 2014. Testing morphodynamic controls on the location and frequency of river avulsions on fans versus deltas: Huanghe (Yellow River), China. Geophysical Research Letters 41, 7882-7890.

Geehan, G. and Underwood, J., 1993. The use of length distributions in geological modelling. In: Flint, S.S. and Bryant, I.D. (Eds.) The Geological Modelling

of Hydrocarbon Reservoirs and Outcrop Analogues. IAS Special Publication, 15, 205–212.

Gersib, G.A., McCabe, P.J., 1981. Continental coal-bearing sediments of the Port Hood Formation (Carboniferous), Cape Linzee, Nova Scotia, Canada, in: Flores, R.M., Ethridge, F.G. (Eds.), *Recent and Ancient Non-Marine Depositional Environments: Models for Exploration*. SEPM, pp. 95-108.

Ghazi, S., Mountney, N.P., Sharif, S., Lower Permian fluvial cyclicity and stratigraphic evolution of the northern margin of Gondwanaland: Warchha Sandstone, Salt Range, Pakistan. *Journal of Asian Earth Sciences* 221, 99-126.

Ghinassi, M., Nemeč, W., Aldinucci, M., Nehyba, S., Özaksoy, V., Fidolini, F., 2014. Plan-form evolution of ancient meandering rivers reconstructed from longitudinal outcrop sections. *Sedimentology* 61, 952-977.

Ghosh, S.K., Chakraborty, C., Chakraborty, T., 2005. Influence of fluvial-tidal interactions on the nature of cross-stratified packages in a deltaic setting: examples from the Barakar Coal Measure (Permian), Satpura Gondwana Basin, central India. *Geological Journal* 40, 65-81.

Gingras, M.K., MacEachern, J.A., Dashtgard, S.E., 2012. The potential of trace fossils as tidal indicators in bays and estuaries. *Sedimentary Geology* 279, 97-106.

Goldstrand, P.M., 1994. Tectonic development of Upper Cretaceous to Eocene strata of Southwestern Utah. *Geological Society of America Bulletin* 106, 145-154.

Gomez-Veroiza, C.A., Steel, R.J., 2010. Iles clastic wedge development and sediment partitioning within a 300-km fluvial to marine Campanian transect (3 my), Western Interior seaway, southwestern Wyoming and northern Colorado. *AAPG Bulletin* 94, 1349-1377.

Gomis-Cartesio, L., Poyatos-More, M., Flint, S., Hodgson, D., Brunt, R., Wickens, H., 2016. Anatomy of a mixed-influence shelf-edge delta, Karoo Basin, South Africa. *Geological Society Special Publications*.

Gowland, S., 1996. Facies characteristics and depositional models of highly bioturbated shallow marine siliciclastic strata: an example from the Fulmar Formation (Late Jurassic), UK Central Graben. *Geological Society, London, Special Publications* 114, 185-214.

Gualtieri, J.L., 1991. Map and cross sections of coal zones in the Upper Cretaceous Neslen Formation, North-Central part of the Westwater 30' * 60' quadrangle, Grand and Uintah counties, Utah. U.S. Geological Survey.

Guion, P.D., Fulton, I.M., Jones, N.S., 1995. Sedimentary facies of the coal-bearing Westphalian A and B north of the Wales-Brabant High. *Geological Society, London, Special Publications* 82, 45-78.

Gugliotta, M., 2016. The Fluvial To Marine Transition Zone And Its Stratigraphic Significance, Earth, Atmospheric and Environmental Sciences. University of Manchester, p. 241.

Gugliotta, M., Kurcinka, C.E., Dalrymple, R.W., Flint, S.S., Hodgson, D.M., 2016. Decoupling seasonal fluctuations in fluvial discharge from the tidal signature in ancient deltaic deposits: an example from the Neuquén Basin, Argentina. *Journal of the Geological Society* 173, 94-107.

Hajek, E.A., Edmonds, D., 2014. Is river avulsion style controlled by floodplain morphodynamics? *Geology* 42, 199-202.

Hajek, E.A., Heller, P.L., Sheets, B.A., 2010. Significance of channel-belt clustering in alluvial basins. *Geology* 38, 535-538.

Hajek, E.A., Heller, P.L., Schur, E.L., 2012. Field test of autogenic control on alluvial stratigraphy (Ferris Formation, Upper Cretaceous–Paleogene, Wyoming). *Geological Society of America Bulletin* 124, 1898-1912.

Halfar, J., Riegel, W., Walther, H., 1998. Facies architecture and sedimentology of a meandering fluvial system: a Palaeogene example from the Weissester Basin, Germany. *Sedimentology* 45, 1-17.

Hampson, G.J., 2016. Towards a sequence stratigraphic solution set for autogenic processes and allogenic controls: Upper Cretaceous strata, Book Cliffs, Utah, USA. *Journal of the Geological Society* 173, 817-836.

Hampson, G.J., Jewell, T.O., Irfan, N., Gani, M.R., Bracken, B., 2013. Modest Change In Fluvial Style With Varying Accommodation In Regressive Alluvial-To-Coastal-Plain Wedge: Upper Cretaceous Blackhawk Formation, Wasatch Plateau, Central Utah, USA. *Journal of Sedimentary Research* 83, 145-169.

Hampson, G.J., Royhan Gani, M., Sahoo, H., Rittersbacher, A., Irfan, N., Ranson, A., Jewell, T.O., Gani, N.D.S., Howell, J.A., Buckley, S.J., Bracken, B., 2012. Controls on large-scale patterns of fluvial sandbody distribution in alluvial to coastal plain strata: Upper Cretaceous Blackhawk Formation, Wasatch Plateau, Central Utah, USA. *Sedimentology* 59, 2226-2258.

Harms, J., 1975. Stratification produced by migrating bed forms, in: Harms, J., Southard, J., Spearing, D., Walker, R. (Eds.), *Depositional Environments as Interpreted from Primary Sedimentary Structures and Stratification Sequences*. SEPM, pp. 45-61.

Harris, J., 1992. Mid-Jurassic lagoonal delta systems in the Hebridean basins: thickness and facies distribution patterns of potential reservoir sandbodies. Geological Society, London, Special Publications 62, 111-144.

Harris, P., Heap, A., Bryce, S., Porter-Smith, R., Ryan, D., Heggie, D., 2002. Classification of Australian clastic coastal depositional environments based upon a quantitative analysis of wave, tidal, and river power. *Journal of Sedimentary Research* 72, 858-870.

Hassan, M.H.A., Johnson, H.D., Allison, P.A., Abdullah, W.H., 2013. Sedimentology and stratigraphic development of the upper Nyalau Formation (Early Miocene), Sarawak, Malaysia: a mixed wave-and tide-influenced coastal system. *Journal of Asian Earth Sciences* 76, 301-311.

Hartley, A.J., Weissmann, G.S., Nichols, G.J., Warwick, G.L., 2010. Large distributive fluvial systems: characteristics, distribution, and controls on development. *Journal of Sedimentary Research* 80, 167-183.

Hartley, A.J., Weissmann, G.S., Scuderi, L., 2016. Controls on the apex location of large deltas. *Journal of the Geological Society*.

Heller, P.L., Paola, C., 1996. Downstream changes in alluvial architecture: an exploration of controls on channel-stacking patterns. *Journal of Sedimentary Research* 66, 297-306.

Hettinger, R.D., Kirshbaum, M.A., 2003. Stratigraphy of the Upper Cretaceous Mancos Shale (Upper Part) and Mesaverde Group in the Southern Part of the Uinta and Piceance Basins, Utah and Colorado, in: Team, U.U.-P.A. (Ed.), *Petroleum Systems and Geologic Assessment of Oil and Gas in the Uinta-Piceance Province, Utah and Colorado*. U.S Geological Survey, pp. 1-16.

Hickin, E.J., 1974. The development of meanders in natural river-channels. *American Journal of Science* 274, 414-442.

High Jr, L.R., Picard, M.D., 1974. Reliability of cross-stratification types as paleocurrent indicators in fluvial rocks. *Journal of Sedimentary Research* 44.

Hobday, D., Jackson, M., 1979. Transgressive shore zone sedimentation and syndepositional deformation in the Pleistocene of Zululand, South Africa. *Journal of Sedimentary Research* 49, 145-158.

Hofmann, M.H., Wroblewski, A., Boyd, R., 2011. Mechanisms controlling the clustering of fluvial channels and the compensational stacking of cluster belts. *Journal of Sedimentary Research* 81, 670-685.

Hogan, I.M., Sutton, S.J., 2014. The Role of Mudstone Baffles In Controlling Fluid Pathways In A Fluvial Sandstone: A Study In the Pennsylvanian–Permian Fountain Formation, Northern Colorado, USA. *Journal of Sedimentary Research* 84, 1064-1078.

Holbrook, J.M., 1996. Complex fluvial response to low gradients at maximum regression: A genetic link between smooth sequence-boundary morphology and architecture of overlying sheet sandstone. *Journal of Sedimentary Research* 66.

Holbrook, J., 2001. Origin, genetic interrelationships, and stratigraphy over the continuum of fluvial channel-form bounding surfaces: an illustration from middle Cretaceous strata, southeastern Colorado. *Sedimentary Geology* 144, 179-222.

Holbrook, J.M., Bhattacharya, J.P., 2012. Reappraisal of the sequence boundary in time and space: case and considerations for an SU (subaerial unconformity) that is not a sediment bypass surface, a time barrier, or an unconformity. *Earth-Science Reviews* 113, 271-302.

Holbrook, J., Scott, R.W., Oboh-Ikuenobe, F.E., 2006. Base-level buffers and buttresses: a model for upstream versus downstream control on fluvial geometry and architecture within sequences. *Journal of Sedimentary Research* 76, 162-174.

Holz, M., Kalkreuth, W., Banerjee, I., 2002. Sequence stratigraphy of paralic coal-bearing strata: an overview. *International Journal of Coal Geology* 48, 147-179.

Homewood, P., Allen, P., 1981. Wave-, tide-, and current-controlled sandbodies of Miocene Molasse, Western Switzerland. *AAPG Bulletin* 65, 2534-2545.

Hooke, J., 1984. Changes in river meanders a review of techniques and results of analyses. *Progress in Physical Geography* 8, 473-508.

Hooke, J., Yorke, L., 2011. Channel bar dynamics on multi-decadal timescales in an active meandering river. *Earth Surface Processes and Landforms* 36, 1910-1928.

Hopkins, J.C., 1985. Channel-fill deposits formed by aggradation in deeply scoured, superimposed distributaries of the Lower Kootenai Formation (Cretaceous). *Journal of Sedimentary Research* 55, 42-52.

Horne, J., Ferm, J., Caruccio, F., Baganz, B., 1978. Depositional models in coal exploration and mine planning in Appalachian region. *AAPG Bulletin* 62, 2379-2411.

Hovikoski, J., RÄSÄNen, M., Gingras, M., Ranzi, A., Melo, J., 2008. Tidal and seasonal controls in the formation of Late Miocene inclined heterolithic stratification deposits, western Amazonian foreland basin. *Sedimentology* 55, 499-530.

Hovius, N., 1998. Controls on sediment supply by large rivers, in: Kocurek, G. (Ed.), *Relative Role of Eustasy, Climate and Tectonism in Continental Rocks*. SEPM Special Publication, pp. 3-16.

Howard, J.D., Frey, R.W., 1984. Characteristic trace fossils in nearshore to offshore sequences, Upper Cretaceous of east-central Utah. *Canadian Journal of Earth Sciences* 21, 200-219.

Howell, J.A., Skorstad, A., MacDonald, A., Fordham, A., Flint, S., Fjellvoll, B., Manocchi, T., 2008. Sedimentological parameterization of shallow-marine reservoirs. *Petroleum Geoscience* 14, 17-34.

Hubbard, S.M., Smith, D.G., Nielsen, H., Leckie, D.A., Fustic, M., Spencer, R.J., Bloom, L., 2011. Seismic geomorphology and sedimentology of a tidally influenced river deposit, Lower Cretaceous Athabasca oil sands, Alberta, Canada. *AAPG Bulletin* 95, 1123-1145.

Huber, B.T., Norris, R.D., MacLeod, K.G., 2002. Deep-sea paleotemperature record of extreme warmth during the Cretaceous. *Geology* 30, 123-126.

Huerta, P., Armenteros, I., Silva, P.G., 2011. Large-scale architecture in non-marine basins: the response to the interplay between accommodation space and sediment supply. *Sedimentology* 58, 1716-1736.

Ielpi, A., Ghinassi, M., 2014. Planform architecture, stratigraphic signature and morphodynamics of an exhumed Jurassic meander plain (Scalby Formation, Yorkshire, UK). *Sedimentology* 61, 1923-1960.

Insole, A.N., Hutt, S., 1994. The palaeoecology of the dinosaurs of the Wessex Formation (Wealden Group, early Cretaceous), Isle of Wight, southern England. *Zoological Journal of the Linnean Society* 112, 197-215.

Jablonski, B.V., Dalrymple, R.W., 2016. Recognition of strong seasonality and climatic cyclicity in an ancient, fluviially dominated, tidally influenced point bar: Middle McMurray Formation, Lower Steepbank River, north-eastern Alberta, Canada. *Sedimentology* 63, 552-585.

Jackson II, R.G., 1976. Depositional model of point bars in the lower Wabash River. *Journal of Sedimentary Research* 46, 579-594.

Jackson II, R.G., 1978. Preliminary evaluation of lithofacies models for meandering alluvial streams, in: Miall, A.D. (Ed.), *Fluvial Sedimentology: Fluvial Facies Models*. Canadian Society of Petroleum Geologists Memoir, pp. 543-576.

Jerolmack, D.J., Paola, C., 2010. Shredding of environmental signals by sediment transport. *Geophysical Research Letters* 37, L19401, 1-5.

Jerolmack, D.J., Swenson, J.B., 2007. Scaling relationships and evolution of distributary networks on wave-influenced deltas. *Geophysical Research Letters* 34, L23402.

Jerrett, R.M., Davies, R.C., Hodgson, D.M., Flint, S.S., Chiverrell, R.C., 2011a. The significance of hiatal surfaces in coal seams. *Journal of the Geological Society* 168, 629-632.

Jerrett, R.M., Flint, S.S., Davies, R.C., Hodgson, D.M., 2011b. Sequence stratigraphic interpretation of a Pennsylvanian (Upper Carboniferous) coal from the central Appalachian Basin, USA. *Sedimentology* 58, 1180-1207.

Jerrett, R.M., Hodgson, D.M., Flint, S.S., Davies, R.C., 2011c. Control of Relative Sea Level and Climate on Coal Character in the Westphalian C (Atokan) Four Corners Formation, Central Appalachian Basin, USA. *Journal of Sedimentary Research* 81, 420-445.

Jin, D., Schumm, S., 1987. A new technique for modeling river morphology. *International Geomorphology, Part I: Chichester, UK, John Wiley & Sons*, 681-690.

Joeckel, R.M., Korus, J.T., 2012. Bayhead delta interpretation of an Upper Pennsylvanian sheetlike sandbody and the broader understanding of transgressive deposits in cyclothem. *Sedimentary Geology* 275-276, 22-37.

Johnson, R.C., 2003. Depositional Framework of the Upper Cretaceous Mancos Shale and the Lower Part of the Upper Cretaceous Mesaverde Group, Western Colorado and Eastern Utah, *Petroleum Systems and Geologic Assessment of Oil and Gas in the Uinta-Piceance Province, Utah and Colorado*. U.S Geological Survey, pp. 1-24.

Johnson, C.L., Stright, L., Purcell, R., Durkin, P., 2016. Stratigraphic evolution of an estuarine fill succession and the reservoir characterization of inclined heterolithic strata, Cretaceous of southern Utah, USA. Geological Society, London, Special Publications 444, SP444. 441.

Johnson, S.M., Dashtgard, S.E., 2012. The Nature of Inclined Heterolithic Stratification in a Mixed Tidal-Fluvial Setting, Fraser River, British Columbia, Canada, AAPG Annual Convention and Exhibition. AAPG, Long Beach, California.

Johnson, S.M., Dashtgard, S.E., 2014. Inclined heterolithic stratification in a mixed tidal-fluvial channel: Differentiating tidal versus fluvial controls on sedimentation. *Sedimentary Geology* 301, 41-53.

Jones, L., Schumm, S., 2009. Causes of avulsion: an overview. *Fluvial sedimentology* VI, 169-178.

Jordan, T.E., 1981. Thrust loads and foreland basin evolution, Cretaceous, Western United States. *AAPG Bulletin* 65, 2506-2520.

Jordt, H., Faleide, J.I., Bjørlykke, K., Ibrahim, M.T., 1995. Cenozoic sequence stratigraphy of the central and northern North Sea Basin: tectonic development, sediment distribution and provenance areas. *Marine and Petroleum Geology* 12, 845-879.

Kamola, D.L., Van Wagoner, J.C., 1995. Stratigraphy and facies architecture of parasequences with examples from the Spring Canyon Member, Blackhawk Formation, Utah, in: Van Wagoner, J.C., Bertram, G.T. (Eds.), *Sequence Stratigraphy of Foreland Basin Deposits* AAPG, pp. 27-54.

Karaman, O., 2012. Shoreline Architecture and Sequence Stratigraphy of Campanian to Cretaceous Clastic Wedge, Piceance Basin, CO: Influence of Laramide Movements in Western Interior Seaway. University of Texas at Austin, Texas, p. 137.

Kasvi, E., Vaaja, M., Alho, P., Hyypä, H., Hyypä, J., Kaartinen, H., Kukko, A., 2013. Morphological changes on meander point bars associated with flow structure at different discharges. *Earth Surface Processes and Landforms* 38, 577-590.

Kauffman, E.G., 1977. Geological and biological overview: Western Interior Cretaceous Basin. *The Mountain Geologist* 14, 75-99.

Keighin, C.W., Fouch, T.D., 1981. Depositional Environments And Diagenesis Of Some Nonmarine Upper Cretaceous Reservoir Rocks Uinta Basin Utah. *SEPM Special Publication* 31, 109-125.

Keller, E., 1972. Development of alluvial stream channels: a five-stage model. *Geological Society of America Bulletin* 83, 1531-1536.

Keogh, K.J., Martinius, A.W. and Osland, R., 2007. The development of fluvial stochastic modelling in the Norwegian oil industry: A historical review, subsurface implementation and future directions. *Sedimentary Geology*, 202, 249-268.

Kieft, R.L., Hampson, G.J., Jackson, C.A.-L., Larsen, E., 2011. Stratigraphic Architecture of a Net-Transgressive Marginal-to Shallow-Marine Succession: Upper Almond Formation, Rock Springs Uplift, Wyoming, USA. *Journal of Sedimentary Research* 81, 513-533.

Kim, W., Paola, C., Voller, V.R., Swenson, J.B., 2006. Experimental measurement of the relative importance of controls on shoreline migration. *Journal of Sedimentary Research* 76, 270-283.

Kirschbaum, M., Hettinger, R., 1998. Stratigraphy and depositional environments of the late Campanian coal-bearing Neslen/Mount Garfield formations, eastern Book Cliffs, Utah and Colorado. US Geological Survey report number 98-43.

Kirschbaum, M.A., Hettinger, R.D., 2004. Facies Analysis and Sequence Stratigraphic Framework of Upper Campanian Strata (Neslen and Mount Garfield Formations, Bluecastle Tongue of the Castlegate Sandstone, and Mancos Shale), Eastern Book Cliffs, Colorado and Utah. U.S. Geological Survey, U.S. Geological Survey Digital Data Series. Report DDS-69-G.

Kirschbaum, M.A., Spear, B.D., 2012. Stratigraphic cross section of measured sections and drill holes of the Neslen Formation and adjacent formations, Book Cliffs Area, Colorado and Utah. US Geological Survey open field report 2012-1260.

Kosters, E.C., Bailey, A., 1983. Characteristics of peat deposits in the Mississippi River delta plain. 33, 311-325.

Kraft, J.C., Chrzastowski, M.J., Belknap, D.F., Toscano, M.A., Fletcher, C.H., 1987. The transgressive barrier-lagoon coast of Delaware: morphostratigraphy, sedimentary sequences and responses to relative rise in sea level, in: Nummedal, D., Pilkey, O.H., Howard, J.D. (Eds.), *Sea-level Fluctuation and Coastal Evolution*. SEPM Special Publication, pp. 129-143.

Krystinik, L.F., Blakeney DeJarnett, B., 1995. Lateral Variability of Sequence Stratigraphic Framework in the Campanian and Lower Maastrichtian of the Western Interior Seaway, in: Bertram, G.T., Van Wagoner, J.C. (Eds.), *AAPG Special Volume: Sequence Stratigraphy of Foreland Basin Deposits* AAPG, pp. 11-25.

Kvale, E.P., 2011. Tidal Constituents of Modern and Ancient Tidal Rhythmites, in: Davis Jr, A.R., Dalrymple, R.W. (Eds.), *Principles of Tidal Sedimentology*. Springer, Netherlands, pp. 1-17.

Labrecque, P.A., Hubbard, S.M., Jensen, J.L., Nielsen, H., 2011. Sedimentology and stratigraphic architecture of a point bar deposit, Lower Cretaceous McMurray Formation, Alberta, Canada. *Bulletin Of Canadian Petroleum Geology* 59, 147-171.

La Croix, A.D., Dashtgard, S.E., 2014. Of sand and mud: Sedimentological criteria for identifying the turbidity maximum zone in a tidally influenced river. *Sedimentology* 61, 1961-1981.

La Croix, A.D., Dashtgard, S.E., 2015. A synthesis of depositional trends in intertidal and upper subtidal sediments across the tidal–fluvial transition in the Fraser River, Canada. *Journal of Sedimentary Research* 85, 683-698.

Lamb, M.P., Nittrouer, J.A., Mohrig, D., Shaw, J., 2012. Backwater and river plume controls on scour upstream of river mouths: Implications for fluvio-deltaic morphodynamics. *Journal of Geophysical Research: Earth Surface* 117, F01002.

Lambiase, J.J., 2013. Sediment Dynamics and Depositional Systems of the Mahakam Delta, Indonesia: Ongoing Delta Abandonment On A Tide-Dominated Coast. *Journal of Sedimentary Research* 83, 503-521.

Lanier, W.P., Feldman, H.R., Archer, A.W., 1993. Tidal sedimentation from a fluvial to estuarine transistion, Douglas Group, Missourian Virgilian, Kansas. *Journal of Sedimentary Petrology* 63, 860-873.

Lavigne, J.M., 2001. Aspects of marginal marine sedimentology, stratigraphy and ichnology of the Upper Cretaceous Horseshoe Canyon Formation, Drumheller, Alberta. University of Alberta, p. 146.

Lawton, T.F., 1983. Late Cretaceous fluvial systems and the age of foreland uplifts in central Utah. *Rocky Mountain foreland basins and uplifts: Denver, Rocky Mountain Association of Geologists*, 181-199.

Lawton, T.F., 1986. Fluvial systems of Upper Cretaceous Mesaverde Group and Paleocene North Horn formation, central Utah: A record of transition from thin-skinned deformation in foreland region, *in: J.A. Peterson, ed., Paleotectonics and sedimentation in the Rocky Mountain region, United States: American Association of Petroleum Geologists Memoir* 41, p. 423-442.

Lawton, T.F., Bradford, B.A., 2011. Correlation and Provenance of Upper Cretaceous (Campanian) Fluvial Strata, Utah, U.S.A., from Zircon U-Pb Geochronology and Petrography. *Journal of Sedimentary Research* 81, 495-512.

Le Blanc, R.J., 1975. Significant studies of modern and ancient deltaic sediments, *in: Broussard, M.L. (Ed.), Deltas: Models for Exploration Houston Geological Society*, pp. 13-85.

Legarreta, L., Uliana, M., Larotonda, C., Meconi, G., 1993. Approaches to nonmarine sequence stratigraphy-theoretical models and examples from Argentine basins. *Collection Colloques Et Seminaires-Institut Francais Du Petrole* 51, 125-125.

Legler, B., Johnson, H.D., Hampson, G.J., Massart, B.Y., Jackson, C.A.L., Jackson, M.D., El-Barkooky, A., Ravnas, R., 2013. Facies model of a fine-grained, tide-dominated delta: Lower Dir Abu Lifa Member (Eocene), Western Desert, Egypt. *Sedimentology*.

Legler, B., Hampson, G.J., Jackson, C.A., Johnson, H.D., Massart, B.Y., Sarginson, M., Ravnås, R., 2014. Facies Relationships and Stratigraphic Architecture of Distal, Mixed Tide-and Wave-Influenced Deltaic Deposits: Lower Sego Sandstone, Western Colorado, USA. *Journal of Sedimentary Research* 84, 605-625.

Leeder, M., 1977. A quantitative stratigraphic model for alluvium, with special reference to channel deposit density and interconnectedness, in: Miall, A.D. (Ed.), *Fluvial Sedimentology*. Canadian Society of Petroleum Geology, pp. 587-596.

Leeder, M., 1999. *Sedimentology and Sedimentary Basins. From Turbulence to Tectonics*, 6 ed. Blackwell Science Ltd. 592 p.

Leeder, M.R., Stewart, M.D., 1996. Fluvial incision and sequence stratigraphy: alluvial responses to relative sea-level fall and their detection in the geologic record, in: Hesselbo, S.P., Parkinson, D.N. (Eds.), *Sequence Stratigraphy in British Geology*. Geological Society Special Publication, pp. 25-39.

Leopold, L.B., Wolman, M.G., 1960. River meanders. *Geological Society of America Bulletin* 71, 769-793.

Leopold, L.B., Wolman, M.G., Miller J.P., 1995. *Fluvial processes in geomorphology*, Courier Dover Publications, 544 p.

Leva López, J., Rossi, V., Olariu, C., Steel, R., 2016. Architecture and recognition criteria of ancient shelf ridges; an example from Campanian Almond Formation in Hanna Basin, USA. *Sedimentology* 63, 1651-1676.

Li, W., Bhattacharya, J.P., Campbell, C., 2010. Temporal evolution of fluvial style in a compound incised-valley fill, Ferron "Notom Delta", Henry Mountains Region, Utah (USA). *Journal of Sedimentary Research* 80, 529-549.

Li, C.-x., Wang, P., Fan, D., Yang, S., 2006. Characteristics and formation of Late Quaternary incised-valley-fill sequences in sediment-rich deltas and estuaries: case studies from China. *SEPM Special Publication* 85, 141.

Longhitano, S.G., Mellere, D., Steel, R.J., Ainsworth, R.B., 2012. Tidal depositional systems in the rock record: A review and new insights. *Sedimentary Geology* 279, 2-22.

Longhitano, S.G., Steel, R.J., 2016. Deflection of the progradational axis and asymmetry in tidal seaway and strait deltas: insights from two outcrop case studies. Geological Society, London, *Special Publications* 444, SP444. 448.

Lynds, R., Hajek, E., 2006. Conceptual model for predicting mudstone dimensions in sandy braided-river reservoirs. *AAPG Bulletin* 90, 1273-1288.

MacEachern, J.A., Bann, K.L., Bhattacharya, J.P., Howell, C.D., 2005. Ichnology of deltas: organism responses to the dynamic interplay of rivers, waves, storms, and tides, in: Giosan, L., Bhattacharya, J.P. (Eds.), *River Deltas - Concepts, Models and Examples*. SEPM Special Publication, pp. 49-85.

Mackey, S.D., Bridge, J.S., 1995. Three-dimensional model of alluvial stratigraphy: theory and application. *Journal of Sedimentary Research* 65, 7-31.

Makhlouf, I.M., 2003. Fluvial/tidal interaction at the southern Tethyan strandline during Triassic Mukheiris times in central Jordan. *Journal of Asian Earth Sciences* 21, 377-385.

Martinius, A.W., Gowland, S., 2011. Tide-influenced fluvial bedforms and tidal bore deposits (Late Jurassic Lourinha Formation, Lusitanian Basin, Western Portugal). *Sedimentology* 58, 285-324.

Martinsen, O.J., Ryseth, A., Helland-Hansen, W., Flesche, H., Torkildsen, G., Idil, S., 1999. Stratigraphic base level and fluvial architecture: Ericson Sandstone (Campanian), Rock Springs Uplift, SW Wyoming, USA. *Sedimentology* 46, 235-259.

McCabe, P.J., 1984. Depositional environments of coal and coal-bearing strata, in: Rahmani, R.A., Flores, R.M. (Eds.), *Sedimentology of Coal and Coal-Bearing Sequences*. Wiley Online Library, Oxford, pp. 13-42.

McCabe, P.J., 1985. Depositional environments of coal and coal-bearing strata, in: Rahmani, R.A., Flores, R.M. (Eds.), *Sedimentology of Coal and Coal-Bearing Sequences*. Blackwell Publishing: IAS Special Publication, pp. 13-42.

McCabe, P.J., 1987. Facies studies of coal and coal-bearing strata. *Geological Society, London, Special Publications* 32, 51-66.

McCarthy, P.J., Faccini, U.F., Plint, A.G., 1999. Evolution of an ancient coastal plain: palaeosols, interfluves and alluvial architecture in a sequence stratigraphic framework, Cenomanian Dunvegan Formation, NE British Columbia, Canada. *Sedimentology* 46, 861-891.

McCave, I., 1970. Deposition of fine-grained suspended sediment from tidal currents. *Journal of Geophysical Research* 75, 4151-4159.

McIlroy, D., 2006. Ichnology of a macrotidal tide-dominated deltaic depositional system: Lajas Formation, Neuquén Province, Argentina. *Special Publication-SEPM* 88, 195.

McLaurin, B.T., Steel, R.J., 2000. Fourth-order nonmarine to marine sequences, middle Castlegate Formation, Book Cliffs, Utah. *Geology* 28, 359-362.

McLaurin, B.T., Steel, R.J., 2007. Architecture and origin of an amalgamated fluvial sheet sand, lower Castlegate Formation, Book Cliffs, Utah. *Sedimentary Geology* 197, 291-311.

McGookey, D.P., Haun, J., Hale, L., Goodell, H., McCubbin, D., Weimer, R., Wulf, G., 1972. Cretaceous system. *Geologic Atlas of the Rocky Mountain Region*: Rocky Mountain Association of Geologists, 190-228.

McGowen, J., Garner, L., 1970. Physiographic Features And Stratification Types Of Coarse-Grained Point bars: Modern And Ancient Examples. *Sedimentology* 14, 77-111.

Medici, G., Boulesteix, K., Mountney, N., West, L., Odling, N., 2015. Palaeoenvironment of braided fluvial systems in different tectonic realms of the Triassic Sherwood Sandstone Group, UK. *Sedimentary Geology* 329, 188-210.

Mellere, D., Steel, R., 1995. Variability of lowstand wedges and their distinction from forced-regressive wedges in the Mesaverde Group, southeast Wyoming. *Geology* 23, 803-806.

Mellere, D., Steel, R., 2000. Style contrast between forced regressive and lowstand/transgressive wedges in the Campanian of south-central Wyoming (Hatfield Member of the Haystack Mountains Formation). Geological Society, London, Special Publications 172, 141-162.

Mellet, C.L., Hodgson, D.M., Lang, A., Mauz, B., Selby, I., Plater, A.J., 2012. Preservation of a drowned gravel barrier complex: A landscape evolution study from the north-eastern English Channel. Marine Geology 315–318, 115-131.

Miall, A.D., 1978. Lithofacies types and vertical profile models in braided river deposits: a summary, in: Miall A.D., (Ed.) Fluvial Sedimentology. Canadian Society of Petroleum Geology Memoir, 5, 597–604.

Miall, A.D., 1985. Architectural-element analysis: A new method of facies analysis applied to fluvial deposits. Earth-Science Reviews 22, 261-308.

Miall, A.D., 1988. Facies architecture in clastic sedimentary basins, in: Kleinspehn, K.L., Paola, C. (Eds.), New perspectives in basin analysis. Springer, pp. 67-81.

Miall, A.D., 1993. The architecture of fluvial-deltaic sequences in the Upper Mesaverde Group (Upper Cretaceous), Book Cliffs, Utah. Geological Society, London, Special Publications 75, 305-332.

Miall, A. D., 1996. The Geology of Fluvial Deposits: Berlin, Springer, 582 p.

Miall, A. D., 2014a. Fluvial Depositional Systems, Springer, 316 p.

Miall, A.D., Arush, M., 2001. The Castlegate Sandstone of the Book Cliffs, Utah: Sequence Stratigraphy, Paleogeography, and Tectonic Controls. Journal of Sedimentary Research 71, 537-548.

Miall, A.D., Catuneanu, O., Vakarelov, B.K., Post, R., 2008. Chapter 9 The Western Interior Basin, in: Andrew, D.M. (Ed.), Sedimentary Basins of the World. Elsevier, pp. 329-362.

Miall, A.D., Jones, B.G., 2003. Fluvial architecture of the Hawkesbury sandstone (Triassic), near Sydney, Australia. Journal of Sedimentary Research 73, 531-545.

Miller, R.L., Fram, M., Fujii, R., Wheeler, G., 2008. Subsidence Reversal in a Re-established Wetland in the Sacramento-San Joaquin Delta, California, USA. San Francisco Estuary and Watershed Science 6, 1-20.

Miller, I.M., Johnson, K.R., Kline, D.E., 2013. A Late Campanian flora from the Kaiparowits, in: Titus, A.L., Loewen, M.A. (Eds.), At the Top of the Grand Staircase: The Late Cretaceous of Southern Utah. Indiana University Press, Bloomington, pp. 107-131.

Miranda, M.C., De Fátima Rossetti, D., Carlos Ruiz Pessenda, L., 2009. Quaternary paleoenvironments and relative sea-level changes in Marajó Island (Northern Brazil): Facies, $\delta^{13}C$, $\delta^{15}N$ and C/N. Palaeogeography, Palaeoclimatology, Palaeoecology 282, 19-31.

Mitchum Jr, R., Vail, P., Thompson III, S., 1977. Seismic stratigraphy and global changes of sea level: Part 2. The depositional sequence as a basic unit for stratigraphic analysis: Section 2. Application of seismic reflection configuration to stratigraphic interpretation, *Seismic Stratigraphy--Applications to Hydrocarbon Exploration*. AAPG Memoir, pp. 53-62.

Mjos, R., Walderhaug, O., Prestholm, E., 2009. Crevasse splay sandstone geometries in the Middle Jurassic Ravenscar Group of Yorkshire, UK. *Alluvial Sedimentation*, International Association of Sedimentologists, Special Publication 17, 167-184.

Mohrig, D., Heller, P.L., Paola, C., Lyons, W.J., 2000. Interpreting avulsion process from ancient alluvial sequences: Guadalope-Matarranya system (northern Spain) and Wasatch Formation (western Colorado). *Geological Society of America Bulletin* 112, 1787-1803.

Moore, P., 1987. Ecological and hydrological aspects of peat formation. *Geological Society, London, Special Publications* 32, 7-15.

Moore, P.D., 1995. Biological processes controlling the development of modern peat-forming ecosystems. *International Journal of Coal Geology* 28, 99-110.

Mulhern, J.S., Johnson, C.L., 2016. Time–space variability of paralic strata deposited in a high accommodation, high sediment supply setting: example from the Cretaceous of Utah. *Geological Society, London, Special Publications* 444, SP444. 447.

Musial, G., Labourdette, R., Franco, J., Reynaud, J.-Y., 2013. Modeling of a tide-influenced point-bar heterogeneity distribution and Impacts on steam-assisted gravity drainage production: Example from Steepbank River, McMurray Formation, Canada, in: Hein, F.J., Leckie, D., Larter, S., Suter, J. (Eds.), *Heavy-oil and oil-sand petroleum systems in Alberta and beyond*. AAPG Studies in Geology, pp. 545-564.

Musial, G., Reynaud, J.-Y., Gingras, M.K., Féliès, H., Labourdette, R., Parize, O., 2012. Subsurface and outcrop characterization of large tidally influenced point bars of the Cretaceous McMurray Formation (Alberta, Canada). *Sedimentary Geology* 279, 156-172.

Muto, T., Steel, R.J., 1992. Retreat of the front in a prograding delta. *Geology* 20, 967-970.

Muto, T., Steel, R.J., 2001. Autostepping during the transgressive growth of deltas: Results from flume experiments. *Geology* 29, 771-774.

Muto, T., Steel, R.J., 2002. Role of autoretreat and A/S changes in the understanding of deltaic shoreline trajectory: a semi-quantitative approach. *Basin Research* 14, 303-318.

Muto, T., Steel, R.J., Swenson, J.B., 2007. Autostratigraphy: a framework norm for genetic stratigraphy. *Journal of Sedimentary Research* 77, 2-12.

Muto, T., Steel, R.J., Burgess, P.M., 2016. Contributions to sequence stratigraphy from analogue and numerical experiments. *Journal of the Geological Society* 173, 837-844.

Nadon, G.C., 1998. Magnitude and timing of peat-to-coal compaction. *Geology* 26, 727-730.

Nami, M., Leeder, M., 1977. Changing channel morphology and magnitude in the Scalby Formation (M. Jurassic) of Yorkshire, England. *Canadian Journal of Petroleum Geologists Memoir* 5, 431-440.

Nardin, T.R., Feldman, H.R., Carter, B.J., 2013. Stratigraphic architecture of a large-scale point-bar complex in the McMurray Formation: Syncrude's Mildred Lake Mine, Alberta, Canada.

Nanson, G.C., 1980. Point bar and floodplain formation of the meandering Beatton River, northeastern British Columbia, Canada. *Sedimentology* 27, 3-29.

Nanson, R.A., Vakarelov, B.K., Ainsworth, R.B., Williams, F.M., Price, D.M., 2013. Evolution of a Holocene, mixed-process, forced regressive shoreline: The Mitchell River delta, Queensland, Australia. *Marine Geology* 339, 22-43.

Neal, J., Abreu, V., 2009. Sequence stratigraphy hierarchy and the accommodation succession method. *Geology* 37, 779-782.

Nelson, C.S., Mildenhall, D.C., Todd, A.J., Pocknall, D.T., 1988. Subsurface stratigraphy, paleoenvironments, palynology, and depositional history of the late Neogene Tauranga Group at Ohinewai, Lower Waikato Lowland, South Auckland, New Zealand. *New Zealand Journal of Geology and Geophysics* 31, 21-40.

Nichols, G.J., 2009. *Sedimentology and Stratigraphy*, 2 ed. Wiley, 419 pp.

Nio, S.-D., Yang, C.-S., 1991. Diagnostic attributes of clastic tidal deposits: a review, in: Smith, D.G., Reinson, G.E., Zaitlin, B.A., Rahmani, R.A. (Eds.), *Clastic Tidal Sedimentology*. Canadian Society of Petroleum Geologists, pp. 3-28.

Nittrouer, J.A., Shaw, J., Lamb, M.P., Mohrig, D., 2012. Spatial and temporal trends for water-flow velocity and bed-material sediment transport in the lower Mississippi River. *Geological Society of America Bulletin* 124, 400-414.

Nummedal, D., Riley, G.W., 1991. Origin of late Turonian and Coniacian unconformities in the San Juan basin, in: Van Wagoner, J.C., Nummedal, D., Jones, C.R., Taylor, A.M., Jenette, D.C., Riley, G.W. (Eds.), *Sequence stratigraphy applications to shelf sandstone reservoirs: outcrop to subsurface examples*. AAPG Field Conference Guide, p. 275.

Nyberg, B., Howell, J.A., 2016. Global distribution of modern shallow marine shorelines. Implications for exploration and reservoir analogue studies. *Marine and Petroleum Geology* 71, 83-104.

O'Brien, K.C., 2015. Stratigraphic architecture of a shallow-water delta deposited in a coastal-plain setting: Neslen Formation, Floy Canyon, Utah. Colorado School of Mines. Arthur Lakes Library, p. 77.

O'Byrne, C.J., Flint, S., 1995. Sequence, parasequence, and intraparasequence architecture of the Grassy Member, Blackhawk Formation, Book Cliffs, Utah, USA. 64, 225-255.

Olariu, M.I., Olariu, C., 2015. Ubiquity of Wave-Dominated Deltas In Outer-Shelf Growth-Faulted Compartments. *Journal of Sedimentary Research* 85, 768-779.

Olariu, C., Steel, R.J., Olariu, M.I., Choi, K.S., 2015. Facies and architecture of unusual fluvial-tidal channels with inclined heterolithic strata: Campanian Neslen Formation, Utah, USA, in: Ashworth, P.J., Best, J.L., Parsons, D.R. (Eds.), *Fluvial-Tidal Sedimentology*, Elsevier, 353-394.

Olsen, T., 1993. Large fluvial systems: the Atane Formation, a fluvio-deltaic example from the Upper Cretaceous of central West Greenland. *Sedimentary Geology* 85, 457-473.

Olsen, T., Steel, R., Hogseth, K., Skar, T., Roe, S.L., 1995. Sequential architecture in a fluvial succession; sequence stratigraphy in the Upper Cretaceous Mesaverde Group, Prince Canyon, Utah. *Journal of Sedimentary Research* 65, 265-280.

Okolo, S.A., 2009. Fluvial distributary channels in the Fletcher Bank Grit (Namurian R 2b), at Ramsbottom, Lancashire, England, in: Collinson, J.D., Lewin, J. (Eds.), *Modern and Ancient Fluvial Systems IAS Special Publication*, pp. 421-433.

Oomkens, E., 1974. Lithofacies relations in the Late Quaternary Niger Delta complex. *Sedimentology* 21, 195-222.

Orton, G., Reading, H., 1993. Variability of deltaic processes in terms of sediment supply, with particular emphasis on grain size. *Sedimentology* 40, 475-512.

Parrish, J.T., Gaynor, G.C., Swift, D.J.P., 1984. Circulation In The Cretaceous Western Interior Seaway Of North America, A Review, in: Stott, D.F., Glass, D.J. (Eds.), *The Mesozoic of Middle North America*. Canadian Society of Petroleum Geologists Memoir 9, pp. 221-231.

Patruyo, D.J., Huang, Haiping , Hubbard, Stephen and Spencer, Ron, 2009. Point Bar Modeling, Middle McMurray Formation, Alberta, CSPG CSEG CWLS Convention. *Frontiers + Innovation*, Alberta Ingenuity Center for In-Situ Energy (AICISE), University of Calgary, pp. 806-809.

Peakall, J., Ashworth, P.J., Best, J.L., 2007. Meander-bend evolution, alluvial architecture, and the role of cohesion in sinuous river channels: a flume study. *Journal of Sedimentary Research* 77, 197-212.

Pearson, N.J., Gingras, M.K., 2006. An ichnological and sedimentological facies model for muddy point-bar deposits. *Journal of Sedimentary Research* 76, 771-782.

Pemberton, S.G., Flach, P.D., Mossop, G.D., 1982. Trace fossils from the Athabasca oil sands, Alberta, Canada. *Science* 217, 825-827.

Pemberton, S.G., MacEachern, J.A., 1995. The Sequence Stratigraphic Significance of Trace Fossils: Examples from the Cretaceous Foreland Basin of Alberta, Canada, in: Van Wagoner, J.C., Bertram, G.T. (Eds.), *Seismic/Sequence Stratigraphy*. AAPG Special Volumes, pp. 429-475.

Pemberton, S.G., Wightman, D.M., 1992. Ichnological characteristics of brackish water deposits. *Applications of Ichnology to Petroleum Engineering* 17, 141-167.

Penland, S., Boyd, R., 1981. Shoreline changes on the Louisiana barrier coast, *OCEANS* 81. IEEE, pp. 209-219.

Penland, S., Suter, J.R., 1983. Transgressive coastal facies preserved in barrier island arc retreat paths in the Mississippi River delta plain. *Gulf Coast Association of Geological Societies Transactions* 33, 367-382.

Penland, S., Suter, J.R., Boyd, R., 1985. Barrier island arcs along abandoned Mississippi River deltas. *Marine Geology* 63, 197-233.

Penland, S., Boyd, R., Suter, J.R., 1988. Transgressive depositional systems of the Mississippi delta plain: a model for barrier shoreline and shelf sand development. *Journal of Sedimentary Research* 58, 932-949.

Penland, S., Suter, J.R., 1989. The geomorphology of the Mississippi River chenier plain. *Marine Geology* 90, 231-258.

Percival, C.J., 1992. The Harthope Ganister--A Transgressive Barrier Island to Shallow-Marine Sand-Ridge from the Namurian of Northern England. *Journal of Sedimentary Petrology* 62, 442-454.

Petersen, H.I., Andsbjerg, J., 1996. Organic facies development within Middle Jurassic coal seams, Danish Central Graben, and evidence for relative sea-level control on peat accumulation in a coastal plain environment. *Sedimentary Geology* 106, 259-277.

Picard, M.D., High Jr, L.R., 1973. *Sedimentary Structures of Ephemeral Streams*. Elsevier. 223 p.

Pitman, J.K., Franczyk, K.J., Anders, D.E., 1986. Marine and Nonmarine gas-bearing rocks in Upper Cretaceous Neslen and Blackhawk formations, Eastern Uinta Basin, Utah--Sedimentology, Diagenesis, and Source rock potential. *AAPG Bulletin* 70, 1052-1052.

Plink-BjÖRklund, P., 2005. Stacked fluvial and tide-dominated estuarine deposits in high-frequency (fourth-order) sequences of the Eocene Central Basin, Spitsbergen. *Sedimentology* 52, 391-428.

Plint, A.G., Hart, B.S., Donaldson, W.S., 1993. Lithospheric flexure as a control on stratal geometry and facies distribution in Upper Cretaceous rocks of the Alberta foreland basin. *Basin Research* 5, 69-77.

Plummer, P., Gostin, V., 1981. Shrinkage cracks: desiccation or syneresis? *Journal of Sedimentary Research* 51, 1147-1156.

Posamentier, H.W., Allen, G.P., 1993. Variability of the sequence stratigraphic model: effects of local basin factors. *Sedimentary Geology* 86, 91-109.

Posamentier, H.W., Allen, G.P., James, D.P., Tesson, M., 1992. Forced regressions in a sequence stratigraphic framework: concepts, examples, and exploration significance (1). *AAPG Bulletin* 76, 1687-1709.

Posamentier, H.W., Morris, W.R., 2000. Aspects of the stratal architecture of forced regressive deposits. Geological Society, London, Special Publications 172, 19-46.

Posamentier, H., Vail, P., 1988. Eustatic controls on clastic deposition II—sequence and systems tract models, in: Wilgus, C., Hastings, B., Posamentier, H., Van Wagoner, J., Ross, C., Kendall, C. (Eds.), *Sea-Level Changes-An Integrated Approach*. SEPM.

Postma, G., 2014. Generic autogenic behaviour in fluvial systems: lessons from experimental studies. *Depositional Systems to Sedimentary Successions on the Norwegian Continental Margin (IAS SP 46)* 46, 1-18.

Pranter, M.J., Ellison, A.I., Cole, R.D., Patterson, P.E., 2007. Analysis and modeling of intermediate-scale reservoir heterogeneity based on a fluvial point-bar outcrop analog, Williams Fork Formation, Piceance Basin, Colorado. *AAPG Bulletin* 91, 1025-1051.

Pranter, M.J., Hewlett, A.C., Cole, R.D., Wang, H. and Gilman, J., 2014. Fluvial architecture and connectivity of the Williams Fork Formation: use of outcrop analogues for stratigraphic characterization and reservoir modelling. Geological Society, London, Special Publications, 387, pp.57-83.

Pranter, M.J., Sommer, N.K., 2011. Static connectivity of fluvial sandstones in a lower coastal-plain setting: An example from the Upper Cretaceous lower Williams Fork Formation, Piceance Basin, Colorado. *AAPG Bulletin* 95, 899-923.

Pranter, M.J., Vargas, M.F. and Davis, T.L., 2008. Characterization and 3D reservoir modelling of fluvial sandstones of the Williams Fork Formation, Rulison field, Piceance basin, Colorado, USA. *Journal of Geophysics and Engineering*, 5, p.158.

Purnachandra Rao, V., Shynu, R., Kessarkar, P.M., Sundar, D., Michael, G.S., Narvekar, T., Blossom, V., Mehra, P., 2011. Suspended sediment dynamics on a seasonal scale in the Mandovi and Zuari estuaries, central west coast of India. *Estuarine, Coastal and Shelf Science* 91, 78-86.

Rasanen, M.E., Linna, A.M., Santos, J.C.R., Negri, F.R., 1995. Late Miocene Tidal Deposits in the Amazonian Foreland Basin. *Science* 269, 386-390.

Reading, H.G., Collinson, J.D., 1996. Clastic coasts, in: H.G., R. (Ed.), *Sedimentary Environments: Processes, Facies and Stratigraphy*, 3 ed. Blackwell Publishing, University of Oxford, pp. 154-231.

Reineck, H.E., Wunderlich, F., 1968. Classification and Origin of Flaser and Lenticular bedding *Sedimentology* 11, 99-104.

Richards, K., Chandra, S., Friend, P., 1993. Avulsive channel systems: characteristics and examples. Geological Society, London, Special Publications 75, 195-203.

Rittersbacher, A., Howell, J.A., Buckley, S.J., 2014. Analysis Of Fluvial Architecture In the Blackhawk Formation, Wasatch Plateau, Utah, U.S.A., Using Large 3D Photorealistic Models. *Journal of Sedimentary Research* 84, 72-87.

Roberts, H.H., 1997. Dynamic changes of the Holocene Mississippi River delta plain: the delta cycle. *Journal of Coastal Research*, 605-627.

Roberts, H.H., Coleman, J.M., 1996. Holocene evolution of the deltaic plain: a perspective—from Fisk to present. *Engineering Geology* 45, 113-138.

Robinson Roberts, L.N., Kirschbaum, M.A., 1995. Paleogeography of the Late Cretaceous of the Western Interior of Middle North America-coal distribution and Sediment accumulation. USGS Professional Paper 1561, 1-65.

Roehler, H.W., 1990. Stratigraphy of the Mesaverde Group in the central and eastern greater Green River Basin, Wyoming, Colorado, and Utah. *Journal Name: United States Geological Survey, Professional Paper; (USA); Journal Volume: 1508, 1-52.*

Rogers, R.R., 1998. Sequence analysis of the Upper Cretaceous Two Medicine and Judith River formations, Montana: nonmarine response to the Claggett and Bearpaw marine cycles. *Journal of Sedimentary Research* 68, 615-631.

Rudolph, K.W., Devlin, W.J., Crabaugh, J.P., 2015. Upper Cretaceous Sequence Stratigraphy of the Rock Springs Uplift, Wyoming. *The Mountain Geologist* 52, 13-157.

Ryer, T.A., 1981. Deltaic coals of Ferron Sandstone Member of Mancos Shale: predictive model for Cretaceous coal-bearing strata of Western Interior. *AAPG Bulletin* 65, 2323-2340.

Ryer, T.A., 1983. Transgressive-regressive cycles and the occurrence of coal in some Upper Cretaceous strata of Utah. *Geology* 11, 207-210.

Ryer, T.A., Langer, A.W., 1980. Thickness change involved in the peat-to-coal transformation for a bituminous coal of Cretaceous age in central Utah. *Journal of Sedimentary Research* 50.

Sanders, J.E., Kumar, N., 1975. Evidence of Shoreface Retreat and In-Place "Drowning" During Holocene Submergence of Barriers, Shelf off Fire Island, New York. *Geological Society of America Bulletin* 86, 65-76.

Santos, M.G., Almeida, R.P., Mountney, N.P., Fragoso-Cesar, A.R., 2012. Seismites as a tool in the palaeoenvironmental reconstruction of fluvial deposits: the Cambrian Guarda Velha Formation, southern Brazil. *Sedimentary Geology* 277, 52-60.

Savrdá, C.E., 1991. Teredolites, wood substrates, and sea-level dynamics. *Geology* 19, 905-908.

Schlager, W., 1993. Accommodation and supply—a dual control on stratigraphic sequences. *Sedimentary Geology* 86, 111-136.

Schmidt, C.W., 2015. Delta Subsidence: An Imminent Threat to Coastal Populations. *Environmental Health Perspectives* 123, A204-A209.

Schubel, J., 1968. Turbidity maximum of the northern Chesapeake Bay. *Science* 161, 1013-1015.

Schumm, S.A., 1963. Sinuosity of alluvial rivers on the Great Plains. *Geological Society of America Bulletin* 74, 1089-1100.

Schumm, S., 1968. Speculations concerning paleohydrologic controls of terrestrial sedimentation. *Geological Society of America Bulletin* 79, 1573-1588.

Schumm, S., 1985. Patterns of alluvial rivers. *Annual Review of Earth and Planetary Sciences* 13, 5.

Schumm, S., Khan, H., 1972. Experimental study of channel patterns. *Geological Society of America Bulletin* 83, 1755-1770.

Shanley, K.W., McCabe, P.J., Hettinger, R.D., 1992. Tidal influence in Cretaceous fluvial strata from Utah, USA: a key to sequence stratigraphic interpretation. *Sedimentology* 39, 905-930.

Shanley, K.W., McCabe, P.J., 1994. Perspectives on the sequence stratigraphy of continental strata *AAPG Bulletin* 78, 544-568.

Shanley, K.W., McCabe, P.J., 1995. Sequence Stratigraphy of Turonian–Santonian Strata, Kaiparowits Plateau, Southern Utah, U.S.A.: Implications for Regional Correlation and Foreland Basin Evolution, in: Van Wagoner J. C., B., George T. (Ed.), *Sequence Stratigraphy of Foreland Basin Deposits: Outcrop and Subsurface examples from the Cretaceous of North America*. American Association of Petroleum Geologists, Tulsa, Oklahoma, USA, pp. 103-136.

Shiers, M., Mountney, N., Hodgson, D., Cobain, S., 2014. Depositional Controls on Tidally Influenced Fluvial Successions, Neslen Formation, Utah, USA. *Sedimentary Geology* 311, 1-16.

Shchepetkina, A., Gingras, M.K., Zonneveld, J.-P., Pemberton, S.G., 2016. Sedimentary fabrics of the macrotidal, mud-dominated, inner estuary to fluvio-tidal transition zone, Petitcodiac River estuary, New Brunswick, Canada. *Sedimentary Geology* 333, 147-163.

Shuster, M.W., Steidtmann, J.R., 1987. Fluvial-sandstone architecture and thrust-induced subsidence, northern Green River Basin, Wyoming, in: Ethridge, F.G., Flores, R.M., Harvey, M.D., Weaver, J.N. (Eds.), *Recent Developments in Fluvial Sedimentology*. SEPM, pp. 279-284.

Simons, D.B., 1960. Sedimentary structures generated by flow in alluvial channels. *SEPM Special Publication Primary Sedimentary Structures*, 34-52.

Silverberg, N., Sundby, B., 1979. Observations in the turbidity maximum of the St. Lawrence Estuary. *Canadian Journal of Earth Sciences* 16, 939-950.

Sisulak, C.F., Dashtgard, S.F., 2012. Seasonal controls on the development and character of inclined heterolithic stratification in a tide-influenced, fluvially dominated channel: Fraser River, Canada. *Journal of Sedimentary Research* 82, 244-257.

Sixsmith, P.J., Hampson, G.J., Gupta, S., Johnson, H.D., Fofana, J.F., 2008. Facies architecture of a net transgressive sandstone reservoir analog: The Cretaceous Hosta Tongue, New Mexico. *AAPG Bulletin* 92, 513-547.

Slingerland, R., Keen, T., 1999. Sediment Transport In The Western Interior Seaway Of North America Predictions From A Climate-Ocean-Sediment Model. *SEPM Special Publication* 64, 179-190.

Slingerland, R., Kump, L.R., Arthur, M.A., Fawcett, P.J., Sageman, B.B., Barron, E.J., 1996. Estuarine circulation in the Turonian western interior seaway of North America. *Geological Society of America Bulletin* 108, 941-952.

Slingerland, R., Smith, N.D., 2004. River avulsions and their deposits. *Annu. Rev. Earth Planet. Sci.* 32, 257-285.

Smith, C.E., 1998. Modeling high sinuosity meanders in a small flume. *Geomorphology* 25, 19-30.

Smith, D.G., 1987. Meandering river point bar lithofacies models: modern and ancient examples compared, in: Ethridge, F.G., Flores, R.M., Harvey, M.D. (Eds.), *Recent developments in Fluvial Sedimentology*. SEPM, pp. 83-91.

Smith, D.G., Hubbard, S.M., Leckie, D.A., Fustic, M., 2009. Counter point bar deposits: lithofacies and reservoir significance in the meandering modern Peace River and ancient McMurray Formation, Alberta, Canada. *Sedimentology* 56, 1655-1669.

Smith, N.D., Cross, T.A., Dufficy, J.P., Clough, S.R., 1989. Anatomy of an avulsion. *Sedimentology* 36, 1-23.

Snedden, J.W., Bergmann, K.M., 1999. Isolated shallow marine sand bodies: deposits for all interpretations, in: Olszewski, T.D. (Ed.), *Isolated Shallow Marine Sand Bodies Sequence Stratigraphic Analysis and Sedimentologic Interpretation*. SEPM Special Publication, pp. 1-11.

Soltan, R., Mountney, N.P., 2016. Interpreting complex fluvial channel and barform architecture: Carboniferous Central Pennine Province, northern England. *Sedimentology* 63, 207-252.

Sønderholm, M., Tirsgaard, H., 1998. Proterozoic fluvial styles: response to changes in accommodation space (Rivieradal sandstones, eastern North Greenland). *Sedimentary Geology* 120, 257-274.

Sornoza, L., Barnolas, A., Arasa, A., Maestro, A., Rees, J.G., Hernandez-Molina, F.J., 1998. Architectural stacking patterns of the Ebro delta controlled by Holocene high-frequency eustatic fluctuations, delta-lobe switching and subsidence processes. *Sedimentary Geology* 117, 11-32.

Spears, D., 1987. Mineral matter in coals, with special reference to the Pennine Coalfields, Coal and coal bearing strata: Recent advances. Geological Society of London Special Publication 32, pp. 171-185.

Steel, R., Aasheim, S.M., 1977. Alluvial sand deposition in a rapidly subsiding basin (Devonian, Norway), in: Miall, A. (Ed.), *Fluvial Sedimentology*. Canadian Society of Petroleum Geologists Memoir, pp. 385-412.

Steel, R.J., Plink-Bjorklund, P., Aschoff, J., 2012. Tidal Deposits of the Campanian Western Interior Seaway, Wyoming, Utah and Colorado, USA, in: Davis Jr, A.R., Dalrymple, W.R. (Eds.), *Principles of Tidal Sedimentology*. Springer Netherlands, Dordrecht, pp. 437-471.

Stewart, D., 1983. Possible Suspended-Load Channel Deposits from the Wealden Group (Lower Cretaceous) of Southern England. *Modern and ancient fluvial systems*, 369-384.

Stouthamer, E., Berendsen, H.J.A., 2007. Avulsion: The relative roles of autogenic and allogenic processes. *Sedimentary Geology* 198, 309-325.

Stouthamer, E., Cohen, K., Gouw, M.J., 2011. Avulsion and its implications for fluvial-deltaic architecture: insights from the Holocene Rhine-Meuse Delta. From River to Rock Record: The Preservation of Fluvial Sediments and Their Subsequent Interpretation, Davidson SK, Leleu S, North CP (eds), *SEPM Special Publication 97*, 215-232.

Straub, K.M., Paola, C., Mohrig, D., Wolinsky, M.A., George, T., 2009. Compensational stacking of channelized sedimentary deposits. *Journal of Sedimentary Research* 79, 673-688.

Stuart, J.Y., 2015. *Subsurface Architecture of Fluvial-Deltaic Deposits in High- and Low-Accommodation Settings*, School of Earth and Environment. University of Leeds, p. 346.

Sun, T., Meakin, P., Jøssang, T., 2001. A computer model for meandering rivers with multiple bed load sediment sizes: 2. Computer simulations. *Water Resources Research* 37, 2243-2258.

Swift, D.J., 1975. Barrier-island genesis: evidence from the central Atlantic shelf, eastern USA. *Sedimentary Geology* 14, 1-43.

Swift, D.J., Niederoda, A.W., Vincent, C.E., Hopkins, T.S., 1985. Barrier island evolution, middle Atlantic shelf, USA Part I: Shoreface dynamics. *Marine Geology* 63, 331-361.

Syvitski, J.P.M., Farrow, G.E., 1983. Structures and processes in bayhead deltas: Knight and bute inlet, British Columbia. *Sedimentary Geology* 36, 217-244.

Syvitski, J.P., Milliman, J.D., 2007. Geology, geography, and humans battle for dominance over the delivery of fluvial sediment to the coastal ocean. *The Journal of Geology* 115, 1-19.

Tabet, D.E., Quick, J.C., Hucka, B.P., 2008. Distribution, Amount, and Maturity of Coal Resources of Most of the Se-go Coalfield, Utah. Rocky Mountain Association of Geologists and Utah Geological Association Publication 37, 339-365.

Taylor, A.M., Goldring, R., 1993. Description and analysis of bioturbation and ichnofabric. *Journal of the Geological Society* 150, 141-148.

Taylor, K.G., Mächent, P.G., 2011. Extensive carbonate cementation of fluvial sandstones: An integrated outcrop and petrographic analysis from the Upper Cretaceous, Book Cliffs, Utah. *Marine and Petroleum Geology* 28, 1461-1474.

Tew, B.H., Mancini, E.A., 1995. An integrated stratigraphic method for paleogeographic reconstruction: examples from the Jackson and Vicksburg Groups of the eastern Gulf Coastal Plain. *Palaios*, 133-153.

Thomas, R.G., Smith, D.G., Wood, J.M., Visser, J., Calverleyrange, E.A., Koster, E.H., 1987. Inclined heterolithic stratification-terminology, description, interpretation and significance. *Sedimentary Geology* 53, 123-179.

Tissot, B.P., Welte, D.H., 1984. From kerogen to petroleum, *Petroleum Formation and Occurrence*. Springer, pp. 160-198.

Tonkin, N.S., 2012. Deltas, in: Knaust, D., Bromley, R.G. (Eds.), Trace fossils as indicators of sedimentary environments. Elsevier, pp. 507-528.

Törnqvist, T.E., Bridge, J.S., 2002. Spatial variation of overbank aggradation rate and its influence on avulsion frequency. *Sedimentology* 49, 891-905.

Törnqvist, T.E., Wallace, D.J., Storms, J.E., Wallinga, J., Van Dam, R.L., Blaauw, M., Derksen, M.S., Klerks, C.J., Meijneken, C., Snijders, E.M., 2008. Mississippi Delta subsidence primarily caused by compaction of Holocene strata. *Nature Geoscience* 1, 173-176.

Trendell, A.M., Atchley, S.C., Nordt, L.C., 2013. Facies Analysis of A Probable Large-Fluvial-Fan Depositional System: The Upper Triassic Chinle Formation At Petrified Forest National Park, Arizona, U.S.A. *Journal of Sedimentary Research* 83, 873-895.

Turner, B., Eriksson, K., 1999. Meander bend reconstruction from an Upper Mississippian muddy point bar at Possum Hollow, West Virginia, USA. *Fluvial sedimentology* VI, 363-379.

Tyler, N., Gholston, J.C., Ambrose, W., 1987. Oil recovery in a low-permeability, wave-dominated, Cretaceous, deltaic reservoir, Big Wells (San Miguel) field, south Texas. *AAPG Bulletin* 71, 1171-1195.

Tyler, N., Finley, R. J., 1991. Architectural controls on the recovery of hydrocarbons from sandstone reservoirs, in: Tyler, N., Miall, A. (Eds.), The three-dimensional facies architecture of terrigenous clastic sediments, and its implications for hydrocarbon discovery and recovery. *Society of Economic Paleontologists and Mineralogists*, pp. 1-5.

Uncles, R., Stephens, J., Law, D., 2006. Turbidity maximum in the macrotidal, highly turbid Humber Estuary, UK: Flocs, fluid mud, stationary suspensions and tidal bores. *Estuarine, Coastal and Shelf Science* 67, 30-52.

Vail, P.R., 1987. Seismic stratigraphy interpretation using sequence stratigraphy: Part 1: Seismic stratigraphy interpretation procedure, in: Bally, A.W. (Ed.), *Atlas of Seismic Stratigraphy*. AAPG Studies in Geology, pp. 1-10.

Vail, P.R., Mitchum Jr, R., Thompson III, S., 1977. Seismic Stratigraphy and Global Changes of Sea Level: Part 4. Global Cycles of Relative Changes of Sea Level.: Section 2. Application of Seismic Reflection Configuration to Stratigraphic Interpretation.

Vakarelov, B.K., Ainsworth, R.B., 2013. A hierarchical approach to architectural classification in marginal marine systems-bridging the gap between sedimentology and sequence stratigraphy. *AAPG Bulletin* 97, 1121-1161.

Valasek, D., 1995. The Tocito Sandstone in a sequence stratigraphic framework: An example of landward-stepping small-scale genetic sequences, in: Van Wagoner, J.C., Bertram, G.T. (Eds.), *Sequence stratigraphy of foreland basin deposits: Outcrop and subsurface examples from the Cretaceous of North America*. AAPG Memoir 64, pp. 349-369.

van Asselen, S., Stouthamer, E., van Asch, T.W.J., 2009. Effects of peat compaction on delta evolution: A review on processes, responses, measuring and modeling. *Earth-Science Reviews* 92, 35-51.

Van de Graaff, F.R., 1972. Fluvial--deltaic facies of the Castlegate Sandstone (Cretaceous), east-central Utah. *Journal of Sedimentary Research* 42, 558-571.

van den Berg, J.H., Boersma, J.R., van Gelder, A., 2007. Diagnostic sedimentary structures of the fluvial-tidal transition zone - Evidence from deposits of the Rhine and Meuse. *Netherlands Journal of Geosciences-Geologie En Mijnbouw* 86, 287-306.

Van Strien, W.J., 2016. Fluvial Sequence Stratigraphy, <http://www.epgeology.com/articles/fluvial-sequence-stratigraphy.html>.

van Wagoner, J.C., 1991. High-frequency sequence stratigraphy and facies architecture of the Sego Sandstone in the Book Cliffs of western Colorado and eastern Utah., in: Van Wagoner J.C., N.D., Jones C.R., Taylor D.R., Jennette D.C., and , G.W., R. (Eds.), *Sequence Stratigraphy Applications to Shelf Sandstone Reservoirs: Outcrop to Subsurface Examples*. American Association of Petroleum Geologists, Tulsa, pp. 1-22.

van Wagoner, J.C., 1995. Sequence Stratigraphy and Marine to Nonmarine Facies Architecture of Foreland Basin Strata, Book Cliffs, Utah, U.S.A., in: Van Wagoner, J.C., Bertram, G.T. (Eds.), *Sequence Stratigraphy of Foreland Basin Deposits: Outcrop and Subsurface Examples from the Cretaceous of North America* American Association of Petroleum Geologists, pp. 137-223.

van Wagoner, J.C., Mitchum, R.M., Campion, K.M., Rahmanian, V.D., 1990. Siliciclastic Sequence Stratigraphy in Well Logs, Cores, and Outcrops: Concepts for High-Resolution Correlation of Time and Facies. AAPG Special Volumes A174, 1-55.

van Wagoner, J.C., Posamentier, H.W., Mitchum Jr, R.M., Vail, P.R., Sarg, J.F., Loutit, T.D., Hardenbol, J., 1988. An overview of the fundamentals of sequence stratigraphy and key definitions. SEPM Special Publication 42, 39-45.

Visher, G.S., 1960. Fluvial processes as interpreted from ancient and recent fluvial deposits, Primary Sedimentary Structures. SEPM, pp. 116-132.

Visher, G.S., 1965. Use of vertical profile in environmental reconstruction. AAPG Bulletin 49, 41-61.

Visher, G.S., 1972. Physical characteristics of fluvial deposits, in: Rigby, J.K., Hamblin, W.K. (Eds.), Recognition of Ancient Sedimentary Environments, pp. 84-97.

Visser, M.J., 1980. Neap-spring cycles reflected in Holocene subtidal large-scale bedform deposits: A preliminary note. *Geology* 8, 543-546.

Wadsworth, J., Boyd, R., Diessel, C., Leckie, D., Zaitlin, B.A., 2002. Stratigraphic style of coal and non-marine strata in a tectonically influenced intermediate accommodation setting: the Mannville Group of the Western Canadian Sedimentary Basin, south-central Alberta. *Bulletin Of Canadian Petroleum Geology* 50, 507-541.

Wadsworth, J., Boyd, R., Diessel, C., Leckie, D., 2003. Stratigraphic style of coal and non-marine strata in a high accommodation setting: Falher Member and Gates Formation (Lower Cretaceous), western Canada. *Bulletin Of Canadian Petroleum Geology* 51, 275-303.

Wakelin-King, G.A., Webb, J.A., 2007. Upper-flow-regime mud floodplains, lower-flow-regime sand channels: sediment transport and deposition in a drylands mud-aggregate river. *Journal of Sedimentary Research* 77, 702-712.

Wallinga, J., Törnqvist, T.E., Busschers, F.S., Weerts, H.J., 2004. Allogenic forcing of the late Quaternary Rhine–Meuse fluvial record: the interplay of sea-level change, climate change and crustal movements. *Basin Research* 16, 535-547.

Walker, R.G., Cant, D.J., 1984. Sandy fluvial systems, Facies models. *Geosci. Can., Repr. ser.* pp. 71-89.

Wang, H., Shao, L., Hao, L., Zhang, P., Glasspool, I.J., Wheeley, J.R., Wignall, P.B., Yi, T., Zhang, M., Hilton, J., 2011. Sedimentology and sequence stratigraphy of the Lopingian (Late Permian) coal measures in southwestern China. *International Journal of Coal Geology* 85, 168-183.

Warner, D.L., 1964. Mancos-Mesaverde (Upper Cretaceous) Intertonguing Relations Southeast Piceance Basin, Colorado. AAPG Bulletin 48, 1091-1107.

Weimer, R.J., 1960. Upper cretaceous stratigraphy, rocky Mountain area. AAPG Bulletin 44, 1-20.

Weimer, R.J., Howard, J.D., Lindsay, D.R., 1982. Tidal flats and associated tidal channels, in: Scholle, P.A., Spearing, D. (Eds.), *Sandstone Depositional Environments* American Association of Petroleum Geologists, Memoir, pp. 191-245.

Weissmann, G., Bennett, G., Lansdale, A., 2005. Factors controlling sequence development on Quaternary fluvial fans, San Joaquin Basin, California, USA. *Geological Society of London* 251, 169.

Weissmann, G. S., A. J. Hartley, G. J. Nichols, L. A. Scuderi, M. Olson, H. Buehler, and R. Banteah, 2010a. Fluvial form in modern continental sedimentary basins: Distributive fluvial systems: *Geology*, v. 38, p. 39-42.

Weissmann, G., Hartley, A., Nichols, G., Scuderi, L., Olson, M., Buehler, H., Massengill, L., 2010b. Alluvial facies distributions in continental sedimentary basins—Distributive fluvial systems. *Rivers to Rock Record: The Society for Sedimentary Geology Special Publication* 97, 327-355.

Weissmann, G., Hartley, A., Scuderi, L., Nichols, G., Davidson, S., Owen, A., Atchley, S., Bhattacharyya, P., Chakraborty, T., Ghosh, P., 2013. Prograding distributive fluvial systems—geomorphic models and ancient examples, in: Driese, S.G., Nordt, L.C., McCarthy, P.J. (Eds.), *New Frontiers in Paleopedology and Terrestrial Paleoclimatology, Paleosols and Soil Surface Analog Systems*, . *SEPM Special Publication*, pp. 131-147.

Wellner, R., Beaubouef, R., Van Wagoner, J., Roberts, H., Sun, T., 2005. Jet-plume depositional bodies—the primary building blocks of Wax Lake delta. *Gulf Coast Association Geological Society Transcripts* 55, 867-909.

Wescott, W.A., 1993. Geomorphic thresholds and complex response of fluvial systems--some implications for sequence stratigraphy. *AAPG Bulletin* 77, 1208-1218.

Thomas, L., 1992. *A handbook on practical coal geology*. Wiley.338 p.

Williams, L., 2015. Sedimentology of the Lower Cretaceous reservoirs of the Sea Lion Field, North Falkland Basin. *Petroleum Geoscience* 21, 183-198.

Williams, G.P., 1986. River meanders and channel size. *Journal of Hydrology* 88, 147-164.

Willis, A.J., Moslow, T.F., 1994. Stratigraphic setting of transgressive barrier-island reservoirs with an example from the Triassic Halfway Formation, Wembley Field, Alberta, Canada. *AAPG Bulletin* 78, 775-791.

Willis, A., 2000. Tectonic control of nested sequence architecture in the Segó Sandstone, Neslen Formation and upper Castlegate Sandstone (Upper Cretaceous), Sevier foreland basin, Utah, USA. *Sedimentary Geology* 136, 277-317.

Willis, B.J., 1989. Palaeochannel reconstructions from point bar deposits: a three-dimensional perspective. *Sedimentology* 36, 757-766.

Willis, B.J., Gabel, S., 2001. Sharp-based, tide-dominated deltas of the Segó Sandstone, Book Cliffs, Utah, USA. *Sedimentology* 48, 479-506.

Willis, B.J., Gabel, S.L., 2003. Formation of Deep Incisions into Tide-Dominated River Deltas: Implications for the Stratigraphy of the Sego Sandstone, Book Cliffs, Utah, U.S.A. *Journal of Sedimentary Research* 73, 246-263.

Willis, B.J., Tang, H., 2010. Three-dimensional connectivity of point-bar deposits. *Journal of Sedimentary Research* 80, 440-454.

Wright, P. V., Marriott, S.B., 1993. The sequence stratigraphy of fluvial depositional systems: the role of floodplain sediment storage. *Sedimentary Geology* 86, 203-210.

Wu, C., Bhattacharya, J.P., Ullah, M.S., 2015. Paleohydrology and 3D Facies Architecture of Ancient Point Bars, Ferron Sandstone, Notom Delta, South-Central Utah, USA. *Journal of Sedimentary Research* 85, 399-418.

Yan, N., Mountney, N.P., 2016. A forward stratigraphic model of fluvial meander-bend evolution for prediction of point-bar lithofacies architecture. *Computers & Geosciences* in review.

Yingling, V.L., Heller, P., 1992. Timing and record of foreland sedimentation during the initiation of the Sevier orogenic belt in central Utah. *Basin Research* 4, 279-290.

Yoshida, S., 2000. Sequence and facies architecture of the upper Blackhawk Formation and the Lower Castlegate Sandstone (Upper Cretaceous), Book Cliffs, Utah, USA. *Sedimentary Geology* 136, 239-276.

Yoshida, S., Johnson, H.D., Pye, K., Dixon, R.J., 2004. Transgressive changes from tidal estuarine to marine embayment depositional systems: The Lower Cretaceous Woburn Sands of southern England and comparison with Holocene analogs. *AAPG Bulletin* 88, 1433-1460.

Yoshida, S., Steel, R.J., Dalrymple, R.W., 2007. Changes in depositional processes—an ingredient in a new generation of sequence-stratigraphic models. *Journal of Sedimentary Research* 77, 447-460.

Yoshida, S., Willis, A., Miall, A.D., 1996. Tectonic control of nested sequence architecture in the Castlegate Sandstone (Upper Cretaceous), Book Cliffs, Utah. *Journal of Sedimentary Research* 66, 737-748.

Young, R.G., 1955. Sedimentary facies and intertonguing in the Upper Cretaceous of the Book Cliffs, Utah- Colorado. *Geological Society of America Bulletin* 66, 177-202.

Young, R.G., 1957. Late Cretaceous cyclic deposits, Book Cliffs, Eastern Utah. *Bulletin of the American Association of Petroleum Geologists* 41, 1790-1774.

Zapp, A., Cobban, W., 1960. Some Late Cretaceous strand lines in northwestern Colorado and northeastern Utah. *US Geological Survey Professional Paper* 400, B246-B249.

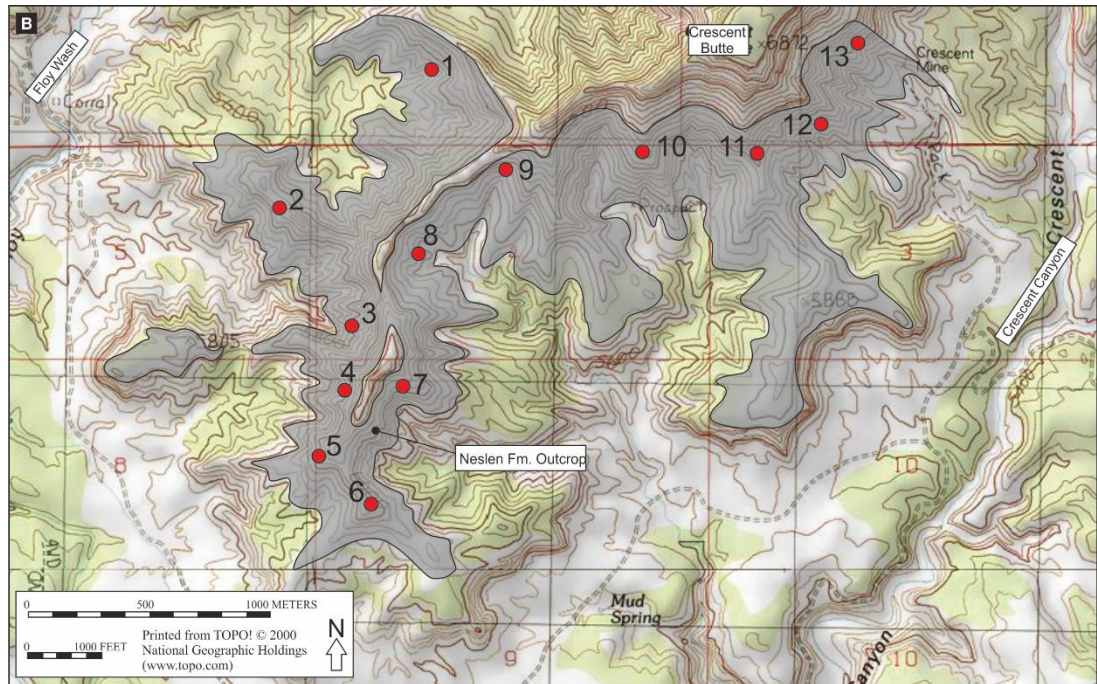
APPENDIX A

A.1: Log co-ordinates

Log locations for logs through at least the lower half of the Neslen Formation around Crescent Butte (Chapter 4; Fig. 4.3), Log locations for smaller logs are displayed on stratigraphic panels (Appendix C).





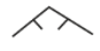



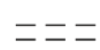
















Season Number	Original Log Name	New Log Name	Lower GPS		Upper GPS		Length m
			N 39	W 109	N 39	W 109	
1	1	13					118
			00.87	48.55			
1	2	12	2	6			47
			00.83	46.67			
1	3	8	9	4			42
1	4	6					43
			00.88	46.33	01.01		
1	6	4	9	2	3	46.098	89
			00.84	48.93	00.95		
2	2.1	10	3	3	6	48.951	75
			00.67	49.60			
2	3.1	9	5	4			89
			00.23	49.85	00.29		
2	4.1	7	0	9	0	49.854	37
			00.06	49.95			
2	10.1	5	4	8			54.5
2	10.2	3					53
			00.69	48.64			
2	11.1	11	0	9			86
2	12.1	2					59
			01.00	49.69			
2/3	P8	1	2	2			64

A.2: Map of log locations



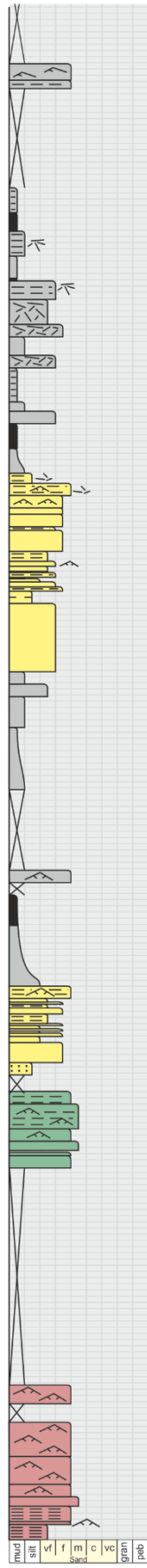
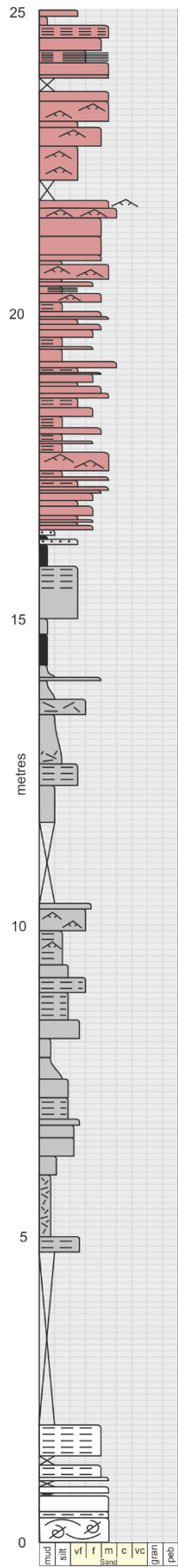
APPENDIX B: LOGS AROUND CRESCENT BUTTE

B.1: Key for logged sections

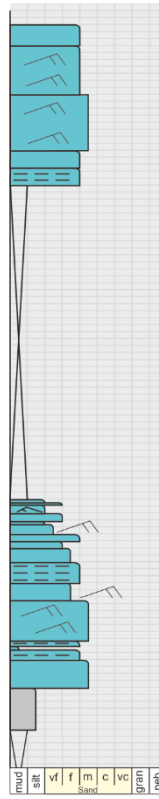
	Planar cross-bedded sandstone		Bioturbation (undifferentiated)
	Trough cross-bedded sandstone	Te	<i>Teredolites</i>
	Convolute lamination	Th	<i>Thalassinoides</i>
	Symmetrical ripple-laminated sandstone (grey if draped)		<i>Ophiomorpha</i>
	Asymmetrical ripple-laminated sandstone (grey if draped)		<i>Arenicolites</i>
	Horizontal lamination		<i>Rhizocorallium</i>
	Wavy lamination		Root traces
	Flaser lamination		
	Intraformational clasts		
	Wood fragments		
	Amalgamated channel-fill element		Distributary channel fill
	Sandstone dominated lateral accretion deposit		Heterolithic lateral accretion deposit
	Amalgamated inclined heterolithic stratification		Reworked shoreface sandstone
	Bay-fill sandstone deposit		Overbank deposits
	Floodplain or Lagoonal fines		Coal-prone floodplain deposit

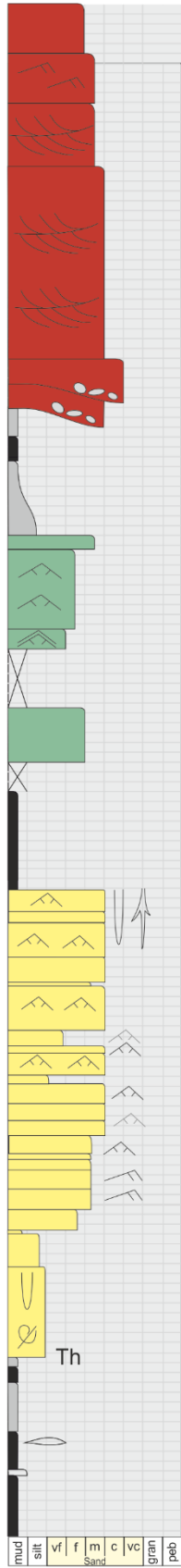
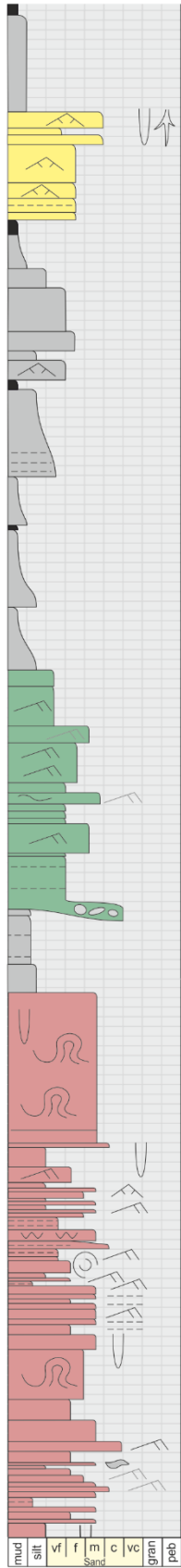
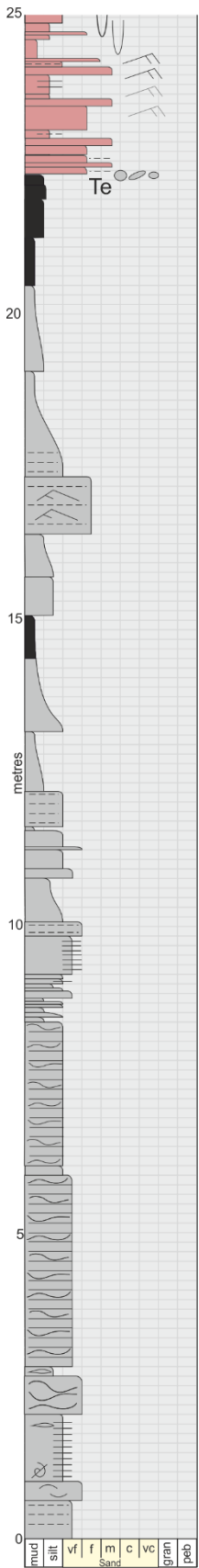
B.2: Logged sections

A selection of logs collected around Crescent Butte are presented below.



Log 2





Point-bar element 21

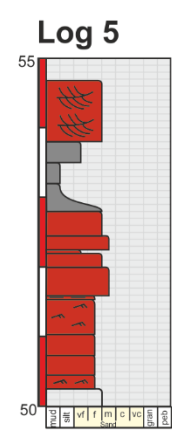
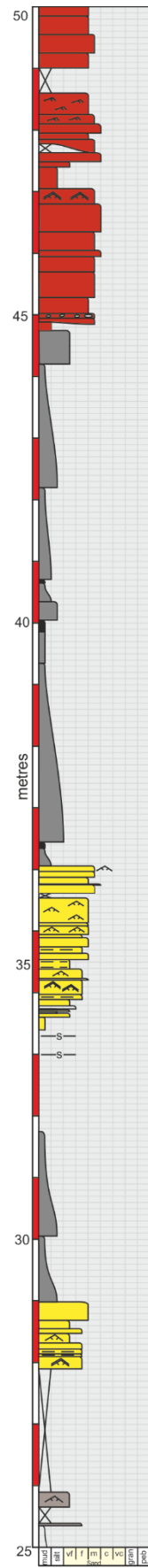
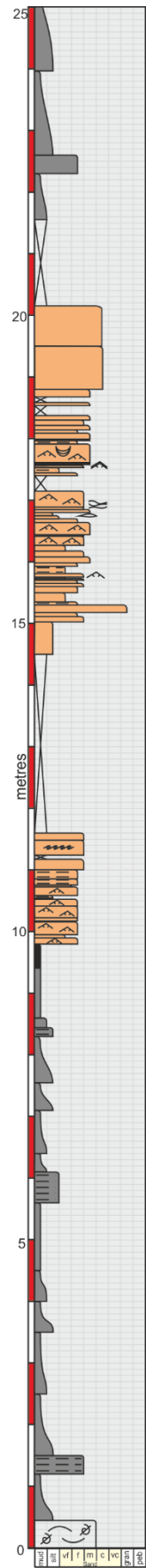


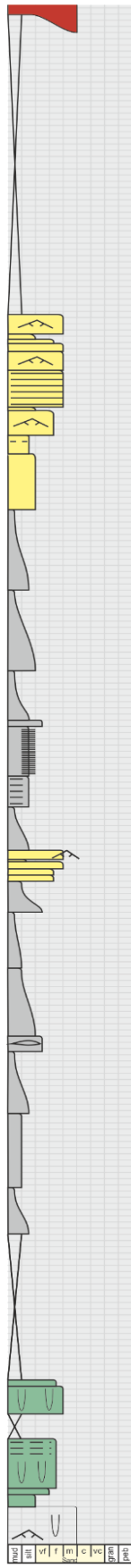
Point-bar element 28

Log 4

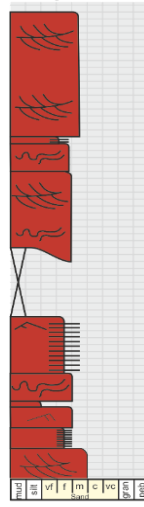


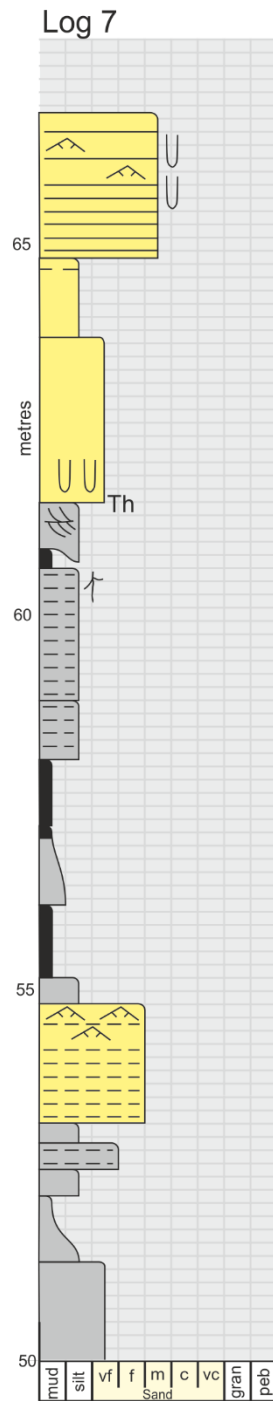
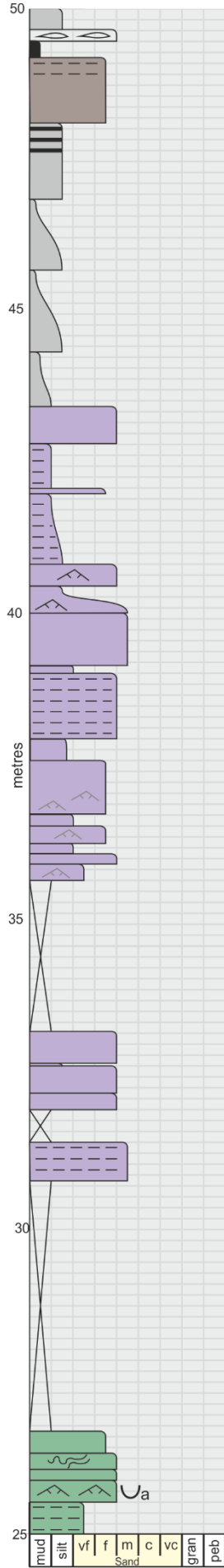
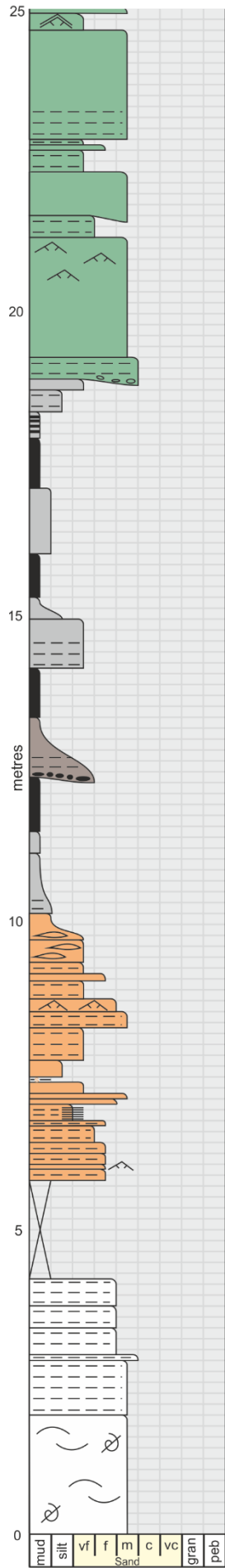
Point-bar element 36

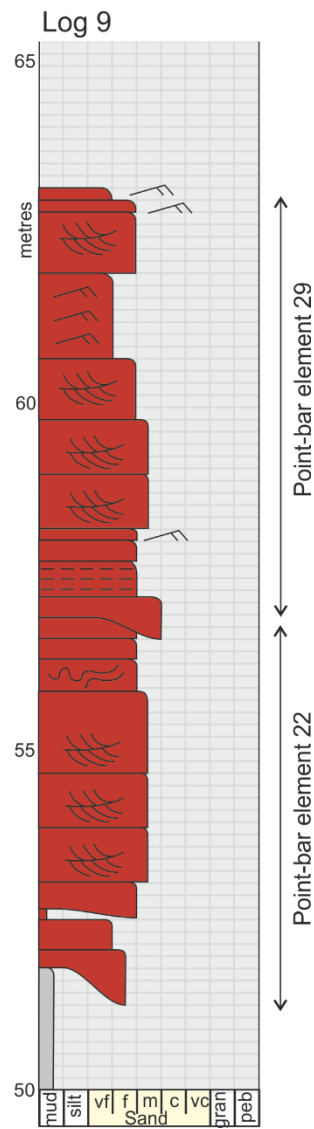
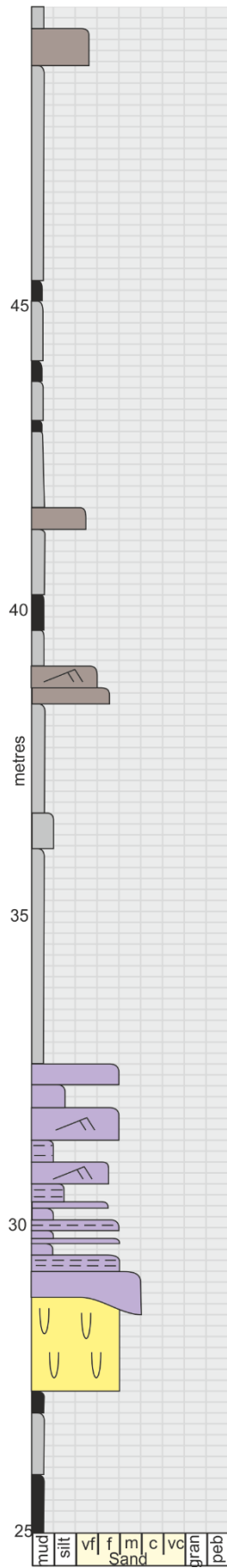
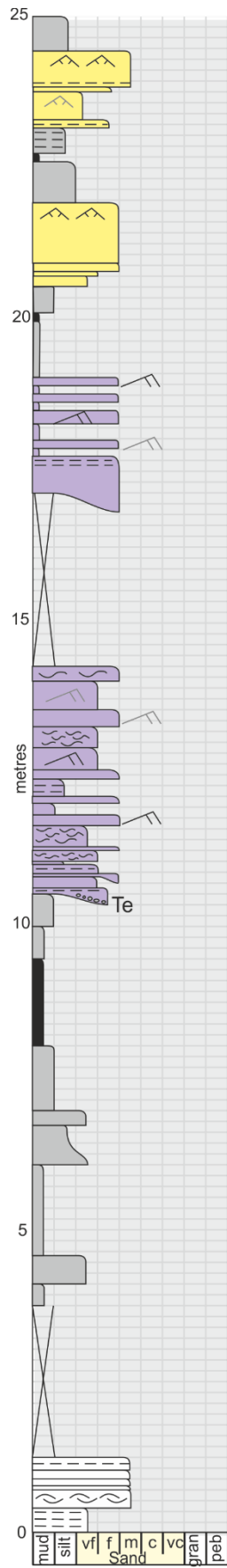


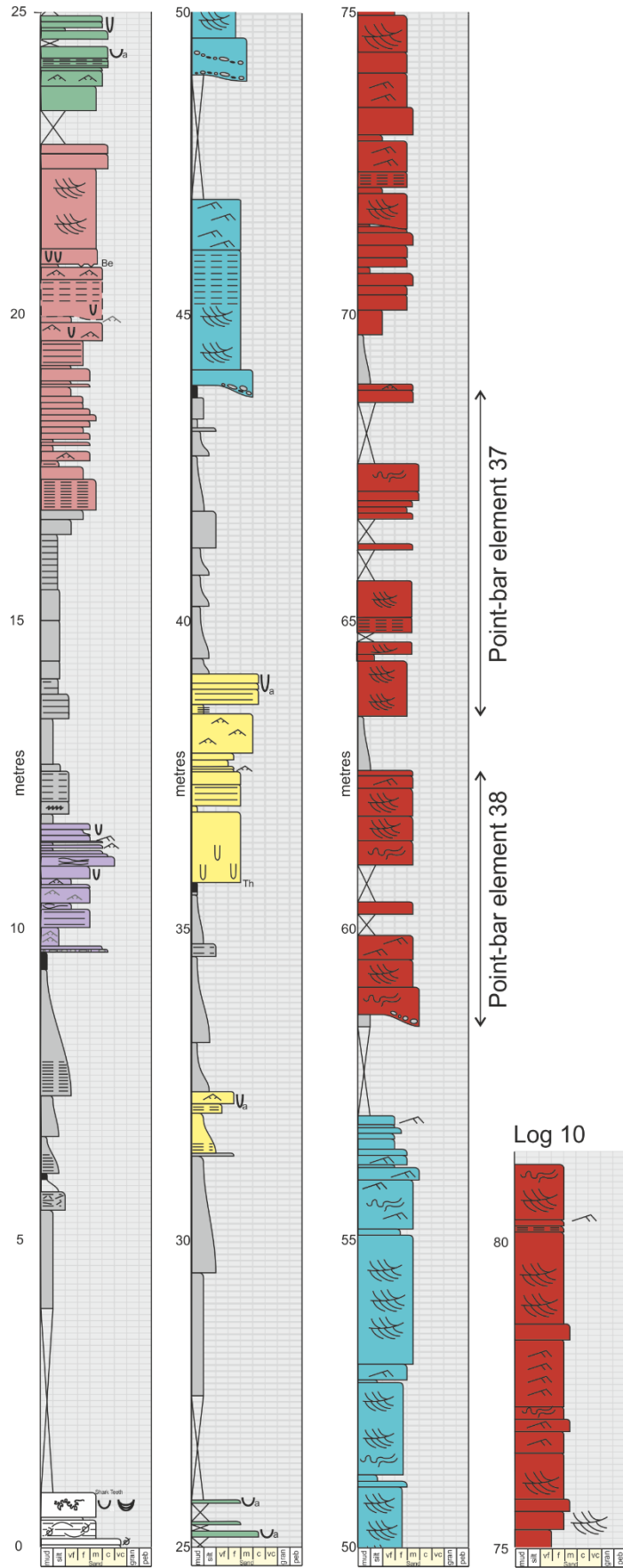


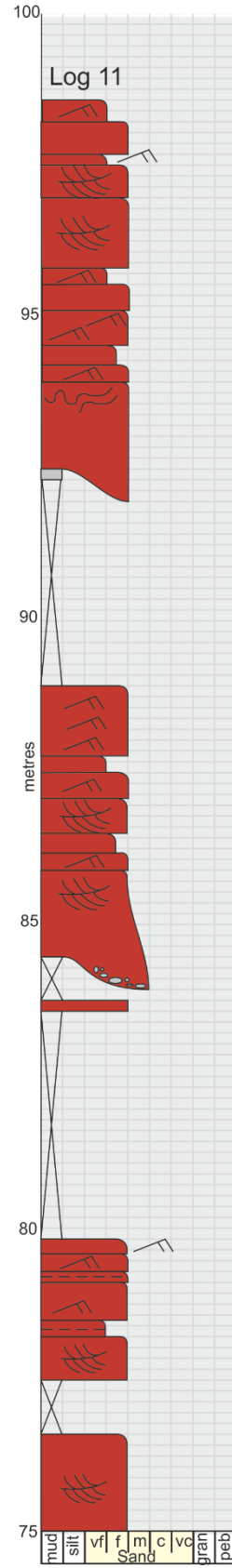
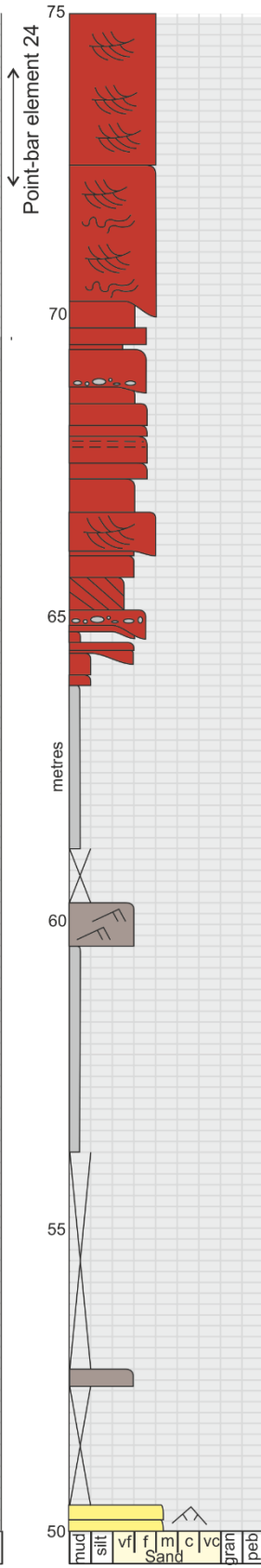
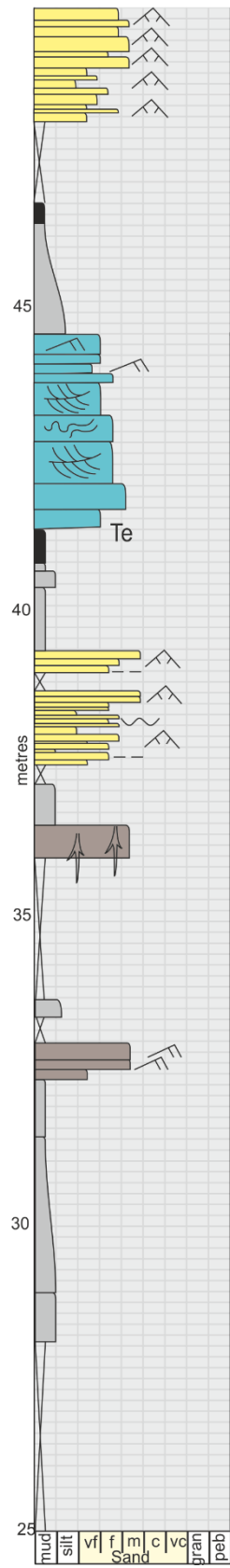
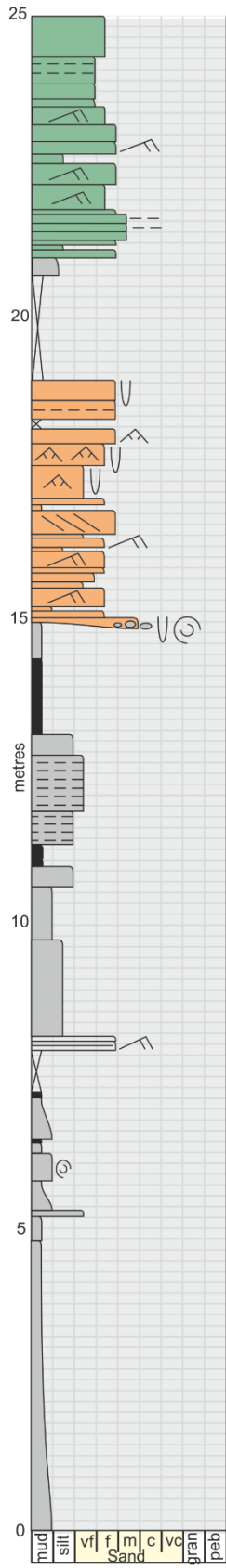
Log 6

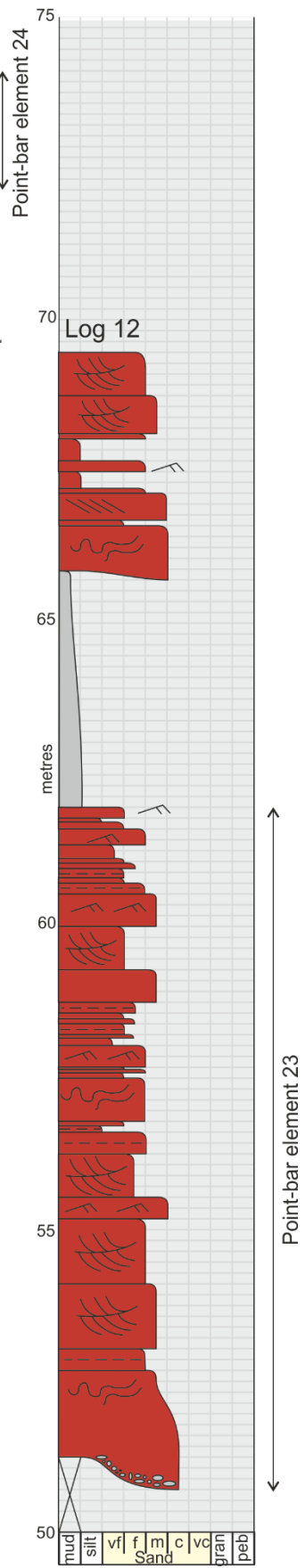
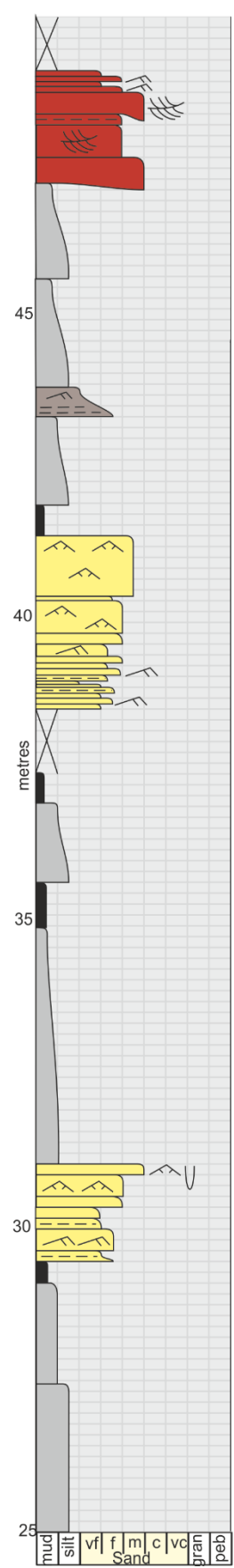
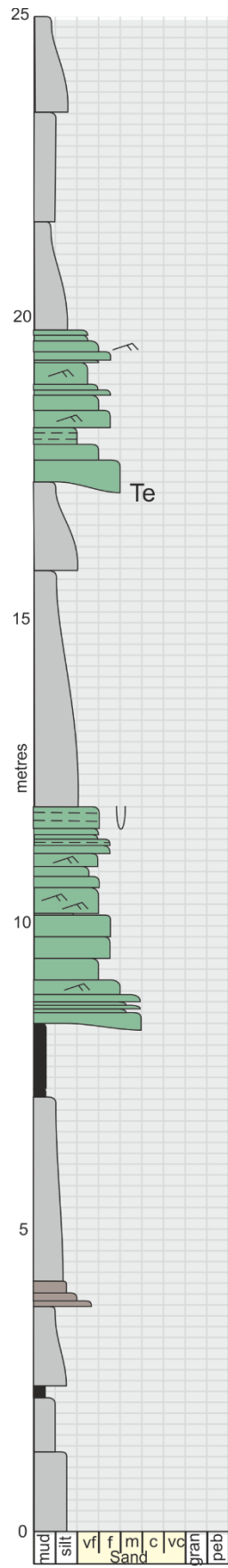


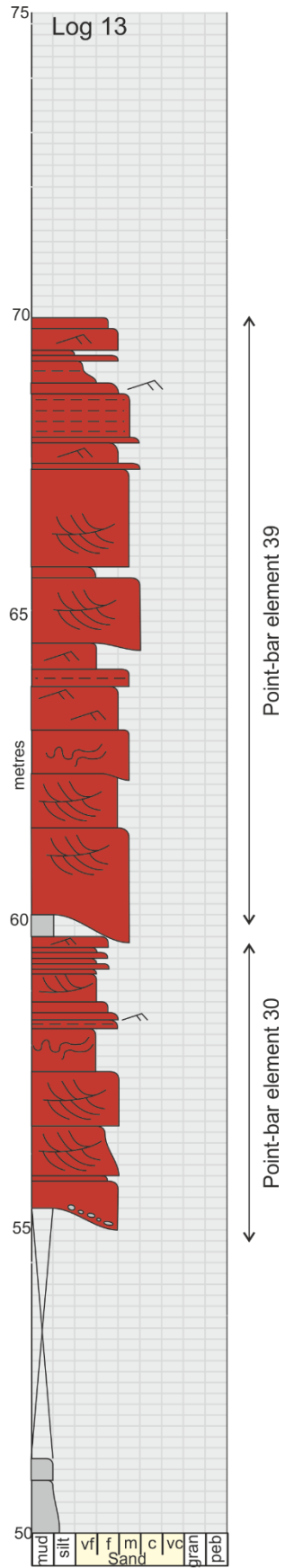
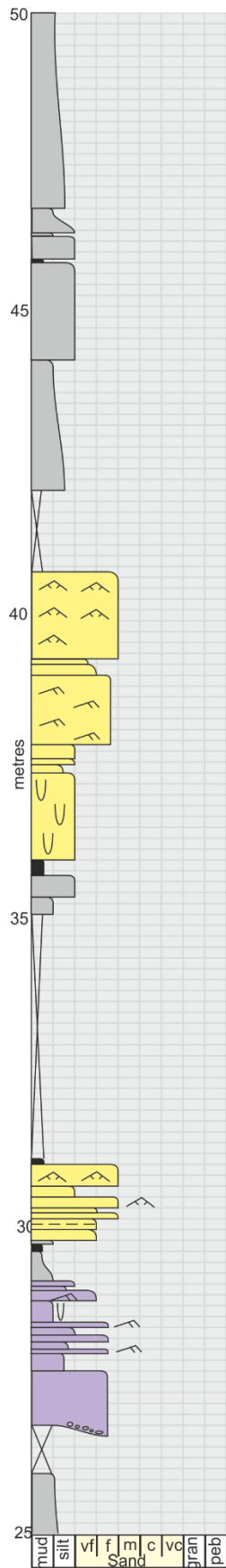
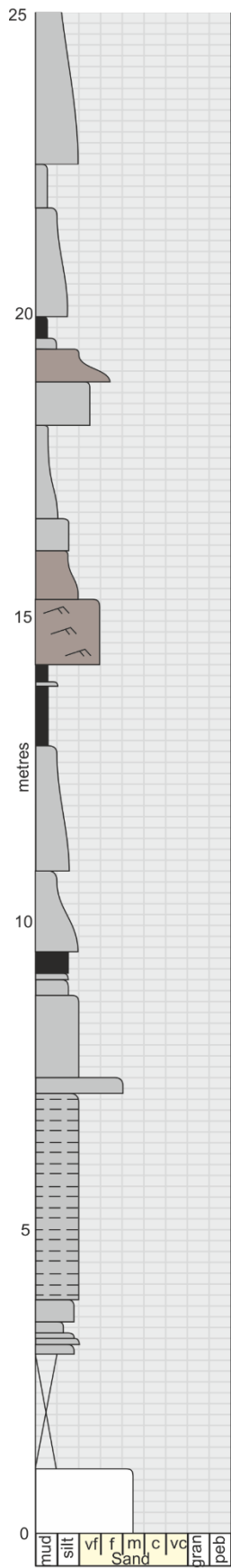






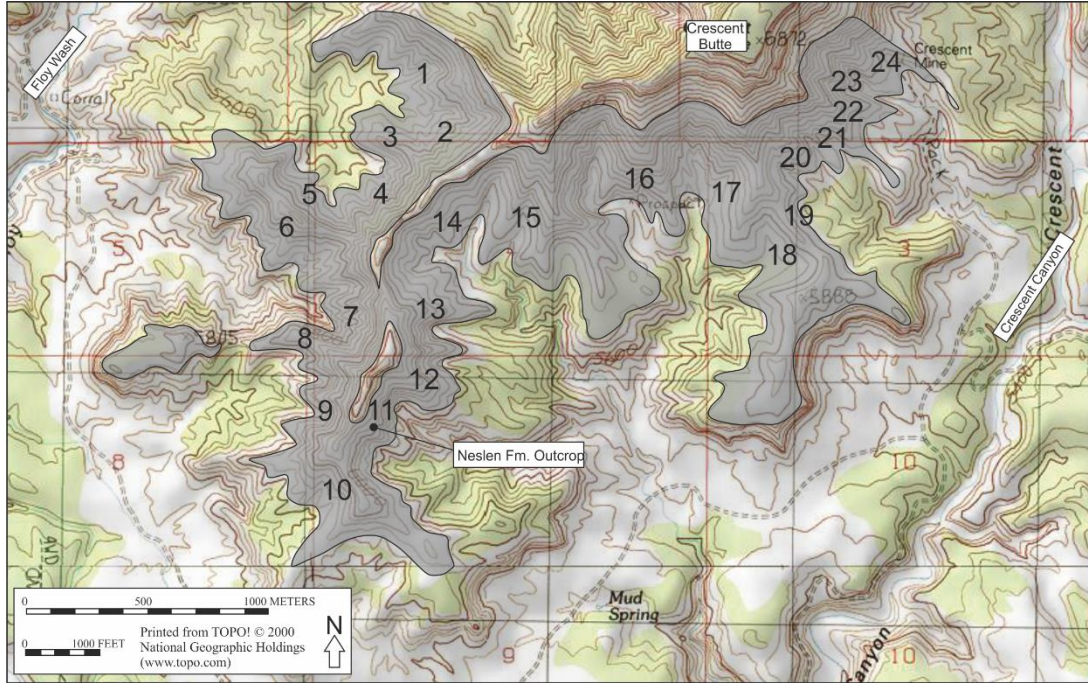






APPENDIX C

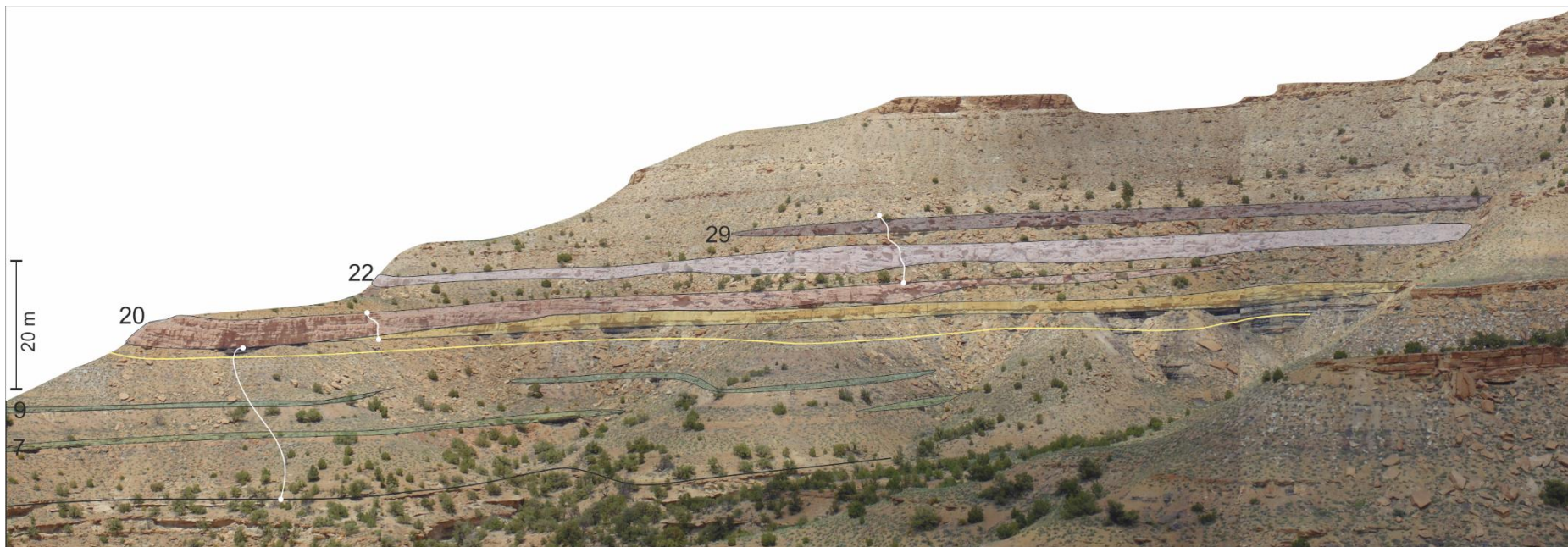
C.1: Map of panel locations



C.2: Panels around Crescent Butte

Panels (numbered above are displayed in the section below, scale bars are approximately 50 m. Numbers refer to point-bar elements in Appendix D. Logs are shown on panels where appropriate.

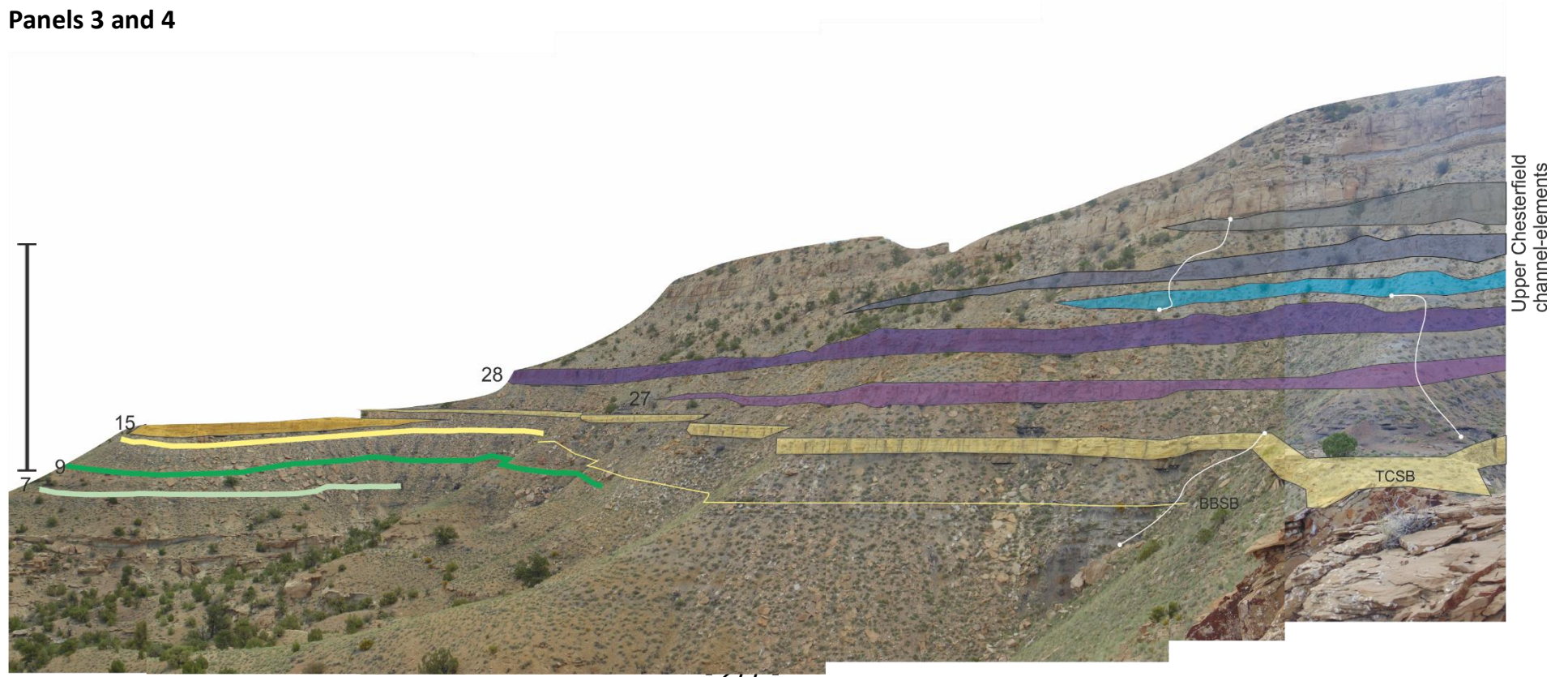
Panel 1



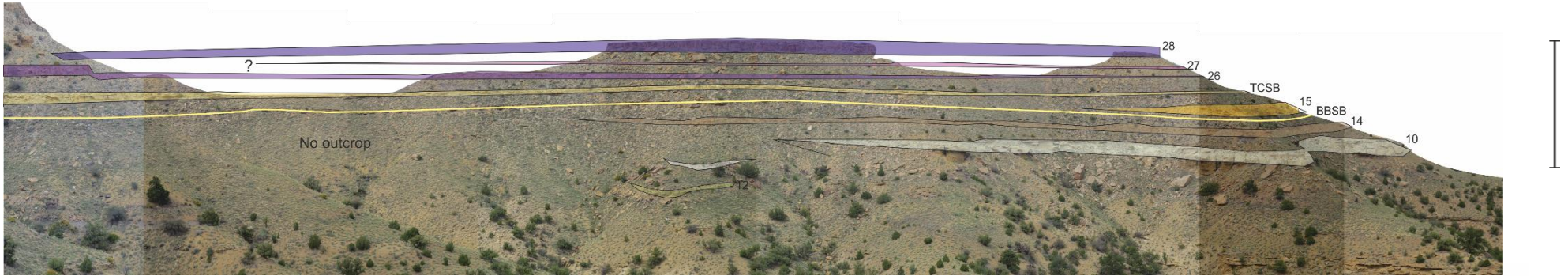
Panel 2



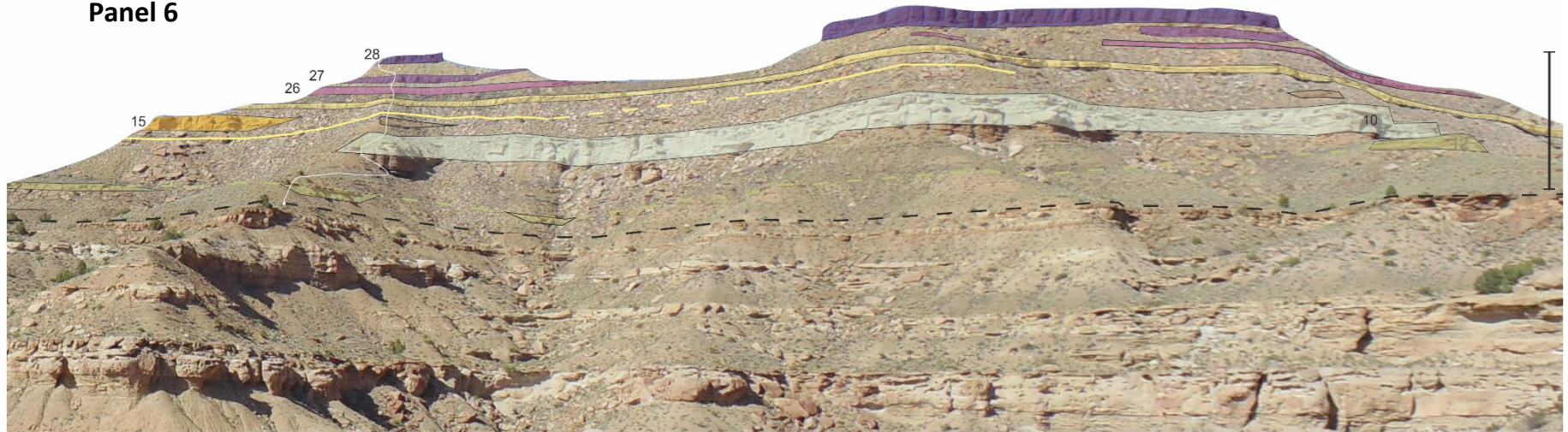
Panels 3 and 4



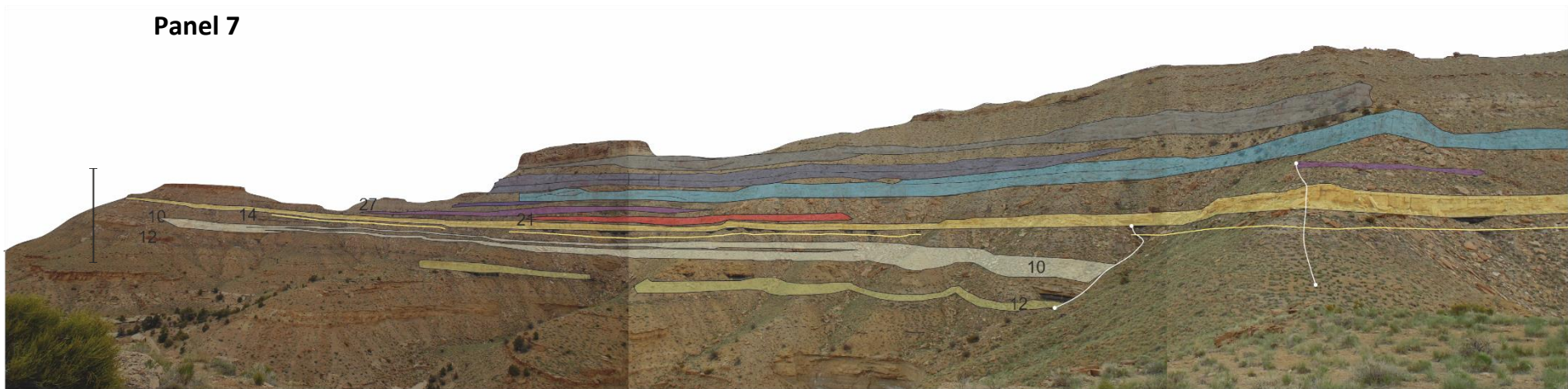
Panel 5



Panel 6



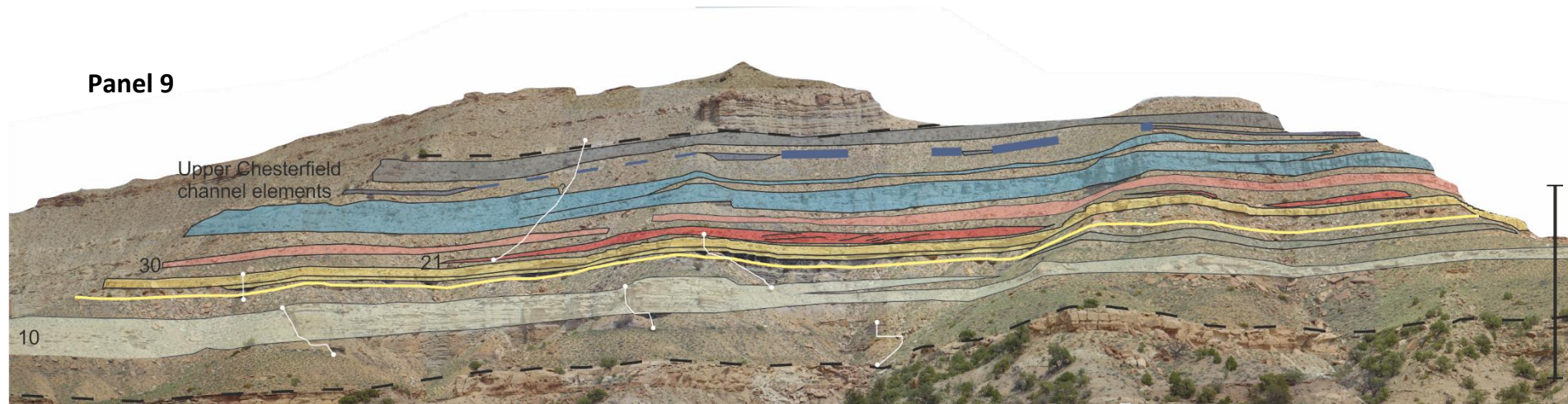
Panel 7



Panel 8



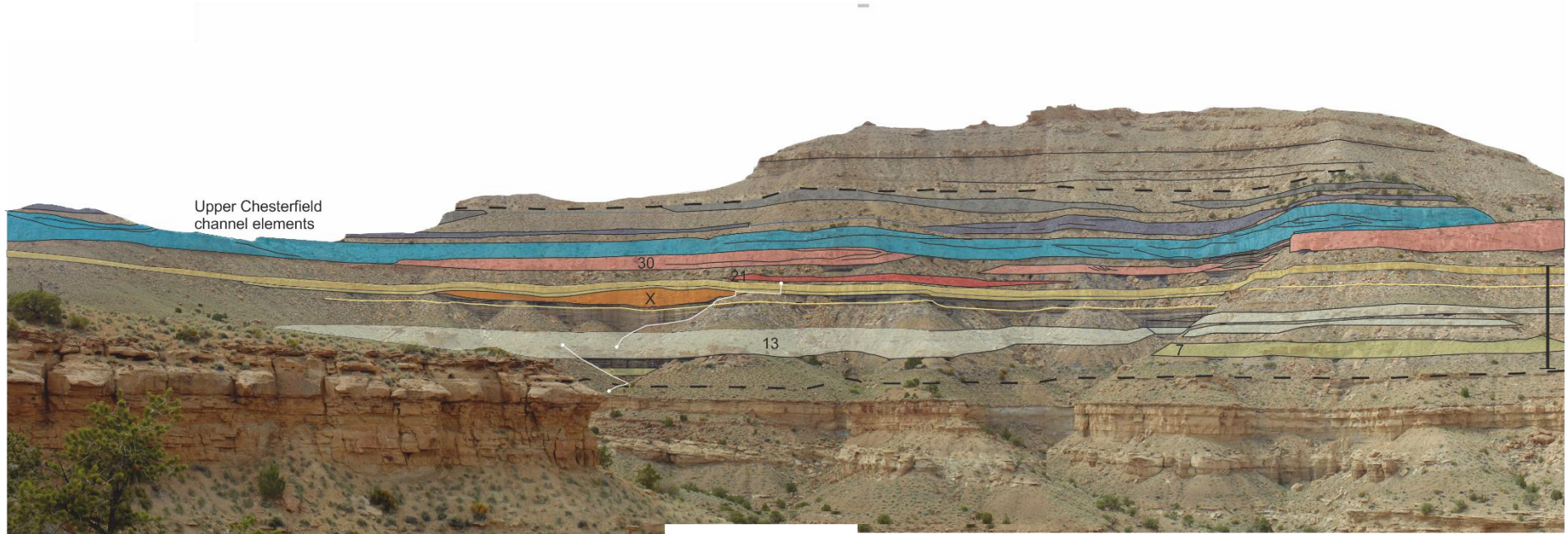
Panel 9



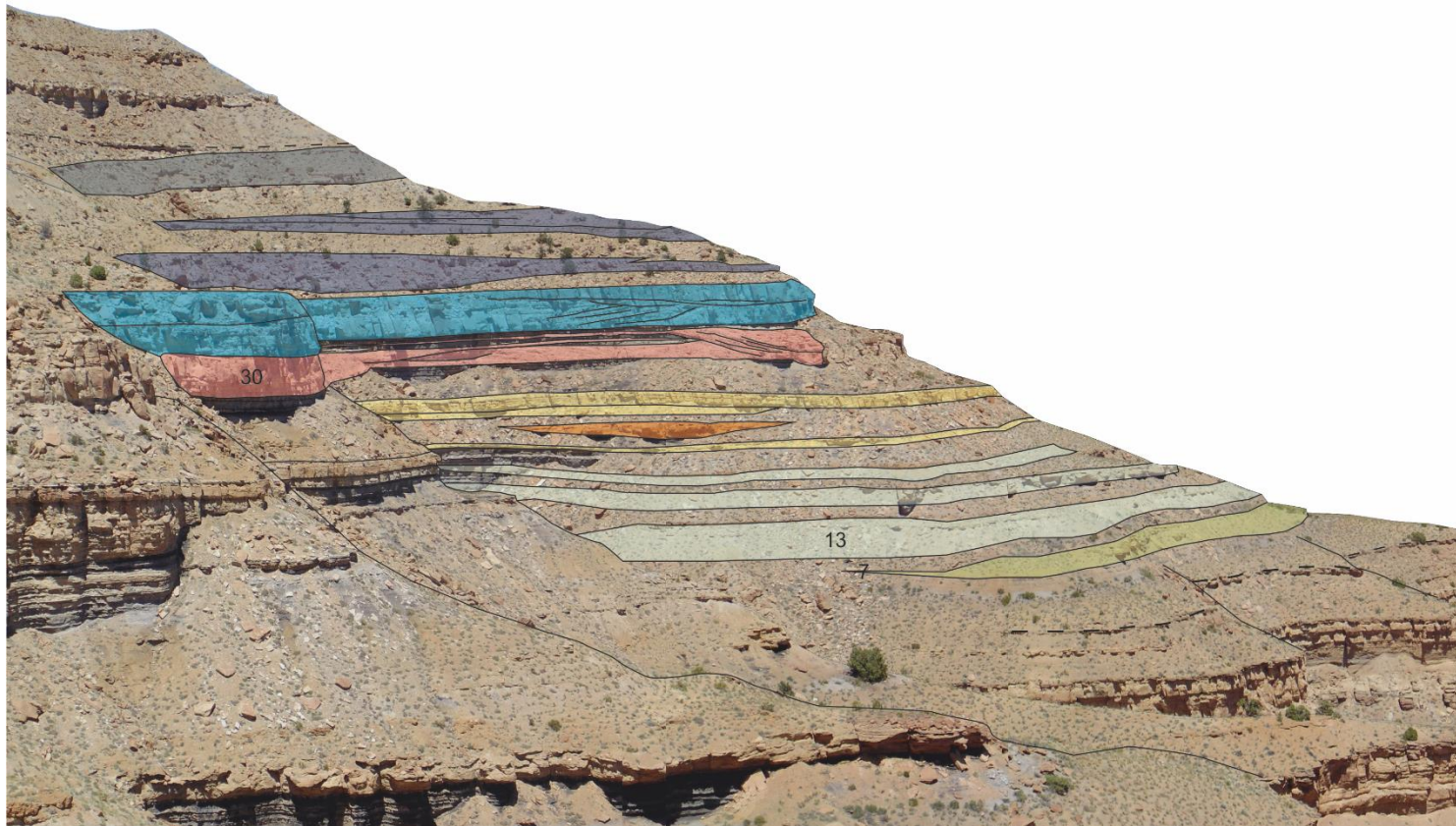
Panel 10



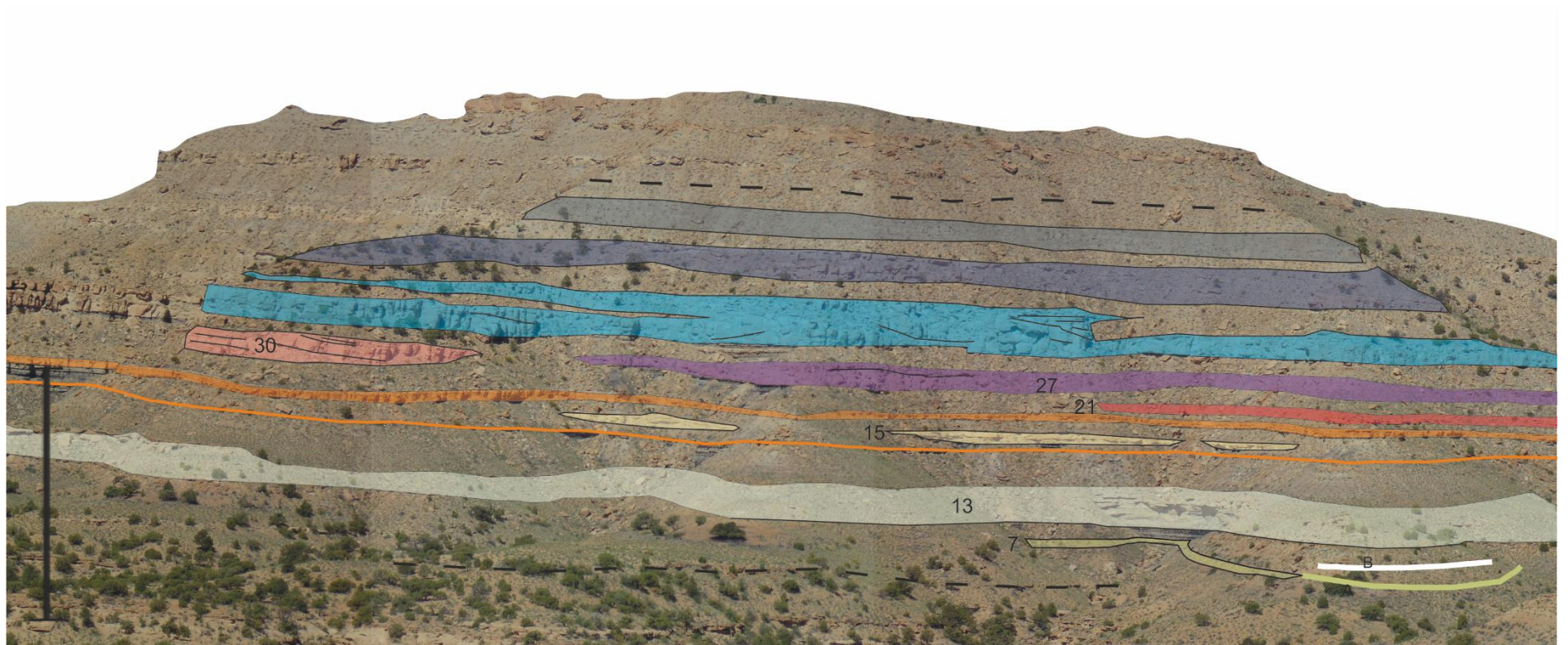
Panel 11



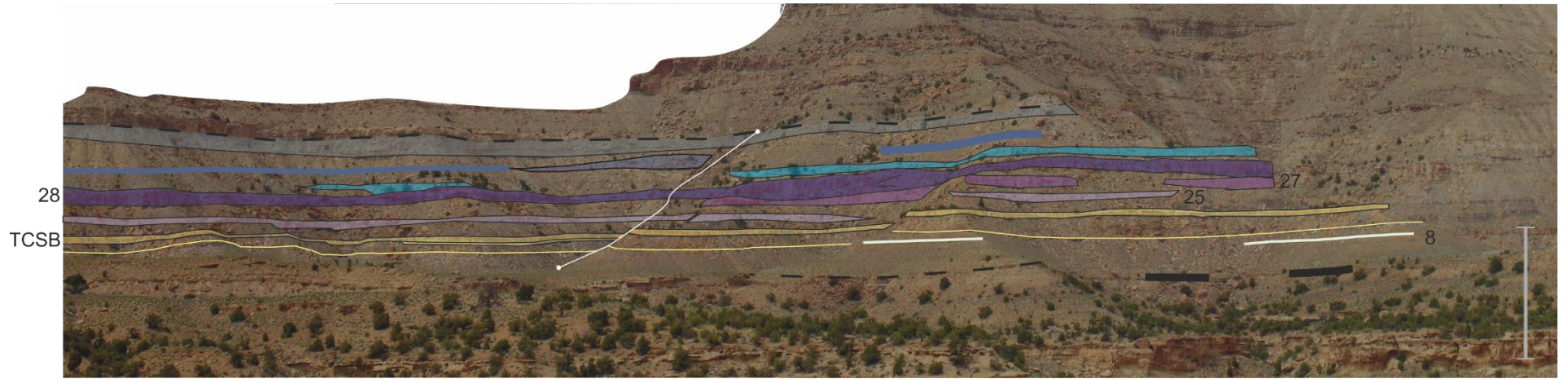
Panel 12



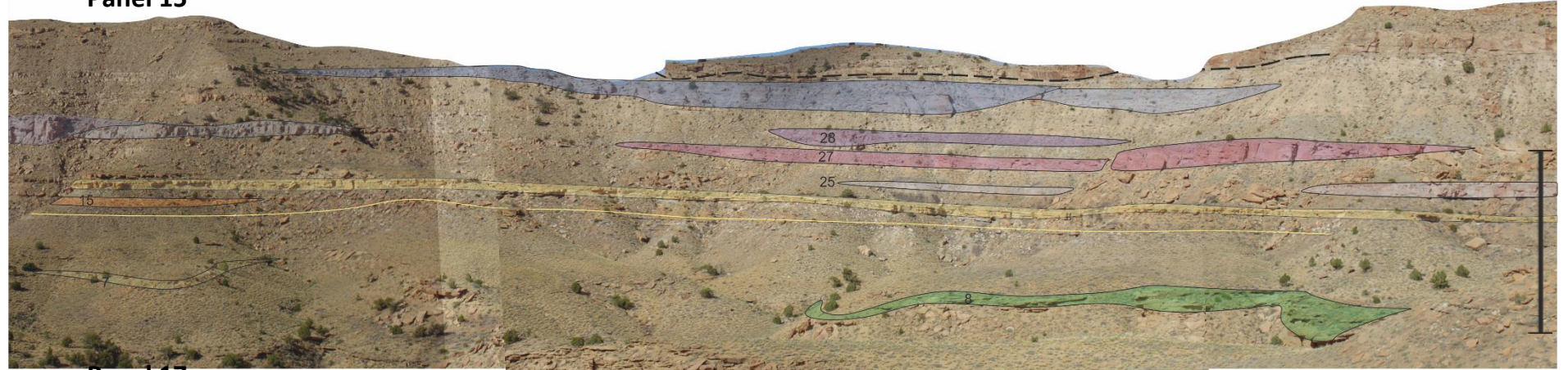
Panel 13



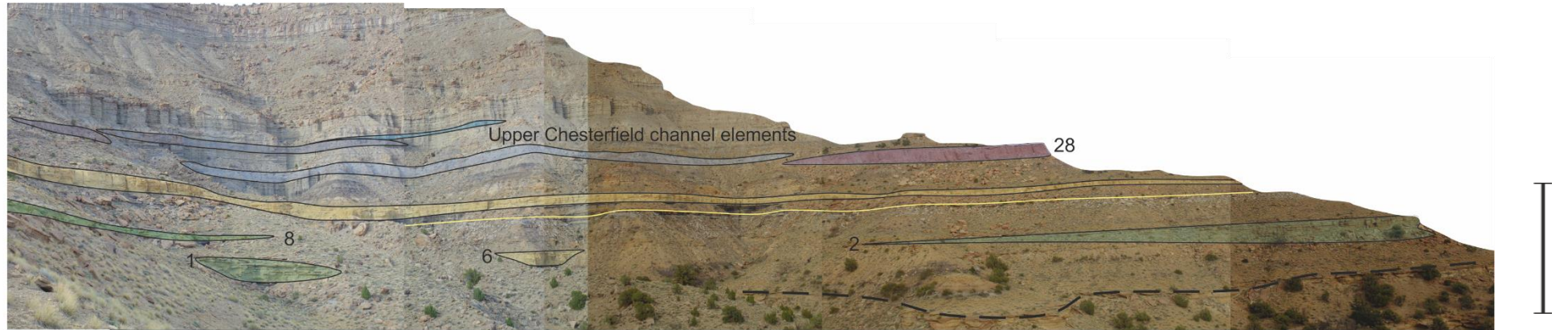
Panel 14



Panel 15



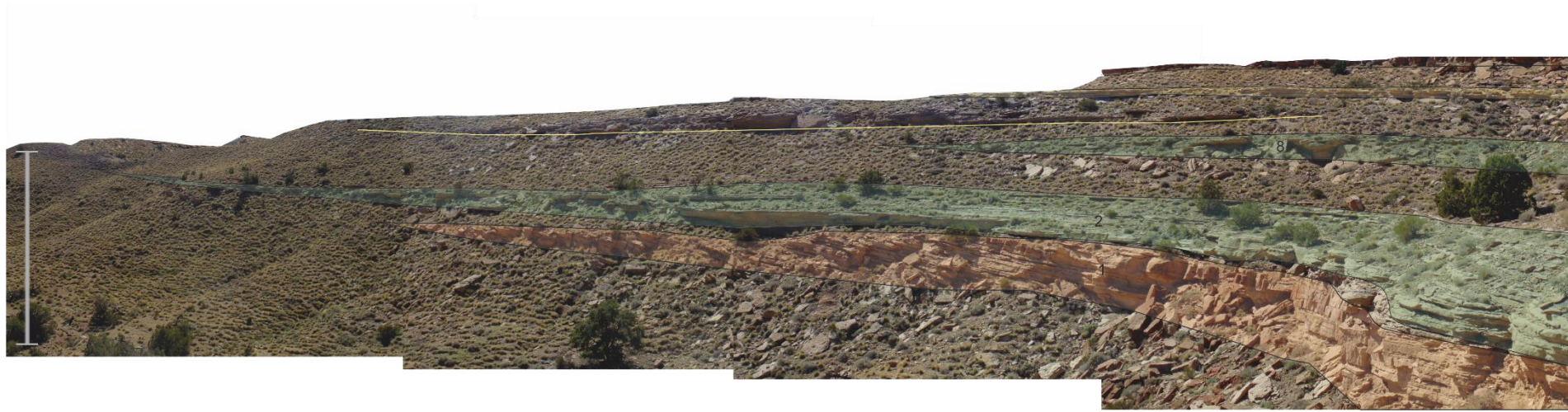
Panel 17



Panel 18



Panel 19



Panel 20 and 21



Panel 22

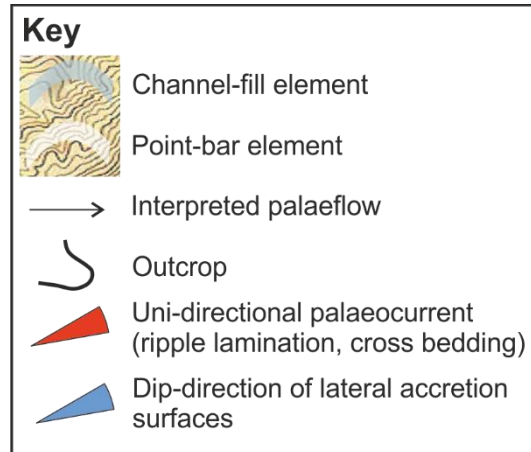


Panel 24

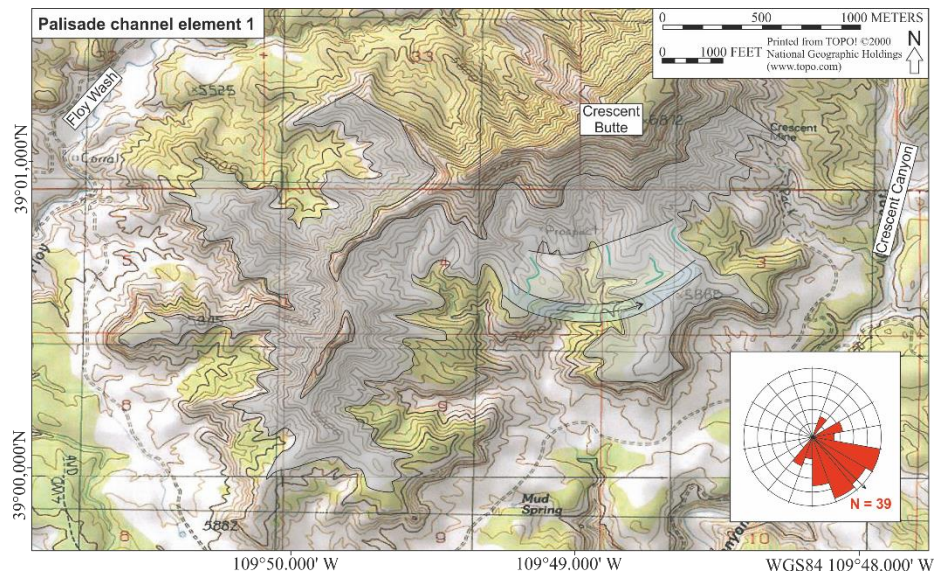


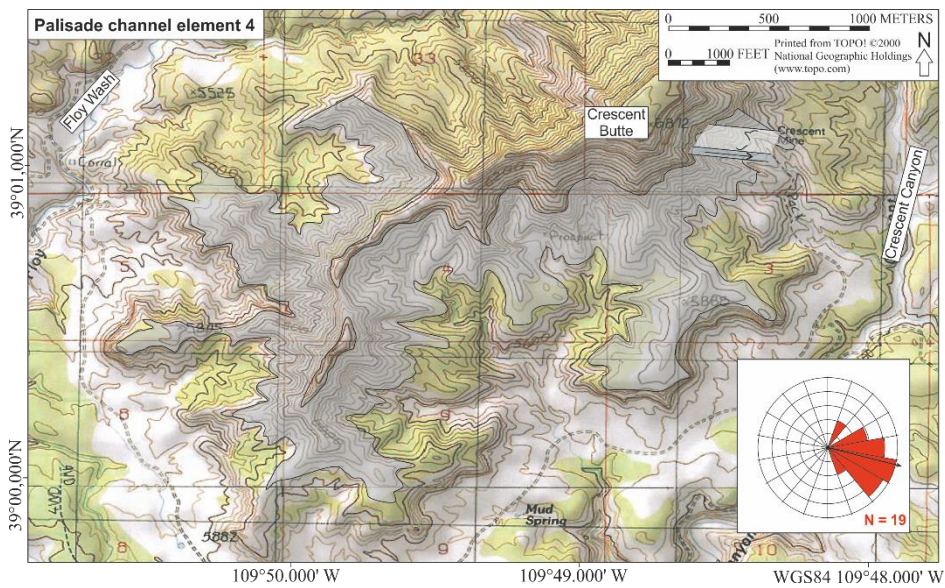
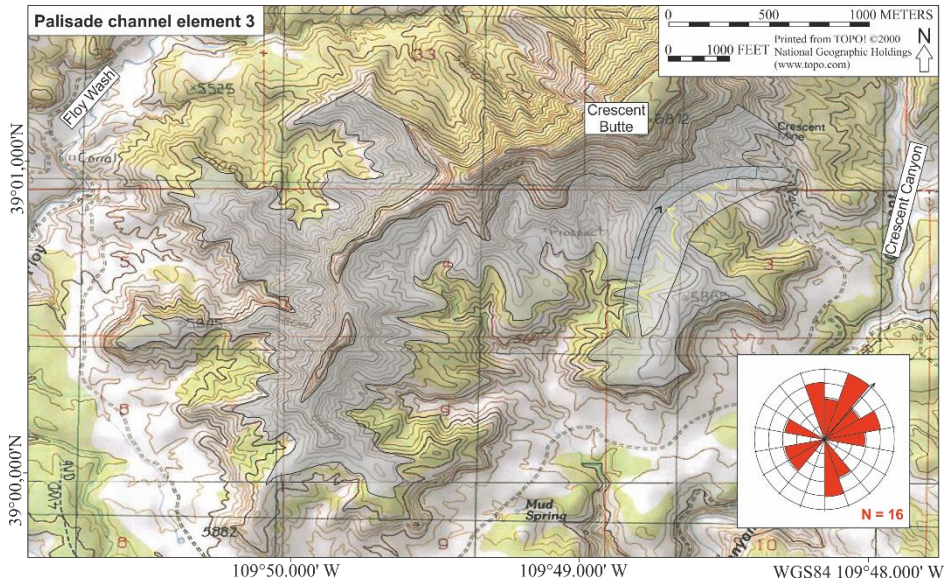
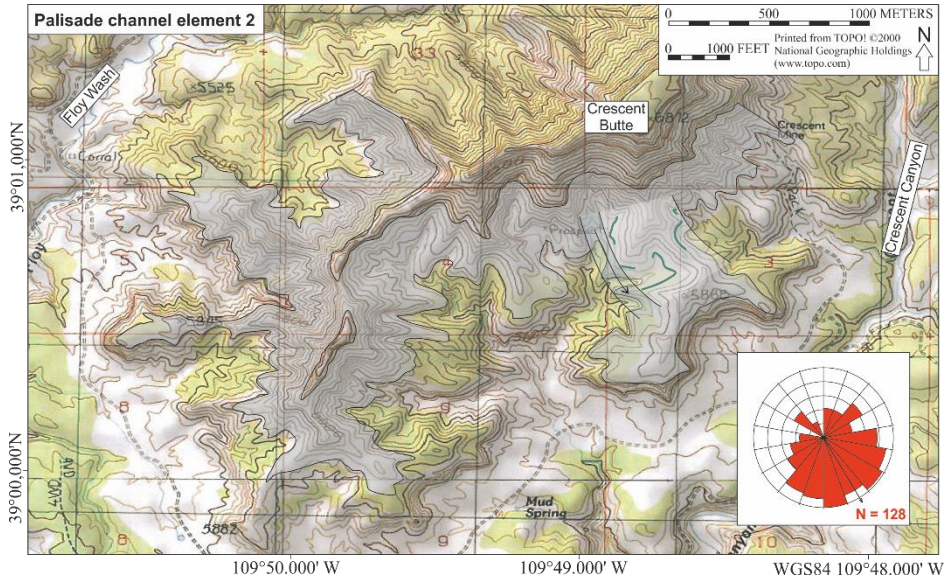
Appendix D

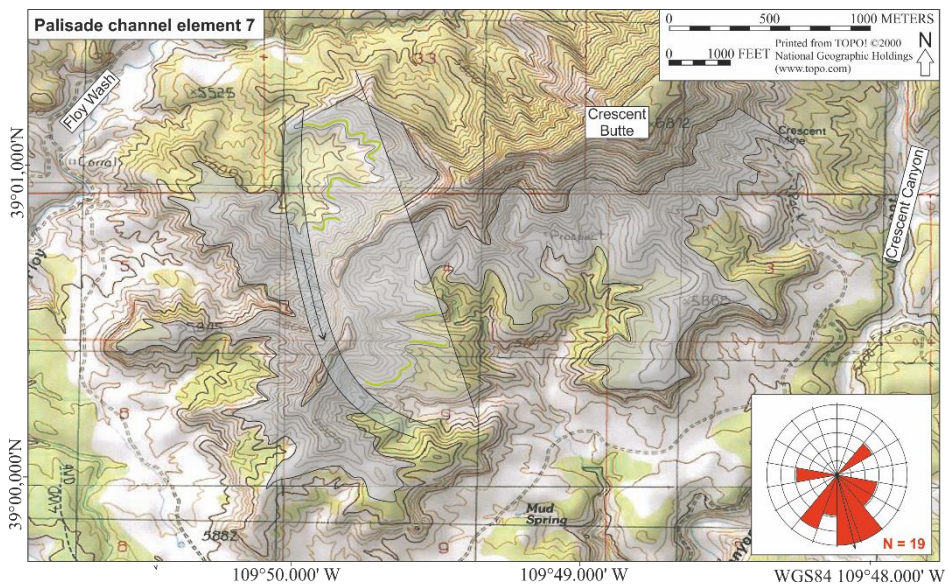
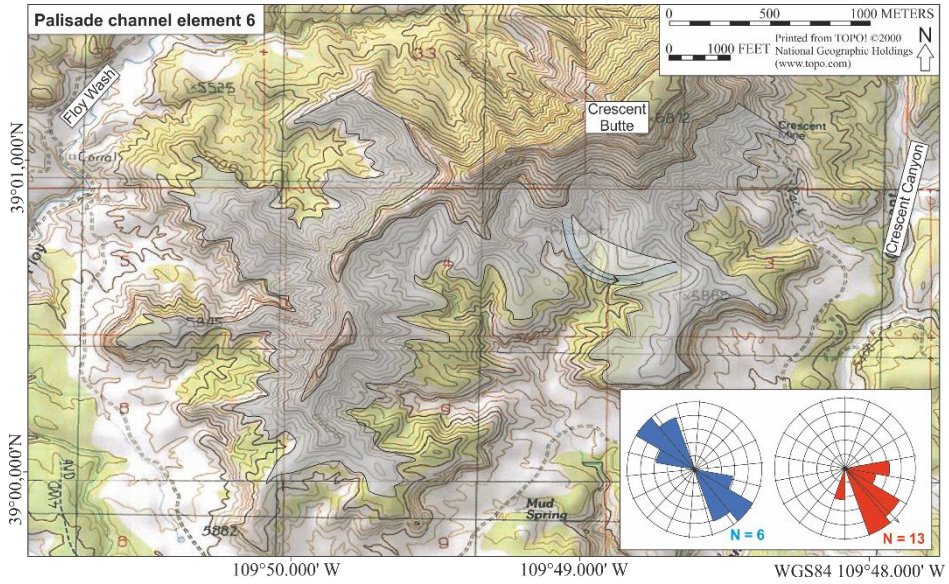
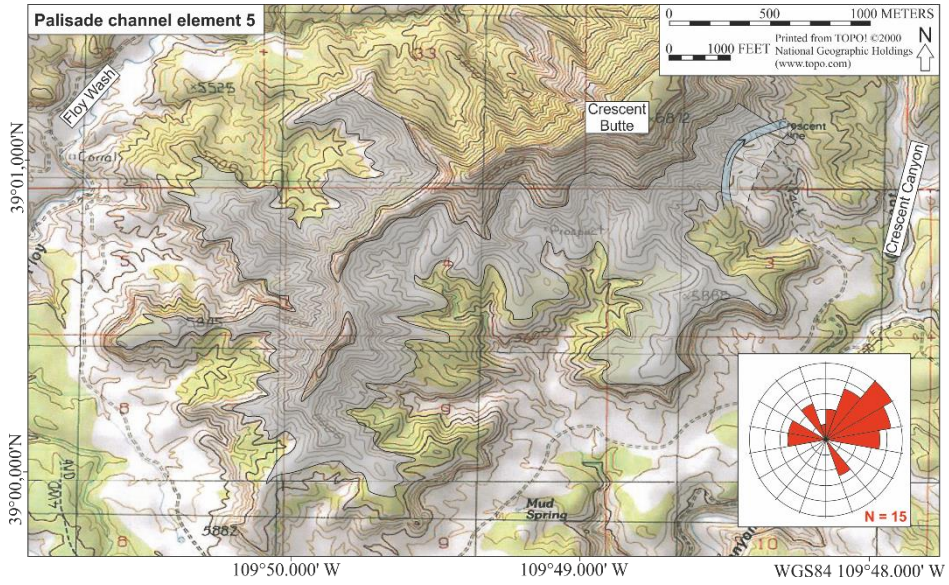
Maps for each channel in the Palisade, Ballard and lower Chesterfield zones analysed in Chapter 4 are presented. It was not possible to map individual channel-bodies for the upper Chesterfield Zone around the study area because they are frequently amalgamated and eroded by successive channel bodies.

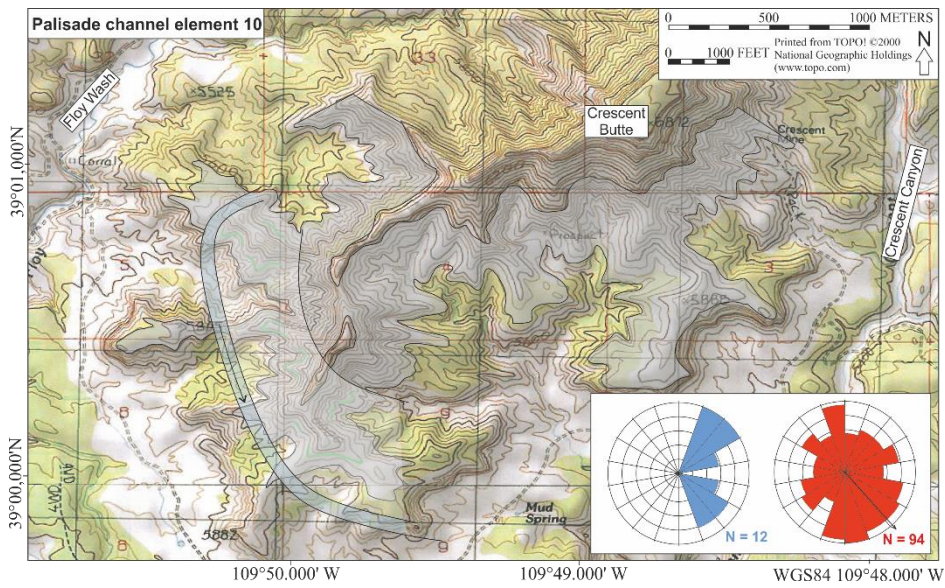
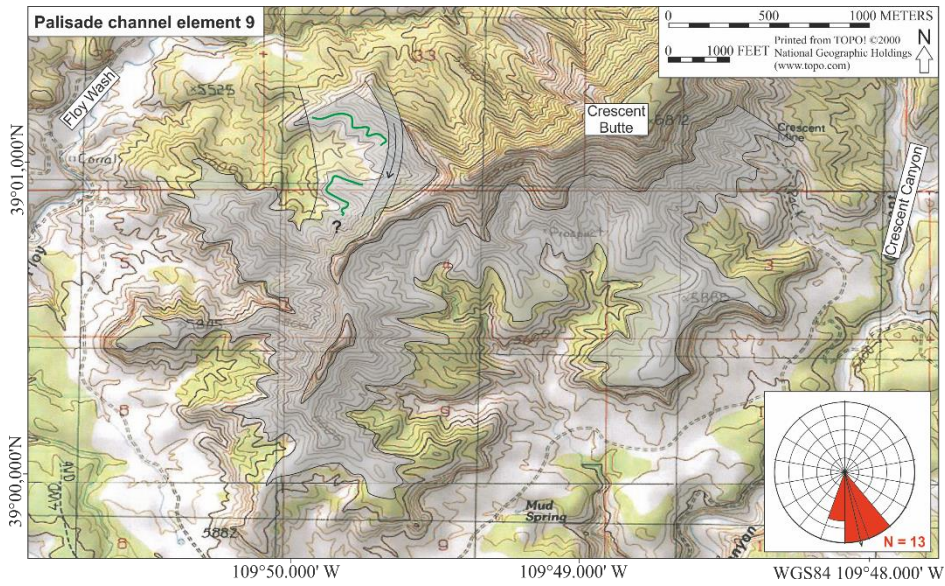
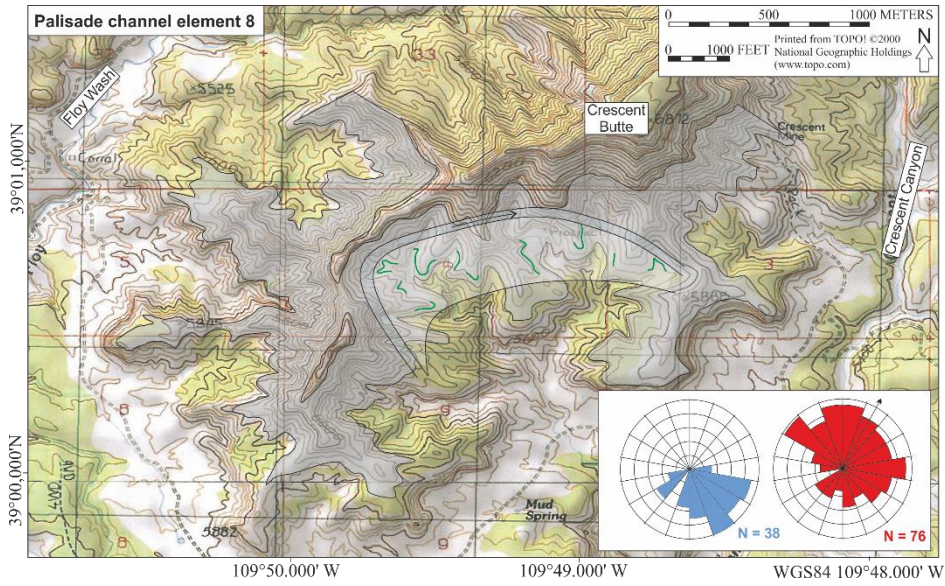


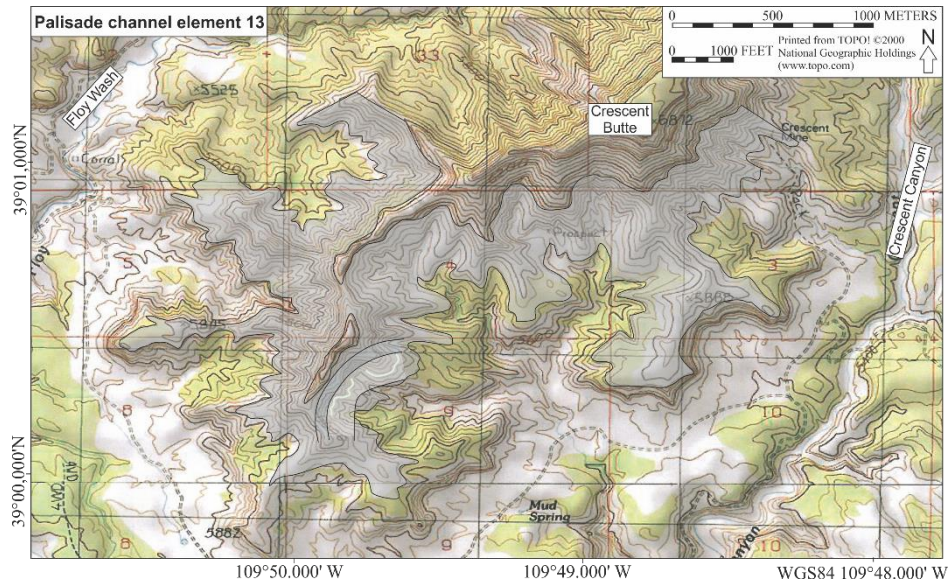
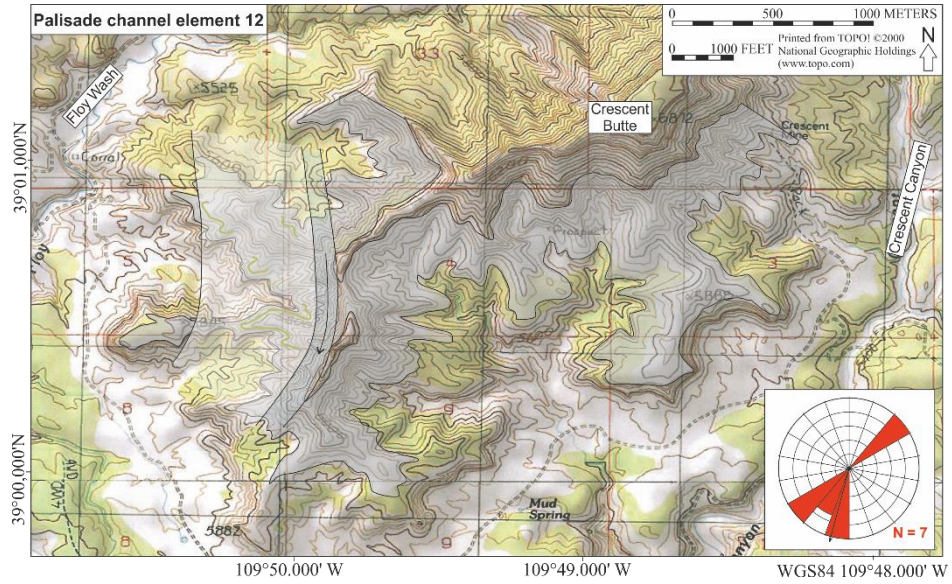
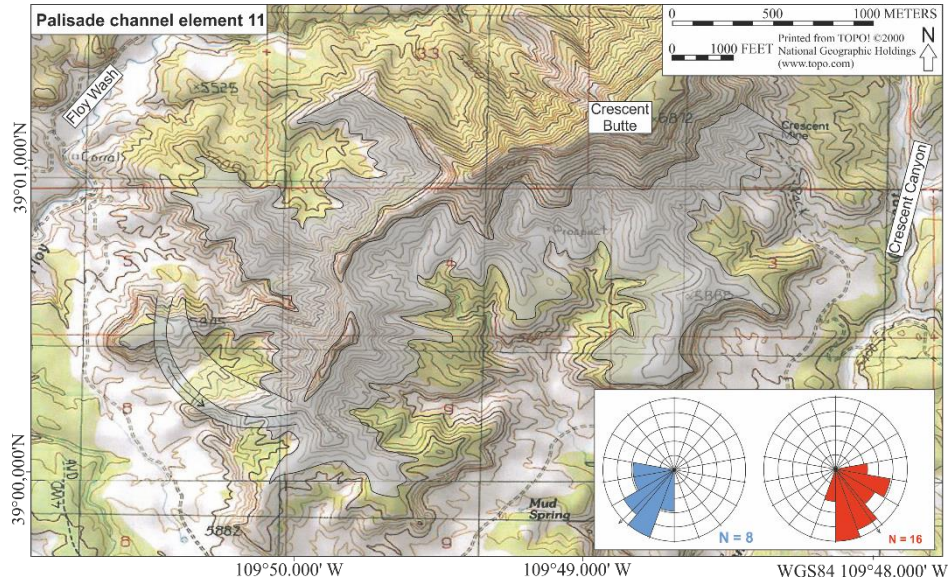
Palisade Zone Channel Elements

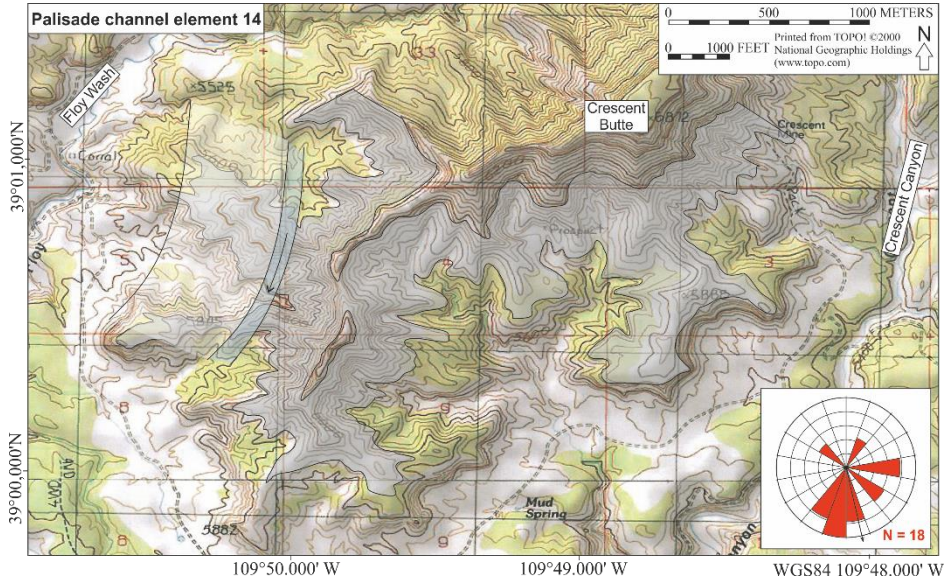




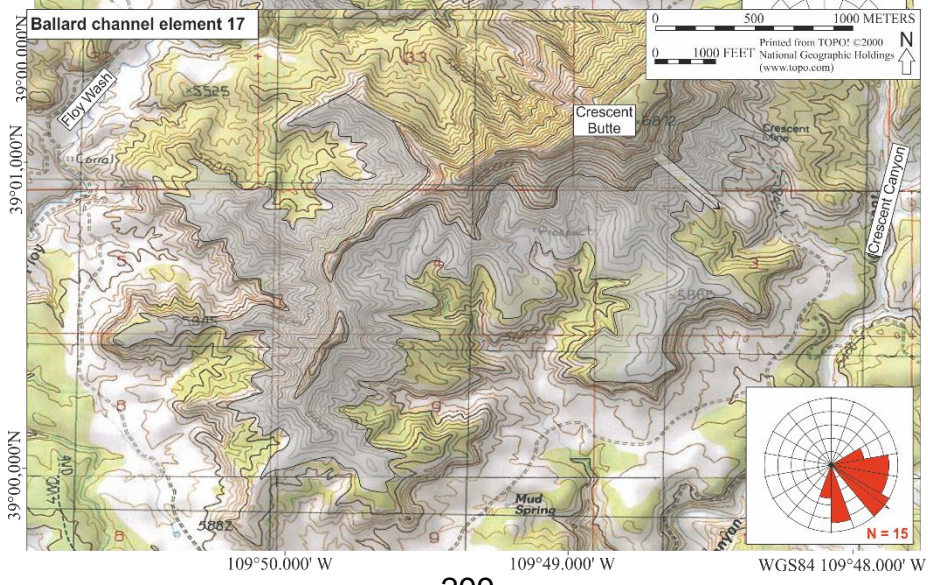
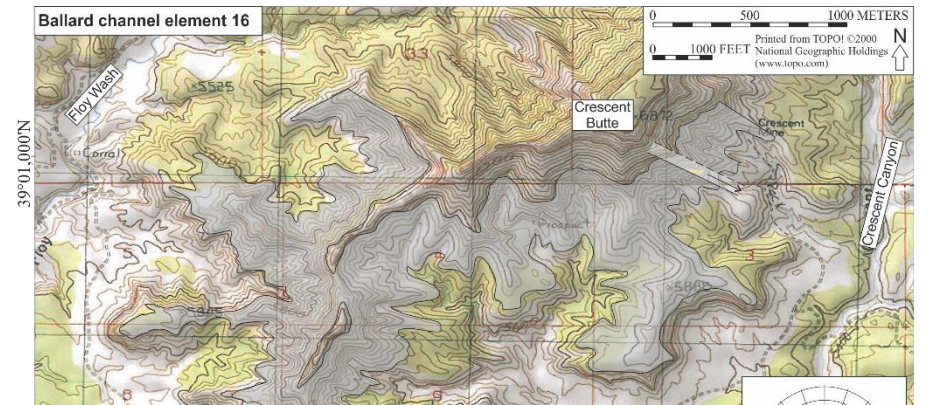
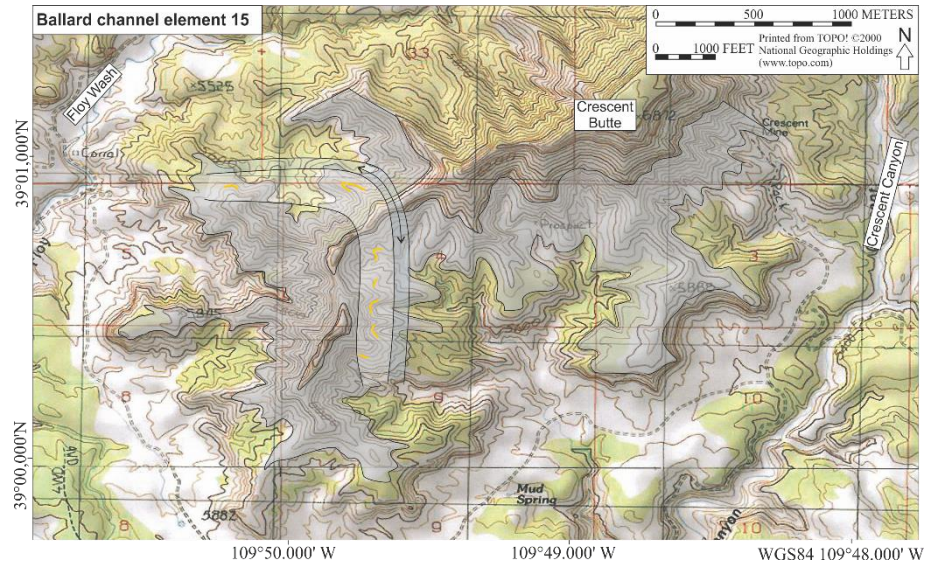


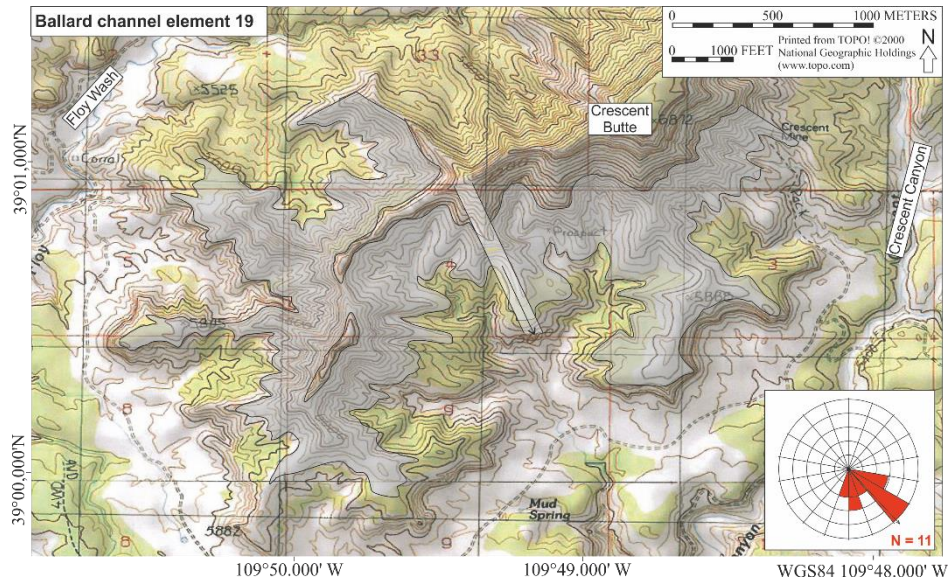
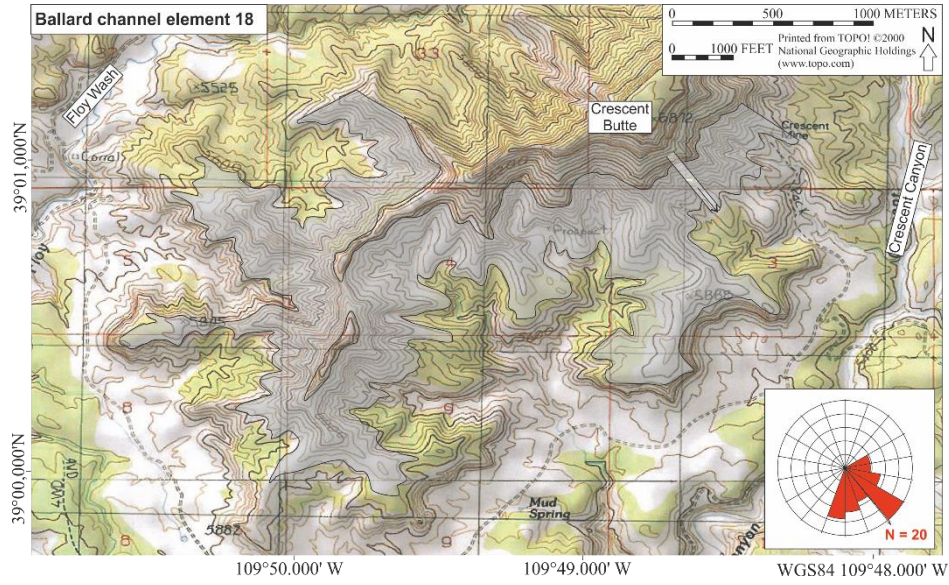




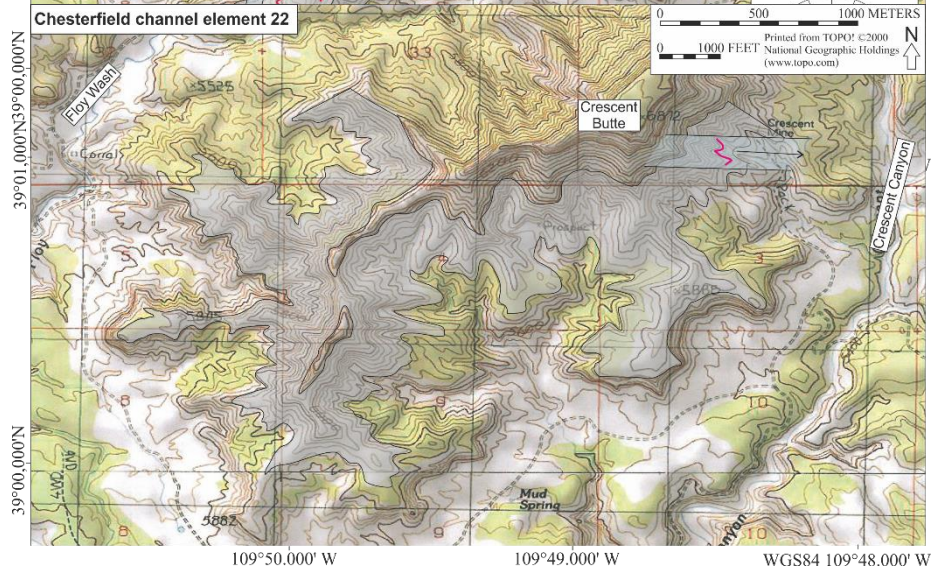
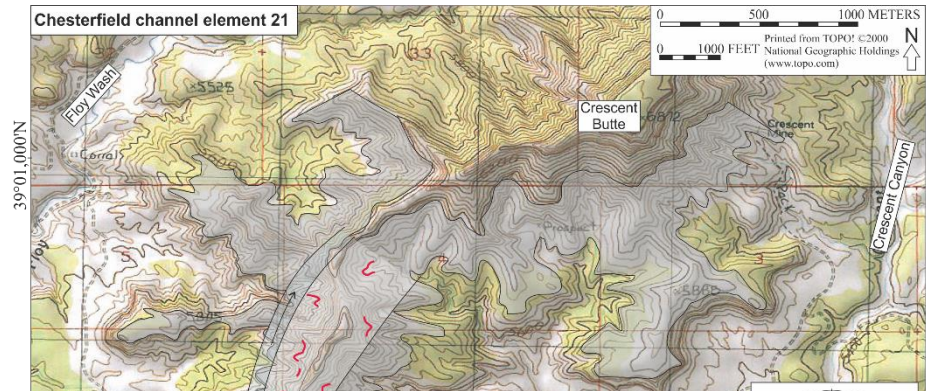
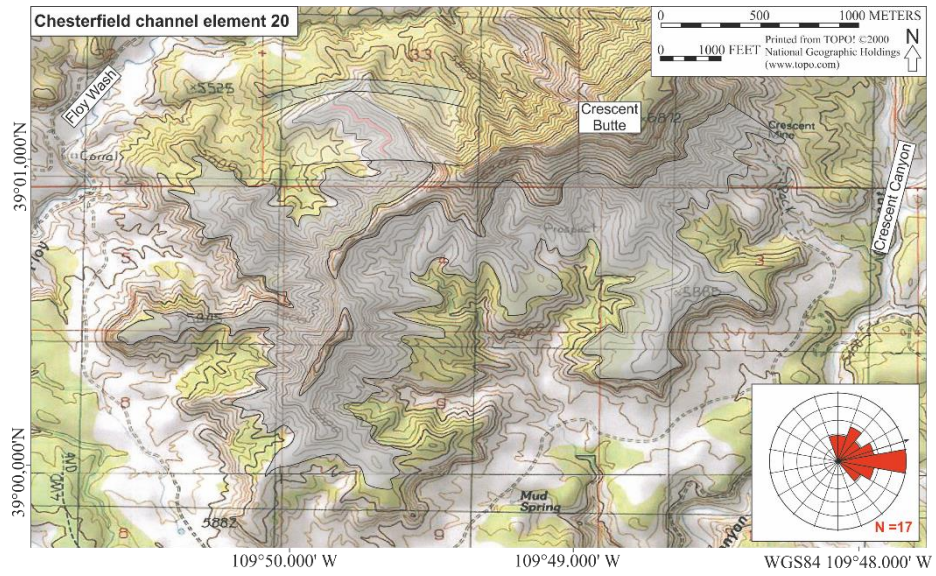


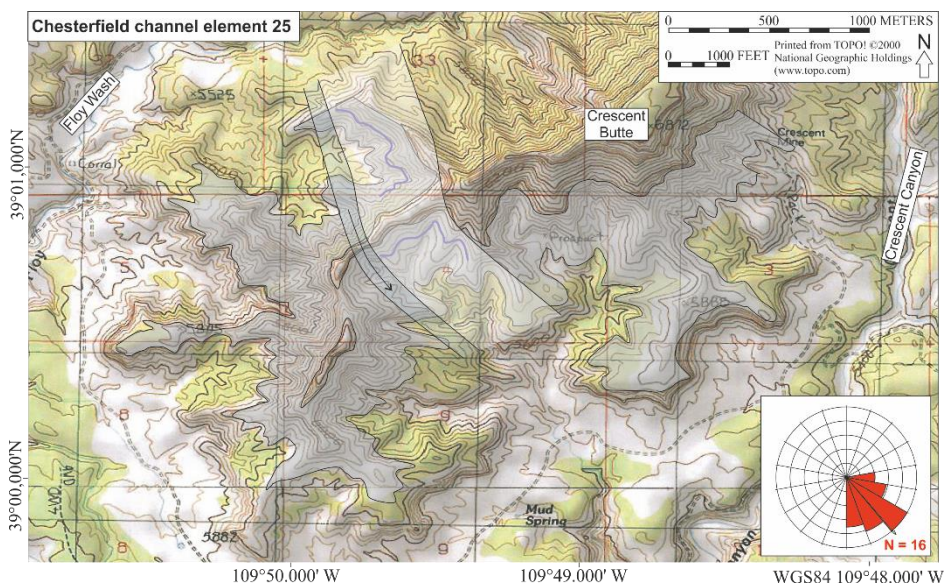
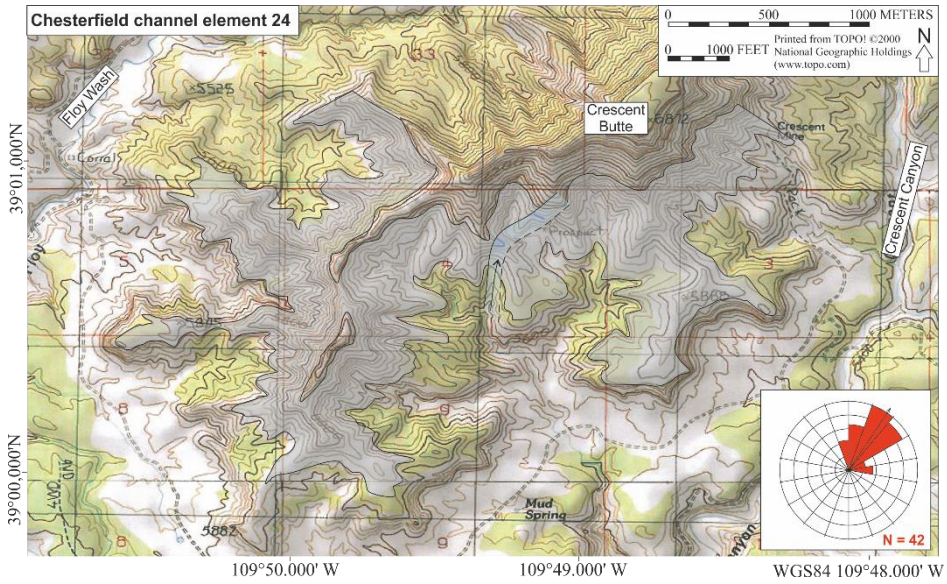
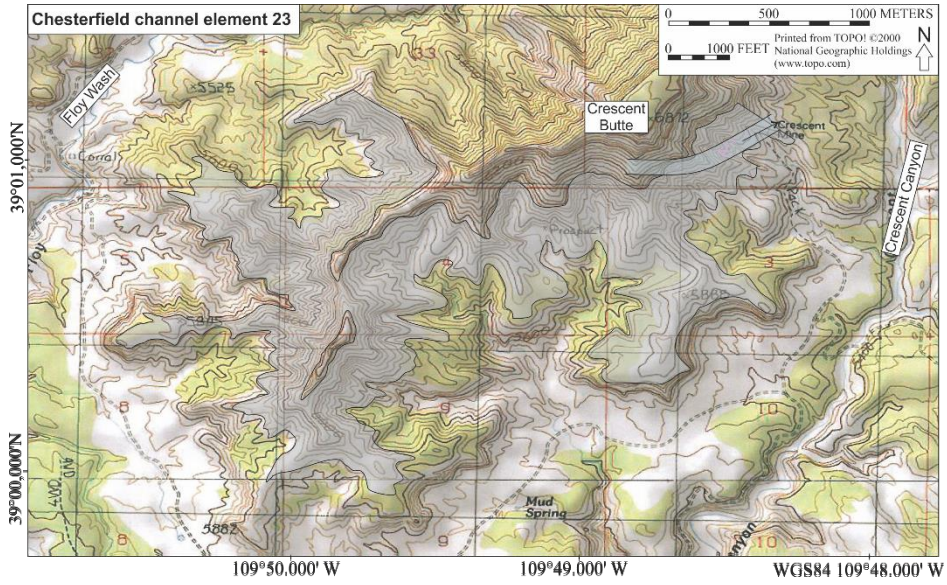
Ballard Zone Channel Elements

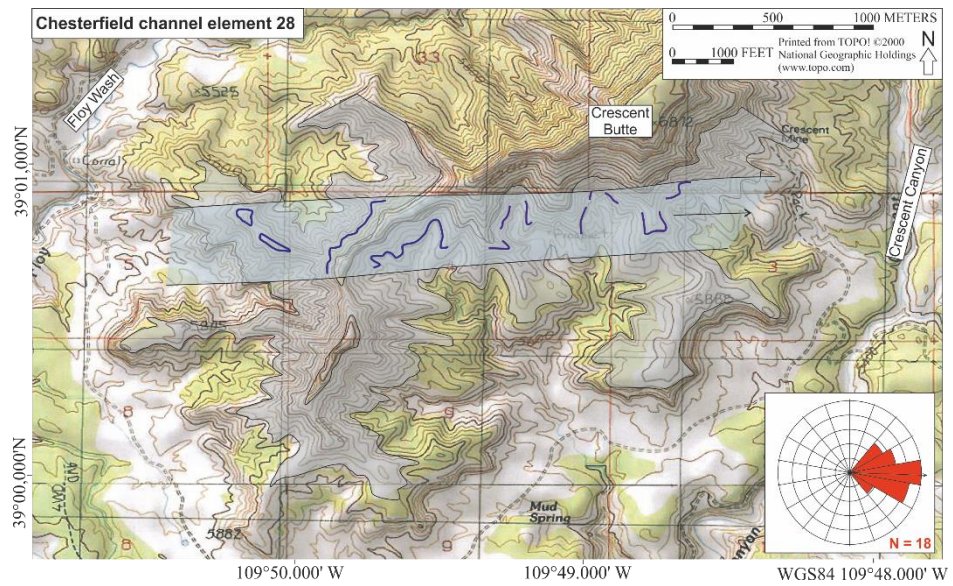
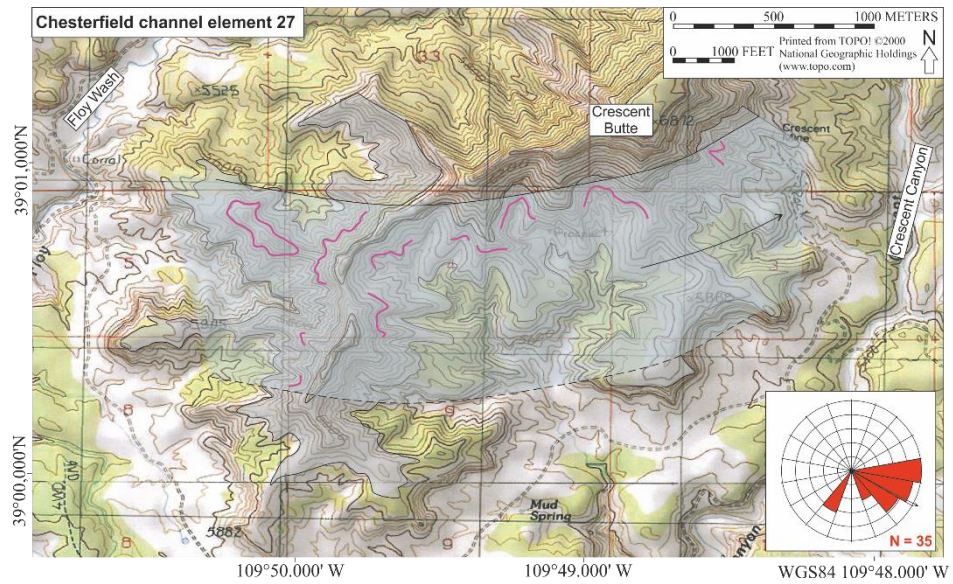
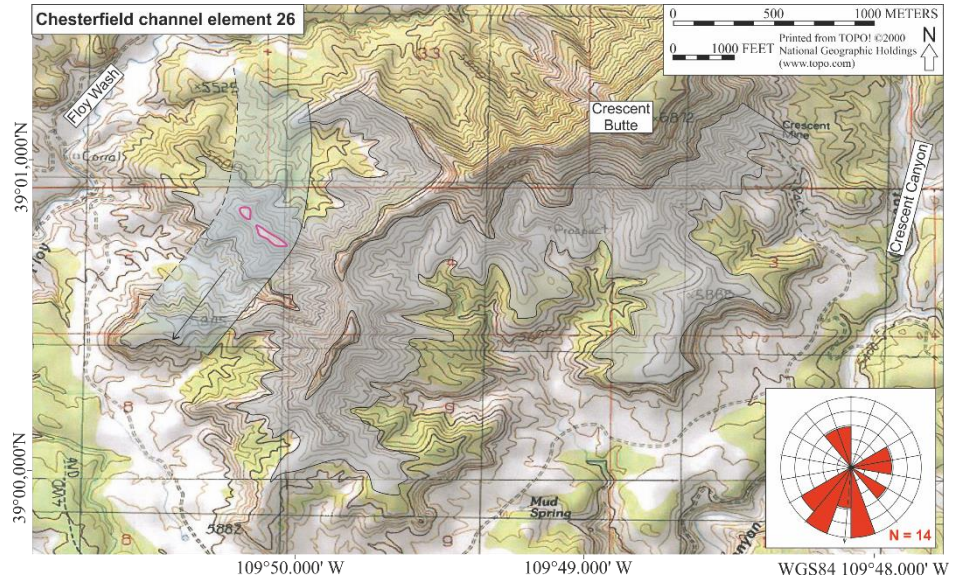


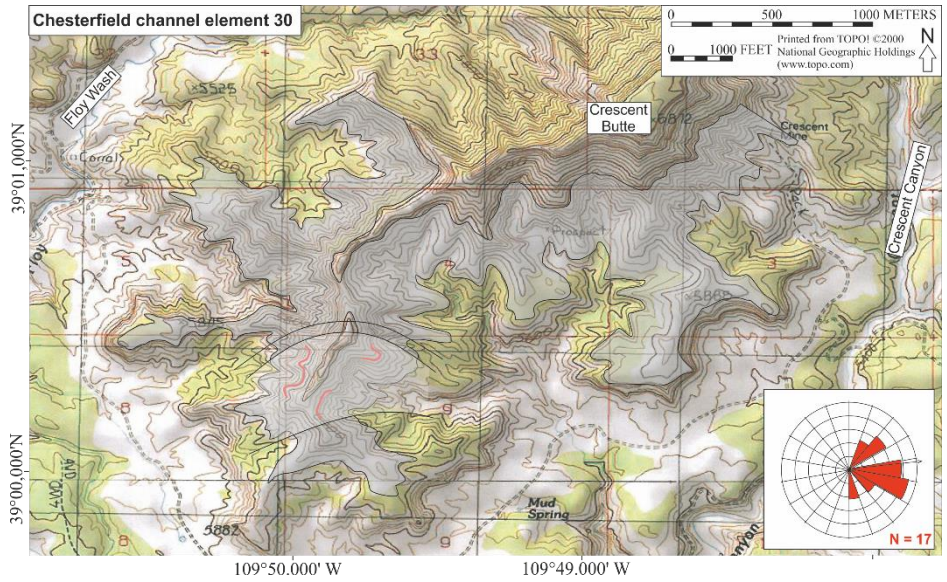
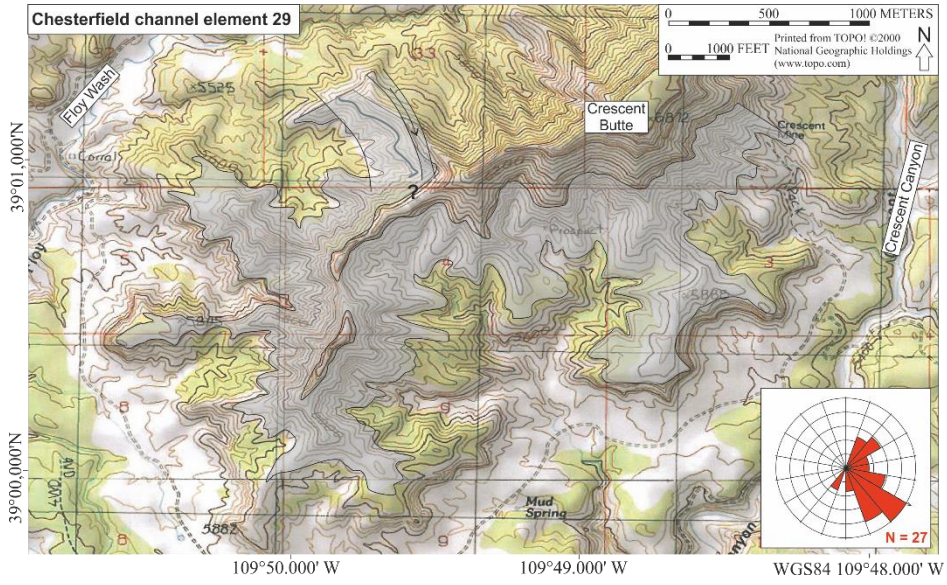


Chesterfield Zone Channel Elements15









Appendix E

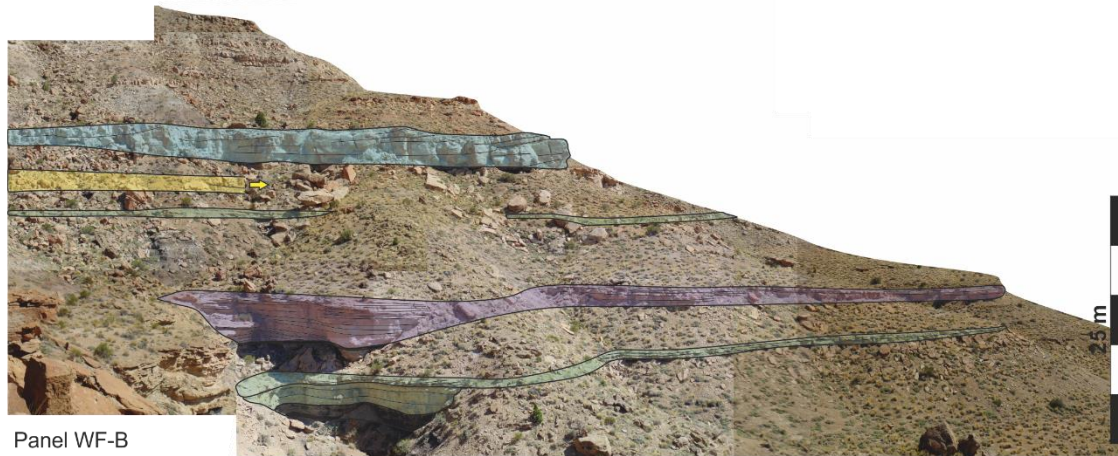
Log locations for logs at each study location shown in Chapter 5 (Figs. 5.5, 5.8). Additional smaller logs were also collected, these are indicated on the panels shown in Appendix F.

Season Number	Log Name	Lower GPS		Upper GPS		Length m
		N	W 109	N 39	W 109	
4	West Floy	01.515	51.944	01.576	51.894	48
1/2	East Floy	00.889	46.332	01.013	46.098	89
2	West Crescent Mine	00.690	48.649	00.539	48.468	85
4	Crescent Canyon	01.965	47.704	01.966	47.673	47
4	Right Hand Crescent	01.388	46.935	01.422	46.892	34
1	East Crescent	00.889	46.332	01.013	46.098	89
1	West Blaze	59.759	46.252	/	/	83
3	Blaze Canyon	01.207	44.674	01.202	44.338	98.5
4	West Thompson	00.933	43.811	00.982	43.753	28
3	East Segoe	01.032	41.333	01.051	41.213	136
4	Salt Wash	01.309	40.824	01.308	40.739	34.5
4	East Salt Wash	01.073	39.943	01.061	39.849	57.5
4	Sagers Canyon	01.521	38.519	/	/	36

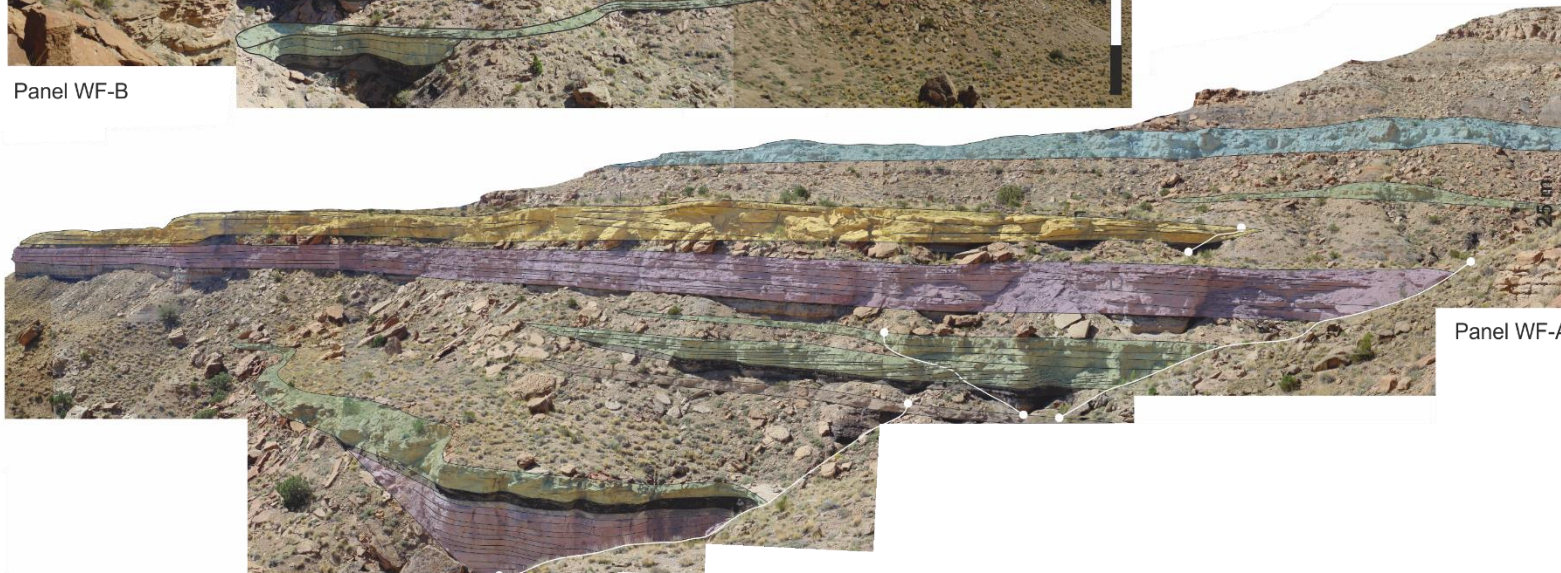
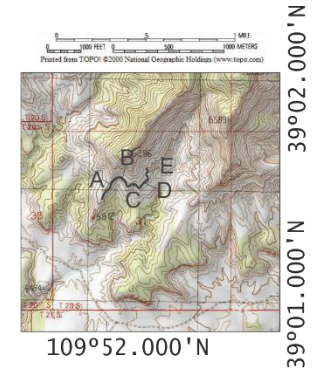
Appendix F

Summary of data collected at each study site analysed for Chapter 5. Logs at each site are presented in Figure 5.5.

West Floy study site

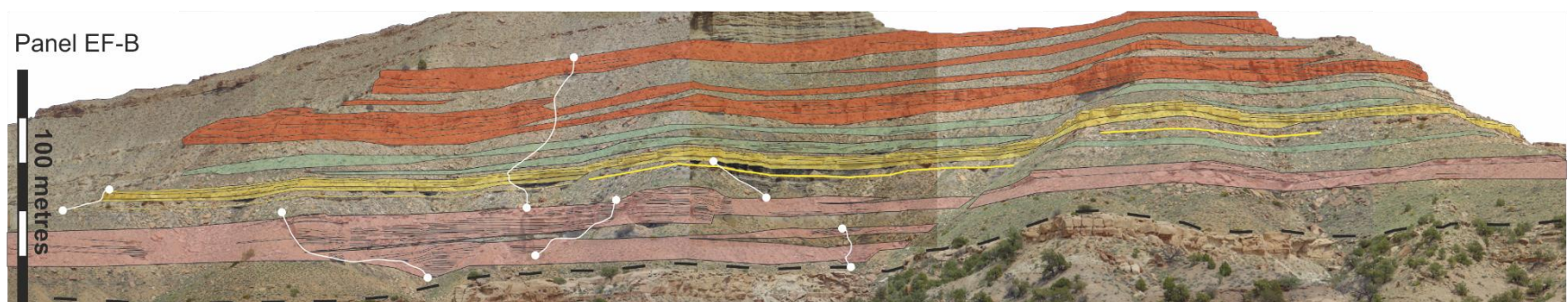
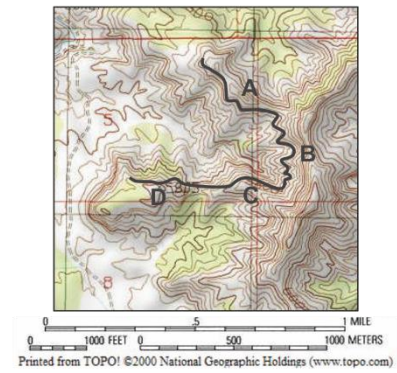


Panel WF-B



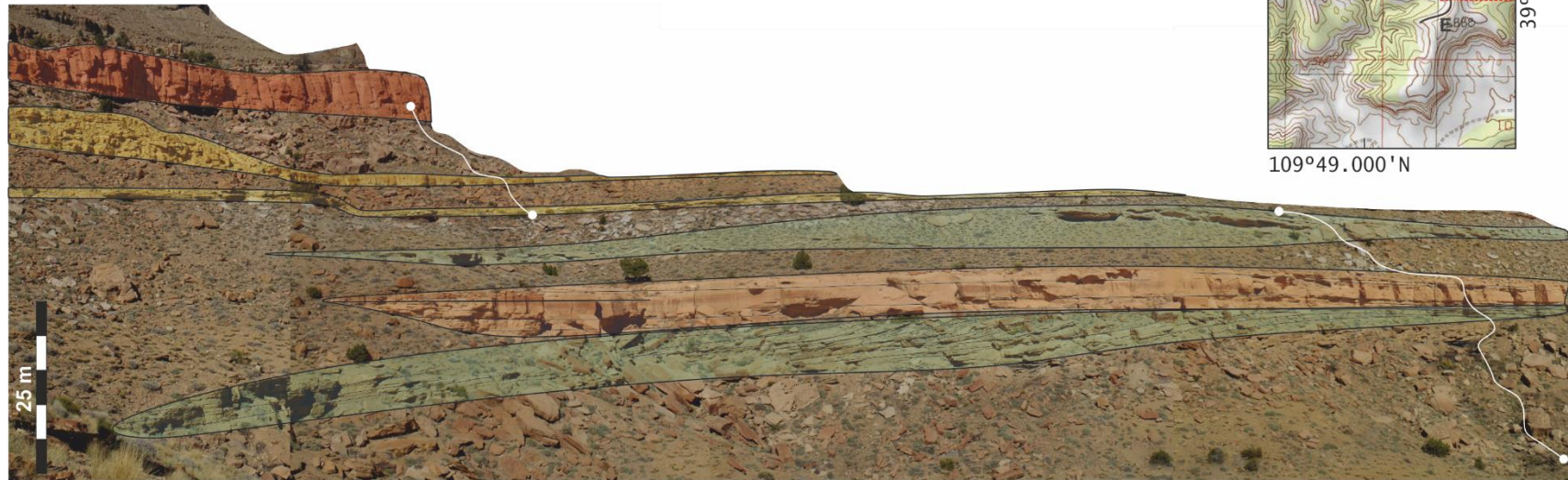
Panel WF-A

East Floy study site

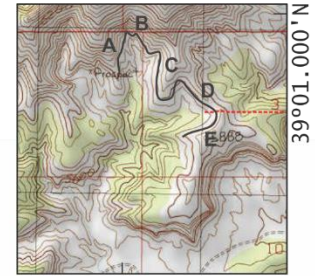


West Crescent study site

Panel WCM-D



0 1000 FEET 0 500 1000 METERS 1 MILE
Printed from TOPO! ©2000 National Geographic Holdings (www.topo.com)



109°49.000' N
39°01.000' N

Panel WCM-E



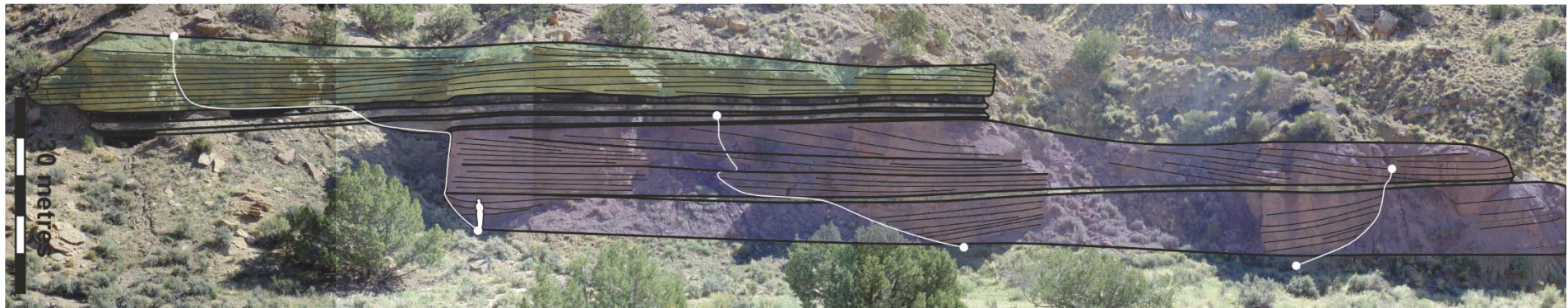
Crescent Canyon study site

Panel CC-C

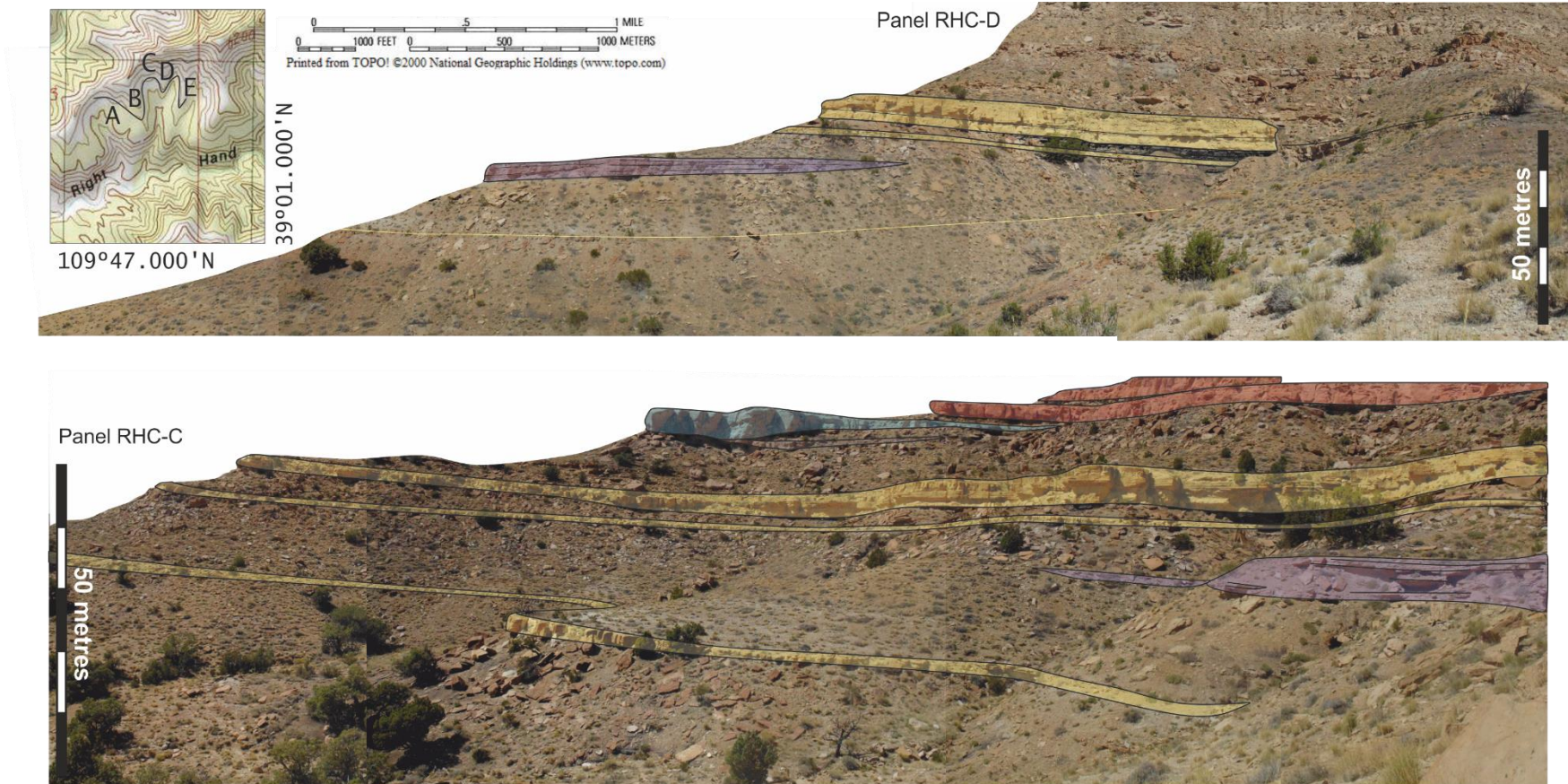


0 5 1 MILE
0 1000 FEET 0 500 1000 METERS
Printed from TOPO! ©2000 National Geographic Holdings (www.topo.com)

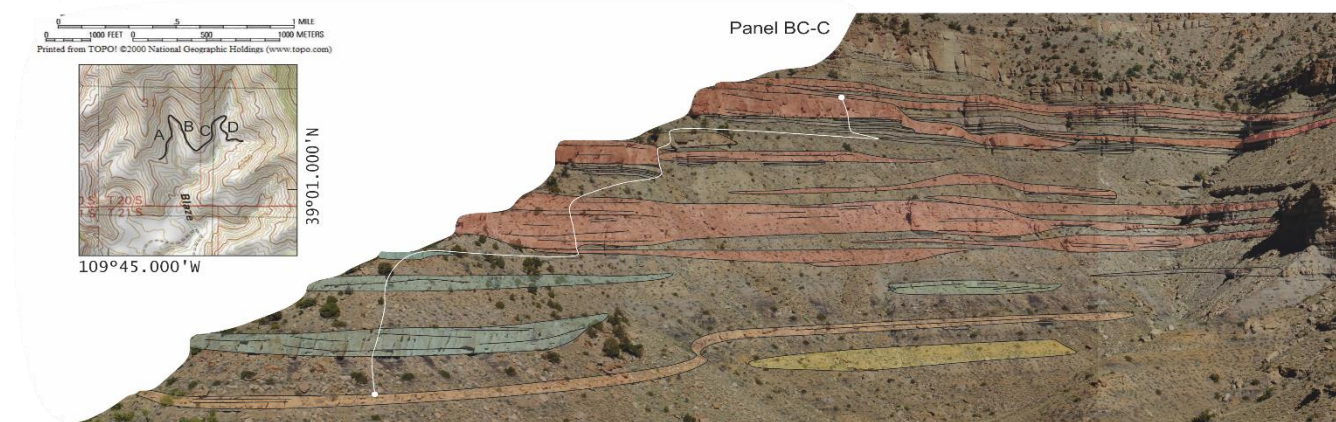
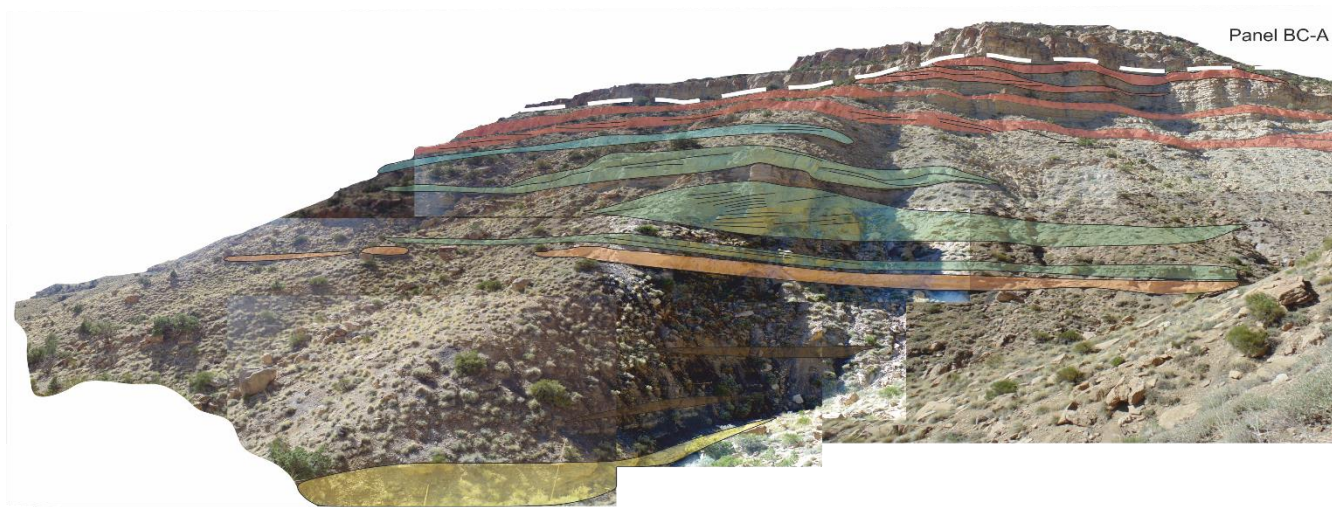
Panel CC-D



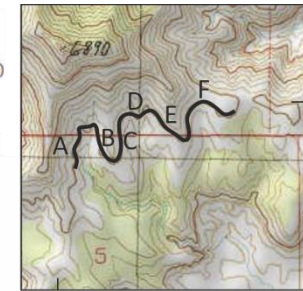
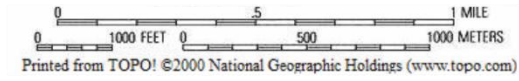
Right Hand Crescent study site



Blaze Canyon study site

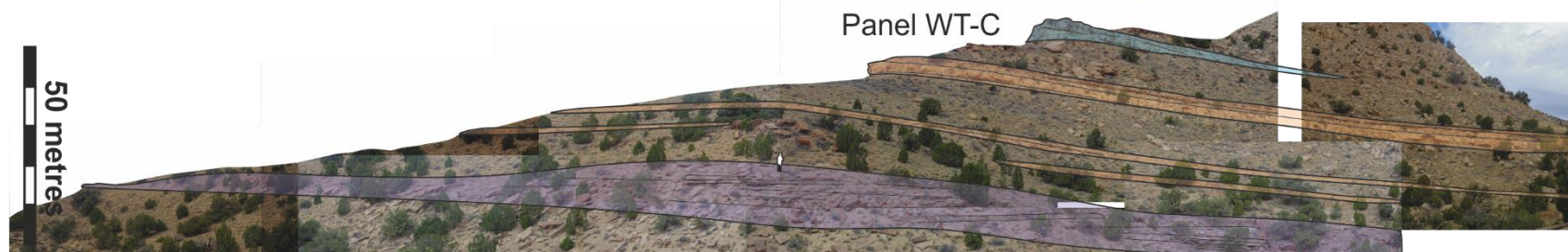
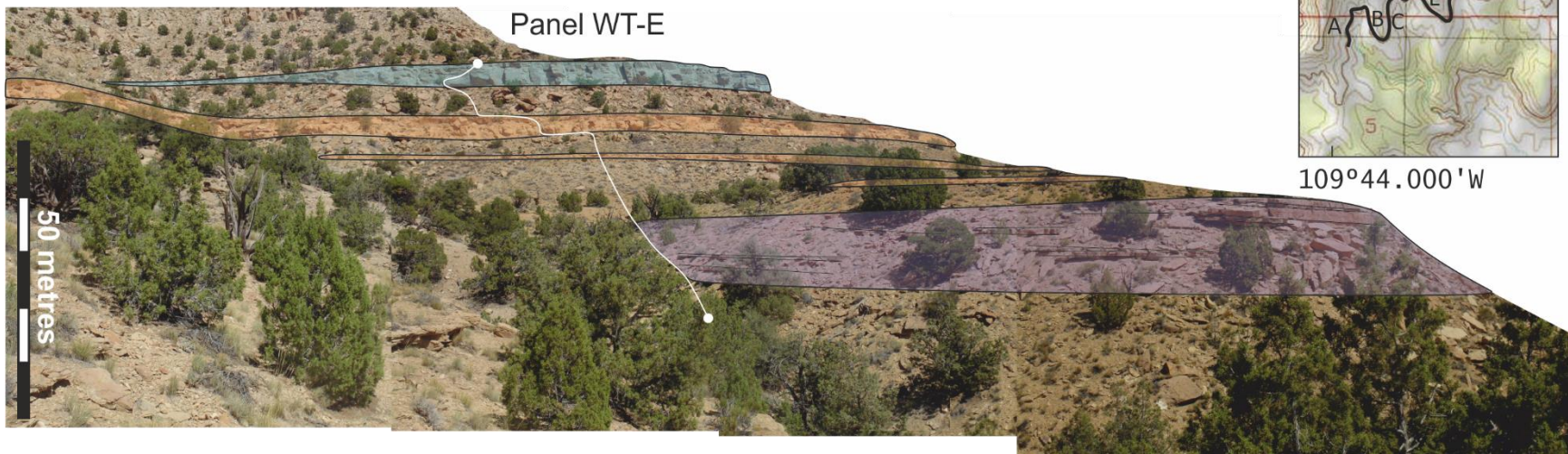


West Thompson study site

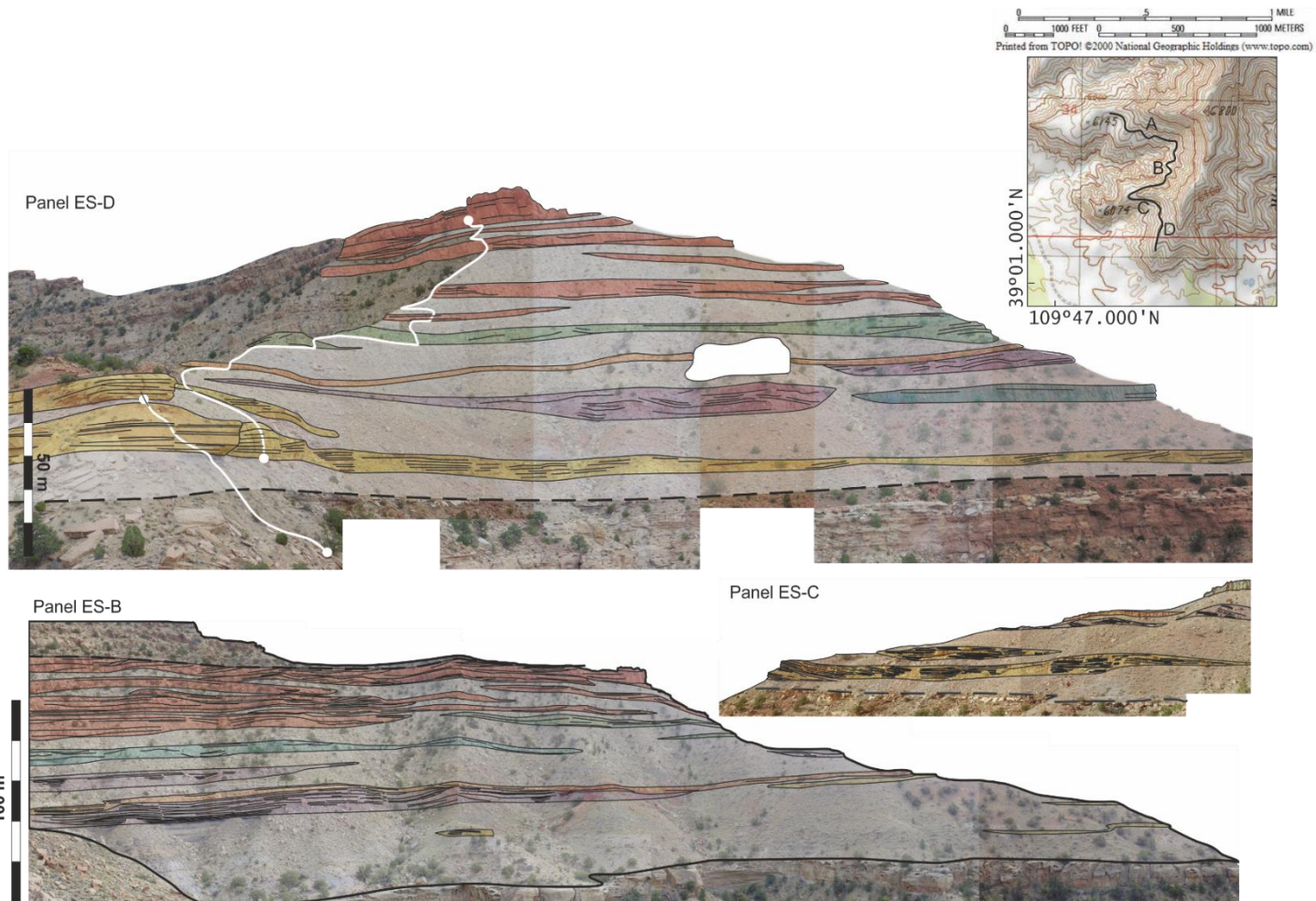


39°01.000'N

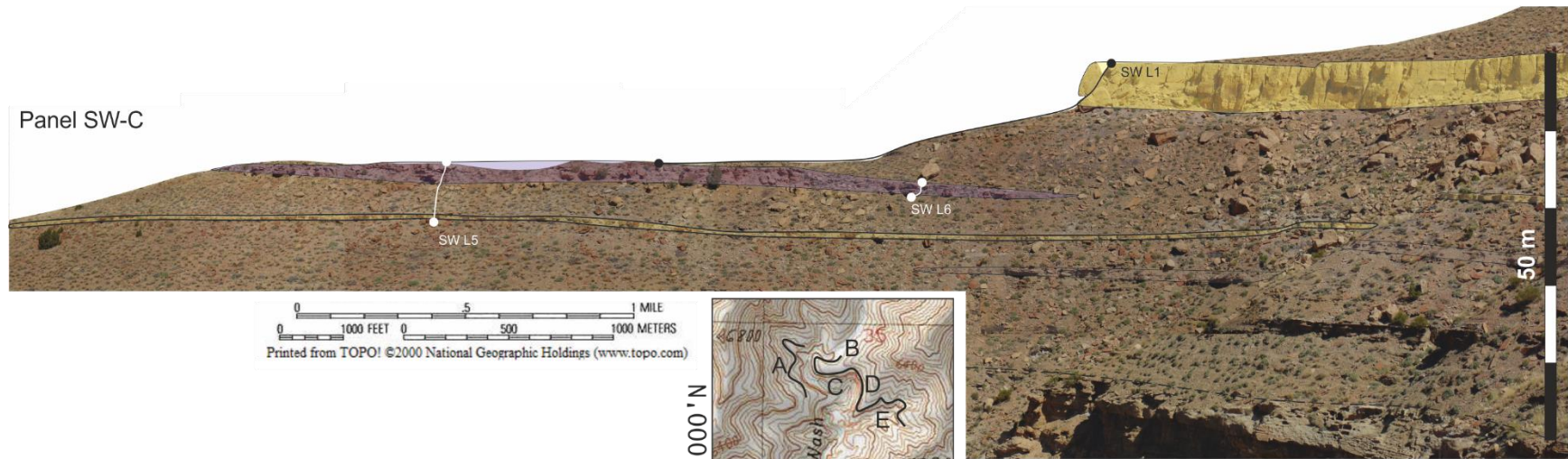
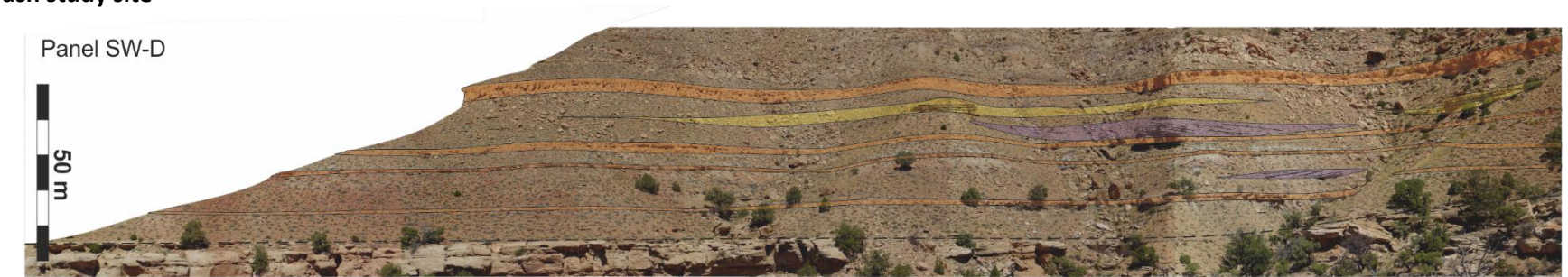
109°44.000'W



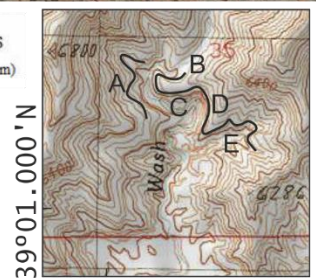
East Sego study site



Salt Wash study site



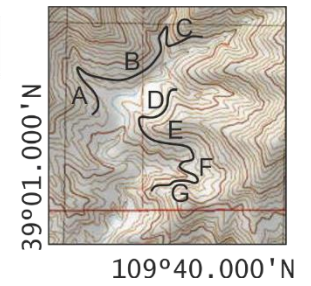
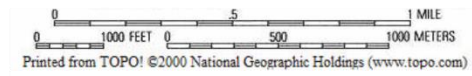
0 5 1 MILE
0 1000 FEET 0 500 1000 METERS
Printed from TOPO! ©2000 National Geographic Holdings (www.topo.com)



39°01.000' N

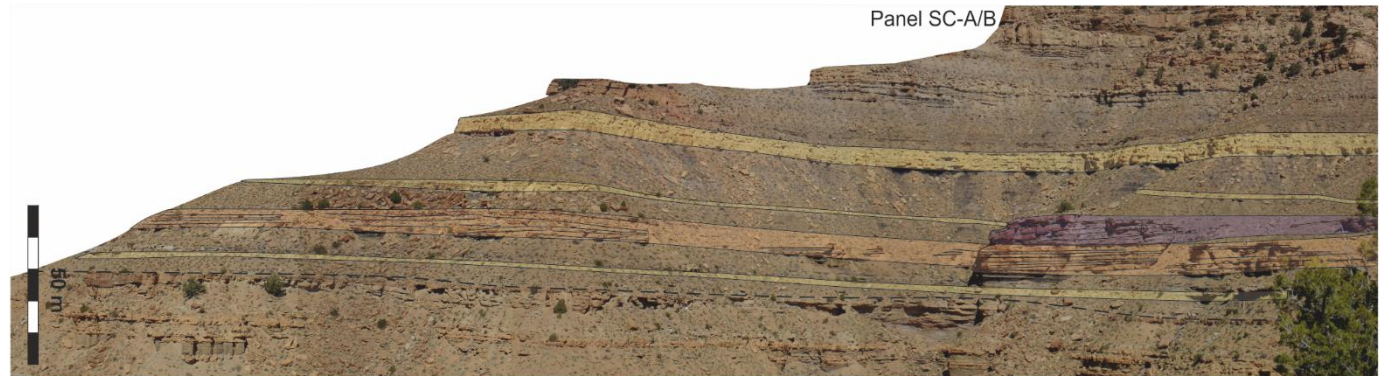
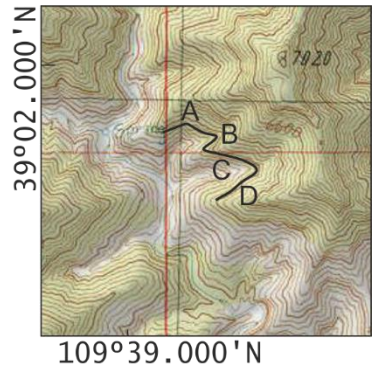
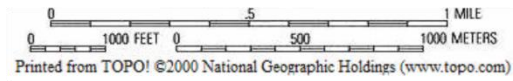
109°41.000' N

East Salt Wash study site

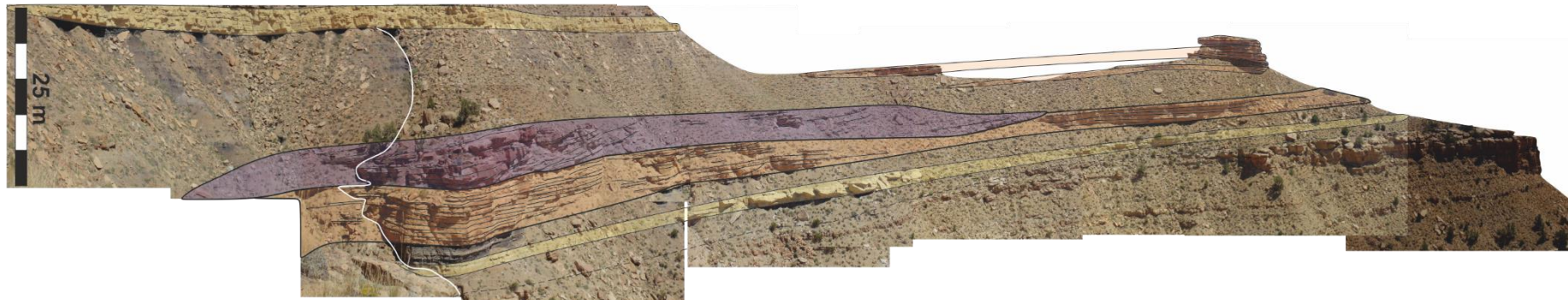


8.5

Sagers canyon study site



Panel SC-D

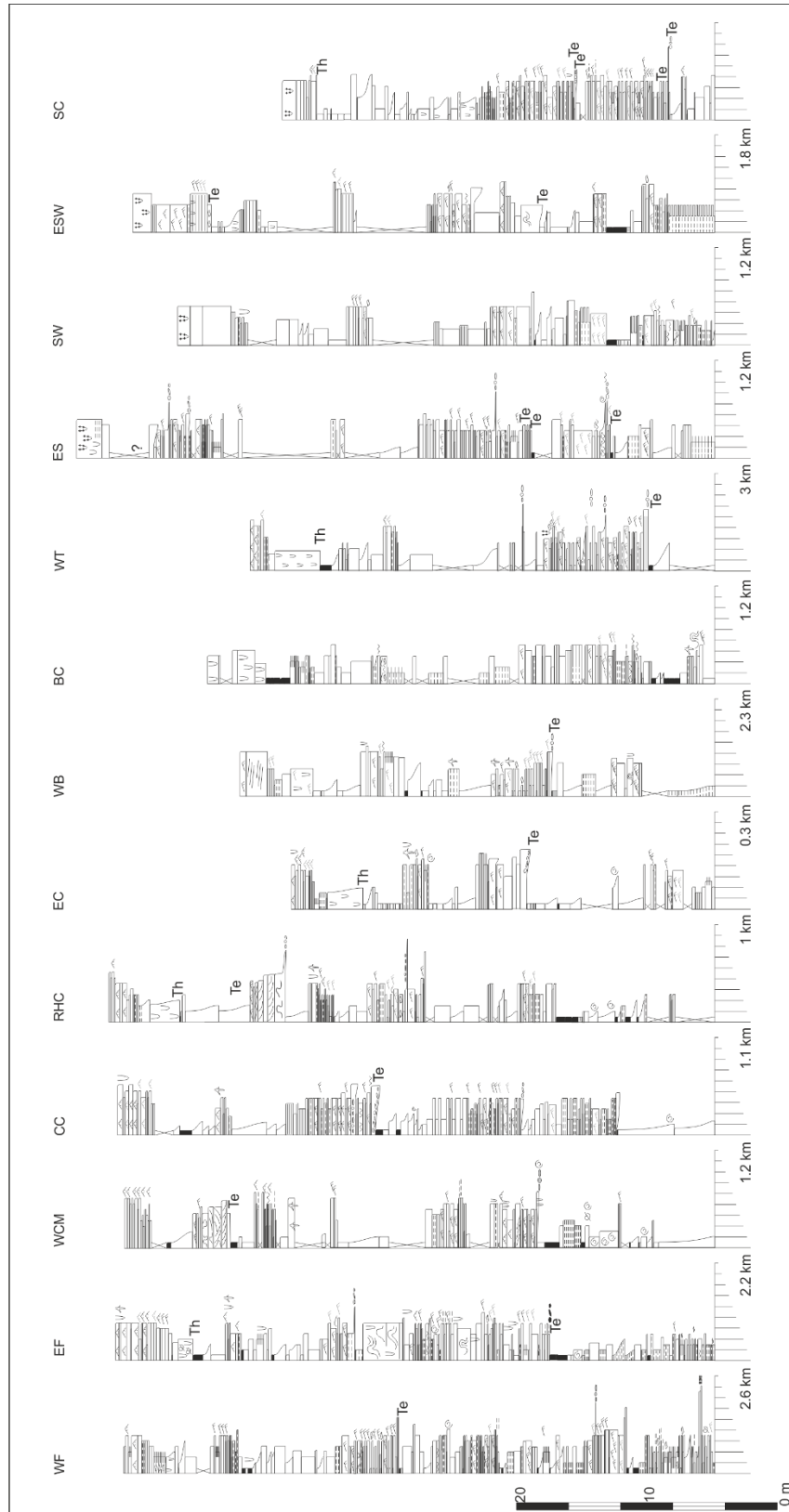


APPENDIX G

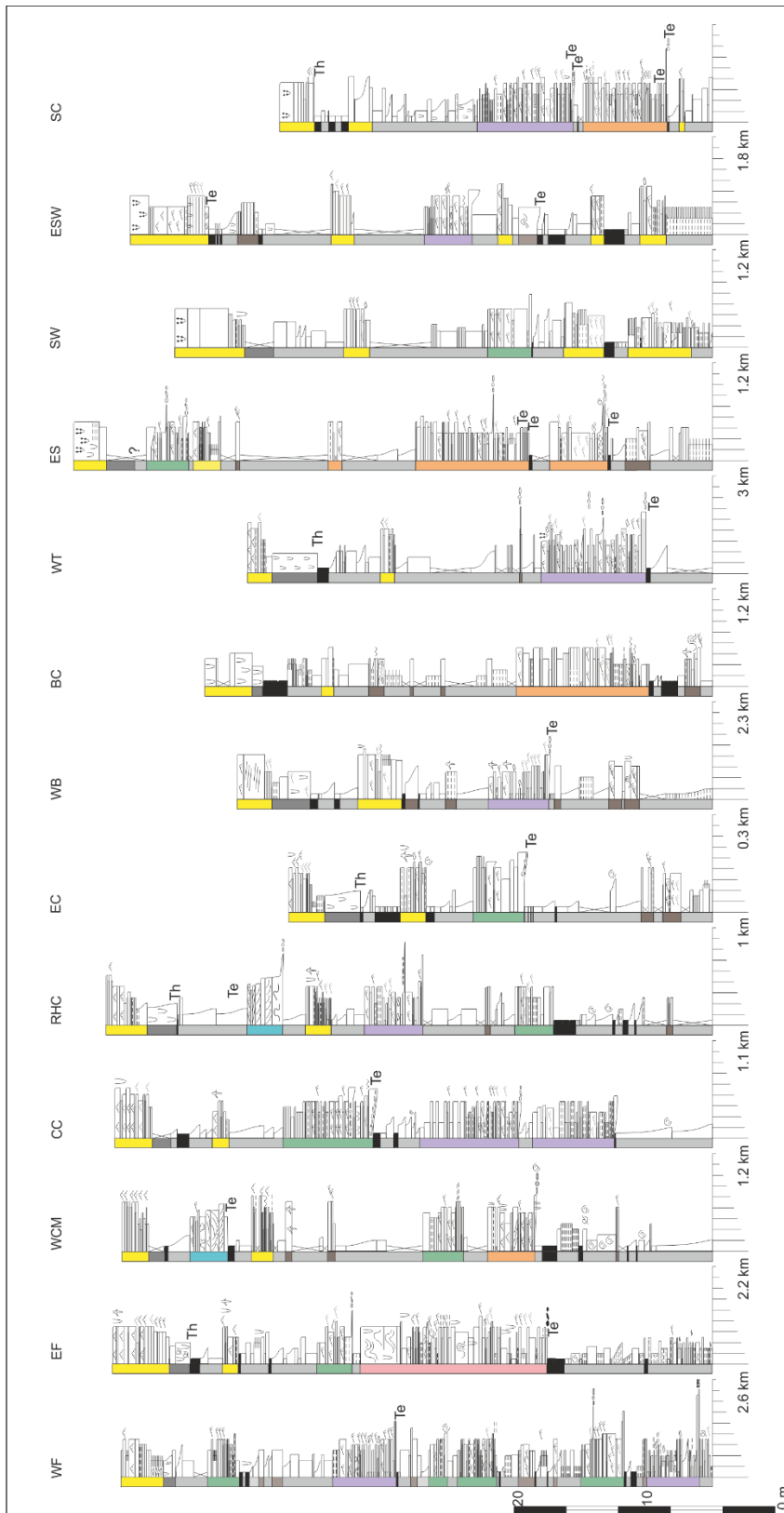
Workflow for the correlation panel presented in Chapter 5. The workflow will be presented in a series of stages:

- 1) Raw data panel showing facies, without any architectural element, correlation or marker bed interpretations included
- 2) Architectural element interpretations are included onto the panel
- 3) Logs are hung from a marker horizon (the base of the TCSB) (cf. Fig. 5.5)
- 4) Logs are spaced correctly
- 5) Confident correlations of marker beds (TCSB and BBSB) and confident coal correlations are included
- 6) Further correlations of coal are interpreted
- 7) The panel is simplified to remove facies data
- 8) The Middle Palisade Zone is interpreted
- 9) Further depositional intervals, as described in the text are interpreted (cf. Fig. 5.8)
- 10) The logs are removed from the panel leaving the interpretation of sandstone-dominated architectural elements and coal
- 11) Coals and marker horizons are correlated across the simplified panel
- 12) The geometry of marker horizons is interpreted and simplified
- 13) A simplified, schematic geometry of other sandstone dominated architectural elements are indicated (cf. Fig. 5.10).

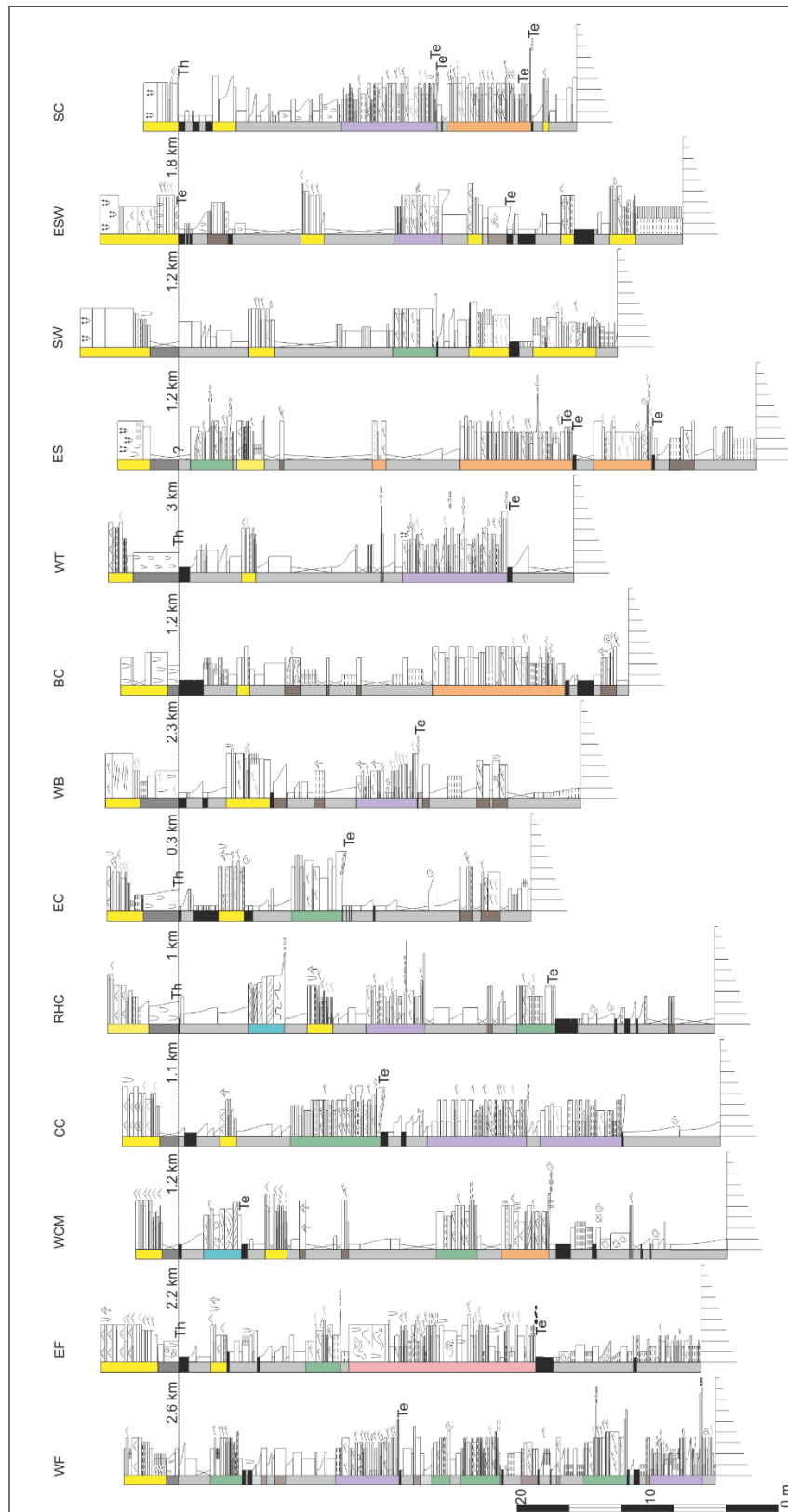
G.1. Raw data panel showing facies, without any architectural element, correlation or marker bed interpretations included



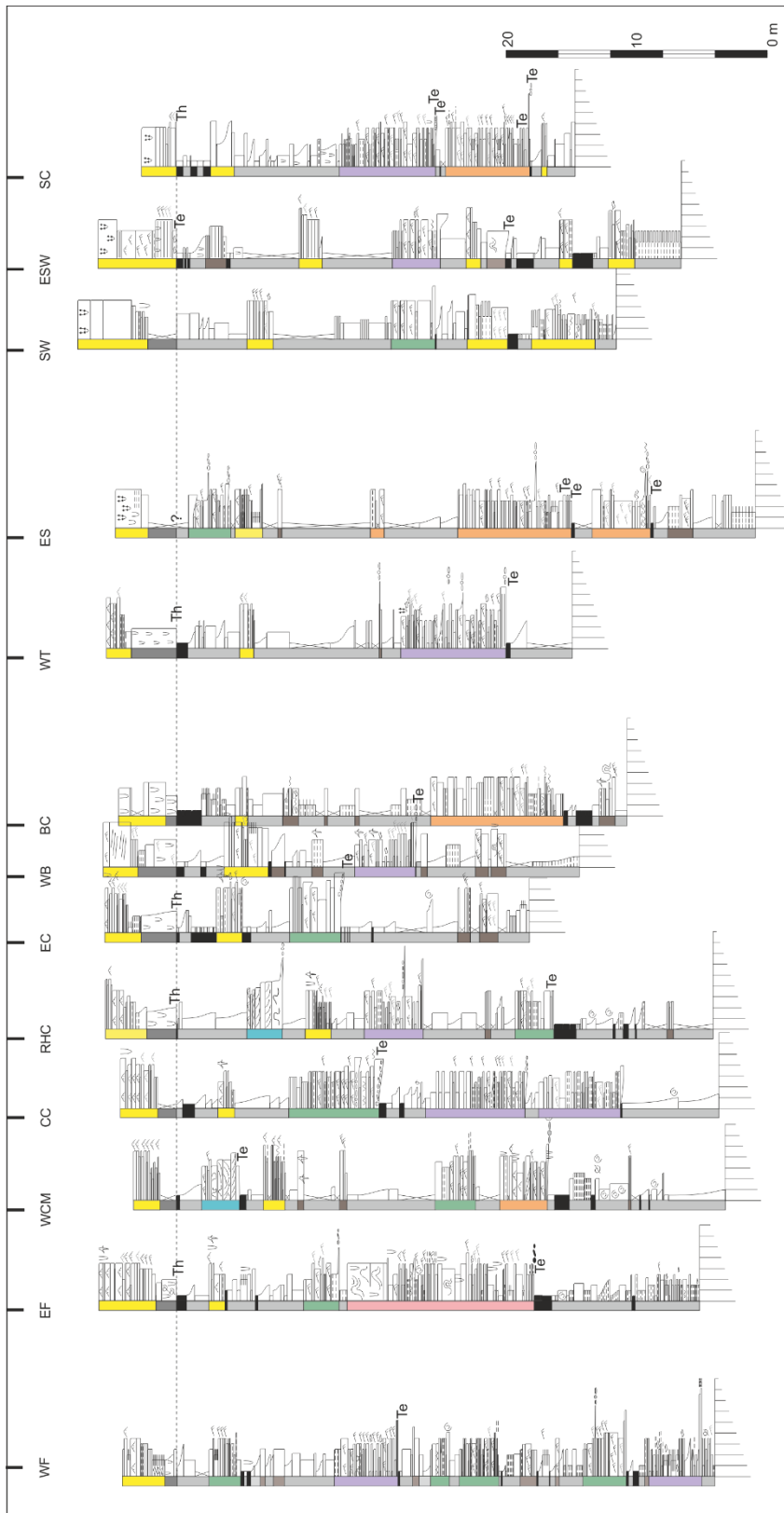
G.2. Architectural element interpretations are included onto the panel



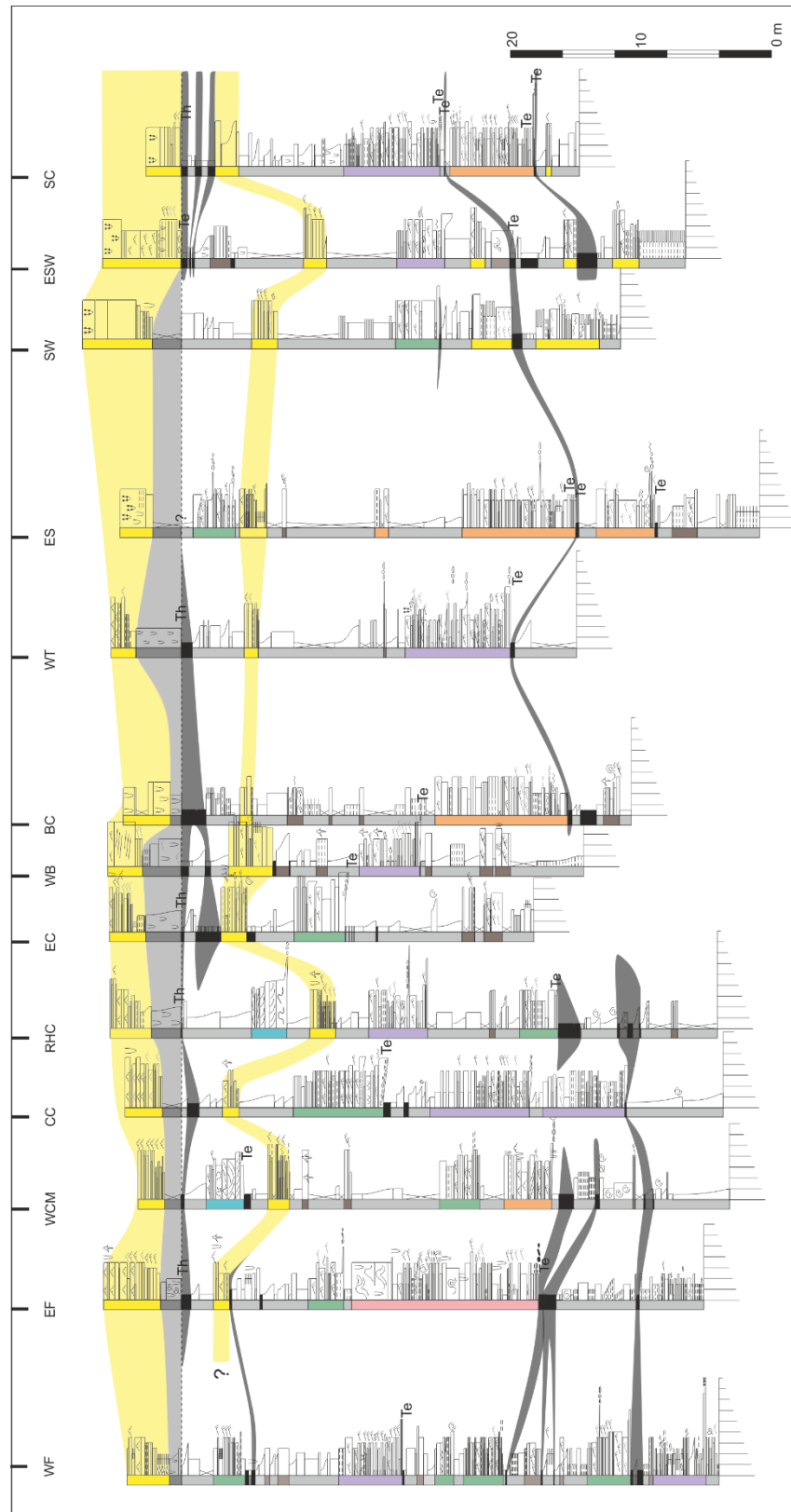
G.3. Logs are hung from a marker horizon



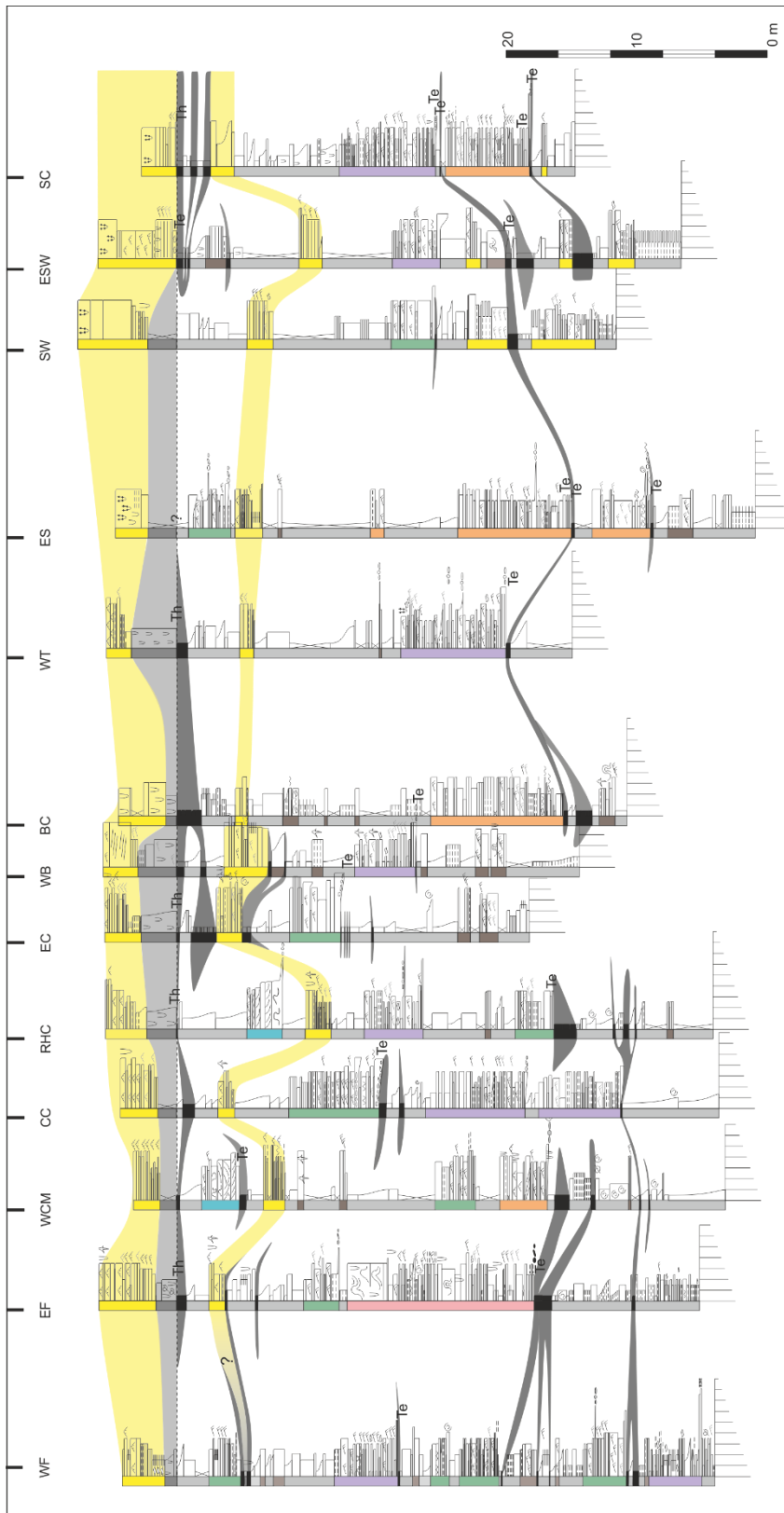
G.4. Logs are correctly spaced



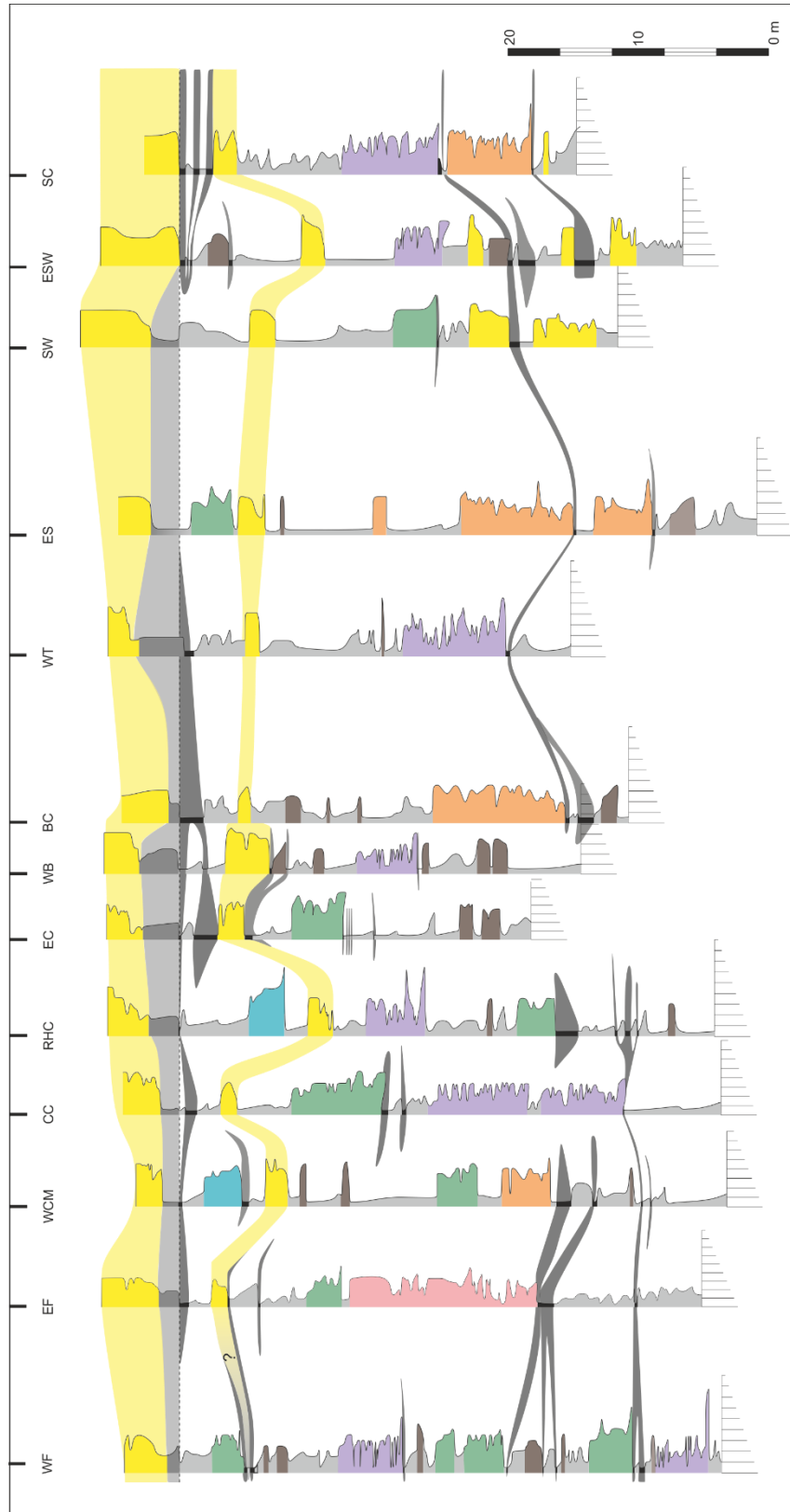
G.5. Confident correlations of marker beds



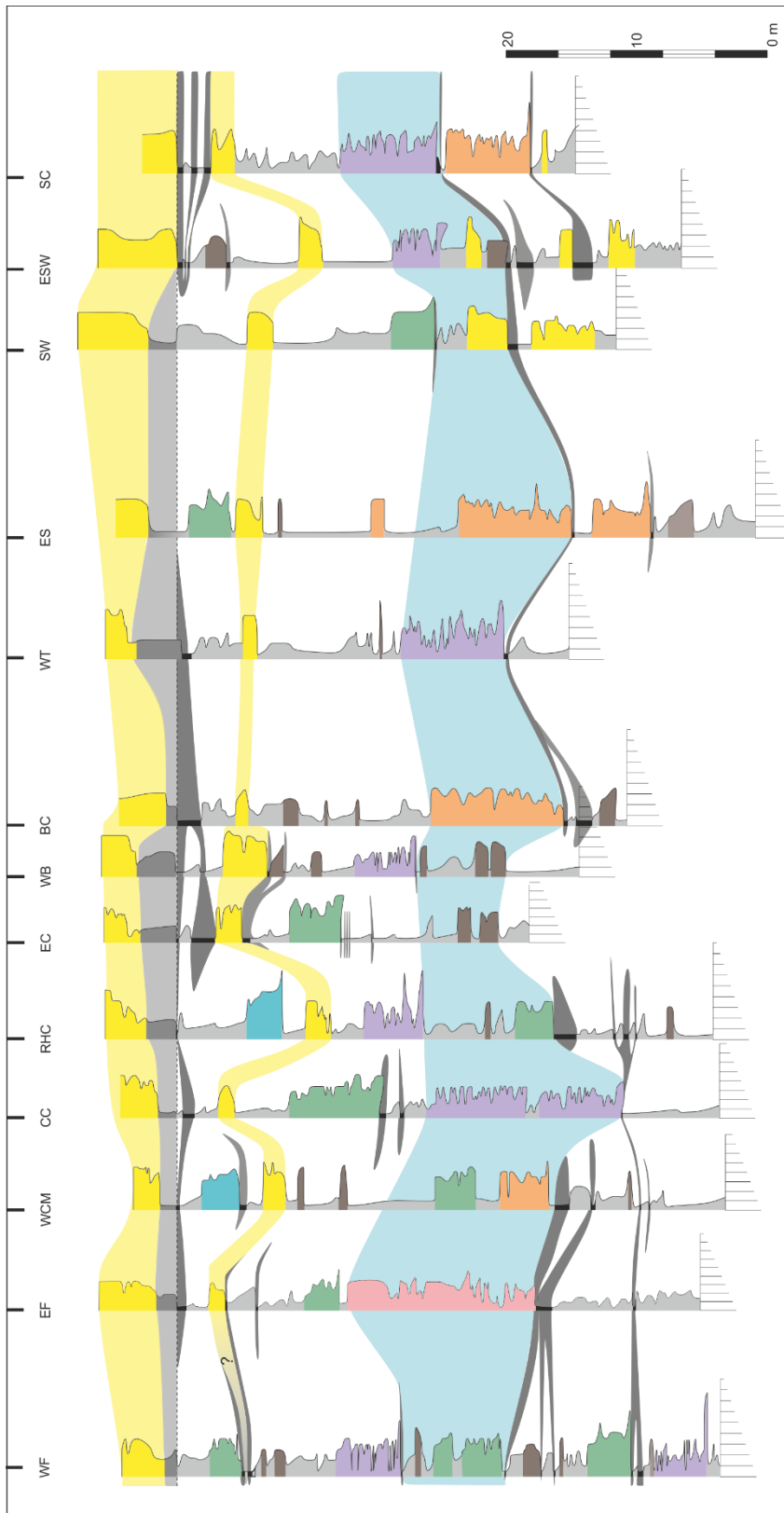
G.6. Further correlations of coal are interpreted



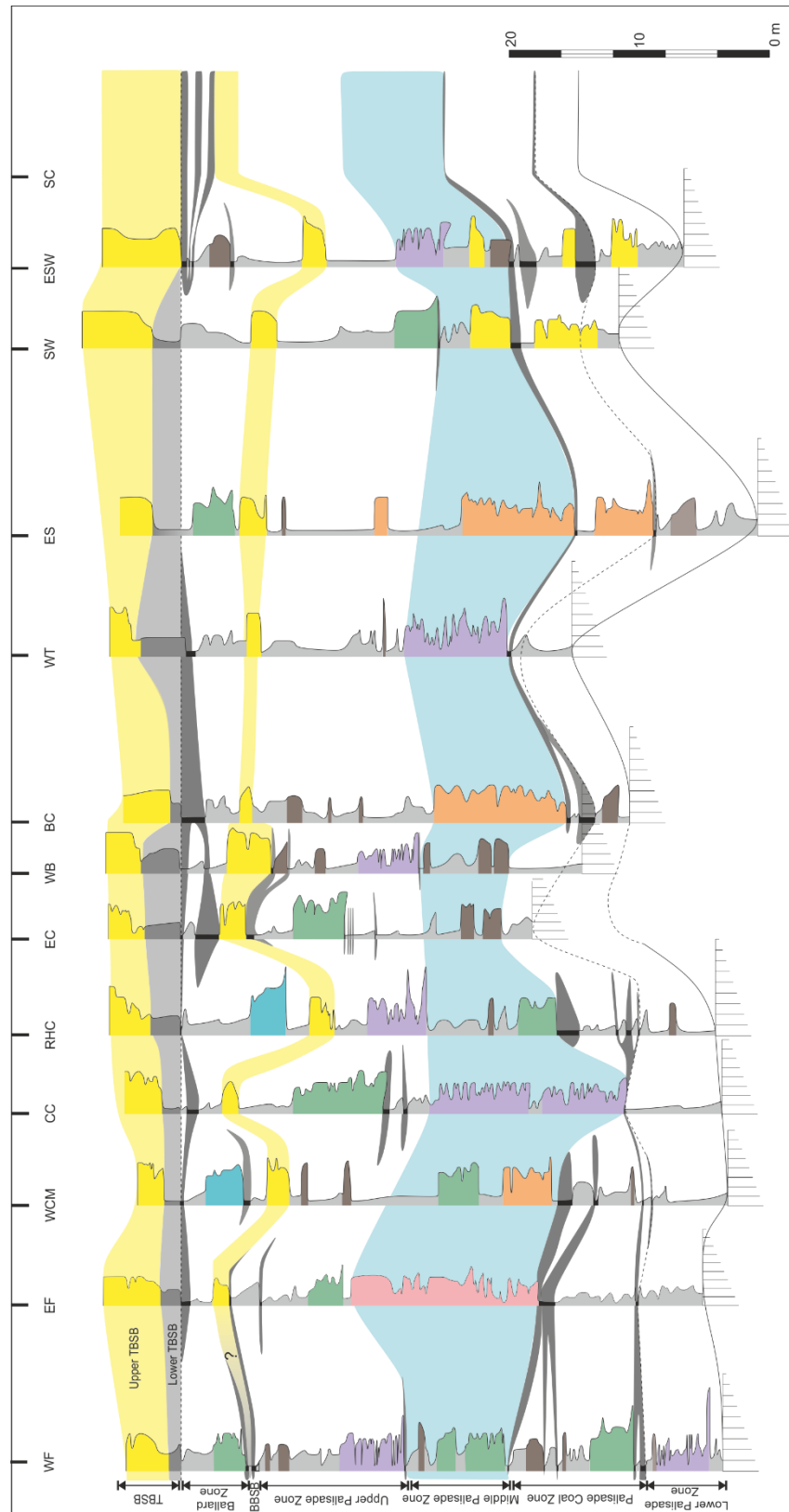
G.7. The panel is simplified to remove facies data



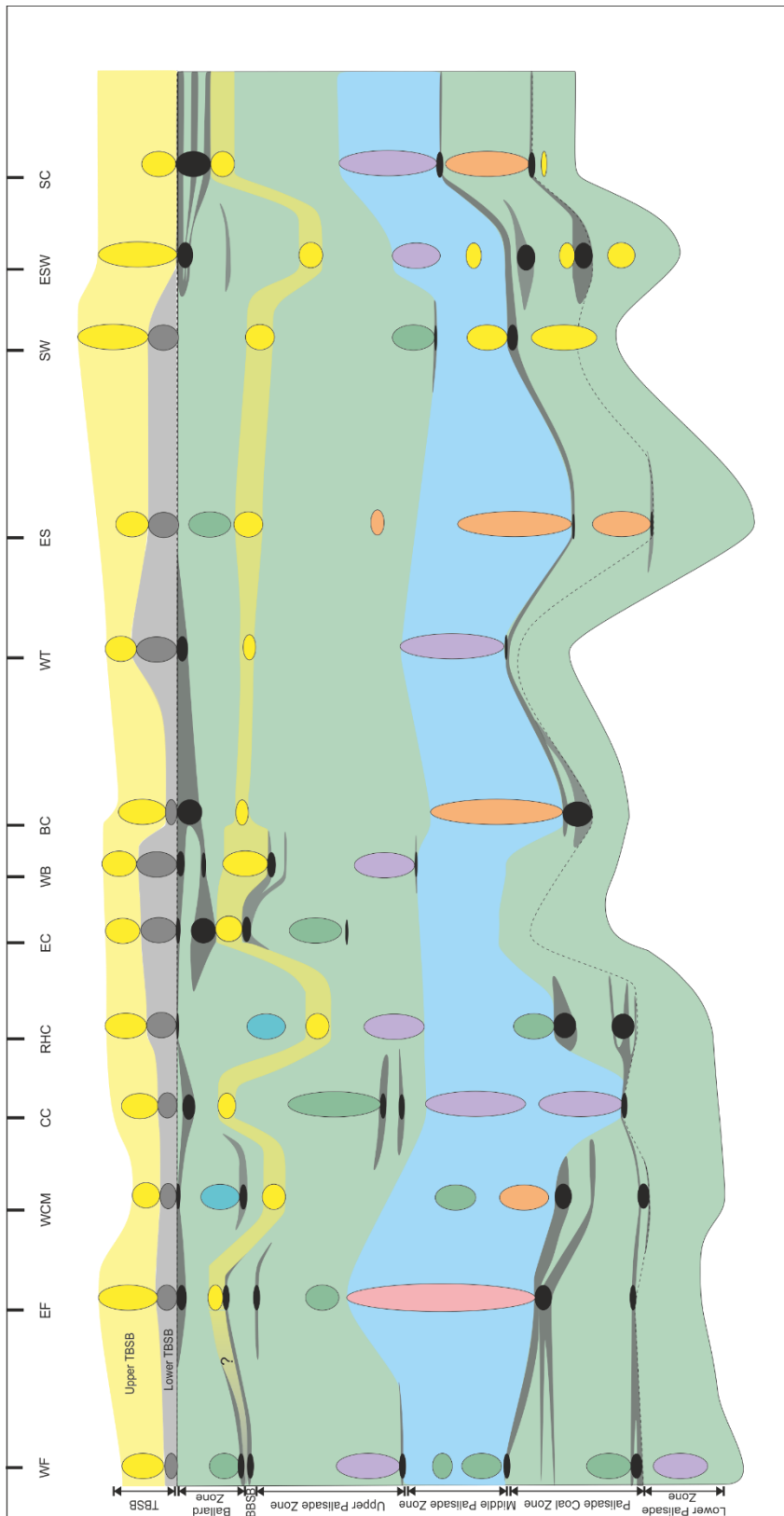
G.8. The Middle Palisade Zone is interpreted



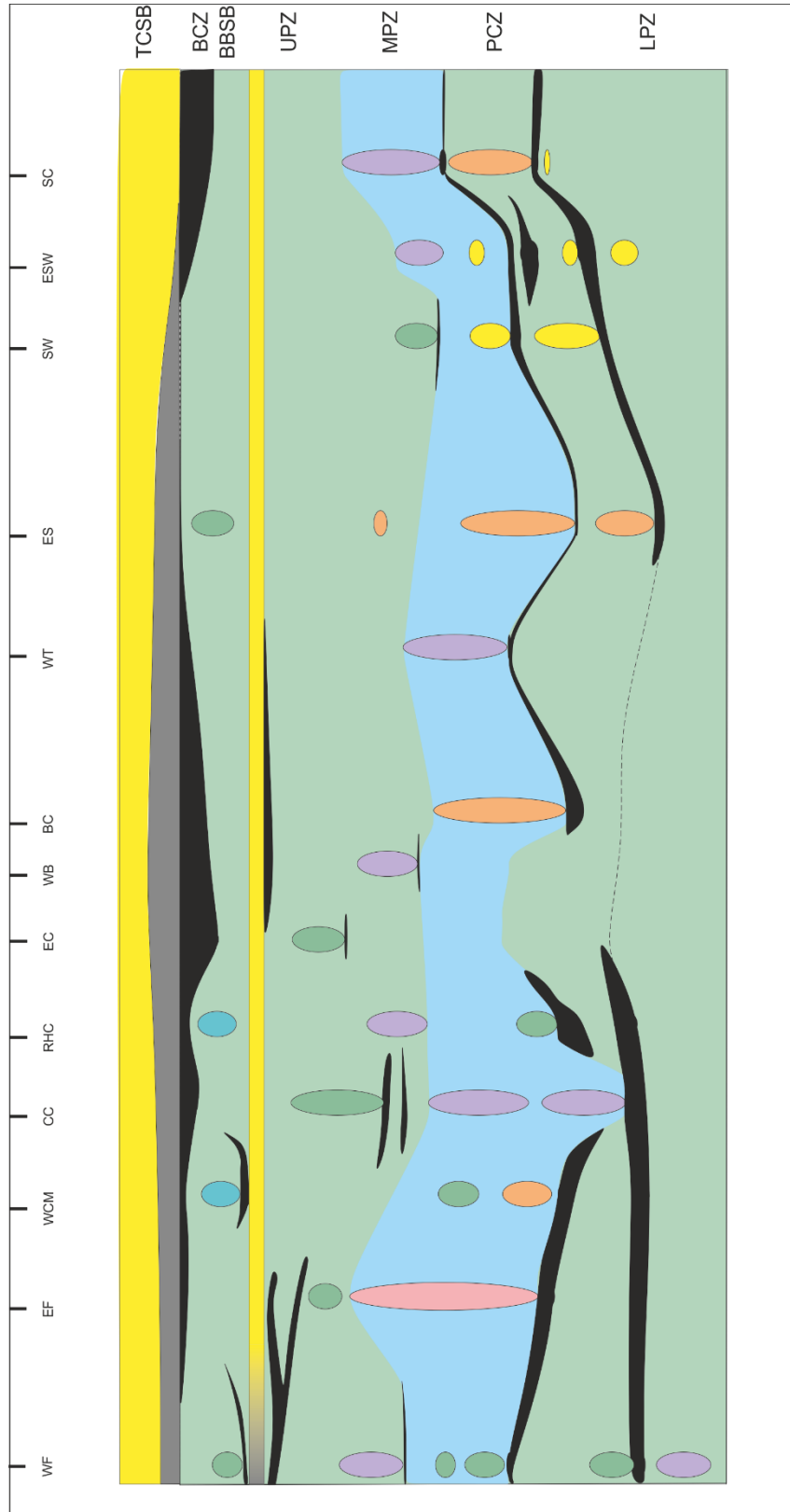
G.9. Interpretation of further depositional intervals



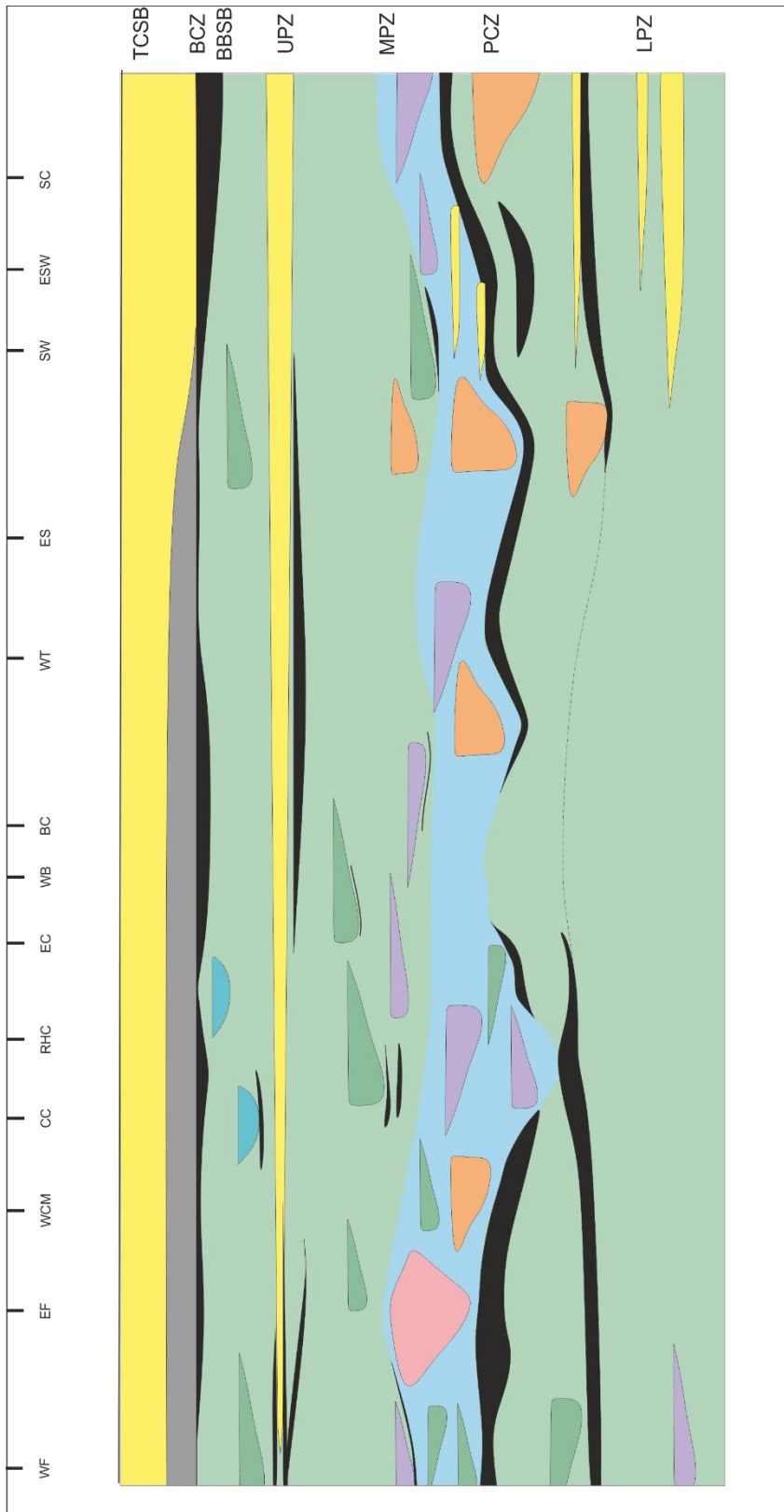
G.10. The logs are removed from the panel



G.12. The geometry of marker horizons is interpreted and simplified

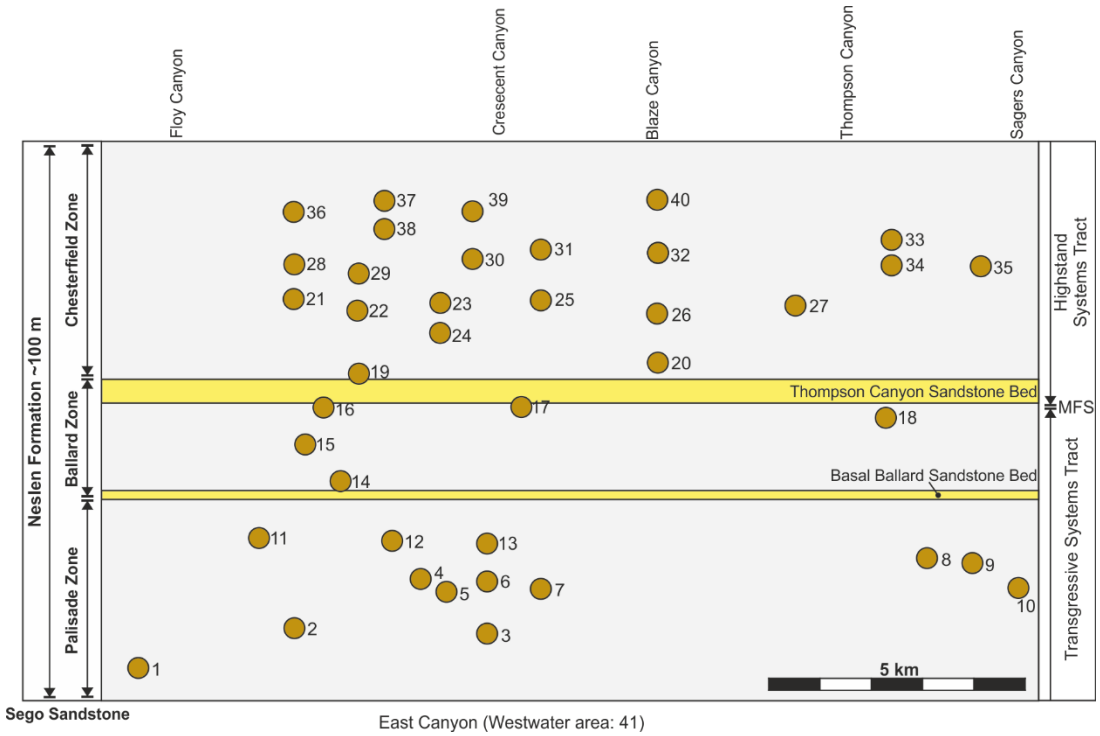


G.13. Simplified geometry of architectural elements are indicated



APPENDIX H

A total of 42 point-bars were analysed in Chapter 6; these are numbered 1-41 on the panel below, and their coordinates are displayed in the table. The data recorded at each point bar is shown in the following sections.



The co-ordinates, or position on a larger logged section (presented in Appendix B or Appendix F) are presented below:

Point bar number	Log number	Lower GPS		Upper GPS		On a larger logged section: Name (Appendix)	Total length (m)
		N	W	N	W		
1	a					West Floy (E) 15-17 m	6.7
2	a						4
3	a	39 01.921	108 47.645				3
	b	39 01.934	109 47.971	39 01.937	109 47.974		3.5
4	a					Log 11 (B) X-X	3
5	a					Log 13 (B) X-X	5
6	a	39 01.965	109 47.704	39 01.367	109 47.712		3.5
	b	39 01.921	108 47.645				3.7
	c	39 01.958	109 47.670				5.6
7	a					Right Hand Crescent (E) 18-23.2	5.2
8	a					Salt Wash (E) 20-23	3
	b	39 01.308	109 40.739				1.5
	c	39 01.298	109 40.959				3
	d	39 01.282	109 40.947				3
	e	39 01.291	109 40.786				1.5
	f	39 01.296	109 40.747				2
9	a					East Salt Wash (E) 27-31	4
	b	39 01.084	109 39.910	39 01.083	109 39.907		1.5
	c	39 01.073	109 39.914	39 01.078	109 39.906		4.5
	d	39 01.069	109 39.902	39 01.075	109 39.892		7
	e	39 01.059	109 39.896	39 01.058	109 39.894		3.75
	f	39 01.050	109 39.905	39 01.048	109 39.902		2
	g	39 01.051	109 39.883	39 01.049	109 39.873		1.5
10	a					Sagers Canyon (E) 10-16	6

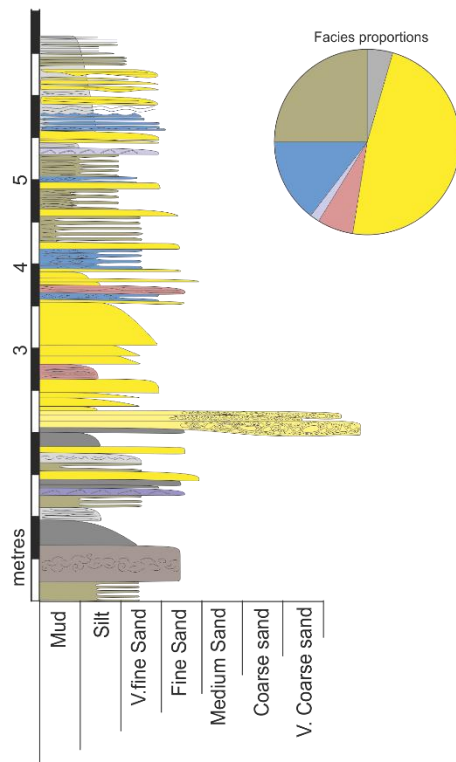
11	a	39 00.504	109 50.110				9.5
	b	39 00.500	109 50.072	39 00.505	109 50.059		8.5
12	a					Log 3 (B) 20-26	5.7
13	a	39 01.976	109 47.715	39 01.979	109 47.727		6.7
	b			39 01.928	109 47.646		3.8
	c			39 01.966	109 47.673		4
14	a						6
15	a					Log X (B) X-X	4.2
16	a					Log 1 (B) X-X	15
17	a	39 01.385	109 47.078	39 01.385	109 47.071		11.8
18	a					Panel X	8
19	a					Log 3 (B) X-X	
20	a					Blaze Canyon (H) 40-53	13
21	a					Log 4 (B) X-X	10.9
22	a					Log 5 (B) X-X	5.3
23	a					Log 12 (B) X-X	11.7
24	a					Log 12 (B) X-X	1.6
25	a					Right Hand Crescent (H) X-X	6
26	a					Blaze Canyon (H) X-X	10
27	a					West Thompson (H) X-X	5
28	a					Log 6 (B) X-X	13.1
29	a					Log 5 (B) X-X	6.4
30	a					Log 13 (B) X-X	4.5
31	a					Right Hand Crescent (H) X-X	8.9
32	a					Blaze Canyon (H) X-X	13
33	a					East Sego (H) X-X	8.2
35	a					Salt Wash (H) X-X	25.5
34	a					East Sego (H) X-X	10
36	a					Log 4 (B) X-X	10.7

37	a					Log 6 (B) X-X	6.3
38	a					Log 6 (B) X-X	3.9
39	a					Log 13 (B) X-X	10.1
40	a					Blaze Canyon (H) X-X	5
41	a	39 18.09	109 16.581	39 18.006	109 16.596		2
	b	39 18.090	109 16.612	39 18.100	109 16.615		2
	c	39 18.034	109 16.718	39 18.042	109 16.725		12
	d	39 18.034	109 16.694	39 18.028	109 16.702		8
	e	39 18.037	109 16.566	39 18.037	109 16.567		6
	f	39 18.059	209 16.637	39 18.036	109 16.638		6
	g	39 17.984	109 16.586	39 17.983	109 16.583		8.5

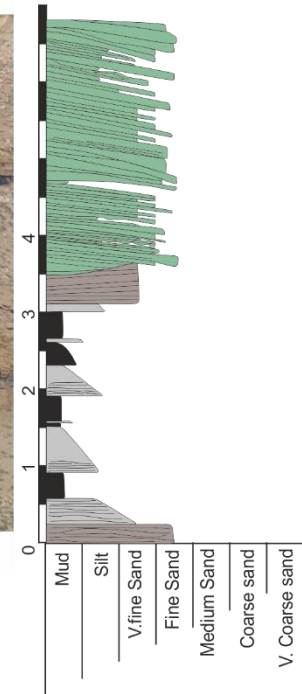
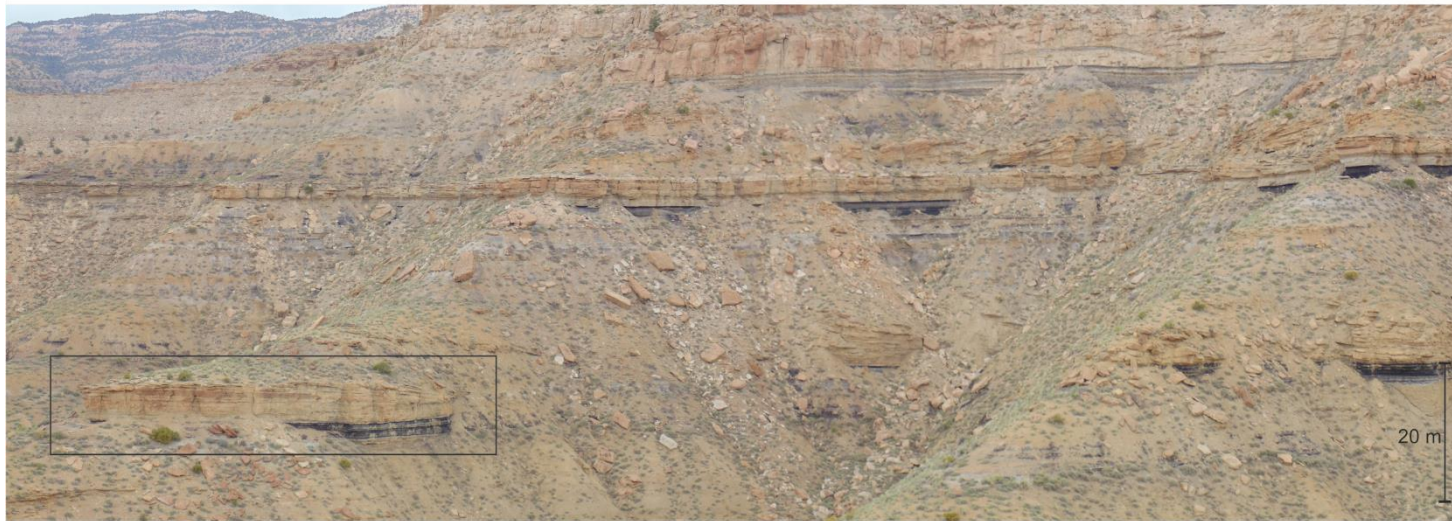
Appendix I

Sedimentary logs and stratigraphic panels, along with their facies proportions and interpreted type are presented for each studied point-bar element (point-bar elements 1-21, 41). Logs for point bar-elements 19, 21-24, 28-30, 36-39 can be found within large scale logs around Crescent Butte; Appendix B. The large-scale logs for other elements can be found within this Appendix. The key for facies is found in Figure 6.7.

Point-bar element 1: Type II



Point-bar element 2: Type I

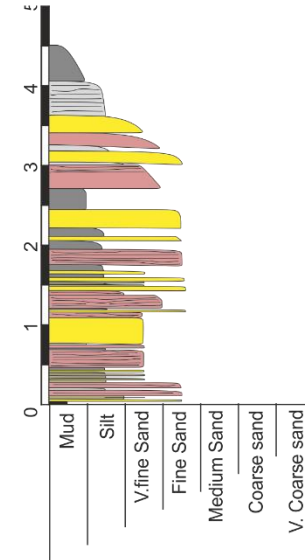
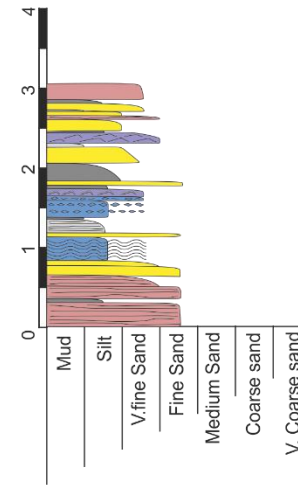
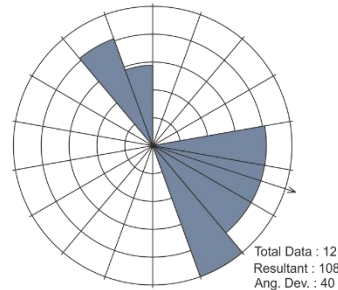
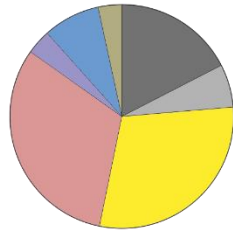


Type III point bar element based on the aspect ratio

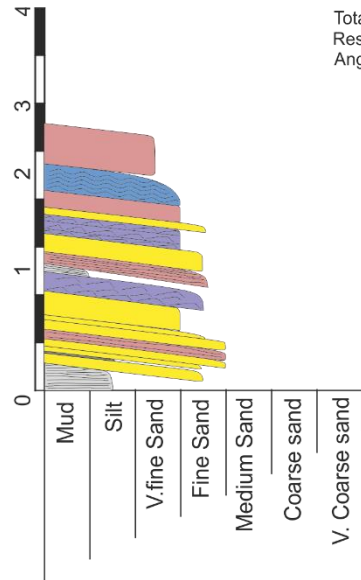
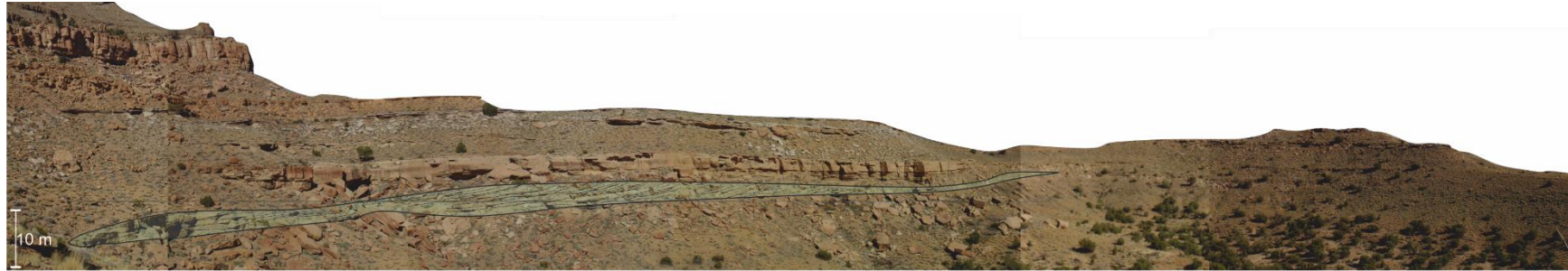
Point-bar element 3: Type II



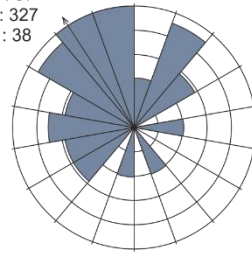
Facies proportions



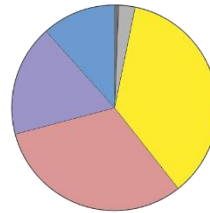
Point-bar element 4: Type I



Total Data : 37
 Resultant : 327
 Ang. Dev. : 38



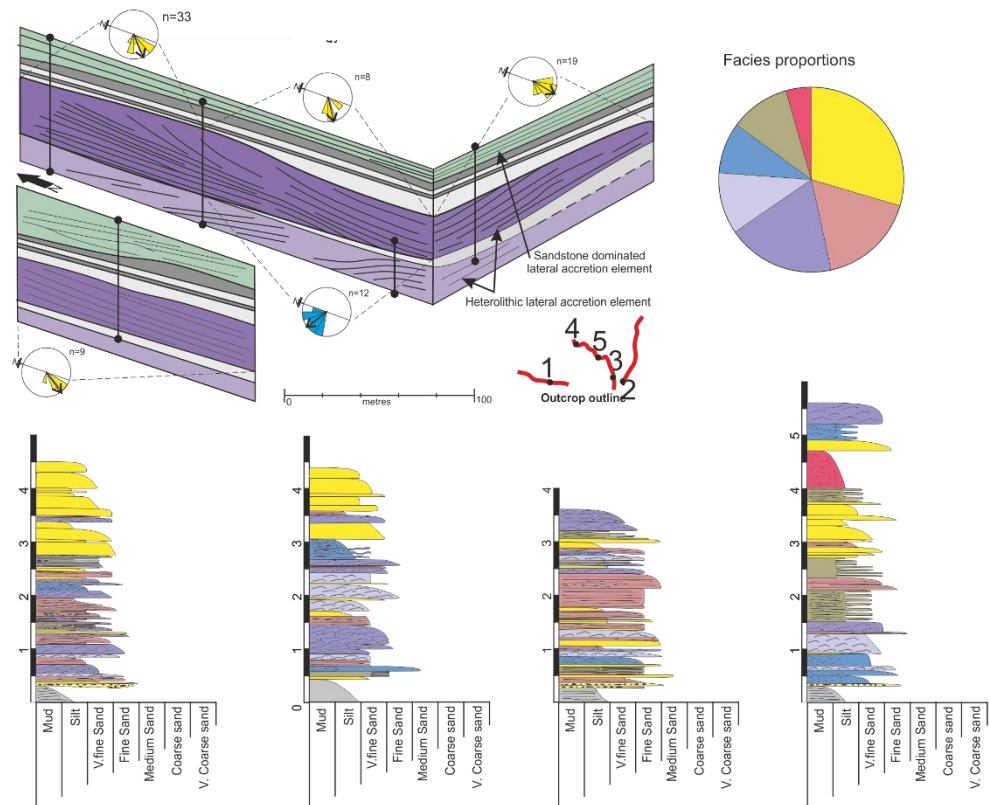
Facies proportions



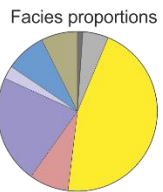
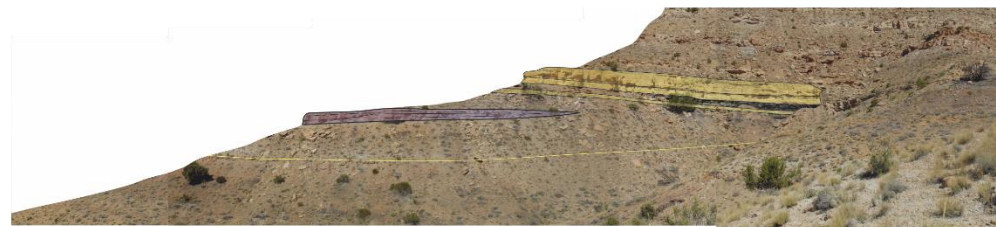
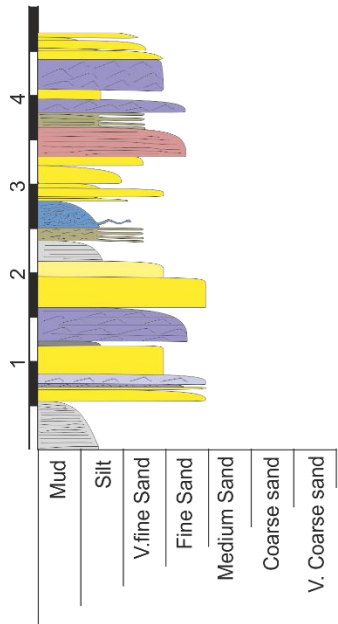
Point-bar element 5: Type II

This point-bar element is displayed in Figure 6.8

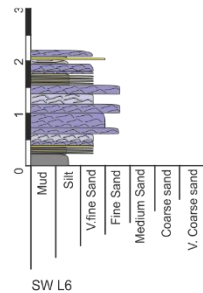
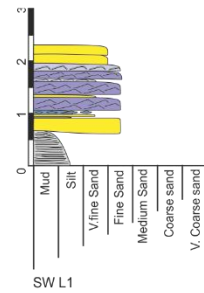
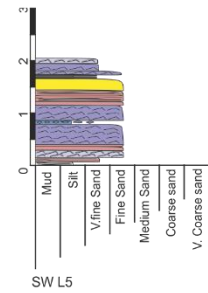
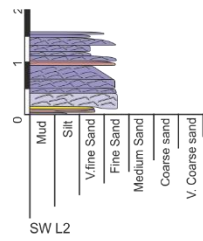
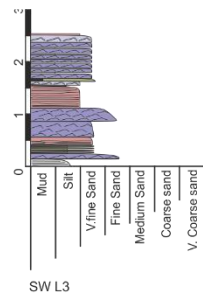
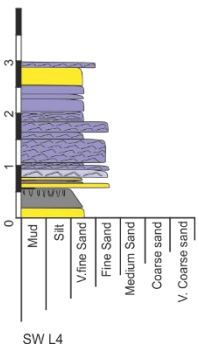
Point-bar element 6: Type I



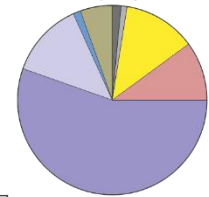
Point-bar element 7: Type I



Point-bar element 8: Type I



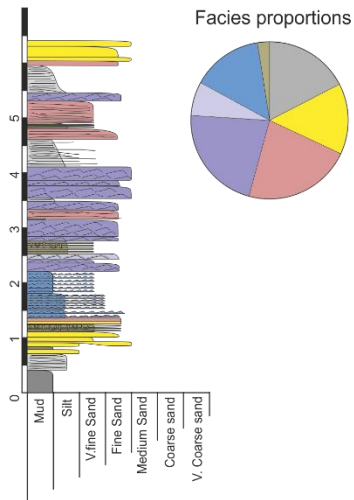
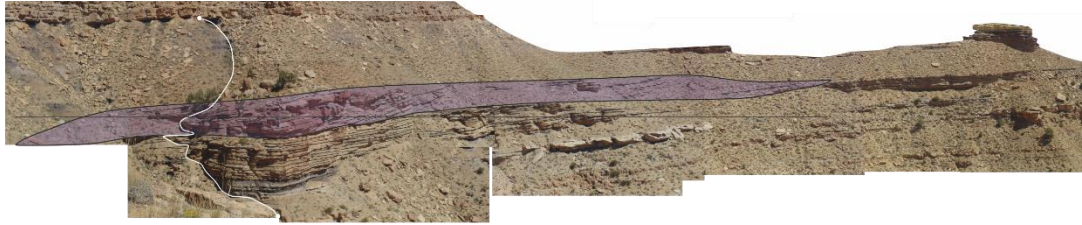
Facies proportions



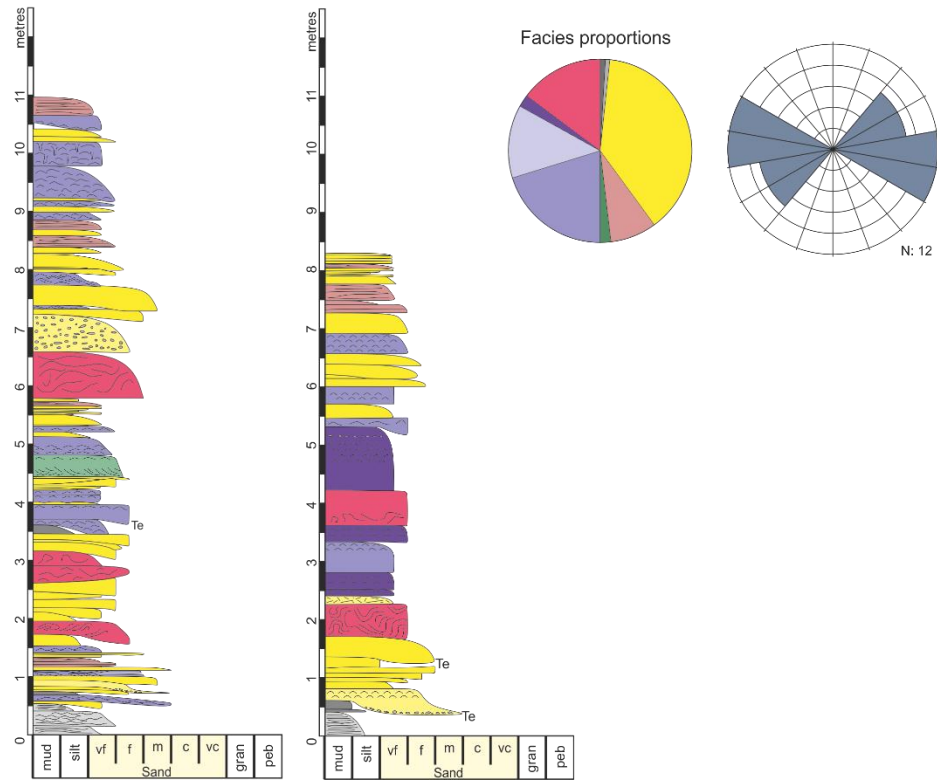
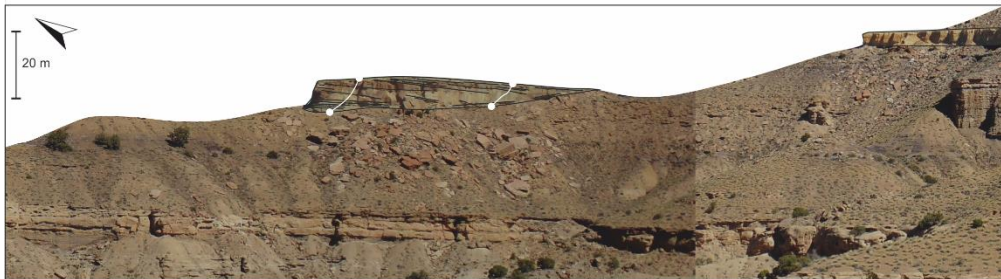
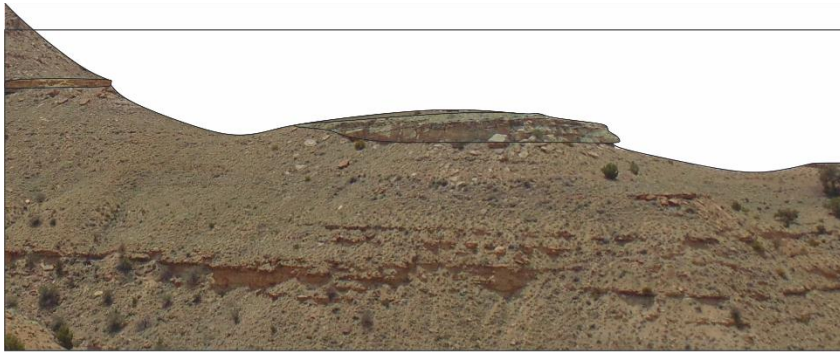
Point-bar element 9: Type I

This element is shown in Figure 6.7

Point-bar element 10: Type II



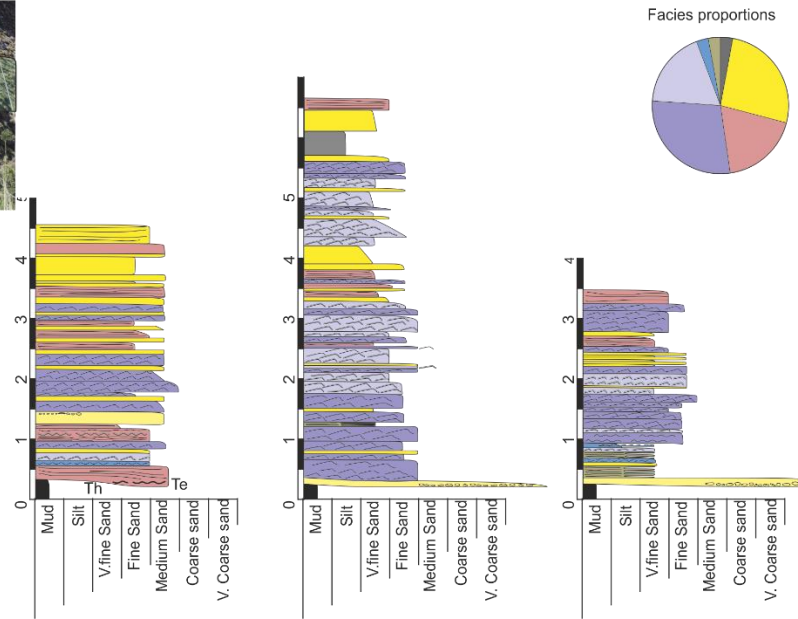
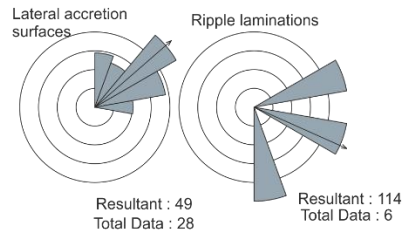
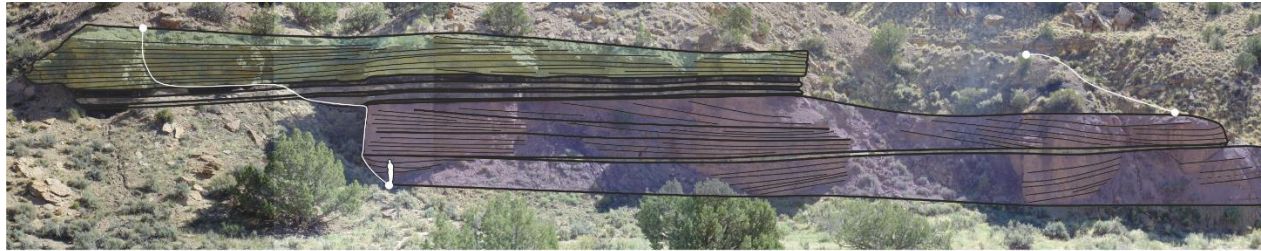
Point-bar element 11: Type II



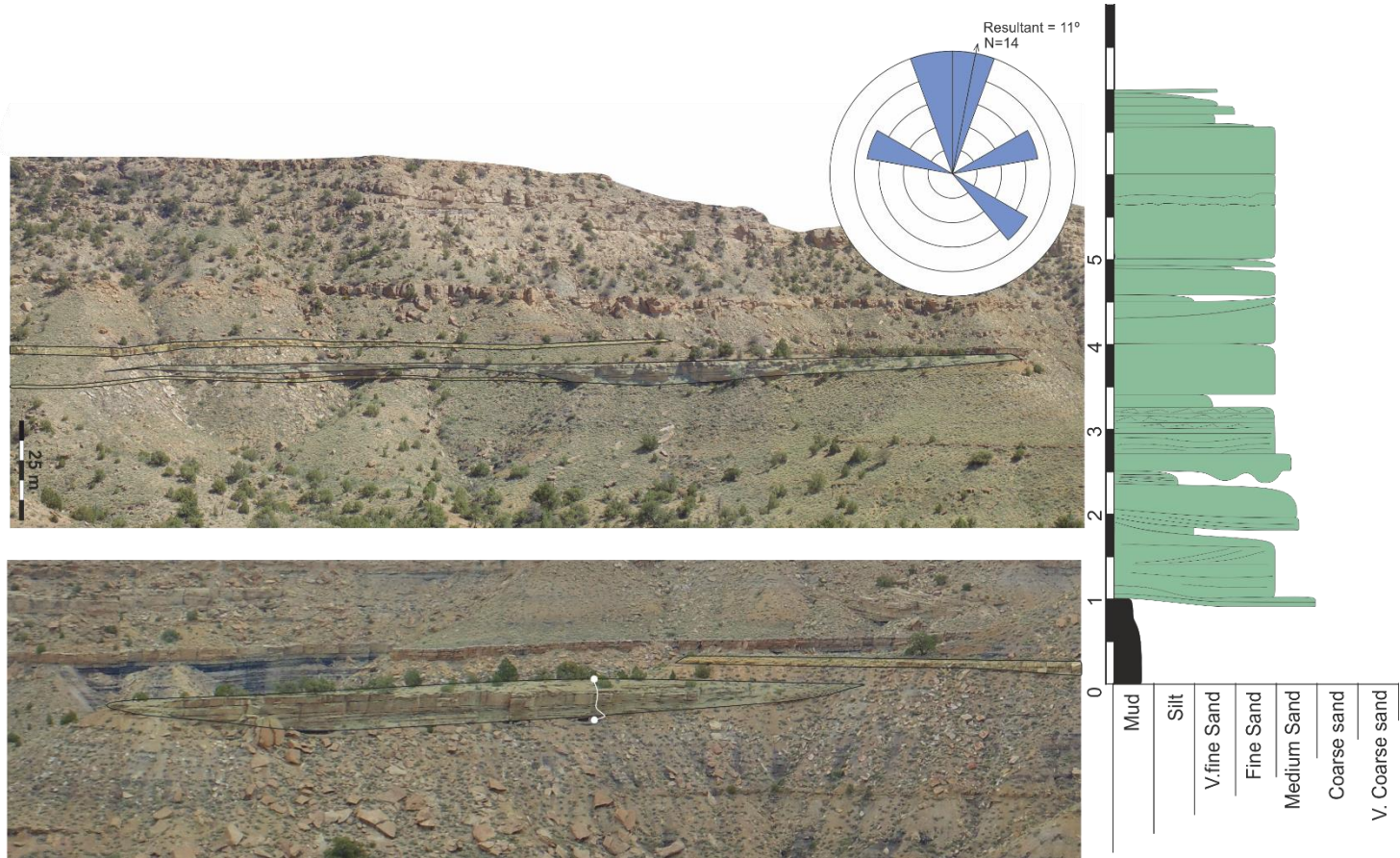
Point-bar element 12: Type III

This element is shown in Figure 6.9

Point-bar element 13: Type II



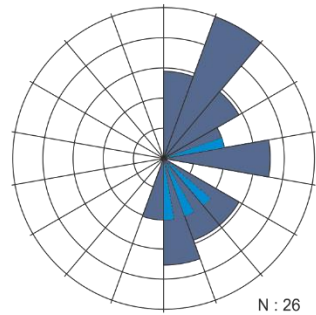
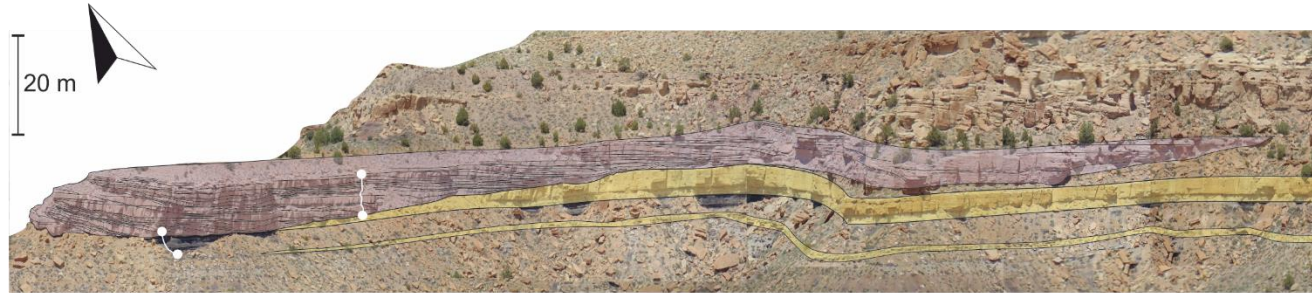
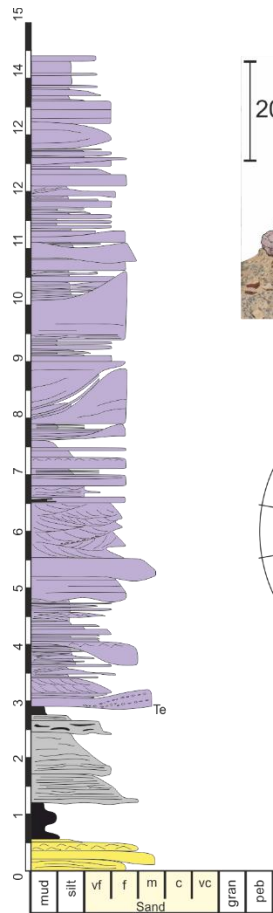
Point-bar element 14: Type I



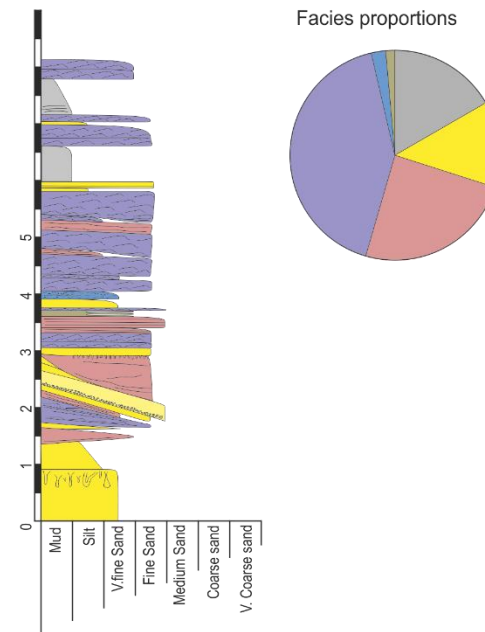
Point-bar element 15: Type I



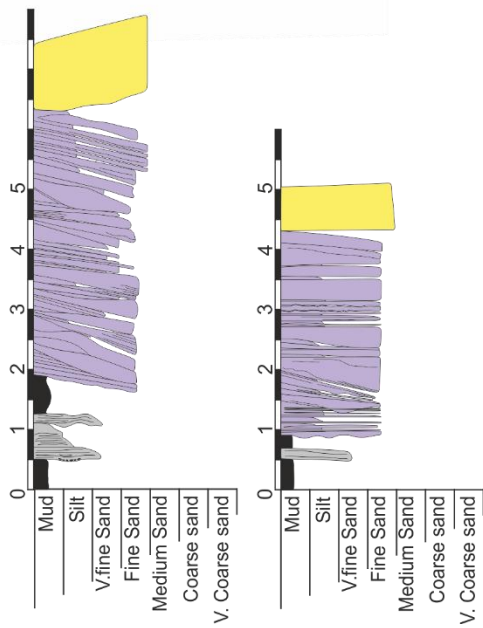
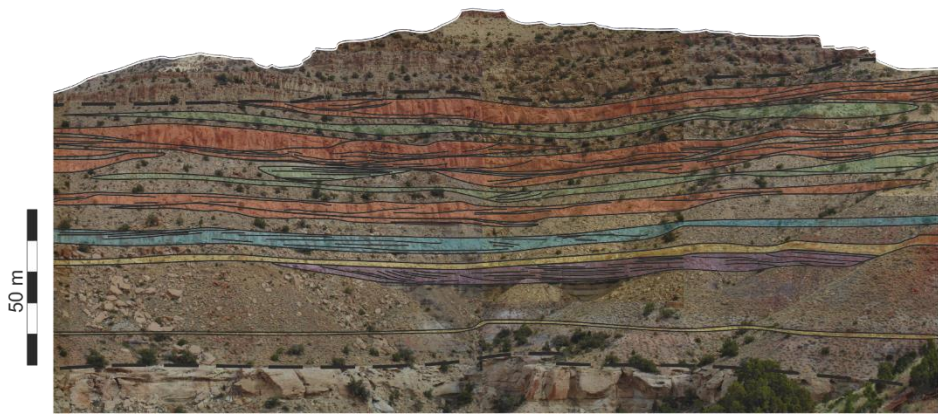
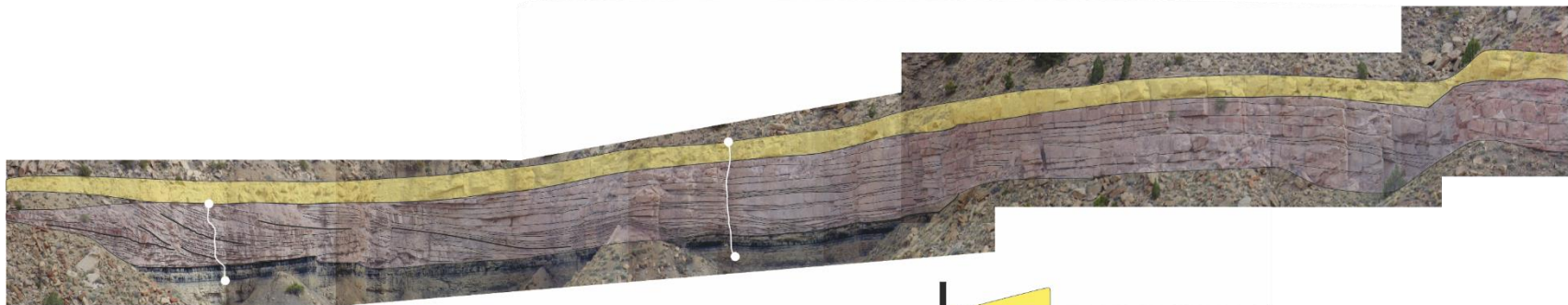
Point-bar element 16: Type III



Accretion surfaces
Ripples

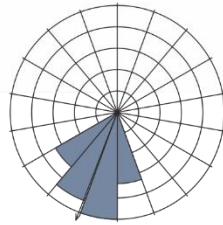
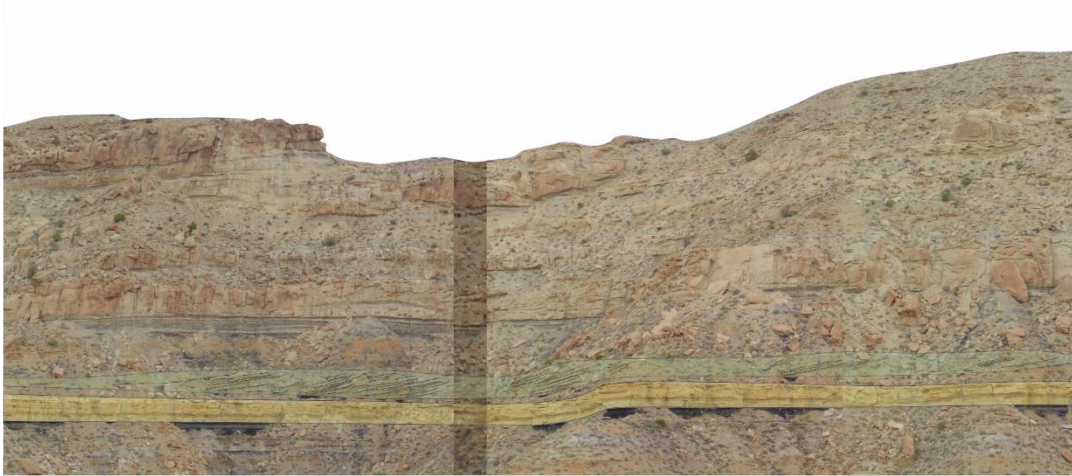


Point-bar element 17: Type I

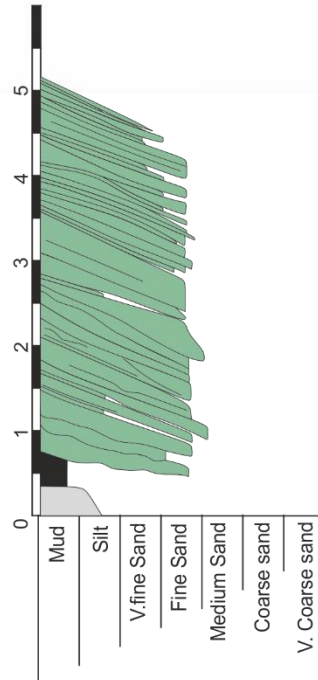


Point-bar element 18: Type I

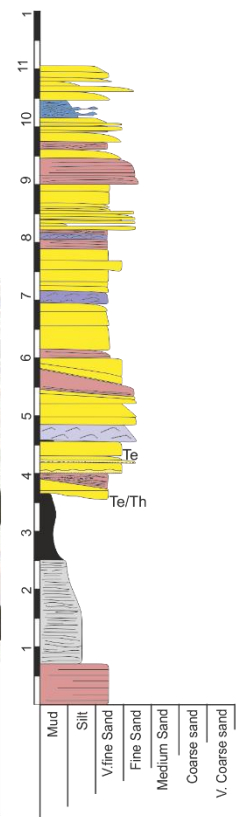
Point-bar element 19: Type I



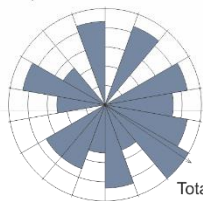
Total Data : 24
Resultant : 201



Point-bar element 20: Type I

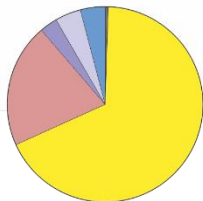


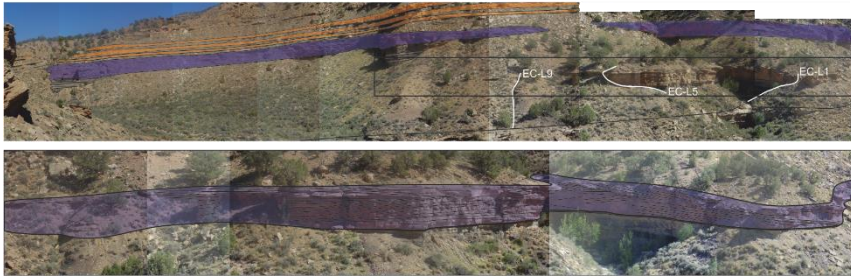
Dip direction of accretion surfaces



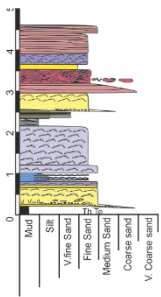
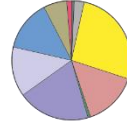
Total Data : 32
Resultant : 124

Facies proportions

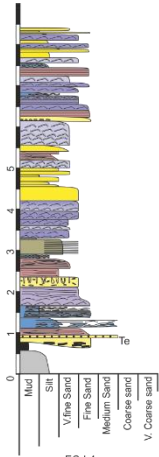




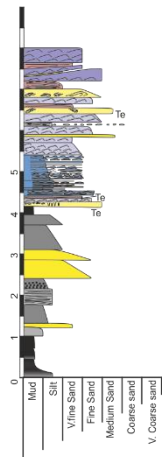
Facies proportions



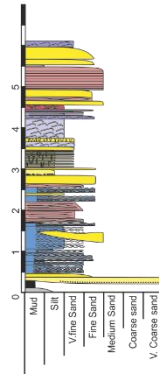
EC-L8



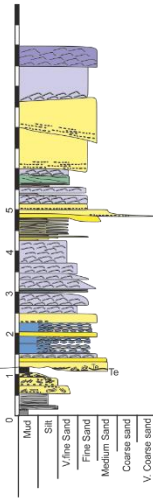
EC-L4



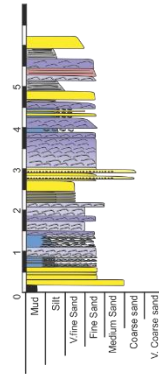
EC-L1



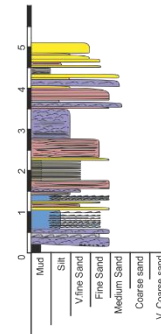
EC-L5



EC-L7



EC-L6



Point-bar element 41: Type I

Point-bar elements within Appendix B: Type IV

Point-bar element 19 can be found on log 3

Point-bar elements 21 and 36 can be found on log 4

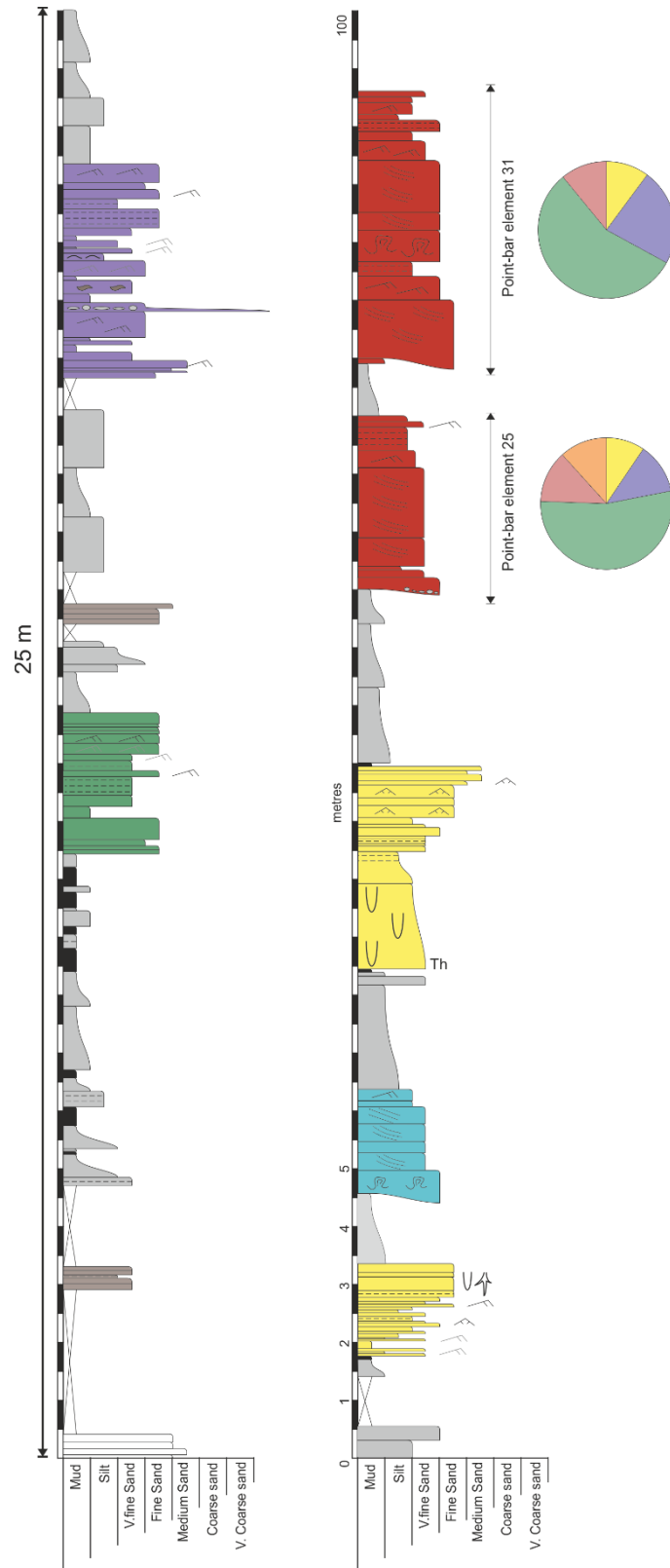
Point-bar elements 22 and 29 can be found on log 5

Point-bar elements 28, 37 and 38 can be found on log 6

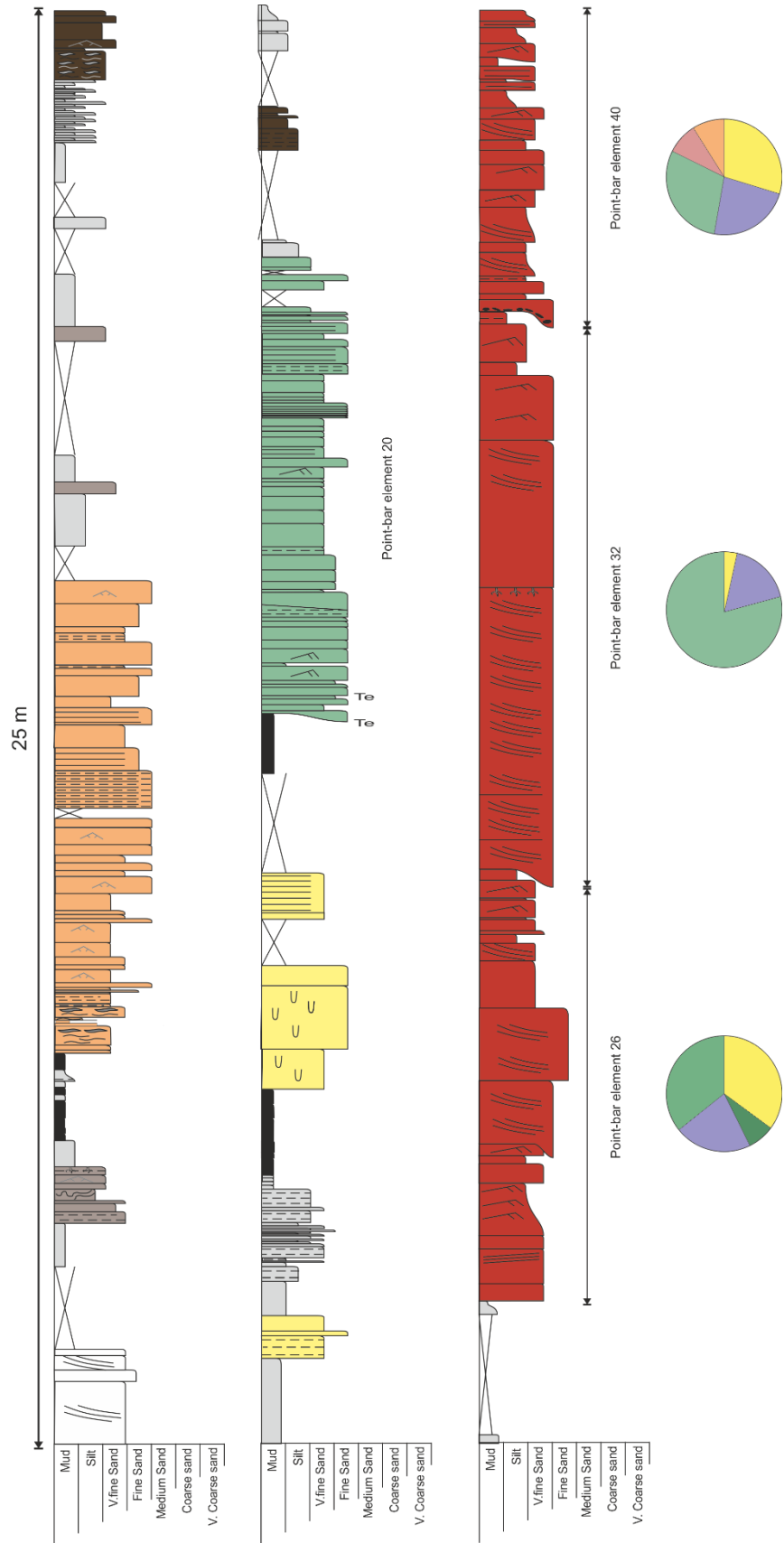
Point-bar element 24 can be found on log 12

Point-bar elements 30 and 39 can be found on log 13

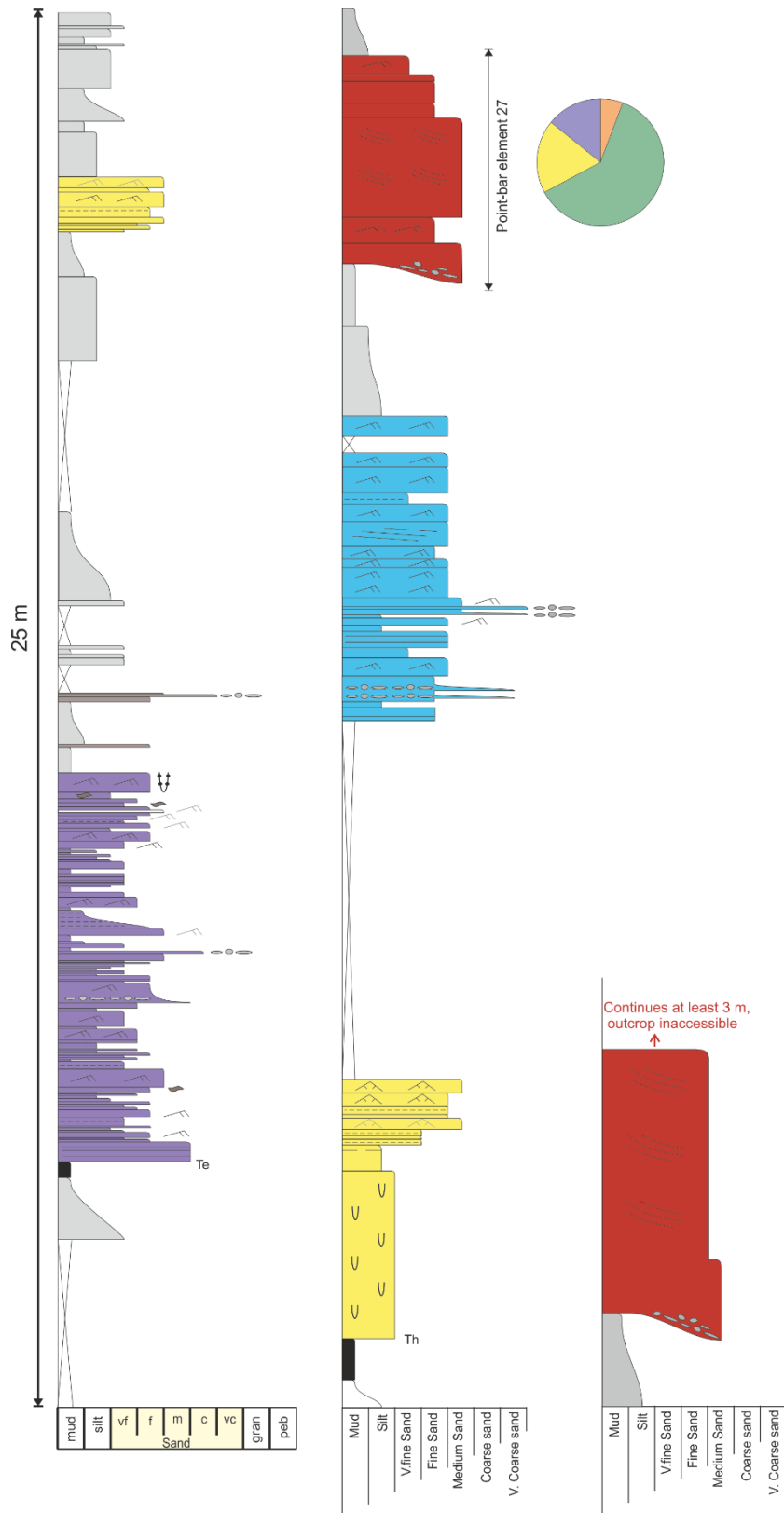
Point-bar elements 25 and 31 (Right Hand Crescent): Type IV



Point-bar elements 26,32 and 40 (Blaze Canyon): Type IV



Point-bar element 27 (West Thompson): Type IV



Point-bar element 35 (Salt Wash): Type I

